Université de Paris

École doctorale ED564 : «Physique en Île-de-France»

Laboratoire Matière et Systèmes Complexes

Infinite dimensional active matter and stochastic calculus for path integration

Par Thibaut Arnoulx de Pirey

Thèse de doctorat de Physique théorique

Dirigée par Frédéric van Wijland

Présentée et soutenue publiquement le 12 novembre 2021

Devant un jury composé de :

David Dean, Professeur, Université de Bordeaux, Rapporteur

Irene Giardina, Associate professor, Sapienza University of Rome, Examinatrice,

Jorge Kurchan, DR, Ecole Normale Supérieure de Paris, Président

Thomas Speck, Professor, Johannes Gutenberg-Universität Mainz, Rapporteur,

Valentina Ros, CR, Université Paris-Saclay, Examinatrice,

Frédéric van Wijland, Professeur, Université de Paris, Directeur.

Université de Paris

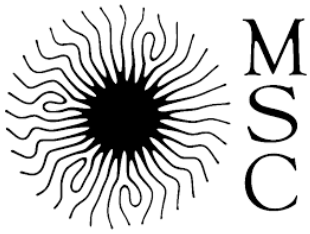

Université de Paris
Laboratoire Matière et Systèmes Complexes

Infinite dimensional active matter and stochastic calculus for path integration

Presented by Thibaut ARNOULX de PIREY SAINT ALBY

PhD thesis in Theoretical physics

November 12th 2021

Matière active en dimension infinie et calcul stochastique appliqué aux intégrales de chemin.

Résumé

Ce travail de thèse se divise en deux parties distinctes. La première est consacrée aux systèmes actifs de particules autopropulsées. Nous commençons par étudier le cas d'une particule dans un potentiel. Nous analysons les déviations par rapport à la dynamique d'équilibre de celle d'une particule active propulsée par un processus d'Ornstein-Ulhenbeck (AOUP) à petit temps de persistance et en présence de bruit thermique ainsi que les propriétés stationnaires d'une particule autopropulsées autour d'un obstacle sphérique dans la limite de grand temps de persistance. Nous nous intéressons ensuite aux propriétés collectives de ces systèmes. D'un point de vue analytique, leur compréhension est pour l'instant entravée par leur diffculté intrinsèque qui combine celles des systèmes hors d'équilibre à celles des liquides fortement corrélés. Depuis le milieu des années 1980, nous savons que les fuides d'équilibres peuvent être étudiés analytiquement dans la limite où la dimension de l'espace ambiant devient infinie. Les gains mathématiques sont alors considérables : non seulement l'énergie libre peut être calculée exactement mais aussi les coeffcients de transport. Ces idées eurent ensuite une influence majeure dans la théorie de la transition vitreuse en champ moyen. L'objectif ici est d'utiliser la limite de grande dimension dans le cas actif. Nous étudions d'abord les équations de la théorie de champ moyen dynamique dans la limite diluée, ce qui nous permet de quantifier la relation entre le déplacement quadratique moyen et la vitesse effective d'autopropulsion. Pour étudier les propriétés des systèmes actifs au-delà de la limite diluée nous proposons ensuite un schéma approché de resommation de la hiérarchie de Born-Bogolioubov-Green-Kirkwood-Yvon des fonctions de corrélation. Celui-ci permet de rendre compte de nombreuses propriétés observées dans les systèmes actifs de dimension finie, en particulier de la transition de phase induite par la motilité et de la décroissance linéaire de la vitesse effective d'autopropulsion des sphères dures actives avec la densité. Ces travaux nous conduisent à introduire le concept d'amplitude effective des interactions potentielles. Nous montrons alors que celle-ci s'annule à la même densité que la vitesse effective d'autopropulsion qui est aussi la densité de transition vitreuse dynamique d'un système colloïdal d'équilibre de structure équivalente. Ces résultats dressent un parallèle intéressant entre la transition vitreuse des systèmes d'équilibre et l'annulation de la vitesse effective d'autopropulsion des systèmes actifs qui est une propriété de la mesure stationnaire d'un système unique. La spécificité soulignée par cette resommation approchée est la présence d'interactions multicorps dans la mesure stationnaire. Contrairement au cas des liquides classiques d'équilibre, celle-ci ne peut en effet pas s'écrire sous la forme d'un produit sur les paires du système. L'importance de ces interactions multicorps dans le diagramme des phases des systèmes actifs a récemment été soulignée en dimension 3. Nous continuons d'explorer cette idée en dimension infinie en étudiant le diagramme des phases de l'approximation dite de bruit coloré unifié de la dynamique AOUP. Nous montrons que celui-ci présente deux régions de coexistence de phase que les interactions de paires seules ne peuvent expliquer. La deuxième partie de cette thèse porte sur des extensions du calcul stochastique dans les intégrales de chemin et généralise des résultats récemment établis dans le cas de processus unidimensionnels. Après avoir expliqué pourquoi il est en général

impossible d'utiliser les règles du calcul stochastique pour changer de variable au sein des intégrales de chemin en temps continu nous montrons comment modifier ces dernières en conséquence. Enfin, nous proposons une discrétisation d'ordre supérieur étendant celle de Stratonovich et rendant utilisable le calcul différentiel au sein des intégrales de chemin.

Mots clés : Physique statistique hors de l'équilibre, Matière active, Transition vitreuse, Champ moyen, Intégrales de chemin, Calcul stochastique, Transition de phase.

Infinite dimensional active matter and stochastic calculus for path integration.

Abstract

The forthcoming work is divided into two distinct parts. The first one deals with self-propelled particles systems. We start by studying the one particle in an external potential case. We derive the nonequilibrium properties of the Active Ornstein-Ulhenbeck Particle model at small persistence time in the presence of thermal noise and the stationary measure of a run-and-tumble particle around a hard spherical obstacle at large persistence time. We then focus on the collective behavior of such systems. From an analytical standpoint, not much is known given their high degree of complexity that combines those of out-of-equilibrium physics to those of strongly correlated liquids. Since the mid-eighties and Frisch's & al. work, we have known that equilibrium fluids can be studied exactly in the limit where the dimension of the embedding space becomes infinite. The mathematical gains are then considerable: not only the free energy can be obtained analytically but also transport coefficients. These ideas later had a groundbreaking influence on the mean-field theory of the glass transition which is naturally expressed in infinite dimension. Here, the goal is to use the large dimension limit to gain theoretical insights into the behavior of active systems. The equations of the dynamical mean field theory are first studied in the dilute limit and we quantify the connections between the mean-square-displacement and the effective propulsion speed. To go beyond the dilute limit, we then propose an approximate resummation scheme of the Born-Bogolioubov-Green-Kirkwood-Yvon hierarchy of correlation functions. The latter allows us to account for various properties observed in finite dimensional systems, in particular for the Motility Induced Phase Separation and for the linear decrease with density of the effective self-propulsion speed of active hard spheres. We also introduce the concept of effective amplitude of potential interactions. We then show that this amplitude vanishes at the same density as the effective propulsion speed which is also that of the dynamical glass transition of an equilibrium colloidal system with equivalent structure. These results draw interesting links between the glass transition of equilibrium systems and the vanishing of the effective self-propulsion speed which is a stationary property of a unique active system. The specificity underlined by this approximate resummation is the presence of multibody interactions in the steady state measure. Unlike its equilibrium counterpart, it cannot be written as a product over the pairs in the system. The importance of these multibody interactions in the phase behavior of active systems was recently demonstrated in dimension 3. We keep exploring this idea by studying the phase diagram of the unified colored noise approximation of the AOUP dynamics. We show that it displays two regions of phase coexistence that the sole pair interactions are unable to account for. The second part of the manuscript deals with the extension of stochastic calculus to path integration and generalizes results recently obtained in the one-dimensional case. After explaining why it is in general impossible to use the rules of stochastic calculus to change variables within continuous time path integrals we show how to modify these rules consequently. We finally propose a higher-order discretization scheme extending that of Stratonovich and making the rules of standard differential calculus compatible with path integration.

Keywords: Out-of-equilibrium statistical physics, Active matter, Mean-field, Glass transition, Phase transitions, Path integrals, Stochastic calculus.

Matière active en dimension infinie et calcul stochastique appliqué aux intégrales de chemin.

Résumé substantiel

Ce travail de thèse se divise en deux parties distinctes. La première est dédiée à l'étude d'une classe de modèles de matière active. Ce terme englobe un vaste ensemble de systèmes qui ont en commun la capacité de leur constituants élémentaires à extraire et consommer de l'énergie de leur milieu dans le but de se mouvoir. À l'échelle de la particule individuelle, la dissipation et l'injection d'énergie suivent alors des processus physico-chimiques distincts ce qui a pour conséquence immédiate de faire évoluer hors de l'équilibre jusqu'aux plus simples systèmes de particules actives en interaction. À l'échelle collective ou macroscopique, la phénoménologie des systèmes composés d'un grand nombre de particules actives est de ce fait extrêmement riche, suscitant ainsi l'intérêt des physiciens tout au long des trente dernières années.

Les systèmes expérimentaux qui viennent le plus naturellement en tête sont pour la plupart issus du monde vivant comme illustré Fig. 1. On peut ainsi penser aux grands groupes d'animaux tels que les vols d'étourneaux [9], les troupeaux de moutons [80] ou les bancs de poissons [111] dont une des particularités remarquable est l'existence d'un mouvement collectif à grande échelle. D'autres exemples existent aussi aux échelles cellulaires et subcellulaires, à l'instar des bactéries auto-propulsées [173] qui peuvent, dans certaines circonstances, se regrouper en clusters denses. Il existe par ailleurs un nombre de plus en plus im-

Figure 1: Exemples de comportements collectifs dans le vivant. **(a)** Vol d'étourneaux. **(b)** Troupeau de mouton. **(c)** Colonies de bactéries (Myxococcus xanthus). [173].

portant de systèmes expérimentaux synthétiques. Ceux-ci ont l'avantage certain d'être plus contrôlés et reproductibles que les systèmes vivants. L'étude des particules Janus [207], des colloïdes auto-propulsés par diffusiophorèse, est ainsi devenue centrale en matière active. Par exemple, dans [19], celles-ci sont recouvertes sur un hémisphère seulement de carbone et sont placées dans un mélange quasi-critique d'eau et de lutidine. Lorsqu'illuminé par un laser de la bonne fréquence, l'hémisphère de carbone chauffe. Ceci induit alors localement un déphasage de la solution ce qui, en retour, exerce une force phorétique sur les colloïdes. Lorsque la densité de particules est suffisamment grande, ces colloïdes, qui ne sont nullement attirés entre eux par aucune interaction potentielle directe, se regroupent alors en cluster denses séparés par des régions presque vides comme montré Fig. 2.

Au sein de ce vaste ensemble de systèmes que forme la matière active, nous nous intéresserons dans cette thèse plus spécifiquement à une classe de modèles visant à décrire

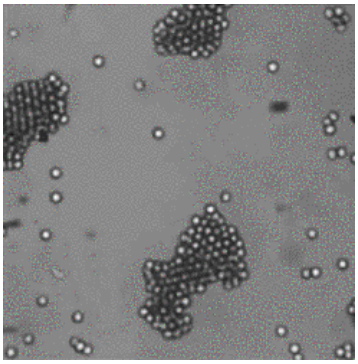

Figure 2: Formation de clusters denses de particule Janus à moitié recouverte de carbone évoluant dans un mélange quasi-critique d'eau et de lutidine [19].

de la façon la plus simple possible la phénoménologie observée dans les expériences sur les particules Janus. Ceux-ci sont définis par les équations du mouvement à N-corps dans une limite suramortie,

$$\dot{\mathbf{r}}_i = \mathbf{v}_i(t) - \boldsymbol{\nabla}_{\mathbf{r}_i}\Phi(\mathbf{r}_1, \ldots, \mathbf{r}_N)\,, \tag{1}$$

chaque particule i évoluant ainsi sous l'action de (i) une force d'autopropulsion $\mathbf{v}_i(t)$ et (ii) une force conservative. L'énergie potentielle totale Φ est donnée comme la somme de contributions à un corps (dans un potentiel extérieur V) et de contributions à deux corps (avec U pour potentiel de paire),

$$\Phi(\mathbf{r}_1, \ldots, \mathbf{r}_N) = \sum_{i=1}^{N} V(\mathbf{r}_i) + \sum_{(i,j)} U(\mathbf{r}_i - \mathbf{r}_j)\,. \tag{2}$$

En l'absence d'interaction, la particule libre, sous l'effet de la force d'autopropulsion, suit une marche aléatoire persistante. On trouve différentes façons de modéliser la statistique de celle-ci dans la littérature en matière active. Par exemple, dans le cas des particules browniennes actives (ou ABP pour Active Brownian Particles), $\mathbf{v}_i(t) = v_0\mathbf{u}_i(t)$ où $\mathbf{u}_i(t)$ est de norme unité et diffuse librement sur la sphère, voir Fig. 3. Dans le cas des particules dites de type RTP (pour Run-and-Tumble Particles), $\mathbf{v}_i(t) = v_0\mathbf{u}_i(t)$ où $\mathbf{u}_i(t)$ est de norme unité et est aléatoirement et uniformément tiré sur la sphère avec un temps caractéristique τ de sorte que le mouvement d'une particule libre est constitué d'une séquence d'excursions balistiques aléatoirement réorientées, voir Fig. 3.

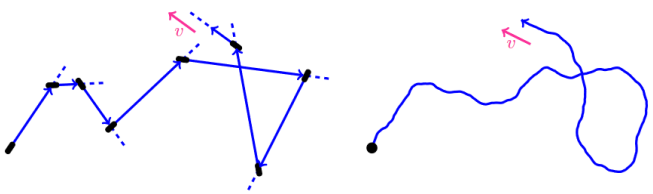

Figure 3: Trajectoire d'une particule libre **(Gauche)** de type RTP et **(Droite)** de type ABP. Extrait de [24].

Dans la limite où la longueur de persistance du marcheur aléatoire libre devient négligeable devant la portée typique des interactions potentielles (tout en conservant un coefficient de diffusion D fini), le système à N-corps défini par l'équation Eq. (1) est bien connu puisqu'il s'agit d'un système colloïdal d'équilibre. La distribution stationaire associée est en particulier donnée par la distribution de Boltzmann à température D, $P_S \propto \mathrm{e}^{-\Phi/D}$. La nature active du système devient manifeste dès lors que la longueur de persistance est de l'ordre de (ou grande devant) la portée des interactions potentielles. Faire des prédictions analytiques dans ce régime n'est cependant pas chose facile, la solution stationaire de l'équation maîtresse associée à la dynamique décrite dans l'équation Eq. (1) étant en général hors de portée. Grâce à de nombreux travaux numériques [39, 162], le diagramme des phases des modèles de particules actives interagissant via un potentiel de paire répulsif de courte portée est néanmoins bien connu. Lorsque l'activé (quantifiée par le rapport entre la longueur de persistance de la particule libre et la portée du potentiel de paire) et la densité sont suffisamment grande, le système devient inhomogène et se sépare en deux phases, l'une dense et l'autre diluée [193] et ceci en dépit du fait que les interactions potentielles entre particules soient purement répulsives : c'est la séparation de phase induite par la motilité (ou MIPS pour Motility-Induced Phase Separation).

Dans cette thèse, ces systèmes sont étudiés analytiquement avec pour objectif de gagner en compréhension quant à leur comportement macroscopique. L'approche que nous adoptons est celle d'une complexité qui augmente tout au long du manuscrit. Nous commençons ainsi par étudier le cas d'une particule dans un potentiel extérieur. Nous analysons d'abord les déviations par rapport à la dynamique d'équilibre de celle d'une particule active propulsée par un processus d'Ornstein-Ulhenbeck (AOUP) à petit temps de persistance et en présence de bruit thermique. Nous montrons en particulier que le courant de probabilité et le taux de production d'entropie peuvent être, suivant le potentiel extérieur, des fonctions non-monotones de la température tranduisant ainsi une relation non-triviale entre le bruit actif et le bruit thermique. Dans un second temps, nous calculons la distribution stationaire d'une particule autopropulsée autour d'un obstacle sphérique dans la limite de grands temps de persistance. Ces résultats mettent en exergue comment la persistance de la force d'autopropulsion peut induire une attraction effective entre la particule et l'obstacle. Celle-ci se manifeste notamment à travers l'existence, dans la distribution stationnaire, d'un delta de Dirac au contact. Nous nous intéressons ensuite aux propriétés collectives de ces systèmes. D'un point de vue analytique, leur compréhension est pour l'instant entravée par leur difficulté intrinsèque qui combine celles des systèmes hors d'équilibre à celles des liquides fortement corrélés. Depuis le milieu des années 1980, nous savons que les fluides d'équilibres peuvent être étudiés analytiquement dans la limite où la dimension de l'espace ambiant devient infinie. Les gains mathématiques sont alors considérables : non seulement l'énergie libre peut être calculée exactement mais aussi les coefficients de transport. Ces idées eurent ensuite une influence majeure dans la théorie de la transition vitreuse en champ moyen. L'objectif ici est d'utiliser la limite de grande dimension dans le cas actif. Nous étudions d'abord les équations de la théorie de champ moyen dynamique dans la limite diluée, ce qui nous permet de quantifier la relation entre le déplacement quadratique moyen et la vitesse effective d'autopropulsion. Pour étudier les propriétés des systèmes actifs au-delà de la limite diluée nous proposons ensuite un schéma approché de resommation de la hiérarchie de Born-Bogolioubov-Green-Kirkwood-Yvon des fonctions de corrélation. Celui-ci permet de rendre compte de nombreuses propriétés observées dans les systèmes ac-

tifs de dimension finie, en particulier de la transition de phase induite par la motilité et de la décroissance linéaire de la vitesse effective d'autopropulsion des sphères dures actives avec la densité. Ces travaux nous conduisent à introduire le concept d'amplitude effective des interactions potentielles. Nous montrons alors que celle-ci s'annule à la même densité que la vitesse effective d'autopropulsion qui est aussi la densité de transition vitreuse dynamique d'un système colloïdal d'équilibre de structure équivalente. Ces résultats dressent un parallèle intéressant entre la transition vitreuse des systèmes d'équilibre et l'annulation de la vitesse effective d'autopropulsion des systèmes actifs qui est une propriété de la mesure stationnaire d'un système unique. La spécificité soulignée par cette resommation approchée est la présence d'interactions multicorps dans la mesure stationnaire. Contrairement au cas des liquides classiques d'équilibre, celle-ci ne peut en effet pas s'écrire sous la forme d'un produit sur les paires du système. L'importance de ces interactions multicorps dans le diagramme des phases des systèmes actifs a récemment été soulignée en dimension 3 [202]. Nous continuons d'explorer cette idée en dimension infinie en étudiant le diagramme des phases de l'approximation dite de bruit coloré unifié de la dynamique AOUP. Nous montrons que celui-ci présente deux régions de coexistence de phase que les interactions de paires seules ne peuvent expliquer.

La deuxième partie de cette thèse porte sur des extensions du calcul stochastique dans les intégrales de chemin et généralise des résultats récemment établis dans le cas de processus unidimensionnels [28, 29]. Depuis leur formalisation par Wiener [208] et les travaux ultérieurs de Feynman [52], les intégrales de chemin sont devenus un outil fondamental en physique théorique, des hautes énergies à la matière molle. Leur utilisation est néanmoins entravée par l'existence de nombreuses difficultés mathématiques. Certaines de celles-ci se retrouvent au niveau des équations différentielles stochastiques. Du fait de la non différentiabilité du mouvement Brownien, il est en effet bien connu que, contrairement aux équations différentielles ordinaires, une prescription de discrétisation est nécessaire pour donner sens aux équations différentielles stochastiques à bruit multiplicatif. En particulier, ceci conduit à introduire les règles du calcul stochastique, dont le fameux lemme d'Itō, qui généralisent le théorème de dérivation des fonctions composées. Dans ce manuscrit, nous commençons par rappeler la construction de la représentation dite de Onsager-Machlup en intégrale de chemin des processus stochastiques diffusifs dans la discrétisation α [103] et nous expliquons, suivant Edwards et Gulyaev [45], que le théorème de dérivation des fonctions composées n'est pas applicable au niveau de l'action en temps continu, et ce même si celle-ci est construite à partir de la discrétisation de Stratonovich. Nous montrons également que les règles du calcul stochastique établies dans le cas des équations différentielles stochastiques ne sont pas non plus applicables en général au niveau de l'action en temps continu. Nous expliquons alors comment les étendre de manière à traiter le terme cinétique $\dot{x}^2$ apparaissant dans le poids trajectoriel. Dans la dernière partie de cette thèse, nous inversons la perspective et nous demandons s'il est possible de construire une discrétisation de l'intégrale de chemin telle que celle-ci soit manifestement covariante en temps continue et donc que le théorème de dérivation des fonctions composées puissent s'appliquer directement. Nous rappelons les travaux de deWitt [36] et Graham [87] qui proposent d'exprimer le propagateur infinitésimal à partir d'une action covariante évaluée le long du chemin classique, infinitésimal lui aussi, ayant les bonnes conditions aux limites. Nous proposons enfin une discrétisation d'ordre supérieur, quadratique dans les incréments Δx, et étendant celle

de Stratonovich, qui permet de rendre utilisable le calcul différentiel ordinaire au sein des intégrales de chemin en temps continu. L'ensemble de ces résultats sont obtenus pour des processus stochastiques de dimension arbitraire d finie et soulèvent de nombreuses question quant à leur généralisation aux théories des champs correspondant formellement à la limite $d \to \infty$.

Contents

Part I

Infinite dimensional active matter

Chapter 1

Introduction

More is different.

– Philip W. Anderson

What are the emerging macroscopic properties of systems made up of many interacting *particles* [1] ? Answering this question and thus bridging the macroscopic world to the microscopic one is the formidable task of statistical physics. The field was born in the second half of the XIXth century, at the instigation of Maxwell, Gibbs and Boltzmann to mention but a few, to link thermodynamics and Newton mechanics and explain the thermodynamic behavior of fluids seen as collections of (nearly) infinitely many interacting atoms. Its scope is today much larger than at the origin and encompasses subjects as diverse as, for instance, superconductivity [10], glassy physics [25], magnetism [152], chemical reactions [104] and active matter [178] that will be one of the main topics of the present thesis. Ideas stemming from statistical physics have even had far-reaching consequences in domains traditionally outside the scope of physics where the interacting particles can be neurons in the brain [76], species in large ecosystems [147], agents in a model economic system [156], or, as it is a topical issue today, contagious and healthy people in disease propagation [23].

One of the key facts in statistical physics is that large scale properties of many-particle systems may not be understood in terms of a mere extrapolation from the small systems ones. How one could guess, just by looking at the behavior of a few H_2O molecules, that water just above 0°C would be liquid and flow while it would freeze and solidify just below ? This is an example of a phase transition, a ubiquitous notion in statistical physics that designates the existence of a sharp and qualitative transition in the properties of the system (quantified by order parameters) as an external parameter (here the temperature) is slightly varied. This also illustrates the idea of symmetry breaking which refers here to the fact that, in some region of parameter space, matter at the macroscopic scale may not exhibit the symmetries that dictates its behavior at the microscopic one. In our previous example, the dynamics of an ensemble of water molecules is described by rotationally

[1] The word particle here is understood in the very generic sense of constitutive element.

and translationally invariant equations, meaning that there is no privileged direction nor location put by hand from the outside, and yet, in ice, water molecules self-organize in a crystalline lattice that breaks these two symmetries. Mathematically speaking, symmetry breaking can only occur in the thermodynamic limit where the number of particles in the system is infinite. In large but finite-size systems the symmetry appears to be effectively broken on experimental time scales. While phase transitions and symmetry breaking are common in our everyday experience of the physical world, they escape the simple intuition solely based on the behavior of few particle systems. These phenomena emerging at large scales challenge the reductionist approach and are the main mechanisms responsible for the qualitative differences between small systems and very large ones. "More is different" coined Philip W. Anderson in 1977 [6].

Given the extraordinary complexity of the many-particle systems that are of interest in statistical physics, experiments and numerical simulations play a role of paramount importance in exploring and understanding their properties. The role of theoretical physics is then to provide the tools to grasp and apprehend these properties that would sometimes escape our intuition otherwise often based on the behavior of small systems. One approach is to devise microscopic models in which the extraordinary complexity of the real physical world in reduced at its maximum and that keep only the very few relevant ingredients that account for the macroscale phenomenology. The goal is therefore not to give an accurate description of a particular real system (*e.g.* a particular piece of ice), but rather to give an intelligible description of the backbone of the experimentally observed phenomenology. The still ubiquitous presence of the Ising model [101], not only as a pedagogical tool but also in the scientific literature, demonstrates how fruitful this approach can be.

1.1 Equilibrium physics

Statistical mechanics was originally developed to study large collections of atoms and molecules that, at least at the classical level, obey Newton's laws of mechanics and have Hamiltonian dynamics. Hamiltonian systems display remarkable properties. In particular, it can be shown from the Liouville equation that the uniform distribution on constant energy surfaces is a stationary distribution of the dynamics: if the initial conditions are distributed uniformly then so will be the distribution of points in phase space at later times.

It is usually believed that generic large Hamiltonian systems ergodically explore the constant energy surface with respect to the uniform distribution on such surfaces. The number of actual dynamical systems, such as Sinaï's billard [191], for which ergodicity can be proven remains extremely restricted. However, the standard mathematical results from dynamical systems theory that object such a statement, such as the existence of finite measure invariant tori in perturbed integrable systems (a result of the Kolmogorov–Arnold–Moser (KAM) theorem [8, 116, 159]), are expected to be of increasingly small relevance as the number of particles in the system becomes large. This idea can be traced back to Boltzmann's ergodic hypothesis and gave rise to the celebrated microcanonical ensemble: if the system is ergodic and follows Hamiltonian dynamics with Hamiltonian $H(\mathbf{q}, \mathbf{p})$, with $\mathbf{q}$ the positions and $\mathbf{p}$ the momenta, then time-averages of single-time observables (that can be measured in real experiments performed on a single system) can be obtained from an ensemble average

with a flat measure on the constant energy surface,

$$P(\mathbf{p},\mathbf{q}) = \frac{\delta\left(H(\mathbf{p},\mathbf{q}) - E\right)}{\Omega(E)}\,, \tag{1.1}$$

with E the energy of the system and $\Omega(E)$ the phase space area accessible to the dynamics[2]:

$$\Omega(E) = \int \mathrm{d}\mathbf{p}\mathrm{d}\mathbf{q}\,\delta\left(H(\mathbf{p},\mathbf{q}) - E\right)\,. \tag{1.2}$$

It is a remarkable feature that in the microcanonical ensemble, the knowledge of the Hamiltonian or accordingly of the (conservative) forces entering Newton's equation of motion directly prescribes the stationary state distribution function from which expectations values of one-time observables can be computed. Equation (1.1) is the founding postulate of equilibrium statistical physics, and, historically, of statistical physics itself. While it can be rationalized from the above mentioned arguments it is mainly its predictive power in real experiments that gave it its credentials.

The rest of equilibrium statistical mechanics can be derived from Eq. (1.1). Let us consider a system in microcanonical equilibrium at energy E that is made of two closed subsystem, say 1 and 2 with phase space coordinates $(\mathbf{q}_1,\mathbf{p}_1)$ and $(\mathbf{q}_2,\mathbf{p}_2)$. The total Hamiltonian of the system then writes,

$$H(\mathbf{p}_1,\mathbf{p}_2,\mathbf{q}_1,\mathbf{q}_2) = H_1(\mathbf{p}_1,\mathbf{q}_1) + H_2(\mathbf{p}_2,\mathbf{q}_2) + H_{12}(\mathbf{p}_1,\mathbf{p}_2,\mathbf{q}_1,\mathbf{q}_2)\,, \tag{1.3}$$

where H_1 is the Hamiltonian of system 1, H_2 the Hamiltonian of system 2 and H_{12} the coupling part of the total Hamiltonian. If we assume (i) that $H_1(\mathbf{p}_1,\mathbf{q}_1) \gg H_2(\mathbf{p}_2,\mathbf{q}_2)$ so that system 1 acts as a thermostat for system 2 and (ii) that H_{12} is negligible (which requires system 2 to be of macroscopic size and the coupling interactions to be short-ranged) then expectations values of one-time observables depending only on system 2 variables can be computed from the Gibbs-Boltzmann distribution:

$$P(\mathbf{p}_2,\mathbf{q}_2) = \frac{\mathrm{e}^{-\beta H_2(\mathbf{p}_2,\mathbf{q}_2)}}{Z(\beta)}\,. \tag{1.4}$$

with $Z(\beta)$ a normalization constant and $\beta = T^{-1}$ the inverse microcanonical temperature of system 1. This defines the canonical ensemble of equilibrium statistical mechanics in which, once more, the subsystem Hamiltonian directly prescribes the stationary state distribution function. Another approach can be taken to study the dynamics of a system coupled to a large bath in equilibrium. This is nicely illustrated by a model of oscillators [217] in which computations can be carried exactly. Consider a system with positions $\mathbf{q}$ and momenta $\mathbf{p}$ in a potential $V(\mathbf{q})$ linearly coupled to an ensemble of N harmonic oscillators. The total Hamiltonian writes

$$H = \frac{\mathbf{p}^2}{2m} + V(\mathbf{q}) + \sum_{j=1}^{N}\left[\frac{\mathbf{p}_j^2}{2} + \frac{1}{2}\omega_j^2\left(\mathbf{q}_j - \frac{\gamma_j}{\omega_j^2}\mathbf{x}_j\right)^2\right]\,. \tag{1.5}$$

[2]In order to properly take into account the quantum nature of the underlying dynamics, $\Omega(E)$ should be renormalized by a constant independent of E to become the true density of states. We do not cover these issues here.

Because of the linearity of the equations of motion of the harmonic oscillators, one can obtain closed equations for the dynamics of $\mathbf{p}$ and $\mathbf{q}$ at $t > 0$ that explicitly depend on the initial positions and momenta of the oscillators at $t = 0$. If one assumes that these initial conditions are sampled randomly from the corresponding Boltzmann distribution $\mathrm{e}^{-\beta H}$ at temperature β^{-1}, then the dynamics of $\mathbf{q}$ and $\mathbf{p}$ follows,

$$\begin{aligned} \dot{\mathbf{q}}(t) &= \frac{\mathbf{p}(t)}{m}\,, \\ \dot{\mathbf{p}}(t) &= -\boldsymbol{\nabla} V(\mathbf{q}) - \int_0^t \mathrm{d}s K(s) \frac{\mathbf{p}(t-s)}{m} + \mathbf{F}(t)\,, \end{aligned} \tag{1.6}$$

with $\mathbf{F}(t)$ a random Gaussian force (the randomness comes from the sampling of the oscillators initial conditions) with zero average,

$$\langle \mathbf{F}(t) \rangle = 0\,, \tag{1.7}$$

and correlations,

$$\langle F^\mu(t) F^\nu(t') \rangle = T K(t-t') \delta^{\mu\nu}\,. \tag{1.8}$$

The action of the bath on the system thus writes as the sum of a deterministic drag with finite memory kernel and a Gaussian random force with variance proportional to that kernel. In the limit where inertial effects are negligible, Eq. (1.6) reduces to the generalized Langevin equation

$$\int_0^t \mathrm{d}s K(s) \dot{\mathbf{q}}(t-s) = -\boldsymbol{\nabla} V(\mathbf{q}) + \mathbf{F}(t)\,. \tag{1.9}$$

Furthermore, if the range of the memory kernel can be neglected with respect to the typical timescale of the variations of $\mathbf{q}$ and $K(s)$ can thus be approximated by a delta function one then obtains the overdamped Langevin equation,

$$\gamma \dot{\mathbf{q}}(t) = -\boldsymbol{\nabla} V(\mathbf{q}) + \sqrt{2\gamma T}\, \boldsymbol{\eta}(t)\,, \tag{1.10}$$

with $\boldsymbol{\eta}(t)$ a Gaussian white noise with zero mean and unit variance. It is then possible to show from the associated Fokker-Planck equation that the stationary distribution associated with Eq. (1.10) is indeed of the Boltzmann type $\mathrm{e}^{-\beta V(\mathbf{q})}$. This could actually be proven directly at the level of Eq. (1.6) but, due to the non-Markovian nature of this equation, the computation is more intricate and mainly involves reintroducing the original model of oscillators to unfold the memory kernel. Now, coupling a system with many harmonic oscillators may seem an abstract game of little experimental relevance. However, Eq. (1.10) was actually introduced for the first time by Paul Langevin [123] in 1908 to quantitatively describe Brownian motion, first observed in the form of the erratic motion of small particles immersed in the fluid within a pollen grain [17]. As for the model of oscillators, Langevin's original idea was that the force exerted by the fluid, that is the result of the many collisions between water molecules and these particles, could be written as the sum of a standard deterministic drag term and a fluctuating part that, by virtue of the central limit theorem, is endowed with Gaussian statistics.

In modern statistical physics, the notion of equilibrium is not restricted to Hamiltonian dynamics. A system is said to be in equilibrium if it obeys the so-called detailed balance

condition that asserts that for any two states A and B in which the system can be found the probability to observe a transition path from A to B is equal to that of observing the time-reversed transition from B to A: the system is thus symmetric under time reversal. Because of the reversibility of Hamilton's equations of motion and the flatness of the microcanonical measure, Hamiltonian systems indeed satisfy the detailed balance condition. The same can be shown for systems whose dynamics obeys the stochastic differential equations Eq. (1.10) and the more general Eq. (1.6) due to the proportionality of noise correlations with the friction memory kernel. The notion of equilibrium extends however far beyond these two cases.

We have just introduced basic facts about equilibrium statistical mechanics. For the scope of this work, one of the key ones is that in equilibrium the knowledge of the dynamical rules that satisfy detailed balance is enough to simply determine the stationary state distribution function. It does not mean that the macroscopic properties of large equilibrium systems are easy to derive; far from it. But at least the N-body distribution function is known and provides a convenient starting point for the study of the phase behavior. In the following, we will however be interested in systems in which the time-reversal symmetry is broken. In these systems, one must study the full dynamics to extract the stationary state distribution function, a mission impossible in most cases.

1.2 Active matter

We now introduce the main framework of the present thesis: active matter. In active systems, the individual *particles* are able to extract and consume energy from the environment in order to self-propel. Breaking the delicate balance between dissipation and injection of energy at the particle level inevitably drives even the simplest versions of such interacting particle systems away from equilibrium. As will be discussed in more detail later, their macroscale phenomenology is very rich and stimulated the interest of physicists over the past 30 years. A lot of experimental realizations of active matter are to be found in the living world, see Fig. 1.1. At the meter scale, this comprises large animal groups such as starling flocks [9], sheep herds [80] or fish schools [111] that can exhibit large-scale collective motion. At the micro-metric scale, common examples of active matter systems are assemblies of self-propelling bacteria [173] that can display, under some circumstances, aggregation behavior.

Figure 1.1: Examples of collective behavior in the living world. **(a)** A starling flock. **(b)** A sheep herd. **(c)** Bacterial (Myxococcus xanthus) colonies [173].

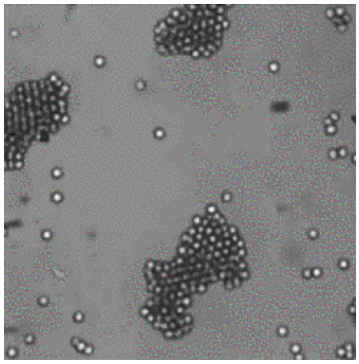

Figure 1.2: Formation of dense clusters of carbon-coated Janus particles embedded in a near critical mixture of water and lutidine [19].

Lots of experiments have also been performed with synthetic elements. These experiments have the great advantage to be more reproducible and more controlled than those on living systems. As such, Janus particles [207], colloids with one coated hemisphere that self-propel due to diffusiophoresis, are commonly used today. For instance, in [19], the particles have one carbon-coated hemisphere and are embedded in a near critical mixture of water and lutidine. When illuminated by a laser beam of precise wavelength, the carbon-coated hemisphere of the colloid heats up and locally induce demixing of the water-lutidine solution that, in turn, induces phoretic forces on the particles. When the light is on and at high enough packing fraction, assemblies of such particles, while displaying no direct attraction, separate into dense clusters separated by a dilute phase, see Fig. 1.2.

1.2.1 Active matter models

When it comes to modelling these active matter systems, lots of ingredients can be taken into account. First, the mechanism that induces self-propulsion can be modeled (*e.g.* the explicit demixing of the water-lutidine mixture at the surface of the colloid in [19]) or the self-propulsion can be put by hand. Particles can be point-like, or spherical as in [19] or can have a more complicated shape, for instance, a rod-like shape as E. Coli bacteria. The effect of the ambient medium can be taken into account through hydrodynamic interactions [214] between the different particles or through an explicit coupling to Navier-Stokes equations [183]. Finally, the particles in the model can interact via different mechanisms: explicit alignment in their self-propulsion [206], quorum sensing [200], steric repulsion [54] ect. The scale at which the description starts is also of prime importance. So far we had in mind microscopic (or agent based) models in which we keep track of the individual units making up the system. Huge efforts were also put in devising phenomenological models that give a description at the mesoscopic scale by postulating hydrodynamic equations satisfied by *e.g* the density or the velocity field (depending on the problem at hand, more fields can obviously be incorporated into the description). One approach can be to write the most general hydrodynamic equations allowed by the symmetries of the problem at hand, as J. Toner and Y. Tu did in their 1998 theory of the flocking transition [201]. In the work presented all along this thesis, our starting point are microscopic models and we briefly

present some of the most standard ones in the following.

1.2.2 The Vicsek model

The model proposed by T. Vicsek & collaborators in 1995 [206] has participated in the recent surge of enthusiasm for active matter in the physics community. It is a simple and yet conceptually powerful model of flocking in the vein of the theoretical physics approach presented at the beginning of this introduction. Particles are point-like and self-propel with a fixed speed. They align their velocity with their neighbors' up to some noise term that causes imperfect alignment. At large noise, the system is disordered and the mean velocity of the flock is zero. Upon decreasing the amplitude of the noise, the system undergoes a transition to collective motion as all the particles start to move in the same direction. The possibility to observe a breaking of the rotational invariance as observed in the two-

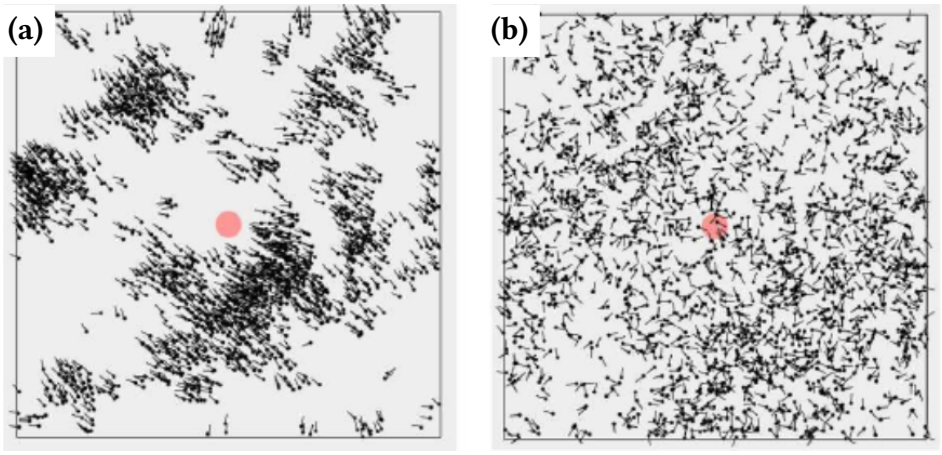

Figure 1.3: Transition to collective motion in the Vicsek model. Reproduced from [4]. **(a)** Ordered phase in the small noise regime: all the particles move in the same direction. **(b)** Disordered phase in the large noise regime: no privileged direction is selected by the dynamics. The shaded circle at the center of each frame indicates the size of the interaction vicinity.

dimensional Vicsek model was the cause of a great interest in the physics community. Indeed, thanks to the seminal work of Mermin and Wagner [151] and Hohenberg [96], it is now understood that the breaking of a continuous symmetry is forbidden in dimension 1 and 2 in equilibrium systems with short-ranged interactions. The flocking transition, despite the short-range nature of the alignment interaction, is therefore a direct consequence of the nonequilibrium nature of the dynamics of the Vicsek model (mainly that the interaction network is continuously modified) that allows the associated stationary state distribution to escape the conditions under which the so-called Mermin-Wagner theorem holds.

1.2.3 Quorum sensing active matter

The term quorum-sensing refers to the ability of a biological entity to adapt its properties in response to the fluctuations in the local density around it. Quorum-sensing is ubiquitous in our everyday life (*e.g.* we use visual inputs to adapt our motion to the presence of obstacles) but also at the cellular scale in which case extracellular signalling molecules are used to carry information on the local density of biological agents. In the active matter literature, the term Quorum Sensing Active Particles (QSAPs) refers to systems in which the particles' self-propulsion amplitude is a function of the local density field. Such mechanism was for instance proven to be at play in E. Coli populations [195]. In the standard models of QSAPs, particles are persistent random walkers whose speed explicitly depends on a convolution of the local density field. In their simplest versions, the corresponding equations of motion for the N-particle system write

$$\dot{\mathbf{r}}_i(t) = v\left[\tilde{\rho}(\mathbf{r}_i)\right]\mathbf{u}_i(t)\,, \tag{1.11}$$

for $i \in [\![1, N]\!]$ where $\tilde{\rho}(\mathbf{r}_i)$ is a convolution of the local density field

$$\tilde{\rho}(\mathbf{r}) = \int \mathrm{d}\mathbf{r}' K(\mathbf{r}' - \mathbf{r})\hat{\rho}(\mathbf{r}) \text{ with } \hat{\rho}(\mathbf{r}) = \sum_i \delta(\mathbf{r} - \mathbf{r}_i)\,, \tag{1.12}$$

where K is a short-ranged kernel and where $\mathbf{u}_i(t)$ is a unit vector that gives the direction of the self-propulsion of particle i. There exists different ways to model the dynamics of the vector $\mathbf{u}_i(t)$ that correspond to different persistent random walker models. The two main models used in that case are the run-and-tumble dynamics [186] (where the particles are said to be run-and-tumble particles or RTPs), which corresponds to $\mathbf{u}_i(t)$ being uniformly reshuffled on the unit sphere at a given rate and the active Brownian dynamics (where the particles are said to be active Brownian particles or ABPs) in which case $\mathbf{u}_i(t)$ freely diffuses on the unit sphere. The run-and-tumble model describes the motion of many bacteria swimming by rotating their flagellar filaments (see [13] for an analysis of the E. Coli motion where the tumble was however shown not to be perfectly uniform) while the ABP model applies to the motion of self-propelled colloids such as the aforementioned Janus particles [121].

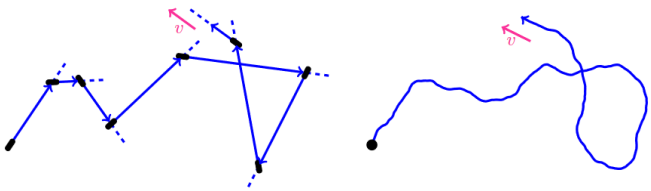

Figure 1.4: Trajectory of a particle performing **(Left)** a run-and-tumble motion and **(Right)** an active Brownian one. Reproduced from [24].

If v decreases fast enough with the density, the system, above a certain density threshold, undergoes a phase transition and separates into a dense and a dilute phase [200], a phenomenon called in the active matter literature the Motility Induced Phase Separation

(MIPS) [24]. The phase diagram of 1 and 2 dimensional QSAPS, both of the ABP and RTP types, is reproduced from [192] in Fig. 1.5. The precise functions $v(\rho)$ and $K(\mathbf{x})$ used to construct the phase diagram are to be found in Eq. (42) and (43) of [192]. The model can be refined to display a richer phenomenology [128] but is as such a remarkable minimal model of sensing-induced aggregation behavior in real active matter systems. The mechanism driving the phase separation in QSAPs is well understood: particles accumulate where they go slower and particles go slower in denser regions, thus leading particles to accumulate in denser regions. Remarkably for an out-of-equilibrium many body system, and as can be seen in Fig. 1.5, it is possible to obtain quantitative analytical predictions of the phase diagram [192]. This notable feature is made possible by the near mean-field nature of the QSAPs [192]: due to the absence of steric repulsion between the particles together with the high densities in the MIPS region for this choice of v and K, one particle indeed interacts at the same time with many others.

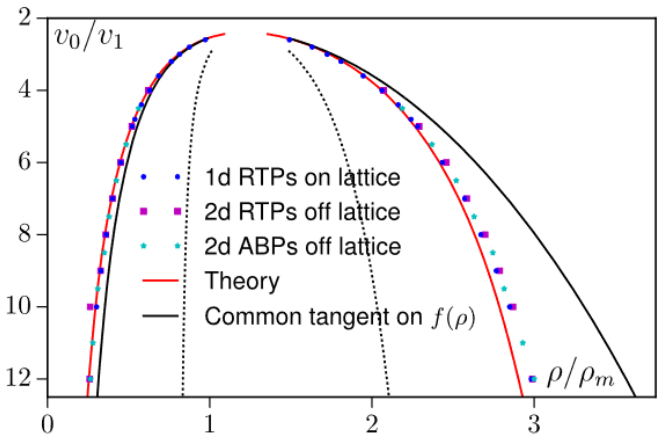

Figure 1.5: Phase diagram of QSAPs. Reproduced from [192]. The parameter v_0 is the low density limit of v and v_1 its high density limit. The transition between the two takes place at densities $\rho \simeq \rho_m$. Above a certain threshold for v_0/v_1, the system phase separates into a dense and a dilute phase. The phase coexistence region lies between the two binodals that give the corresponding coexistence densities. The binodals are given by the continuous red line (theoretical prediction) and squares and circles (numerical simulations).

1.2.4 Pairwise forces interacting active particles

We now introduce a broad class of minimal models of steric-hindering-induced aggregation behavior that we will study in this thesis. These are models of persistent random walkers interacting via pairwise conservative forces, and possibly evolving in an external potential. One can think about this forces as representing a hard core repulsion between the particles even though other types of potentials will be explored throughout the present thesis. The models we consider are defined by the N-body equations of motion

$$\dot{\mathbf{r}}_i(t) = \mathbf{v}_i(t) - \boldsymbol{\nabla}_{\mathbf{r}_i} \Phi\left(\mathbf{r}_1, \ldots, \mathbf{r}_N\right) , \tag{1.13}$$

with $\mathbf{v}_i(t)$ the self-propulsion of particle i and where the total potential energy is the sum of one body contributions (with external potential V) and two-body ones (with pairwise potential U)

$$\Phi(\mathbf{r}_1, \dots, \mathbf{r}_N) = \sum_{i=1}^{N} V(\mathbf{r}_i) + \sum_{(i,j)} U(\mathbf{r}_i - \mathbf{r}_j)\,. \tag{1.14}$$

For simplicity, we restrict to spherically symmetric pair potentials, *i.e.* $U(\mathbf{r}_i - \mathbf{r}_j) = U\left(|\mathbf{r}_i - \mathbf{r}_j|\right)$. As pointed out before, there exist in the active matter literature different ways to model the statistics of the self-propulsion forces. In the ABPs case, $\mathbf{v}_i(t) = v_0\mathbf{u}_i(t)$ with $\mathbf{u}_i(t)$ unitary and freely diffusing on the unit-sphere with diffusion coefficient D_r,

$$\dot{\mathbf{u}}_i(t) \overset{\text{Stratonovich}}{=} -\mathbf{u}_i(t)\left(\mathbf{u}_i(t)\cdot\boldsymbol{\eta}_i(t)\right) + \boldsymbol{\eta}_i(t)\,, \tag{1.15}$$

where $\boldsymbol{\eta}_i$ is a zero mean Gaussian white noise with variance $\langle \eta_i^\mu(t)\eta_i^\nu(t')\rangle = 2D_r\delta(t-t')\delta^{\mu\nu}$. In the RTPs one, $\mathbf{v}_i(t) = v_0\mathbf{u}_i(t)$ with $\mathbf{u}_i(t)$ unitary and uniformly reshuffled on the unit sphere with rate τ^{-1},

$$\dot{\mathbf{u}}_i(t) = \sum_k \delta(t - t_k)\left(\tilde{\mathbf{u}}_k - \mathbf{u}_i(t^-)\right)\,, \tag{1.16}$$

where the τ_k's are Poisson distributed with rate τ^{-1} and the $\tilde{\mathbf{u}}_k$'s are independent random vectors uniformly distributed on the unit sphere. In both cases, in the steady-state dynamics, the self-propulsion force is exponentially correlated in time and we have

$$\begin{aligned}
\left\langle u_i^\mu(t)u_j^\nu(t')\right\rangle_{RTP} &= \frac{1}{d}\exp\left(-\frac{|t-t'|}{\tau}\right)\delta^{\mu\nu}\delta_{ij}\,,\\
\left\langle u_i^\mu(t)u_j^\nu(t')\right\rangle_{ABP} &= \frac{1}{d}\exp\left(-D_r(d-1)\,|t-t'|\right)\delta^{\mu\nu}\delta_{ij}\,,
\end{aligned} \tag{1.17}$$

where d is the space dimension. These correlations are identical under the replacement $(d-1)D_r \leftrightarrow \tau^{-1}$. There exists a third much used model in the active matter literature in which the self-propulsion follows an Ornstein-Ulhenbeck process [145] (in which case the particles are called active Ornstein-Ulhenbeck particles or AOUPs),

$$\dot{\mathbf{v}}_i(t) = -\frac{\mathbf{v}_i(t)}{\tau} + \frac{\sqrt{2D}}{\tau}\boldsymbol{\eta}_i(t)\,, \tag{1.18}$$

with $\boldsymbol{\eta}_i(t)$ a zero mean Gaussian white noise with unit variance. This model in which the modulus of $\mathbf{v}_i(t)$ itself fluctuates has been used to model collective cell dynamics [88, 34]. It has also the advantage to endow the self-propulsion force with Gaussian statistics that makes it more suitable for analytical calculations than ABPs or RTPs. The self-propulsion correlations in this case are also exponentially decaying with time,

$$\left\langle v_i^\mu(t)v_j^\nu(t')\right\rangle = \frac{D}{\tau}\exp\left(-\frac{|t-t'|}{\tau}\right)\delta^{\mu\nu}\,. \tag{1.19}$$

In numerical simulations, the phase behavior of active particles interacting via short-ranged repulsive pairwise forces was shown to be similar to the QSAPs one. At high enough activity (as quantified by what is called the Peclet number in the literature that measures the ratio between the run length of a free particle to the interaction range of the pair potential) and high enough density, the system phase separates into a dense and a dilute phase

[193]. This similarity between QSAPs and active particles interacting via pairwise short-ranged repulsive conservative forces can heuristically be rationalized by the expectation that collisions effectively reduce the self-propulsion amplitude of the particles thus fueling the nonlinear feedback mechanism responsible for the formation of high-density regions. The phase diagram of AOUPs with Weeks-Chandler-Andersen (WCA) interactions is reproduced from [145] in Fig 1.6. It displays, at fixed D and large enough τ, a region of phase separation with coexisting densities given by the blue (low density branch) and the red (high density branch) lines. Extensive studies of the phase diagram of ABPs both in the

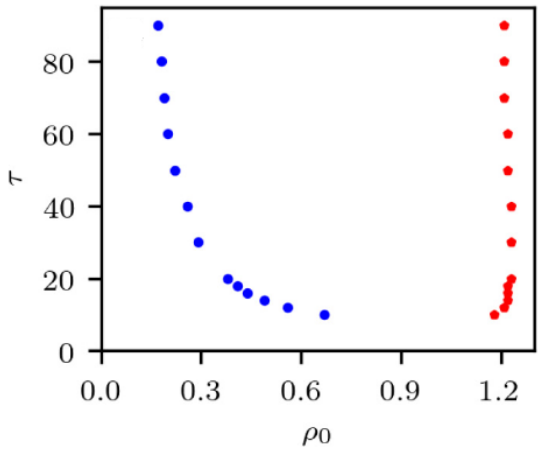

Figure 1.6: Phase diagram of AOUPs interacting via a WCA potential. Reproduced from [145]. Distances are measured in units of the natural scale of the WCA potential and $D = 10$. The blue and red lines are the low and high density binodals, respectively.

near-equilibrium and in the high activity regimes have been conducted in [40] (dimension 2) and [162] (dimension 3). These in particular show that the equilibrium solid/liquid phase transition survives in the small activity regime and extends at high activities where it eventually crosses the MIPS domain. We still however lack a first principle theory of the phase diagram as is often the case with many-body systems evolving far from equilibrium.

Let us now stress what elements of realistic active matter systems these models neglect. It first appears clear that the self-propulsion is added by hand in the dynamics and that internal mechanisms (*e.g.* diffusiophoresis, rotation of a flagella ect.) causing it are not modeled but are effectively encapsulated in the statistics of the self-propulsion force. We believe this is a reasonable level of coarse-graining, especially given the similarities between AOUPs, RTPs and ABPs on thermodynamic scales. There exist however some circumstances in which these different types of particles behave qualitatively differently (for instances noninteracting AOUPs in a harmonic potential have a Gaussian stationary state probability distribution centered at the bottom of the trap while that RTPs or ABPs can display an off-centered peak, see [33] and [199]). Furthermore, because of the rotational symmetry of the pair potential, the elementary constituents we describe are spherical. These models do not aim to capture the rich phenomenology of active nematics, *i.e.* assemblies of self-propelled elongated particles as are, at the subcellular scale, microtubule and motor protein mixtures. Striking deviations from the behavior of standard liquid crystals, such as self-sustained generation of topological defects [82] and the associated large-scale

complex flow patterns emerging in steady state [42], have been reported both in experiments and numerical simulations of hydrodynamic models of active nematics. Beside, in [204], the authors investigated the behavior of 2 dimensional hard-rods self-propelling in their elongated direction by taking into account, on top of the short-ranged repulsion of Eq. (1.18), the alignment torques caused by the hard-rods collisions. They reported a gradual destruction of the MIPS phase with increasing aspect ratio. While Eq. (1.18) completely disregards alignment interactions in the self-propulsion direction, it has nevertheless been shown that the dense phases of this model are characterized by local velocity alignment in steady state [20]. Moreover, Eq. (1.18) is first order in time: it is thus assumed that viscous drag dominates inertial effects. The influence of inertia in self-propelled particle systems has been recently investigated [163] showing that, while finite inertia effects are subtle and non-generic, the nonequilibrium phenomenology is destroyed at large inertia. Finally, the above defined models of active particles interacting through pairwise forces belong to the broad class of dry active matter in which hydrodynamic interactions are neglected. Such effects have been extensively studied in squirmer models, in which the particles move in a low Reynolds fluid by imposing at their surface a given velocity field [14] that can account, for instance, for ciliary propulsion. Hydrodynamic interactions then play an important role in shaping the large scale behavior of theses systems that appears to depend on the chosen type of surface flow [216]. In the spirit of studying a minimal model of steric-hindering-induced aggregation behavior, we will nevertheless neglect hydrodynamic interactions as they need not be taken into account to observe the phase separation.

1.2.5 Self-propelling away from equilibrium

Systems made of interacting self-propelled particles are generically out-of-equilibrium in the sense that their steady state dynamics is not symmetric under time-reversal. The deviations from the detailed balance condition can be quantitatively measured by the entropy production rate, which however comes with its share of subtleties [161, 57]. This generic breaking of time-reversal symmetry in active systems can be understood by inspecting Eq. (1.13) on one side and Eqs. (1.9) and (1.10) on the other. In the Langevin approach for equilibrium systems evolving in contact with a thermostat, both the viscous friction and the fluctuating force have the same physical origin - hence the proportionality between the friction kernel and the noise correlation function in Eq. (1.8), an identity called the Fluctuation-Dissipation relation. In active systems, the friction still emerges from the surrounding viscous medium but the self-propulsion is induced by other processes, such as the consumption of internally stored energy. As clearly seen in Eq. (1.13), the noise memory kernel violates the fluctuation-dissipation relation and thus even some the simplest versions of such systems evolve away from equilibrium.

Let us nevertheless investigate the similarities existing between active systems whose dynamics obey Eq. (1.13) and equilibrium ones with dynamics given by Eq. (1.10). First, we remark that Eq. (1.19) reduces in the $\tau \to 0$ limit to

$$\langle v^\mu(t) v^\nu(t') \rangle = 2D\delta(t-t')\delta^{\mu\nu} \,. \tag{1.20}$$

Thus the active dynamics becomes, in the limit of zero persistence, an equilibrium Langevin one with temperature D. Similar statements can be made in the RTP case (respectively the

ABP case) provided $v_0^2\tau$ (respectively v_0^2/D_r) remains finite as $\tau \to 0$ (respectively $D_r \to \infty$). The small τ regime therefore allows us to probe the deviations from the equilibrium Langevin equation and the emergence of the non-equilibrium properties of the dynamics [60]. Let us now consider a free AOUP particle,

$$\dot{\mathbf{r}} = \mathbf{v}(t)\,, \tag{1.21}$$

with $\mathbf{v}(t)$ obeying Eq. (1.18). The Mean Square Displacement (MSD) of the particle can be computed and reads, after equilibration of the $\mathbf{v}(t)$ degrees of freedom,

$$\left\langle \Delta\mathbf{r}(t)^2 \right\rangle = 2dD\left(t + \tau\left(-1 + \mathrm{e}^{-\frac{t}{\tau}}\right)\right)\,. \tag{1.22}$$

Over short time scales $t \ll \tau$, the MSD is ballistic with velocity dD/τ,

$$\left\langle \Delta\mathbf{r}(t)^2 \right\rangle \simeq \frac{dD}{\tau}t^2\,, \tag{1.23}$$

which is a signature of the persistent nature of the random process. On long time scales $t \gg \tau$, the MSD becomes diffusive with diffusion constant D

$$\left\langle \Delta\mathbf{r}(t)^2 \right\rangle \simeq 2dDt\,, \tag{1.24}$$

exactly as one would expect for a free Brownian particle at temperature D. It actually appears that if one keeps track only of the position $\mathbf{r}$, the process defined in Eq. (1.21) is an equilibrium one. From these considerations, one could be tempted to endow D with the meaning of a true thermodynamic temperature. However, as soon as one adds interaction into the game between different particles or with an external potential (and except for the peculiar case of an AOUP in a harmonic trap [60]), the process becomes out-of-equilibrium and the identification of D with a temperature ceases to be operative.

1.3 Outline of the thesis

The goal of the present work is to gain analytical insights on the properties of systems made of many self-propelled particles interacting via pairwise conservative forces. The outline of the thesis follows the increasing complexity of the systems we consider. We start our investigation in Chapter 2 by that of one active particle in an external potential. Based on the results of a collaboration with D. Martin [143], we first work out the emergence of the nonequilibrium signatures of an AOUP subjected to thermal noise. This will allow us to quantify the non-trivial interplay between the thermal and active noises. We then review the stationary probability distribution of a one-dimensional RTP in a soft and hard confining potential. Lastly, we derive the stationary distribution function for a single RTP around a fixed spherical obstacle in the ballistic limit. In Chapter 3, we introduce some useful concepts in view of Chap.4. We start by defining various observables such as the n-point distribution function, the effective self-propulsion or the mechanical pressure that can be used to describe the stationary properties of large active matter systems. We then use results from Chap. 2 to compute these observables for highly ballistic run-and-tumble particles in the dilute limit. We finally move to another subject and review the Mayer expansion of standard equilibrium liquid and in particular its truncation in infinite dimension. We follow the

steps of [67] and explain why the infinite dimensional limit is a powerful organizing device to derive approximate expressions for physical observables in classical fluids. In order to prepare the forthcoming chapter, we show that the results of [67, 68] can be recovered not only from the Mayer expansion of the free energy but also using the Born-Bogolioubov-Green-Kirkwood-Yvon (BBGKY) hierarchy of correlation functions as a starting point. In Chapter 4, we study self-propelled particle systems in the limit of infinite dimension with a particular emphasis on the role of multibody interactions that are defined at the beginning of the chapter. In this work, we first characterize the low density dynamics of sticky hard spheres within the Dynamical Mean Field Theory framework of [2]. In particular this allows us to make predictions for the mean-square displacement to first order in the density. These results were obtained in collaboration with F. Zamponi and A. Manacorda [176]. Next, we derive an approximate resummation of the infinite dimensional BBGKY hierarchy. These results were first presented in [175]. However, one of the claims of that paper was that the resummation scheme was exact in the large d limit which we know now not to be the case. An erratum is being written out. Within this closure scheme, standard results concerning the phenomenology of active hard spheres in finite dimension are recovered. As opposed to what happens in standard equilibrium fluids in infinite dimension, this closure highlights the importance of multibody interactions in explaining the phase behavior of active particle systems, at least at the mean-field level. This idea is finally studied in an approximate equilibrium model of active matter, namely the Unified Colored Noise Approximation (UCNA) of the AOUPs dynamics, where we show analytically that the system undergoes a phase transition that is driven by multibody interactions.

Chapter 2

One particle in an external potential

Contents

As a first step towards understanding the collective behavior of interacting active particle systems, we study the simpler case of one particle in an external potential. For a passive particle in an external potential $V(\mathbf{r})$ subjected to a thermal noise at temperature T the stationary distribution is the Boltzmann one,

$$\rho(\mathbf{r}) \propto \mathrm{e}^{-\beta V(\mathbf{r})} \,. \tag{2.1}$$

This is no longer true in the case of self-propelled particles and this one-body phenomenology already displays some puzzling features as the tendency to be attracted to otherwise repulsive obstacles as was reported in many experimental [184] and theoretical [49] works. From a purely analytical standpoint, instances in which the stationary distribution can be

found exactly are scarce. A single RTP in an arbitrary external potential in one space dimension [194] is a notable exception. Remarkably, the stationary distribution of [194] is not a local function of the potential $V(r)$, at odds with the Boltzmann distribution Eq. (2.1).

In Sec. 2.1, we start by considering a one-dimensional AOUP in an external potential subjected to thermal noise. We reproduce the results published in [143] in collaboration with D. Martin in which we studied the emergence of the nonequilibrium signatures in the small τ regime such as the deviations from the Boltzmann distribution, the steady currents in periodic potentials and the entropy production rate. The appendices of [143] are reproduced in App. A. These findings extend the analysis published in [145] that disregarded the presence of Brownian noise and disentangle the respective roles of the passive and active noises on the steady state of AOUPs, showing nonequilibrium-driven surprising behaviors emerge as the temperature is varied. Indeed, depending on the potential in which the particle evolves, both the current and the entropy production rate can be non-monotonic functions of the temperature.

In Sec. 2.2, we reproduce the computation of [194] of the stationary distribution of a single one-dimensional RTP confined to the right half-line by an external potential $V(x)$. By studying the case of an exponential potential $V(x) = V_0 \mathrm{e}^{-x/\epsilon}$ with $\epsilon > 0$, we identify a transition between an equilibrium-like behavior where the probability density is depleted in the vicinity of the obstacle (when ϵ the range of the potential is larger than $v_0\tau$, the run-length of an isolated particle) and a regime where the particle is effectively attracted by the repulsive obstacle for $\epsilon < v_0\tau$. The hard wall limit $\epsilon \to 0^+$, where the stationary distribution function develops a delta peak contribution at contact, is then studied. We finally adapt a method we presented in [175] to solve for the hard wall case directly from the Fokker-Planck equation. This approach will be useful when dealing with cases in which the distribution in an arbitrary potential is not known, as in the rest of this chapter.

In Sec. 2.3, we derive the stationary distribution of a single run-and-tumble particle evolving around a hard spherical obstacle in the ballistic regime where $v_0\tau \gg \sigma$, with σ the size of the obstacle. This computation clearly shows the activity induced attraction often referred to in the active matter literature, in particular in the form of a delta peak contribution at contact, and is at the basis of our later study of interacting self-propelled spheres.

Contributions

Section 2.1

- perturbative expansion at small τ of the stationary distribution of an AOUP in an external potential in the presence of thermal noise,
- perturbative expansion at small τ of the current in an asymmetric potential of an AOUP in the presence of thermal noise. Non-monotonous behavior as a function of T.
- perturbative expansion at small τ of the entropy production rate of an AOUP in an external potential in the presence of thermal noise. Non-monotonous behavior as a function of T.

Section 2.2

- a method to compute the stationary state probability distribution directly in the hard sphere limit.

Section 2.3

- a self-consistent equation for the density field of a RTP around a hard spherical obstacle,
- density field in the vicinity of the obstacle exhibiting a square root plus a logarithmic divergence,
- stationary distribution function in the ballistic limit $v_0\tau/\sigma \gg 1$.

2.1 Emergence of the nonequilibrium signatures of an Active-Ornstein Uhlenbeck particle subjected to thermal noise

In this section, we focus on an Active Ornstein Uhlenbeck Particle (AOUP) evolving in one space dimension, subjected to an external potential $\phi(x)$ and further experiencing an additional thermal noise. Its position $x(t)$ and self-propulsion $v(t)$ evolve according to the following system of Langevin equations [84, 30]:

$$\dot{x} = -\partial_x\phi + \sqrt{2T}\,\eta_1 + v \tag{2.2}$$

$$\dot{v} = -\frac{v}{\tau} + \frac{\sqrt{2D}}{\tau}\,\eta_2\,. \tag{2.3}$$

In the above dynamics Eqs. (2.2)-(2.3), η_1 and η_2 are two uncorrelated Gaussian white noises of unit variance, T is the amplitude of the thermal noise while D and τ control the amplitude and the persistence of the self-propulsion. When $T = 0$, Eqs. (2.2)-(2.3) correspond to the workhorse AOUP model which has been used to model transport properties of active

colloids [117] as well as collective cell dynamics [88, 34]. On the theoretical side, there has been fundamental interest in its steady-state distribution, which has been characterized both in the limit of small τ [59, 15, 144, 212, 105] and in the limit of high τ [53, 212, 105]. However, these theoretical approaches ignore the potentially physically relevant presence of an underlying thermal noise and the steady state distribution of Eqs. (2.2)-(2.3) remains elusive for a generic combination of T and D. Indeed, such a combination of both active and thermal noise sources arises in multiple experiments: passive tracers embedded in living cells [210, 58, 3] or immersed in a bath of active colloids [133], fluctuations of cellular membrane in red blood cells [203, 12]...

In this section, we aim at filling this gap by computing perturbatively the stationary probability density of an AOUP experiencing an additional thermal noise in the small-persistence-time limit. Note that for $\tau = 0$, the self-propulsion v falls back onto a Wiener process of amplitude D. In this particular case, the dynamics Eqs. (2.2)-(2.3) is an equilibrium one with temperature $T + D$. Thus, intuitively, one could hope to find analytical formulas that smoothly departs from thermal equilibrium when τ is small. We develop here such a perturbative expansion and our main result is an analytical prediction of the steady-state distribution $\mathcal{P}_s(x, v)$ as a series in $\tau^{1/2}$. Building on it, we make quantitative predictions about three emerging quantities: the marginal in space of the probability density, the current in an asymmetric periodic ratchet, and the entropy production rate. Depending on the boundary conditions and on the potential $\phi(x)$, we find that the interplay between passive and active noises leads to a rich phenomenology for the current and the entropy production rate when the temperature is varied: decline or non-monotonicity, divergence or decay at high T.

2.1.1 Systematic construction of the probability density function

To perform the derivation of the steady-state distribution $\mathcal{P}_s(x, v)$ as a series in powers of $\tau^{1/2}$, we proceed in several steps as follows. First, we conveniently rescale the Fokker-Planck operator. Then, we look for its stationary solution by expanding $\mathcal{P}_s$ on the basis of Hermite polynomials and we show how the Fokker-Planck equation imposes a recursion relation between the coefficients of this expansion. Finally, we solve this recursion by expanding these coefficients as power series in $\tau^{1/2}$. We now detail the derivation starting from the Fokker-Planck operator $\mathcal{L}$ corresponding to Eqs. (2.2)-(2.3), which reads

$$\mathcal{L}\cdot = \partial_x(\cdot\,\partial_x\phi) - v\partial_x\cdot + \partial_v\left(\frac{v}{\tau}\cdot\right) + \frac{D}{\tau^2}\partial_{vv}\cdot + T\partial_{xx}\cdot \tag{2.4}$$

Because the steady-state distribution of Eq. (2.3) is proportional to $\exp(-\frac{\tau v^2}{2D})$, we now rescale v as $\tilde{v} = \sqrt{\tau}v$ in order to expand $\mathcal{P}_s$ in series of $\tau^{1/2}$ around the equilibrium measure. When expressed in terms of the rescaled variable, $\mathcal{P}_s(x, \tilde{v})$ satisfies

$$\tilde{\mathcal{L}}\mathcal{P}_s(x, \tilde{v}) = 0\,, \tag{2.5}$$

with the operator $\tilde{\mathcal{L}}$ defined as :

$$\tilde{\mathcal{L}}\cdot = \partial_x(\cdot\,\partial_x\phi) - \frac{\tilde{v}}{\sqrt{\tau}}\partial_x\cdot + \partial_{\tilde{v}}\left(\frac{\tilde{v}}{\tau}\cdot\right) + \frac{D}{\tau}\partial_{\tilde{v}\tilde{v}}\cdot + T\partial_{xx}\cdot \tag{2.6}$$

In the remainder of this work, the tilde notation for v and $\mathcal{L}$ will be omitted for notational simplicity. We first note that the Fokker-Planck operator (2.6) can be written as :

$$\mathcal{L} = \frac{1}{\tau}\mathcal{L}_1 + \frac{1}{\sqrt{\tau}}\mathcal{L}_2 + \mathcal{L}_3 \,, \tag{2.7}$$

where $\mathcal{L}_1$, $\mathcal{L}_2$ and $\mathcal{L}_3$ are given by

$$\mathcal{L}_1 \cdot = D\frac{\partial^2}{\partial^2 v}\cdot + \frac{\partial}{\partial v} v \cdot \qquad \mathcal{L}_2 \cdot = -v\frac{\partial}{\partial x}\cdot \qquad \mathcal{L}_3 \cdot = \frac{\partial}{\partial x}\left(\cdot\, \partial_x \phi\right) + T\frac{\partial^2}{\partial^2 x}\cdot \tag{2.8}$$

$\mathcal{L}_1$ is the Fokker-Planck generator of the Ornstein-Uhlenbeck process, and its n^{th} eigenfunction P_n is related to the n^{th} physicists' Hermite polynomial $H_n(v) = (-1)^n e^{v^2}\partial_v^n e^{-v^2}$:

$$P_n(v) \;=\; \frac{e^{-\frac{v^2}{2D}} H_n\left(\frac{v}{\sqrt{2D}}\right)}{\sqrt{2^n n! 2\pi D}} \,. \tag{2.9}$$

The family $\{P_n\}$ are eigenfunctions of the operator $\mathcal{L}_1$ satisfying

$$\mathcal{L}_1 P_n \;= -nP_n \,, \tag{2.10}$$

and they are further orthogonal to the family $\{H_n\}$ as

$$\delta_{k,n} \;= \int_{-\infty}^{+\infty} \frac{H_k\left(\frac{v}{\sqrt{2D}}\right)}{\sqrt{2^k k!}} P_n(v)\mathrm{d}v \,. \tag{2.11}$$

We use the P_n's to search for the solution of the stationary distribution $\mathcal{P}_s$ under the form of:

$$\mathcal{P}_s(x,v) \;=\; \sum_n P_n(v) A_n(x) \,. \tag{2.12}$$

Using the orthogonality property (2.11), the A_n's can be obtained as

$$A_n(x) \;=\; \int \mathcal{P}_s(x,v)\frac{H_n\left(\frac{v}{\sqrt{2D}}\right)}{\sqrt{2^n n!}} dv \,. \tag{2.13}$$

Inserting (2.12) into (2.5) and using (2.10), we find that A_n is a solution of

$$\sum_n P_n(v)\partial_x\left(\partial_x\phi A_n\right) + \sum_n P_n(v) T\partial_{xx} A_n - \sum_n \frac{nP_n(v)}{\tau} A_n - \sum_n \frac{vP_n(v)}{\sqrt{\tau}}\partial_x A_n = 0 \,. \tag{2.14}$$

Using the recurrence property of Hermite polynomials, $H_{n+1}(v) = 2vH_n(v) - 2nH_{n-1}(v)$, we decompose vP_n into a sum of P_{n+1} and P_{n-1}

$$vP_n = \sqrt{(n+1)D}P_{n+1} + \sqrt{nD}P_{n-1} \,. \tag{2.15}$$

We are now in position to project equation (2.14) onto H_k and use the orthogonality relation (2.11). This leads us to the following recursion relation for the A_n's

$$0 = -nA_n - \sqrt{\tau}\sqrt{(n+1)D}\partial_x A_{n+1} - \sqrt{\tau}\sqrt{nD}\,\partial_x A_{n-1} + \tau\partial_x\left(\partial_x\phi A_n\right) + \tau T\partial_{xx} A_n \,. \tag{2.16}$$

We now look for the A_n's as series in powers of $\tau^{1/2}$. Because (2.6) is formally invariant upon the reversal $\{\tilde{v}, \sqrt{\tau}\} \to -\{\tilde{v}, \sqrt{\tau}\}$, so is the stationary distribution $\mathcal{P}_s$. Consequently, A_{2k} contains only integer powers of τ while A_{2k+1} contains only half-integer powers of τ. We shall further assume that the first nonzero contribution to A_k is of order $\tau^{k/2}$. This hierarchical ansatz is necessary to disentangle and solve, starting from A_0 and order by order in powers of $\tau^{1/2}$, the recursion equation (2.16). Its validity is a posteriori confirmed by inserting our final result for $\mathcal{P}_s$ into (2.6) and checking that $\mathcal{L}\mathcal{P}_s$ vanishes order by order in τ. We thus propose the scaling ansatz

$$\begin{aligned} A_0 &= A_0^0(x) + \tau A_0^2(x) + \tau^2 A_0^4(x) + ... && (2.17)\\ A_1 &= \tau^{1/2} A_1^1(x) + \tau^{3/2} A_1^3(x) + \tau^{5/2} A_1^5(x) + ... && (2.18)\\ A_2 &= \tau A_2^2(x) + \tau^2 A_2^4(x) + \tau^3 A_2^6(x) + ... && (2.19)\\ &\vdots \end{aligned}$$

Let us now show that the A_i^j can be computed recursively. Looking at (2.16) for $n = 0$, we get

$$\partial_x A_1 = \sqrt{\frac{\tau}{D}} \left[\partial_x \left(\partial_x \phi A_0\right) + T \partial_{xx} A_0\right] . \tag{2.20}$$

Equating coefficients of order $\tau^{k/2}$ on both sides of (2.20) and integrating once over the position leads to:

$$A_1^k = \frac{1}{\sqrt{D}} \left[\partial_x \phi A_0^{k-1} + T \partial_x A_0^{k-1}\right] + b_k . \tag{2.21}$$

with b_k an integration constant. Further equating coefficients of order $\tau^{k/2}$ in (2.16), we obtain:

$$A_n^k = -\frac{\sqrt{(n+1)D}}{n} \partial_x A_{n+1}^{k-1} - \sqrt{\frac{D}{n}} \partial_x A_{n-1}^{k-1} + \frac{\partial_x \left(\partial_x \phi A_n^{k-2}\right)}{n} + \frac{T}{n} \partial_{xx} A_n^{k-2} . \tag{2.22}$$

Taking $k = n$ in (2.22) and using that $A_n^j = 0$ for $j \leq n$ yields the expression of A_n^n as a function of A_0^0:

$$A_n^n = -\sqrt{\frac{D}{n}} \partial_x A_{n-1}^{n-1} = (-1)^n \frac{D^{n/2}}{\sqrt{n!}} \partial_x^n A_0^0 . \tag{2.23}$$

Using expression (2.21) for $k = 1$ and expression (2.23) for $n = 1$, we obtain a closed equation on A_0^0:

$$\partial_x \phi \; A_0^0 + (T + D) \partial_x A_0^0 = -b_1 \sqrt{D} . \tag{2.24}$$

Since A_0^0 corresponds to the equilibrium stationary measure when $\tau = 0$ we must have

$$\int_{-\infty}^{+\infty} \mathcal{P}_s(x, v)|_{\tau=0} \, dv = A_0^0 = c_0 \, e^{-\frac{\phi}{T+D}} , \tag{2.25}$$

with c_0 fixed by normalization:

$$c_0 = \left(\int_{-\infty}^{+\infty} e^{-\frac{\phi}{T+D}} dx \right)^{-1} . \tag{2.26}$$

The constant b_1 is self-consistently fixed to zero such that (2.25) is a solution of (2.24). We now set out to compute the next order correction A_0^2. Applying (2.22) for $n = 1$ and $k = 3$ gives:

$$A_1^3 = -\sqrt{2D}\partial_x A_2^2 - \sqrt{D}\partial_x A_0^2 + \partial_x \left(\partial_x \phi A_1^1\right) + T\partial_{xx} A_1^1 \,. \tag{2.27}$$

In (2.27), we can use (2.23) to express A_1^1 and A_2^2 as a function of A_0^0 and (2.21) to express A_1^3 as a function of A_0^2. We thus obtain a differential equation for A_0^2:

$$\frac{\partial_x \phi}{T+D} A_0^2 + \partial_x A_0^2 \;=\; -\frac{D^2 \partial_x^3 A_0^0}{T+D} + \frac{D\partial_x \left(\partial_x \phi \partial_x A_0^0\right)}{T+D} + \frac{TD\partial_x^3 A_0^0}{T+D} - \frac{b_3\sqrt{D}}{T+D} \,. \tag{2.28}$$

Using (2.25), we can integrate (2.28) and determine the expression of A_0^2

$$A_0^2 = c_0 e^{-\frac{\phi}{T+D}} \left(\frac{D\partial_{xx}\phi}{T+D} - \frac{D\left(\partial_x \phi\right)^2}{2(T+D)^2} \right) + c_2 e^{-\frac{\phi}{T+D}} - \frac{b_3\sqrt{D}}{T+D} e^{-\frac{\phi}{T+D}} \int_0^x e^{\frac{\phi}{T+D}} \mathrm{d}x \,, \tag{2.29}$$

where c_0 is defined in (2.26). Equation (2.29) involves two integration constants: c_2 and b_3. While c_2 is found by normalization, requiring $\int_{-\infty}^{+\infty} A_0^2(x)dx = 0$, b_3 is fixed by boundary conditions on A_0^2 as we shall see in the next sections. The recursion can be iterated up to an arbitrary order in τ to find both the A_0^{2k}'s and the A_i^k's for $i > 0$. In addition to the previous constants c_{2i} and b_{2i+1} for $i < k$, which were determined for lower orders, A_0^{2k} generically depends on two new integration constants: c_{2k} and b_{2k+1}. The former, c_{2k}, is found by requiring the normalization of A_0^{2k} while the latter b_{2k+1} is fixed by boundary conditions for A_0^{2k}. For example, the differential equation on A_0^4 is found by applying (2.22) for $(n = 2, k = 4)$ and $(n = 1, k = 5)$. Its solution not only depends on c_2 and b_3, which were previously determined upon computing A_0^2, but also on two new integration constants : c_4 and b_5. The constant c_4 is found by requiring normalization $\int_{-\infty}^{+\infty} A_0^4 = 0$ and b_5 is fixed by enforcing the correct boundary conditions for A_0^4. While the explicit expressions of the A_0^{2k} rapidly become cumbersome, their systematic derivation can be implemented with a software such as Mathematica [100]. For illustration purposes, we report the complete expression of $\mathcal{P}_s(x, v)$, with its integration constants, up to order τ^2 in (A.1). We remark that (2.29) shares a common feature with the distribution of other active models [16, 212]: it is non-local. Indeed, a perturbation of the potential $\delta\phi(x)$ localized around position x will affect the steady-state at position x' located far away from x. This strongly differs from the Boltzmann distribution and leads to intriguing phenomena, for example in bacterial suspensions [73].

2.1.2 Confining potential: explicit computation and numerics

The marginal in space of $\mathcal{P}_s(x, v)$ can be used to quantify how the steady-state distribution departs from the Boltzmann weight as τ increases :

$$\mathcal{P}_s(x) = \int_{-\infty}^{+\infty} \mathcal{P}_s(x, v)dv = A_0 = \sum_k A_0^{2k}\tau^k \,. \tag{2.30}$$

Here we consider the special case of a confining potential ϕ, and we require that, for all $k \geq 1$,

$$\lim_{x\to\pm\infty} A_0^{2k}(x) = 0 \tag{2.31}$$

$$\int_{-\infty}^{+\infty} A_0^{2k}(x) = 0\,. \tag{2.32}$$

For a simple harmonic confinement, we note that the complete steady-state distribution $\mathcal{P}_s(x,v)$ remains Gaussian and we report its expression in A.2. In the remainder of this paper, we will focus on the more general case of anharmonic potentials. We remark that equation (2.31) imposes $b_{2k+1} = 0$ for all $k \geq 1$ while (2.32) fixes c_{2k} for all $k \geq 1$. The function A_0^{2k} is then uniquely determined. For example, using (2.29) and the definition of c_0 (2.26), A_0^2 reads

$$A_0^2 = c_0\, e^{-\frac{\phi}{T+D}} \left(\frac{D\partial_{xx}\phi}{T+D} - \frac{D\left(\partial_x\phi\right)^2}{2(T+D)^2} \right) - \frac{3\, c_0^2\, D}{2(T+D)}\, e^{-\frac{\phi}{T+D}} \int_{-\infty}^{+\infty} \partial_{xx}\phi\, e^{-\frac{\phi}{T+D}} dx \tag{2.33}$$

In expression (2.33), we can readily extract the first correction to the Gibbs-Boltzmann measure

$$\frac{\mathcal{P}_s(x) - c_0 e^{-\frac{\phi}{T+D}}}{c_0 e^{-\frac{\phi}{T+D}}} = \tau \left[\frac{D}{T+D}\partial_{xx}\phi - \frac{3D}{T+D} \frac{\int_{-\infty}^{+\infty} \partial_{xx}\phi\, e^{-\frac{\phi}{T+D}} dx}{\int_{-\infty}^{+\infty} e^{-\frac{\phi}{T+D}} dx} \right] + o(\tau)\,. \tag{2.34}$$

which reduces at $T = 0$ to the steady-state of an Active Ornstein-Uhlenbeck (AOUP) particle [59] to this order in τ. The expression of the full marginal in space $\mathcal{P}_s(x)$ up to order τ^2 is reported in (A.2). Note that our ansatz (2.17) rests on the hypothesis that $\mathcal{P}_s(x)$ is an analytic function in $\tau^{1/2}$, which need not necessarily hold for an arbitrary potential. To check this hypothesis, we have to verify whether the series admits a finite radius of convergence. We do this for a potential $\phi(x) = x^4/4$, at fixed D and T and for two different values of τ. For $\tau = 0.01$, we show in Fig.2.1 that the truncation of Eq.(2.30) to order τ^8 is well-behaved and quantitatively agrees with the stationary distribution obtained numerically. However, for $\tau = 0.2$, Fig.2.1 shows the successive orders of the truncation to be typical of asymptotic series: adding one order in τ increases the series by a larger amount than the sum of the previous terms, leading to wild oscillations. While such a result seems disappointing, it does not mean that the full series fails in capturing the steady state. Mathematically speaking, it only entails that the finite truncation yields a poor approximation of the full series and that more work should be carried out to extract physical behaviors. To regularize our diverging truncated sequence, we resort to a Padé-Borel summation method. We first introduce the Borel transform B_N associated to Eq. (2.30):

$$B_N(\tau) = \sum_{k=0}^{N} \frac{A_0^{2k}}{k!}\tau^k\,. \tag{2.35}$$

The finite-N truncation of the series Eq. (2.30) is exactly recovered from its N^{th}-Borel transform B_N by applying a Laplace inversion :

$$\sum_{k=0}^{N} A_0^{2k}\tau^k = \int_0^{\infty} B_N(\omega\tau)e^{-\omega}d\omega\,. \tag{2.36}$$

The Laplace inversion of expression Eq. (2.35) for B_N indeed leads back to the divergent finite truncation that we wanted to regularize. To avoid such a fate, one has to find a nonpolynomial approximation of $B_N(\tau)$ whose Taylor expansion coincides with the known terms in Eq. (2.35). In the Padé-Borel method, it is achieved by approximating B_N with a rational fraction $F_N = Q_N/R_N$, where Q_N and R_N are polynomials in τ of order $N/2$ chosen such that $B_N(\tau) = Q_N(\tau)/R_N(\tau) + o(\tau^N)$. The Borel resummation at order N of Eq. (2.30), B_N^r, is defined by replacing B_N in Eq. (2.36) by its Padé approximant F_N:

$$B_N^r = \int_0^\infty \frac{Q_N(\omega\tau)}{R_N(\omega\tau)} e^{-\omega} d\omega \ . \tag{2.37}$$

Finally, the series Eq. (2.30) is formally obtained from the limit of B_N^r when $N \to \infty$. In this article, we estimate Eq. (2.30) while keeping N finite and we will not evaluate B_N^r beyond $N = 8$. Interestingly, for $\tau = 0.2$, while the truncated sequence of Eq. (2.30) is divergent, its Borel resummation B_8^r agrees quantitatively with numerical estimates of the steady-state distribution as shown in the bottom right corner of Fig. 2.1. In Fig. 2.2, we plot the Borel resummations B_8^r and the corresponding numerics for different values of T. When $T \ll D$, the dynamics Eqs. (2.2)-(2.3) is strongly out-of-equilibrium and the probability density differs significantly from the Boltzmann weight with the presence of two humps. When $T \gg D$, self-propulsion is washed out by thermal noise, the dynamics draws closer to equilibrium and the two humps of the distribution are smoothed out. Note that the Borel resummation B_8^r accurately fits the numerics without any free parameter.

2.1.3 Ratchet current: analytical formula and numerics

An interesting signature of nonequilibrium dynamics is the ratchet mechanism by which asymmetric periodic potentials generically lead to steady-state currents. Here, we consider such a potential ϕ of period L and we use our perturbative expansion to compute the steady-state current J, defined as

$$\begin{aligned} J &= \langle \dot{x} \rangle & (2.38)\\ &= \int_0^L \int_{-\infty}^{\infty} \left(-\partial_x \phi + \frac{v}{\sqrt{\tau}} \right) \mathcal{P}_s(x,v) dx dv & (2.39)\\ &= -\sum_{k\geq 0} \tau^k \int_0^L \partial_x \phi A_0^{2k} dx + \frac{\sqrt{D}}{\sqrt{\tau}} \sum_{k\geq 0} \tau^{k+1/2} \int_0^L A_1^{2k+1} dx & (2.40)\\ &= \sum_{k\geq 0} T\tau^k \int_0^L \partial_x A_0^{2k} dx + L\sqrt{D} \sum_{k>0} b_{2k+1} \tau^k \ . & (2.41) \end{aligned}$$

To go from Eq. (2.40) to Eq. (2.41), we used the expression of A_1^{2k+1} in Eq. (2.21). We require the marginal in space $\mathcal{P}_s(x)$ to be periodic, which entails A_0^{2k} to be periodic for all $k \geq 0$. The current J then simplifies into:

$$J = L\sqrt{D} \sum_{k>0} b_{2k+1} \tau^k \ . \tag{2.42}$$

While the $\{b_k\}$ all vanished in the previous section as a result of confinement Eq. (2.31), they do not for a periodic potential. Indeed, the value of b_k is fixed upon requiring the

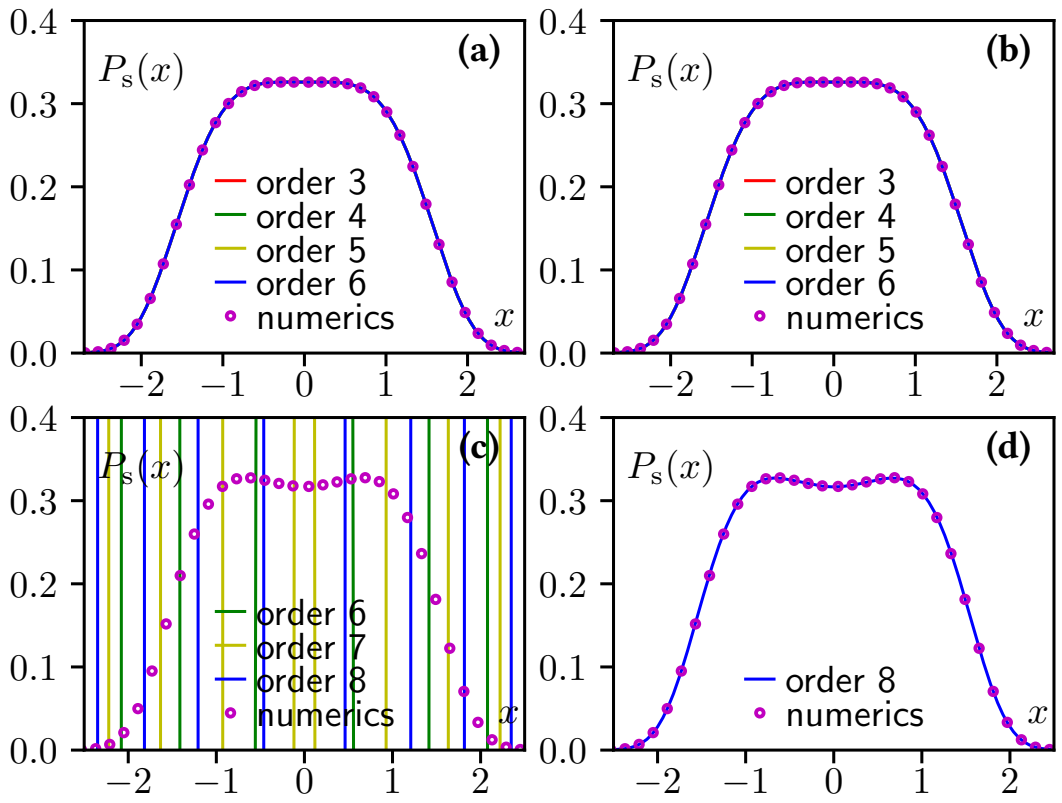

Figure 2.1: Steady-state distribution of Eqs. (2.2)-(2.3) in a confining potential $\phi(x) = x^4/4$. **Top:** For $\tau = 0.01$, the finite truncation of Eq. (2.30) converges and agrees with the numerics **(a)**. Its corresponding Borel resummation B_N^r also coincides with simulation data **(b)**. **Bottom:** For $\tau = 0.2$, the finite truncation of Eq. (2.30) is rapidly diverging **(c)**. However, the Borel resummation B_8^r accurately follows the data **(d)**. Parameters : $D = T = 1$, $dt = 10^{-4}$, time $= 10^8$.

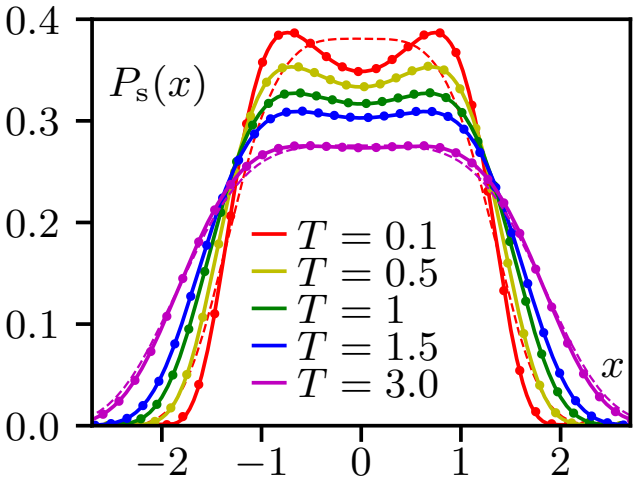

Figure 2.2: Steady-state distribution of Eqs. (2.2)-(2.3) in a confining potential $\phi(x) = x^4/4$ for different values of T. Plain curves correspond to Borel resummations B_8^r while symbols are obtained from numerical simulations of Eqs. (2.2)-(2.3). In dashed lines, we plot the Gibbs-Boltzmann distributions for the two limiting cases $T = 0.1$ and $T = 3.0$ to highlight the activity-induced deviation. The Borel resummation B_8^r always fits the data accurately without any free parameter. Parameters: $\tau = 0.2$, $D = 1$, $dt = 10^{-4}$, time $= 10^8$.

periodicity of A_0^{k-1}. Thus, different boundary conditions lead to different distributions, highlighting once again the nonlocal nature of the steady state. We report the expression of the marginal in space $\mathcal{P}_s(x)$ for a periodic potential up to order τ^2 in Eqs. (A.3)-(A.4). Using it, we find that $Lb_5\tau^2$ is the first non-vanishing contribution to the current:

$$J = \frac{DL\tau^2}{2(T+D)} \frac{\int_0^L \phi^{(1)2}\phi^{(3)}dx}{\int_0^L e^{\frac{\phi}{T+D}}dx \int_0^L e^{-\frac{\phi}{T+D}}dx} + o(\tau^2)\,. \tag{2.43}$$

The above formula reduces to the recently computed expression of J for an AOUP particle when $T = 0$ [144]. It is interesting to note that, as $T \to \infty$, J always vanishes as $J \propto 1/T$. Physically, when the thermal noise is much stronger than the self-propulsion, the nonequilibrium part of the dynamics becomes irrelevant and J dies out. However, as shown in the left part of Fig. 2.3, this intuitive picture is misleading at intermediate values of T. In this regime, the interplay between passive and active noises can, depending on the potential, make the current J non-monotonic: ramping up the temperature might drive the particle further away from equilibrium. In the right part of Fig. 2.3, we compare our quantitative prediction Eq. (2.43) with the results of numerical simulations for a potential $\phi(x) = \sin(\pi x/2) + \alpha \sin(\pi x)$ with α a constant. We find quantitative agreement at small τ for $\tau < 0.01$, which confirms our conclusion in the previous section for the radius of convergence of our ansatz Eq. (2.12). Note that J in Eq. (2.42) could also be regularized using Borel resummation to extend the quantitative range of agreement between theory and simulations to higher values of τ, but we leave such a regularization for future works.

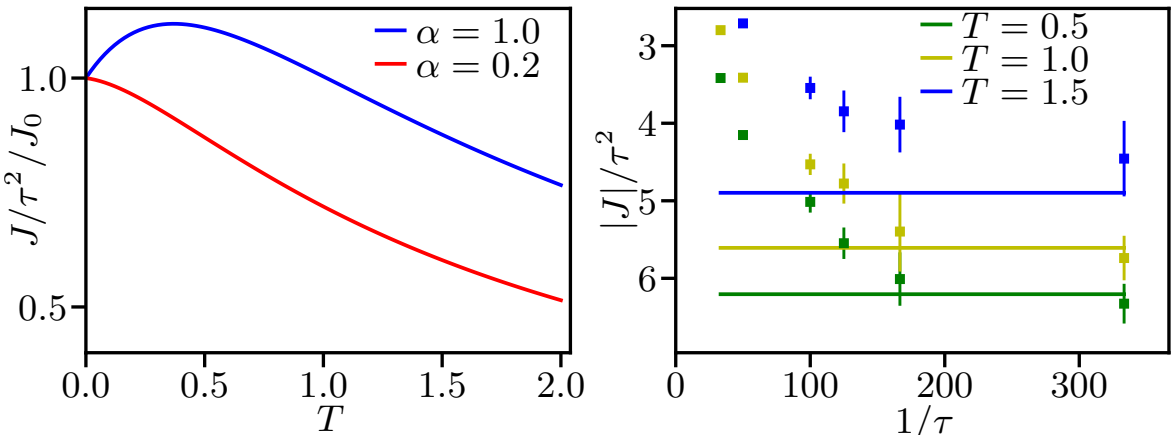

Figure 2.3: Current J induced by a ratchet potential $\phi(x) = \sin(\pi x/2) + \alpha \sin(\pi x)$ for different values of T and α. Plain curves correspond to prediction Eq. (2.43) while dots are numerical simulations with error bars given by the standard deviation. **Left:** J/τ^2 normalized by $J_0 = J(T = 0)$ as a function of T for different values of α. **Right:** J/τ^2 as a function of $1/\tau$ for $\alpha = 1$. Parameters: $D = 1$, $dt = 15.10^{-4}$, time $= 5.10^8$.

2.1.4 Entropy production rate

Another signature of nonequilibrium processes is the existence of a non-zero entropy production rate σ, which is defined as the long time limit of the logarithm of the ratio between the probability of a trajectory and that of its time-reversed counterpart (to which we refer as "forward" and "backward" trajectories) divided by the duration of the trajectory. It thus measures the dynamics' irreversibility. Somehow counter-intuitively, it has already been shown that σ might exhibit a nonmonotonic behaviour when τ is varied [30, 56]. In this part, in the same spirit, we would like to assess the dependency of the entropy production rate on the temperature and explore its possible behaviors in different contexts. More generally, the computation of σ for the AOUP dynamics Eqs. (2.2)-(2.3) remains a hot topic [31, 22, 59, 56] and it has triggered a debate about the parity of the self-propulsion v under time-reversal [21]. Following [22], we choose here to focus instead on the non Markovian process $x(t)$ obtained after integrating out the active degrees of freedom $v(t)$. In this case, a trajectory over the time interval $[0, t_f]$ is solely defined as a set of positions $x(t)$ for $t \in [0, t_f]$ and its backward counterpart is given by the set of positions $\mathcal{R}x(t) = x(t_f - t)$. After equilibration of the process $v(t)$, Eqs. (2.2)-(2.3) can be rewritten in position space only as

$$\frac{dx}{dt} = -\phi'(x) + \psi(t) \,, \tag{2.44}$$

where $\psi(t) = \sqrt{2T}\eta_1(t) + v(t)$ is a zero mean Gaussian noise with variance

$$\langle \psi(t_1)\psi(t_2)\rangle = \frac{D}{\tau} \exp\left(-\frac{|t_1 - t_2|}{\tau}\right) + 2T\delta(t_1 - t_2) = \Gamma(t_1 - t_2) \,. \tag{2.45}$$

To derive σ, we use a path-integral formalism. Since ψ is Gaussian, we obtain the steady-state Itō probability of a trajectory over the time interval $[0, t_f]$ as:

$$\mathcal{P}[x(t)] \propto P_s(x(0)) \exp\left(-\frac{1}{2}\int_0^{t_f}\int_0^{t_f} dt_1\, dt_2\, \mathcal{S}[\dot{x}, x]\right), \tag{2.46}$$

with the action

$$\mathcal{S}[\dot{x}, x] = \left[\dot{x}(t_1) + \phi'(x(t_1))\right] \Gamma^{-1}(t_1 - t_2) \left[\dot{x}(t_2) + \phi'(x(t_2))\right] , \tag{2.47}$$

and where P_s is the stationary state probability distribution and $\Gamma^{-1}(t)$ the functional inverse of the noise time correlation. It writes

$$\Gamma^{-1}(t) = \frac{1}{2T}\delta(t) - \frac{G(t)}{\tau} , \tag{2.48}$$

with

$$G(t) = \frac{D}{4T^2}\sqrt{\frac{T}{D+T}} \exp\left(-\sqrt{\frac{D+T}{T}}\frac{|t|}{\tau}\right) . \tag{2.49}$$

By definition, the entropy production rate σ over a path $x(t)$ is given by

$$\sigma = \lim_{t_f \to \infty} \frac{1}{t_f}\int_0^{t_f}\int_0^{t_f} dt_1\, dt_2\, \frac{1}{2}\left(\mathcal{S}\left[\dot{\mathcal{R}}x, \mathcal{R}x\right] - \mathcal{S}\left[\dot{x}, x\right]\right) . \tag{2.50}$$

with $\mathcal{R}x$ the reverse path. Note that in Eq. (2.50), even terms under time reversal cancels while exact derivatives yield no contribution to σ in the limit $t_f \to \infty$. Taking into account these simplifications, as well as the ergodicity of the dynamics that allows us to replace long-time averages by dynamical ensemble averages, we obtain the entropy production rate as

$$\sigma = -2\int_{-\infty}^{+\infty} \Gamma^{-1}(t) \left\langle \dot{x}(0)\phi'(x(t))\right\rangle dt , \tag{2.51}$$

where the stochastic integral is now understood in the Stratonovich scheme and the average is computed using Eq. (2.46). Note that formula Eq. (2.51) for σ is general and extends to any additive SDE with Gaussian colored noise. Lastly, as the local part of the kernel does not contribute to the entropy production rate, σ expresses as

$$\sigma = \frac{2}{\tau}\int_{-\infty}^{+\infty} G(t) \left\langle \dot{x}(0)\phi'(x(t))\right\rangle dt . \tag{2.52}$$

So far, the entropy production rate Eq. (2.51) involves two-time correlation functions, and our approach will be to reduce it to averages taken from the steady-state distribution computed in Section 2.1.1. To this aim, we use the particle displacement as a small-τ expansion parameter. Indeed, over times of order τ, for which the kernel $G(t)$ is non-vanishing, we have $x(t) - x(0) \sim \sqrt{\tau}$. The details of this expansion are given in A.3. In particular, Eq. (2.52) leads to the following expansion of σ

$$\sigma = \frac{2}{\tau}\sum_{n=2}^{+\infty}\frac{1}{n!}\int_0^{+\infty} dt\, G(t) \left\langle \dot{x}(0)\phi^{(n+1)}(x(0)) \left[x(-t) - x(0)\right]^n\right\rangle . \tag{2.53}$$

where the discretization is of the Stratonovich type and where $\phi^{(k)}$ is the k-th derivative of ϕ. In agreement with [32], Eq. (2.53) allows us to show that additive SDEs with Gaussian colored noise have vanishing entropy production rates when the potential is harmonic. Moreover, as shown in A.3, the equation of motion Eq. (2.44) can be integrated recursively in powers of τ to yield a series expansion in $\tau^{1/2}$ of σ. Our main result is the first non-vanishing order in τ of this expansion

$$\sigma = D\tau^2 H\left(\frac{T}{D}\right)\frac{\int_{-\infty}^{+\infty}\phi^{(3)2}\, e^{-\frac{\phi}{T+D}}dx}{\int_{-\infty}^{+\infty}e^{-\frac{\phi}{T+D}}dx} + O(\tau^{\frac{5}{2}})\,, \tag{2.54}$$

where the function H is given by

$$H(x) = \frac{4\sqrt{\frac{x}{x+1}} + x\left(4\sqrt{\frac{x}{x+1}}+2\right)+1}{8\sqrt{x(x+1)}+2x\left(6x+6\sqrt{x(x+1)}+7\right)+2}\,. \tag{2.55}$$

When $T \to 0$, the entropy production rate Eq. (2.54) brings us back to the expected findings of [59] for an AOUP particle. Furthermore, in a system endowed with periodic boundary conditions at $-L$ and $+L$, the entropy production rate vanishes as $1/T$ at large temperature and

$$\sigma \simeq \frac{D^2\tau^2}{4T}\frac{\int_{-L}^{+L}\phi^{(3)2}dx}{2L}\,. \tag{2.56}$$

Physically, this supports the idea that thermal noise is washing out activity and nonequilibrium signatures. However, this intuitive picture is challenged by the rich behavior of σ with T, which strongly depends on the nature of ϕ and need not be a monotonic decreasing function. For an unbounded system in a confining potential, the entropy production rate might even diverge at high temperature: increasing T might thus drive the system further away from equilibrium. In order to illustrate this idea, let us assume that $\phi(x) = \lambda x^{2p}/2p!$ with p an integer great than 1. For $T \gg D$,

$$\begin{aligned}\frac{\int_{-\infty}^{+\infty}\phi^{(3)2}\, e^{-\frac{\phi}{T+D}}dx}{\int_{-\infty}^{+\infty}e^{-\frac{\phi}{T+D}}dx} &\sim \lambda\frac{(2p)!}{(2p-3)!}\frac{\int_{-\infty}^{+\infty}x^{4p-6}\, e^{-\lambda\frac{x^{2p}}{T}}dx}{\int_{-\infty}^{+\infty}e^{-\lambda\frac{x^{2p}}{T}}dx}\\ &\propto T^{2-3/p}\,,\end{aligned} \tag{2.57}$$

which shows that the entropy production rate behaves at high T as

$$\sigma \propto T^{1-3/p}\,. \tag{2.58}$$

As $T \to \infty$, it thus goes to 0 for $p = 2$ and diverges for $p > 3$ as the particle explores steeper regions of the potential. In Figure 2.4, we plot σ/τ^2 in the $\tau \to 0$ limit, as given by Eq. (2.54), as a function of temperature in the three potentials characterized by $p = 2$, $p = 3$ and $p = 4$ and for $D = 1$ and $\lambda = 1$. Depending on the potential, it shows the rich phenomenology displayed by σ when T is varied: monotonic decrease or non-monotonicity, divergence or decay at high temperature...

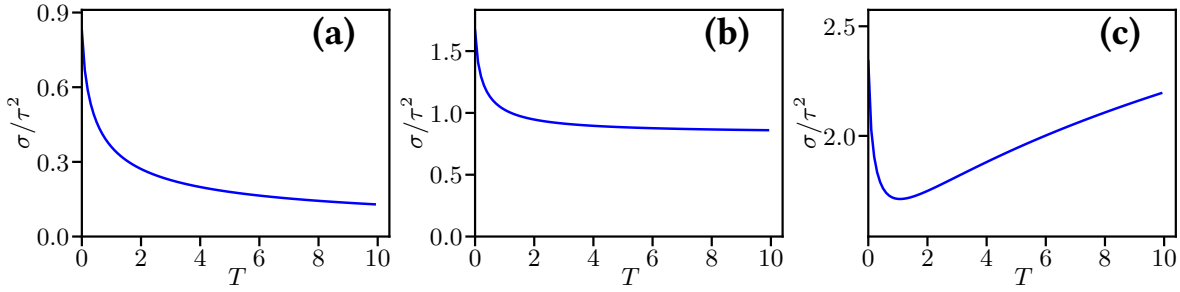

Figure 2.4: Entropy production rate of the process Eqs. (2.2)-(2.3) divided by the persistence time squared in the small persistence time limit for different confining potential $\phi(x) = \lambda x^{2p}/2p!$ as a function of temperature at $D = 1$ and $\lambda = 1$. For $p = 2$, the entropy production rate decreases as a function of T and converges to 0 at large T **(a)**. For $p = 3$, the entropy production rate decreases as a function of T and converges to a non vanishing constant at large T **(b)**. For $p = 4$, the entropy production rate is a non monotonous function of T and diverges at large T **(c)**.

2.1.5 Conclusion

We have developed theoretical insights for an AOUP subjected to an additional Brownian noise Eqs. (2.2)-(2.3). First, we devised a recursion scheme allowing us to compute its stationary distribution to an arbitrary order in $\tau^{1/2}$. We then used this result to derive quantitative expressions for activity-induced phenomena such as the emergence of current and the entropy production rate. We find that the interplay between passive and active noises produces a rich phenomenology for these nonequilibrium signatures when T is varied: monotonic, non-monotonic, diverging or decaying behaviors. The intuitive picture of a passive noise hindering activity is thus challenged in many cases where switching on translational diffusion instead drives the particle further away from equilibrium. As an alternative to our derivation, it is possible to obtain the marginal in space $\mathcal{P}_s(x)$ up to order τ^2 by using a Markovian approximation for the evolution operator: such a method has been developed in parallel to this work [177].

2.2 A one-dimensional run-and-tumble particle in an external potential

Following [194], we study here the fully solvable case of a single run and tumble particle on the real line in an arbitrary external potential V. The equation of motion of the particle writes

$$\dot{x} = v_0 u(t) - \partial_x V \tag{2.59}$$

where $u(t) = \pm 1$ is a dichotomous telegraphic noise [107] with flipping rate τ^{-1}. Two coupled equations for the evolution of the probability densities of being at point x with

orientation ± 1 can be obtained and read

$$\begin{aligned} \partial_t P_+ &= -v_0 \partial_x P_+ + \partial_x \left(P_+ \partial_x V \right) + \frac{1}{\tau} \left(P_- - P_+ \right) , \\ \partial_t P_- &= \quad v_0 \partial_x P_- + \partial_x \left(P_- \partial_x V \right) + \frac{1}{\tau} \left(P_+ - P_- \right) , \end{aligned} \tag{2.60}$$

with $P_+(x)$ (respectively $P_-(x)$) the probability density to be at x with $u = +1$ (respectively -1). We now define $\rho = P_+ + P_-$ the total local density and $g = P_+ - P_-$ measuring the local orientation of the system. The system in Eq. (2.60) can then be rewritten as

$$\begin{aligned} \partial_t \rho &= -v_0 \partial_x g + \partial_x \left(\rho \partial_x V \right) , \\ \partial_t g &= -v_0 \partial_x \rho + \partial_x \left(g \partial_x V \right) - 2\tau^{-1} g \, . \end{aligned} \tag{2.61}$$

In the steady state, the absence of density current (as is the case in a confining potential) allows us to obtain a closed equation for the stationary density ρ,

$$\partial_x \rho \left(v_0^2 - \left(\partial_x V \right)^2 \right) + 2\rho \left(\tau^{-1} \partial_x V - \partial_x V \partial_x^2 V \right) = 0 \, . \tag{2.62}$$

This differential equation displays a singularity whenever $v_0^2 - \left(\partial_x V \right)^2 = 0$ whose origin can be understood from the microscopic dynamics. Let us assume that V represents a soft wall confining the particle in the $x > 0$ half line. From the equation of motion of the particle in the left going state, one concludes that $\dot{x}$ vanishes for $\partial_x v|_{x^*} = -v_0$ (which we assume for simplicity to define a unique x^*) meaning that the particle can not penetrate the wall beyond that point. The particle density ρ is thus non-vanishing only for $x > x^*$ and we obtain, imposing a density ρ_∞ at $x \to +\infty$,

$$\rho(x) = \frac{\rho_\infty}{1 - \left(\partial_x V / v_0 \right)^2} \exp \left(\int_x^\infty \frac{2\tau^{-1} \partial_x V}{v_0^2 - \left(\partial_x V \right)^2} \right) \Theta(x - x^*) \, . \tag{2.63}$$

One of the most prominent features of the obtained probability distribution is its non locality in the potential $V(x)$. As already discussed, it also displays a cutoff at x^* which depends on both the potential and v_0: the larger the self-propulsion amplitude the deeper the particle can penetrate the wall. We now choose $V(x) = V_0 \exp\left(-x/\epsilon\right)$ with $\epsilon > 0$, the $\epsilon \to 0^+$ limit later allowing us to probe the hard wall regime. Equation (2.63) then becomes

$$\rho(x^* + r) = \frac{\rho_\infty}{1 - \exp\left(-2r/\epsilon\right)} \left\{ \frac{1 - \exp\left(-r/\epsilon\right)}{1 + \exp\left(-r/\epsilon\right)} \right\}^{\epsilon / v_0 \tau} , \tag{2.64}$$

with $x^* = -\epsilon \ln\left(\epsilon v_0 / V_0\right)$ and $r \geq 0$. If $\epsilon > v_0 \tau$, *i.e.* if the range of the potential is larger than the run length of the RTP, the density profile does not show anything spectacular and is depleted in the vicinity of the obstacle. However, if $\epsilon < v_0 \tau$, meaning that the persistent nature of the random walk can be probed over the typical scale of the potential, then the density profile diverges at $r = 0$ thus displaying a strong accumulation at the wall. This is summarized in Fig. 2.5.

2.2.1 The hard-wall limit

We now study in detail the hard wall $\epsilon \to 0^+$ limit. For this, let us consider an observable $f(x)$ independent of ϵ. We assume that f is integrable over $[0, +\infty[$ and of bounded absolute

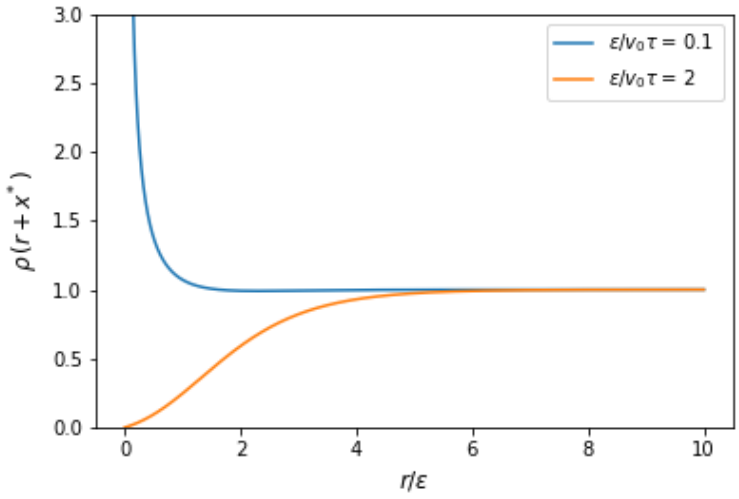

Figure 2.5: Stationary distribution function of a single one-dimensional RTP confined to the $x > 0$ half-line by a soft repulsive exponential potential of range ϵ. Distances are measured in units of ϵ and $\rho_\infty = 1$. **(Orange)** $\epsilon = 2v_0\tau$: the stationary distribution function vanishes at $r = 0$. **(Blue)** $\epsilon = 0.1\, v_0\tau$: the stationary distribution function diverges at $r = 0$.

value. Its average over the ρ distribution is given by :

$$\begin{aligned}
\langle f \rangle &= \int_{x^*}^{\infty} \rho(x) f(x)\, \mathrm{d}x\,, \\
&= \int_{0}^{\infty} \rho(x^*+r) f(x^*+r)\, \mathrm{d}r\,, \\
&= \int_{0}^{\epsilon\sqrt{\epsilon}} \rho(x^*+r) f(x^*+r)\, \mathrm{d}r + \int_{\epsilon\sqrt{\epsilon}}^{\epsilon} \rho(x^*+r) f(x^*+r)\, \mathrm{d}r + \int_{\epsilon}^{\sqrt{\epsilon}} \rho(x^*+r) f(x^*+r)\, \mathrm{d}r \\
&\quad + \int_{\sqrt{\epsilon}}^{\infty} \rho(x^*+r) f(x^*+r)\, \mathrm{d}r\,,
\end{aligned} \tag{2.65}$$

where we have split the integral in such a way that the $\epsilon \to 0$ limit can be carefully studied. First, it is easy to remark that, $\forall x \geq \sqrt{\epsilon}\,,\ \rho(x^*+r) \to \rho_\infty$ as $\epsilon \to 0$. Therefore,

$$\int_{\sqrt{\epsilon}}^{\infty} \rho(x^*+r) f(x^*+r)\, \mathrm{d}r \to \rho_\infty \int_{0}^{\infty} f(x)\, \mathrm{d}x\,. \tag{2.66}$$

Moreover,

$$\rho(x^*+\epsilon) = \frac{\rho_\infty}{1-\exp(-2)} \left\{ \frac{1-\exp(-1)}{1+\exp(-1)} \right\}^{\epsilon/v_0\tau}\,. \tag{2.67}$$

which is finite. Hence the third integral yields a vanishing contribution in the $\epsilon \to 0^+$ limit,

$$\int_{\epsilon}^{\sqrt{\epsilon}} \rho(x^*+r) f(x^*+r)\, \mathrm{d}r \to 0\,. \tag{2.68}$$

Furthermore, we have :

$$\begin{aligned}\int_{\epsilon\sqrt{\epsilon}}^{\epsilon} \rho(x^*+r)f(x^*+r)\,\mathrm{d}r &\leq \epsilon\rho(x^*+\epsilon\sqrt{\epsilon})f(x^*+\epsilon\sqrt{\epsilon})\,,\\ &= \epsilon\frac{\rho_\infty}{1-\exp\left(-2\sqrt{\epsilon}\right)}\left\{\frac{1-\exp\left(-\sqrt{\epsilon}\right)}{1+\exp\left(-\sqrt{\epsilon}\right)}\right\}^{\epsilon/v_0\tau} f(x^*+\epsilon\sqrt{\epsilon})\,,\\ &\xrightarrow[\epsilon\to 0^+]{} 0\,.\end{aligned} \tag{2.69}$$

Thus the second integral also vanishes in the hard sphere limit. The contribution from the vicinity of the obstacle thus only comes from the first one that evaluates to,

$$\begin{aligned}\int_0^{\epsilon\sqrt{\epsilon}} \rho(x^*+r)f(x^*+r)\,\mathrm{d}r &= \epsilon\int_0^{\sqrt{\epsilon}} \rho(x^*+\epsilon r)f(x^*+\epsilon r)\,\mathrm{d}r\\ &\simeq \epsilon\rho_\infty f(0)\int_0^{\sqrt{\epsilon}} \frac{r^{\epsilon/v_0\tau}}{2r}\\ &\xrightarrow[\epsilon\to 0^+]{} \frac{v_0\tau}{2}\rho_\infty f(0)\,.\end{aligned} \tag{2.70}$$

Note that we could perform exactly the same computation for this last integral with ϵ^q, for any $q>1$, as an upper bound. From this, we can first conclude that :

$$\rho(x) \xrightarrow[\epsilon\to 0^+]{} \frac{v_0\tau}{2}\rho_\infty\delta(x)+\rho_\infty\Theta(x)\,, \tag{2.71}$$

in agreement with [137] where the hard wall limit is rather obtained by studying a RTP with zero-current boundary condition in the presence of thermal noise and later setting the temperature to 0. The stationary distribution function therefore displays a delta peak accumulation at the wall and a flat bulk part. Note that all the weight of the δ function is at $x=0^+$, *i.e.* the convention is such that

$$\int_0^1 \mathrm{d}x\,\delta(x)=1\,. \tag{2.72}$$

Moreover, for finite ϵ, the solution displays an accumulation boundary layer close to the wall with thickness smaller than any polynomial in ϵ. Within the accumulation boundary layer we therefore always have $(\partial_x v)^2 = v_0^2$, an identity that allows to regularize products of the type $\rho(x)\partial_x V$ that often arise when computing, for instance, the mechanical pressure exerted on the wall.

2.2.2 The hard-wall limit again

Here, we present a way of directly obtaining Eq. (2.71) without having to solve first for an arbitrary external potential. This is adapted from the method we presented in [175] and will be useful later when studying more complex geometries where general solutions of

the type Eq. (2.63) are not available. We start from Eq. (2.60) that we rewrite in stationary state as

$$0 = -v_0\sigma\partial_x P_\sigma + \partial_x\left(P_\sigma \partial_x V\right) + \frac{1}{\tau}\left(P_{-\sigma} - P_\sigma\right)\,, \tag{2.73}$$

with $\sigma = \pm 1$. Furthermore, we know that the probability current vanishes at $x = x^*$, *i.e.* $\lim_{x\to x^*}\left(v_0\sigma - \partial_x V\right)P_\sigma(x) = 0$. Thus, by integrating Eq. (2.73) between x^* and $x^* + \delta x$ we get

$$-v_0\sigma P_\sigma\left(x^*+\delta x\right) + P_\sigma\left(x^*+\delta x\right)\partial_x V\left(x^*+\delta x\right) + \frac{1}{\tau}\int_{x^*}^{x^*+\delta x} \mathrm{d}x'\left(P_{-\sigma}\left(x'\right) - P_\sigma\left(x'\right)\right) = 0\,. \tag{2.74}$$

We then take the hard wall limit $\epsilon \to 0^+$ and afterwards the limit $\delta x \to 0$. This procedure kills the potential term and we obtain

$$\lim_{\delta x\to 0^+}\lim_{\epsilon\to 0^+}\left[-v_0\sigma P_\sigma\left(x^*+\delta x\right) + \frac{1}{\tau}\int_{x^*}^{x^*+\delta x}\mathrm{d}x'\left(P_{-\sigma}\left(x'\right) - P_\sigma\left(x'\right)\right)\right] = 0\,. \tag{2.75}$$

This equation shows us that, in the hard wall limit, the probability density can indeed be decomposed as the sum of a bulk part at $x > 0$ and a delta peak contribution at $x = 0$,

$$\lim_{\epsilon\to 0^+} P_\sigma(x) = \Gamma_\sigma\delta(x) + f_\sigma(x)\Theta(x)\,, \tag{2.76}$$

with, from Eq. (2.75),

$$-v_0\sigma f_\sigma\left(0^+\right) + \frac{1}{\tau}\left(\Gamma_{-\sigma} - \Gamma_\sigma\right) = 0\,, \tag{2.77}$$

which takes the form of a flux-balance equation at the surface of the wall. Furthermore, the bulk equation can be derived straightforwardly from the original Fokker-Planck one,

$$-v_0\sigma\partial_x f_\sigma + \frac{1}{\tau}\left(f_{-\sigma} - f_\sigma\right) = 0\,, \tag{2.78}$$

from which we recover the flatness of the bulk distribution $f_\sigma(x) = \rho_\infty/2$. The surface flux-balance equations then reduces to

$$\left(\Gamma_- - \Gamma_+\right) = \frac{v_0\tau}{2}\rho_\infty\,. \tag{2.79}$$

It appears natural to close the system by setting $\Gamma_+ = 0$ as right going particles do not accumulate at the left confining wall. This finally yields

$$\Gamma_- = \frac{v_0\tau}{2}\rho_\infty\,, \tag{2.80}$$

from which one recovers Eq. (2.71). The vanishing of Γ_+ can actually be proven by integrating Eq. (2.74) over $\delta x \in [0, \delta x']$ and taking first the $\epsilon \to 0^+$ limit and afterwards the $\delta x' \to 0^+$ one. This yields,

$$\lim_{\delta x\to 0^+}\lim_{\epsilon\to 0^+}\int_0^{\delta x'}\mathrm{d}s P_\sigma\left(x^*+s\right)\partial_x V\left(x^*+s\right) = v_0\sigma\,\Gamma_\sigma\,. \tag{2.81}$$

The non negativity of the probability together with the negativity of $\partial_x V$ finally imposes $\Gamma_+ = 0$. This construction overall shows that the precise form of the potential used to build the hard wall limit is irrelevant. To sum things up, we obtain in the end

$$\begin{cases} P_-(x) = \dfrac{\rho_\infty}{2}\Theta(x) + \dfrac{v_0\tau}{2}\rho_\infty\delta(x)\,, \\ P_+(x) = \dfrac{\rho_\infty}{2}\Theta(x)\,. \end{cases} \tag{2.82}$$

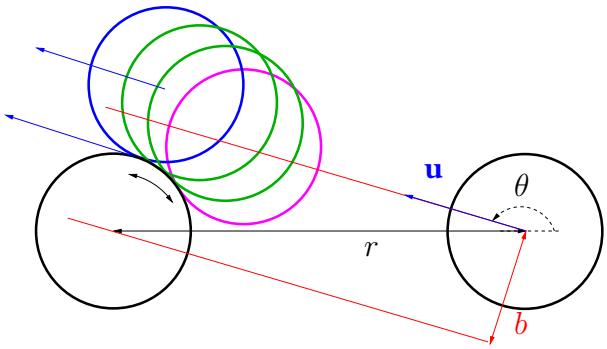

Figure 2.6: A collision of an active hard-sphere (black, rightmost) with diameter σ and impact parameter $b = r\sin\theta < \sigma$ (with $\cos\theta < 0$) onto a pinned (black, leftmost) one. In the following we introduce the notation $w = \cos\theta$. The incoming particle with direction $\mathbf{u}$ hits the target sphere (at the magenta position) and then skids around by occupying the sequence of green positions. It eventually takes off at the blue position when its orientation $\mathbf{u}$ becomes tangent to the target sphere. In the highly ballistic limit, no tumble can occur over the typical skidding distances.

2.3 A run-and-tumble particle around a hard spherical obstacle

We now address the case of an RTP in contact with a hard spherical obstacle in arbitrary space dimension $d > 1$ in the highly ballistic limit $v_0\tau \gg \sigma$ with σ the size of the obstacle. Incidentally, the highly ballistic limit turns out to be relevant for studying collective phenomena such as the motility-induced phase separation, as can be seen from the phase diagrams of [196] in which the MIPS critical point in a WCA system arises when the run length equals a few tens of the potential range both in $d = 2$ and $d = 3$. This regime has also been studied for its connections with sheared granular systems [1, 155]. Our main results are as follows. For all $\sigma/v_0\tau$, the stationary distribution function is shown to exhibit a delta peak accumulation at contact and a bulk contribution that diverges at $r = \sigma$. The structure of this divergence is elucidated. The distribution is then fully characterized in $d \geq 2$ as $\sigma/v_0\tau \to 0$.

The equation of motion of a RTP evolving in a spherically symmetric potential reads

$$\frac{\mathrm{d}\mathbf{r}}{\mathrm{d}t} = v_0\mathbf{u}(t) - \boldsymbol{\nabla}V(\mathbf{r})\,, \tag{2.83}$$

where $\mathbf{u}(t)$ is the standard RTP propulsion vector: it is normalized and uniformly reoriented on the unit sphere with rate τ^{-1}. The physical picture for the interaction between the particle and the obstacle is depicted in Fig. 2.6. The stationary state distribution function $P(\mathbf{r},\mathbf{u})$ solves the master equation,

$$-v_0\mathbf{u}\cdot\boldsymbol{\nabla}_{\mathbf{r}}P + \boldsymbol{\nabla}_{\mathbf{r}}\left(P\boldsymbol{\nabla}_{\mathbf{r}}V(\mathbf{r})\right) + \frac{1}{\tau}\left(\int\frac{\mathrm{d}\mathbf{u}'}{\Omega_d}P(\mathbf{r},\mathbf{u}') - P\right) = 0\,. \tag{2.84}$$

Using rotational symmetry, and denoting $r = ||\mathbf{r}||$ and $w = \mathbf{r}\cdot\mathbf{u}/r$, the above equation is written as

$$\begin{aligned} 0 =& -v_0\left(w\partial_r P + \frac{1-w^2}{r}\partial_w P\right) + \frac{1}{r^{d-1}}\partial_r\left(r^{d-1}P\partial_r V(r)\right) \\ &+ \frac{1}{\tau}\left(\int_{-1}^{1}\frac{\mathrm{d}w'}{2W_{d-2}}\left(1-w'^2\right)^{\frac{d-3}{2}}P(r,w') - P(r,w)\right), \end{aligned} \tag{2.85}$$

with W_n the n^{th} Wallis integral. We assume that $V(r)$ corresponds to a hard sphere potential of exclusion diameter σ. In other words, as in Sec. 2.2, we choose

$$V(r) = V_0\,\mathrm{e}^{-\frac{r-\sigma}{\epsilon\sigma}}, \tag{2.86}$$

and we take the hard sphere limit $\epsilon \to 0^+$ by following the program explained in Sec. 2.2.2. First, from the equation of motion Eq. (2.83), we know that $\forall\epsilon > 0$, $P(r,w) = 0$ for $r \leq r^*$ with r^* defined by $V'(r^*) = -v_0$. Upon multiplying Eq. (2.85) by r^{d-1} and integrating it between r^* and $r > r^*$ we obtain

$$\begin{aligned} 0 =& -v_0 w r^{d-1}P(r,w) + v_0(d-1)w\int_{r^*}^{r}\mathrm{d}r' r'^{d-2}P(r',w) \\ &- v_0(1-w^2)\partial_w\int_{r^*}^{r}\mathrm{d}r' r'^{d-2}P(r',w) + r^{d-1}P(r,w)V'(r) \\ &+ \frac{1}{\tau}\int_{r^*}^{r}\mathrm{d}r' r'^{d-1}\left(\int_{-1}^{1}\frac{\mathrm{d}w'}{2W_{d-2}}\left(1-w'^2\right)^{\frac{d-3}{2}}P(r,w') - P(r,w)\right), \end{aligned} \tag{2.87}$$

At fixed r, we take the limit $\epsilon \to 0^+$. We then take the $r \to \sigma$ limit. This shows that the probability distribution function develops in the hard sphere limit a singular part at contact in the form of a delta peak at $r = \sigma$. Denoting $z = r/\sigma$, the stationary distribution function takes the form

$$P(\mathbf{r},\mathbf{u}) = f(z,w)\Theta(z-1) + \Gamma(w)\delta(z-1), \tag{2.88}$$

where $f(z,w)$ and $\Gamma(w)$ are solutions of the two coupled partial integro-differential equations

$$w\partial_z f + \frac{1-w^2}{z}\partial_w f + \eta f = \eta\rho(z), \tag{2.89}$$

and

$$\Gamma'(w) - \frac{w}{1-w^2}(d-1)\Gamma(w) + \frac{\eta}{1-w^2}\Gamma(w) = -\frac{w}{1-w^2}f(1,w) + \frac{\eta}{1-w^2}\hat{\Gamma}, \tag{2.90}$$

with $\eta = 1/\mathrm{Pe} = \sigma/v_0\tau$ and

$$\rho(z) = \int_{-1}^{1}\frac{\mathrm{d}w}{2W_{d-2}}(1-w^2)^{\frac{d-3}{2}}f(z,w), \tag{2.91}$$

the bulk density and

$$\hat{\Gamma} = \int_{-1}^{1}\frac{\mathrm{d}w}{2W_{d-2}}(1-w^2)^{\frac{d-3}{2}}\Gamma(w), \tag{2.92}$$

the surface density. Equations (2.89) and (2.90) can be understood as two coupled flux balance equations : one for the bulk and one for the surface of the obstacle. We also regularize the product $P(r,w)V'(r)$ in the hard sphere limit. We integrate once more Eq. (2.87) over $r \in [r^*, r']$, take the $\epsilon \to 0^+$ limit at fixed r' and later the $r' \to \sigma$ limit. In Eq. (2.87), only the first and the fourth term yield non vanishing contributions, thus showing that

$$\begin{aligned}\lim_{r'\to\sigma}\lim_{\epsilon\to 0^+}\int_{r^*}^{r'} \mathrm{d}r P(r,w)V'(r) &= v_0 w \lim_{r\to\sigma}\lim_{\epsilon\to 0^+}\int_{r^*}^{r'} \mathrm{d}r P(r,w) \\ &= v_0\sigma w\Gamma(w)\end{aligned} \tag{2.93}$$

proving that $\Gamma(w>0)=0$: particles leaving the obstacle do not accumulate on it. This in particular yields the following boundary condition for the bulk equation

$$f(1,w>0) = \frac{\eta\hat{\Gamma}}{w}\,. \tag{2.94}$$

2.3.1 A self-consistent equation over the density field

At fixed $\rho(z)$, the bulk equation Eq. (2.89) is a first order linear partial differential equation that can be solved by the method of characteristics. The function $\rho(z)$ is then determined self-consistently. The goal of this section is to obtain this self-consistent equation satisfied by the density field. The characteristics of the bulk equation are given by

$$\begin{cases} z'(s) = w(s) \\ w'(s) = \dfrac{1-w^2(s)}{z(s)} \end{cases} \tag{2.95}$$

and are thus lines such that $z\sqrt{1-w^2} = b =$ cste with b the impact parameter. They correspond to free streaming trajectories and are depicted in Fig. 2.7. Equation (2.89) is furthermore supplemented with the boundary condition $f(L, w<0)=1$ that implements an homogeneous reservoir of incoming particles. L is sent to infinity in the end. As $L\to\infty$, the actual form of the boundary condition at $z=L$ is irrelevant.

Domain 1 : $w>0$ **and** $z\sqrt{1-w^2}<1$

By definition, along a characteristic, the bulk equation writes

$$f'(s) + \eta f(s) = \eta K(s) \text{ with } K(s) = \rho(z(s))\,, \tag{2.96}$$

and hence can be integrated as

$$f(s,b) = f(s=0,b)\mathrm{e}^{-\eta s} + \eta \mathrm{e}^{-\eta s}\int_0^s \mathrm{d}s' K(s')\mathrm{e}^{\eta s'}\,. \tag{2.97}$$

A boundary condition must then be implemented to express $f(s=0,b)$ and the (s,b) variables that parametrize the characteristic must be replaced by their (z,w) counterparts. We

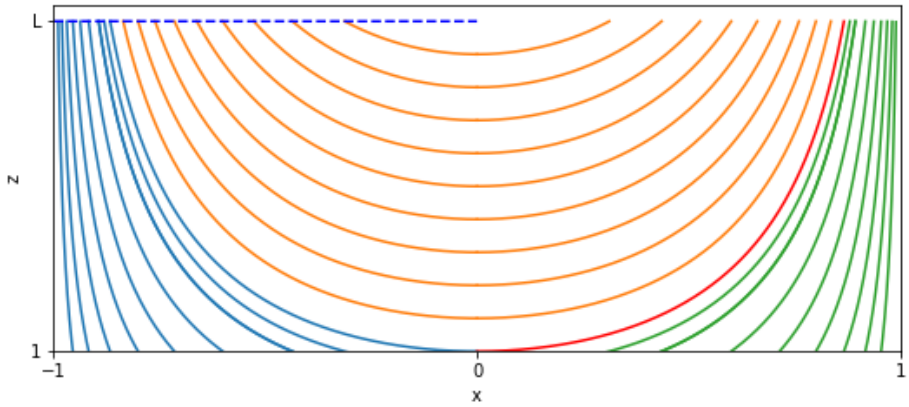

Figure 2.7: Characteristics of the bulk equation in Eq. (2.89). (**Blue and Orange**) Characteristics that are connected to the boundary condition at $z = L$ (dashed blue line). (**Green**) Characteristics that are connected to the boundary condition at $z = 1$ Eq. (2.94). (**Red**) Characteristic that originates from $(z = 1, w = 0)$. After each collision, the particle leaves the obstacle exactly along this line (except when it has flipped in course of skidding).

first solve the equation on the domain $w > 0$ and $z\sqrt{1-w^2} < 1$. This domain is generated by characteristics corresponding to trajectories leaving the obstacle after a collision. These are depicted in green in Fig. 2.7. On each characteristic we have

$$\begin{aligned} z\sqrt{1-w^2} &= b < 1\,, \\ \Rightarrow\ w(s) &= \sqrt{1-\frac{b^2}{z(s)^2}}\,. \end{aligned} \tag{2.98}$$

Thus

$$\begin{aligned} z'(s) &= \sqrt{1-\frac{b^2}{z(s)^2}}\,, \\ \Rightarrow\ z(s)\sqrt{1-\frac{b^2}{z(s)^2}} &= s + \sqrt{1-b^2}\,, \end{aligned} \tag{2.99}$$

as we choose to parametrize the characteristics such that $z(s=0) = 1$. This leads to

$$\begin{cases} z(s,b) = \sqrt{s^2 + 2s\sqrt{1-b^2} + 1}\,, \\ w(s,b) = \dfrac{s+\sqrt{1-b^2}}{s^2 + 2s\sqrt{1-b^2}+1}\,, \end{cases} \tag{2.100}$$

which can be inverted so as to get

$$\begin{cases} b = z\sqrt{1-w^2}\,, \\ s = zw - \sqrt{1-z^2(1-w^2)}\,. \end{cases} \tag{2.101}$$

Lastly, from Eq. (2.94) and Eq. (2.100), the boundary condition writes

$$f(s=0,b) = \frac{\eta\hat{\Gamma}}{\sqrt{1-b^2}}\,. \tag{2.102}$$

This finally leads to

$$\begin{aligned} f(z,w) = &\frac{\eta\hat{\Gamma}}{\sqrt{1-z^2(1-w^2)}}\mathrm{e}^{-\eta(zw-\sqrt{1-z^2(1-w^2)})} \\ &+ \eta\mathrm{e}^{-\eta zw}\int_1^z \mathrm{d}z'\rho(z')\frac{z'}{\sqrt{z'^2-z^2(1-w^2)}}\mathrm{e}^{\eta\sqrt{z'^2-z^2(1-w^2)}}\,. \end{aligned} \tag{2.103}$$

Domain 2 : $w<0$

This domain is generated by characteristics that are connected to the boundary condition at $z=L$. These are depicted in blue and orange in Fig. 2.7. Following the same route as above, we obtain along a characteristic

$$\begin{cases} z(s,b) = \sqrt{b^2+\left(s-L\sqrt{1-\dfrac{b^2}{L^2}}\right)^2}\,, \\ w(s,b) = \dfrac{-L\sqrt{1-\frac{b^2}{L^2}}+s}{\sqrt{b^2+(s-L\sqrt{1-\frac{b^2}{L^2}})^2}}\,, \end{cases} \tag{2.104}$$

with $z(s=0,b)=L$. These equations can be inverted to yield

$$\begin{cases} b = z\sqrt{1-w^2}\,, \\ s = zw + L\sqrt{1-\dfrac{z^2(1-w^2)}{L^2}}\,. \end{cases} \tag{2.105}$$

Hence,

$$\begin{aligned} f(z,w) = &\eta\mathrm{e}^{-\eta zw}\int_z^L \mathrm{d}z'\rho(z')\exp\left\{-\eta z'\sqrt{1-\frac{z^2(1-w^2)}{z'^2}}\right\}\frac{1}{\sqrt{1-\frac{z^2(1-w^2)}{z'^2}}} \\ &+ \mathrm{e}^{-\eta\left(zw+L\sqrt{1-\frac{z^2(1-w^2)}{L^2}}\right)}\,, \\ \underset{L\to\infty}{=} &\eta\mathrm{e}^{-\eta zw}\int_z^{+\infty}\mathrm{d}z'\rho(z')\exp\left\{-\eta\sqrt{z'^2-z^2(1-w^2)}\right\}\frac{z'}{\sqrt{z'^2-z^2(1-w^2)}}\,. \end{aligned} \tag{2.106}$$

The above equation shows, as expected, the irrelevance of the boundary condition at $z=L$ as L is sent to infinity.

Domain 3 : $w > 0$ **and** $z\sqrt{1-w^2} > 1$

This domain is generated by the extension of the orange characteristics of Fig. 2.7 studied in the previous paragraph to the $w > 0$ domain. In this domain we use the continuity requirement at $w = 0$ inferred from Eq. (2.106) as an initial condition at $s = 0$. The characteristics are parametrized by

$$\begin{cases} w(s,b) = \dfrac{s}{\sqrt{b^2+s^2}}\,, \\ z(s,b) = \sqrt{b^2+s^2}\,, \end{cases} \tag{2.107}$$

as $w(s=0,b) = 0$. These equations can be inverted to yield

$$\begin{cases} b = z\sqrt{1-w^2}\,, \\ s = zw\,. \end{cases} \tag{2.108}$$

Furthermore, we have by continuity,

$$f(s=0,b) = \eta \int_b^{+\infty} \mathrm{d}z' \rho(z') \exp\left\{ -\eta z' \sqrt{1-\frac{b^2}{z'^2}} \right\} \frac{1}{\sqrt{1-\frac{b^2}{z'^2}}}\,, \tag{2.109}$$

and hence

$$\begin{aligned} f(z,w) = \eta \mathrm{e}^{-\eta z w} \int_{z\sqrt{1-w^2}}^{+\infty} \mathrm{d}z' \rho(z') \exp\left\{ -\eta \sqrt{z'^2 - z^2(1-w^2)} \right\} \frac{z'}{\sqrt{z'^2 - z^2(1-w^2)}} \\ + \eta \mathrm{e}^{-\eta z w} \int_{z\sqrt{1-w^2}}^{z} \mathrm{d}z' \rho(z') \exp\left\{ \eta \sqrt{z'^2 - z^2(1-w^2)} \right\} \frac{z'}{\sqrt{z'^2 - z^2(1-w^2)}}\,. \end{aligned} \tag{2.110}$$

Domain 4 : $w > 0$ **and** $z\sqrt{1-w^2} = 1$

The line defined by $z\sqrt{1-w^2} = 1$ with $w > 0$ which is depicted in red in Fig. 2.7 plays a special role. Indeed, after each collision, the particle leaves the obstacle exactly along this line (except when it has flipped in course of skidding). This strongly suggests that the bulk distribution function $f(z,w)$ displays a delta peak contribution along this characteristic line. To check this, let us write the ansatz,

$$f(z,w) = f_0(z,w) + \phi(z)\delta(z\sqrt{1-w^2} - 1)\Theta(w)\,, \tag{2.111}$$

with $f_0(z,w)$ a piece-wise continuous function (as f_0 might not be continuous when crossing the characteristic line $z\sqrt{1-w^2} = 1$ at $w > 0$). By inserting the above expression in Eq. (2.89), we get for $z > 1$

$$\left[\sqrt{1-\frac{1}{z^2}}\phi'(z) + \eta\phi(z) \right] \delta(z\sqrt{1-w^2} - 1) + w\partial_z f_0 + \frac{1-w^2}{z}\partial_w f_0 + \eta(f_0 - \rho) = 0\,, \tag{2.112}$$

which in particular yields

$$\phi(z) = \phi(1)\mathrm{e}^{-\eta\sqrt{z^2-1}}\,. \tag{2.113}$$

The value of $\phi(1)$ is given by Eq. (2.90). By integrating it between $w = 0^-$ and $w = 0^+$, we indeed obtain

$$\Gamma(0^-) = \lim_{\epsilon\to 0}\int_{-\epsilon}^{+\epsilon} \mathrm{d}w\; w f(1,w)\,. \tag{2.114}$$

Hence

$$f(1,w) = \frac{\Gamma(0^-)}{w}\delta(w) + ... = \Gamma(0^-)\delta(\sqrt{1-w^2}-1) + ...\,, \tag{2.115}$$

where the ... stands for something more regular than $\delta(w)/w$. We therefore get

$$\phi(z) = \Gamma(0^-)\mathrm{e}^{-\eta\sqrt{z^2-1}}\,. \tag{2.116}$$

The existence of a Dirac delta singularity in the distribution function, not only at the surface of the obstacle but also in the bulk of the (w,z) plane, is a remarkable feature of this problem that, up to our knowledge, has not so far been pointed out in the literature. We believe this effect, that would be smoothed by a soft-potential, is a generic feature of active particles around strictly convex rigid obstacles.

A self-consistent equation for the bulk density $\rho(z)$

The self-consistent equation for the bulk density $\rho(z)$ is obtained by integrating Eqs. (2.103)-(2.106)-(2.110)-(2.116) over w. It takes the form of an integral equation

$$\rho(z) = \rho_0(z) + \mathcal{L}[\rho](z)\,, \tag{2.117}$$

where

$$\begin{aligned}\rho_0(z) = \eta\hat{\Gamma}\int_{\frac{\sqrt{z^2-1}}{z}}^1 \frac{\mathrm{d}w}{2W_{d-2}}(1-w^2)^{\frac{d-3}{2}}\frac{\exp\left\{-\eta\left(zw-\sqrt{1-z^2(1-w^2)}\right)\right\}}{\sqrt{1-z^2(1-w^2)}} \\ + \frac{\Gamma(0^-)}{2W_{d-2}}\frac{\mathrm{e}^{-\eta\sqrt{z^2-1}}}{\sqrt{z^2-1}}z^{2-d}\,,\end{aligned} \tag{2.118}$$

and where the operator $\mathcal{L}$ is defined as

$$\mathcal{L}[\rho](z) = \mathcal{L}_1[\rho](z) + \mathcal{L}_2[\rho](z) + \mathcal{L}_3[\rho](z)\,, \tag{2.119}$$

with

$$\mathcal{L}_1[\rho](z) = \eta\int_1^z \mathrm{d}z' z'\rho(z')\int_{\frac{\sqrt{z^2-1}}{z}}^1 \frac{\mathrm{d}w}{2W_{d-2}}(1-w^2)^{\frac{d-3}{2}}\frac{\mathrm{e}^{-\eta z w}\exp\left(\eta\sqrt{z'^2-z^2(1-w^2)}\right)}{\sqrt{z'^2-z^2(1-w^2)}}\,, \tag{2.120}$$

and

$$\mathcal{L}_2[\rho](z) = 2\eta\int_1^z \mathrm{d}z' z'\rho\left(z'\right)\int_{\frac{\sqrt{z^2-z'^2}}{z}}^{\frac{\sqrt{z^2-1}}{z}} \frac{\mathrm{d}w}{2W_{d-2}}\left(1-w^2\right)^{\frac{d-3}{2}}\frac{\mathrm{e}^{-\eta z w}\cosh\left(\eta\sqrt{z'^2-z^2(1-w^2)}\right)}{\sqrt{z'^2-z^2(1-w^2)}}\,, \tag{2.121}$$

and finally

$$\mathcal{L}_3[\rho](z) = \eta \int_z^{+\infty} \mathrm{d}z' z' \rho(z') \int_{-1}^{\frac{\sqrt{z^2-1}}{z}} \frac{\mathrm{d}w}{2W_{d-2}} \left(1-w^2\right)^{\frac{d-3}{2}} \frac{\mathrm{e}^{-\eta z w} \exp\left(-\eta\sqrt{z'^2 - z^2(1-w^2)}\right)}{\sqrt{z'^2 - z^2(1-w^2)}} \,. \tag{2.122}$$

To our knowledge, Eq. (2.117) can in general only be solved formally,

$$\rho(z) = \sum_{n=0}^{+\infty} \mathcal{L}^n[\rho_0](z) \,. \tag{2.123}$$

Progresses can nevertheless be made in some limiting cases. The first one we study is the near obstacle regime $z-1 \ll 1$. We then focus on the highly ballistic limit $\eta \to 0$ where the size of the obstacle is much smaller than the persistence length of the self-propelled particle. At the other side of the spectrum, the first η^{-1} correction to the $\eta \to \infty$ equilibrium limit is equivalent to the case of one particle against a hard wall that has been studied in a two-dimensional geometry in [49].

2.3.2 Behavior of the density field in the vicinity of the obstacle

We start by studying the behavior of the density field in the vicinity of the obstacle. We denote $h = z - 1$ and assume that $h << 1$. We first have,

$$\rho_0(1+h) = \frac{\Gamma(0^-)}{2W_{d-2}} \frac{1}{\sqrt{2h}} - \frac{\eta\hat{\Gamma}}{4W_{d-2}} \ln h + O(1) \,. \tag{2.124}$$

Indeed, the last term of Eq. (2.118) writes in the small h limit,

$$\begin{aligned}
&\eta\hat{\Gamma} \int_{\frac{\sqrt{z^2-1}}{z}}^1 \frac{\mathrm{d}w}{2W_{d-2}} (1-w^2)^{\frac{d-3}{2}} \frac{\exp\left\{-\eta\left(zw - \sqrt{1-z^2(1-w^2)}\right)\right\}}{\sqrt{1-z^2(1-w^2)}} \\
=& \eta\hat{\Gamma} \int_0^{1/z^2} \frac{\mathrm{d}s}{4W_{d-2}} \left(\frac{1}{z^2} - s\right)^{\frac{d-3}{2}} \frac{\exp\left(-\eta\sqrt{z^2-1+z^2 s} + \eta z\sqrt{s}\right)}{\sqrt{s}\sqrt{z^2-1+z^2 s}} \,, \\
=& \frac{\eta\hat{\Gamma}}{4W_{d-2}} \left(\int_0^1 \mathrm{d}s \frac{(1-s)^{\frac{d-3}{2}}}{\sqrt{s}\sqrt{s+2h}} \left[1 + O(h)\right] \right. \\
&\left. - \int_{1/z^2}^1 \mathrm{d}s \left(\frac{1}{z^2} - s\right)^{\frac{d-3}{2}} \frac{\exp\left(-\eta\sqrt{z^2-1+z^2 s} + \eta z\sqrt{s}\right)}{\sqrt{s}\sqrt{z^2-1+z^2 s}} \right) , \\
=& -\frac{\eta\hat{\Gamma}}{4W_{d-2}} \ln h + O(1) \,.
\end{aligned} \tag{2.125}$$

Our claim is that Eq. (2.124) gives the leading order behavior of the actual density field, *i.e.*

$$\rho(1+h) = \frac{\Gamma(0^-)}{2W_{d-2}} \frac{1}{\sqrt{2h}} - \frac{\eta\hat{\Gamma}}{4W_{d-2}} \ln h + O(1) \,. \tag{2.126}$$

To prove the validity of the above equation, we now investigate the small h behavior of $\mathcal{L}[\tilde{\rho}](1+h)$ for a generic function $\tilde{\rho}(z)$ integrable at $z=1$. We start by noting that upon a change of variables

$$\mathcal{L}_1[\tilde{\rho}](z) = \frac{\eta z^{4-d}}{4W_{d-2}} \int_1^z \mathrm{d}z'\, z' \tilde{\rho}(z') g_1(z', z)\,, \tag{2.127}$$

with

$$g_1(z', z) = \int_0^{\frac{1}{z^2}} \mathrm{d}s \frac{(1-z^2 s)^{\frac{d-3}{2}}}{\sqrt{z^2-1+z^2 s}} \frac{\exp\left(-\eta\sqrt{z^2-1+z^2 s} + \eta\sqrt{z'^2-1+z^2 s}\right)}{\sqrt{z'^2-1+z^2 s}}\,. \tag{2.128}$$

Thus, in the vicinity of the obstacle,

$$\mathcal{L}_1[\tilde{\rho}](1+h) = \frac{\eta(1+h)h}{4W_{d-2}} \int_0^1 \mathrm{d}u\, (1+uh)\, \tilde{\rho}\,(1+uh)\, g_1\,(1+uh, 1+h)\ , \tag{2.129}$$

with

$$\begin{aligned} g_1\,(1+uh, 1+h) &\simeq \int_0^1 \mathrm{d}s \frac{1}{\sqrt{s}\sqrt{s+2h(1+u)}}\,, \\ &\simeq -\ln h\,. \end{aligned} \tag{2.130}$$

Therefore,

$$\mathcal{L}_1[\tilde{\rho}](1+h) \simeq -\frac{\eta}{4W_{d-2}} h \ln h \int_0^1 \mathrm{d}u\, \tilde{\rho}\,(1+uh)\ . \tag{2.131}$$

We proceed accordingly for $\mathcal{L}_2$. We have,

$$\mathcal{L}_2[\tilde{\rho}](z) = 2\eta \int_1^z \mathrm{d}z' z' \tilde{\rho}\,(z')\, g_2\,(z', z)\ , \tag{2.132}$$

with

$$g_2(z', z) = \int_{\frac{\sqrt{z^2-z'^2}}{z}}^{\frac{\sqrt{z^2-1}}{z}} \frac{\mathrm{d}w}{2W_{d-2}} \left(1-w^2\right)^{\frac{d-3}{2}} \frac{\exp\left(-\eta z w\right)}{\sqrt{z'^2 - z^2(1-w^2)}} \cosh\left(\eta\sqrt{z'^2 - z^2(1-w^2)}\right). \tag{2.133}$$

Thus,

$$\mathcal{L}_2[\tilde{\rho}](1+h) = 2\eta h \int_0^1 \mathrm{d}u\, (1+uh)\, \tilde{\rho}\,(1+uh)\, g_2\,(1+uh, 1+h)\ , \tag{2.134}$$

with

$$\begin{aligned} g_2\,(1+uh, 1+h) &\simeq \int_{\sqrt{2h(1-u)}}^{\sqrt{2h}} \frac{\mathrm{d}w}{2W_{d-2}} \frac{1}{\sqrt{2h(u-1)+w^2}}\,, \\ &\simeq \operatorname{arctanh}\left(\sqrt{u}\right)\ . \end{aligned} \tag{2.135}$$

Hence we obtain,

$$\mathcal{L}_2[\tilde{\rho}](1+h) \simeq 2\eta h \int_0^1 \mathrm{d}u\, \tilde{\rho}\,(1+uh) \operatorname{arctanh}\left(\sqrt{u}\right)\ . \tag{2.136}$$

Lastly, we study the conditions under which $\mathcal{L}_3[\tilde{\rho}](1)$ is finite. The latter indeed yields a finite result if

$$\tilde{\rho}\,(z')\int_{-1}^{0}\frac{\mathrm{d}w}{2W_{d-2}}\left(1-w^2\right)^{\frac{d-3}{2}}\frac{\exp\left(\eta w-\eta\sqrt{z'^2-1+w^2)}\right)}{\sqrt{z'^2-1+w^2}}\,, \tag{2.137}$$

is integrable at $z'=1$. By denoting $u=\sqrt{z'^2-1}\ll 1$ we obtain,

$$\int_{-1}^{0}\frac{\mathrm{d}w}{2W_{d-2}}\left(1-w^2\right)^{\frac{d-3}{2}}\frac{\exp\left(\eta w-\eta\sqrt{z'^2-1+w^2)}\right)}{\sqrt{z'^2-1+w^2}}\simeq\frac{-1}{4W_{d-2}}\ln u\,, \tag{2.138}$$

thus showing that $\mathcal{L}_3[\tilde{\rho}](1)$ is finite if

$$\tilde{\rho}\,(1+h)\ln(h) \tag{2.139}$$

is integrable at $h=0$. It thus appears from Eqs. (2.131)-(2.136)-(2.139) that $\mathcal{L}[\rho_0](z)$ has a finite limit at $z=1$. Recursively, the same can be said for $\mathcal{L}^n[\rho_0](z)$ for any $n>0$. Let us assume that ϵ is the typical amplitude of the operator $\mathcal{L}$ (which can be formally put by hand by setting $\mathcal{L}\to\epsilon\mathcal{L}$ and letting $\epsilon\to 1$). Then to any finite order in ϵ we have,

$$\rho(1+h)\underset{h\to 0}{=}\frac{\Gamma(0^-)}{2W_{d-2}}\frac{1}{\sqrt{2h}}-\frac{\eta\hat{\Gamma}}{4W_{d-2}}\ln h+O(1)\,. \tag{2.140}$$

We assume that the latter holds after resummation, which then implies Eq. (2.126). This equation relates exactly the divergences of the bulk distribution function on the obstacle to properties of the surface distribution function. We have simulated the dynamics Eq. (2.83) in dimension $d=2$ and numerically measured $\Gamma(w)$ and $\rho(z)$. The simulation is performed in a spherical box of radius $L=100v_0\tau$. The boundary condition is such that when the particle hits the outer boundary it is reflected with a random (inward) orientation. In Fig. 2.8, we plot the function $\Gamma(w)$ at $\eta=1$ and deduce $\Gamma(0^-)$ from it. We then show that the measured $\rho(z)$ indeed exhibits the square root divergence predicted by Eq.(2.140).

2.3.3 Behavior of the density field in the highly ballistic limit

We now study the solution of Eq. (2.117) in the highly ballistic limit $\eta\to 0$. We first define $K(z)=\rho(z)-1$ such that $\lim_{z\to\infty}K(z)=0$. From Eq. (2.117), one obtains

$$K(z)=K_0(z)+\mathcal{L}[K](z)\,, \tag{2.141}$$

with

$$K_0(z)=\rho_0(z)-\int_{\frac{\sqrt{z^2-1}}{z}}^{1}\frac{\mathrm{d}w}{2W_{d-2}}\left(1-w^2\right)^{\frac{d-3}{2}}\exp\left(-\eta zw+\eta\sqrt{1-z^2(1-w^2)}\right). \tag{2.142}$$

Our claim is then the following. In any dimension $d\geq 2$, $K_0(z)$ gives the leading order behavior of $K(z)$,

$$K(z)\underset{\eta\to 0}{=}\frac{\Gamma(0^-)}{2W_{d-2}}\frac{z^{2-d}}{\sqrt{z^2-1}}-\int_{\frac{\sqrt{z^2-1}}{z}}^{1}\frac{\mathrm{d}w}{2W_{d-2}}\left(1-w^2\right)^{\frac{d-3}{2}}+o(1)\,. \tag{2.143}$$

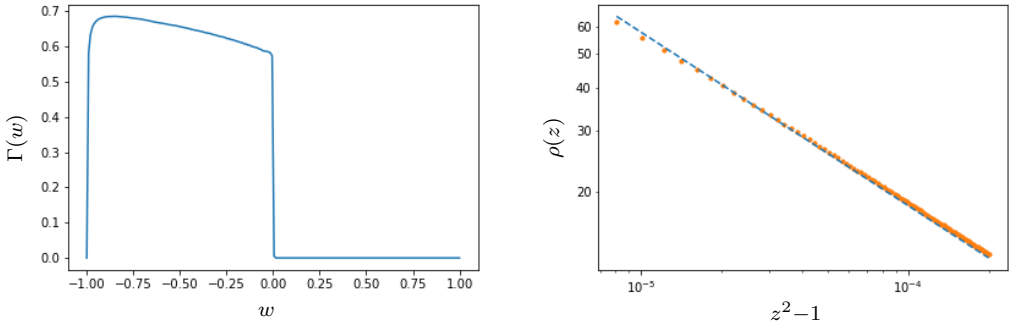

Figure 2.8: Steady-state distribution of Eq. (2.83) for the hard sphere case at $\eta = 1$ in dimension $d = 2$. **(Left)** Numerically measured surface distribution $\Gamma(w)$. It is non-vanishing for $w < 0$ only and yields $\Gamma(0^-) \simeq 0.57$. **(Right)** Log-log plot of the bulk space density $\rho(z)$ as a function of $z^2 - 1$ in the vicinity of the obstacle. The dashed blue line is the theoretical prediction of Eq. (2.140) with $2W_0 = \pi$ and using the measured value of $\Gamma(0^-)$. The orange dots correspond to numerical simulations. Parameters: $v = 1$, $\tau = 1$, $\sigma = 1$, $L = 100$ $T = 10^{10}$ with T the total physical time.

Interestingly, this leading order behavior can be obtained quite simply from the $\eta \to 0$ limit of Eq. (2.89) supplemented with the boundary condition $f(L, w < 0) = 1$ at some fixed L and afterwards sending $L \to \infty$, *i.e.* by extending all along each characteristic its prescribed value at the corresponding boundary condition. In other words, the $\eta \to 0$ and $L \to \infty$ limits commute. The result in Eq. (2.143) can be understood from a visual inspection of Eq. (2.119) from which $\mathcal{L}$ can be expected to scale as $O(\eta)$. As we prove next, this scaling is correct in all dimension $d \geq 3$. Equation Eq. (2.143) also holds in $d = 2$. However, the small η result reads

$$K(z) = \frac{\Gamma(0^-)}{\pi} \frac{1}{\sqrt{z^2-1}} - \left(\frac{1}{2} - \frac{1}{\pi} \arcsin\left(\frac{\sqrt{z^2-1}}{z} \right) \right) + O(\eta \ln \eta) \,, \tag{2.144}$$

showing that the η expansion is not regular. We interpret this as being related to the recurrence of two-dimensional random walks.

Leading order corrections at z fixed

We show that both $\mathcal{L}_1$ and $\mathcal{L}_2$ yield $O(\eta)$ corrections in the $\eta \to 0$ limit for all z fixed. We first notice that

$$\lim_{\eta \to 0} \frac{1}{\eta} \mathcal{L}_1[K](z) = \int_1^z \mathrm{d}z' \, z' \, K_{\eta=0}(z') \int_{\frac{z^2-1}{z}}^1 \frac{\mathrm{d}w}{2W_{d-2}} \frac{(1-w^2)^{\frac{d-3}{2}}}{\sqrt{z'^2 - z^2(1-w^2)}} \,. \tag{2.145}$$

The above integral is indeed well-defined as

$$\int_{\frac{z^2-1}{z}}^1 \frac{\mathrm{d}w}{2W_{d-2}} \frac{(1-w^2)^{\frac{d-3}{2}}}{\sqrt{z'^2 - z^2(1-w^2)}} \,, \tag{2.146}$$

has finite value at $z'=1$ and $\rho_{\eta=0}(z')$ is integrable at $z'=1$ as can be seen from Eq. (2.126). Accordingly, the same scaling holds for $\mathcal{L}_2$,

$$\lim_{\eta\to 0}\frac{1}{\eta}\mathcal{L}_2[K](z)=2\int_1^z \mathrm{d}z' z' K_{\eta=0}(z')\int_{\frac{\sqrt{z^2-z'^2}}{z}}^{\frac{\sqrt{z^2-1}}{z}}\frac{\mathrm{d}w}{2W_{d-2}}\frac{(1-w^2)^{\frac{d-3}{2}}}{\sqrt{z'^2-z^2(1-w^2)}}\,. \tag{2.147}$$

As a preliminary result, we thus obtain $\forall z$ fixed,

$$K(z)=K_0(z)+\mathcal{L}_3[K](z)+\eta\lim_{\eta\to 0}\frac{1}{\eta}\mathcal{L}_1[K](z)+\eta\lim_{\eta\to 0}\frac{1}{\eta}\mathcal{L}_2[K](z)+o(\eta)\,. \tag{2.148}$$

We now turn to the study of $\mathcal{L}_3[\rho](z)$. We recall Eq. (2.122),

$$\mathcal{L}_3[K](z)=\eta\int_z^{+\infty}\mathrm{d}z' z' K(z')\int_{-1}^{\frac{\sqrt{z^2-1}}{z}}\frac{\mathrm{d}w}{2W_{d-2}}\left(1-w^2\right)^{\frac{d-3}{2}}\times \\ \cdots\times\frac{\exp\left(-\eta z w-\eta\sqrt{z'^2-z^2(1-w^2)}\right)}{\sqrt{z'^2-z^2(1-w^2)}}\,. \tag{2.149}$$

from which it appears that if $K_{\eta=0}(z')$ is integrable at $+\infty$, then

$$\lim_{\eta\to 0}\frac{1}{\eta}\mathcal{L}_3[K](z)\ \text{ exists.} \tag{2.150}$$

Result in $d\geq 3$: In the limits where $\eta\to 0$, $z\to\infty$ with $\eta z\to 0$, one has

$$K_0(z)\simeq\frac{\Gamma(0^-)}{2W_{d-2}}\frac{1}{z^{d-1}}\,, \tag{2.151}$$

which is integrable in $d\geq 3$ at $z'\to\infty$. Therefore,

$$\mathcal{L}_3[K_0](z)=O(\eta)\,. \tag{2.152}$$

Equation (2.143) is therefore a solution of the self-consistent equation Eq. (2.141). The small η corrections are obtained as

$$K(z)=K_0(z)+\eta\lim_{\eta\to 0}\frac{1}{\eta}\mathcal{L}[K_0](z)+o(\eta)\,. \tag{2.153}$$

These corrections are not studied in detail here.

Result in $d=2$: In $d=2$, $K_0(z)$ in Eq. (2.151) is not integrable at $z\to\infty$. We obtain the leading order behavior of $\mathcal{L}_3[K_0](z)$ at finite z by decomposing it into the sum of a near-field contribution and a far-field one,

$$\mathcal{L}_3[K_0](z)=I_1+I_2\,, \tag{2.154}$$

with

$$I_1 = \eta \int_z^{\frac{1}{\sqrt{\eta}}} \mathrm{d}z' z' K_0(z') \int_{-1}^{\frac{\sqrt{z^2-1}}{z}} \frac{\mathrm{d}w}{2W_{d-2}} \left(1-w^2\right)^{\frac{d-3}{2}} \frac{\exp\left(-\eta z w - \eta\sqrt{z'^2 - z^2(1-w^2)}\right)}{\sqrt{z'^2 - z^2(1-w^2)}}\,, \tag{2.155}$$

and

$$I_2 = \eta \int_{\frac{1}{\sqrt{\eta}}}^{+\infty} \mathrm{d}z' z' K_0(z') \int_{-1}^{\frac{\sqrt{z^2-1}}{z}} \frac{\mathrm{d}w}{2W_{d-2}} \left(1-w^2\right)^{\frac{d-3}{2}} \frac{\exp\left(-\eta z w - \eta\sqrt{z'^2 - z^2(1-w^2)}\right)}{\sqrt{z'^2 - z^2(1-w^2)}}\,. \tag{2.156}$$

The leading order behavior of the near field contribution is given by

$$\begin{aligned} I_1 &\simeq \eta \int^{\frac{1}{\sqrt{\eta}}} \mathrm{d}z' K_0(z') \int_{-1}^{\frac{\sqrt{z^2-1}}{z}} \frac{\mathrm{d}w}{2W_{d-2}} \left(1-w^2\right)^{\frac{-1}{2}}\,, \\ &\simeq -\frac{1}{2}\eta \ln\eta \,\frac{\Gamma(0^-)}{\pi}\left(\frac{1}{2} + \frac{1}{\pi}\arcsin\left(\frac{\sqrt{z^2-1}}{z}\right)\right)\,. \end{aligned} \tag{2.157}$$

Accordingly, the leading order behavior of the far-field contribution is obtained as

$$\begin{aligned} I_2 &\simeq \int_{\sqrt{\eta}}^{+\infty} \mathrm{d}u\, K_0\left(\frac{u}{\eta}\right) \mathrm{e}^{-u} \int_{-1}^{\frac{\sqrt{z^2-1}}{z}} \frac{\mathrm{d}w}{2W_{d-2}} \left(1-w^2\right)^{\frac{d-3}{2}}\,. \\ &\simeq -\frac{1}{2}\eta \ln\eta \,\frac{\Gamma(0^-)}{\pi}\left(\frac{1}{2} + \frac{1}{\pi}\arcsin\left(\frac{\sqrt{z^2-1}}{z}\right)\right)\,, \end{aligned} \tag{2.158}$$

thus yielding at leading order

$$\mathcal{L}_3[K_0](z) \simeq -\eta \ln\eta \,\frac{\Gamma(0^-)}{\pi}\left(\frac{1}{2} + \frac{1}{\pi}\arcsin\left(\frac{\sqrt{z^2-1}}{z}\right)\right)\,. \tag{2.159}$$

Equation (2.159) proves Eq. (2.144). We remark that this $\eta \ln\eta$ behavior emerges from the non integrability at infinity of the $\eta \to 0$ limit of the last term in the expression of $\rho_0(z)$ in Eq. (2.118). This term accounts for the particles that have left the obstacle after a collision (see Sec. 2.3.1). This $\eta \ln\eta$ correction can thus be thought as originating from a return in the vicinity of the obstacle of far away particles that have already collided with it, which is all the more likely as random walks are recurrent in the low dimension $d = 2$.

Stationary distribution in the (z, w) space

Accordingly, in all dimension $d \geq 2$, the stationary distribution in the (z, w) plane can be obtained in the $\eta \to 0$ limit. In domain 1 defined by $w > 0$ and $z\sqrt{1-w^2} < 1$, Eq. (2.103) reduces to

$$f(z, w) = 0\,. \tag{2.160}$$

In domain 2 defined by $w < 0$, Eq. (2.106) is given in this limit by

$$\begin{aligned} f(z, w) &= 1 + \eta \mathrm{e}^{-\eta z w} \int_z^{+\infty} \mathrm{d}z' K(z') \exp\left\{-\eta\sqrt{z'^2 - z^2(1-w^2)}\right\} \frac{z'}{\sqrt{z'^2 - z^2(1-w^2)}}\,, \\ &= 1\,. \end{aligned} \tag{2.161}$$

Finally, in domain 3 defined by $w > 0$ and $z\sqrt{1-w^2} > 1$ we obtain accordingly from Eq. (2.110),

$$f(z,w) = 1\,. \tag{2.162}$$

Therefore, the full bulk distribution reads

$$f(z,w) = \Theta(-w) + \Theta(w)\left[\Theta(z\sqrt{1-w^2}-1) + \Gamma(0^-)\delta(z\sqrt{1-w^2}-1)\right]\,. \tag{2.163}$$

The surface density

The system of equations can then be closed by studying Eq. (2.90) for the surface density. In the limit $\eta \to 0$, and using Eq. (2.161)

$$\Gamma(w) = \frac{1}{d-1}\Theta(-w)\,. \tag{2.164}$$

We therefore obtain the full probability distribution in the ballistic $\eta \to 0$ limit,

$$\begin{aligned} P(z,w) = &\Theta(z-1)\left(\Theta(-w) + \Theta(w)\left[\Theta(z\sqrt{1-w^2}-1) + \frac{1}{d-1}\delta(z\sqrt{1-w^2}-1)\right]\right) \\ &+ \frac{1}{d-1}\delta(z-1)\Theta(-w)\,. \end{aligned} \tag{2.165}$$

Accordingly, the spatial distribution function reads

$$\begin{aligned} P(z) &= \int_{-1}^{1} \frac{\mathrm{d}w}{2W_{d-2}}(1-w^2)^{\frac{d-3}{2}} P(z,w) \\ &= \frac{\delta(z-1)}{2(d-1)} + \Theta(z-1)\left[\frac{1}{2} + \int_0^{\frac{\sqrt{z^2-1}}{z}} \frac{\mathrm{d}x}{2W_{d-2}}\left(1-x^2\right)^{\frac{d-3}{2}} + \frac{1}{2W_{d-2}(d-1)}\frac{z^{2-d}}{\sqrt{z^2-1}}\right]\,. \end{aligned} \tag{2.166}$$

In Fig. 2.9, we plot the evolution of $\hat{\Gamma}$ as a function of τ at fixed $\sigma = 1$ and $v_0 = 1$ in dimension $d = 2$ obtained from the numerical simulation of Eq. (2.83). Figure 2.9 shows in particular the convergence to $1/2$ at large τ as can be seen from Eq. (2.166).

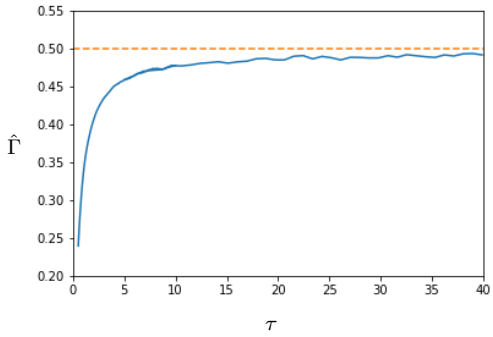

Figure 2.9: Evolution of $\hat{\Gamma}$ as a function of τ at fixed $\sigma = 1$ and $v_0 = 1$ in dimension $d = 2$. $\hat{\Gamma}$ converges to $1/2$ at large τ as predicted by Eq. (2.166). Parameters: $v_0 = 1$, $\sigma = 1$, $L = 100 v_0 \tau$, $T = 10^{10}$ with T the total physical time.

Chapter 3

Intermezzo: thermodynamics of self-propelled particle systems and equilibrium fluids in infinite dimension

Contents

The purpose of this chapter is mainly to introduce some useful concepts for Chap. 4. In Sec. 3.1, we present the main tools we will use to study and characterize the macroscopic behavior of self-propelled particle systems. Among the concepts introduced are: the BBGKY hierarchy of correlation functions, the radial pair-distribution function, the effective self-propulsion [55] and the mechanical pressure [193]. We use the results obtained in

Chap.2 to derive low density estimates for these observables in hard sphere systems in the ballistic limit.

In Sec. 3.2 we turn to the different subject of infinite dimensional equilibrium fluids. We first review the standard Mayer expansion of the free energy. We then show that in the limit of large dimension the free energy is truncated, up to exponentially small corrections, to second order in density. This is at the basis of [68] in which the authors first derived an exact equation of state for infinite dimensional hard spheres. We finally show that the results obtained through the Mayer expansion, for which we have no equivalent at hand in active matter systems, can actually be recovered by an exact resummation of the BBGKY hierarchy to all order in the density. This new dynamics-based derivation is an alternative to the original approach of [68].

Contributions

Section 3.1

- low density estimates of the pair-distribution function, effective self-propulsion and mechanical pressure of self-propelled hard spheres in the ballistic limit.

Section 3.2

- resummation of the BBGKY hierarchy that allows to recover the truncation of the free energy functional to second order.

3.1 Collective properties of self-propelled particle systems and macroscopic observables

Prior to delving specifically into the limit of infinite dimension, we introduce some useful concepts to describe the macroscopic properties of large active matter systems. The equations of motion that describe the behavior of an N-body system made of self-propelled particles interacting via pairwise forces have been introduced in Sec. 1.2.4 and read

$$\dot{\mathbf{r}}_i = v_0 \mathbf{u}_i(t) - \sum_{j(\neq i)} \boldsymbol{\nabla}_{\mathbf{r}_i} U\left(\mathbf{r}_i - \mathbf{r}_j\right) \,, \tag{3.1}$$

where the self-propulsion $\mathbf{u}_i(t)$ can be either of the AOUP, ABP or RTP type. Note that the $\mathbf{u}_i(t)$ evolve independently from each other: there is no alignment interactions in the models we consider. The corresponding N-body master equation that evolves the probability density to observe a configuration of $\{\mathbf{r}_i, \mathbf{u}_i\}_{i=1\ldots N}$ can be derived from Eq. (3.1) and it reads,

$$\partial_t P = \sum_i \boldsymbol{\nabla}_{\mathbf{r}_i} \cdot \left(P \sum_{j \neq i} \boldsymbol{\nabla}_{\mathbf{r}_i} U\left(\mathbf{r}_i - \mathbf{r}_j\right) \right) + v_0 \sum_i \mathbf{u}_i \cdot \boldsymbol{\nabla}_{\mathbf{r}_i} P + \sum_i \mathcal{R}_i P \,, \tag{3.2}$$

where the operator $\mathcal{R}_i$ accounts for the reorientation of the self-propulsion of particle i. The normalization of the N-body distribution function is chosen such that

$$\int \mathrm{d}\mathbf{r}_1 \frac{\mathrm{d}\mathbf{u}_1}{\Omega_d} \dots \mathrm{d}\mathbf{r}_N \frac{\mathrm{d}\mathbf{u}_N}{\Omega_d} P\left(\mathbf{r}_1, \mathbf{u}_1; \dots; \mathbf{r}_N, \mathbf{u}_N, t\right) = 1\,. \tag{3.3}$$

For RTPs, each $\mathbf{u}_i$ is a unit vector uniformly picking a random orientation at random times drawn from a Poisson distribution with density τ^{-1}. The evolution operator $\mathcal{R}_i$ thus writes

$$\mathcal{R}_i P = \frac{1}{\tau}\left(\int \frac{\mathrm{d}\mathbf{u}_i}{\Omega_d} P - P\right)\,, \tag{3.4}$$

from which one obtains the two-point correlation $\langle \mathbf{u}_i(t)\cdot\mathbf{u}_i(t')\rangle = \mathrm{e}^{-|t-t'|/\tau}$. Had we chosen to describe active Brownian particles (ABPs) instead, the evolution operator $\mathcal{R}_i$ would have been given by

$$\mathcal{R}_i P = D_r \Delta_{\mathbf{u}_i} P\,, \tag{3.5}$$

where $\Delta_{\mathbf{u}_i}$ is the Laplacian on the unit sphere and thus $\langle \mathbf{u}_i(t)\cdot\mathbf{u}_i(t')\rangle = \mathrm{e}^{-(d-1)D_r|t-t'|}$. Finally, for AOUPs, the vectors $\mathbf{u}_i$ don't have a fixed norm. They are however chosen to be unitary on average $\langle \mathbf{u}_i^2\rangle = 1$ in the stationary state to link with the above introduced RTP and ABP models. Given this constraint, Eq. (1.18) of the introduction has to be slightly modified and now reads

$$\frac{\mathrm{d}\mathbf{u}_i}{\mathrm{d}t} = -\frac{\mathbf{u}_i}{\tau} + \sqrt{\frac{2}{d\tau}}\,\boldsymbol{\xi}_i\,, \tag{3.6}$$

where the Gaussian white noises have correlations $\langle \xi_i^\alpha(t)\xi_j^\beta(t')\rangle = \delta^{\alpha\beta}\delta_{ij}\delta(t-t')$. The corresponding $\mathcal{R}_i$ operator is then obtained as

$$\mathcal{R}_i P = \frac{1}{\tau}\left(\boldsymbol{\nabla}_{\mathbf{u}_i}\cdot(\mathbf{u}_i P) + \frac{1}{d}\boldsymbol{\nabla}^2_{\mathbf{u}_i} P\right)\,. \tag{3.7}$$

from which one recovers $\langle \mathbf{u}_i(t)\cdot\mathbf{u}_i(t')\rangle = \mathrm{e}^{-|t-t'|/\tau}$. Interestingly, we remark that the stationary distribution of $\mathbf{u}_i$ reads

$$p_{\mathrm{st}}(\mathbf{u}_i) = \frac{1}{\sqrt{2\pi/d}}\mathrm{e}^{-d\mathbf{u}_i^2/2}\,, \tag{3.8}$$

so that the probability distribution of its norm u_i is given by

$$p_{\mathrm{st}}(u_i) = \frac{\Omega_d}{\sqrt{2\pi/d}} u_i^{d-1}\mathrm{e}^{-du_i^2/2}\,. \tag{3.9}$$

with Ω_d the surface of the $(d-1)$-dimensional unit hypersphere in d dimension. In the $d \gg 1$ limit that we will consider later on, this shows that the value $u_i = 1$, up to vanishingly small fluctuations as $d \to \infty$, eventually dominates the statistics, thus making a link with RTPs and ABPs. At odds with equilibrium systems for which the N-body stationary distribution function is known and is given by the Boltzmann distribution, the solution to Eq. (3.2) remains elusive.

3.1.1 Correlation functions and the BBGKY hierarchy

The N-body master equation in Eq. (3.2) can be analyzed through the introduction of the n-body correlation functions,

$$\rho^{(n)}\left(\mathbf{r}_1,\mathbf{u}_1;\dots;\mathbf{r}_n,\mathbf{u}_n;t\right)=\frac{N!}{(N-n)!}\int \mathrm{d}\mathbf{r}_{n+1}\frac{\mathrm{d}\mathbf{u}_{n+1}}{\Omega_d}\dots\mathrm{d}\mathbf{r}_N\frac{\mathrm{d}\mathbf{u}_N}{\Omega_d}P\left(\mathbf{r}_1,\mathbf{u}_1;\dots;\mathbf{r}_N,\mathbf{u}_N;t\right)\,. \tag{3.10}$$

From the $\rho^{(n)}$ we also define the n-body distribution functions $g^{(n)}$ by

$$\rho^{(n)}\left(\mathbf{r}_1,\mathbf{u}_1;\dots;\mathbf{r}_n,\mathbf{u}_n;t\right)=\left[\prod_{i=1}^{n}\rho\left(\mathbf{r}_i,\mathbf{u}_i;t\right)\right]g^{(n)}\left(\mathbf{r}_1,\mathbf{u}_1;\dots;\mathbf{r}_n,\mathbf{u}_n;t\right)\,, \tag{3.11}$$

with $\rho(\mathbf{r},\mathbf{u};t)=\rho^{(1)}(\mathbf{r},\mathbf{u};t)$ the local density field in the $(\mathbf{r},\mathbf{u})$ space. In the thermodynamic limit, their exists an infinite hierarchy of equations relating n-body distribution functions $g^{(n)}(\mathbf{r}_1,\dots,\mathbf{r}_n;\mathbf{u}_1,\dots,\mathbf{u}_n)$ to $(n+1)$-body ones, known as the Bogoliubov–Born–Green–Kirkwood–Yvon (BBGKY) hierarchy. In the stationary state and in a homogeneous phase of density ρ, it reads

$$\begin{aligned}&-v_0\sum_{i=1}^{n}\mathbf{u}_i\cdot\boldsymbol{\nabla}_{\mathbf{r}_i}g^{(n)}+\sum_{i=1}^{n}\sum_{j\neq i}^{n}\boldsymbol{\nabla}_{\mathbf{r}_i}\left(g^{(n)}\boldsymbol{\nabla}_{\mathbf{r}_i}U(\mathbf{r}_i-\mathbf{r}_j)\right)+\sum_{i=1}^{n}\mathcal{R}_i g^{(n)}\\&+\rho\sum_{i=1}^{n}\boldsymbol{\nabla}_{\mathbf{r}_i}\int\mathrm{d}\mathbf{r}'\,\frac{\mathrm{d}\mathbf{u}'}{\Omega_d}g^{(n+1)}(\mathbf{r}_1,\mathbf{u}_1;\dots;\mathbf{r}_n,\mathbf{u}_n;\mathbf{r}',\mathbf{u}')\boldsymbol{\nabla}_{\mathbf{r}_i}U(\mathbf{r}_i-\mathbf{r}')=0\,.\end{aligned} \tag{3.12}$$

The above equation displays a term like

$$\rho\int\mathrm{d}\mathbf{r}'\,\frac{\mathrm{d}\mathbf{u}'}{\Omega_d}\frac{g^{(n+1)}(\mathbf{r}_1,\mathbf{u}_1;\dots;\mathbf{r}_n,\mathbf{u}_n;\mathbf{r}',\mathbf{u}')}{g^{(n)}(\mathbf{r}_1,\mathbf{u}_1;\dots;\mathbf{r}_n,\mathbf{u}_n)}\boldsymbol{\nabla}_{\mathbf{r}_i}U(\mathbf{r}_i-\mathbf{r}')\,, \tag{3.13}$$

which is the mean force exerted by all the $N-1-n$ other particles on the particle sitting at $\mathbf{r}_i$ with orientation $\mathbf{u}_i$ conditioned on the presence of the n particles at positions $\mathbf{r}_k$ with orientations $\mathbf{u}_k$. In a standard equilibrium fluid, most of the thermodynamic properties, as the equation of state for the pressure, can be inferred from the two-point distribution function. In an active fluid, the knowledge of $g^{(2)}(\mathbf{r}_1,\mathbf{u}_1;\mathbf{r}_2,\mathbf{u}_2)$ also allows to compute relevant thermodynamic observables and to get insights into the phase behavior of the system, with however some restrictions compared to the equilibrium case as we explain next. Given its crucial role, and in order to lighten the notations, the two-point distribution function will simply be called $g(\mathbf{r}_1,\mathbf{u}_1;\mathbf{r}_2,\mathbf{u}_2)$ in the following. Throughout this discussion, we will restrict ourselves to the case of run-and-tumble particles even though similar statements can be made for the other models of ABPs and AOUPs.

3.1.2 The effective self-propulsion:

The effective self-propulsion is probably the most natural observable to consider in a system made of self-propelled particles interacting via pair-wise forces [55]. The speed (or mean

quadratic speed in the case of AOUPs) of a free particle is given by v_0. In the presence of other particles, the speed is expected to be reduced by collisions. This leads to defining a density dependent speed $v(\rho)$ as the norm of the mean (in a homogeneous phase of density ρ) of $\dot{\mathbf{r}}_i$ at fixed $\mathbf{u}_i$. Averaging Eq. (3.1) over all the $N-1$ degrees of freedom attached to particles j for $j \neq i$ yields,

$$\begin{aligned}\langle \dot{\mathbf{r}}_i \rangle_{\mathbf{u}_i} &= v_0 \mathbf{u}_i + \rho \int \mathrm{d}\mathbf{r} \frac{\mathrm{d}\mathbf{u}'}{\Omega_d} g^{(2)}\left(0, \mathbf{u}_i; \mathbf{r}, \mathbf{u}'\right) \boldsymbol{\nabla}_{\mathbf{r}} U(\mathbf{r}) \,, \\ &= \left(v_0 + \rho \int \mathrm{d}\mathbf{r} \frac{\mathrm{d}\mathbf{u}'}{\Omega_d} g^{(2)}\left(0, \mathbf{u}_i; \mathbf{r}, \mathbf{u}'\right) \boldsymbol{\nabla}_{\mathbf{r}} U(\mathbf{r}) \cdot \mathbf{u}_i \right) \mathbf{u}_i \,, \\ &= v(\rho) \mathbf{u}_i \,,\end{aligned} \tag{3.14}$$

where we have used the translational and rotational invariance of $g^{(2)}$ within homogeneous phases and with the density dependent speed,

$$v(\rho) = \left(v_0 + \rho \int \mathrm{d}\mathbf{r} \frac{\mathrm{d}\mathbf{u}'}{\Omega_d} g^{(2)}\left(\mathbf{0}, \mathbf{u}_i; \mathbf{r}, \mathbf{u}'\right) \boldsymbol{\nabla}_{\mathbf{r}} U(\mathbf{r}) \cdot \mathbf{u}_i \right) . \tag{3.15}$$

In numerical simulations of ABPs interacting via a strongly repulsive WCA potential, the effective velocity has been found, both in 2 and 3 dimensions, to decay linearly with ρ over a wide range of densities until a given near close-packing density after which it roughly vanishes. This was reported in [193, 196]. A finer description of the decay of $v(\rho)$ in the dense regime can be found in the appendix of [192]. Deviations from this linear decay at moderate densities have been reported in simulations with softer potentials, such as for harmonic disks in [55].

3.1.3 The mechanical pressure:

Another interesting macroscopic quantity that can be derived from the two-point distribution function is the mechanical pressure defined as the mean normal stress exerted by an active fluid on the wall of a container. For some time, pressure remained an elusive quantity in active matter. Indeed, in many active matter systems, the mechanical pressure is not a state function: it does not depend solely on the bulk properties of the system but also depends on the details of the interaction with the wall. This is the case, for instance, in systems of particles interacting via quorum-sensing or in systems made of elongated particles [194]. However, it can be shown that the process in Eq. (3.1) (supplemented with an interaction with an external potential to mimic the confining wall) admits and equation of state for the mechanical pressure [193]. For the RTP model, the latter reads

$$P(\rho) = \rho \frac{v_0 v(\rho) \tau}{d} - \frac{\rho^2}{2d} \int \mathrm{d}\mathbf{r} \frac{\mathrm{d}\mathbf{u}_1}{\Omega_d} \frac{\mathrm{d}\mathbf{u}_2}{\Omega_d} g^{(2)}(\mathbf{0}, \mathbf{u}_1; \mathbf{r}, \mathbf{u}_2)\, \mathbf{r} \cdot \boldsymbol{\nabla}_{\mathbf{r}} U(\mathbf{r}) \,. \tag{3.16}$$

This is reminiscent of the equation of state for the pressure in an equilibrium system at temperature T with Hamiltonian

$$H = \sum_{i \neq j} U(\mathbf{r}_i - \mathbf{r}_j) \,, \tag{3.17}$$

for which the pressure in a homogeneous phase writes

$$P(\rho) = \rho T - \frac{\rho^2}{2d} \int \mathrm{d}\mathbf{r}\, g^{(2)}(\mathbf{0}\,;\mathbf{r})\, \mathbf{r} \cdot \boldsymbol{\nabla}_{\mathbf{r}} U(\mathbf{r})\,. \tag{3.18}$$

The main qualitative difference between Eq. (3.16) and Eq. (3.18) is that in equilibrium the first term reads ρ times the diffusion constant of a free particle while in the active case the free diffusion constant $v_0^2\tau/d$ is replaced by $v_0 v(\rho)\tau/d$. This modification is however of great relevance. Indeed, the decay of $v(\rho)$ with the density tends to decrease the pressure as attractive interactions in equilibrium would do. There actually exist quite deep similarities between the pressure of active fluids in Eq. (3.16) and the pressure of passive ones in Eq. (3.18). First, and this is a direct consequence of the existence of an equation of state, in a phase separated fluid the coexistence pressures must be equal [193]. Second, the relaxation of the local density field in position space

$$\phi(\mathbf{r}, t) = \int \frac{\mathrm{d}\mathbf{u}}{\Omega_d} \rho(\mathbf{r}, \mathbf{u}, t)\,, \tag{3.19}$$

is given [192] to leading order in the gradient expansion, by

$$\partial_t \phi(\mathbf{r}, t) = \boldsymbol{\nabla}^2 P\left(\phi(\mathbf{r}, t)\right)\,, \tag{3.20}$$

where the function P is the same as in Eq. (3.16). Thus, as in standard equilibrium physics, the spinodal region, which corresponds to the region of linear instability of homogeneous phases, is also the region of negative compressibility $P'(\rho) < 0$. In [193], ABPs interacting via a WCA potential were numerically shown to display a region of negative compressibility. However, the resemblance with the equilibrium pressure does not extend any further. In particular, it is not possible to use an equal-area law à la Maxwell on the equation of state for the pressure to predict the binodals of the MIPS region [193]. The equation of state for the pressure does not contain all the information needed to predict the phase diagram of active systems but it only provides one equation that the coexisting densities must satisfy. We do not know yet of any observable that could be measured in a homogeneous phase and that would yield the second constraint.

3.1.4 Low density thermodynamics in the ballistic regime

In this section, we explicitly derive the first density corrections to the ideal gas effective velocity

$$v(\rho) = v_0\,, \tag{3.21}$$

and ideal gas pressure

$$P = \rho \frac{v_0^2 \tau}{d}\,, \tag{3.22}$$

for d-dimensional run-and-tumble particles in the ballistic limit $v_0\tau \gg \sigma$. This regime, that is the only one we could obtain analytical predictions for in the one-particle against a hard spherical obstacle case in Sec. 2.3, has however its own share of interesting features given that it is the locus of the MIPS. For instance, in [162], the MIPS critical point of a system of

3 dimensional active Brownian hard spheres was found to lie at a ratio $v_0\tau/\sigma \simeq 18.8$, with σ the diameter of a sphere. The low density behavior of the system can be extracted from the 0^{th} order of the virial expansion of $g(\mathbf{0}, \mathbf{u}_1; \mathbf{r}, \mathbf{u}_2)$ given as the solution of

$$-\frac{v_0}{2}\left(\mathbf{u}_2-\mathbf{u}_1\right)\cdot\boldsymbol{\nabla}_{\mathbf{r}}g+\boldsymbol{\nabla}_{\mathbf{r}}\left(g\boldsymbol{\nabla}_{\mathbf{r}}U(\mathbf{r})\right)+\frac{1}{2}\left(\mathcal{R}_1 g+\mathcal{R}_2 g\right)=0\,. \tag{3.23}$$

Denoting $\hat{\mathbf{u}}_{12}=\left(\mathbf{u}_2-\mathbf{u}_1\right)/\left|\mathbf{u}_1-\mathbf{u}_2\right|$, the solution of Eq. (3.23) in the ballistic limit is that of Eq. (2.84) in the same limit under the substitution $v_0 \to v_0\left|\mathbf{u}_1-\mathbf{u}_2\right|/2$, *i.e*

$$g(\mathbf{0}, \mathbf{u}_1; \mathbf{r}, \mathbf{u}_2) = P(\mathbf{r}, \hat{\mathbf{u}}_{12})\big|_{v_0\to v_0|\mathbf{u}_1-\mathbf{u}_2|/2}\,. \tag{3.24}$$

From Eq. (2.165) of Sec.2.3, we therefore obtain in the dilute limit

$$\begin{aligned} g(\mathbf{0}, \mathbf{u}_1; \mathbf{r}, \mathbf{u}_2) = \frac{1}{d-1}\delta\left(z-1\right)\Theta\left(-w\right)+\Bigg[\Theta\left(-w\right)+\Theta\left(w\right)\Big(\Theta\left(z\sqrt{1-w^2}-1\right)\\ +\frac{1}{d-1}\delta\left(z\sqrt{1-w^2}-1\right)\Big)\Bigg]\Theta(z-1)\,, \end{aligned} \tag{3.25}$$

with $z=r/\sigma$ and $w=\hat{\mathbf{r}}\cdot\hat{\mathbf{u}}_{12}$. Equation (2.93) furthermore yields

$$\lim_{\text{hard sphere}} g(\mathbf{0}, \mathbf{u}_1; \mathbf{r}, \mathbf{u}_2)U'(r) = \frac{v_0\left|\mathbf{u}_1-\mathbf{u}_2\right|}{2}\frac{w}{d-1}\Theta(-w)\delta(z-1)\,. \tag{3.26}$$

Radial distribution function The radial distribution function $g(\mathbf{r})$ is found upon integrating the two-point distribution one $g(\mathbf{0}, \mathbf{u}_1; \mathbf{r}, \mathbf{u}_2)$ over $\mathbf{u}_1$ and $\mathbf{u}_2$. Using Eq. (3.25), we therefore obtain

$$\begin{aligned} g(z) = \int_{-1}^{1}\mathrm{d}w\, m(w)\Bigg\{\frac{1}{d-1}\delta\left(z-1\right)\Theta\left(-w\right)+\Bigg[\Theta\left(-w\right)+\Theta\left(w\right)\Big(\Theta\left(z\sqrt{1-w^2}-1\right)\\ +\frac{1}{d-1}\delta\left(z\sqrt{1-w^2}-1\right)\Big)\Bigg]\Theta(z-1)\Bigg\}, \end{aligned} \tag{3.27}$$

with the Jacobian $m(w)$,

$$\begin{aligned} m(w) &= \int\frac{\mathrm{d}\mathbf{u}_1}{\Omega_d}\frac{\mathrm{d}\mathbf{u}_2}{\Omega_d}\delta\left(w-\hat{\mathbf{u}}_{12}\cdot\hat{\mathbf{r}}\right)\,,\\ &= \int\frac{\mathrm{d}\hat{\mathbf{r}}}{\Omega_d}\int\frac{\mathrm{d}\mathbf{u}_1}{\Omega_d}\frac{\mathrm{d}\mathbf{u}_2}{\Omega_d}\delta\left(w-\hat{\mathbf{u}}_{12}\cdot\hat{\mathbf{r}}\right)\\ &= \int_{-1}^{1}\frac{\mathrm{d}w'}{2W_{d-2}}\left(1-w'^2\right)^{\frac{d-3}{2}}\delta(w'-w)\,,\\ &= \frac{1}{2W_{d-2}}\left(1-w\right)^{\frac{d-3}{2}}\,. \end{aligned} \tag{3.28}$$

The low density radial distribution function thus reads,

$$g(z) = \frac{\delta(z-1)}{2(d-1)} + \Theta(z-1)\left[\frac{1}{2} + \int_0^{\frac{\sqrt{z^2-1}}{z}} \frac{\mathrm{d}w}{2W_{d-2}}\left(1-w^2\right)^{\frac{d-3}{2}} + \frac{1}{2W_{d-2}(d-1)}\frac{z^{2-d}}{\sqrt{z^2-1}}\right] . \tag{3.29}$$

Specializing the result in physical dimensions yields

$$g(z) = \frac{\delta(z-1)}{2} + \Theta(z-1)\left[\frac{1}{2} + \frac{1}{\pi}\arcsin\left(\frac{\sqrt{z^2-1}}{z}\right) + \frac{1}{\pi\sqrt{z^2-1}}\right] , \tag{3.30}$$

in two dimensions and

$$g(z) = \frac{\delta(z-1)}{4} + \Theta(z-1)\left[\frac{1}{2} + \frac{\sqrt{z^2-1}}{2z} + \frac{1}{4z\sqrt{z^2-1}}\right] , \tag{3.31}$$

in three dimensions. Note that in any dimension the radial distribution function is the sum of a delta peak accumulation at contact and a bulk term at $z > 1$. The bulk value of the distribution function is monotonically decreasing and has a square root divergence at $z = 1$. Effectively, in the stationary state, there is a strong attraction between the particles. We next specify the result in the case $d \gg 1$ that will be in the end our main focus. Introducing

$$h = d\,(z-1) , \tag{3.32}$$

the scale over which the radial distribution decays, the latter takes takes the form

$$g(h) = \frac{\delta(h)}{2} + \Theta(h)\left[\frac{1}{2}\left(1 + \mathrm{erf}\left(\sqrt{h}\right)\right) + \frac{\mathrm{e}^{-h}}{\sqrt{4\pi h}}\right] . \tag{3.33}$$

The effective self-propulsion We now compute the small density corrections to the effective self-propulsion of run-and-tumble hard spheres. Using Eq.(3.26), the formula for the effective self-propulsion Eq. (3.15) reduces to,

$$v(\rho) = v_0\left[1 + \frac{\rho\sigma^d}{2(d-1)}\int \mathrm{d}\hat{\mathbf{r}}\frac{\mathrm{d}\mathbf{u}_2}{\Omega_d}\left(\hat{\mathbf{r}}\cdot\mathbf{u}_1\right)\left|\mathbf{u}_2-\mathbf{u}_1\right|\left(\hat{\mathbf{r}}\cdot\hat{\mathbf{u}}_{12}\right)\Theta\left(-\hat{\mathbf{r}}\cdot\hat{\mathbf{u}}_{12}\right)\right] . \tag{3.34}$$

The above integral can be computed as follows,

$$\begin{aligned}
&\int \mathrm{d}\hat{\mathbf{r}}\frac{\mathrm{d}\mathbf{u}_2}{\Omega_d}\left(\hat{\mathbf{r}}\cdot\mathbf{u}_1\right)\left|\mathbf{u}_2-\mathbf{u}_1\right|\left(\hat{\mathbf{r}}\cdot\hat{\mathbf{u}}_{12}\right)\Theta\left(-\left(\hat{\mathbf{r}}\cdot\hat{\mathbf{u}}_{12}\right)\right)\\
&= \int \frac{\mathrm{d}\mathbf{u}_2}{\Omega_d}\left|\mathbf{u}_2-\mathbf{u}_1\right|\left(\int \mathrm{d}\hat{\mathbf{r}}\ \left(\hat{\mathbf{r}}\cdot\hat{\mathbf{u}}_{12}\right)\Theta\left(-\hat{\mathbf{r}}\cdot\hat{\mathbf{u}}_{12}\right)\hat{\mathbf{r}}\right)\cdot\mathbf{u}_1\\
&= \int \frac{\mathrm{d}\mathbf{u}_2}{\Omega_d}\left|\mathbf{u}_2-\mathbf{u}_1\right|\left(\int \mathrm{d}\hat{\mathbf{r}}\ \left(\hat{\mathbf{r}}\cdot\hat{\mathbf{u}}_{12}\right)^2\Theta\left(-\hat{\mathbf{r}}\cdot\hat{\mathbf{u}}_{12}\right)\right)\mathbf{u}_1\cdot\hat{\mathbf{u}}_{12}\\
&= -\frac{\Omega_d}{2d} .
\end{aligned} \tag{3.35}$$

Thus the effective self-propulsion is given by,

$$v(\rho) = v_0\left(1 - \frac{\rho\mathcal{V}_d(\sigma)}{4(d-1)}\right) , \tag{3.36}$$

with $V_d(\sigma)$ the volume of a sphere of radius σ thus making explicit the decrease of the self-propulsion due to collisions. In terms of the packing fraction

$$\varphi = \rho \mathcal{V}_d \left(\frac{\sigma}{2}\right) , \tag{3.37}$$

the result reads, both in 2 and 3 dimensions, as

$$v(\varphi) = v_0 \left(1 - \varphi\right) . \tag{3.38}$$

It is very interesting to note that in numerical simulations of ABPs interacting via a WCA potential, the linear decay of the effective self-propulsion extends beyond the small φ regime. Furthermore, as $d \to \infty$, it appears natural from Eq. (3.36) to work in density regimes in which

$$\frac{\rho \mathcal{V}_d(\sigma)}{d} = \frac{2^d \varphi}{d} = \widehat{\varphi} , \tag{3.39}$$

is held fixed. As we will see in our study of infinite dimensional fluids, starting in Sec. 3.2, this is indeed the correct infinite dimensional density scaling. As a function of $\widehat{\varphi}$, the effective self-propulsion thus writes in large dimension

$$v(\widehat{\varphi}) = v_0 \left(1 - \frac{\widehat{\varphi}}{4}\right) . \tag{3.40}$$

The mechanical pressure We compute the ρ^2 term of the density expansion of the mechanical pressure of run-and-tumble hard spheres. From Eqs. (3.16) and (3.26), computing the latter reduces to evaluating,

$$\begin{aligned} &\int \mathrm{d}\hat{\mathbf{r}} \frac{\mathrm{d}\mathbf{u}_1 \mathrm{d}\mathbf{u}_2}{\Omega_d^2} \left|\mathbf{u}_1 - \mathbf{u}_2\right| \left(\hat{\mathbf{r}} \cdot \hat{\mathbf{u}}_{12}\right) \Theta\left(-\hat{\mathbf{r}} \cdot \hat{\mathbf{u}}_{12}\right) \\ &= \left[\int \frac{\mathrm{d}\mathbf{u}_1 \mathrm{d}\mathbf{u}_2}{\Omega_d^2} \sqrt{1 - \mathbf{u}_1 \cdot \mathbf{u}_2}\right] \int_{-1}^{0} \frac{\mathrm{d}w}{2W_{d-2}} w \left(1 - w^2\right)^{\frac{d-3}{2}} , \\ &= - \frac{\sqrt{2} A_d \Omega_d}{2W_{d-2}(d-1)} , \end{aligned} \tag{3.41}$$

with

$$\begin{aligned} A_d &= \int \frac{\mathrm{d}\mathbf{u}_1 \mathrm{d}\mathbf{u}_2}{\Omega_d^2} \sqrt{1 - \mathbf{u}_1 \cdot \mathbf{u}_2} , \\ &= \int_{-1}^{1} \frac{\mathrm{d}w}{2W_{d-2}} \left(1 - w^2\right)^{\frac{d-3}{2}} \sqrt{1 - w} . \end{aligned} \tag{3.42}$$

While a general formula for A_d can be found in terms of hypergeometric functions, here we display only its value in some particular dimensions,

$$A_d = \begin{cases} \frac{2\sqrt{2}}{\pi} & \text{if} \quad d = 2 , \\ \frac{2\sqrt{2}}{3} & \text{if} \quad d = 3 , \\ 1 & \text{if} \quad d \to \infty . \end{cases} \tag{3.43}$$

We thus obtain the equation of state for the pressure as

$$P = \rho \frac{v_0^2 \tau}{d} \left(1 - \frac{\rho \mathcal{V}_d(\sigma)}{4(d-1)} \right) + \frac{\rho^2 \mathcal{V}_d(\sigma)}{2(d-1)} \frac{v_0 \sigma A_d}{\sqrt{2}(d-1) 2 W_{d-2}} \,. \tag{3.44}$$

Therefore, the equilibrium like-term in the equation of state gives a positive contribution to the second coefficient of the virial expansion, which is natural for repulsive potentials, while the $v(\rho)$ term gives a negative contribution, thus accounting for the effective attraction between the particles. The positivity of the second virial coefficient directly depends on the value of the Peclet number $\mathrm{Pe} = v_0 \tau / \sigma$: it is positive at small Pe, *i.e.* at low activity, and negative at high Pe. Expressed in terms of the packing fraction φ, it reads in physical dimensions,

$$\frac{P}{\rho} = \frac{v_0^2 \tau}{2} + \frac{\varphi v_0 \sigma}{\pi^2} \left(1 - \frac{\pi^2}{8} Pe \right) \tag{3.45}$$

in $d = 2$ and,

$$\frac{P}{\rho} = \frac{v_0^2 \tau}{3} + \frac{\varphi v_0 \sigma}{3} \left(1 - Pe \right) \,, \tag{3.46}$$

in $d = 3$. The critical Pe one could try to estimate from the change of sign in the second virial coefficient in Eqs. (3.45) and (3.45) are around 1 and are therefore much lower than the actual critical Peclet number observed in numerical simulations. Thus, if it describes quite correctly the actual $v(\rho)$ part of the equation of state, at least for hard potentials, the low density estimates tend to significantly underestimate the amplitude of the (repulsive) equilibrium-like term of the equation of state. Lastly, at large d, and using the density scaling of Eq. (3.39), the equation of state writes

$$\frac{P}{\rho} = \frac{v_0}{\sqrt{d}} \left(\frac{v_0 \tau}{\sqrt{d}} \left(1 - \frac{\widehat{\varphi}}{4} \right) + \frac{\widehat{\varphi}}{4} \frac{\sigma}{\sqrt{\pi}} \right) \,. \tag{3.47}$$

The above equation thus suggests that the proper infinite-dimensional scalings of the model parameters so as to maintain a competition between activity and repulsive pairwise interactions leading to a complex spatial organization keep the ratio $v_0 \tau / \sqrt{d}$ fixed.

3.2 The Mayer expansion of standard equilibrium fluids and the infinite dimensional limit

3.2.1 Mayer expansion of the grand canonical potential

The Mayer expansion is a standard tool of liquid theory. Many good and thorough reviews [92, 158, 135] on the subject can be found in the literature. The present section contains no original material but instead it intends to present the key ideas of the Mayer expansion with a particular emphasis on the role of the infinite dimensional limit. Let us start by considering an equilibrium system at temperature $T = \beta^{-1}$ in a box of volume V made of interacting particles with Hamiltonian

$$H(\mathbf{r}_i) = \sum_i V(\mathbf{r}_i) + \sum_{i<j} U(\mathbf{r}_i - \mathbf{r}_j) \,, \tag{3.48}$$

where the Hamiltonian comprises an external potential V and a pairwise interaction potential U. For the sake of lightness, the momenta degrees of freedom are forgotten throughout this presentation. The system is studied in the grand-canonical ensemble with chemical potential μ for which the grand-canonical partition function writes

$$\Xi = \sum_{N=0}^{+\infty} \frac{1}{N!} \int \prod_{i=1}^{n} \mathrm{d}\mathbf{r}_i \prod_{i=1}^{N} \mathrm{e}^{\beta\mu - \beta V(\mathbf{r}_i)} \prod_{i<j}^{N} \mathrm{e}^{-\beta U(\mathbf{r}_i - \mathbf{r}_j)} \,. \tag{3.49}$$

Hereafter, we interpret the latter as a functional of the generalized chemical potential

$$\mu(\mathbf{r}_i) = \beta\mu - \beta V(\mathbf{r}_i) \,, \tag{3.50}$$

and we introduce the Mayer function

$$f(\mathbf{r}_i, \mathbf{r}_j) = -1 + \mathrm{e}^{-\beta U(\mathbf{r}_i - \mathbf{r}_j)} \,, \tag{3.51}$$

so that the grand-canonical partition functional writes

$$\Xi[\mu] = \sum_{N=0}^{+\infty} \frac{1}{N!} \int \prod_{i=1}^{N} \mathrm{d}\mathbf{r}_i \prod_{i=1}^{N} \mathrm{e}^{\mu(\mathbf{r}_i)} \prod_{i<j}^{N} \left(1 + f(\mathbf{r}_i, \mathbf{r}_j)\right) \,. \tag{3.52}$$

The idea of the Mayer expansion is to expand the product over the (i, j) pairs. Thus, its very core rests on the pair-structure of the stationary distribution. This is important given that, while this structure is very natural in standard equilibrium fluids, it is expected not to hold in active ones (see for instance the small τ expansion in [60]). This will be discussed more in depth in Sec. 4.2 and Sec. 4.3. The resulting series is better captured by a diagrammatic expansion [148],

$$\Xi[\mu] = \sum_{N=0}^{+\infty} \frac{1}{N!} \sum_{G \in \mathcal{U}_N} \Gamma(G) \,, \tag{3.53}$$

where $\mathcal{U}_N$ is the ensemble of labeled graphs with N vertices and $\Gamma(G)$ is the corresponding amplitude of such a graph. The latter is computed as follows,

$$\Gamma(G) = \int \prod_{i=1}^{N_G} \left[\mathrm{d}\mathbf{r}_i \, \mathrm{e}^{\mu(\mathbf{r}_i)}\right] \prod_{(i,j) \in E(G)} f(\mathbf{r}_i, \mathbf{r}_j) \,, \tag{3.54}$$

with N_G the number of vertices of G and $E(G)$ its set of edges. The set of vertices of G is called $V(G)$. Thus, each vertex i of G corresponds to a $\mathrm{e}^{\mu(\mathbf{r}_i)}$ term and each edge, say between vertices i and j, corresponds to $f(\mathbf{r}_i, \mathbf{r}_j)$. The $N = 1$ contribution is trivial and is represented by a graph with a single vertex

$$= \int \mathrm{d}\mathbf{r} \, \mathrm{e}^{\mu(\mathbf{r})} \,. \tag{3.55}$$

The $N = 2$ term is made of two two-vertex graphs,

$$= \int \mathrm{d}\mathbf{r}_1 \mathrm{d}\mathbf{r}_2 \, \mathrm{e}^{\mu(\mathbf{r}_1)} \mathrm{e}^{\mu(\mathbf{r}_1)} + \int \mathrm{d}\mathbf{r}_1 \mathrm{d}\mathbf{r}_2 \, \mathrm{e}^{\mu(\mathbf{r}_1)} \mathrm{e}^{\mu(\mathbf{r}_1)} f(\mathbf{r}_1, \mathbf{r}_2) \,, \tag{3.56}$$

and the $N = 3$ contribution already contains 8 three-vertex ones,

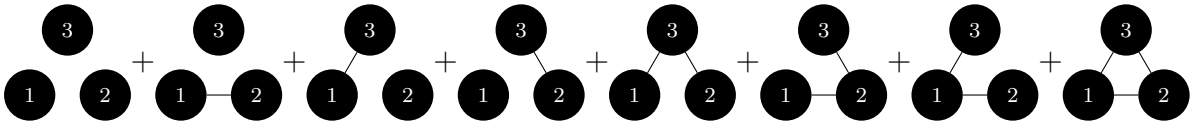

(3.57)

Two graphs are said to be isomorphic if they are the same up to a permutation of the vertices labels: they hence correspond to the same unlabeled graph. Two isomorphic graphs have equal amplitude. Such graphs can therefore be grouped together and the series in Eq. (3.53) can be rewritten as a sum over unlabeled graphs,

$$\Xi[\mu] = \sum_{N=0}^{+\infty} \sum_{g \in \mathcal{V}_N} A(g)\,, \tag{3.58}$$

where $\mathcal{V}_N$ is the set of unlabeled graphs with N vertices and the graph amplitude $A(g)$ is given as

$$A(g) = \frac{1}{S_g}\Gamma(G)\,, \tag{3.59}$$

where G is any labeling of g (we will keep this notation in the following) and S_g its symmetry factor. The latter is defined as the number of permutations of the vertex labels of any labeling G of g that leave the graph invariant, *i.e.* that preserves the set of vertices and edges. Indeed, one has from Eq. (3.53),

$$A(g) = \frac{n_g}{N!}\Gamma(G)\,, \tag{3.60}$$

with n_g the number of topologically inequivalent (*i.e.* with a different set of edges) labeling of g, thus yielding Eq. (3.59). The series in Eq. (3.58) thus writes as,

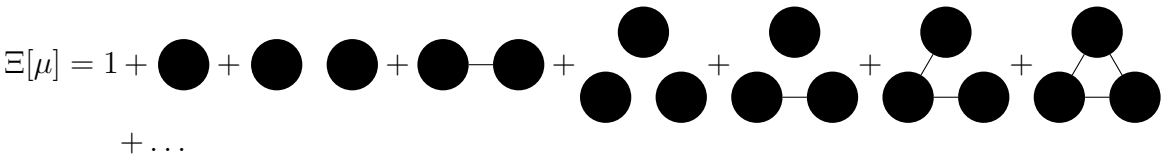

(3.61)

A huge number of such diagrams can be further simplified by considering the logarithm of the functional $\Xi[\mu]$ that, as is common in statistical and quantum field theory [215], suppresses the disconnected diagrams in an instance of the linked-cluster theorem. Let $\mathcal{C}$ be the set of connected diagrams and denote its elements by $\mathcal{C}_q$ for $q \in \mathbb{N}$. Any disconnected diagram g can then be parametrized by the number of times n_q each diagram $\mathcal{C}_q$ in $\mathcal{C}$ appears in g. The symmetry factor S_g can then be expressed as

$$\prod_{q=1}^{+\infty} n_q!\, S_{\mathcal{C}_q}^{n_q}\,, \tag{3.62}$$

where the first term in the product accounts for permutations of the indices between the different instances of $\mathcal{C}_q$ and the second for the ones within single instances. Thus,

$$\begin{aligned} A(g) &= \prod_{q=1}^{+\infty} \frac{\Gamma(\mathcal{C}_q)^{n_q}}{n_q!\, S_{\mathcal{C}_q}^{n_q}}\,, \\ &= \prod_{q=1}^{+\infty} \frac{A(\mathcal{C}_q)^{n_q}}{n_q!}\,. \end{aligned} \tag{3.63}$$

and so the functional $\Xi[\mu]$ writes

$$\begin{aligned} \Xi[\mu] &= \sum_{n_1=0}^{+\infty}\sum_{n_2=0}^{+\infty}\cdots\sum_{n_q=0}^{+\infty}\prod_{q=1}^{+\infty}\frac{A(\mathcal{C}_q)^{n_q}}{n_q!} \\ &= \exp\left(\sum_{q=1}^{+\infty} A(\mathcal{C}_q)\right) = \mathrm{e}^{W[\mu]}\,, \end{aligned} \tag{3.64}$$

where the grand canonical potential $W[\mu]$ is defined as the sum over the connected diagrams,

$W[\mu] =$ 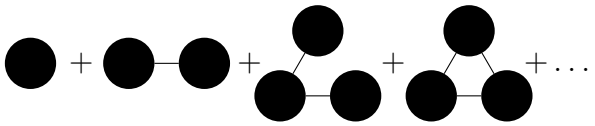 $+\ldots$ (3.65)

3.2.2 The free energy functional

Taking the functional derivative of the grand canonical potential $W[\mu]$ yields the mean density field,

$$\frac{\delta W[\mu]}{\delta\mu(\mathbf{r})} = \left\langle \sum_{i=1}^{N} \delta(\mathbf{r}-\mathbf{r}_i) \right\rangle = \rho(\mathbf{r})\,, \tag{3.66}$$

where the average is taken with respect to the grand-canonical measure in Eq. (3.49). We thus define the free energy functional $F[\rho]$ as the Legendre transform of $W[\mu]$,

$$\beta F[\rho] = \sup_{\mu}\left(-W[\mu] + \int \mathrm{d}\mathbf{r}\rho(\mathbf{r})\mu(\mathbf{r})\right)\,. \tag{3.67}$$

The grand canonical potential $W[\mu]$ being a convex functional of $\mu(\mathbf{r})$ [83], the supremum is unique and is reached at $\mu^*[\rho]$ defined such that

$$\rho(\mathbf{r}) = \left.\frac{\delta W[\mu]}{\delta\mu(\mathbf{r})}\right|_{\mu^*[\rho]}\,, \tag{3.68}$$

i.e. at the appropriate generalized chemical potential $\mu(\mathbf{r})$ such that the grand canonical measure yields $\rho(\mathbf{r})$ as a mean density field. Hence, we have

$$\beta F[\rho] = -W[\mu^*[\rho]] + \int \mathrm{d}\mathbf{r}\rho(\mathbf{r})\mu^*[\rho](\mathbf{r})\,, \tag{3.69}$$

and accordingly

$$\beta \frac{\delta F[\rho]}{\delta \rho(\mathbf{r})} = \mu^*[\rho](\mathbf{r}) \,. \tag{3.70}$$

Let us finally introduce, for some function $\mu(\mathbf{r})$, the functional $G[\rho]$ defined as,

$$G[\rho] = F[\rho] - T \int \mathrm{d}\mathbf{r} \rho(\mathbf{r}) \mu(\mathbf{r}) \,. \tag{3.71}$$

From Eq. (3.70) and from the convexity of G, it appears that G is minimal at the mean density field corresponding to the chemical potential $\mu(\mathbf{r})$.

3.2.3 Graph expansion of the free energy functional

Taking the Legendre transform of Eq. (3.65) suppresses the diagrams that are not 1-particle irreducible, *i.e.* the diagrams that can be disconnected upon the removal of a vertex (if it exists such a vertex is called an articulation one). As we will prove next, the free energy functional indeed writes

$-\beta F[\rho] = \int \mathrm{d}\mathbf{r} \rho(\mathbf{r}) \left(1 - \ln \rho(\mathbf{r})\right) +$ 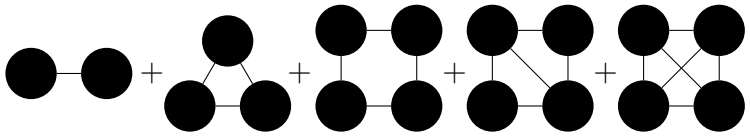 $+ \ldots$

(3.72)

where the dots stand for the summation over all the remaining 1-particle irreducible diagrams and where the vertices are understood as $\rho(\mathbf{r})$ vertices and not $\mathrm{e}^{\mu(\mathbf{r})}$ ones anymore as in Eq. (3.65). The proof of this identity goes as follows. First, we differentiate Eq. (3.65) to get an expansion of $\rho(\mathbf{r})$ as a function of $\mu(\mathbf{r})$,

$\rho(\mathbf{r})\mathrm{e}^{-\mu(\mathbf{r})} = 1 +$ 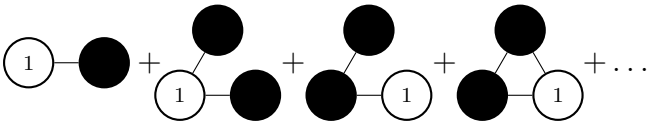 $+ \ldots$

(3.73)

The white vertex sits at position $\mathbf{r}$. It is not integrated upon and its value is fixed to one. The dots stand for a summation over all the remaining connected diagrams with a white unit-valued vertex. In computing the amplitude of a graph in Eq. (3.73), the symmetry factor is that of the black vertices only. The combinatorics indeed work out nicely [92] as we show now. We have indeed,

$$\begin{aligned} \rho(\mathbf{r}) &= \frac{\delta}{\delta \mu(\mathbf{r})} \left(\sum_{g \in \mathcal{C}} \frac{1}{S_g} \Gamma(G) \right) \,, \\ &= \sum_{g \in \mathcal{C}} \frac{1}{S_g} \mathrm{e}^{\mu(\mathbf{r})} \sum_{i \in V(G)} \Gamma\left(G_i\right) \,, \end{aligned} \tag{3.74}$$

where G_i is the labeled graph extracted from G by replacing vertex i by a unit-valued white vertex. Different G_i (for different i) can have the same amplitude and the series can

be rearranged as a sum over the unlabeled connected diagrams with a white unit-valued vertex (which form the set called $\mathcal{C}_w$),

$$\rho(\mathbf{r})\mathrm{e}^{-\mu(\mathbf{r})} = \sum_{g\in\mathcal{C}_w} \frac{n_g}{S_{\tilde{g}}}\,\Gamma\left(G\right)\,, \tag{3.75}$$

where $\tilde{g}$ is the graph obtained from g by blackening the white vertex and n_g is the number of vertices i of $\tilde{G}$ such that $\Gamma(G) = \Gamma(\tilde{G}_i)$. Let i_1 be such a vertex. As $\Gamma(\tilde{G}_{i_1}) = \Gamma(\tilde{G}_j)$ iff there exists a permutation of the vertices of $\tilde{G}_{i_1}$ that brings $\tilde{G}_{i_1}$ to $\tilde{G}_j$, we obtain

$$n_g = \mathrm{card}\left\{j\in[\![1,n_V]\!] \text{ s.t. } \exists \text{ an invariant permutation of the indices of } \tilde{G} \text{ with } i_1\to j\right\}\,, \tag{3.76}$$

with n_V the number of vertices of G. This exactly reconstructs the symmetry factor S_g of the graph $g\in\mathcal{C}_w$ in Eq. (3.75), thus proving Eq. (3.73). Next, we take the logarithm of Eq. (3.73). The reason that this is so is that if the white vertex is an articulation vertex, then the amplitude of the corresponding (labeled) graph is the product of the amplitude of the (labeled) ones attached to the white vertex. Thus, the linked-cluster theorem applies as in Eq. (3.65) and we obtain

$$-\mu(\mathbf{r}) = -\ln\rho(\mathbf{r}) + \Sigma[\mu]\,. \tag{3.77}$$

where $\Sigma[\mu]$ is the sum over all the diagrams in $\mathcal{C}_w$ where the white vertex is not an articulation one. Now, the goal is to invert Eq. (3.77) so as to express $\mu(\mathbf{r})$ as a functional of $\rho(\mathbf{r})$. Following Eq. (3.70), this relation can then be integrated to yield the free energy functional Eq. (3.72). Inverting the relation in Eq. (3.77) indeed yields ,

$-\mu^*[\rho](\mathbf{r}) = -\ln\rho(\mathbf{r}) +$ 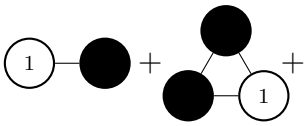 $+\ldots$ (3.78)

where the black vertices are now $\rho(\mathbf{r})$ ones and the sum extends over all the remaining 1-particle irreducible diagrams (thus also excluding those for which a black vertex is an articulation one). This formula can be checked order by order [102] using the Mayer function f as an organizing device for the series in Eq. (3.77). A more systematic derivation of Eq. (3.78) was presented in [158]. We briefly sketch their argument without entering into further details of the combinatorics. Any diagram in $\Sigma[\mu]$ can be uniquely described by a 1-particle irreducible diagram containing the white vertex (precisely its maximally irreducible subdiagram containing it) to the black vertices of which are attached diagrams of $\mathcal{C}_w$ in such a way that the white vertex of these diagrams in $\mathcal{C}_w$ is superimposed to a black one of the 1-particle irreducible one. This is better seen on an example,

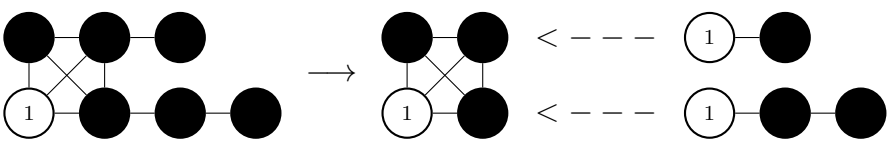 (3.79)

Thus the series in $\Sigma[\mu]$ can be reorganized as a sum over all 1-particle irreducible diagrams for which the vertices $\mathrm{e}^{\mu(\mathbf{r})}$ are replaced by a sum over all the diagrams that can be connected

to the black vertices of the 1-particle irreducible ones, *i.e.* all the diagrams in $\mathcal{C}_w$,

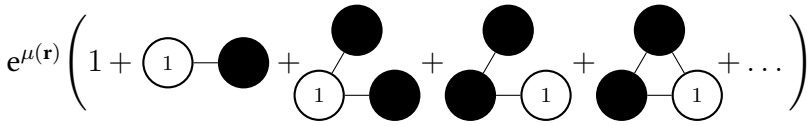

(3.80)

But according to Eq. (3.73), the series between parenthesis in the above equation exactly equals $\rho(\mathbf{r})\mathrm{e}^{-\mu(\mathbf{r})}$. Thus $\Sigma[\mu]$ can be replaced by a sum over 1-particle irreducible diagrams with one white unit-valued vertex and $\rho(\mathbf{r})$ black vertices. This hence proves Eq. (3.78) and from it Eq. (3.72). Once again, the combinatorial aspects of the proof in [158] are quite tedious and were not detailed in the above. As we will see in Sec. 3.2.5, the key aspect in Eq. (3.72) is the absence, apart from the two-vertex one, of tree graphs in the Mayer expansion of the free energy functional.

3.2.4 The Ornstein-Zernike equation

We stress that not only the first derivative of the free energy functional prescribes the mean density field but its second derivative also tells us about the structure of the fluid. This is this relation, known as the Ornstein-Zernike equation [166], that we phrase out in what follows. First, differentiating one more time Eq. (3.70) yields

$$\beta \frac{\delta^2 F[\rho]}{\delta\rho(\mathbf{r})\delta\rho(\mathbf{r}')} = \frac{\delta\mu^*[\rho](\mathbf{r})}{\delta\rho(\mathbf{r}')} \tag{3.81}$$

Furthermore, differentiating Eq. (3.68) we obtain,

$$\int \left.\frac{\delta^2 W[\mu]}{\delta\mu(\mathbf{r})\delta\mu(\mathbf{r}'')}\right|_{\mu^*[\rho]} \frac{\delta\mu^*[\rho](\mathbf{r}'')}{\delta\rho(\mathbf{r}')}\,\mathrm{d}\mathbf{r}'' = \delta(\mathbf{r}-\mathbf{r}')\,. \tag{3.82}$$

As in Sec. 3.1, we introduce the pair-distribution function $g(\mathbf{r},\mathbf{r}')$ and $h(\mathbf{r},\mathbf{r}')$ defined by

$$g(\mathbf{r},\mathbf{r}') = 1 + h(\mathbf{r},\mathbf{r}') \tag{3.83}$$

so that $h(\mathbf{r},\mathbf{r}')$ vanishes as $|\mathbf{r}-\mathbf{r}'| \to \infty$. It can be obtained from the second-derivative of the grand canonical potential $W[\mu]$ with respect to μ,

$$\left.\frac{\delta^2 W[\mu]}{\delta\mu(\mathbf{r})\delta\mu(\mathbf{r}')}\right|_{\mu^*[\rho]} = \rho(\mathbf{r})\rho(\mathbf{r}')h(\mathbf{r},\mathbf{r}') + \rho(\mathbf{r})\delta(\mathbf{r}-\mathbf{r}')\,. \tag{3.84}$$

We then introduce $c^{(2)}(\mathbf{r},\mathbf{r}')$, the direct pair-correlation function defined as the second derivative of $F[\rho]$ with the ideal gas contribution subtracted,

$$-\beta \frac{\delta^2 F[\rho]}{\delta\rho(\mathbf{r})\delta\rho(\mathbf{r}')} = c^{(2)}(\mathbf{r},\mathbf{r}') - \frac{1}{\rho(\mathbf{r})}\delta(\mathbf{r}-\mathbf{r}')\,. \tag{3.85}$$

Inserting Eq. (3.84) and Eq. (3.85) into Eq. (3.82) we ultimately obtain the Ornstein-Zernike equation

$$h(\mathbf{r},\mathbf{r}') = c^{(2)}(\mathbf{r},\mathbf{r}') + \int \mathrm{d}\mathbf{r}''\rho(\mathbf{r}'')h(\mathbf{r},\mathbf{r}'')c^{(2)}(\mathbf{r}',\mathbf{r}'')\,. \tag{3.86}$$

3.2.5 The infinite dimensional limit of the Mayer expansion

A geometrical argument:

In [68], Frisch and collaborators computed exactly the equation of state of infinite dimensional equilibrium hard spheres. This important work paved the way for the high dimensional limit to become instrumental in devising mean field theories of interacting particle systems. The key feature of their work is the understanding that in Eq. (3.65), only tree diagrams contribute to the Mayer expansion in this limit. Indeed, each diagram with a loop is exponentially suppressed as $d \to \infty$. As we explain in more details below, the reason is geometric and can be understood from the following facts. We do not intend to provide a rigorous proof of the results of [68] but rather to give some intuition about the peculiarities of the large d limit. First, consider n uniformly and independently distributed unit vectors $\hat{\mathbf{u}}_i$ for $i \in [\![1, n]\!]$. It is well-known that for any pair $(i \neq j)$, $\hat{\mathbf{u}}_i \cdot \hat{\mathbf{u}}_j = O\left(d^{-1/2}\right)$ in the sense that this scalar product becomes Gaussian distributed in the large d limit,

$$\lim_{d\to\infty} P\left(x = \sqrt{d}\,\hat{\mathbf{u}}_i \cdot \hat{\mathbf{u}}_j\right) = \frac{1}{\sqrt{2\pi}} \mathrm{e}^{-\frac{x^2}{2}} \,. \tag{3.87}$$

with $P(x)$ the probability distribution of x. We are now interested in a rough estimate of the probability that the $\{\hat{\mathbf{u}}_i\}_{i\in[\![1,n]\!]}$ form a "closed loop", *i.e.* that there exists a subset $\mathcal{U}$ of $[\![1, n]\!]$ such that

$$\left| \sum_{i\in\mathcal{U}} \hat{\mathbf{u}}_i \right| < \epsilon \,, \tag{3.88}$$

where ϵ is some fixed constant smaller than 1, as illustrated in Fig. 3.1. The above condition requires that there exists at least a pair $(i \neq j)$ such that $\hat{\mathbf{u}}_i \cdot \hat{\mathbf{u}}_j = O(1)$. But as shown in Eq. (3.87), the probability for this to occur is exponentially suppressed as $d \to \infty$. Thus the probability of observing a "closed loop" decays exponentially to zero as the number of directions in which the $\hat{\mathbf{u}}_i$'s can point increases. To complete the argument, consider

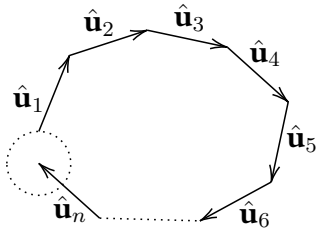

Figure 3.1: A configuration of the $\hat{\mathbf{u}}_i$ displaying a closed loop. The dashed circle has radius less than ϵ.

a graph in the expansion of the free energy functional that contains a loop $\mathbf{r}_1 \to \mathbf{r}_2 \to \mathbf{r}_3 \cdots \to \mathbf{r}_n \to \mathbf{r}_1$ where $\mathbf{r}_i \to \mathbf{r}_j$ simply means that there exists an edge between vertices i and j. For $i \in [\![1, n-1]\!]$ we introduce $\mathbf{u}_i = \mathbf{r}_{i+1} - \mathbf{r}_i$. In the hard sphere case, the presence of an edge constrains the integration volume to

$$u_i \leq \sigma \,, \tag{3.89}$$

whereas the closing loop edge $\mathbf{r}_n \to \mathbf{r}_1$ imposes in a way similar to Eq. (3.88),

$$\left| \sum_{i=1}^{n-1} \mathbf{u}_i \right| \leq \sigma \, . \tag{3.90}$$

Now, in a high dimensional space, all the volume of a ball of finite radius R is concentrated within a shell of thickness $O(1/d)$ around its surface. Then, in an overwhelming fraction of the integration volume, the constraint in Eq. (3.89) becomes

$$u_i \simeq \sigma \, , \tag{3.91}$$

in the sense that $d\,(u_i - \sigma)$ is finite as $d \to \infty$. And we are back to first case of loop-closing with unit vectors that is exponentially unlikely. These ideas are at the basis of the results in [68]. This is confirmed by an explicit computation of the first terms of the Mayer expansion. However, prior to this, we show how to scale appropriately the interaction potential, or equivalently the Mayer function, as well as the density in order to get meaningful results as the dimension increases.

Scalings in the infinite dimensional limit:

In [68], the authors focused on the behavior of classical hard spheres of diameter σ. Their conclusions can nevertheless be generalized beyond the hard sphere case by studying spherically symmetric potentials

$$U\,(\mathbf{r}_i, \mathbf{r}_j) = U\,(\mathbf{r}_i - \mathbf{r}_j) = U\,(|\mathbf{r}_i - \mathbf{r}_j|) \, , \tag{3.92}$$

that scale, together with the temperature, appropriately with the dimension in such a way that [136]

$$\lim_{d\to\infty} \beta U(r) = \widehat{\beta}\widehat{U}(h) \;\text{ with }\; h = \mathrm{d}\,(r/\sigma - 1) \, , \tag{3.93}$$

with both $\widehat{\beta}$ and $\widehat{U}$ finite and $\widehat{U}(-\infty) = +\infty$ and $\widehat{U}(+\infty) = 0$. The considered potentials are thus short-ranged with hard core at $r \simeq \sigma$ and the Mayer function in Eq. (3.51) interpolates between -1 and 0 over a shell of thickness $O(1/d)$ located around $r = \sigma$. This allows the qualitative arguments of Sec. 3.2.5 to hold for a generic rescaled potential $\widehat{U}(h)$. We denote the rescaled Mayer function by

$$\lim_{d\to\infty} f(r) = \widehat{f}(h) = -1 + \mathrm{e}^{-\widehat{\beta}\widehat{U}(h)} \, . \tag{3.94}$$

While the corresponding potential is singular, hard spheres indeed belong to this class given that their Mayer function writes

$$f_{\text{HS}}(r) = -\,\Theta\,(\sigma - r) \Rightarrow \widehat{f}_{\text{HS}}(h) = -\,\Theta(-h) \, . \tag{3.95}$$

This scaling implies that each particle interacts at a given time with roughly $\rho\mathcal{V}_d(\sigma)$ other particles where ρ is the mean local density. Indeed, all the particles another particle can interact with are located in a shell of thickness $O(1/d)$ around σ and the volume of such a

shell is $O\left(\mathcal{V}_d(\sigma)\right)$. This is a peculiarity of large dimensional hyperspheres whose volume is concentrated near their surface. As in [2, 136, 171] we focus on density regimes for which each particles interacts at a given time with $O(d)$ other particles, *i.e.* in a regime where

$$\frac{\rho \mathcal{V}_d(\sigma)}{d} = \widehat{\varphi}\,, \tag{3.96}$$

is held fixed, as already conjectured in Sec. 3.1. This scaling leaves room for nontrivial collective behavior. For example, infinite dimensional equilibrium hard spheres undergo a dynamical glass transition at $\widehat{\varphi} = 4.807$ [136]. Nevertheless, it still allows for considerable simplification of the thermodynamics. The truncation of the free energy functional conjectured in [68] to second order in its density expansion is indeed expected to break down only at much larger densities $\widehat{\varphi} \sim (e/2)^{d/2}$ [67].

First terms of the Mayer expansion in the infinite dimensional limit:

We now explicitly compute the amplitude of the first two graphs of the Mayer expansion of the free energy functional in a homogeneous phase of density $\rho(\mathbf{r}) = \rho$. This will illustrate the exponential suppression of the loop diagrams and the truncation of the free energy. The two-vertex diagram is given by

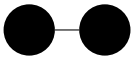

$$\begin{aligned} &= \tfrac{1}{2} \int \mathrm{d}\mathbf{r}_1 \mathrm{d}\mathbf{r}_2\, \rho(\mathbf{r}_1)\rho(\mathbf{r}_2) f(\mathbf{r}_1, \mathbf{r}_2)\,, \\ &= \tfrac{V}{2}\rho^2 \int \mathrm{d}\mathbf{r} f(\mathbf{r})\,, \\ &= \tfrac{N}{2}\rho \mathcal{V}_d(\sigma) \int \mathrm{d}h\, \mathrm{e}^h \left(-1 + \mathrm{e}^{-\widehat{\beta U}(h)}\right)\,, \end{aligned} \tag{3.97}$$

where $\mathcal{V}_d(\sigma)$ is the volume of a sphere of radius σ. Accordingly, the three-vertex one is obtained as

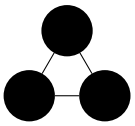

$$\begin{aligned} &= \tfrac{V}{3!}\rho^3 \int \mathrm{d}\mathbf{r}\mathrm{d}\mathbf{r}' f(\mathbf{r}) f(\mathbf{r}') f(\mathbf{r}-\mathbf{r}')\,, \\ &\simeq \tfrac{N}{3!}\left(\rho \mathcal{V}_d(\sigma)\right)^2 \int \mathrm{d}h\, \mathrm{d}h' \mathrm{e}^h \mathrm{e}^{h'} \widehat{f}(h) \widehat{f}\,(h') \int_{-1}^{1} \tfrac{\mathrm{d}x}{2W_{d-2}} \left(1 - \tfrac{x^2}{2}\right)^{\frac{d-3}{2}} \widehat{f}\left(d\left(\sqrt{2-2x} - 1\right)\right)\,. \end{aligned} \tag{3.98}$$

where the last line is obtained to leading order by neglecting small corrections in the argument of the third $\widehat{f}$ and where x denotes $\hat{\mathbf{r}} \cdot \hat{\mathbf{r}}'$. The formula in Eq. (3.98) is quite transparent. On the one hand, the angular measure on the $(d-1)$-dimensional unit sphere concentrates x around $1/\sqrt{d}$. On the other hand, the last $\hat{f}$ factor vanishes unless $x > 1/2$, *i.e.* $x = \cos(\theta)$ with $\theta < \pi/3$ (this comes as no surprise as this is the value of the angles in an equilateral triangle). Being more explicit requires knowing more about the function $\hat{f}$. If we take the

hard sphere Mayer function of Eq. (3.95) we obtain,

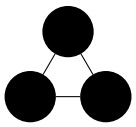

$$\begin{aligned} &\simeq \tfrac{N}{3!}\left(\rho\mathcal{V}_d(\sigma)\right)^2 \int_{1/2}^1 \tfrac{\mathrm{d}x}{2W_{d-2}} \left(1-\tfrac{x^2}{2}\right)^{\frac{d-3}{2}} , \\ &\simeq \tfrac{N}{3!}\left(\rho\mathcal{V}_d(\sigma)\right)^2 \tfrac{3}{2\pi\sqrt{d}} \left(\tfrac{\sqrt{3}}{2}\right)^{d-3} . \end{aligned} \tag{3.99}$$

The above diagram thus decays to zero as α^d with $\alpha = \sqrt{3}/2 < 1$. Indeed, it is only in density ranges in which $\rho\mathcal{V}_d(\sigma)$ is exponential in d, much denser that the scalings considered in this work, that the effect of the above diagram can become relevant. By extending this argument to all the remaining loop diagrams of Eq. (3.72) and upon assuming that the sum over the diagrams and the large d limit can be commuted (a proof of this statement can be found in [67]), we conclude that the free energy is truncated to second order in its density expansion

$$\lim_{N\to\infty} \frac{\beta F[\rho(\mathbf{r})=\rho]}{N} = (\ln\rho - 1) + \frac{\rho\mathcal{V}_d(\sigma)}{2}\int \mathrm{d}h\, \mathrm{e}^h \left(1-\mathrm{e}^{-\widehat{\beta U}(h)}\right) . \tag{3.100}$$

The pressure of a homogeneous phase can be derived from the above equation,

$$P = \rho T\left(1+\frac{d\widehat{\varphi}}{2}\int \mathrm{d}h\, \mathrm{e}^h \left(1-\mathrm{e}^{-\widehat{\beta U}(h)}\right)\right) , \tag{3.101}$$

thus reproducing the main result of [68]. This reasoning extends beyond the homogeneous phase case and writes for a generic density profile locally satisfying the scaling hypothesis Eq. (3.96),

$$\beta F[\rho] = \int \mathrm{d}\mathbf{r}\rho(\mathbf{r})\left(\ln(\rho(\mathbf{r}))-1\right) + \frac{1}{2}\int \mathrm{d}\mathbf{r}_1\mathrm{d}\mathbf{r}_2\rho(\mathbf{r}_1)\rho(\mathbf{r}_2)f(\mathbf{r}_1,\mathbf{r}_2) . \tag{3.102}$$

3.2.6 The Ornstein-Zernike equation again

We are now in position to use the Ornstein-Zernike equation in Eq. (3.86) in order to predict the structure of the infinite dimensional fluid. In any dimension d, an expansion the of the direct pair-correlation function $c^{(2)}(\mathbf{r}_1,\mathbf{r}_2)$ can be obtained by differentiating Eq. (3.72). Making the position of the white vertices explicit, the latter reads

$c^{(2)}(\mathbf{r}_1,\mathbf{r}_2) =$ 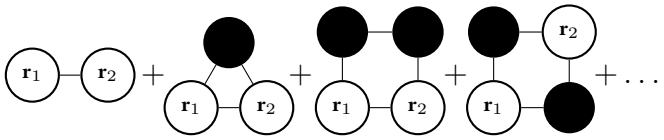

(3.103)

where the sum extends over all 1-particle irreducible diagrams with two white vertices at $\mathbf{r}_1$ and $\mathbf{r}_2$. If $|\mathbf{r}_1-\mathbf{r}_2| \simeq \sigma$, in the sense that $d\left(|\mathbf{r}_1-\mathbf{r}_2|-\sigma\right)$ is kept finite as $d\to\infty$, then following the same path as in the above leads to truncating the expansion at first order and to neglecting all loop diagrams, *i.e.*

$$\lim_{d\to\infty} c^{(2)}\left(|\mathbf{r}_1-\mathbf{r}_2| = \sigma\left(1+\frac{h}{d}\right)\right) = \widehat{f}(h) . \tag{3.104}$$

Accordingly, if $\mathbf{r}_1$ and $\mathbf{r}_2$ are "far away" so that $d\left(|\mathbf{r}_1-\mathbf{r}_2|-\sigma\right)\to+\infty$ all the diagrams yield vanishingly small contributions and

$$c^{(2)}\left(\mathbf{r}_1,\mathbf{r}_2\right)=0\,. \tag{3.105}$$

The vanishing of the first three diagrams is indeed immediate since they all display a $(\mathbf{r}_1,\mathbf{r}_2)$ edge. The result can then be confirmed by explicit computation of the fourth one, the argument being the same for all the others. In the hard sphere case, it reads

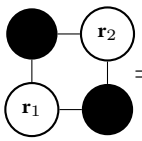

$$\begin{aligned}&=\frac{\rho^2}{2}\left(\int \mathrm{d}\mathbf{r} f(\mathbf{r}) f\left(\mathbf{r}_1-\mathbf{r}_2-\mathbf{r}\right)\right)^2\\ &=\frac{\rho^2}{2}\left(\int \mathrm{d}r\mathrm{d}\hat{\mathbf{r}}\, r^{d-1}\,\Theta(\sigma-r)\Theta\left(\sigma-\sqrt{|\mathbf{r}_1-\mathbf{r}_2|^2+r^2-2\,|\mathbf{r}_1-\mathbf{r}_2|\,r\,\hat{n}_{12}\cdot\hat{\mathbf{r}}}\right)\right)^2\\ &=0\,,\end{aligned} \tag{3.106}$$

up to exponentially small corrections. However, no such simplification occurs in the regime where the two points $\mathbf{r}_1$ and $\mathbf{r}_2$ nearly superimposes and $d\,|\mathbf{r}_1-\mathbf{r}_2|$ is fixed as $d\to\infty$. This can be seen on the second diagram that at $\mathbf{r}_1=\mathbf{r}_2$ simply reduces to

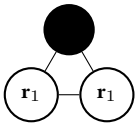

$$=-d\widehat{\varphi}\int \mathrm{d}h \mathrm{e}^{h}\widehat{f}(h)^2\,. \tag{3.107}$$

Notice that this cannot be anticipated directly from Eq. (3.102). This is however not an obstacle for solving the Ornstein-Zernike equation Eq. (3.86) as we know on general grounds that, due to the hard-core exclusion, $h(\mathbf{r})=-1$ whenever $\lim_{d\to\infty} d\left(\sigma-r\right)=+\infty$. Taking advantage of the translational and rotational symmetries of homogeneous phases, Eq. (3.86) can be rewritten as

$$h(r)=c^{(2)}(r)+\int \mathrm{d}\mathbf{r}' c^{(2)}\left(|\mathbf{r}-\mathbf{r}'|\right)h(r')\,, \tag{3.108}$$

which needs to be studied only for $r\gtrsim\sigma$. This equation can be solved by noting that for $r\gtrsim\sigma$,

$$\int \mathrm{d}\mathbf{r}' c^{(2)}\left(|\mathbf{r}-\mathbf{r}'|\right)c^{(2)}(r')=0\,, \tag{3.109}$$

up to exponentially small corrections provided there exists $\alpha\in[0,1[$ such that $r^{\alpha d}c^{(2)}(r)\to 0$ as $r\to 0$. Given that none of the graphs contributing to the expansion of $c^{(2)}(\mathbf{r}_1,\mathbf{r}_2)$ diverges as $\mathbf{r}_2\to\mathbf{r}_1$, this is a reasonable assumption. For $r\gtrsim\sigma$ we therefore obtain,

$$h(r)=c^{(2)}(r)\,, \tag{3.110}$$

from which one can deduce the 2-body distribution function,

$$\lim_{d\to\infty} g\left(r=\sigma\left(1+\frac{h}{d}\right)\right)=\mathrm{e}^{-\widehat{\beta}\widehat{U}(h)}\,. \tag{3.111}$$

and $g(r)=1$ whenever $\lim_{d\to\infty} d\left(r-\sigma\right)=+\infty$. The latter thus reduces to its value in the dilute limit, consistently with the expression for the pressure shown in Eq. (3.101).

3.2.7 Equilibrium infinite dimensional fluids from the BBGKY hierarchy

In this section, we present a dynamics-based alternative derivation of the aforementioned results starting from the BBGKY hierarchy of distribution functions. The equations of motion for the N-particle equilibrium system read

$$\dot{\mathbf{r}}_i = -\sum_{j(\neq i)} \boldsymbol{\nabla}_{\mathbf{r}_i} U\left(\mathbf{r}_i - \mathbf{r}_j\right) + \sqrt{2T}\boldsymbol{\eta}_i \,, \tag{3.112}$$

with $\boldsymbol{\eta}$ a zero mean Gaussian white noise with unit variance and where the potential U is rotationally invariant. The scalings introduced in Sec. 3.2 are assumed to hold in the large dimensional limit, *i.e.* $\beta = T^{-1}$ is held fixed with

$$\lim_{d\to\infty} U(r) = \widehat{U}(h) \;\text{ with }\; h = \mathrm{d}\left(r/\sigma - 1\right) \,, \tag{3.113}$$

and

$$\lim_{d\to\infty} \frac{\rho \mathcal{V}_d(\sigma)}{d} = \widehat{\varphi} \,. \tag{3.114}$$

In equilibrium, the BBGKY hierarchy of distribution functions reads,

$$\begin{aligned} &T\sum_{i=1}^{n} \boldsymbol{\nabla}_{\mathbf{r}_i} g^{(n)} + \sum_{i=1}^{n}\sum_{j\neq i}^{n} \left(g^{(n)} \boldsymbol{\nabla}_{\mathbf{r}_i} U(\mathbf{r}_i - \mathbf{r}_j)\right) \\ &+ \rho \sum_{i=1}^{n} \int \mathrm{d}\mathbf{r}'\, g^{(n+1)}(\mathbf{r}_1, \ldots, \mathbf{r}_n, \mathbf{r}') \boldsymbol{\nabla}_{\mathbf{r}_i} U(\mathbf{r}_i - \mathbf{r}') = \mathbf{0} \,. \end{aligned} \tag{3.115}$$

We find it convenient to introduce an infinite, virial-like, series expansion of the correlation functions in powers of $\widehat{\varphi}$. For the two-point function, we thus write

$$g^{(2)}(\mathbf{r}_1, \mathbf{r}_2) = \sum_{p=0}^{+\infty} \widehat{\varphi}^p \gamma_p^{(2)}(\mathbf{r}_1, \mathbf{r}_2) \,, \tag{3.116}$$

while similar expansion can be written for any n-body distribution function. To the lowest order in the density we have,

$$\gamma_0^{(2)}(\mathbf{r}_1, \mathbf{r}_2) = g_0(\mathbf{r}_1 - \mathbf{r}_2) = \mathrm{e}^{-\beta U(\mathbf{r}_1 - \mathbf{r}_2)} \,, \tag{3.117}$$

where the above equation defines g_0. By truncating the hierarchy to order $n \geq 2$, we have access to all $\gamma_p^{(2)}(\mathbf{r}_1, \mathbf{r}_2)$ for $p \leq n-2$. We thus start by assuming such a truncation holds, *i.e.* we look for $g^{(n)}(\mathbf{r}_1, \ldots, \mathbf{r}_n)$ such that

$$T\sum_{i=1}^{n} \boldsymbol{\nabla}_{\mathbf{r}_i} g^{(n)} + \sum_{i=1}^{n}\sum_{j\neq i}^{n} \left(g^{(n)} \boldsymbol{\nabla}_{\mathbf{r}_i} U(\mathbf{r}_i - \mathbf{r}_j)\right) = \mathbf{0} \,. \tag{3.118}$$

The solution to this equation is given by the n-body Boltzmann weight,

$$g^{(n)}(\mathbf{r}_1, \ldots, \mathbf{r}_n) = \prod_{i<j}^{n} g_0(\mathbf{r}_i - \mathbf{r}_j) \,. \tag{3.119}$$

We can now insert this solution into the hierarchical equation at order $n-1$. This will give us the first order term of the density expansion of $g^{(n-1)}$. We thus have to compute for any $k \in [\![1, n-1]\!]$,

$$\begin{aligned}
&\rho \left(\prod_{i<j}^{n-1} g_0 \left(\mathbf{r}_i - \mathbf{r}_j \right) \right) \int \mathrm{d}\mathbf{r}' \left(\prod_{i\neq k}^{n-1} g_0 \left(\mathbf{r}_i - \mathbf{r}' \right) \right) g_0 \left(\mathbf{r}_k - \mathbf{r}' \right) \boldsymbol{\nabla}_{\mathbf{r}_k} U \left(\mathbf{r}_k - \mathbf{r}' \right) \\
&= -\rho \left(\prod_{i<j}^{n-1} g_0 \left(\mathbf{r}_i - \mathbf{r}_j \right) \right) \int \mathrm{d}\mathbf{r}' \left(\prod_{i\neq k}^{n-1} g_0 \left(\mathbf{r}_i - \mathbf{r}_k - \mathbf{r}' \right) \right) g_0 \left(\mathbf{r}' \right) \boldsymbol{\nabla}_{\mathbf{r}'} U \left(\mathbf{r}' \right) , \\
&= \rho T \sigma^{d-1} \int \mathrm{d}h' \mathrm{e}^{h'} \mathrm{d}\hat{\mathbf{r}}' \left(\prod_{i\neq k}^{n-1} g_0 \left(\sqrt{\left| \mathbf{r}_i - \mathbf{r}_k \right|^2 + \sigma^2 - 2 \left| \mathbf{r}_i - \mathbf{r}_k \right| \sigma \hat{\mathbf{r}} \cdot \hat{n}_{ik}} \right) \right) \widehat{f}'(h') \, \hat{\mathbf{r}}' \\
&\quad \times \left(\prod_{i<j}^{n-1} g_0 \left(\mathbf{r}_i - \mathbf{r}_j \right) \right) .
\end{aligned} \tag{3.120}$$

with $\hat{n}_{ik} = \left(\mathbf{r}_i - \mathbf{r}_k \right) / \left| \mathbf{r}_i - \mathbf{r}_k \right|$ and where we have neglected the irrelevant $O(1/d)$ corrections in the argument of the g_0's inside the integral. First, due the product of g_0's outside the integral, the above term is non-vanishing only if $|\mathbf{r}_i - \mathbf{r}_k| \gtrsim \sigma$. Thus, as seen in Sec. 3.2, and except in an exponentially small fraction of the integration volume,

$$g_0 \left(\sqrt{\left| \mathbf{r}_i - \mathbf{r}_k \right|^2 + \sigma^2 - 2 \left| \mathbf{r}_i - \mathbf{r}_k \right| \sigma \hat{\mathbf{r}} \cdot \hat{n}_{ik}} \right) = 1 , \tag{3.121}$$

as typically $\hat{\mathbf{r}} \cdot \hat{n}_{ik} = O(1/\sqrt{d})$. Therefore, up to corrections that are exponentially small in d,

$$\begin{aligned}
&\rho \left(\prod_{i<j}^{n-1} g_0 \left(\mathbf{r}_i - \mathbf{r}_j \right) \right) \int \mathrm{d}\mathbf{r}' \left(\prod_{i\neq k}^{n-1} g_0 \left(\mathbf{r}_i - \mathbf{r}' \right) \right) g_0 \left(\mathbf{r}_k - \mathbf{r}' \right) \boldsymbol{\nabla}_{\mathbf{r}_k} U \left(\mathbf{r}_k - \mathbf{r}' \right) \\
&= \rho T \sigma^{d-1} \left(\prod_{i<j}^{n-1} g_0 \left(\mathbf{r}_i - \mathbf{r}_j \right) \right) \int \mathrm{d}h' \mathrm{e}^{h'} \mathrm{d}\hat{\mathbf{r}}' \widehat{f}'(h') \, \hat{\mathbf{r}}' , \\
&= 0 .
\end{aligned} \tag{3.122}$$

Hence, the mean force exerted by the surrounding fluid on each of the $n-1$ tagged particles vanishes in the infinite dimensional limit. At finite d such a mean force emerges on particle k as the distribution of the $n-2$ other tagged ones biases in an anisotropic way that of the remaining particles of the fluid. This effect is exponentially suppressed at $d \gg 1$. Consequently, the expression of $g^{(n-1)}$ to the first order in $\widehat{\varphi}$ reduces, up to exponentially small corrections, to its 0^{th} order one,

$$g^{(n-1)}(\mathbf{r}_1, \ldots, \mathbf{r}_n) = \prod_{i<j}^{n-1} g_0(\mathbf{r}_i - \mathbf{r}_j) . \tag{3.123}$$

The same argument can then be repeated for the hierarchical equation to order $n-2$ and then all the way down to the equation for $g^{(2)}$ thus showing that at order $\widehat{\varphi}^{n-2}$, the density

expansion of $g^{(2)}$ is truncated after the first term. This holds for any $n > 2$ thus in the end showing

$$g^{(2)}(\mathbf{r}_1, \mathbf{r}_2) = g_0\left(\mathbf{r}_1 - \mathbf{r}_2\right) \,, \tag{3.124}$$

in agreement with the result obtained from the Ornstein-Zernike equation in Eq. (3.111). The same argument can be used to study higher order distribution functions and obtain $\forall n > 2$,

$$g^{(n)}(\mathbf{r}_1, \ldots, \mathbf{r}_n) = \prod_{i<j}^{n} g_0(\mathbf{r}_i - \mathbf{r}_j) \,, \tag{3.125}$$

thus completely elucidating the structure of the infinite dimensional fluid. In particular, the Kirkwood approximation

$$g^{(3)}(\mathbf{x}_1, \mathbf{x}_2, \mathbf{x}_3) = g^{(2)}(\mathbf{x}_1, \mathbf{x}_2) g^{(2)}(\mathbf{x}_1, \mathbf{x}_3) g^{(2)}(\mathbf{x}_2, \mathbf{x}_3) \,, \tag{3.126}$$

holds in this limit.

Chapter 4

Active matter in infinite dimension

Contents

Understanding the collective behavior of simple liquids has been a fundamental statistical mechanical challenge since its early days [92]. The absence of a well-defined and versatile approximation method able to capture collective effects in liquids has led to the development of a branch in its own right: the art of elaborating approximations leading to correlations in fluids is almost as old as statistical mechanics itself [149, 180]. It is only in the mid-eighties that Frisch, Rivier and Wyler [66] were able to devise a *bona fide* mean-field approximation. The latter, that we reviewed in Sec.3.2, takes the form of a controlled large dimensionality limit in which they could derive, among other thermodynamical properties, an exact equation of state for classical hard-spheres. The physical price to pay by going to large space dimensions is heftily compensated by the mathematical gain: not only the equation of state [66, 213] but also thermodynamic quantities, such as the entropy [64] and even transport coefficients inferred from the collision dynamics [47] can be determined exactly. Perhaps more importantly, the greatest insight is to be found in the pair-correlation function in that it, alone, controls the spatial organization of the fluid [65], and can thus be used as an educated starting point for density functional approaches [48] (see [131] for a recent overview).

The realization that classical infinite-dimensional hard-spheres lent themselves to analytical treatment, especially regarding the determination of entropy, laid the ground for the idea that they could also be used to investigate metastability issues (understood in terms of free energy minima) [170, 172, 120]. They have thus become the workhorse of the theory of jamming and of the static approach to glasses. More recent inroads into dynamical behavior [99, 185, 136, 119] address relaxation properties, including with nonequilibrium evolutions [2]. The associated Dynamical Mean Field Theory (DMFT) framework will be the subject of the first section of this chapter. For some of these glassy-behavior-related questions, the high-dimensionality comes with its own share of hotly debated issues as to what exactly survives finite dimensions [95].

A pivotal starting point common to all static approaches is the celebrated equilibrium Boltzmann weight. In stark contrast, no such shortcut exists for the stationary properties of active matter systems and it is thus no surprise that a many-body exactly solvable model of particles interacting with pairwise forces has so far remained elusive. Understanding collective behavior in active matter thus combines the hurdles of strongly correlated liquids with those of nonequilibrium physics.

One of the remarkable properties of standard equilibrium fluids is the pairwise structure of their N-body stationary distribution, *i.e.* the possibility to express it as a product over all the pairs of particles. We stress that the question to know whether the former is true in a many-body interacting system is a priori transverse to the, dynamical in nature, question of being or not in equilibrium. In general, we say that a many-body distribution admits a pairwise structure if there exists some functions $g_1(\mathbf{r})$ and $g_2(\mathbf{r})$ such that it can be written

in the form

$$P_N(\mathbf{r}_1, \mathbf{r}_2, \dots, \mathbf{r}_N) = \prod_{i=1}^{N} g_1(\mathbf{r}_i) \prod_{i>j}^{N} g_2(\mathbf{r}_i - \mathbf{r}_j)\,. \tag{4.1}$$

If the latter holds, and whether or not the original system is in equilibrium, then their is a direct mapping between its static properties and that of a standard equilibrium one.

Equation (4.1) is however expected not to hold in in active matter systems, thus making their stationary state distribution genuinely different from that of standard equilibrium fluids. We say that the system displays many-body interactions in the steady state. Even though there is no known formula for the stationary distribution of interacting self-propelled particle systems, the breaking of Eq. (4.1) can already be seen in its small τ expansion for AOUPs [60]. For the dynamics defined by Eq. (1.13) in the absence of external potential together with Eq. (1.18), the stationary state distribution indeed writes,

$$\begin{aligned} -D \ln P_N(\mathbf{r}_1, \dots, \mathbf{r}_N) = &\sum_{i<j} \left[U(\mathbf{r}_i - \mathbf{r}_j) - 2D\tau \boldsymbol{\nabla}^2_{\mathbf{r}_i} U(\mathbf{r}_i - \mathbf{r}_j)\right] \\ &+ \frac{\tau}{2} \sum_i \left(\sum_{j \neq i} \boldsymbol{\nabla}_{\mathbf{r}_i} U(\mathbf{r}_i - \mathbf{r}_j) \right)^2 + O(\tau^2)\,. \end{aligned} \tag{4.2}$$

The last term of the above formula generates 3-body interactions and breaks the structure of Eq. (4.1). Several attempts have been made in the literature to describe the properties of active fluids using approximate measures of the form Eq. (4.1) with well chosen effective pair potential [51, 141]. Such mappings however tend to work quantitatively or even qualitatively only in the near-equilibrium regime [179]. In a recent work [202], Turci and collaborators shed a new light on the importance of multibody interactions in self-propelled particles system. In particular, they showed that a system described by the many-body distribution

$$P_N(\mathbf{r}_1, \dots, \mathbf{r}_N) = \prod_{i<j} g_2(\mathbf{r}_i - \mathbf{r}_j)\,, \tag{4.3}$$

where $g_2(\mathbf{r})$ is the stationary distribution of two ABPs interacting via a WCA potential, does not experience phase separation whereas it is known that the original ABP system undergoes MIPS at high enough activity. This is particularly interesting given the Lennard-Jones like shape of $\ln g_2$. Lastly, we underline the fact that all the (static) thermodynamic properties of any system respecting Eq. (4.1) are known exactly in the limit of infinite dimension (provided the correct scalings are taken). It is not so in systems with multibody interactions in the steady state. This will be one of the main concerns of this work.

In this chapter, our purpose is to show how working in infinite dimension allows to gain theoretical insights into the thermodynamic behavior of active matter systems and particularly on the role of multibody interactions. Section 4.1 is the result of a collaboration [176] with A. Manacorda and F. Zamponi. There, we first introduce the correct scalings of the active dynamics in the infinite dimensional limit. We then introduce the family of sticky sphere potentials that generalize the hard sphere one by adding short-ranged attraction on top of it. The low density thermodynamic properties of an infinite dimensional system of RTPs are then derived in the ballistic limit. Next, we study the active DMFT equations in the same regime. We compute to the first order in $\widehat{\varphi}$ the different dynamical kernels.

We recover the above mentioned static results and obtain a formula for the Mean Square Displacement (MSD). We show that at long times it is that of a free particle with the bare self-propulsion replaced by the effective one.

In Sec. 4.2, we investigate the steady state behavior of infinite dimensional active systems beyond the dilute limit. This part is based on the results of a collaboration with G. Lozano [175]. The starting point is the BBGKY hierarchy of correlation functions Eq.(3.12) that we showed in Sec.3.2.7 to be amenable to an exact closure in equilibrium systems. We originally thought the resummation scheme of [175] was exact but we now know that it is not the case as it only partially takes into account the effect of multibody interactions in steady state. We present here this resummation scheme and clearly highlight which contributions are kept and which are neglected. I would like to thank here G. Biroli, A. Manacorda, C. Liu and F. Zamponi for extremely insightful discussions regarding these issues. The work of [175] on active hard spheres is here extended to the family of sticky spheres. The result is the description of the local structure of n-point correlation functions that is shown to be that of an equilibrium fluid with density dependent interaction pair potential. From this we derive the effective self-propulsion $v(\widehat{\varphi})$. While that of hard spheres decays linearly with $\widehat{\varphi}$ as already shown in [175] and consistently with numerical observations of finite dimensional systems [196], we show that the latter does not hold in general. We also introduce the concept of effective amplitude of potential interactions $\mu(\widehat{\varphi})$. Both the effective self-propulsion and the effective amplitude of potential interactions are found to vanish at the same finite crowding density $\widehat{\varphi}_{cr}$. Interestingly, we remark that the predicted density coincides with the dynamic glass transition one of an equilibrium colloidal system with a density dependent pair potential that reproduces the local structure of the active fluid.

Lastly, in Sec. 4.3, we conclude our investigation on the behavior of infinite dimensional active systems and the role of multibody interactions. We study the Unified Colored Noise Approximation (UCNA) of the AOUPs dynamics for which the N-body stationary distribution function is known and exhibits multibody interactions. Using a mapping to a system with pairwise structure, we are able to predict the density dependence of the radial distribution function as well as the phase behavior of the UCNA. The latter displays two regions of phase coexistence for which a simple two-body approximation of the distribution is unable to account for.

Contributions

Section 4.1

- introduction of the family of sticky sphere potentials,
- solution of the two-body problem in the ballistic limit and computation of the low density pair-correlation function, effective self-propulsion, mechanical pressure,
- first order in density of the dynamical kernels of the active DMFT equations,
- computation of the MSD that at long-times equals that of a free particle with v_0 replaced by $v(\widehat{\varphi})$.

Section 4.2

- failure of the Kirkwood approximation at large d,
- approximate resummation scheme of the hierarchy of correlation functions in infinite dimensional RTPs systems in the ballistic limit,
- prediction for the fluid structure and correspondence with that of an equilibrium fluid with density dependent pair potential,
- computation of the effective velocity and effective amplitude of pair interactions,
- puzzling correspondence between the crowding density $\widehat{\varphi}_{cr}$ and the dynamical glass transition one $\widehat{\varphi}_d$ of the equivalent equilibrium fluid.

Section 4.3

- proof of the absence of phase transition in the two-body approximation of the infinite dimensional UCNA,
- mapping of the UCNA to a system with pairwise structure,
- predictions for the fluid structure and correspondence with that of an equilibrium fluid with density dependent interaction potential,
- phase diagram of the UCNA.

4.1 Sticky hard spheres in the dilute and ballistic limit

We start with this section our study of infinite dimensional systems made of interacting self-propelled particles with a particular emphasis on their dynamical properties within the DMFT framework. First, we specify the scalings of the model parameters with the dimension. These are the scalings we will also use in Sec. 4.2. We then introduce a family of

potentials called the sticky sphere potentials that generalize the hard sphere case of Sec. 2.3 by adding an attractive well to the repulsive hard core. In the fashion of Sections 2.3 and 3.1, the stationary state of the two body problem is computed in the ballistic limit and low density radial distribution function, effective self-propulsion and mechanical pressure are derived. The DFMT equations for the dynamics of the two-particle process are next studied in the low density/high persistence regime. The relaxation to the stationary state is studied and the stationary distribution function previously derived is recovered. The dynamical kernels of the DMFT framework are then computed to first order in the density: this constitutes the basis of a more systematic study of the active dynamics. In particular, this allows us to show that after the first density iteration, the long time limit of the MSD is given by that of a free particle with the bare velocity v_0 replaced by the effective self-propulsion $v(\widehat{\varphi})$, as observed numerically in [196] for 2 and 3 dimensional ABPs in a large density range.

4.1.1 Definition of the model and infinite dimensional scalings

We consider the dynamics of N interacting d-dimensional self-propelled particles with equations of motion that follow Eq. (1.13),

$$\zeta \dot{\mathbf{r}}_i(t) = \mathbf{v}_i(t) - \sum_{j(\neq i)} \boldsymbol{\nabla}_{\mathbf{r}_i} U\left(\mathbf{r}_i(t) - \mathbf{r}_j(t)\right) . \tag{4.4}$$

In Eq.(4.4), motion is induced by (i) a self-propulsion force $\mathbf{v}_i(t)$ and (ii) pairwise conservative forces deriving from the potential $U\left(\mathbf{r}_i - \mathbf{r}_j\right)$. The latter is taken radially symmetric, $U\left(\mathbf{r}\right) = U(r)$ with $r = |\mathbf{r}|$. There exist different descriptions of the driving force, each of them corresponding to a particular model of self-propelled particles. In the following, we choose to work with run-and-tumble particles (RTPs) in which case the active force reads $\mathbf{v}_i(t) = v_0 \mathbf{u}_i(t)$ with $\mathbf{u}_i(t)$ a unit vector randomly and uniformly reshuffled on the $(d-1)$-dimensional unit sphere with rate τ^{-1}, thus yielding $\left\langle u_i^\mu(t) u_j^\nu(s) \right\rangle = \delta_{ij}\delta^{\mu\nu} \exp\left(-|t-s|/\tau\right)/d$. Note however that, as shown in [175] and reviewed in Sec. 3.1, the three standard models of self-propelled particles, *i.e.* RTPs, active Brownian particles and active Ornstein-Ulhenbeck particles, are equivalent in the limit where the space dimension d is sent to infinity and the persistence time is large. In the present section, we study the dynamics Eq. (4.4) at low densities in the limit $d \to \infty$. Following our earlier study of infinite-dimensional equilibrium fluids in Sec. 3.2, we consider first the following scalings,

- the pair potential is assumed to decay over a short length scale as $\lim_{d\to\infty} U(r) = \widehat{U}(h)$ with $h = d(r/\sigma - 1)$. The length scale σ can be viewed as the particle diameter;
- the number density ρ is such that each particle interacts with $O(d)$ other particles, *i.e.* $\widehat{\varphi} = \rho\, \mathcal{V}_d(\sigma)/d$ is kept finite with $\mathcal{V}_d(\sigma)$ the volume of the d-dimensional ball of radius σ.

The active dynamics parameters also have to be scaled in the large d limit [2, 175, 176]. This is what we discuss now. As a consequence of the above mentioned scalings, we have

$$|\boldsymbol{\nabla}_{\mathbf{r}_i} U(\mathbf{r}_i - \mathbf{r}_j)| \sim d\,, \tag{4.5}$$

so that

$$\boldsymbol{\nabla}_{\mathbf{r}_i} U(\mathbf{r}_i - \mathbf{r}_j) \cdot \mathbf{u}_i \sim d^{1/2} \,, \tag{4.6}$$

with the additional $d^{-1/2}$ factor between the latter and the former brought about by the scalar product between $\mathbf{u}_i$ and $\hat{\mathbf{r}}_{ij}$. Hence we expect the projection of the total potential force along $\mathbf{u}_i$ to scale as,

$$\sum_{j(\neq i)} \boldsymbol{\nabla}_{\mathbf{r}_i} U(\mathbf{r}_i - \mathbf{r}_j) \cdot \mathbf{u}_i \sim d^{3/2} \,, \tag{4.7}$$

because the above sum contains $O(d)$ terms. The projection of the total potential force on the $(d-1)$-dimensional hyperplane orthogonal to $\mathbf{u}_i$ is also expected to scale in the same way

$$\left| \sum_{j(\neq i)} \boldsymbol{\nabla}^{\perp}_{\mathbf{r}_i} U(\mathbf{r}_i - \mathbf{r}_j) \right| \sim d^{3/2} \,. \tag{4.8}$$

It is indeed the sum $O(d)$ vectors of norm $O(d)$ that are expected to be isotropically distributed and weakly correlated in the large d limit (remember that if both j and k interact with i then it becomes extremely unlikely that j and k also interact together as d grows) so that by central limit theorem-type arguments the above mentionned scaling is recovered. Thus, we propose the following scaling for the self-propulsion speed v_0,

- the norm of the active drive is rescaled as $v_0 = (\sqrt{2} d^{3/2}/\sigma)\widehat{v}_0$. In Eq. (4.4), this equates the scaling of the norms of the conservative force and of the active force;

We finally note that the scaling form of the potential suggests that the relevant time scale of the problem is that over which particle i move by an amount $O(1/d)$ along each direction $\hat{\mathbf{r}}_{ij}$ [130, 2, 136]. Thus,

- the friction coefficient is rescaled as $\zeta = (2d^2/\sigma^2)\widehat{\zeta}$. In this scaling, the variations of the rescaled separation h between two particles over finite time scales are $O(1)$.
- the times t and τ are left unchanged.

Note that in order to maintain a competition between activity and repulsive pairwise interactions in the equation of state, we will sometimes work in the ultraballistic scaling $\tau = d\hat{\tau}$. We also remark that in this settings the equilibrium dynamics can be recovered in the limit $\tau \to 0$ by setting $\widehat{v}_0^2 = \widehat{\zeta} T/\tau$. With this prescription, the active force becomes a thermal noise at temperature T in the limit of vanishing persistence.

4.1.2 Sticky spheres: stationary state properties

The two-body problem in the infinite dimensional limit:

We start by addressing the dynamics of two interacting self-propelled particles. The interaction is carried through a spherically symmetric potential U and both particles are subject

to an external active drive. Following Eq. (4.4), their equations of motion read

$$\begin{aligned}\zeta\dot{\mathbf{r}}_1(t) &= v_0\mathbf{u}_1(t) - \boldsymbol{\nabla}_{\mathbf{r}_1}U\left(\mathbf{r}_1(t)-\mathbf{r}_2(t)\right)\,,\\ \zeta\dot{\mathbf{r}}_2(t) &= v_0\mathbf{u}_2(t) - \boldsymbol{\nabla}_{\mathbf{r}_2}U\left(\mathbf{r}_2(t)-\mathbf{r}_1(t)\right)\,,\end{aligned} \tag{4.9}$$

with $\mathbf{u}_1(t)$ and $\mathbf{u}_2(t)$ two independent run-and-tumble noises. We then introduce $\mathbf{r} = \mathbf{r}_2 - \mathbf{r}_1$, the relative separation, and $P(\mathbf{r},\mathbf{u}_1,\mathbf{u}_2)$, the stationary state probability density associated to the process in Eq. (4.9). The latter obeys the following integro-differential equation

$$\begin{aligned}&-v_0\left(\mathbf{u}_2-\mathbf{u}_1\right)\cdot\boldsymbol{\nabla}_{\mathbf{r}}P + 2\boldsymbol{\nabla}_{\mathbf{r}}\cdot\left(P\boldsymbol{\nabla}_{\mathbf{r}}V(\mathbf{r})\right)\\ &+\frac{\zeta}{\tau_p}\left[\int\frac{\mathrm{d}\mathbf{u}'}{\Omega_d}P(\mathbf{r},\mathbf{u}',\mathbf{u}_2)+\int\frac{\mathrm{d}\mathbf{u}'}{\Omega_d}P(\mathbf{r},\mathbf{u}_1,\mathbf{u}')-2P(\mathbf{r},\mathbf{u}_1,\mathbf{u}_2)\right]=0\,.\end{aligned} \tag{4.10}$$

Taking advantage of the rotational symmetry of P we introduce the variables

$$\begin{aligned}r &= |\mathbf{r}|\,,\\ w_1 &= \left(\mathbf{u}_1\cdot\mathbf{r}\right)/r\,,\\ w_2 &= \left(\mathbf{u}_2\cdot\mathbf{r}\right)/r\,,\\ z &= \mathbf{u}_1\cdot\mathbf{u}_2\,,\end{aligned} \tag{4.11}$$

the use of which allows us to rewrite to Fokker-Planck equation in terms of four (instead of $3d$) coordinates as

$$\begin{aligned}0 =& -v_0\left(w_2-w_1\right)\partial_r P - \frac{v_0}{r}\left[\left(1+w_1w_2-z\right)\left(\partial_{w_2}-\partial_{w_1}\right)P - \left(w_2^2\,\partial_{w_2}-w_1^2\,\partial_{w_1}\right)P\right]\\ &+\frac{2}{r^{d-1}}\partial_r\left(r^{d-1}U'(r)P\right)+\frac{\zeta}{\tau_p}\left[\frac{\Omega_{d-2}}{\Omega_d}\frac{1}{\sqrt{1-w_2^2}}\int_{-1}^{1}\mathrm{d}w_1'\int_{w_1'w_2-\sqrt{1-w_2^2}\sqrt{1-w_1'^2}}^{w_1'w_2+\sqrt{1-w_2^2}\sqrt{1-w_1'^2}}\mathrm{d}z'\times\ldots\right.\\ &\times P(r,w_1',w_2,z')\left(1-w_1'^2-\frac{z'^2+w_1'^2w_2^2-2z'w_1'w_2}{1-w_2^2}\right)^{\frac{d-4}{2}}+\frac{\Omega_{d-2}}{\Omega_d}\frac{1}{\sqrt{1-w_1^2}}\times\ldots\\ &\times\int_{-1}^{1}\mathrm{d}w_2'\int_{w_1w_2'-\sqrt{1-w_2'^2}\sqrt{1-w_1^2}}^{w_1w_2'+\sqrt{1-w_2'^2}\sqrt{1-w_1^2}}\mathrm{d}z'P(r,w_1,w_2',z')\left(1-w_2'^2-\frac{z'^2+w_2'^2w_1^2-2z'w_2'w_1}{1-w_1^2}\right)^{\frac{d-4}{2}}\\ &\left.-2P(r,w_1,w_2,z)\right]\,.\end{aligned} \tag{4.12}$$

The limit of infinite dimension $d\to\infty$ is then taken in Eq. (4.12) with:

$$\begin{aligned}r &= \sigma\left(1+h/d\right)\,,\\ w_1 &\to w_1/\sqrt{d}\,,\\ w_2 &\to w_2/\sqrt{d}\,,\\ z &\to z/\sqrt{d}\,.\end{aligned} \tag{4.13}$$

while keeping h, and the redefined w_1, w_2, z fixed. The infinite dimensional limit of Eq. (4.12) is obtained to leading order in d as:

$$\begin{aligned} &-\frac{\widehat{v}_0}{\sqrt{2}}\left(w_2-w_1\right)\partial_h P-\frac{\widehat{v}_0}{\sqrt{2}}\left(\partial_{w_2}-\partial_{w_1}\right)P+e^{-h}\partial_h\left(e^h\frac{\widehat{U}'(h)}{\sigma}P\right)\\ &+\frac{\widehat{\zeta}}{\tau_p}\left[\int_{-\infty}^{+\infty}\frac{\mathrm{d}w_1'\,\mathrm{d}z'}{2\pi}\exp\left(-\frac{w_1'^2}{2}-\frac{z'^2}{2}\right)P\left(h,w_1',w_2,z'\right)\right.\\ &\left.+\int_{-\infty}^{+\infty}\frac{\mathrm{d}w_2'\,\mathrm{d}z'}{2\pi}\exp\left(-\frac{w_2'^2}{2}-\frac{z'^2}{2}\right)P\left(h,w_1,w_2',z'\right)-2P\left(h,w_1,w_2,z\right)\right]=0\,. \end{aligned} \tag{4.14}$$

It appears from the above equation that the probability density becomes independent of z in this scaling.

Analytical solution with infinite persistence

Equation (4.14) can be solved analytically for certain classes of potentials in the ballistic limit $\tau\to\infty$. Beside providing nice analytical simplifications, this limit is conjectured to be of particular interest regarding the phase behavior of macroscopic systems of interacting active particles, see [196] for a discussion in $d=2$ and $d=3$ and [175] for a discussion in $d\to\infty$. At $\tau\to\infty$, only the relative speed $w=\left(w_2-w_1\right)/\sqrt{2}$ enters the game and

$$-\widehat{v}_0\left(w\partial_h P+\partial_w P\right)+e^{-h}\partial_h\left(e^h\frac{\widehat{U}'(h)}{\sigma}P\right)=0 \tag{4.15}$$

with $P(h\to\infty,w)=1$ as a boundary condition. The class of potentials we work with in the following is that of sticky-sphere potentials. These potentials have hard-sphere repulsion at $h<0$ while displaying an infinitely short ranged attractive well at $h=0^+$ and are vanishing at $h>0$. Such potentials are similar in spirit to the Baxter potential sometimes used as a model for passive colloids with short ranged attraction [11]. However, we make use of a slightly different mathematical construction for these sticky-sphere potentials. Indeed, the pairwise force, when attractive, must always be finite for the stationary state to be well-defined. Were this not to be true, then the two particles whose dynamics is given in Eq. (4.9) would never separate after a collision, the driving forces being unable to counterbalance the attractive force created by the potential. The sticky sphere potential is constructed as follows:

$$\widehat{U}(h)=\begin{cases}\widehat{v}_0\,w_0\left(\frac{\lambda}{2}h^2+h-\frac{1}{2\lambda}\right)\,, & h<0\,,\\ \widehat{v}_0\,w_0\left(-\frac{\lambda}{2}h^2+h-\frac{1}{2\lambda}\right)\,, & 0<h<1/\lambda\,,\\ 0\,, & h>1/\lambda\,,\end{cases} \tag{4.16}$$

in the limit $\lambda\to\infty$, where w_0 is a real positive parameter and $2\widehat{v}_0 w_0$ is the maximal attractive force between two particles. The results shown in the following are however independent of the precise procedure used to construct the sticky-sphere potential as the limit of a regular one. In general, w_0 is defined as

$$w_0=\max_h\left(\frac{\widehat{U}'(h)}{\widehat{v}_0}\right)\,. \tag{4.17}$$

Concretely, when colliding, the two spheres skid one onto each other until they are free to go. In the hard-sphere case, this occurs whenever the relative driving force is orthogonal to the relative separation, *i.e.* at $w = 0$, see Fig. 2.6. In the sticky-sphere case, they keep skidding and only detach at $w = w_0$, when the projection of the relative driving on the separation direction $2\,\widehat{v}_0\,w$ compensates the maximal attractive force, as depicted in Fig. 4.1. Finding the stationary distribution in that case amounts at generalizing the computation we

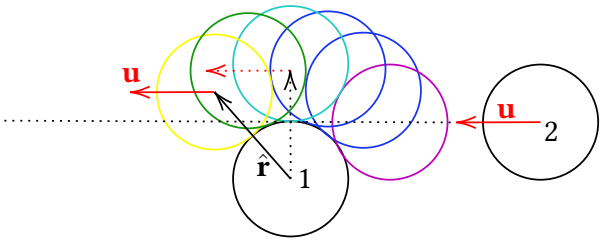

Figure 4.1: A collision between two active sticky hard spheres labeled 1 and 2 in the reference frame where particle labeled 1 is held fixed. Particle 2 with incoming relative self-propulsion $\mathbf{u} = \mathbf{u}_2 - \mathbf{u}_1$ hits particle 1 (at the magenta position) and then skids around. It eventually takes off at the yellow position where the self-propulsion compensates the attractive interaction between the two spheres, *i.e.* $\hat{\mathbf{r}} \cdot \mathbf{u} = \sqrt{2}w_0/\sqrt{d}$. The light blue position is where the relative self-propulsion is tangent to the separation between the two spheres and marks the end of the collision in the hard sphere case $w_0 = 0$.

made in Sec. 2.3 in the hard sphere case. As shown in Appendix B.1, in the limit $\lambda \to \infty$, the stationary probability distribution splits into a bulk part at $h > 0$ and a delta peak accumulation at $h = 0$,

$$P(h, w) = P_b(h, w)\Theta(h) + \Gamma(w)\delta(h)\,, \tag{4.18}$$

where $\Theta(h)$ is the Heaviside step function and $\delta(h)$ is a Dirac delta, with

$$w\partial_h P_b + \partial_w P_b = 0\,, \tag{4.19}$$

and

$$\Gamma'(w) - w\Gamma(w) = -wP_b(0, w) \text{ with } \Gamma(w > w_0) = 0\,. \tag{4.20}$$

The stationary distribution function is shown to be given by (see Appendix B.1 for details of the derivation)

$$P_b(h, w) = \Theta(h)\left[1 - \Theta(w)\Theta\left(\frac{w^2}{2} - h\right) + \Theta(w)e^{\frac{w_0^2}{2}}\delta\left(h - \frac{w^2}{2} + \frac{w_0^2}{2}\right)\right] \tag{4.21}$$

and

$$\Gamma(w) = \Theta(-w) + \Theta(w)\Theta(w_0 - w)e^{\frac{w^2}{2}}\,. \tag{4.22}$$

As discussed in the Appendix B.1, the $2h - w^2 = \text{cst}$ parabolas correspond to the deterministic trajectories (excluding collision events) in the h, w plane. In this plane, the

$\{h > 0,\, w > 0\,, w^2 - 2h > 0\}$ domain is made of trajectories emanating from a collision event. Equation (4.21) thus states that the probability to find the system in this region is concentrated on the $w^2 - 2h = w_0^2$ branch: all trajectories with a collision collapse on this line when the two particles detach. As $w_0 \to 0$ (this limit being taken after the $\lambda \to \infty$ one), one obtains the ballistic limit of the stationary probability distribution of two active hard spheres. The marginal in space probability distribution can then be obtained from equations (4.21)-(4.22) as,

$$\begin{aligned} P(h) &= \int_{-\infty}^{+\infty} \frac{\mathrm{d}w_1 \mathrm{d}w_2}{2\pi} \exp\left(-\frac{w_1^2}{2} - \frac{w_2^2}{2}\right) P\left(h, w = \frac{w_2 - w_1}{\sqrt{2}}\right) , \\ &= \int_{-\infty}^{+\infty} \frac{\mathrm{d}w}{\sqrt{2\pi}} e^{-\frac{w^2}{2}} P(h, w)\,, \\ &= \Theta(h) \left[\frac{1}{2}\left(1 + \mathrm{erf}\left(\sqrt{h}\right)\right) + \frac{e^{-h}}{\sqrt{2\pi\,(2h + w_0^2)}}\right] + \left(\frac{1}{2} + \frac{w_0}{\sqrt{2\pi}}\right) \delta(h)\,. \end{aligned} \tag{4.23}$$

The distribution in Eq. (4.23) clearly shows an activity induced attraction between the two particles. The w_0 parameter of the sticky sphere potential allows to tune the amplitude of the attractive delta peak at contact. We remark that the purely repulsive case $w_0 = 0$ displays a $h^{-1/2}$ divergence of its bulk part while the latter has finite value at $h = 0$ in the attractive $w_0 > 0$ case. The attractive force monotonically depletes the small h region favoring adhesion at $h = 0$, as shown by the delta peak amplitude increasing with w_0.

Thermodynamic properties in the dilute limit

We return to the above mentioned general N-body dynamics Eq. (4.4). Deriving the macroscopic properties of the system, such as its two-point function, directly from the set of equations in Eq. (4.4) is in general a formidable task. Here we use the results obtained above to describe the thermodynamic properties of the stationary state of the process in Eq. (4.4) in the dilute limit. In the limits $\widehat{\varphi} \to 0$ and $\tau \to \infty$, the two point function of the system is given by that of the two-particle one,

$$g\left(\mathbf{r}, \mathbf{u}_1; \mathbf{r}', \mathbf{u}_2\right) = P(h, w)\,, \tag{4.24}$$

where the distribution P was previously derived in Eq. (4.18) with $h = d(|\mathbf{r} - \mathbf{r}'|/\sigma - 1)$ and $w = \sqrt{d}\,(\mathbf{u}_2 - \mathbf{u}_1) \cdot (\mathbf{r}' - \mathbf{r})/(\sqrt{2}|\mathbf{r} - \mathbf{r}'|)$. From Eq. (4.24), we compute the two important quantities introduced in Sec. 3.1: the effective self-propulsion $v(\widehat{\varphi})$ and the mechanical

pressure $p(\widehat{\varphi})$. From Eq. (3.15), the effective self-propulsion writes to first order in $\widehat{\varphi}$

$$\begin{aligned} v(\widehat{\varphi}) &= v_0 + \rho \int \mathrm{d}\mathbf{r} \frac{\mathrm{d}\mathbf{u}'}{\Omega_d} g(\mathbf{0}, \mathbf{u}; \mathbf{r}, \mathbf{u}') U'(r) \hat{\mathbf{r}} \cdot \mathbf{u} \\ &= v_0 + d^{3/2} \widehat{\varphi} \int \mathrm{d}h \, e^h \, \frac{\mathrm{d}w_1 \mathrm{d}w_2}{2\pi} \exp\left(-\frac{w_1^2}{2} - \frac{w_2^2}{2}\right) P\left(h, w = \frac{w_2 - w_1}{\sqrt{2}}\right) \frac{\widehat{U}'(h)}{\sigma} w_1 \\ &= v_0 \left(1 + \frac{\widehat{\varphi}}{\sqrt{2}} \int \frac{\mathrm{d}w_1 \mathrm{d}w_2}{2\pi} \exp\left(-\frac{w_1^2}{2} - \frac{w_2^2}{2}\right) \Gamma\left(w = \frac{w_2 - w_1}{\sqrt{2}}\right) \frac{w_2 - w_1}{\sqrt{2}} \, w_1\right) \\ &= v_0 \left(1 - \frac{\widehat{\varphi}}{2} \int \frac{\mathrm{d}w}{\sqrt{2\pi}} \exp\left(-\frac{w^2}{2}\right) \Gamma(w) \, w^2\right) \\ &= v_0 \left(1 - \frac{\widehat{\varphi}}{4} \left(1 + \frac{\sqrt{2} \, w_0^3}{3\sqrt{\pi}}\right)\right) , \end{aligned} \tag{4.25}$$

from which it appears clearly that at small density the slow-down of the effective self-propulsion induced by collisions increases with the stickiness of the potential. In order to go from the second to the third line of Eq. (4.25), we have used the regularization of the product $P\widehat{U}'(h)$ in the hard $\lambda \to \infty$ limit:

$$\lim_{\lambda \to \infty} P(h, w) \frac{\widehat{U}'(h)}{\sigma} = \widehat{v}_0 w \, \Gamma(w) \, \delta(h) \, . \tag{4.26}$$

A proof of Eq. (4.26) is given in Appendix B.1. Next we compute the equation of state for the mechanical pressure associated to Eq. (4.4). For a generic ζ (as opposed to Eq. (3.16) that was given for $\zeta = 1$), the expression reads

$$p(\widehat{\varphi}) = \rho \frac{v_0^2 \tau}{d\zeta} \frac{v(\widehat{\varphi})}{v_0} - \frac{\rho^2}{2d} \int \mathrm{d}\mathbf{r} \frac{\mathrm{d}\mathbf{u}_1}{\Omega_d} \frac{\mathrm{d}\mathbf{u}_2}{\Omega_d} g\left(0, \mathbf{u}; \mathbf{r}, \mathbf{u}'\right) U'(r) r \, . \tag{4.27}$$

which indeed reduces to Eq. (3.16) at $\zeta = 1$. Within the considered scalings,

$$\begin{aligned} &\frac{\rho^2}{2d} \int \mathrm{d}\mathbf{r} \frac{\mathrm{d}\mathbf{u}_1}{\Omega_d} \frac{\mathrm{d}\mathbf{u}_2}{\Omega_d} g\left(0, \mathbf{u}; \mathbf{r}, \mathbf{u}'\right) V'(r) r \, , \\ &= d\rho \frac{\widehat{\varphi}}{2} \sigma \widehat{v}_0 \int \frac{\mathrm{d}w_1}{\sqrt{2\pi}} \frac{\mathrm{d}w_2}{\sqrt{2\pi}} \exp\left(-\frac{w_1^2}{2} - \frac{w_2^2}{2}\right) \Gamma\left(w = \frac{w_2 - w_1}{\sqrt{2}}\right) w \\ &= d\rho \frac{\widehat{\varphi}}{2} \sigma \widehat{v}_0 \int \frac{\mathrm{d}w}{\sqrt{2\pi}} \exp\left(-\frac{w^2}{2}\right) \Gamma(w) \, w \\ &= -d\rho \frac{\widehat{\varphi}}{4} \frac{\sqrt{2} \sigma \widehat{v}_0}{\sqrt{\pi}} \left(1 - \frac{w_0^2}{2}\right) \, . \end{aligned} \tag{4.28}$$

Thus, up to second order in $\widehat{\varphi}$, we obtain the equation of state for the mechanical pressure in the presence of attractive attraction between the particles

$$\left(\frac{\Omega_d \sigma^d}{d^2}\right) \frac{p(\widehat{\varphi})}{d} = \widehat{\varphi} \frac{\widehat{v}_0^2 \widehat{\tau}_p}{\widehat{\zeta}} \left[1 - \frac{\widehat{\varphi}}{4} \left(1 + \frac{\sqrt{2} \, w_0^3}{3\sqrt{\pi}}\right)\right] + \frac{\widehat{\varphi}^2}{4} \frac{\sqrt{2} \sigma \widehat{v}_0}{\sqrt{\pi}} \left(1 - \frac{w_0^2}{2}\right) \, . \tag{4.29}$$

Note that in order for the two terms in the above expression to have the same scaling in d, we had to rescale the persistence time consistently with the ballistic hypothesis $\tau \gg 1$ as $\tau = d\widehat{\tau}$. We denote this scaling the ultraballistic one. For τ = O(1), the equation of state is indeed dominated by the second, equilibrium-like, term as we explained in the hard sphere case Eq. (3.47). Note also the manifestly destabilizing role of the sticky-sphere parameter w_0 on the homogeneous state suggested by this low density computation.

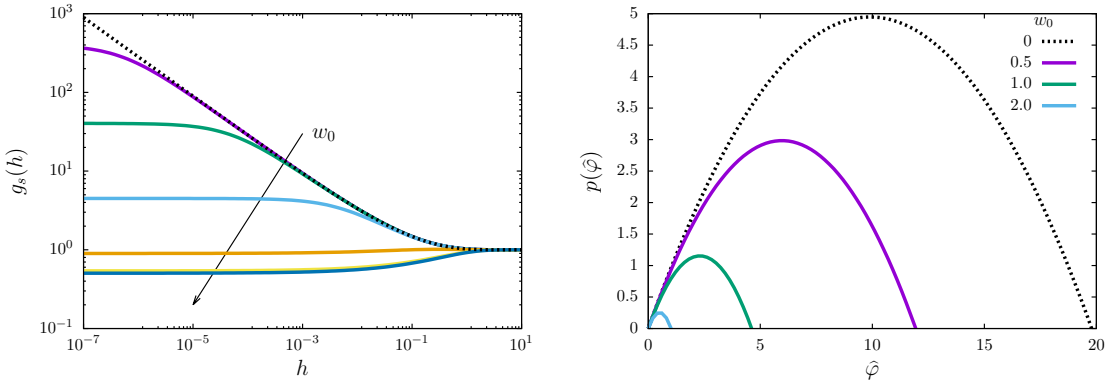

Figure 4.2: Left: pair distribution function $g_s(h) = P(h)$ vs h in the steady state for $w_0 = 0$ (purely repulsive case, black dashed line) and $w_0 = 10^{-3}, 10^{-2}, \ldots, 10^{2}$ (colored lines), Eq. (4.23). The repulsive case displays the $h^{-1/2}$ divergence, while the attractive $w_0 > 0$ curves have a finite limit at $h = 0$; the attractive force monotonically depletes the small h region favoring adhesion at $h = 0$, as shown by the delta peak amplitude increasing with w_0. Right: Pressure vs rescaled density as from Eq. (4.29), with $\widehat{\zeta} = \widehat{\tau}_p = \widehat{v}_0 = \sigma = 1$. Its behavior is non-monotonic and the decreasing region $p'(\widehat{\varphi}) < 0$ is a possible signal of motility-induced phase separation. The pressure becomes negative after a threshold value of $\widehat{\varphi}$, signaling the unphysical behavior of the computed result.

4.1.3 Results from dynamical mean-field theory

Microscopic dynamics and infinite-dimensional limit

The general DMFT of infinite-dimensional particle systems interacting through pair potentials and subject to external drivings has been derived in [2]. Here we address the dynamics of active particles introduced in Eq. (4.4). The dimensional scaling of self-propulsion, viscosity and density follows the prescriptions introduced in Sec. 4.1.1.

The DMFT framework allows one to describe the N-body, d-dimensional process in Eq. (4.4) by means of a two-body scalar process. It is a remarkable feature of the large dimensional limit that extends to the realm of the dynamics the results presented in Sec. 3.2 in the statics. Let us now briefly sketch the idea behind these equations [169]. Consider an arbitrary particle labeled 0. The force it experiences, beside the one-body self-propulsion one, is a sum over the many pairwise forces exerted by its neighbors. Conditioned on the knowledge of the trajectory of particle 0 from time 0 to time t, the latter can be seen as a

function of all the noises and initial positions of the other particles $i = 1, \dots, N$. It can thus be decomposed as the sum of its average plus a zero mean fluctuating part. On the one hand, because of the small displacement $|\delta \mathbf{r}_0(t)| \sim d^{-1/2}$ of particle 0 over time scales of order 1, the average part can be written to leading order in linear response theory and takes the form of a retarded friction. On the other hand, the fluctuating part is obtained as the sum over many weakly correlated pairwise forces and thus becomes Gaussian in the large d limit. Both the induced friction kernel and noise correlation function depend on the statistical properties of $U(\mathbf{r}_0 - \mathbf{r}_i)$ for any $i = 1, \dots, N$, *i.e.* on the properties of the two-body dynamics. The latter can be analyzed by repeating the same procedure while isolating two arbitrary particles. This closes the system by yielding self-consistent equations for the friction kernel and noise correlations. In [136], these equations have actually been originally derived in equilibrium using the dynamical partition function as a starting point. Its form indeed allows to adapt, in the space of trajectories instead of the configuration space, the analysis of Sec. 3.2. Alternative cavity-based proofs whose spirit was given in the above discussion have later been obtained [2, 130].

More precisely, it is known that when $d \to \infty$ the two-particle process can be determined self-consistently by analyzing the behavior of the rescaled inter-particle gap, *i.e.*

$$h(t) = h_0 + y(t) + \Delta_r(t) \approx d \left(\frac{r(t)}{\sigma} - 1 \right) , \tag{4.30}$$

where $r(t)$ is the relative distance between two reference particles (say i and j), $y(t) = (d/\sigma)\, \hat{\mathbf{r}}_0 \cdot (\mathbf{r}(t) - \mathbf{r}_0)$ is the rescaled projection of the relative displacement along the initial relative direction, and $\Delta_r(t) = (d/\sigma^2) \langle |\mathbf{r}_i(t) - \mathbf{r}_i(0)|^2 \rangle$ is the mean-square displacement (MSD) contribution given by the $d-1$ transverse components. The equation of motion for $y(t)$ can be shown to take the following form:

$$\begin{aligned} &\widehat{\zeta} \dot{y}(t) = -\kappa(t) y(t) + \int_0^t \mathrm{d}s\, \mathcal{M}_R(t,s)\, y(s) - \widehat{U}'(h_0 + y(t) + \Delta_r(t)) + \Xi(t) , \qquad y(0) = 0 , \\ &\langle \Xi(t) \rangle = 0 , \quad \langle \Xi(t) \Xi(s) \rangle = \mathcal{G}_C(t-s) + \mathcal{M}_C(t,s) , \qquad \mathcal{G}_C(t) = \widehat{v}_0^2 e^{-|t|/\tau} . \end{aligned} \tag{4.31}$$

The colored noise $\Xi(t)$ has two contributions: (i) the active self-propulsion with stationary time correlations $\mathcal{G}_C(t-s)$ and (ii) the kernel $\mathcal{M}_C(t,s)$, accounting for the force-force correlation given by pairwise interactions. The term $-\widehat{U}'(h(t))$ is the rescaled two-particle interaction force. Finally, as discussed above, DMFT also introduces the instantaneous and retarded response kernels, respectively $\kappa(t)$ and $\mathcal{M}_R(t,s)$, to describe the reaction of the N-body system on the two-particle process. The response and correlation kernels $\kappa(t)$,

$\mathcal{M}_R(t,s)$ and $\mathcal{M}_C(t,s)$ need to be determined self-consistently with the definitions

$$\begin{aligned}
\kappa(t) &= \frac{\widehat{\varphi}}{2}\int_{-\infty}^{\infty} \mathrm{d}h_0\, e^{h_0} g_0(h_0) \left\langle \widehat{U}''(h(t)) + \widehat{U}'(h(t)) \right\rangle_h \ , \\
\mathcal{M}_C(t,t') &= \frac{\widehat{\varphi}}{2}\int_{-\infty}^{\infty} \mathrm{d}h_0\, e^{h_0} g_0(h_0) \langle \widehat{U}'(h(t))\widehat{U}'(h(t'))\rangle_h \ , \\
\mathcal{M}_R(t,t') &= \frac{\widehat{\varphi}}{2}\int_{-\infty}^{\infty} \mathrm{d}h_0\, e^{h_0} g_0(h_0) \left.\frac{\delta\langle \widehat{U}'(h(t))\rangle_{h,\mathcal{P}}}{\delta\mathcal{P}(t')}\right|_{\mathcal{P}=0} \\
&= \frac{\widehat{\varphi}}{2}\int_{-\infty}^{\infty} \mathrm{d}h_0\, e^{h_0} g_0(h_0) \langle \widehat{U}''(h(t)) H(t,s)\rangle_h \ ,
\end{aligned} \tag{4.32}$$

where $g_0(h_0)$ is the initial gap distribution function, the perturbation $\mathcal{P}(t)$ acts in the pairwise interaction as $\widehat{U}'(h_0 + y(t) + \Delta_r(t)) \to \widehat{U}'(h_0 + y(t) + \Delta_r(t) - \mathcal{P}(t))$, and the fluctuating response is defined as $H(t,s) = \delta h(t)/\delta\mathcal{P}(s)|_{\mathcal{P}=0}$; its evolution is given by

$$\widehat{\zeta}\frac{\partial}{\partial t}H(t,t') = -\kappa(t)H(t,t') - \widehat{U}''(h(t))\left[H(t,t') - \delta(t-t')\right] + \int_{t'}^{t} \mathrm{d}s\, \mathcal{M}_R(t,s)H(s,t') \ . \tag{4.33}$$

The system is not yet closed, because of the MSD contribution given by $\Delta_r(t)$ in Eq. (4.31); the latter can be determined through the dynamical correlation and response. We introduce

$$\mathcal{C}(t,t') = \frac{d}{N}\sum_i \langle [\mathbf{r}_i(t) - \mathbf{r}_i(0)] \cdot [\mathbf{r}_i(t') - \mathbf{r}_i(0)]\rangle \ , \tag{4.34}$$

the rescaled two-times correlation function and

$$\mathcal{R}(t,t') = \frac{d}{N}\sum_{i,\mu}\left\langle \frac{\delta r_i^\mu(t)}{\delta\lambda_i^\mu(t')}\right\rangle \tag{4.35}$$

the rescaled response function of the one-body process. The perturbation acts in a standard way as $\zeta\dot{r}_i^\mu(t) = \ldots \to \zeta\dot{r}_i^\mu(t) = \cdots + \lambda_i^\mu(t)$. The correlation and response function obeys,

$$\begin{aligned}
\widehat{\zeta}\frac{\partial}{\partial t}\mathcal{C}(t,t') =& 2\widehat{\zeta}T\mathcal{R}(t',t) - \kappa(t)\mathcal{C}(t,t') + \int_0^t \mathrm{d}s\, \mathcal{M}_R(t,s)\mathcal{C}(s,t') \\
&+ \int_0^{t'} \mathrm{d}s\, \left[\mathcal{G}_C(t-s) + \mathcal{M}_C(t,s)\right]\mathcal{R}(t',s) \ , \\
\widehat{\zeta}\frac{\partial}{\partial t}\mathcal{R}(t,t') =& \frac{\delta(t-t')}{2} - \kappa(t)\mathcal{R}(t,t') + \int_{t'}^t \mathrm{d}s\, \mathcal{M}_R(t,s)\mathcal{R}(s,t') \ .
\end{aligned} \tag{4.36}$$

By definition, one has $\Delta_r(t) = \mathcal{C}(t,t)$, and the dynamical equations are at this stage closed. The evolution equation for the MSD $\Delta(t,t') = \frac{d}{\sigma^2}\langle|\mathbf{r}_i(t) - \mathbf{r}_i(t')|^2\rangle$ and $\Delta_r(t) \equiv \Delta(t,0)$

therefore read

$$\begin{aligned}\widehat{\zeta}\frac{\partial}{\partial t}\Delta(t,t') =& -\kappa(t)\left[\Delta(t,t')+\Delta_r(t)-\Delta_r(t')\right]-4\widehat{\zeta}T\,\mathcal{R}(t',t)\\ &+\int_0^t \mathrm{d}s\,\mathcal{M}_R(t,s)\left[\Delta_r(t)-\Delta_r(t')+\Delta(s,t')-\Delta(s,t)\right]\\ &+2\int_0^{\max(t,t')}\mathrm{d}s\,\left[\mathcal{G}_C(t-s)+\mathcal{M}_C(t,s)\right]\left[\mathcal{R}(t,s)-\mathcal{R}(t',s)\right]\,, \qquad (4.37)\\ \widehat{\zeta}\dot{\Delta}_r(t) =& -2\kappa(t)\Delta_r(t)+\int_0^t \mathrm{d}s\,\mathcal{M}_R(t,s)\left[\Delta_r(t)+\Delta_r(s)-\Delta(s,t)\right]\\ &+2\int_0^t \mathrm{d}s\,\left[\mathcal{G}_C(t-s)+\mathcal{M}_C(t,s)\right]\mathcal{R}(t,s)\,.\end{aligned}$$

Dilute solution with infinite persistence

The analytical solution of the problem determined by Eqs. (4.31-4.36) is currently out of reach. In the equilibrium case, these equations simplify thanks to fluctuation-dissipation relations and a numerical solution has been found [138]. In the present case, a numerical solution must deal with strong technical difficulties, the main one being the sampling efficiency at long times: indeed, particles with infinite persistence time eventually collide with a rate that is exponentially decaying in time. Therefore, the amount of trajectories needed to compute the dynamical kernels at long time is exponentially high. A possible solution may involve the generation of biased trajectories to increase efficiency, but its design goes beyond the scope of this article.

It is however possible to derive an analytical solution in the dilute limit: indeed, the implicit equations (4.32) for the kernels depend on the density only through a global multiplicative coefficient. Therefore, a solution for *e.g.* the instantaneous response $\kappa(t)$ reads

$$\kappa(t) = \widehat{\varphi}\,\mathcal{F}\left[\kappa, \mathcal{M}_R, \mathcal{M}_C\right](t)\,. \qquad (4.38)$$

The self-consistent kernels are given by the fixed points of Eq. (4.38). An iterative solution can be found assuming that the low-density limit is continuous and that the series

$$\kappa(t) = \widehat{\varphi}\,\kappa^{(1)}(t) + \widehat{\varphi}^2\kappa^{(2)}(t) + \dots\,. \qquad (4.39)$$

converges.

When $\widehat{\varphi} = 0$, the kernels are trivially vanishing because no interaction occurs. In the dilute limit $\widehat{\varphi} \ll 1$, the solution can be approximated by the first-order expansion in Eq. (4.39). The latter can be analytically computed in the infinite persistence time limit $\tau \to \infty$: indeed, in that case the active force reduces to a constant driving and, in absence of dynamical kernels, the trajectories in Eq. (4.31) are fully determined by the self-propulsion $\Xi(t) \equiv \Xi_0$ drawn at $t = 0$.

The solution of the fluctuating equations (4.31) and (4.33) can be then computed imposing $\kappa(t) = \mathcal{M}_R(t,t') = \mathcal{M}_C(t,t') = 0$ and plugging the trajectories $h(t)$ into Eqs. (4.32) to compute the first-order kernels.

Analytical solution in the dilute limit: trajectories and pair distribution function

In the case of vanishing kernels, the response and correlation read

$$\begin{aligned} \mathcal{R}(t,t') &= \frac{1}{2\widehat{\zeta}}\,\theta(t-t')\;, \\ \mathcal{C}(t,t') &= \frac{\widehat{v}_0^2}{2\widehat{\zeta}^2}\,t\,t' \quad \Rightarrow \quad \Delta(t,t') = \frac{\widehat{v}_0^2}{2\widehat{\zeta}^2}(t-t')^2\;. \end{aligned} \tag{4.40}$$

This result depends on a natural time scale $\tau_0 = \widehat{\zeta}/\widehat{v}_0$, which represents the typical duration of a collision, as it is the time needed to traverse a distance σ/d at speed v_0. This time scale must not be confused with τ, which we recall to be the persistence time of the active self-propulsion. In the following, we will set $\widehat{\zeta} = \widehat{v}_0 = 1$, setting τ_0 as unit of time and $\widehat{v}_0$ as unit of energy; the dimensional coefficients will be reinstated in the final results. The solution in Eq. (4.40) leads to the dynamical equation for $h(t) = h_0 + y(t) + \Delta_r(t)$

$$\begin{gathered} \dot{h}(t) = -\widehat{U}'(h(t)) + \xi_0 + t\;, \quad h(0) = h_0 \\ \langle \xi_0 \rangle = 0\;, \quad \langle \xi_0^2 \rangle = 1\;, \end{gathered} \tag{4.41}$$

having now called $\Xi(t) = \Xi_0 = \widehat{v}_0\,\xi_0$. The equation for the fluctuating response $H(t,t')$ now reads

$$\frac{\partial}{\partial t} H(t,t') = -\widehat{U}''(h(t))\,[H(t,t') - \delta(t-t')]\;. \tag{4.42}$$

The last equations must be solved with an appropriate choice of the potential. We consider a sticky-sphere potential as defined in Eq. (4.16), always taking $\widehat{v}_0 = 1$, and will study the dynamics in the same limit with $\lambda \to \infty$ corresponding to a hard core and an infinitely narrow attractive region, with a constant adhesive force when $h = 0$.

Our goal is to compute the pair distribution function and the dynamical kernels based on the dynamical equations above. The first one is given by [2]

$$g(h,t) = e^{-h} \int \mathrm{d}h_0\, g_0(h_0)\, e^{h_0}\, \langle \delta(h(t) - h) \rangle_{h_0}\;, \tag{4.43}$$

where $\langle \ldots \rangle_{h_0}$ refers to an average over the trajectory realizations conditioned to the initial condition $h(0) = h_0$. In our settings, this average is equivalent to the average over the unitary normal variable ξ_0. The pair distribution evolution depends on the initial distribution $g_0(h_0)$; however, the steady state limit must not depend on its choice, so we choose to work with $g_0(h_0) = \theta(h_0 - 1/\lambda)$, so that the particles are not interacting at the initial time.

Given these premises, the pair distribution function can be directly computed in the hard-sphere limit. Indeed, when $\lambda \to \infty$, the particles are unable to overlap at $h < 0$, and feel a finite attractive force with strength w_0 when $h = 0$. The trajectories can be then divided into external and colliding ones. The former simply follow a ballistic motion with initial velocity ξ_0 and unitary acceleration; the latter are divided in three zones: (i) a ballistic motion for $t < t_1$, being t_1 the starting time of the collision; (ii) the sticky collision, *i.e.* $h(t) = 0$ for $t_1 < t < t_2$, being t_2 the time when the particle leaves the barrier; (iii) a ballistic motion for $t > t_2$. Namely,

$$h(t) = h_0 + \xi_0\, t + \frac{1}{2}t^2 \qquad \text{for external trajectories,} \tag{4.44}$$

and

$$h(t) = \begin{cases} h_0 + \xi_0\, t + \frac{1}{2}t^2 & t < t_1 = -\xi_0 - \sqrt{\xi_0^2 - 2h_0} \\ 0 & t_1 < t < t_2 = -\xi_0 + w_0 \\ \frac{1}{2}\left[(t+\xi_0)^2 - w_0^2\right] & t > t_2 \end{cases} \qquad \text{for colliding trajectories.} \tag{4.45}$$

At any time t, $h(t)$ is determined by the values of ξ_0 and h_0; the trajectories at contact with the barrier will contribute to the delta peak in $h = 0$, while the trajectories with $h > 0$ will give the regular part of the pair distribution function. Injecting the solution above into the equation for $g(h,t)$ one has the time-dependent solution

$$\begin{aligned} g(h,t) &= G(t)\,\delta(h) + g_r(h,t)\ , \\ G(t) &= \begin{cases} \frac{t}{\sqrt{2\pi}} & \text{for } t < w_0 \\ \frac{1}{2} + \frac{w_0}{\sqrt{2\pi}} - \frac{1}{2}\mathrm{erfc}\frac{t-w_0}{\sqrt{2}} & \text{for } t > w_0 \end{cases}\ , \\ g_r(h,t) &= \begin{cases} \frac{1}{2}\left(1 + \mathrm{erf}\sqrt{h}\right) + \frac{e^{-h}}{\sqrt{2\pi(2h+w_0^2)}}\left[1 - e^{-\frac{1}{2}\left(t-\sqrt{2h+w_0^2}\right)^2}\right] & \text{for } 0 < h < \frac{t^2-w_0^2}{2}\ , \\ \frac{1}{2}\left(1 + \mathrm{erf}\sqrt{h}\right) & \text{for } \frac{t^2-w_0^2}{2} < h < \frac{t^2}{2}\ , \\ \frac{1}{2}\left[1 + \mathrm{erf}\left(\frac{2h+t^2}{2\sqrt{2}\,t}\right)\right] & \text{for } h > \frac{t^2}{2}\ , \end{cases} \end{aligned} \tag{4.46}$$

leading to the steady state limit for $t \to \infty$:

$$g_s(h) = \Theta(h)\left[\frac{1}{2}\left(1 + \mathrm{erf}\sqrt{h}\right) + \frac{e^{-h}}{\sqrt{2\pi(2h+w_0^2)}}\right] + \left(\frac{1}{2} + \frac{w_0}{\sqrt{2\pi}}\right)\delta(h)\ . \tag{4.47}$$

This result is equivalent to Eq. (4.23) in the steady state, and adds new information on the transient behavior of the pair distribution function. In particular, the delta peak emerges continuously with time and has a singular behavior at $t = w_0$, exactly when the particles can start to detach after a collision.

Dynamical kernels

The computation of dynamical kernels requires the evaluation of the potential and its derivatives, and thus cannot be performed in the hard limit $\lambda \to \infty$, since in that case all these terms are singular. We then need to solve the equations of motion for the regular potential in Eq. (4.16). Those can be solved by parts for three interaction scenarios: (i) the external case $h(t) > 1/\lambda$ for all t, (ii) the colliding case $h(t) < 0$ at some t and (iii) an intermediate, tangential case for which there exists $h(t) < 1/\lambda$ but $h(t) > 0$ at any t, which means that the particles enter the mutual attraction region but never get to the repulsive core. This case disappears in the hard potential limit, where the width of the attractive region vanishes, but must be nevertheless accounted for in the course of the kernel computation.

The details of the computation are reported in Appendix B.2.1. As can be foreseen from Eqs. (4.32) the response kernels $\kappa(t)$ and $\mathcal{M}_R(t,s)$ are divergent in the hard-sphere limit;

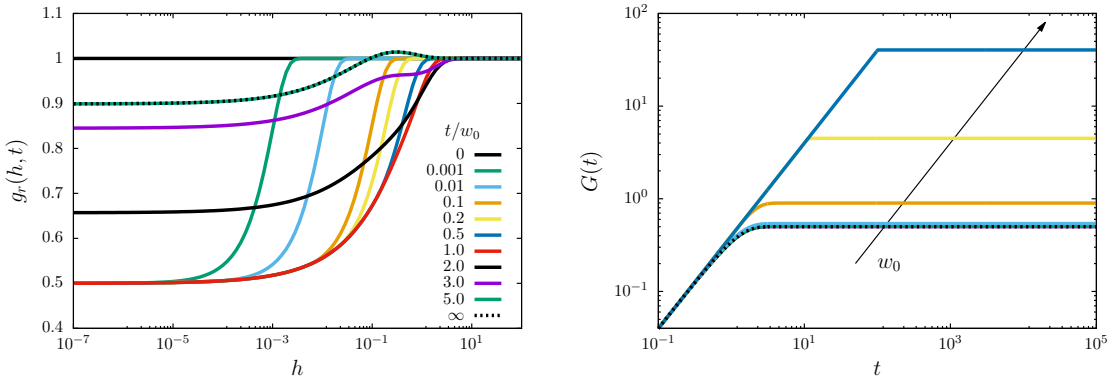

Figure 4.3: Left: the regular part of the pair distribution function $g_r(h,t)$ vs h at several times (see key), given by Eq. (4.46) with $w_0 = 1$. The small-gap region $h \ll 1$ is rapidly depleted by means of adhesive collisions. When $t > w_0$, the self-propulsion overcomes the attractive force, the particles leave the adhesive boundary and the small h region becomes populated again. Right: the delta peak amplitude $G(t)$ vs t for $w_0 = 0$ (purely repulsive case, black dashed line) and $w_0 = 10^{-3}, 10^{-2}, \ldots, 10^{2}$ (colored lines). The linear growth at short times is followed by a steady state at longer times, where $G(t) \to 1/2 + w_0/\sqrt{2\pi}$.

however, their divergences compensate in that limit, as shown in Appendix B.2.3. We also argue that in the hard-sphere limit the repulsive interactions give rise to a short-ranged memory kernel $\mathcal{M}_R(t,s)$: as shown in Appendix B.2.2, the fluctuating response vanishes over a time scale proportional to λ^{-1} and therefore only the near past of a dynamical variable contributes to the response term. The integrated response can be then expanded as

$$\begin{aligned}\int_0^t \mathrm{d}s\, \mathcal{M}_R(t,s)\, f(s) &= \int_0^t \mathrm{d}s\, \mathcal{M}_R(t,s) \left[f(t) - \dot{f}(t)(t-s) + \frac{1}{2}\ddot{f}(t)(t-s)^2 + \ldots \right] \\ &= \chi_0(t)\, f(t) - \chi_1(t)\, \dot{f}(t) + \frac{1}{2}\chi_2(t)\, \ddot{f}(t) + \ldots \,,\end{aligned} \tag{4.48}$$

being $f(s)$ is a continuous function of time. The latter equation is nothing but a Taylor expansion of the function $f(s)$ in the integral for $s \approx t^-$, assuming that the response kernel $\mathcal{M}_R(t,s)$ is peaked at $s = t$ and rapidly decaying over time. The integrated response moments $\chi_n(t)$ are defined as

$$\chi_n(t) \equiv \int_0^t \mathrm{d}s\, \mathcal{M}_R(t,s)\, (t-s)^n \,. \tag{4.49}$$

It is shown in Appendix B.2.4 that the moments with $n \geq 2$ vanish in the hard-sphere limit. The physical picture behind the short-rangeness of the memory kernel is the following. Whenever, in the original dynamics, the interaction potential between any two particles, say i and j, is non-vanishing then it must exactly compensate the projection of their relative instantaneous velocity along the direction $\hat{\mathbf{r}}_{ij}$. It thus comes as no surprise that in the DMFT framework too the average force exerted on the particle does not depend on the remote past of the trajectory. Using this property, the general motion equation (4.31) for $y(t)$ can be approximated for $\lambda \gg 1$ as

$$\widehat{\zeta}\dot{y}(t) = -\gamma(t)\, y(t) - \chi_1(t)\, \dot{y}(t) - \widehat{U}'(h(t)) + \Xi(t) \,, \tag{4.50}$$

where $\gamma(t) \equiv \kappa(t) - \chi_0(t)$, and the same transformation can be applied to all the dynamical equations containing the two reaction terms $\kappa(t)$ and $\mathcal{M}_R(t,s)$. Their physical meaning is transparent: the first coefficient $\gamma(t)$ is an elastic coefficient and we expect it to vanish in the long-time limit, since we are in the dilute phase and the individual trajectories are not dynamically arrested near their initial position. The second coefficient gives the first-order density correction to the bare friction coefficient $\widehat{\zeta}$, the main information needed to understand how a small density affects the dynamics. We also underline that this expansion does not depend on the low density assumption but on the hard-sphere interactions, and holds at any density.

The computation of the dynamical kernels is tedious and mostly technical, and is therefore deferred to Appendix B.2.3. It relies on the computation of the two-particle process $h(t)$ and on the fluctuating response $H(t,s)$, which are respectively performed in Appendix B.2.1 and B.2.2. Altogether, in the long-time limit one gets

$$\gamma_\infty = 0\,, \quad \chi_1^\infty = \frac{\widehat{\varphi}}{4}\widehat{\zeta}\left(1 + \frac{\sqrt{2}}{3\sqrt{\pi}} w_0^3\right) \equiv \frac{\widehat{\varphi}}{\widehat{\varphi}_0(w_0)}\,\widehat{\zeta}\,. \tag{4.51}$$

Effective self-propulsion

The last result allows us to compute the effective self-propulsion in the steady state, namely the velocity along the self-propulsion direction. To do so, we write the equation for the displacement of a generic particle $\delta\mathbf{r}_i(t) = \mathbf{r}_i(t) - \mathbf{r}_i(0)$, derived through a dynamical cavity method, before the infinite-dimensional rescaling [2]. Since all particles are equivalent the label i is dropped in the following. This reads

$$\begin{aligned} \zeta\dot{\delta\mathbf{r}}(t) &= -k(t)\delta\mathbf{r}(t) + \int_0^t \mathrm{d}s M_R(t,s)\delta\mathbf{r}(s) + \mathbf{v}(t) + \boldsymbol{\xi}(t)\,, \\ \langle f_\mu(t)\rangle &= 0\,, \quad \langle f_\mu(t) f_\nu(t')\rangle = \delta_{\mu\nu}\,\Gamma_C(t-t')\,, \\ \langle \xi_\mu(t)\rangle &= 0\,, \quad \langle \xi_\mu(t)\xi_\nu(t')\rangle = \delta_{\mu\nu} M_C(t,t')\,. \end{aligned} \tag{4.52}$$

Note that, as we mentioned while presenting the spirit of the DMFT framework, the one-particle equation has the same functional form as the two-particle one Eq. (4.31) (without of course the pair potential $\widehat{U}$). Indeed, as we have seen before in the static equilibrium case, if a particle of the active fluid interacts with a given tagged particle i, it has no way to interact (nor to have interacted in the past over time scales of order $O(1)$) with another given tagged particle j next to i. The only thing the fluid particle knows about is the trajectory of particle i, which can however be modified by the presence of particle j through their direct pair interaction. This is in spirit the argument that allows to obtain the two-body process Eq. (4.31) from a mere subtraction of two independent one-body ones coupled by a pair-potential (subsequent projections are needed to reach the scalar form in Eq. (4.31)). We then define the dynamical observable $A(t,t')$

$$A(t,t') = \frac{\zeta}{v_0}\,\langle \delta\mathbf{r}(t)\cdot\mathbf{v}(t')\rangle\,, \tag{4.53}$$

measuring the total displacement at time t along the direction of the active force at time t'. This quantity leads to the definition of the effective propulsion $v(\widehat{\varphi})$ as

$$v(\widehat{\varphi}) = \frac{\partial}{\partial t} A(t,t') \bigg|_{t=t'} = \frac{1}{v_0} \left\langle \zeta \dot{\delta \mathbf{r}}(t) \cdot \mathbf{v}(t) \right\rangle \ . \tag{4.54}$$

At zero density, the free-particle is moving at the bare self-propulsion speed v_0, and we expect $v(\widehat{\varphi})$ to decrease monotonically with the density. The quantity $A(t,t')$ follows the dynamical equation

$$\partial_t A(t,t') = -k(t)A(t,t') + \int_0^t \mathrm{d}s\, M_R(t,s)A(s,t') + \frac{d\zeta}{v_0}\Gamma_C(t-t') \ , \tag{4.55}$$

having exploited the independence between the active noise and the bath noise, *i.e.* $\langle \boldsymbol{\xi}(t) \cdot \mathbf{v}(t') \rangle = 0$. When $t, t' \to \infty$, we obtain the steady-state dynamical equation

$$\zeta \partial_t A(t,t') = -g(t)A(t,t') - c_1(t)\partial_t A(t,t') + \frac{d\zeta}{\hat{v}_0}\Gamma_C(t-t') \ , \tag{4.56}$$

where $g(t) = k(t) - \int_0^t \mathrm{d}s\, M_R(t,s) = (2d^2/\sigma^2)\gamma(t) \to 0$ and $c_1(t) = \int_0^t \mathrm{d}s\, M_R(t,s)\,(t-s) = (2d^2/\sigma^2)\chi_1(t) \to c_1^\infty$ when $t \to \infty$. The last results hold for $\Gamma_C(t-t') = v_0^2/d$, and the stationary friction correction reads $c_1^\infty = \zeta(1 + \widehat{\varphi}/\widehat{\varphi}_0)$. So, Eq. (4.54) gives us

$$v(\widehat{\varphi}) = \frac{v_0}{1 + \widehat{\varphi}/\widehat{\varphi}_0(w_0)} \ . \tag{4.57}$$

This is the fundamental result of this calculation. We show then that, to the first order in $\widehat{\varphi}$, the effective propulsion in a dilute media is damped by a factor $1 + \widehat{\varphi}/\widehat{\varphi}_0(w_0)$, accounting for the slowing down of particles' velocity caused by interactions. Considering the dilute limit approximation $\widehat{\varphi} \ll 1$, its first-order expansion in $\widehat{\varphi}$ coincides with the result obtained from Fokker-Planck equation in Eq. (4.25).

4.1.4 Transient behavior of Hard Spheres

When $w_0 = 0$, we recover the purely repulsive hard-sphere interaction potential, namely

$$\widehat{U}_{\mathrm{HS}}(h) = \begin{cases} \infty & h < 0 \\ 0 & h > 0 \end{cases} \ . \tag{4.58}$$

All calculations above are valid for the case $w_0 = 0$. Furthermore, in this case one can also compute the transient dynamics of the dynamical kernels defined in Eqs. (4.32), which were analytically unattainable in the general sticky spheres case. With the same procedure as in the previous section, we approximate the hard-sphere potential with a soft-sphere one, namely $\widehat{U}(h) = \frac{\epsilon}{2} h^2 \theta(-h)$. The hard-sphere potential is recovered in the $\epsilon \to \infty$ limit. This soft-sphere potential is equivalent to the sticky-sphere one defined in Eq. (4.16), in the limit $w_0 \to 0$ and $\lambda \to \infty$ keeping $\lambda w_0 = \epsilon$ fixed, and it is the same interaction potential already analyzed in the solution of equilibrium dynamics presented in [138].

This choice makes the analytical computation of the dynamical kernels much easier; indeed, one can follow the same scheme described for sticky spheres to access the pair distribution function $g(h,t)$ and the dynamical kernels $\kappa(t)$, $\mathcal{M}_R(t,t')$ and $\mathcal{M}_C(t,t')$. The pair distribution function evolution is given by Eq. (4.46), setting $w_0 = 0$ (and so its steady state). For the dynamical kernels, we can avoid the limit $t \to \infty$ in their calculation; we get then the first integrated response moments, finally leading to

$$\begin{aligned}
\gamma(t) &= \frac{\widehat{\varphi}}{2}\widehat{v}_0 \left[\frac{e^{-t^2/2}}{\sqrt{2\pi}} - \frac{t}{2}\operatorname{erfc}\left(\frac{t}{\sqrt{2}}\right)\right] , \\
\chi_1(t) &= \frac{\widehat{\varphi}}{4}\widehat{\zeta}\operatorname{erf}\left(\frac{t}{\sqrt{2}}\right) , \\
\mathcal{M}_C(t,t') &= \frac{\widehat{\varphi}}{4}\widehat{v}_0^2 \left[\operatorname{erfc}\left(\frac{|t-t'|}{\sqrt{2}}\right) + \operatorname{erfc}\left(\frac{t}{\sqrt{2}}\right)(1+tt') - \sqrt{\frac{2}{\pi}}t'\, e^{-t^2/2}\right] ,
\end{aligned} \tag{4.59}$$

always expressing the time t in units of the natural time scale $\tau_0 = \widehat{\zeta}/\widehat{v}_0$. The steady-state limit is the same as that described for the sticky-sphere case, *i.e.* $\gamma_\infty = 0$ and $\chi_1^\infty = \widehat{\varphi}\widehat{\zeta}/4 \equiv \widehat{\varphi}\widehat{\zeta}/\widehat{\varphi}_0$. Furthermore, we can characterize the noise correlation in the long-time limit, where it only depends on the time difference $s = t - t'$, namely

$$\mathcal{M}_C^\infty(s) = \frac{\widehat{\varphi}}{4}\widehat{v}_0^2 \operatorname{erfc}\frac{|s|}{\sqrt{2}} . \tag{4.60}$$

The above result thus reintroduces in the steady state dynamics to first order in $\widehat{\varphi}$ a colored noise that hampers our attempts to go further in the density expansion. The time scale over which this noise is correlated is set by the typical duration of a collision. Equation (4.60) allows us to derive the behavior of the MSD in the long-time limit; indeed, with the kernels computed in Eq. (4.59), the correlation-response equations now read

$$\begin{aligned}
\widehat{\zeta}\frac{\partial}{\partial t}\mathcal{R}(t,t') &= \frac{\delta(t-t')}{2} - \gamma(t)\mathcal{R}(t,t') - \chi_1(t)\frac{\partial}{\partial t}\mathcal{R}(t,t') , \\
\widehat{\zeta}\frac{\partial}{\partial t}\mathcal{C}(t,t') &= -\gamma(t)\mathcal{C}(t,t') - \chi_1(t)\frac{\partial}{\partial t}\mathcal{C}(t,t') + \int_0^{t'} \mathrm{d}s\, \left[\mathcal{G}_C(t-s) + \mathcal{M}_C(t,s)\right]\mathcal{R}(t',s) .
\end{aligned} \tag{4.61}$$

The first equation can be explicitly solved in the steady-state limit, giving

$$\mathcal{R}^\infty(s) = \frac{1}{2\widehat{\zeta}(1+\widehat{\varphi}/\widehat{\varphi}_0)}\theta(s) . \tag{4.62}$$

With this result, and from Eq. (4.37), one can derive an equation for the MSD in the steady-state limit $t, t' \gg 1$, as a function of the dimensionless time difference $s = t - t'$, *i.e.*

$$\dot{\Delta}(s) = \frac{1}{(1+\widehat{\varphi}/\widehat{\varphi}_0)^2}\left\{s + \frac{\widehat{\varphi}}{\widehat{\varphi}_0}\left[s\operatorname{erfc}\frac{s}{\sqrt{2}} + \sqrt{\frac{2}{\pi}}\left(1 - e^{-s^2/2}\right)\right]\right\} , \tag{4.63}$$

and this equation can be easily integrated, yielding

$$\Delta(s) = \frac{1}{(1+\widehat{\varphi}/\widehat{\varphi}_0)^2}\left\{\frac{s^2}{2} + \frac{\widehat{\varphi}}{\widehat{\varphi}_0}\left[\frac{s}{\sqrt{2\pi}}\left(2 - e^{-s^2/2}\right) - \frac{1}{2}\operatorname{erf}\frac{s}{\sqrt{2}} + \frac{s^2}{2}\operatorname{erfc}\frac{s}{\sqrt{2}}\right]\right\} . \tag{4.64}$$

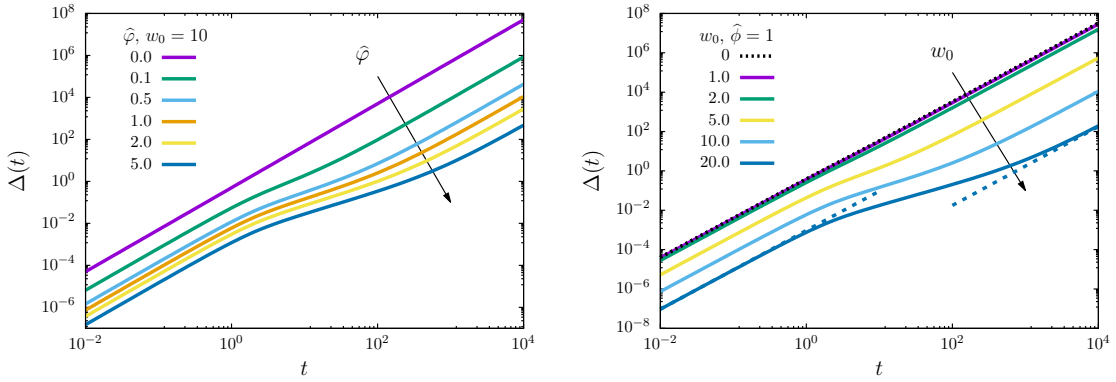

Figure 4.4: Mean squared displacement $\Delta(t)$ vs t from Eq. (4.64) for several values of rescaled density $\widehat{\varphi}$ (left, $w_0 = 10$) and attractive force w_0 (right, $\widehat{\varphi} = 1$). The MSD is ballistic at short and long times, but the increase in density or in adhesion induces a slowdown at intermediate times, respectively given by the many-body interactions or the duration of an adhesive collision. We compare the short and long time behavior from Eq. (4.65) for the case $w_0 = 20$ in the right panel (dashed blue lines).

The solution above shows that the dynamics is ballistic at short and long times (this comes as no surprise given that we have taken the limit $\tau \to \infty$), with a slowdown at intermediate times given by the presence of interactions. With the effective propulsion definition computed in Eq. (4.57), it is clear that

$$\Delta(s) \sim \frac{v(\widehat{\varphi})^2}{2\widehat{\zeta}^2} s^2 \times \begin{cases} 1 + \widehat{\varphi}/\widehat{\varphi}_0 & s \ll \tau_0 \\ 1 & s \gg \tau_0 \end{cases} \tag{4.65}$$

with $\tau_0 = \widehat{\zeta}/\widehat{v}_0$. The last result contains two pieces of information: one is the MSD at short times, which is ballistic with a contribution from the self-propulsion $\mathbf{v}(t)$ and from the force exerted by the surrounding particles $\boldsymbol{\xi}(t)$; the equal-time variance of the latter gives the additional contribution $\widehat{\varphi}/\widehat{\varphi}_0$ in the first line. At long times, interactions decorrelate (at least in the dilute phase) and the MSD is dominated by the ballistic contribution from the infinitely persistent self-propulsion, so the particle maintains its velocity $v(\widehat{\varphi})$. To first order in the density, the long-time MSD is thus the same as that of a free particle with a rescaled self-propulsion speed $v_0 \to v(\widehat{\varphi})$. This is in agreement with the numerical observation of [196].

4.1.5 Conclusions

In this section, we studied, in the low density/high persistence time regime, the behavior of self-propelled sticky spheres in infinite dimension. The considered sticky sphere potential generalizes the hard-sphere one and introduces a new parameter w_0 with which the propensity of two particles to stick together increases. We derived the associated stationary two-point distribution function and the corresponding effective self-propulsion both from the dilute limit of the BBGKY hierarchy and within the DMFT framework. In particular, we

have shown that the larger w_0 is the fastee the decay of the effective self-propulsion with the density $\widehat{\varphi}$ is.

The last part of our analysis has been dedicated to the transient behavior of hard spheres by means of dynamical mean-field theory; it has been shown how, starting from an equilibrium configuration, the system relaxes towards a stationary state. This relaxation is described by the transient part of the dynamical coefficients, and in this limit we computed the MSD in the steady state, elucidating how the interplay between active self-propulsion and interactions affects its short-time behavior, while the infinitely persistent self-propulsion dominates at long times.

These results constitute a starting point for a more complete analysis of active systems in high dimensions. The next step along this line of research is its extension to higher densities and finite persistence times. This task being severely hard to accomplish via analytical tools, a numerical solution of DMFT equations must be found, in line with previous results [181, 138]. However, if the self-propulsion is too strong or too persistent, the trajectories drift away and the solution relies on the statistics of exponentially rare events. The development of importance-based algorithms is then required and would give an important edge in the solution of the problem at any density.

Another approach that may be tackled in the future concerns the limit of small persistence time; in that case, often studied in active matter systems [60, 57], the dynamics can be perturbatively studied starting from the equilibrium solution. Its analysis would lead to understand how a small amount of activity affects the dynamics, *i.e.* the behavior of dynamical kernels, the interplay between the dynamical transition and the crowding transition, and the effects on fluctuation-dissipation relations.

4.2 An approximate resummation scheme for active matter in the ballistic limit

In this section, we study the steady state of infinite dimensional RTPs beyond the dilute limit. The N-body stationary distribution function being unknown in that case, the approach of Frisch and collaborators [68], based on an exact truncation of the density expansion of the free energy functional of standard equilibrium fluids at large d, is not available. Instead we use the BBGKY hierarchy of correlation functions as a starting point. In Sec. 3.2, we showed that one could recover the results of [68] for equilibrium systems through its exact resummation at large d. Here we start by using the Kirkwood approximation as a closure of the BBGKY hierarchy. We show that in infinite dimension the latter is unable to account for the rich behavior of self-propelled particle systems observed in low dimension. We claim that this is not a peculiarity of the infinite dimensional limit but rather a failure of the Kirkwood approximation to accurately describe the system. In Sec. 4.2.2, we devise a strategy for resumming the BBGKY hierarchy that clearly highlights the role of multibody interactions. This strategy was presented in [175]. We originally believed the induced resummation was exact in the limit $d \to \infty$ and that was one of the claims of [175]. We now know that the proposed resummation only partially takes into account these effects.

An erratum is being written out. I would like to stress here that my understanding of the importance of multibody effects in infinite dimensional systems, in particular in regards with the results of Dynamical Mean Field Theory, greatly benefited from discussions with Francesco Zamponi and Giulio Biroli, Alessandro Manacorda and Chen Liu. Here we give an account of the proposed resummation scheme with a particular emphasis on which contributions are taken into account and which are not. While [175] was restricted to the study of hard spheres, we extend here these results by considering the sticky sphere potential introduced in Sec. 4.1. The results we obtain are hence the fruit of a partial resummation of the density expansion in infinite dimension. They should thus be taken with caution by the reader and presented with modesty by us. They however allow to grasp some interesting physical effects and yield equally interesting results. We therefore hope they can bring some insights into the structure of active fluid beyond two-body (a field that has not been much studied, a notable exception being [93]) and the importance of multibody interactions in active matter.

Throughout this section, we use scalings very similar to those of Sec. 4.1. However, we set $\zeta = 1$. The friction coefficient ζ can indeed be absorbed into a redefinition of time. In the scalings of Sec. 4.1, this would amount to working with $\tau = \hat{\tau}/d^2$. Instead, here, we choose to work in the ultra ballistic limit $\tau = \hat{\tau}/d$. Together with $v_0 = \sqrt{2}\hat{v}_0 d^{3/2}$, this guarantees that the product $v_0\tau/\sqrt{d}$ remains finite in the large d limit, so as to maintain a competition between activity and repulsive pairwise interactions in the equation of state, see Eq. (3.47). In these scalings, the typical duration of a collision between two particles is $O(1/d^2)$ (it was $O(1)$ in Sec. 4.1), $O(1/d)$ less than the time it takes for a particle to flip its orientation.

4.2.1 Kirkwood approximation in infinite dimensional active matter

In Sec. 3.2, we have completely characterized the structure of standard equilibrium infinite dimensional fluids. In particular, the Kirkwwod approximation becomes exact is this limit as a direct consequence of (i) the geometrical properties of large dimensional spaces and (ii) the underlying pair structure of the N-body stationary distribution. We start our study of self-propelled hard spheres in large d by assuming that such a structure holds at the 3-body level, *i.e.* that

$$g^{(3)}\left(\mathbf{r}_1,\mathbf{u}_1;\mathbf{r}_2,\mathbf{u}_2;\mathbf{r}_3,\mathbf{u}_3\right) = g\left(\mathbf{r}_1,\mathbf{u}_1;\mathbf{r}_2,\mathbf{u}_2\right) g\left(\mathbf{r}_1,\mathbf{u}_1;\mathbf{r}_3,\mathbf{u}_3\right) g\left(\mathbf{r}_2,\mathbf{u}_2;\mathbf{r}_3,\mathbf{u}_3\right) \ . \tag{4.66}$$

Following the same reasoning as in the equilibrium case, Eq. (4.66) holds if the N-body measure can be written as a product over pair functions,

$$P\left(\mathbf{r}_1,\mathbf{u}_1;\cdots:\mathbf{r}_N,\mathbf{u}_N\right) = \prod_{i<j} g\left(\mathbf{r}_i,\mathbf{u}_i;\mathbf{r}_j,\mathbf{u}_i\right) \ , \tag{4.67}$$

provided g has the correct scaling as $d \to \infty$ given in terms of the associated Mayer function $f = g - 1$ in Eq. (3.94). This hypothesis about the scaling of g is supported by our result on the low density limit of the two-point correlation function in Eqs. (4.21)-(4.22). We further

note that the DMFT equations explicitly show that $h = d\,(r/\sigma - 1)$ is indeed correct scale to describe the decay of f even at finite $\widehat{\varphi}$. This hypothesis about the scaling of g is self-consistently checked at the end of the calculation. In other words, Eq. (4.66) is expected to hold if one can effectively neglect more-than-two body contributions in the stationary state measure that would break structure of Eq. (4.67). Assuming that Eq. (4.66) holds truncates the BBGKY hierarchy to second order, thus providing a closed form equation for the two-point function $g\,(\mathbf{r}_1, \mathbf{u}_1; \mathbf{r}_2, \mathbf{u}_2)$. From Eq. (3.12), the second order hierarchy equation reads,

$$\begin{aligned} &- v_0 \mathbf{u}_1 \cdot \boldsymbol{\nabla}_{\mathbf{r}_1} g - v_0 \mathbf{u}_2 \cdot \boldsymbol{\nabla}_{\mathbf{r}_2} g + \boldsymbol{\nabla}_{\mathbf{r}_1} \left(g \boldsymbol{\nabla}_{\mathbf{r}_1} U(\mathbf{r}_1 - \mathbf{r}_2) \right) + \boldsymbol{\nabla}_{\mathbf{r}_2} \left(g \boldsymbol{\nabla}_{\mathbf{r}_2} U(\mathbf{r}_2 - \mathbf{r}_1) \right) \\ &+ \mathcal{R}_1 g + \mathcal{R}_2 g + \rho \boldsymbol{\nabla}_{\mathbf{r}_1} \int \mathrm{d}\mathbf{r}_3 \frac{\mathrm{d}\mathbf{u}_3}{\Omega_d} g^{(3)}\left(\mathbf{r}_1, \mathbf{u}_1; \mathbf{r}_2, \mathbf{u}_2; \mathbf{r}_3, \mathbf{u}_3\right) \boldsymbol{\nabla}_{\mathbf{r}_1} U\left(\mathbf{r}_1 - \mathbf{r}_3\right) \\ &+ \rho \boldsymbol{\nabla}_{\mathbf{r}_2} \int \mathrm{d}\mathbf{r}_3 \frac{\mathrm{d}\mathbf{u}_3}{\Omega_d} g^{(3)}\left(\mathbf{r}_1, \mathbf{u}_1; \mathbf{r}_2, \mathbf{u}_2; \mathbf{r}_3, \mathbf{u}_3\right) \boldsymbol{\nabla}_{\mathbf{r}_2} U\left(\mathbf{r}_2 - \mathbf{r}_3\right) = 0\,, \end{aligned} \tag{4.68}$$

where

$$\mathbf{F}_1 = \rho \int \mathrm{d}\mathbf{r}_3 \frac{\mathrm{d}\mathbf{u}_3}{\Omega_d} \frac{g^{(3)}\left(\mathbf{r}_1, \mathbf{u}_1; \mathbf{r}_2, \mathbf{u}_2; \mathbf{r}_3, \mathbf{u}_3\right)}{g\left(\mathbf{r}_1, \mathbf{u}_1; \mathbf{r}_2, \mathbf{u}_2\right)} \boldsymbol{\nabla}_{\mathbf{r}_1} U\left(\mathbf{r}_1 - \mathbf{r}_3\right)\,, \tag{4.69}$$

is the mean force exerted by all the $N-2$ remaining particles on the particle sitting at $\mathbf{r}_1$ conditioned on the fact that is has a self-propulsion vector $\mathbf{u}_1$ and that there is another particle at $\mathbf{r}_2$ with self-propulsion vector $\mathbf{u}_2$. Within the Kirkwood closure approximation Eq. (4.66), it is expressed as

$$\mathbf{F}_1 = \rho \int \mathrm{d}\mathbf{r}_3 \frac{\mathrm{d}\mathbf{u}_3}{\Omega_d} g\left(\mathbf{r}_1, \mathbf{u}_1; \mathbf{r}_3, \mathbf{u}_3\right) g\left(\mathbf{r}_2, \mathbf{u}_2; \mathbf{r}_3, \mathbf{u}_3\right) \boldsymbol{\nabla}_{\mathbf{r}_1} U\left(\mathbf{r}_1 - \mathbf{r}_3\right)\,. \tag{4.70}$$

which has a structure very similar to the mean force we computed in the equilibrium case in Eq. (3.120) from which we can conclude that $g\left(\mathbf{r}_2, \mathbf{u}_2; \mathbf{r}_3, \mathbf{u}_3\right) = 1$ everywhere in the integration volume of the above integral but in an exponentially small fraction of it. Let us now repeat the argument. We are only interested in configurations in which $|\mathbf{r}_1 - \mathbf{r}_2| \gtrsim \sigma$ as the two particles cannot overlap. The integral in Eq. (4.70) is furthermore restricted to regions where $|\mathbf{r}_1 - \mathbf{r}_3| \simeq \sigma$. Therefore, $|\mathbf{r}_2 - \mathbf{r}_3| \simeq \sigma$ implies that $\hat{\mathbf{r}}_{12} \cdot \hat{\mathbf{r}}_{13} = O(1)$, an event that has vanishingly small probability in the large d limit. The situation is summarized in Fig. 4.5. which shows all the particles that surround the one at $\mathbf{r}_1$. The dashed particles are all the ones that contribute to the conditional mean force $\mathbf{F}_1$ and none of them interacts directly with $\mathbf{r}_2$, *i.e.* $g\left(\mathbf{r}_2, \mathbf{u}_2; \mathbf{r}_i, \mathbf{u}_i\right) = 1$. Incidentally and for the same reason, there is no direct interactions between the different particles contributing to $\mathbf{F}_1$: the interaction network is tree-like. Up to exponentially small corrections, the conditional mean force is then obtained as

$$\begin{aligned} \mathbf{F}_1 &= \rho \int \mathrm{d}\mathbf{r}_3 \frac{\mathrm{d}\mathbf{u}_3}{\Omega_d} g\left(\mathbf{r}_1, \mathbf{u}_1; \mathbf{r}_3, \mathbf{u}_3\right) \boldsymbol{\nabla}_{\mathbf{r}_1} U\left(\mathbf{r}_1 - \mathbf{r}_3\right) \\ &= \left(v_0 - v(\widehat{\varphi})\right) \mathbf{u}_1\,, \end{aligned} \tag{4.71}$$

with $v(\widehat{\varphi})$ the effective self-propulsion defined in Eq. (3.15). Note that within the Kirkwood approximation, and as in equilibrium, the mean force exerted by the rest of the fluid on the particle at $\mathbf{r}_1$ with orientation $\mathbf{u}_1$ conditioned on the presence of another particle at $\mathbf{r}_2$ with orientation $\mathbf{u}_2$ is exactly equal to that exerted by the rest of the fluid on a particle at $\mathbf{r}_1$ with orientation $\mathbf{u}_1$ in the absence of conditioning. The main difference between the

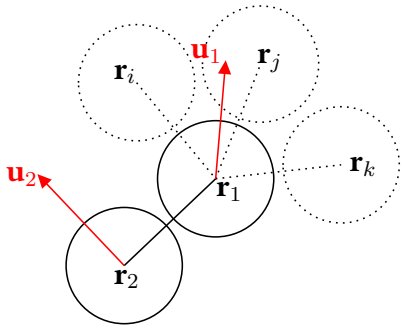

Figure 4.5: A sketch of the different particles surrounding the one at $\mathbf{r}_1$. The dashed particles are the ones contributing to the conditional mean force $\mathbf{F}_1$. None of them interacts directly with the one at $\mathbf{r}_2$.

equilibrium and the active cases being that in the latter the isotropy of space is broken at the one particle level by the self-propulsion vector $\mathbf{u}_1$, thus making the mean force non vanishing. One therefore obtains a self-consistent equation for the two-point distribution function,

$$\begin{aligned} &- v(\widehat{\varphi})\,\mathbf{u}_1\cdot\boldsymbol{\nabla}_{\mathbf{r}_1} g + \boldsymbol{\nabla}_{\mathbf{r}_1}\left(g\boldsymbol{\nabla}_{\mathbf{r}_1} U(\mathbf{r}_1-\mathbf{r}_2)\right) + \mathcal{R}_1 g \\ &- v(\widehat{\varphi})\,\mathbf{u}_2\cdot\boldsymbol{\nabla}_{\mathbf{r}_2} g + \boldsymbol{\nabla}_{\mathbf{r}_2}\left(g\boldsymbol{\nabla}_{\mathbf{r}_2} U(\mathbf{r}_2-\mathbf{r}_1)\right) + \mathcal{R}_2 g = 0\,. \end{aligned} \tag{4.72}$$

In the hard sphere case, the two-point distribution function is thus given by its dilute limit counterpart, Eqs. (4.21)-(4.22) at $w_0 = 0$. The regularization of the product gU' is however modified with respect to the dilute limit case with v_0 becoming $v(\widehat{\varphi})$ in Eq. (4.26). This leads to the following self-consistent equation for the effective self-propulsion,

$$v\left(\widehat{\varphi}\right) = v_0 - v\left(\widehat{\varphi}\right)\frac{\widehat{\varphi}}{4}\,, \tag{4.73}$$

thus yielding

$$v\left(\widehat{\varphi}\right) = \frac{v_0}{1+\frac{\widehat{\varphi}}{4}}\,. \tag{4.74}$$

The rescaled mechanical pressure can accordingly be computed within this truncation scheme and read,

$$P = \hat{v}_0\sigma\left(\frac{\hat{v}_0\tau}{\sigma}\frac{\widehat{\varphi}}{1+\frac{\widehat{\varphi}}{4}} + \frac{\widehat{\varphi}^2}{4\sqrt{\pi}\left(1+\frac{\widehat{\varphi}}{4}\right)}\right)\,. \tag{4.75}$$

Several observations are now in order. First, the obtained effective self-propulsion speed does not reproduce the linear decay at moderate packing fraction measured [196] in finite dimensional simulations of strongly repulsive self-propelled particles. Second, the mechanical pressure does not display any spinodal instability as $P'(\widehat{\varphi}) > 0$ for all $\widehat{\varphi}$ and Péclet number. The infinite dimensional Kirkwood approximation thus performs rather poorly in reproducing the properties of low dimensional active systems. This is not intrinsic to the infinite dimensional limit but this is a feature of the Kirkwood approximation that remains at this level, just an... approximation.

4.2.2 An approximate truncation scheme of the hierarchy

The reason for this failure of the Kirkwood approximation in infinite dimensional active systems lies in the fact that, in Fig. 4.5, the particle sitting at $\mathbf{r}_2$ influences the conditional mean force through its direct influence on the particle sitting at $\mathbf{r}_1$, à la Onsager reaction term. This sheds the light on the importance of multibody interactions in active matter, at least at the mean-field level. In this section, we propose a resummation scheme of the BBGKY hierarchy that partially takes them into account.

A virial expansion:

We follow the route paved in Sec. 3.2.7. We express the n-point distribution functions as power series of the rescaled density $\widehat{\varphi}$,

$$g^{(n)}(\mathbf{r}_1,\mathbf{u}_1;\ldots;\mathbf{r}_n,\mathbf{u}_n)=\sum_{p=0}^{+\infty}\widehat{\varphi}^{\,p}\gamma_p^{(n)}(\mathbf{r}_1,\mathbf{u}_1;\ldots;\mathbf{r}_n,\mathbf{u}_n)\,, \tag{4.76}$$

and introduce the partial sums $g_p^{(n)}$

$$g_p^{(n)}(\mathbf{r}_1,\mathbf{u}_1;\ldots;\mathbf{r}_n,\mathbf{u}_n)=\sum_{q=0}^{p}\widehat{\varphi}^{\,q}\gamma_q^{(n)}(\mathbf{r}_1,\mathbf{u}_1;\ldots;\mathbf{r}_n,\mathbf{u}_n)\,. \tag{4.77}$$

We later self-consistently show that $\widehat{\varphi}$ is the correct expansion parameter so that for all $p\geq 0$ and all $n\geq 2$ the functions $g_p^{(n)}(\mathbf{r}_1,\mathbf{u}_1;\ldots;\mathbf{r}_n,\mathbf{u}_n)$ remain $O(1)$ as d increases. The BBGKY hierarchy Eq. (3.12) provides relations between the different partial sums $g_p^{(n)}$,

$$\begin{aligned}&-v_0\sum_{i=1}^{n}\mathbf{u}_i\cdot\boldsymbol{\nabla}_{\mathbf{r}_i}g_p^{(n)}+\sum_{i=1}^{n}\sum_{j\neq i}^{n}\boldsymbol{\nabla}_{\mathbf{r}_i}\left(g_p^{(n)}\boldsymbol{\nabla}_{\mathbf{r}_i}U(\mathbf{r}_i-\mathbf{r}_j)\right)+\sum_{i=1}^{n}\mathcal{R}_i g_p^{(n)}\\&+\rho\sum_{i=1}^{n}\boldsymbol{\nabla}_{\mathbf{r}_i}\int\mathrm{d}\mathbf{r}'\,\frac{\mathrm{d}\mathbf{u}'}{\Omega_d}g_{p-1}^{(n+1)}(\mathbf{r}_1,\mathbf{u}_1;...;\mathbf{r}_n,\mathbf{u}_n;\mathbf{r}',\mathbf{u}')\boldsymbol{\nabla}_{\mathbf{r}_i}U(\mathbf{r}_i-\mathbf{r}')=0\,.\end{aligned} \tag{4.78}$$

for all $n\geq 2$ and $p\geq 1$ together with the 0^{th} order equations,

$$-v_0\sum_{i=1}^{n}\mathbf{u}_i\cdot\boldsymbol{\nabla}_{\mathbf{r}_i}g_0^{(n)}+\sum_{i=1}^{n}\sum_{j\neq i}^{n}\boldsymbol{\nabla}_{\mathbf{r}_i}\left(g_0^{(n)}\boldsymbol{\nabla}_{\mathbf{r}_i}U(\mathbf{r}_i-\mathbf{r}_j)\right)+\sum_{i=1}^{n}\mathcal{R}_i g_0^{(n)}=0\,, \tag{4.79}$$

for all $n\geq 2$. Note that we start to work with regular potentials that obey the infinite dimensional scalings of Sec. 4.1. From there, the infinitely short-ranged limit is taken step by step as the BBGKY hierarchy is resummed.

Zeroth order solution:

As for the equilibrium case, we start by solving the zeroth order equations in (4.79). We investigate first the scalings with d of the different terms appearing in these equations. We

recall that the n-body distribution varies over scales $|\delta\mathbf{r}_i| = O(1/d)$, so that gradients of $g_0^{(n)}$ are typically of order $O(d)$,

$$\left|\boldsymbol{\nabla}_{\mathbf{r}_i} g_0^{(n)}\right| \sim d\,. \tag{4.80}$$

Furthermore, the scalar product of the gradient with $\mathbf{u}_i$ yields a $1/\sqrt{d}$ factor. Taking into account the scaling of the self-propulsion $v_0 = O(d^{3/2})$, we obtain

$$\left|v_0\,\mathbf{u}_i \cdot \boldsymbol{\nabla}_{\mathbf{r}_i} g_0^{(n)}\right| \sim d^2\,. \tag{4.81}$$

The terms in Eq. (4.79) induced by the potential interaction have the same amplitude. Indeed, we work with pair-potential defined in such a way that $\lim_{d\to\infty} U(\mathbf{r}) = \widehat{U}(h)$ with $h = d\,(r/\sigma - 1)$. Therefore,

$$|\boldsymbol{\nabla}_{\mathbf{r}_i} U(\mathbf{r}_i - \mathbf{r}_j)| \sim d\,. \tag{4.82}$$

The divergence $\boldsymbol{\nabla}_{\mathbf{r}_i}$ then brings in an additional $O(d)$ factor as explained above. There is no additional $1/\sqrt{d}$ factor as $g_0^{(n)}$ seen as a function of $\mathbf{r}_i$ varies over $1/d$ scales in the directions set by the relative separations $\hat{\mathbf{r}}_{ij} = (\mathbf{r}_i - \mathbf{r}_j)\,/\,|\mathbf{r}_i - \mathbf{r}_j|$. Therefore,

$$\left|\boldsymbol{\nabla}_{\mathbf{r}_i} \cdot \left(g_0^{(n)} \boldsymbol{\nabla}_{\mathbf{r}_i} U(\mathbf{r}_i - \mathbf{r}_j)\right)\right| \sim d^2\,. \tag{4.83}$$

An important comment is now in order. We have seen that,

$$|v_0 \mathbf{u}_i| \gg |\boldsymbol{\nabla}_{\mathbf{r}_i} U(\mathbf{r}_i - \mathbf{r}_j)|\ , \tag{4.84}$$

as the latter is $O(d)$ while the former is $O(d^{3/2})$. However, inside the $\boldsymbol{\nabla}_{\mathbf{r}_i}$ operators, both vectors yield the same amplitude as the divergence projects along components that are roughly aligned with $\boldsymbol{\nabla}_{\mathbf{r}_i} U(\mathbf{r}_i - \mathbf{r}_j)$ and almost orthogonal to $\mathbf{u}_i$. Therefore, when comparing two quantities, we should be cautious to compare scalar ones and not vectorial ones. Finally, we recall that $\tau = O(1/d)$. Consequently, the flipping terms in the equation for the n-body correlation function scale as $O(d)$,

$$\left|\frac{1}{\tau}\sum_i \left(\int \frac{\mathrm{d}\mathbf{u}_i'}{\Omega_d} g^{(n)} - g^{(n)}\right)\right| \sim d\,. \tag{4.85}$$

Thus, in Eq. (4.79), the potential and the convective terms have the same amplitude d^2. The flipping terms are $1/d$ smaller, a signature that the considered scalings automatically place us in the ultraballistic limit. We now look for a solution of Eq. (4.79). Let us single out arbitrarily the particle labeled n and propose the following ansatz,

$$\begin{aligned} g_0^{(n)}(\mathbf{r}_1, \mathbf{u}_1; \ldots; \mathbf{r}_n; \mathbf{u}_n) =& g_0^{(n-1)}(\mathbf{r}_1, \mathbf{u}_1; \ldots; \mathbf{r}_{n-1}; \mathbf{u}_{n-1}) \left[\prod_{i=1}^{n-1} g_0^{(2)}(\mathbf{r}_i, \mathbf{u}_i; \mathbf{r}_n, \mathbf{u}_n)\right] \times \ldots \\ & \cdots \times \Big(1 + K_0(\mathbf{r}_1, \mathbf{u}_1; \ldots; \mathbf{r}_n; \mathbf{u}_n)\Big)\,, \end{aligned} \tag{4.86}$$

schematically illustrated in Fig.4.6 and where K_0 is yet to be determined. We then insert Eq. (4.86) into Eq. (4.79). In order to lighten up notations, the arguments of $g_0^{(n-1)}$ and K_0

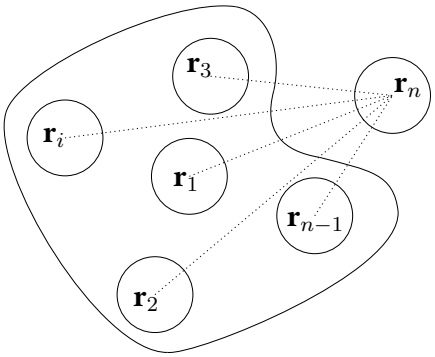

Figure 4.6: A schematic representation of the ansatz Eq. (4.86). The particle labeled n is singled out. Particles labeled $i \in [\![1, n-1]\!]$ are grouped together in a $g_0^{(n-1)}$ term while couplings between particle n and particles i is taken into account by two-body distribution functions $g_0^{(2)}$.

are dropped and we write $g_0^{(2)}(\mathbf{r}_i, \mathbf{u}_i; \mathbf{r}_j, \mathbf{u}_j) = g_0^{(2)}(i,j)$. We eventually obtain the (nasty-looking) equation obeyed by K_0,

$$
\begin{aligned}
& g_0^{(n-1)} \prod_{j=1}^{n-1} g_0^{(2)}(j,n) \left[-v_0 \sum_{i=1}^{n} \mathbf{u}_i \boldsymbol{\nabla}_{\mathbf{r}_i} K_0 + \sum_{i=1}^{n} \sum_{j \neq i}^{n} \boldsymbol{\nabla}_{\mathbf{r}_i} K_0 \cdot \boldsymbol{\nabla}_{\mathbf{r}_i} U(\mathbf{r}_i - \mathbf{r}_j) \right] \\
& + (1+K_0) \left[g_0^{(n-1)} \sum_{i=1}^{n-1} \sum_{j \neq i}^{n-1} \left(\prod_{k \neq i}^{n-1} g_0^{(2)}(k,n) \right) \boldsymbol{\nabla}_{\mathbf{r}_i} g_0^{(2)}(i,n) \cdot \boldsymbol{\nabla}_{\mathbf{r}_i} U(\mathbf{r}_i - \mathbf{r}_j) \right. \\
& + g_0^{(n-1)} \sum_{i=1}^{n-1} \sum_{j \neq i}^{n-1} \left(\prod_{k \neq j}^{n-1} g_0^{(2)}(k,n) \right) \boldsymbol{\nabla}_{\mathbf{r}_n} g_0^{(2)}(j,n) \cdot \boldsymbol{\nabla}_{\mathbf{r}_n} U(\mathbf{r}_n - \mathbf{r}_i) \\
& \left. + \prod_{j=1}^{n-1} g_0^{(2)}(j,n) \sum_{i=1}^{n-1} \boldsymbol{\nabla}_{\mathbf{r}_i} g_0^{(n-1)} \cdot \boldsymbol{\nabla}_{\mathbf{r}_i} U(\mathbf{r}_i - \mathbf{r}_n) \right] \\
& + \sum_{i=1}^{n} \mathcal{R}_i \left(g_0^{(n-1)} \prod_{i=1}^{n-1} g_0^{(2)}(i,n)(1+K_0) \right) - (1+K_0) \prod_{j=1}^{n-1} g_0^{(2)}(j,n) \sum_{i=1}^{n-1} \mathcal{R}_i g_0^{(n-1)} \\
& - g_0^{(n-1)} (1+K_0) \sum_{i=1}^{n-1} \prod_{j \neq i}^{n-1} g_0^{(2)}(j,n) \left(\mathcal{R}_i g_0^{(2)}(i,n) + \mathcal{R}_n g_0^{(2)}(i,n) \right) = 0 \,.
\end{aligned}
\tag{4.87}
$$

We will not attempt to solve Eq. (4.87). It is however instructive to determine the order in d of the various terms appearing in it. We use the same arguments as for determining the scaling of those in Eq. (4.79). In the first two lines, they are of order $O(d^2 K_0)$ with the order of K_0 yet unspecified. In the next three lines they are all of order $O((1+K_0)d^{3/2})$. Indeed, both gradients

$$
\left| \boldsymbol{\nabla}_{\mathbf{r}_i} g_0^{(2)}(i,k) \right| \sim d \,, \tag{4.88}
$$

and

$$
|\boldsymbol{\nabla}_{\mathbf{r}_i} U(\mathbf{r}_i - \mathbf{r}_j)| \sim d \,, \tag{4.89}
$$

are of order $O(d)$ but point in typically orthogonal directions, so that

$$\boldsymbol{\nabla}_{\mathbf{r}_i} g_0^{(2)}(i,k) \cdot \boldsymbol{\nabla}_{\mathbf{r}_i} U(\mathbf{r}_i - \mathbf{r}_j) \sim d^{3/2}\,, \tag{4.90}$$

for $k \neq i$. Finally the flipping terms in the last two lines scale as $O(d)$. Consequently, the unknown function K_0 scales as $O(d^{-1/2})$. As a conclusion, to zeroth order in density, we have

$$\begin{aligned} g_0^{(n)}(\mathbf{r}_1,\mathbf{u}_1;\dots;\mathbf{r}_n;\mathbf{u}_n) =& g_0^{(n-1)}(\mathbf{r}_1,\mathbf{u}_1;\dots;\mathbf{r}_{n-1};\mathbf{u}_{n-1}) \left[\prod_{i=1}^{n-1} g_0^{(2)}(\mathbf{r}_i,\mathbf{u}_i;\mathbf{r}_n,\mathbf{u}_n)\right] \times \dots \\ & \cdots \times \left(1 + \frac{\hat{K}_0(\mathbf{r}_1,\mathbf{u}_1;\dots;\mathbf{r}_n;\mathbf{u}_n)}{\sqrt{d}}\right), \end{aligned} \tag{4.91}$$

with $\hat{K}_0$ an $O(1)$ function. Note that the choice of particle n is purely arbitrary. The zeroth order distribution function can indeed be written to leading order as a product of $g_0^{(2)}$ over all the pairs,

$$g_0^{(n)}(\mathbf{r}_1,\mathbf{u}_1;\dots;\mathbf{r}_n;\mathbf{u}_n) = \left[\prod_{i<j}^{n} g_0^{(2)}(\mathbf{r}_i,\mathbf{u}_i;\mathbf{r}_j,\mathbf{u}_j)\right] \left(1 + \frac{\tilde{K}_0(\mathbf{r}_1,\mathbf{u}_1;\dots;\mathbf{r}_n;\mathbf{u}_n)}{\sqrt{d}}\right), \tag{4.92}$$

with $\tilde{K}_0$ a different $O(1)$ function. The functional form in Eq. (4.91) will however be more convenient in the resummation of the hierarchy. At this level, the difference with the purely pairwise structure of standard equilibrium fluids Eq. (3.125) is seemingly vanishing as it scales as $O(d^{-1/2})$. It is however no longer exponentially decaying with d. As we explain now, this leaves room for non trivial effects.

The sticky sphere potential

We use the solution Eq. (4.91) of Eq. (4.79) as a starting point for the resummation of the hierarchy. In order to get the first $\widehat{\varphi}$ term of the density expansion of $g^{(n-1)}$, one needs to solve the hierarchy equation Eq. (4.78) at $p = 1$ *i.e.* to compute the force term

$$\mathbf{G}_{i,1} = \rho \int \mathrm{d}\mathbf{r}_n \frac{\mathrm{d}\mathbf{u}_n}{\Omega_d} g_0^{(n)}(\mathbf{r}_1,\mathbf{u}_1;...;\mathbf{r}_n,\mathbf{u}_n) \boldsymbol{\nabla}_{\mathbf{r}_i} U(\mathbf{r}_i - \mathbf{r}_n) \tag{4.93}$$

for any $i = 1,\dots,n-1$ and where the index 1 stands for first iteration in the virial resummation. Note that we did not call the above integral $\mathbf{F}_i$ on purpose as it only takes the meaning of a conditional mean force when divided by $g^{(n-1)}$. We now restrict our study to the case of infinitely short ranged potentials of the sticky sphere type introduced in Sec. 4.1. Performing the integral in Eq. (4.93) thus requires regularizing the product $g_0^{(n)} \boldsymbol{\nabla}_{\mathbf{r}_i} U(\mathbf{r}_i - \mathbf{r}_n)$. In the vein of Eq. (2.93), we now derive such a formula that holds independently of the large d limit and for which we give a simple interpretation. For the sake of simplicity of the notations we choose $i = 1$ but all $i's$ are of course equivalent. We first go back to Eq. (4.79)

where we change variables and define $\mathbf{x}_i = \mathbf{r}_i - \mathbf{r}_1$ for $i \in [\![2, n]\!]$. Isolating the variable $\mathbf{x}_n$ and taking advantage of the translational invariance of the distribution function we obtain

$$
\begin{aligned}
&- v_0 \sum_{i=2}^{n-1} (\mathbf{u}_i - \mathbf{u}_1) \cdot \boldsymbol{\nabla}_{\mathbf{x}_i} g_0^{(n)} - v_0 \, (\mathbf{u}_n - \mathbf{u}_1) \cdot \boldsymbol{\nabla}_{\mathbf{x}_n} g^{(n)} + \sum_{i=1}^{n} \mathcal{R}_i g_0^{(n)} \\
&+ \sum_{i=2}^{n-1} \boldsymbol{\nabla}_{\mathbf{x}_i} \cdot \left[g^{(n)} \left(\sum_{j \neq i}^{n-1} \boldsymbol{\nabla}_{\mathbf{x}_i} U(\mathbf{x}_i - \mathbf{x}_j) + \boldsymbol{\nabla}_{\mathbf{x}_i} U(\mathbf{x}_i - \mathbf{x}_n) + 2 \boldsymbol{\nabla}_{\mathbf{x}_i} U(\mathbf{x}_i) + \sum_{j \neq i}^{n-1} \boldsymbol{\nabla}_{\mathbf{x}_j} U(\mathbf{x}_j) \right. \right. \\
&\left. \left. + \boldsymbol{\nabla}_{\mathbf{x}_n} U(\mathbf{x}_n) \right) \right] + \boldsymbol{\nabla}_{\mathbf{x}_n} \cdot \left[g_0^{(n)} \left(\sum_{i=2}^{n-1} \boldsymbol{\nabla}_{\mathbf{x}_n} U(\mathbf{x}_n - \mathbf{x}_i) + 2 \boldsymbol{\nabla}_{\mathbf{x}_n} U(\mathbf{x}_n) + \sum_{i=2}^{n-1} \boldsymbol{\nabla}_{\mathbf{x}_i} U(\mathbf{x}_i) \right) \right] = 0 \, .
\end{aligned}
\tag{4.94}
$$

As shown in Eqs. (2.93) and in App. B.1, in the limit where $U(\mathbf{x}_n)$ becomes infinitely short-ranged, the integrated normal flux vanishes at $x_n = \sigma$, *i.e.*

$$
\begin{aligned}
&2 \lim_{\text{short-ranged}} \int_{\sigma}^{+\infty} \mathrm{d}x_n \, g_0^{(n)}(\mathbf{0}, \mathbf{u}_1; \mathbf{x}_2, \mathbf{u}_2; \ldots; \mathbf{x}_n, \mathbf{u}_n) U'(x_n) = \\
&\lim_{\epsilon \to 0^+} \lim_{\text{short-ranged}} \int_{\sigma}^{\sigma(1+\epsilon)} \mathrm{d}x_n \left(v_0 (\mathbf{u}_n - \mathbf{u}_1) - \sum_{i=2}^{n-1} \boldsymbol{\nabla}_{\mathbf{x}_n} U(\mathbf{x}_n - \mathbf{x}_i) - \sum_{i=2}^{n-1} \boldsymbol{\nabla}_{\mathbf{x}_i} U(\mathbf{x}_i) \right) \cdot \hat{\mathbf{x}}_n \times \ldots \\
&\qquad \ldots \times g_0^{(n)}(\mathbf{0}, \mathbf{u}_1; \mathbf{x}_2, \mathbf{u}_2; \ldots; \mathbf{x}_n, \mathbf{u}_n) \, .
\end{aligned}
\tag{4.95}
$$

This can be demonstrated by splitting the divergence $\boldsymbol{\nabla}_{\mathbf{x}_n}$ into a radial and a non radial part and integrating over the radial distance x_n as in Eqs. (2.87) and (2.93). Equation (4.95) quantifies the idea that (i) the force $U(x_n)$ is zero whenever $x_n > \sigma$ and (ii) when non-zero it must exactly compensate the normal relative velocity between particle 1 and particle n. This relative velocity depends both on the relative self-propulsion velocity $\mathbf{u}_n - \mathbf{u}_1$ and on the potential interactions with the other tagged particles. Independently of the large d limit, $\mathbf{G}_{1,1}$ can thus be evaluated as

$$
\begin{aligned}
\mathbf{G}_{1,1} = - \frac{\rho \Omega_d \sigma^d}{2} \int \frac{\mathrm{d}\hat{\mathbf{x}}_n}{\Omega_d} \frac{\mathrm{d}\hat{\mathbf{u}}_n}{\Omega_d} \hat{\mathbf{x}}_n \left[\lim_{\epsilon \to 0^+} \lim_{\text{short-ranged}} \int_{\sigma}^{\sigma(1+\epsilon)} \frac{\mathrm{d}x_n}{\sigma} \left(v_0 \, (\mathbf{u}_n - \mathbf{u}_1) \right. \right. \\
\left. \left. - \sum_{i=2}^{n-1} \boldsymbol{\nabla}_{\mathbf{x}_n} U(\mathbf{x}_n - \mathbf{x}_i) - \sum_{i=2}^{n-1} \boldsymbol{\nabla}_{\mathbf{x}_i} U(\mathbf{x}_i) \right) \cdot \hat{\mathbf{x}}_n \, g_0^{(n)}(\mathbf{0}, \mathbf{u}_1; \mathbf{x}_2, \mathbf{u}_2; \ldots; \mathbf{x}_n, \mathbf{u}_n) \right] ,
\end{aligned}
\tag{4.96}
$$

Let us now go back to the infinite dimensional case. First we stress that the particles are non overlapping so that $|\mathbf{x}_i| \gtrsim \sigma$. Therefore,

$$
\begin{aligned}
d \left(|\mathbf{x}_i - \mathbf{x}_n| - \sigma \right) &= d \left(\sqrt{x_i^2 + \sigma^2 - 2 x_i \sigma \hat{\mathbf{x}}_i \cdot \hat{\mathbf{x}}_n} - \sigma \right) \\
&\underset{d \to \infty}{\longrightarrow} + \infty \, ,
\end{aligned}
\tag{4.97}
$$

but in an exponentially small fraction of phase space. While computing $\mathbf{G}_{1,1}$ we can thus neglect the potential interactions between the particle at $\mathbf{r}_n$ and those at $\mathbf{r}_i$ for $i = 2, \ldots, n-$

1 as is usual in infinite dimensional systems of interacting spherical particles. We define $\mathbf{F}_{i,1}$ the conditional mean force exerted on particle i at the first iteration of the resummation,

$$\mathbf{F}_{i,1} = \frac{\mathbf{G}_{i,1}}{g_0^{(n-1)}(\mathbf{r}_1, \mathbf{u}_1; \dots; \mathbf{r}_n; \mathbf{u}_n)}\,, \tag{4.98}$$

that we thus express for $i = 1$ as

$$\mathbf{F}_{1,1} = -\frac{\rho\Omega_d\sigma^d}{2}\int \frac{\mathrm{d}\hat{\mathbf{x}}_n}{\Omega_d}\frac{\mathrm{d}\hat{\mathbf{u}}_n}{\Omega_d}\hat{\mathbf{x}}_n\left[\lim_{\epsilon\to 0^+}\int_\sigma^{\sigma(1+\epsilon)}\frac{\mathrm{d}x_n}{\sigma}\left(v_0\left(\mathbf{u}_n-\mathbf{u}_1\right)-\sum_{i=2}^{n-1}\boldsymbol{\nabla}_{\mathbf{x}_i}U(\mathbf{x}_i)\right)\cdot\hat{\mathbf{x}}_n\right.$$
$$\left.\times\lim_{\text{short-ranged}} g_0^{(2)}(\mathbf{0},\mathbf{u}_1;\mathbf{x}_n,\mathbf{u}_n)\left(1+\frac{\hat{K}_0}{\sqrt{d}}\right)\right]. \tag{4.99}$$

In the above equation we have commuted the short-range limit and the gradients of $U(\mathbf{x}_i)$. We are thus taking this limit for the potential interactions of particle n with the $(n-1)$ other particles (dashed lines in Fig.4.6) while keeping regular the potential interactions between particles $i = 1, \dots, n-1$ (within the continuous line in Fig.4.6). The infinitely-short ranged limit is then taken layer by layer as the hierarchy is resummed. We recall that that the norm of the potential gradients is $O(d^{-1/2})$ smaller than that of $v_0\left(\mathbf{u}_n - \mathbf{u}_1\right)$ so that to leading order Eq. (4.99) writes,

$$\mathbf{F}_{1,1} = -v_0\frac{\rho\Omega_d\sigma^d}{2}\int \frac{\mathrm{d}\hat{\mathbf{x}}_n}{\Omega_d}\frac{\mathrm{d}\hat{\mathbf{u}}_n}{\Omega_d}\hat{\mathbf{x}}_n\left[\lim_{\epsilon\to 0^+}\int_\sigma^{\sigma(1+\epsilon)}\frac{\mathrm{d}x_n}{\sigma}\left(\mathbf{u}_n-\mathbf{u}_1\right)\cdot\hat{\mathbf{x}}_n\, g_0^{(2)}(\mathbf{0},\mathbf{u}_1;\mathbf{x}_n,\mathbf{u}_n)\right], \tag{4.100}$$

consistently with Eq. (4.91) and where the $\lim_{\text{short-ranged}}$ is implicit. As explained after Eq. (4.84), the subleading terms are however non-negligible and give rise to leading order terms in the BBGKY hierarchy through the action of the divergence operator $\boldsymbol{\nabla}_{\mathbf{r}_i}$.

Equation (4.99), which is exact up to exponentially small corrections, is an important preliminary result of this work. It shows that the leading order Eq. (4.100) of the mean force, conditioned on the positions and orientations of $n-1$ tagged particles, exerted on any of these by the surrounding fluid made of the $N-n+1$ others, is equal to that exerted on any particle in the absence of conditioning but on its own orientation. The presence of the $n-2$ other tagged particles slightly modifies the result in two ways that are clearly disentangled in the infinitely short-ranged limit. First, from the point of view of the surrounding fluid, the apparent self-propulsion of particle 1 is not $v_0\mathbf{u}_1$ but is dressed by the interactions with the other tagged particles. This is depicted in Fig.4.7. This in turn modifies the distribution of the fluid particles at contact with particle 1 with respect to the untagged case, hence the $\hat{K}_0$ correction.

Approximate resummation scheme:

Equation (4.99) does not allow a full determination of the conditional force since $\hat{K}_0$, defined by the solution of Eq. (4.87), remains undetermined. In order to get further insights into

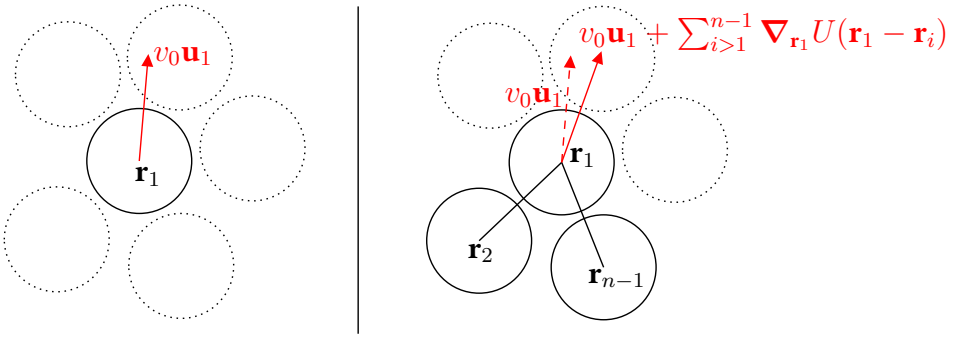

Figure 4.7: **(Left)** A tagged particle moves in the fluid made of the $N-1$ remaining ones. From the point of view of the latter, its apparent self-propulsion is $v_0\mathbf{u}_1$. **(Right)** A tagged particle with $n-2$ neighboring tagged ones moves in the fluid made of the $N-n+1$ others. From the point of view of the fluid its apparent driving is dressed by the interactions with particles i for $i = 2, \dots, n-1$.

the behavior of active fluids we need to make some approximation. We choose to neglect the contributions coming from $\hat{K}_0$ and we will propagate this approximation at each step of the resummation of the virial series. This yields,

$$\mathbf{F}_{1,1} = -\frac{\rho\Omega_d\sigma^d}{2}\int \frac{\mathrm{d}\hat{\mathbf{x}}_n}{\Omega_d}\frac{\mathrm{d}\hat{\mathbf{u}}_n}{\Omega_d}\hat{\mathbf{x}}_n\left[\lim_{\epsilon\to 0^+}\int_\sigma^{\sigma(1+\epsilon)}\frac{\mathrm{d}x_n}{\sigma}\left(v_0\left(\mathbf{u}_n-\mathbf{u}_1\right)-\sum_{i=2}^{n-1}\boldsymbol{\nabla}_{\mathbf{x}_i}U(\mathbf{x}_i)\right)\cdot\hat{\mathbf{x}}_n\times\dots\right.$$
$$\left.\cdots\times g_0^{(2)}(\mathbf{0},\mathbf{u}_1;\mathbf{x}_n,\mathbf{u}_n)\right]. \tag{4.101}$$

We stress that this truncation is approximate and prevents the derivation of [175] from being exact, at odds with the claim originally made in that paper. We recall from Eq. (4.79) that $g_0^{(2)}(\mathbf{0},\mathbf{u}_1;\mathbf{r},\mathbf{u}_2)$ is the solution of,

$$-v_0\left(\mathbf{u}_1-\mathbf{u}_2\right)\boldsymbol{\nabla}_{\mathbf{r}}g_0^{(2)}+2\boldsymbol{\nabla}_{\mathbf{r}}\left(g_0^{(2)}\boldsymbol{\nabla}_{\mathbf{r}}U(\mathbf{r})\right)=0\,, \tag{4.102}$$

in the infinitely short-ranged limit and where we have dropped the subleading flipping terms. With the potential U given by

$$\lim_{d\to\infty}U(r)=\widehat{U}(h)\ \text{ with }\ h=d\left(r/\sigma-1\right)\,, \tag{4.103}$$

and $\widehat{U}$ the sticky sphere potential of Eq. (4.16), the solution of the above equation was given in Sec. 4.1.2. In terms of the rescaled variables $h = d(r/\sigma - 1)$ and $w = \sqrt{d}\,\hat{\mathbf{u}}_{1n}\cdot\hat{\mathbf{r}}$ it reads

$$g_0^{(2)}\left(\mathbf{0},\mathbf{u}_1;\mathbf{r},\mathbf{u}_n\right)=\Theta(h)f_0(h,w)+\delta(h)\Gamma_0(w)\,, \tag{4.104}$$

with the bulk term obtained as

$$f_0(h,w)=\left[1-\Theta(w)\Theta\left(\frac{w^2}{2}-h\right)+\Theta(w)e^{\frac{w_0^2}{2}}\delta\left(h-\frac{w^2}{2}+\frac{w_0^2}{2}\right)\right]\,, \tag{4.105}$$

and the surface term given by

$$\Gamma_0(w) = \Theta(-w) + \Theta(w)\Theta(w_0 - w)e^{\frac{w^2}{2}} . \tag{4.106}$$

We recall that in Eqs. (4.105) and Eqs. (4.106), w_0 is defined as

$$w_0 = \max\left(\frac{\widehat{U}'(h)}{\widehat{v}_0}\right) , \tag{4.107}$$

with $v_0 = (\sqrt{2}d^{3/2}/\sigma)\widehat{v}_0$. We are now in position to compute the zeroth order conditional mean in this truncated scheme. We first note that for any unit vector $\mathbf{u}$ and in any dimension d,

$$\int \frac{\mathrm{d}\hat{\mathbf{x}}}{\Omega_d}\hat{x}^\mu\hat{x}^\nu\,\Gamma\left(\sqrt{d}\hat{\mathbf{x}}\cdot\mathbf{u}\right) = \frac{1}{d}\left(Au^\mu u^\nu + B\delta^{\mu\nu}\right) , \tag{4.108}$$

where the above tensorial form is a direct consequence of the symmetries of the integral and with the coefficients A and B given by

$$\begin{aligned} A &= \int \frac{\mathrm{d}w}{2W_{d-2}}\left(1-w^2\right)^{\frac{d-3}{2}}\left[dw^2 - \frac{d}{d-1}\right]\Gamma(\sqrt{d}w)\,, \\ &\underset{d\to\infty}{=} \int \frac{\mathrm{d}w}{\sqrt{2\pi}}\mathrm{e}^{-\frac{w^2}{2}}\left(w^2-1\right)\Gamma(w)\,, \end{aligned} \tag{4.109}$$

and

$$\begin{aligned} B &= \frac{d}{d-1}\int \frac{\mathrm{d}w}{2W_{d-2}}\left(1-w^2\right)^{\frac{d-3}{2}}\Gamma(\sqrt{d}w)\,, \\ &\underset{d\to\infty}{=} \int \frac{\mathrm{d}w}{\sqrt{2\pi}}\mathrm{e}^{-\frac{w^2}{2}}\Gamma(w)\,. \end{aligned} \tag{4.110}$$

We can therefore write the component μ of the conditional mean force as,

$$\begin{aligned} F^\mu_{1,1} &= -\frac{\rho\mathcal{V}_d(\sigma)}{2}\int\frac{\mathrm{d}\hat{\mathbf{u}}_n}{\Omega_d}\left[v_0\left(u^\nu_n - u^\nu_1\right) + \sum_{i=2}^{n-1}\nabla^\mu_{\mathbf{r}_1}U(\mathbf{r}_1-\mathbf{r}_i)\right]\int\frac{\mathrm{d}\hat{\mathbf{x}}_n}{\Omega_d}\hat{x}^\mu_n\hat{x}^\nu_n\Gamma\left(\sqrt{d}\hat{\mathbf{x}}_n\cdot\hat{\mathbf{u}}_{1n}\right) , \\ &= -\frac{\widehat{\varphi}}{2}\int\frac{\mathrm{d}\hat{\mathbf{u}}_n}{\Omega_d}\left[v_0\left(u^\nu_n - u^\nu_1\right) + \sum_{i=2}^{n-1}\nabla^\mu_{\mathbf{r}_1}U(\mathbf{r}_1-\mathbf{r}_i)\right]\left(Au^\mu_{1n}u^\nu_{1n} + B\delta^{\mu\nu}\right) , \\ &= -\frac{\widehat{\varphi}}{2}\int\frac{\mathrm{d}\hat{\mathbf{u}}_n}{\Omega_d}\left[v_0(A+B)\left(u^\mu_n - u^\mu_1\right) + Au^\mu_{1n}\sum_{i=2}^{n-1}\boldsymbol{\nabla}_{\mathbf{r}_1}U(\mathbf{r}_1-\mathbf{r}_i)\cdot\hat{\mathbf{u}}_{1n}\right. \\ &\qquad\qquad\left. + B\sum_{i=2}^{n-1}\nabla^\mu_{\mathbf{r}_1}U(\mathbf{r}_1-\mathbf{r}_i)\right] , \\ &= -\frac{\widehat{\varphi}}{2}\left[-v_0(A+B)u^\mu_1 + B\sum_{i=2}^{n-1}\nabla^\mu_{\mathbf{r}_1}U(\mathbf{r}_1-\mathbf{r}_i)\right] , \end{aligned} \tag{4.111}$$

where the last line is obtained by keeping only the leading order component along $\mathbf{u}_1$. Note that the conditional mean force is non-vanishing along the self-propulsion vector $\mathbf{u}_1$, which

is the idea behind the effective self-propulsion, but also along the total force exerted by the $n-2$ other tagged particles. The latter effect is not due to some steric hindering exerted by these particles on the remaining $N-n+1$ ones but to the modification of the apparent speed of particle 1 in their presence. Of course, in deriving Eq. (4.111), the number $n-1$ of tagged particles was completely arbitrary.

Resumming the hierarchy:

Using Eq. (4.111), the first order density corrections of the n-body distribution functions are obtained as solutions of,

$$\begin{aligned} &- v_0 \sum_{i=1}^{n} \mathbf{u}_i \boldsymbol{\nabla}_{\mathbf{r}_i} g_1^{(n)} + \sum_{i=1}^{n} \sum_{i \neq j}^{n} \boldsymbol{\nabla}_{\mathbf{r}_i} \left(g_1^{(n)} \boldsymbol{\nabla}_{\mathbf{r}_i} U(\mathbf{r}_i - \mathbf{r}_j) \right) \\ &+ \frac{\widehat{\varphi}}{2} \sum_{i=1}^{n} \boldsymbol{\nabla}_{\mathbf{r}_i} \left[g_0^{(n)} \left(v_0 \left(A + B \right) \mathbf{u}_i - B \sum_{j \neq}^{n} \boldsymbol{\nabla}_{\mathbf{r}_i} U \left(\mathbf{r}_i - \mathbf{r}_j \right) \right) \right] = 0 \,, \end{aligned} \tag{4.112}$$

for any $n \geq 2$ and where the subleading flipping terms have been suppressed. In a way perfectly consistent with the order 1 density expansion we consider here, we can replace $g_0^{(n)}$ by $g_1^{(n)}$ and get,

$$- v_1 \sum_{i=1}^{n} \mathbf{u}_i \boldsymbol{\nabla}_{\mathbf{r}_i} g_1^{(n)} + \mu_1 \sum_{i=1}^{n} \sum_{i \neq j}^{n} \boldsymbol{\nabla}_{\mathbf{r}_i} \left(g_1^{(n)} \boldsymbol{\nabla}_{\mathbf{r}_i} U(\mathbf{r}_i - \mathbf{r}_j) \right) = 0 \,, \tag{4.113}$$

with

$$\begin{aligned} v_1 &= v_0 - \frac{\widehat{\varphi}}{2} v_0 \int \frac{\mathrm{d}w}{\sqrt{2\pi}} \mathrm{e}^{-\frac{w^2}{2}} w^2 \Gamma_0(w) \\ &= v_0 - \frac{\widehat{\varphi}}{4} v_0 \left(1 + \frac{\sqrt{2} w_0^3}{3\sqrt{\pi}} \right) , \end{aligned} \tag{4.114}$$

and

$$\begin{aligned} \mu_1 &= 1 - \frac{\widehat{\varphi}}{2} \int \frac{\mathrm{d}w}{\sqrt{2\pi}} \mathrm{e}^{-\frac{w^2}{2}} \Gamma_0(w) \\ &= 1 - \frac{\widehat{\varphi}}{4} \left(1 + \frac{\sqrt{2} w_0}{\sqrt{\pi}} \right) . \end{aligned} \tag{4.115}$$

Remarkably, after one iteration in the density expansion, the hierarchical equations have the same functional form as their zeroth order counterpart with renormalized coefficients v_1 and μ_1 respectively in front of the self-propulsion and potential interaction terms. Note the difference with respect to the Kirkwood approximation scheme in which only the speed, and not the amplitude of the potential, was renormalized by the interactions. Equation (4.113) moreover shows that $\widehat{\varphi}$ is indeed the correct expansion parameter of the virial series. We can now use the same strategy as above to (i) solve for $g_1^{(n)}$ and (ii) obtain the hierarchy

equations after two iterations in the virial series. We know that the solution to Eq. (4.113) writes

$$g_1^{(n)}(\mathbf{r}_1,\mathbf{u}_1;\dots;\mathbf{r}_n;\mathbf{u}_n) = g_1^{(n-1)}(\mathbf{r}_1,\mathbf{u}_1;\dots;\mathbf{r}_{n-1};\mathbf{u}_{n-1})\left[\prod_{i=1}^{n-1} g_1^{(2)}(\mathbf{r}_i,\mathbf{u}_i;\mathbf{r}_n,\mathbf{u}_n)\right]\times\dots \\ \dots\times\left(1+\frac{\hat{K}_1(\mathbf{r}_1,\mathbf{u}_1;\dots;\mathbf{r}_n;\mathbf{u}_n)}{\sqrt{d}}\right). \tag{4.116}$$

Furthermore, following Eq. (4.95), we get in the infinite dimensional limit

$$\begin{aligned}&2\lim_{\text{short-ranged}}\mu_1\int_\sigma^{+\infty}\mathrm{d}x_n\, g_1^{(n)}(\mathbf{0},\mathbf{u}_1;\mathbf{x}_2,\mathbf{u}_2;\dots;\mathbf{x}_n,\mathbf{u}_n)\mu_1 U'(x_n) = \\ &\lim_{\epsilon\to0^+}\lim_{\text{short-ranged}}\int_\sigma^{\sigma(1+\epsilon)}\mathrm{d}x_n\left(v_1(\mathbf{u}_n-\mathbf{u}_1)-\mu_1\sum_{i=2}^{n-1}\boldsymbol{\nabla}_{\mathbf{x}_i}U(\mathbf{x}_i)\right)\cdot\hat{\mathbf{x}}_n\times\dots \\ &\qquad\dots\times g_1^{(n)}(\mathbf{0},\mathbf{u}_1;\mathbf{x}_2,\mathbf{u}_2;\dots;\mathbf{x}_n,\mathbf{u}_n)\,,\end{aligned} \tag{4.117}$$

Therefore, at the second iteration of the virial series, the conditional mean force exerted on particle 1 conditioned on the presence of the $n-2$ neighboring ones reads,

$$\mathbf{F}_{1,2} = \frac{\hat{\varphi}}{2}\frac{v_1}{\mu_1}\int\frac{\mathrm{d}w}{\sqrt{2\pi}}\mathrm{e}^{-\frac{w^2}{2}}w^2\Gamma_1(w)\mathbf{u}_1 - \frac{\hat{\varphi}}{2}\int\frac{\mathrm{d}w}{\sqrt{2\pi}}\mathrm{e}^{-\frac{w^2}{2}}\Gamma_1(w)\sum_{i\neq1}\boldsymbol{\nabla}_{\mathbf{r}_1}U(\mathbf{r}_1-\mathbf{r}_i)\,. \tag{4.118}$$

with $\Gamma_1(w)$ the surface term of the infinitely short-ranged limit of the solution of the two-body equation after the first iteration,

$$-v_1\left(\mathbf{u}_2-\mathbf{u}_1\right)\boldsymbol{\nabla}_{\mathbf{r}}g_1^{(2)} + 2\mu_1\boldsymbol{\nabla}_{\mathbf{r}}\left(g_1^{(2)}\boldsymbol{\nabla}_{\mathbf{r}}U(\mathbf{r})\right) = 0\,. \tag{4.119}$$

Equation (4.119) having the same functional form as Eq. (4.102), we obtain Γ_1 as,

$$\Gamma_1(w) = \Theta(-w) + \Theta(w)\Theta\left(\frac{v_0\mu_1}{v_1}w_0 - w\right)e^{\frac{w^2}{2}} \tag{4.120}$$

The renormalized coefficients v_1 and μ_1 modify the stationary two-point distribution by rescaling w_0. At small w_0, the effective amplitude of the potential diminishes faster (as w_0) than does the effective speed (as w_0^3) so that after one iteration of the virial series the sitcky nature of the potential is reduced. One can now use Eq. (4.118) to go one order further in the virial series so that the $g_2^{(n)}$'s are obtained as the solutions of,

$$-v_2\sum_{i=1}^{n}\mathbf{u}_i\boldsymbol{\nabla}_{\mathbf{r}_i}g_1^{(n)} + \mu_2\sum_{i=1}^{n}\sum_{i\neq j}^{n}\boldsymbol{\nabla}_{\mathbf{r}_i}\left(g_1^{(n)}\boldsymbol{\nabla}_{\mathbf{r}_i}U(\mathbf{r}_i-\mathbf{r}_j)\right) = 0\,, \tag{4.121}$$

with

$$v_2 = v_0 - \frac{\hat{\varphi}}{4}\frac{v_1}{\mu_1}\left(1+\frac{\sqrt{2}w_0^3}{3\sqrt{\pi}}\left(\frac{v_0\mu_1}{v_1}\right)^3\right), \tag{4.122}$$

and

$$\mu_2 = 1 - \frac{\hat{\varphi}}{4}\left(1 + \frac{\sqrt{2}w_0}{\sqrt{\pi}}\frac{v_0\mu_1}{v_1}\right) . \tag{4.123}$$

This procedure can be iterated to get, after full resummation of this truncated scheme, the equation for the n-body correlation functions,

$$-v(\widehat{\varphi})\sum_{i=1}^{n}\mathbf{u}_i\boldsymbol{\nabla}_{\mathbf{r}_i}g^{(n)} + \mu(\widehat{\varphi})\sum_{i=1}^{n}\sum_{i\neq j}^{n}\boldsymbol{\nabla}_{\mathbf{r}_i}\left(g^{(n)}\boldsymbol{\nabla}_{\mathbf{r}_i}U(\mathbf{r}_i-\mathbf{r}_j)\right) = 0\,. \tag{4.124}$$

The functions $v(\widehat{\varphi})$ and $\mu(\widehat{\varphi})$ are the fixed points of the iteration scheme shown in Eqs. (4.122) and (4.123),

$$v(\widehat{\varphi}) = v_0 - \frac{\hat{\varphi}}{4}\frac{v(\widehat{\varphi})}{\mu(\widehat{\varphi})}\left(1 + \frac{\sqrt{2}w_0^3}{3\sqrt{\pi}}\left(\frac{v_0\mu(\widehat{\varphi})}{v(\widehat{\varphi})}\right)^3\right) , \tag{4.125}$$

and

$$\mu(\widehat{\varphi}) = 1 - \frac{\hat{\varphi}}{4}\left(1 + \frac{\sqrt{2}w_0}{\sqrt{\pi}}\frac{v_0\mu(\widehat{\varphi})}{v(\widehat{\varphi})}\right) . \tag{4.126}$$

Following Eq. (4.92), the solution to Eq. (4.124) can be cast to leading order in the form of a product over pair functions,

$$g^{(n)}(\mathbf{r}_1,\mathbf{u}_1;\ldots;\mathbf{r}_n;\mathbf{u}_n) = \left[\prod_{i<j}^{n} g^{(2)}(\mathbf{r}_i,\mathbf{u}_i;\mathbf{r}_j,\mathbf{u}_j)\right] , \tag{4.127}$$

with the two-point function solution of

$$-v(\widehat{\varphi})\left(\mathbf{u}_2-\mathbf{u}_1\right)\boldsymbol{\nabla}_{\mathbf{r}}g^{(2)} + 2\mu(\widehat{\varphi})\boldsymbol{\nabla}_{\mathbf{r}}\left(g^{(2)}\boldsymbol{\nabla}_{\mathbf{r}}U(\mathbf{r})\right) = 0\,. \tag{4.128}$$

In the infinitely short-ranged limit, it reads

$$g^{(2)}\left(\mathbf{0},\mathbf{u}_1;\mathbf{r},\mathbf{u}_2\right) = \Theta(h)f(h,w) + \delta(h)\Gamma(w)\,, \tag{4.129}$$

with the bulk term obtained as

$$f(h,w) = \left[1 - \Theta(w)\Theta\left(\frac{w^2}{2}-h\right) + \Theta(w)e^{\frac{w(\widehat{\varphi})^2}{2}}\delta\left(h - \frac{w^2}{2} + \frac{w(\widehat{\varphi})^2}{2}\right)\right] , \tag{4.130}$$

and the surface term given by

$$\Gamma(w) = \Theta(-w) + \Theta(w)\Theta(w(\widehat{\varphi})-w)e^{\frac{w^2}{2}}\,. \tag{4.131}$$

The function $w(\widehat{\varphi})$ that quantifies the strength of the attractive sticky part of the pair-potential is given by

$$w(\widehat{\varphi}) = w_0\frac{v_0\mu(\widehat{\varphi})}{v(\widehat{\varphi})}\,. \tag{4.132}$$

In this truncated scheme, the structure of the fluid is thus very similar to that of a standard equilibrium one with the notable distinction that all the coefficients are renormalized by the interactions. We furthermore stress that Eq. (4.125) together with Eq. (4.128) show that $v(\widehat{\varphi})$ is indeed the true effective self-propulsion defined in Eq. (3.15).

Solutions of the fixed point equations:

We now solve the fixed point equations (4.125) and (4.126). We define $c(\widehat{\varphi}) = v(\widehat{\varphi})/v_0$ the ratio between the effective self-propulsion at density $\widehat{\varphi}$ over its dilute limit counterpart. We first study the purely hard-sphere case, $w_0 = 0$. There Eqs. (4.125) and (4.126) simplify and yield,

$$c(\widehat{\varphi}) = \mu(\widehat{\varphi}) = 1 - \frac{\widehat{\varphi}}{4}\,. \tag{4.133}$$

The above equation was the main result of [175]. It immediately defines the range of validity of our calculation, *i.e.* $\widehat{\varphi} < 4$. Indeed $\widehat{\varphi} > 4$ would lead to a nonphysical negative effective self-propulsion $v(\widehat{\varphi})$. We conjecture that for larger densities the hard sphere system is characterized by vanishing $v(\widehat{\varphi})$ and $\mu(\widehat{\varphi})$ for which the self-consistency equation Eq. (4.128) is also satisfied. We cannot however elucidate the structure of the fluid in this regime. We denote by $\widehat{\varphi}_{cr}$ the crowding density at which both $v(\widehat{\varphi})$ and $\mu(\widehat{\varphi})$ vanish. Remarkably, we recover in this truncated scheme the linear decay of the effective self-propulsion speed for strongly repulsive interaction potentials observed in numerical simulations of self-propelled particles in dimension 2 and 3 [193, 196]. Numerics also show the vanishing of $v(\rho)$ at a threshold that was observed to be independent of dynamical parameters [192, 193], at least in the large Péclet regime, as it is the case here. This effect is a fine property of the hard sphere potential and not a dilute limit result and that Eqs. (4.125) and (4.126), while being only approximate, are non-perturbative in $\widehat{\varphi}$. An immediate consequence of the equality between $\mu(\widehat{\varphi})$ and $c(\widehat{\varphi})$ is that the two-point function at non-vanishing $\widehat{\varphi}$ is equal to the dilute limit two-point function as can be seen from Eq. (4.128). In particular, the equation of state for the mechanical pressure obtained in the dilute limit in Eq. (3.47) extends for $0 < \widehat{\varphi} < 4$,

$$P \propto \frac{\widehat{v}_0\widehat{\tau}}{\sigma}\left(1 - \frac{\widehat{\varphi}}{4}\right)\frac{\widehat{\varphi}}{4} + \sqrt{\frac{2}{\pi}}\left(\frac{\widehat{\varphi}}{4}\right)^2\,. \tag{4.134}$$

It allows for a spinodal instability when $\widehat{\varphi} < 4$ and $P'(\widehat{\varphi}) < 0$, hence for

$$\widehat{Pe} = \frac{\widehat{v}_0\widehat{\tau}}{\sigma} > \frac{2\sqrt{2}}{\sqrt{\pi}}\,, \tag{4.135}$$

in line with the numerical observation [196] that the instability threshold for the Péclet number increases with the dimension (we recall that $v_0\tau \sim \sqrt{d}\widehat{v}_0\widehat{\tau}$). When this criterion is fulfilled the spinodal region is defined by

$$\frac{\widehat{Pe}}{2\left(\widehat{Pe} - \sqrt{2/\pi}\right)} < \frac{\widehat{\varphi}}{4} < 1\,. \tag{4.136}$$

The spinodal boundaries of the phase diagram are shown in Fig. 4.8. We now study the sticky-sphere case $w_0 \neq 0$. Equation (4.126) allows to express $\mu(\widehat{\varphi})$ as a function of $c(\widehat{\varphi})$,

$$\mu(\widehat{\varphi}) = \frac{\sqrt{\pi}c(\widehat{\varphi})(4 - \widehat{\varphi})}{4\sqrt{\pi}c(\widehat{\varphi}) + \sqrt{2}w_0\widehat{\varphi}}\,, \tag{4.137}$$

which in particular show that the effective amplitude of potential forces $\mu(\widehat{\varphi})$ and the effective self-propulsion $v_0c(\widehat{\varphi})$ vanish at the same density $\widehat{\varphi}_{cr}$ that now depends on w_0. When

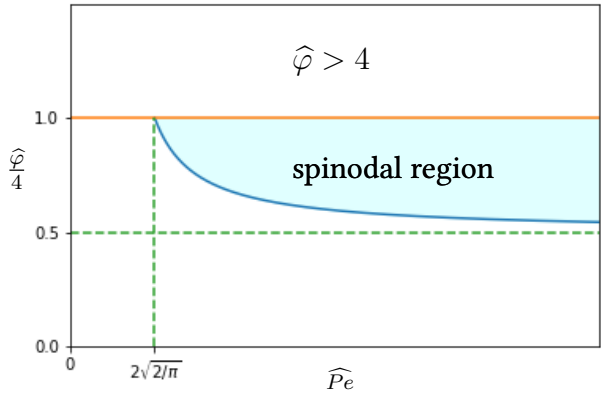

Figure 4.8: Phase boundaries of a system of infinite dimensional active hard-spheres within the approximate resummation scheme in the $(\widehat{Pe}, \widehat{\varphi}/4)$ plane. Cyan: Spinodal region for $\widehat{\varphi} < 4$.

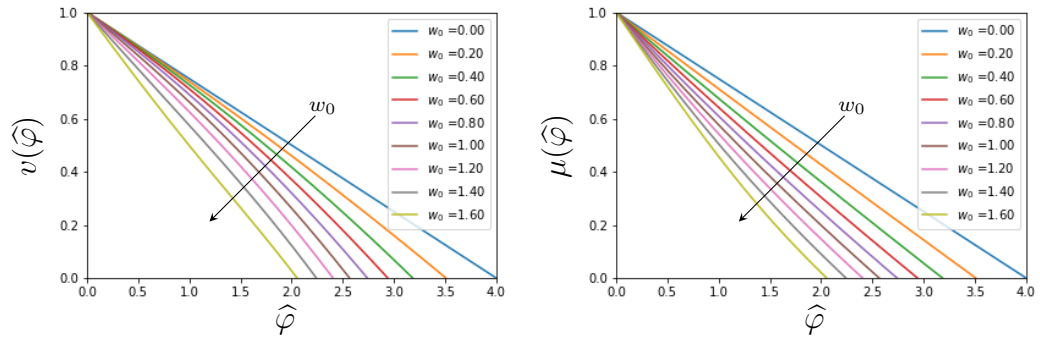

Figure 4.9: (Left) Effective self-propulsion as a function of the rescaled density $\widehat{\varphi}$ for increasing values of w_0. (Right) Effective potential force amplitude as a function of the rescaled density $\widehat{\varphi}$ for increasing values of w_0.

inserted in Eq. (4.125), the above equation yields an equation for $c(\widehat{\varphi})$ as a function of $\widehat{\varphi}$ and w_0. The latter takes the form of a third degree polynomial equation that we solve numerically by selecting the root continuously linked to $c = 1$ at $\widehat{\varphi} = 0$. We show the obtained solution at moderate sticking strength w_0 for both $c(\widehat{\varphi})$ and $\mu(\widehat{\varphi})$ in Fig. 4.9. It shows that for $w_0 \neq 0$ both $c(\widehat{\varphi})$ and $\mu(\widehat{\varphi})$ decay non-linearly to zero with the density and that the larger is the bare attraction strength the faster is the decay. Attraction thus enhances the freezing of the system. For larger w_0, the branch of the solution continuously linked to 1 at $\widehat{\varphi} = 0$ develops an imaginary part before reaching zero. This might be the signature of a discontinuous decay to 0 of the effective self-propulsion and effective potential force amplitude at strong enough attraction. We don't know however of any numerical work that would have reported such a behavior. Upon integrating the self-propulsion degrees of freedom, and according to Eq. (3.33), the radial distribution function reads,

$$g(h) = \Theta(h)\left[\frac{1}{2}\left(1 + \text{erf}\left(\sqrt{h}\right)\right) + \frac{e^{-h}}{\sqrt{2\pi\left(2h + w(\widehat{\varphi})^2\right)}}\right] + \left(\frac{1}{2} + \frac{w(\widehat{\varphi})}{\sqrt{2\pi}}\right)\delta(h)\,, \quad (4.138)$$

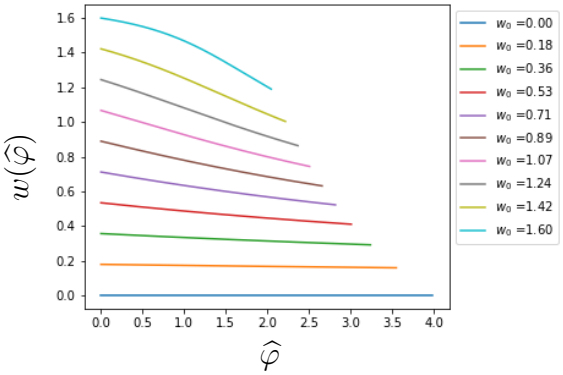

Figure 4.10: Decay of the effective sticking strength $w(\widehat{\varphi})$ as a function of the rescaled density $\widehat{\varphi}$ for different values of w_0. The curves end when the effective self-propulsion vanishes.

with $w(\widehat{\varphi}) = w_0\mu(\widehat{\varphi})/c(\widehat{\varphi})$ introduced in Eq. (4.132). It has the same functional form as the dilute case, with the coefficient $w(\widehat{\varphi})$ renormalized by the interactions. The latter quantifies the amplitude of the sticking strength and is plotted for different w_0 as a function of the density in Fig. 4.10. The curves end when the effective self-propulsion vanishes. This shows in particular, that the interactions tend to diminish the attraction between the particles induced by the attractive part of the potential as was already conjectured after the first resummation of the virial series in Eq. (4.120). This is an interesting and counter-intuitive result of our resummation scheme that would deserve numerical analysis in finite dimensional systems.

4.2.3 Concluding remarks

Let us now make an interesting connection between infinite dimensional active fluids and infinite dimensional passive ones and let us first restrict ourselves to the case of hard spheres with $w_0 = 0$. In position space, and as far as we are only concerned with the statics, the active fluid is completely similar to a passive one with a well chosen interaction pair potential. This can be see upon integrating Eq. (4.127) over all the self-propulsion degrees of freedom. Indeed, the structure of the n-point position-space distribution functions is the same as in an infinite-dimensional passive fluid with rescaled temperature and pairwise potential $\widehat{U}_p(h)$ chosen such that the dilute two-point function is reproduced, *i.e.*

$$\mathrm{e}^{-\widehat{\beta}\widehat{U}_p(h)} = g_0(h)\,. \tag{4.139}$$

This analytically supports the relevance of the Baxter model [11] as a proxy for analyzing of the structure of active fluids as suggested in [81]. Equation (4.139) indeed defines a dressed Baxter potential $\widehat{U}_p(h)$,

$$\widehat{\beta}\widehat{U}_p(h) = \begin{cases} +\infty \ \text{ if } h < 0\,, \\ -U_0 \ \text{ if } 0 < h < \hat{h}\,, \\ -\ln\left(\dfrac{1}{2}\left(1+\mathrm{erf}\left(\sqrt{h}\right)\right) + \dfrac{e^{-h}}{\sqrt{4\pi h}}\right) \ \text{ if } h > \hat{h}\,, \end{cases} \tag{4.140}$$

with $U_0 \to \infty$ and $\hat{h} \to 0$ such that $\ln \hat{h} + U_0 = 1/2$ in order to account for the delta peak accumulation. Now, the behavior of standard infinite dimensional equilibrium fluids as the one defined by Eq. (4.140), in particular regarding the glass transition [169], is well understood. In [189], Sellito and Zamponi showed using the Franz-Parisi potential approach that colloidal particles interacting through a Baxter potential of the type,

$$\mathrm{e}^{-\widehat{\beta}\widehat{U}_p(h)} = \theta(h) + \mathrm{e}^{-\alpha}\delta(h)\,, \tag{4.141}$$

experience a dynamical glass transition at a density $\widehat{\varphi}_d = 2\mathrm{e}^{\alpha}$. Their computation can be extended to the more general potential in Eq. (4.140). In particular, the bulk part of the potential does not modify the value of the predicted glass transition, as we show in App. C. Therefore, an equilibrium fluid with pair potential interactions given so as to reproduce the structure of the active hard sphere fluid experiences a dynamical glass transition at $\widehat{\varphi} = 4$, which is exactly the density at which the effective self-propulsion of the original active hard sphere model vanishes. Due to the delta peak attraction, the cage size at the corresponding glass transition vanishes so that the particles are completely frozen. This is consistent with the simultaneous vanishing of the effective self-propulsion speed and of the effective amplitude of potential interactions that deprives the particles from all sources of motion. Upon reversing the point of view, we also see emerging the dynamical glass transition, that, as the name says, is a dynamical concept in equilibrium and can be approached within the statics only through the coupling of different replicas of the system à la Franz-Parisi, as a property of a one-time observable (the effective self-propulsion or the effective amplitude of the potential forces) computed from the stationary measure of a single system with however an increased number of degrees of freedom.

A similar statement can be made about the sticky sphere case $w_0 \neq 0$ with however an important modification. Indeed, at a given density, the position-space structure of the active fluid is the same as that of a passive one with a pair potential that now explicitly depends on the density. We stress here that this feature can only be caused by multibody interactions. In their absence, the structure of the fluid, quantified by the n-body distribution functions, would be density-independent. The glass transition of this unusual equilibrium system can be studied once again following the work of [189]. At density $\widehat{\varphi}$, it remains indeed described by a dressed Baxter pair potential with the delta peak coefficient $\mathrm{e}^{-\alpha}$ given by,

$$\mathrm{e}^{-\alpha} = \left(\frac{1}{2} + \frac{w(\widehat{\varphi})}{\sqrt{2\pi}}\right)\,, \tag{4.142}$$

for which we know [190] that the onset of the dynamical glass transition is given by the solution of

$$\widehat{\varphi}_d = 4\left[1 + \frac{\sqrt{2}w(\widehat{\varphi}_d)}{\sqrt{\pi}}\right]^{-1}\,. \tag{4.143}$$

It is very puzzling that we can recognize in the above equation just a rewriting of the condition $\mu(\widehat{\varphi}) = 0$ in Eq. (4.126) for the freezing of the corresponding active system. We believe this correspondence advocates for the correctness of the physical picture we obtained within this approximate resummation scheme. Note that in Sec. 4.1, we have indeed proved that at first order in $\widehat{\varphi}$ the long-time MSD is directly proportional to the square of the effective self-propulsion $v(\widehat{\varphi})$. In App. D, we show that within the approximate resummation

scheme of the present section we expect the ultraballistic limit of the diffusion coefficient to be proportional to $v(\widehat{\varphi})^2$, thus rationalizing this correspondence between the Franz-Parisi result and the vanishing of $v(\widehat{\varphi})$. The computation is done in the case of purely hard spheres but can be generalized to sticky ones. This also strongly suggests that the mean-field glass transition of some out-of-equilibrium systems may be described through the Franz-Parisi approach upon replacing the bare pair-potential by the density renormalized one extracted from the stationary two-point distribution. It would be extremely enlightening to study this question within the framework of dynamical mean field theory and to understand under which conditions such an assertion could indeed hold beyond equilibrium.

4.3 Phase separation in effective equilibrium models of active matter: a transition driven by multibody interactions

We conclude our study on the role of multibody interactions by studying the AOUPs N-body dynamics within the Unified Colored Noise Approximation (UCNA). The UCNA has been widely used to study the behavior of active systems [51, 134, 211]. From an analytical standpoint, the great benefit of the UCNA, which is exact in the small persistence-time limit, is that the N-body stationary distribution is known [134]. The impossibility to obtain stationary distribution function of many-body active systems beyond the small persistence-time limit has indeed plagued our understanding of these systems so far. From our point of view, the main relevance of the UCNA approximation lies in that the many-body stationary distribution displays multi-body interactions. It has interestingly been found that keeping track only of the 2-body ones in the fashion of Eq. (4.3) performs poorly in reproducing the behavior of active systems [179]. It is nevertheless not known yet if the picture provided by the UCNA gets better upon conserving higher order interaction terms.

We attempt to give a first answer to this question by studying the phase behavior of the UCNA in the large d limit. After introducing the UCNA dynamics, we show that keeping track only of two-body interactions does not allow to account for phase separation in the limit $d \to \infty$, in line with the findings of [202]. The role of multibody interactions in the large dimensional thermodynamics is then worked out. The computation rests on the possibility, upon introducing additional auxiliary degrees of freedom, to map the problem onto a purely pairwise interacting one in an extended phase space. This opens the door to extending the results from Sec. 3.2. We find, in agreement with the picture drawn in Sec. 4.2, that the structure of the fluid quantified by the n-body distribution functions is the same as that of an infinite dimensional standard equilibrium fluid with density-dependent pair potential that we compute explicitly. The phase diagram of the UCNA is derived. It shows a rich phase behavior with two different phases with different symmetries and coexistence regions between them.

4.3.1 The Unified Colored Noise Approximation (UCNA)

One of the standard model of active matter is the AOUPs one. Considering N interacting particles in dimension d labeled by $i \in [\![1, N]\!]$, the dynamics of the i^{th} particle follows

$$\dot{\mathbf{r}}_i = \mathbf{v}_i - \sum_{j \neq i} \boldsymbol{\nabla}_i U(\mathbf{r}_i - \mathbf{r}_j)\,, \tag{4.144}$$

where U is the pairwise interparticle potential and the active driving $\mathbf{v}_i$ is modeled as a d-dimensional Ornstein-Ulhenbeck process

$$\dot{\mathbf{v}}_i = -\frac{\mathbf{v}_i}{\tau} + \frac{\sqrt{2D}}{\tau}\boldsymbol{\eta}_i(t)\,, \tag{4.145}$$

with $\boldsymbol{\eta}_i(t)$ a Gaussian white noise with correlations $\left\langle \eta_i^\mu(s)\eta_j^\nu(t)\right\rangle = \delta_{ij}\delta^{\mu\nu}\delta(t-s)$. In the steady state, the process $\mathbf{v}_i(t)$ is Gaussian and exponentially correlated in time with correlation time τ. The potential U is assumed to be radially symmetric, $U(\mathbf{r}) = U(r)$ with $r = |\mathbf{r}|$. Introducing the momentum $\mathbf{p}_i = \dot{\mathbf{r}}_i$, the dynamics Eqs. (4.144)-(4.145) can be written as

$$\tau\dot{p}_i^\mu + \left[\delta^{\mu\nu} + \tau\sum_{j\neq i}\partial^\mu\partial^\nu U(\mathbf{r}_i - \mathbf{r}_j)\right] p_i^\nu = -\sum_{j\neq i}\partial^\mu U(\mathbf{r}_i - \mathbf{r}_j) + \sqrt{2D}\,\eta_i^\mu(t)\,, \tag{4.146}$$

where summation over repeated indices is assumed. Equation (4.146) is at the basis of the UCNA approximation of the AOUPs dynamics. Concretely, one drops the inertial term $\tau\dot{p}_i^\mu$ to get the overdamped equation of motion

$$\left[\delta^{\mu\nu} + \tau\sum_{j\neq i}\partial^\mu\partial^\nu U(\mathbf{r}_i - \mathbf{r}_j)\right] \dot{r}_i^\nu = -\sum_{j\neq i}\partial^\mu U(\mathbf{r}_i - \mathbf{r}_j) + \sqrt{2D}\,\eta_i^\mu(t)\,, \tag{4.147}$$

understood as Stratonovich discretized. The Stratonovich prescription allows the dynamics in Eq. (4.147) to be consistent with the original dynamics Eqs. (4.144)-(4.145) to first order in τ at small persistence time. This approximation was actually not introduced first in the context of active matter but to study the properties of driven dye lasers [106] that obey similar dynamics. Interestingly, the UCNA dynamics Eq. (4.147) is an equilibrium dynamics. Despite the complicated form of Eq. (4.147), this allows to find the stationary distribution with respect to which detailed balance holds [134]:

$$P_s(\{\mathbf{r}_i\}) = \frac{1}{Z}\mathrm{e}^{-\beta\sum_{i<j}U(\mathbf{r}_i-\mathbf{r}_j) - \frac{\beta\tau}{2}\sum_i\left(\sum_{j\neq i}\boldsymbol{\nabla}_i U(\mathbf{r}_i-\mathbf{r}_j)\right)^2}\left|\det\left(\mathbb{1} + \mathrm{H}\right)\right|\,, \tag{4.148}$$

with $\beta = D^{-1}$ and where H is a $Nd \times Nd$ matrix with coefficients

$$\mathrm{H}_{i\alpha,j\beta} = \tau\left(\sum_{k\neq i}\partial^\alpha\partial^\beta U(\mathbf{r}_i - \mathbf{r}_k)\delta_{ij} - \partial^\alpha\partial^\beta U(\mathbf{r}_i - \mathbf{r}_j)\left[1-\delta_{ij}\right]\right)\,. \tag{4.149}$$

The UCNA approximation is, together with the Fox approximation [62], one of the main effective equilibrium approximations of active systems interacting via pairwise forces. While

leading to different predictions at the dynamical level, the Fox approximation of Eqs. (4.144)-(4.145) is described in the steady state by the same distribution Eqs. (4.148)-(4.149). As mentioned above, the probability distribution in Eq. (4.148) agrees in a small τ expansion to order $O(\tau)$ with the stationary distribution of the AOUPs dynamics Eqs. (4.144)-(4.145). Equation (4.148) can nevertheless be treated non-perturbatively in τ and is at the basis of our analytical study on the importance of multibody interactions in the phase diagram of active systems. Indeed, the measure in Eq. (4.148) cannot be factorized as a product over pair functions. As already discussed at the beginning of this chapter, we believe this to be a generic feature of active matter systems, as can already be seen from the order $O(\tau)$ expansion of Eq. (4.148) that exhibits 3-body interactions [60], thus making their position-space stationary distribution genuinely different from that of standard equilibrium fluids.

4.3.2 The infinite dimensional limit

Following the pioneering approach of [66] for the liquid phase of classical hard spheres, and later successfully extended to the statics and dynamics of glassy systems [120, 136], we study analytically the thermodynamic properties of the position space stationary measure in Eq. (4.148) in the limit of infinite space dimension $d \to \infty$. The interaction potential is assumed to be short ranged and scales as before as

$$U(r) = \widehat{U}(h) \text{ with } h = d\,(r/\sigma - 1)\ , \tag{4.150}$$

and where σ is the diameter of a particle. In order to keep the product $\beta U(r)$ finite, the coefficient β is kept fixed. Furthermore, each particle is assumed to have roughly d neighbors, *i.e.* for each particle there is $O(d)$ particles with which the rescaled interaction potential $\widehat{U}$ is finite

$$\frac{\rho \mathcal{V}_d(\sigma)}{d} = \widehat{\varphi}\,, \tag{4.151}$$

with $\widehat{\varphi}$ finite. Lastly, the correlation time τ is scaled as $\tau = \hat{\tau}/d^2$. Note that from Eq. (4.145),

$$\left\langle \mathbf{v}_i(t)^2 \right\rangle = \frac{d}{\beta\tau} = \frac{d^3}{\beta\hat{\tau}}\,. \tag{4.152}$$

Hence, over timescales of order τ, the variations of r_i^μ scale as $O(1/d)$ which is the natural length scale due to Eq. (4.150). This scaling is actually the same as that of Sec.4.1 upon setting $\zeta = 1$ by a redefinition of time. In standard equilibrium fluids, where the stationary measure is written as a product over pair functions, the effect of the infinite dimensional limit is an exact truncation (up to corrections exponentially small in the dimension) of the virial expansion of the free energy functional to second order. As we have seen, the reason for this simplification is geometrical. Assume that two particles, say i and j, have a finite rescaled interaction potential $\widehat{U}$. Then the probability that there exists a third particle such that its rescaled interaction potential is non vanishing with both i and j becomes vanishingly small as $d \to \infty$. While this geometrical argument still holds in the case under study, it turns out that the density expansion of the free energy functional associated to Eq. (4.148) can not be truncated exactly to any order even in the limit of infinite space dimension due to the presence of multibody interactions in the stationary distribution. In the remainder of

this article, we extend the work of [66] to the stationary measure in Eq. (4.148) by expressing the later as a product over pair functions in an extended phase space with auxiliary variables, thus allowing us to use the standard machinery of the Mayer expansion and of its truncation in $d \to \infty$. This treatment is akin to the one of [136] for the dynamics of interacting particle systems in which the introduction of the Janssen-de Dominicis response fields allows to write the dynamical partition function as a product over pair functions.

4.3.3 Absence of transition at the two body level

Before studying the full phase diagram of Eq. (4.148) we restrict in the present section our attention to the case $N = 2$. This allows to define the effective bare pair potential $U_{\text{eff}}(\mathbf{r})$ as

$$P_s^{N=2}(\mathbf{r}_1, \mathbf{r}_2) \propto \mathrm{e}^{-\beta U_{\text{eff}}(\mathbf{r}_1 - \mathbf{r}_2)} , \tag{4.153}$$

defined in such a way that $\lim_{|\mathbf{r}|\to\infty} U_{\text{eff}}(\mathbf{r}) = 0$. The effective pair potential also describes the structure of a thermodynamic system in the limit of vanishing density ρ as,

$$\lim_{\rho\to 0} g(\mathbf{r}) = \mathrm{e}^{-\beta U_{\text{eff}}(\mathbf{r})} . \tag{4.154}$$

with $g(\mathbf{r})$ the two-point function. $U_{\text{eff}}(\mathbf{r})$ can be inferred from Eq. (4.148) and was given in [134]

$$U_{\text{eff}}(\mathbf{r}) = U(r) + \tau U'(r)^2 - \frac{(d-1)}{\beta} \ln \left| 1 + 2\tau \frac{U'(r)}{r} \right| - \beta^{-1} \ln |1 + 2\tau U''(r)| , \tag{4.155}$$

In a small τ expansion we get

$$U_{\text{eff}}(r) = U(r) + \tau U'(r)^2 - \frac{2\tau(d-1)}{\beta} \frac{U'(r)}{r} - 2\beta^{-1}\tau U''(r) + O(\tau^2) . \tag{4.156}$$

Let us assume that the interaction potential $U(r)$ is purely repulsive and convex. The first three terms in the right-hand side of Eq. (4.156) then correspond to purely repulsive contributions. The last one yields a purely attractive contribution that accounts for the activity-induced attraction commonly referred to in active matter systems. At arbitrary τ, the expression in Eq. (4.155) however yields unphysical results for generic classes of potentials [134] due to the appearance of negative eigenvalues in the spectrum of $\mathbb{1} + \mathrm{H}$. This problem is cured in the limit of infinite dimension in which the effective pair potential becomes well behaved for convex potentials at arbitrary values of $\hat{\tau}$ and β as one gets to leading order in d, and using the notations introduced previously for rescaled quantities,

$$\widehat{U}_{\text{eff}}(h) = \widehat{U}(h) + \frac{\hat{\tau}}{\sigma^2} \widehat{U}'(h)^2 - \frac{2\hat{\tau}}{\beta\sigma^2} \widehat{U}'(h) - \beta \ln \left| 1 + \frac{2\hat{\tau}}{\sigma^2} \widehat{U}''(h) \right| . \tag{4.157}$$

In Fig. 4.11, we plot the effective pair potential for different values of $\hat{\tau}$ in the case of an exponentially repulsive bare pair potential $\widehat{U}(h) = u_0 \, \mathrm{e}^{-\lambda h}$ (left panel) and of a harmonic sphere one $\widehat{U}(h) = u_0 \, h^2 \Theta(-h)/2$ (right panel). At $\hat{\tau} = 0$ the effective pair potential equals the bare one. For large enough $\hat{\tau} > 0$, the effective potential develops an attractive part due to the logarithmic term in Eq. (4.157).

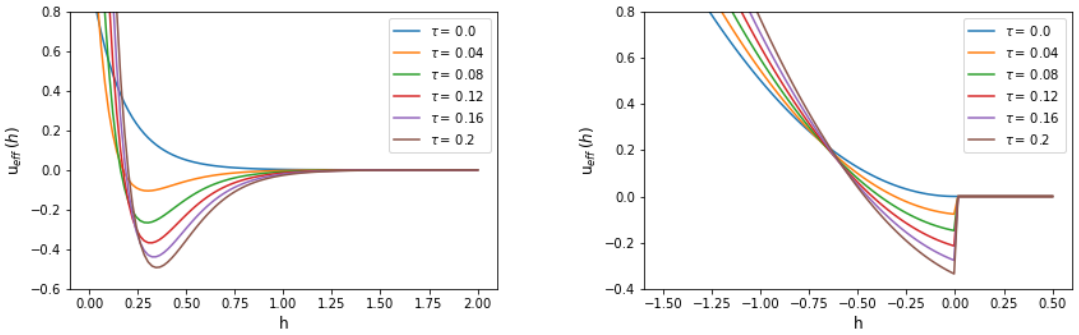

Figure 4.11: Effective pair potential for different values of $\hat{\tau}$ for $\beta = 1$ and $\sigma = 1$. **(Left)** The bare potential is taken of the form $\widehat{U}(h) = u_0\, \mathrm{e}^{-\lambda h}$ with $u_0 = 1$ and $\lambda = 6$. **(Right)** The bare potential is taken of the form $\widehat{U}(h) = u_0\, h^2\Theta(-h)/2$ with $u_0 = 1$.

Interestingly, it turns out that this effective pair potential, while displaying for convex potentials an attractive part due to the logarithmic term, is not able on its own to induce phase separation. To be more precise, let us consider a system of N particles with position space stationary distribution retaining only the pair interactions

$$P_s'\left(\{\mathbf{r}_i\}\right) = \frac{1}{Z'}\prod_{i<j} \mathrm{e}^{-\beta U_{\text{eff}}(\mathbf{r}_i - \mathbf{r}_j)}\,, \tag{4.158}$$

as would be the one of an equilibrium system with temperature β^{-1} and pair potential $U_{\text{eff}}(\mathbf{r})$. As said before, it is known that in the limit of infinite space dimension the free energy functional is truncated to second order in its density expansion,

$$\mathcal{F}[\rho(\mathbf{r})] = \int \mathrm{d}\mathbf{r}\, \rho(\mathbf{r})\left(\ln \rho(\mathbf{r}) - 1\right) - \frac{1}{2}\int \mathrm{d}\mathbf{r}\, \mathrm{d}\mathbf{r}'\, \rho(\mathbf{r})\rho(\mathbf{r}') f\left(\mathbf{r}, \mathbf{r}'\right)\,, \tag{4.159}$$

up to corrections exponentially small in d and with $f(\mathbf{r}) = \mathrm{e}^{-\beta U_{\text{eff}}(\mathbf{r})} - 1$ the Mayer function. For homogeneous systems with density ρ, the thermodynamic pressure thus reads

$$\beta\frac{P(\varphi)\mathcal{V}_d(\sigma)}{d} = \varphi\left(1 + \frac{d\varphi}{2}B(\hat{\beta},\hat{\tau})\right) \simeq d\,\frac{\varphi^2}{2}B(\hat{\beta},\hat{\tau})\,, \tag{4.160}$$

with the second virial coefficient

$$B(\hat{\beta},\hat{\tau}) = \int \mathrm{d}h\, \mathrm{e}^h\left(1 - \mathrm{e}^{-\hat{\beta}\widehat{U}_{\text{eff}}(h)}\right)\,. \tag{4.161}$$

We assume that the pair potential is that of harmonic spheres $\widehat{U}(h) = (u_0/2)h^2\Theta(-h)$. We introduce the constants $c_1 = 2\hat{\tau}u_0/\sigma^2$ and $c_2 = \beta u_0$. The latter is the ratio between the pair potential energy scale and the effective temperature of the $\tau = 0$ dynamics whereas $\sqrt{c_1/c_2}$ controls the ratio between the run length of the original non-interacting AOUPs dynamics to the size of a particle, often called the Péclet number in the literature. The effective potential then reads,

$$\beta\,\widehat{U}_{\text{eff}}(h) = \left[c_2(1+c_1)\frac{h^2}{2} - c_1 h - \ln\left(1 + c_1\right)\right]\Theta(-h)\,. \tag{4.162}$$

Hence the second virial coefficient, seen as a function of c_1 and c_2, is found to be

$$B(c_1, c_2) = 1 - \sqrt{\pi} \exp\left(\frac{1+c_1}{2c_2}\right) \operatorname{erfc}\left(\sqrt{\frac{1+c_1}{2c_2}}\right) \sqrt{\frac{1+c_1}{2c_2}} > 0 \;\; \forall\, c_1, c_2 > 0\,. \quad (4.163)$$

Thus, the second virial coefficent being positive in all regions of parameter space, the system described by the stationary measure Eq.(4.158) has stable homogeneous phases in all its parameter space for all densities in the regime defined by Eq. (4.151). Similar conclusions can be derived for the potential used to construct the left panel of Fig. 4.11. Effective pair interactions are thus not able to account solely for phase separation. This may come as a surprise given the shape of the effective pair potential in Fig. 4.11 (especially on the left panel) that visually resembles the standard Lennard-Jones potential that is well known to account for phase separation in equilibrium simple liquids. However, in such a system, the depth of the attractive well of $\beta\widehat{U}(h)$ can be made arbitrarily large by increasing β, *i.e.* by lowering the temperature. This is not the case here as the amplitude of the attractive part of the attractive term in Eq. (4.157) is itself proportional to β^{-1}. Furthermore, by increasing $\hat{\tau}$ at fixed β, the depth of the attractive part of the effective pair potential can not be made arbitrary large neither. As shown in Fig (4.12), the depth of the attractive well indeed saturates in the case of the exponentially repulsive potential at large $\hat{\tau}$. For the harmonic potential, the situation is slightly different as the depth of the attractive well increases with $\hat{\tau}$ but its width shrinks at the same time. All in all, this is reminiscent of what we showed earlier about the active hard spheres two-particle stationary distribution function that admits a finite limit (in the distribution sense) as the persistence time is sent to infinity. We think this observation is at the basis of the results presented in [202] about the role of multibody interactions in active particle systems.

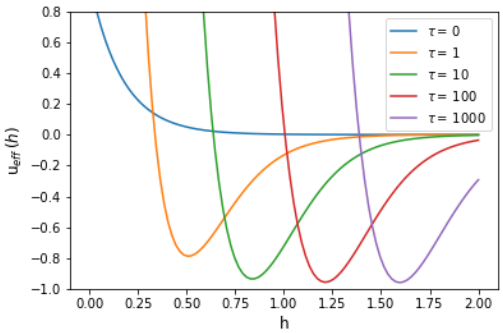

Figure 4.12: Effective pair potential for different values of $\hat{\tau}$ for $\beta = 1$ and $\sigma = 1$ and $\widehat{U}(h) = u_0\, \mathrm{e}^{-\lambda h}$ with $u_0 = 1$ and $\lambda = 6$. The depth of the attractive well saturates as $\hat{\tau}$ increases.

4.3.4 Mapping towards a pairwise interacting system

The thermodynamics properties of the measure in Eq. (4.148) are better captured in the grand-canonical ensemble. We introduce the grand canonical partition functional $\Xi[\mu]$ de-

fined by

$$\Xi[\mu] = \sum_{N=0}^{+\infty} \frac{1}{N!} \int \prod_i \mathrm{d}\mathbf{r}_i \left[\prod_i \mathrm{e}^{\mu(\mathbf{r}_i)} \right] \mathrm{e}^{-\beta \sum_{i<j} U(\mathbf{r}_i - \mathbf{r}_j) - \frac{\beta\tau}{2} \sum_i \left(\sum_{j \neq i} \boldsymbol{\nabla}_i U(\mathbf{r}_i - \mathbf{r}_j) \right)^2} \left| \det \left(\mathbb{1} + \mathrm{H} \right) \right| , \tag{4.164}$$

with $\mu(\mathbf{r})$ the generalized chemical potential. As such, the formula in Eq. (4.164) is not suitable for performing a standard Mayer expansion because of the multibody nature of the stationary distribution function. In this section, we map the problem under consideration onto a problem with purely pairwise interactions in an extended phase space. Doing so will then allow us to use and adapt the machinery of Mayer expansions and of infinite dimensional equilibrium fluids. First, we introduce N d-dimensional vectors $\boldsymbol{\psi}_i$, one attached to each particle, and write

$$\mathrm{e}^{-\frac{\beta\tau}{2} \sum_i \left(\sum_{j \neq i} \boldsymbol{\nabla}_i U(\mathbf{r}_i - \mathbf{r}_j) \right)^2} = \int \prod_i \frac{\mathrm{d}^d \boldsymbol{\psi}_i}{(2\pi)^{d/2}} \mathrm{e}^{-\sum_i \frac{\boldsymbol{\psi}_i^2}{2}} \mathrm{e}^{-i\sqrt{\beta\tau} \sum_{i<j} \left(\boldsymbol{\psi}_i - \boldsymbol{\psi}_j \right) \cdot \boldsymbol{\nabla}_i U(\mathbf{r}_i - \mathbf{r}_j)} , \tag{4.165}$$

so that the 3-body interaction term in the left-hand side of Eq. (4.165) is represented in terms of a two-body one. We proceed along the same lines with the absolute value of the determinant in Eq. (4.148) that we compute through a replica calculation. First, we use the identity valid for any real symmetric matrix H

$$\left| \det \left(\mathbb{1} + \mathrm{H} \right) \right| = \lim_{\epsilon \to 0^+} \lim_{n \to 0} \mathrm{K}_\epsilon^{n-1} , \tag{4.166}$$

with

$$\begin{aligned} \mathrm{K}_\epsilon &= \frac{1}{\left| \det \left((1 + i\epsilon)\, \mathbb{1} + \mathrm{H} \right) \right|} \\ &= \int \prod_{i=1}^{N} \prod_{\alpha=1}^{d} \frac{\mathrm{d}\phi_i^\alpha \mathrm{d}\varphi_i^\alpha}{2\pi} \exp \left(-\frac{\epsilon - i}{2} \sum_i \boldsymbol{\phi}_i^2 - \frac{\epsilon + i}{2} \sum_i \boldsymbol{\varphi}_i^2 \right. \\ &\qquad \left. + \frac{i}{2} \sum_{i,j=1}^{N} \sum_{\alpha,\beta=1}^{d} \left(\phi_i^\alpha \phi_j^\beta - \varphi_i^\alpha \varphi_j^\beta \right) \mathrm{H}_{i\alpha,j\beta} \right) . \end{aligned} \tag{4.167}$$

Hence we obtain,

$$\Xi[\mu] = \lim_{\epsilon \to 0^+} \lim_{n \to 0} \Xi_{\epsilon,n}[\mu(\mathbf{r})] , \tag{4.168}$$

with

$$\Xi_{\epsilon,n}[\mu] = \sum_{N=0}^{+\infty} \frac{1}{N!} \int \prod_i \mathrm{d}\mathbf{r}_i \left[\prod_i \mathrm{e}^{\mu(\mathbf{r}_i)} \right] \mathrm{e}^{-\beta \sum_{i<j} U(\mathbf{r}_i - \mathbf{r}_j) - \frac{\beta\tau}{2} \sum_i \left(\sum_{j \neq i} \boldsymbol{\nabla}_i U(\mathbf{r}_i - \mathbf{r}_j) \right)^2} \mathrm{K}_\epsilon^{n-1} . \tag{4.169}$$

For $n \in \mathbb{N}$ with $n > 1$, the above formula can be evaluated by introducing for each particle $n-1$ sets of replicated fields $\{\boldsymbol{\phi}_i^a, \boldsymbol{\varphi}_i^a\}_{a=1,\dots,n-1}$

$$\Xi_{\epsilon,n}[\mu] = \sum_{N=0}^{+\infty} \frac{1}{N!} \int \prod_{i=1}^{N} \mathrm{d}\mathbf{r}_i \, \mathrm{d}\boldsymbol{\xi}_i \prod_{i=1}^{N} \exp\left[\mu(\mathbf{r}_i) - \sum_{a=1}^{n-1} \left(\frac{\epsilon - i}{2} (\boldsymbol{\phi}_i^a)^2 + \frac{\epsilon + i}{2} (\boldsymbol{\varphi}_i^a)^2 \right) \right.$$
$$\left. -\frac{1}{2}\boldsymbol{\psi}_i^2 - d\left(n - \frac{1}{2}\right) \ln(2\pi) \right] \prod_{i<j} \exp\left[-\beta U(\mathbf{r}_i - \mathbf{r}_j) + i\sqrt{\beta\tau}(\boldsymbol{\psi}_i - \boldsymbol{\psi}_j) \boldsymbol{\nabla} U(\mathbf{r}_i - \mathbf{r}_j) \right.$$
$$\left. + \frac{i\tau}{2} \sum_{a=1}^{n-1} \left[\left(\phi_i^{a,\alpha} - \phi_j^{a,\alpha}\right) \left(\phi_i^{a,\beta} - \phi_j^{a,\beta}\right) - \left(\varphi_i^{a,\alpha} - \varphi_j^{a,\alpha}\right) \left(\varphi_i^{a,\beta} - \varphi_j^{a,\beta}\right) \right] \partial^\alpha \partial^\beta U(\mathbf{r}_i - \mathbf{r}_j) \right] , \tag{4.170}$$

where we used the reduced notation $\boldsymbol{\xi}_i$ for the set of auxiliary fields $\{\boldsymbol{\psi}_i, \boldsymbol{\phi}_i^a, \boldsymbol{\varphi}_i^a\}$ attached to particle i with

$$\mathrm{d}\boldsymbol{\xi}_i = \mathrm{d}\boldsymbol{\psi}_i \prod_{a=1}^{n-1} \mathrm{d}\boldsymbol{\phi}_i^a \mathrm{d}\boldsymbol{\varphi}_i^a \, . \tag{4.171}$$

At the end, we take the limit $n \to 0$. The validity of the method depends on whether it is possible to analytically continue the function from larger than one integers to $n = 0$. $\Xi_n[\mu]$ is finally promoted from a functional of the chemical potential $\mu(\mathbf{r})$ to a functional of the generalized chemical potential $j(\mathbf{r}, \boldsymbol{\xi})$ as

$$\Xi_n[j] = \sum_{N=0}^{+\infty} \frac{1}{N!} \int \prod_{i=1}^{N} \mathrm{d}\mathbf{r}_i \, \mathrm{d}\boldsymbol{\xi}_i \left[\prod_{i=1}^{N} \mathrm{e}^{j(\mathbf{r}_i, \boldsymbol{\xi}_i)} \right] \prod_{i<j} \left(1 + f(\mathbf{r}_i, \boldsymbol{\xi}_i; \mathbf{r}_j, \boldsymbol{\xi}_j)\right) \, , \tag{4.172}$$

where the Mayer function can be read from Eq. (4.170)

$$1 + f(\mathbf{r}_i, \boldsymbol{\xi}_i; \mathbf{r}_j, \boldsymbol{\xi}_j) = \exp\left[-\beta U(\mathbf{r}_i - \mathbf{r}_j) + i\sqrt{\beta\tau}(\boldsymbol{\psi}_i - \boldsymbol{\psi}_j) \boldsymbol{\nabla} U(\mathbf{r}_i - \mathbf{r}_j) \right]$$
$$\exp\left[\frac{i\tau}{2} \sum_{a=1}^{n-1} \left[\left(\phi_i^{a,\alpha} - \phi_j^{a,\alpha}\right) \left(\phi_i^{a,\beta} - \phi_j^{a,\beta}\right) - \left(\varphi_i^{a,\alpha} - \varphi_j^{a,\alpha}\right) \left(\varphi_i^{a,\beta} - \varphi_j^{a,\beta}\right) \right] \partial^\alpha \partial^\beta U(\mathbf{r}_i - \mathbf{r}_j) \right] . \tag{4.173}$$

Hence we managed to express $\Xi[\mu]$ in terms of the grand-canonical partition function of a model with only pairwise interactions. The cost is the introduction of these auxiliary fields attached to each particle. The gain is the possibility to resort to Mayer expansion and mean field theory of simple fluids. In App. E, in a completely different context, we show that such a replica representation of the absolute value of a determinant can be used to recover the results of [70] about the number of stationary points in a family of large random dynamical system. Alternatively, instead of the replicated fields, and following [69], one could use a mix of complex and Grassmann variables to represent the absolute value of the determinant in Eq. (4.148). In the present case we however found this interesting approach to be less fruitful.

4.3.5 The free energy functional

In standard liquid theory, the free energy, seen as a functional of the one-body density field, is defined as the Legendre transform of the logarithm of the grand canonical partition function with respect to the chemical potential $\mu(r)$. However in the present case Eq.(4.172), both the physical generalized chemical potential and the Mayer function are complex valued. The construction of the free energy functional can however be adapted using the graph expansion we showed in Sec. 3.2. Let $\rho(\mathbf{r},\boldsymbol{\xi})$ be the one-body density associated to $\Xi_n[j]$. It is indeed clear that both Eq. (3.64) and Eq. (3.73) hold in the present case upon replacing $\mu(\mathbf{r})$ by $j(\mathbf{r},\boldsymbol{\xi})$. We can then use the linked cluster theorem to state that

$$\rho(\mathbf{r},\boldsymbol{\xi}) = \mathrm{e}^{h(\mathbf{r},\boldsymbol{\xi})}\,, \tag{4.174}$$

with

$$h(\mathbf{r},\boldsymbol{\xi}) = j(\mathbf{r},\boldsymbol{\xi}) + \Sigma[j] \tag{4.175}$$

and $\Sigma[j]$ the sum over all the connected diagrams with a unit-valued white vertex which is not an articulation one and black e^j vertices. The above relation can be inverted as in the standard liquid case to obtain $j(\mathbf{r},\boldsymbol{\xi})$ as a function of $h(\mathbf{r},\boldsymbol{\xi})$. Following the notations introduced in Sec. 3.2, we denote it $j^*[h](\mathbf{r},\boldsymbol{\xi})$ that reads

$$j[h]^*(\mathbf{r},\boldsymbol{\xi}) = h(\mathbf{r},\boldsymbol{\xi}) - \hat{\Sigma}[\rho] \tag{4.176}$$

with $\hat{\Sigma}[\rho]$ the sum over all one-particle irreducible diagrams with $\rho(\mathbf{r},\boldsymbol{\xi})$ black vertices and one white unit-valued one. We thus introduce as before, for a given generalized chemical potential $j(\mathbf{r},\boldsymbol{\xi})$, the free energy functional

$$\mathcal{G}[h] = -W[j^*[h]] + \int \mathrm{d}\mathbf{r}\mathrm{d}\boldsymbol{\xi}\mathrm{e}^{h(\mathbf{r},\boldsymbol{\xi})} j^*[\rho](\mathbf{r},\boldsymbol{\xi}) - \int \mathrm{d}\mathbf{r}\mathrm{d}\boldsymbol{\xi}\mathrm{e}^{h(\mathbf{r},\boldsymbol{\xi})} j(\mathbf{r},\boldsymbol{\xi})\,, \tag{4.177}$$

with $W[j]$ the sum over all connected diagrams with e^j vertices. It has by construction the same graph expansion as its standard liquid counterpart Eq. (3.72)

$$\begin{aligned}\mathcal{G}[h] = &\int \mathrm{d}\mathbf{r}\mathrm{d}\boldsymbol{\xi}\mathrm{e}^{h(\mathbf{r},\boldsymbol{\xi})}\left[h(\mathbf{r},\boldsymbol{\xi}) - 1 - j(\mathbf{r},\boldsymbol{\xi})\right] \\ &- \frac{1}{2}\int \mathrm{d}\mathbf{r}\,\mathrm{d}\boldsymbol{\xi}\,\mathrm{d}\mathbf{r}'\,\mathrm{d}\boldsymbol{\xi}'\,\mathrm{e}^{h(\mathbf{r},\boldsymbol{\xi})}\mathrm{e}^{h(\mathbf{r}',\boldsymbol{\xi}')} f(\mathbf{r},\boldsymbol{\xi};\mathbf{r}',\boldsymbol{\xi}') + \dots\,,\end{aligned} \tag{4.178}$$

where the $\dots$ stand for a summation over all the remaining one-particle irreducible diagrams with $\rho(\mathbf{r},\boldsymbol{\xi})$ vertices. The functional $\mathcal{G}$ is such that the stationarity condition

$$\frac{\delta\mathcal{G}[h]}{\delta h(\mathbf{r},\boldsymbol{\xi})} = 0 \tag{4.179}$$

yields the field $h(\mathbf{r},\boldsymbol{\xi})$ that solves Eq. (4.175), *i.e.* the field $h(\mathbf{r},\boldsymbol{\xi})$ such that $\mathrm{e}^{h(\mathbf{r},\boldsymbol{\xi})}$ is the physical one-body density at chemical potential $j(\mathbf{r},\boldsymbol{\xi})$. Hereafter, we denote by $j(\mathbf{r},\boldsymbol{\xi})$ the generalized chemical potential which corresponds to the UCNA dynamics and that reads in a homogeneous phase with $\mu(\mathbf{r}) = \mu = cst$

$$\begin{aligned} j(\mathbf{r},\boldsymbol{\xi}) &= \mu - \frac{\boldsymbol{\psi}^2}{2} - d\left(n-\frac{1}{2}\right)\ln(2\pi) - \frac{\epsilon - i}{2}\sum_{a=1}^{n-1}\frac{(\boldsymbol{\phi}^a)^2}{2} - \frac{\epsilon + i}{2}\sum_{a=1}^{n-1}\frac{(\boldsymbol{\varphi}^a)^2}{2}\,, \\ &\equiv \mu + j(\boldsymbol{\xi})\,. \end{aligned} \tag{4.180}$$

In the limit of infinite spatial dimension, the density expansion of the free energy functional is truncated at second order,

$$\begin{aligned}\mathcal{G}[h] = &\int \mathrm{d}\mathbf{r}\mathrm{d}\boldsymbol{\xi}\mathrm{e}^{h(\mathbf{r},\boldsymbol{\xi})}\left[h(\mathbf{r},\boldsymbol{\xi}) - 1 - j(\mathbf{r},\boldsymbol{\xi})\right] \\ &- \frac{1}{2}\int \mathrm{d}\mathbf{r}\,\mathrm{d}\boldsymbol{\xi}\,\mathrm{d}\mathbf{r}'\,\mathrm{d}\boldsymbol{\xi}'\,\mathrm{e}^{h(\mathbf{r},\boldsymbol{\xi})}\mathrm{e}^{h(\mathbf{r}',\boldsymbol{\xi}')}f(\mathbf{r},\boldsymbol{\xi};\mathbf{r}',\boldsymbol{\xi}')\,.\end{aligned} \tag{4.181}$$

Therefore, the physical one-body distribution $\rho^*(\mathbf{r},\boldsymbol{\xi})$ obeys the stationarity equation

$$\frac{\delta\mathcal{G}}{\delta h(\mathbf{r},\boldsymbol{\xi})} = 0 \;\Rightarrow\; \rho^*(\mathbf{r},\boldsymbol{\xi}) = \mathrm{e}^{j(\boldsymbol{\xi})}\exp\left(\int \mathrm{d}\mathbf{r}'\mathrm{d}\boldsymbol{\xi}'\rho^*(\mathbf{r}',\boldsymbol{\xi}')f(\mathbf{r},\boldsymbol{\xi};\mathbf{r}',\boldsymbol{\xi}')\right). \tag{4.182}$$

Equation (4.182) can't nevertheless be solved analytically. Fortunately, as explained in [120] in the context of glassy physics, the details of the physical one-body distribution $\rho^*(\mathbf{r},\boldsymbol{\xi})$, or equivalently the details of the physical $h^*(\mathbf{r},\boldsymbol{\xi})$, are not needed to predict the phase diagram of the system nor its structure factor. Indeed, to leading order in the dimension d, the free energy functional $\mathcal{G}[h]$ depends only on a restricted number of moments of the distribution $\rho(\mathbf{r},\boldsymbol{\xi})$. The macroscopic properties of the system under study can therefore be infered from a stationarity condition on this set of moments instead of dealing with the full distribution that generates them. This will be the object of the next three sections. Before diving into these aspects, let us assume for a moment that we know the physical density field, *i.e.* that we know the physical $h^*(\mathbf{r},\boldsymbol{\xi})$ solution to Eq. (4.182). Let us also assume that the corresponding phase is homogeneous with density ρ so that the solution can be put under the form

$$h^*(\mathbf{r},\boldsymbol{\xi}) = \ln\rho + \Gamma^*(\boldsymbol{\xi}) \text{ with } \int \mathrm{d}\boldsymbol{\xi}\,\mathrm{e}^{\Gamma^*(\boldsymbol{\xi})} = 1\,, \tag{4.183}$$

with the one-body distribution that reads

$$\rho^*(\mathbf{r},\boldsymbol{\xi}) = \rho\,\mathrm{e}^{\Gamma^*(\boldsymbol{\xi})} \text{ with } \int \mathrm{d}\boldsymbol{\xi}\,\rho^*(\mathbf{r},\boldsymbol{\xi}) = \rho\,. \tag{4.184}$$

The two-point function $\rho^{(2)}$ of the system, or accordingly its structure factor, can then be computed from the Ornstein-Zernike equation, see Sec. 3.2.6,

$$\rho^{(2)}(\mathbf{r},\boldsymbol{\xi},\mathbf{r}',\boldsymbol{\xi}') = \rho^2\,\mathrm{e}^{\Gamma^*(\boldsymbol{\xi})}\mathrm{e}^{\Gamma^*(\boldsymbol{\xi}')}\left(1 + f(\mathbf{r},\boldsymbol{\xi},\mathbf{r}',\boldsymbol{\xi}')\right)\,, \tag{4.185}$$

and we can derive from it the position space two-point function of the system

$$g(\mathbf{r}) = \int \mathrm{d}\boldsymbol{\xi}\,\mathrm{d}\boldsymbol{\xi}'\mathrm{e}^{\Gamma^*(\boldsymbol{\xi})}\mathrm{e}^{\Gamma^*(\boldsymbol{\xi}')}\left(1 + f(0,\boldsymbol{\xi},\mathbf{r},\boldsymbol{\xi}')\right)\,. \tag{4.186}$$

It is thus expected that the two-point position-space function of the systems depends on the density in a non trivial way. Remark that higher order n-point correlation functions in the $(\mathbf{r},\boldsymbol{\xi})$ space are inferred from Eq. (4.185) using the pair structure Eq. (3.125) of standard infinite dimensional fluid. Finally, we note that at the physical one-body distribution $\Gamma^*[\rho](\boldsymbol{\xi})$ (where the notation stresses the density dependence of the auxiliary fields distribution), the volumic free energy g(ρ) of a homogeneous phase of density ρ thus reads

$$\mathrm{g}(\rho) = \left[\rho\left(\ln\rho - 1\right) - \rho\,\mu\right] - \frac{\rho^2}{2}\int \mathrm{d}\mathbf{r}\;\left(g[\rho](\mathbf{r}) - 1\right) + \rho\int \mathrm{d}\boldsymbol{\xi}\,\mathrm{e}^{\Gamma^*[\rho](\boldsymbol{\xi})}\left[\Gamma^*[\rho](\boldsymbol{\xi}) - j(\boldsymbol{\xi})\right]\,, \tag{4.187}$$

which differs from the conventional expression of the free energy of pairwise interacting systems in infinite dimension in, first, that the pair-correlation function in position space may depend on the density and, second, because the Kullback-Liebler divergence of the distribution $\mathrm{e}^{\Gamma^*(\boldsymbol{\xi})}$ with respect to the distribution $\mathrm{e}^{j(\boldsymbol{\xi})}$ appears explicitly, thus accounting for the entropy of the auxiliary degrees of freedom.

4.3.6 Scaling of the one-body distribution

We start by investigating the behavior of the solution of Eq. (4.182). In particular, we take advantage of the scalings described in Sec. 4.3.2 to elucidate the scaling form of the solution of Eq. (4.182). From the latter equation, we have

$$\begin{aligned}\Gamma^*(\boldsymbol{\xi}) &= \mu - \ln\rho - d\left(n-\frac{1}{2}\right)\ln 2\pi - \frac{\boldsymbol{\psi}^2}{2} - \frac{1}{2}\sum_{a=1}^{n-1}\left[(\epsilon-i)\,(\boldsymbol{\phi}^a)^2 + (\epsilon+i)\,(\boldsymbol{\varphi}^a)^2\right] \\ &\quad + \rho\int \mathrm{d}\mathbf{r}\,\mathrm{d}\boldsymbol{\xi}'\mathrm{e}^{\Gamma^*(\boldsymbol{\xi}')} f(0,\boldsymbol{\xi};\mathbf{r},\boldsymbol{\xi}')\,, \\ &= \mu - \ln\rho - d\left(n-\frac{1}{2}\right)\ln 2\pi - \frac{\boldsymbol{\psi}^2}{2} - \frac{1}{2}\sum_{a=1}^{n-1}\left[(\epsilon-i)\,(\boldsymbol{\phi}^a)^2 + (\epsilon+i)\,(\boldsymbol{\varphi}^a)^2\right] \\ &\quad + \rho\mathcal{V}_d(\sigma)\int \mathrm{d}h\,\mathrm{e}^h\frac{\mathrm{d}\hat{\mathbf{r}}}{\Omega_d}\,\mathrm{d}\boldsymbol{\xi}'\mathrm{e}^{\Gamma^*(\boldsymbol{\xi}')} f(0;\boldsymbol{\xi};h,\hat{\mathbf{r}},\boldsymbol{\xi}')\,.\end{aligned} \tag{4.188}$$

We rescale the auxiliary variables according to $\boldsymbol{\xi} \to \sqrt{d}\,\hat{\boldsymbol{\xi}}$. We furthermore define

$$\hat{\Gamma}(\hat{\boldsymbol{\xi}}) = d\left(n-\frac{1}{2}\right)\ln d + \Gamma^*(\sqrt{d}\,\hat{\boldsymbol{\xi}})\,, \tag{4.189}$$

so that the distribution $\hat{\Gamma}$ is well normalized,

$$\int \mathrm{d}\hat{\boldsymbol{\xi}}\,\mathrm{e}^{\hat{\Gamma}(\hat{\boldsymbol{\xi}})} = 1\,. \tag{4.190}$$

In the following we drop the hat superscript over $\hat{\boldsymbol{\xi}}$ but hereafter the auxiliary fields always are understood to be the rescaled ones. We first make use of

$$\begin{aligned}\partial^\alpha\partial^\beta U(\mathbf{r}) &= \frac{U'(r)}{r}\delta^{\alpha\beta} + \left(U''(r) - \frac{U'(r)}{r}\right)\hat{r}^\alpha\hat{r}^\beta\,, \\ &\simeq \frac{\widehat{U}'(h)}{\sigma^2}\delta^{\alpha\beta} + d\frac{\widehat{U}''(h)}{\sigma^2}\hat{r}^\alpha\hat{r}^\beta\,,\end{aligned} \tag{4.191}$$

so that we obtain from Eq. (4.188),

$$\hat{\Gamma}(\boldsymbol{\xi}) = d\Bigg\{ \frac{\mu - \ln\rho}{d} - \left(n - \frac{1}{2}\right)\ln(2\pi d) - \frac{\boldsymbol{\psi}^2}{2} - \frac{1}{2}\sum_{a=1}^{n-1}\left[(\epsilon - i)\left(\boldsymbol{\phi}^a\right)^2 + (\epsilon + i)\left(\boldsymbol{\varphi}^a\right)^2\right] \\ + \widehat{\varphi}\int \mathrm{d}h\, \mathrm{e}^h \frac{\mathrm{d}\hat{\mathbf{r}}}{\Omega_d}\, \mathrm{d}\boldsymbol{\xi}' \mathrm{e}^{\hat{\Gamma}(\boldsymbol{\xi}')}\Bigg[-1 + \exp\Bigg(-\beta\widehat{U}(h) + i\frac{\sqrt{\beta\hat{\tau}}}{\sigma}\sqrt{d}\,\widehat{U}'(h)\,(\boldsymbol{\psi} - \boldsymbol{\psi}')\cdot\hat{\mathbf{r}} \\ + \frac{i\hat{\tau}}{2}\frac{\widehat{U}'(h)}{\sigma^2}\sum_{a=1}^{n-1}\left(\left(\boldsymbol{\phi}^a - \boldsymbol{\phi}'^a\right)^2 - \left(\boldsymbol{\varphi}^a - \boldsymbol{\varphi}'^a\right)^2\right) \\ + \frac{i\hat{\tau}}{2}\frac{d\,\widehat{U}''(h)}{\sigma^2}\sum_{a=1}^{n-1}\left(\left(\boldsymbol{\phi}^a - \boldsymbol{\phi}'_a\right)\cdot\hat{\mathbf{r}}\right)^2 - \left(\left(\boldsymbol{\varphi}^a - \boldsymbol{\varphi}'_a\right)\cdot\hat{\mathbf{r}}\right)^2\Bigg)\Bigg]\Bigg\}. \tag{4.192}$$

Since scalar products between independent unit vectors scale as $d^{-1/2}$ as $d \to \infty$, we obtain the scaling form of $\hat{\Gamma}$,

$$\hat{\Gamma}(\boldsymbol{\xi}) = d\,\Gamma(\boldsymbol{\xi})\,, \tag{4.193}$$

with $\Gamma(\boldsymbol{\xi})$ an $O(1)$ function. Furthermore, due to rotational symmetry, that we assume unbroken, Γ depends only on the set of scalar products between the different auxiliary vectors, *i.e.* we have

$$\Gamma(\boldsymbol{\xi}) = \Gamma(S)\,, \tag{4.194}$$

with the $(2n-1)\times(2n-1)$ matrix S given by

$$S = \left(\begin{array}{c|ccc} \boldsymbol{\psi}^2 & Y_1 & \cdots & Y_{2(n-1)} \\ \hline Y_1 & & & \\ \vdots & & Q & \\ Y_{2(n-1)} & & & \end{array}\right), \tag{4.195}$$

and

$$Q = \left[\begin{array}{c|c} \boldsymbol{\phi}^a\cdot\boldsymbol{\phi}^b & \boldsymbol{\phi}^a\cdot\boldsymbol{\varphi}^b \\ \hline \boldsymbol{\phi}^b\cdot\boldsymbol{\varphi}^a & \boldsymbol{\varphi}^a\cdot\boldsymbol{\varphi}^b \end{array}\right], \tag{4.196}$$

and

$$Y = \left[\begin{array}{c} \boldsymbol{\varphi}^a\cdot\boldsymbol{\psi} \\ \boldsymbol{\phi}^a\cdot\boldsymbol{\psi} \end{array}\right]. \tag{4.197}$$

Crucially, rotational symmetry reduces the number of variables Γ depends on and makes it finite even in the limit $d \to \infty$. Hence, the one-body distribution function writes

$$\rho(\mathbf{r}, \boldsymbol{\xi}) = \rho\,\mathrm{e}^{d\,\Gamma(S)} \tag{4.198}$$

and therefore admits a large deviation form. Thanks to this, we are now in position to compute the free energy functional in an analytically handleable form.

4.3.7 Computing the free energy

In this section, we evaluate explicitly the free energy functional Eq. (4.181). We restrict the computation of Eq. (4.181) to the space of functions respecting the homogeneity of the associated phase in Eq. (4.183) and the scaling form Eqs. (4.193)-(4.194) to which the physical one-body distribution belongs. We will see that due to the large deviation principle shown in Eq. (4.198), the free energy functional does not depend on the details of the function $\Gamma(S)$ but only on the value S^* of the matrix S at the corresponding saddle point. The result of this computation is displayed in Eqs. (4.215)-(4.216). We decompose the free energy per unit volume into an ideal gas part

$$\mathrm{g}_{IG}[\rho,\Gamma(\boldsymbol{\xi})] = d\rho \int \mathrm{d}\boldsymbol{\xi} \mathrm{e}^{d\Gamma(\boldsymbol{\xi})} \left[\Gamma(\boldsymbol{\xi}) + \frac{\boldsymbol{\psi}^2}{2} + \left(n-\frac{1}{2}\right)\ln 2\pi + \frac{\epsilon - i}{2}\sum_{a=1}^{n-1}(\boldsymbol{\phi}^a)^2 + \frac{\epsilon + i}{2}\sum_{a=1}^{n-1}(\boldsymbol{\varphi}^a)^2 \right], \tag{4.199}$$

and an interacting part

$$\mathrm{g}_{int}[\rho,\Gamma(\boldsymbol{\xi})] = -\frac{d\rho}{2}\varphi \int \mathrm{d}h\, \mathrm{e}^h\, \mathrm{d}\boldsymbol{\xi}\mathrm{d}\boldsymbol{\xi}' \mathrm{e}^{d\Gamma(\boldsymbol{\xi})}\mathrm{e}^{d\Gamma(\boldsymbol{\xi}')} \int \frac{\mathrm{d}\hat{\mathbf{r}}}{\Omega_d} f(0,\boldsymbol{\xi};h,\hat{\mathbf{r}},\boldsymbol{\xi}), \tag{4.200}$$

that we evaluate separately in the following. At the saddle point S_{sp} of the distribution $\mathrm{e}^{d\Gamma(S)}$, we furthermore introduce the notations

$$\boldsymbol{\psi}^2_{sp} = m, \tag{4.201}$$

and

$$Q_{sp} = \left[\begin{array}{c|c} p_{ab} & r_{ab} \\ \hline r_{ba} & q_{ab} \end{array}\right], \tag{4.202}$$

and

$$Y^\alpha_{sp} = Z^\alpha, \tag{4.203}$$

for $\alpha \in [\![1, 2(n-1)]\!]$.

The ideal gas part

We introduce $J(S)$ the Jacobian of the change of variables when going from the fields $\boldsymbol{\xi}$ to the matrix S of scalar products. Performing the change of variable in Eq. (4.199), we obtain

$$\begin{aligned}\mathrm{g}_{IG}[\rho,\Gamma(\boldsymbol{\xi})] &= d\rho \int_{S>0} \mathrm{d}S J(S)\, \mathrm{e}^{d\Gamma(S)} \left[\Gamma(S) + \frac{\boldsymbol{\psi}^2}{2} + \left(n-\frac{1}{2}\right)\ln 2\pi + \frac{\epsilon - i}{2}\sum_{a=1}^{n-1}(\boldsymbol{\phi}^a)^2 + \frac{\epsilon + i}{2}\sum_{a=1}^{n-1}(\boldsymbol{\varphi}^a)^2 \right], \\ &= d\rho \left[\Gamma(S_{sp}) + \frac{m}{2} + \left(n-\frac{1}{2}\right)\ln 2\pi + \frac{\epsilon - i}{2}\sum_{a=1}^{n-1} p_{aa} + \frac{\epsilon + i}{2}\sum_{a=1}^{n-1} q_{aa} \right]\end{aligned} \tag{4.204}$$

where the integration domain is restricted to positive definite S matrices and with S_{sp} the associated saddle point as $d \to \infty$. Note that we used the normalization condition

$$\int \mathrm{d}S J(S)\, \mathrm{e}^{d\Gamma(S)} = 1\,. \tag{4.205}$$

This same normalization condition allows to simplify further Eq. (4.204). The jacobian $J(S)$ (see *e.g.* [72]) is given by

$$J(S) \underset{d\to\infty}{\sim} \exp\left\{ d\left[\left(n - \frac{1}{2}\right)(1 + \ln 2\pi) + \frac{1}{2} \ln\det S \right] \right\}. \tag{4.206}$$

Thus the normalization condition imposes at the associated saddle point

$$\Gamma(S_{sp}) + \frac{1}{2}\,\mathrm{Log}\det S_{sp} + \left(n - \frac{1}{2}\right)(1 + \ln 2\pi) = 0\,. \tag{4.207}$$

Hence, the ideal gas part of the free energy reads

$$\mathrm{g}_{IG}[\rho, \Gamma(\boldsymbol{\xi})] = -\frac{d\rho}{2}\left[\mathrm{Log}\det S_{sp} + (2n-1) - m - (\epsilon - i)\sum_{a=1}^{n-1} p_{aa} - (\epsilon + i)\sum_{a=1}^{n-1} q_{aa} \right]. \tag{4.208}$$

We see that the above expression depends only on the saddle-point matrix S_{sp}.

The interacting part

We start by performing the integral over $\hat{\mathbf{r}}$ so as to make the S dependence explicit in the integrand of Eq. (4.200). From the expression of the Mayer function f, we define the integral

$$\mathrm{I}(\boldsymbol{\xi}_1, \boldsymbol{\xi}_2; h) = \int \frac{\mathrm{d}\hat{\mathbf{r}}}{\Omega_d} \exp\left(i\sqrt{\beta\hat{\tau}}\,\frac{\widehat{U}'(h)}{\sigma}\sqrt{d}\,(\boldsymbol{\psi}_1 - \boldsymbol{\psi}_2)\cdot\hat{\mathbf{r}} + \frac{i\hat{\tau}}{2}\frac{\widehat{U}''(h)}{\sigma^2} d \sum_{a=1}^{n-1}\left[\Big((\boldsymbol{\phi}_1^a - \boldsymbol{\phi}_2^a)\cdot\hat{\mathbf{r}} \Big)^2 - \Big((\boldsymbol{\varphi}_1^a - \boldsymbol{\varphi}_2^a)\cdot\hat{\mathbf{r}} \Big)^2 \right] \right). \tag{4.209}$$

The integral I is evaluated as follows,

$$
\begin{aligned}
I(\boldsymbol{\xi}_1,\boldsymbol{\xi}_2;h) &= \int \frac{\mathrm{d}\hat{\mathbf{r}}}{\Omega_d}\int \mathrm{d}z\,\delta\left(z-\sqrt{d}\,(\boldsymbol{\psi}_1-\boldsymbol{\psi}_2)\cdot\hat{\mathbf{r}}\right)\int\prod_a \mathrm{d}x_a\mathrm{d}y_a\,\delta\left(x_a-\sqrt{d}\,(\boldsymbol{\phi}_1^a-\boldsymbol{\phi}_2^a)\cdot\hat{\mathbf{r}}\right)\\
&\quad \delta\left(y_a-\sqrt{d}\,(\boldsymbol{\varphi}_1^a-\boldsymbol{\varphi}_2^a)\cdot\hat{\mathbf{r}}\right)\exp\left(i\sqrt{\beta\hat{\tau}}\,\frac{\widehat{U}'(h)}{\sigma}z+\frac{i\hat{\tau}}{2}\frac{\widehat{U}''(h)}{\sigma^2}\sum_{a=1}^{n-1}\left(x_a^2-y_a^2\right)\right),\\
&= \int \frac{\mathrm{d}\hat{\mathbf{r}}}{\Omega_d}\int \mathrm{d}z\frac{\mathrm{d}\lambda}{2\pi}\prod_a \mathrm{d}x_a\mathrm{d}y_a\frac{\mathrm{d}\omega_a}{2\pi}\frac{\mathrm{d}\Omega_a}{2\pi}\exp\left(i\sqrt{\beta\hat{\tau}}\,\frac{\widehat{U}'(h)}{\sigma}z+\frac{i\hat{\tau}}{2}\frac{\widehat{U}''(h)}{\sigma^2}\sum_{a=1}^{n-1}\left(x_a^2-y_a^2\right)\right)\\
&\quad \exp\left(i\lambda\left(z-\sqrt{d}\,(\boldsymbol{\psi}_1-\boldsymbol{\psi}_2)\cdot\hat{\mathbf{r}}\right)+i\sum_{a=1}^{n-1}\omega_a\left(x_a-\sqrt{d}\,(\boldsymbol{\phi}_1^a-\boldsymbol{\phi}_2^a)\cdot\hat{\mathbf{r}}\right)\right.\\
&\quad \left.+i\sum_a\Omega_a\left(y_a-\sqrt{d}\,(\boldsymbol{\varphi}_1^a-\boldsymbol{\varphi}_2^a)\cdot\hat{\mathbf{r}}\right)\right),\\
&= \int\prod_a \mathrm{d}x_a\mathrm{d}y_a\frac{\mathrm{d}\omega_a}{2\pi}\frac{\mathrm{d}\Omega_a}{2\pi}\exp\left(i\sum_a\omega_a x_a+i\sum_a\Omega_a y_a+\frac{i\hat{\tau}}{2}\frac{\widehat{U}''(h)}{\sigma^2}\sum_a\left(x_a^2-y_a^2\right)\right)\\
&\quad \exp\left(-\frac{1}{2}\left|-\sqrt{\beta\hat{\tau}}\frac{\widehat{U}'(h)}{\sigma}(\boldsymbol{\psi}_1-\boldsymbol{\psi}_2)+\sum_a\omega_a(\boldsymbol{\phi}_1^a-\boldsymbol{\phi}_2^a)+\sum_a\Omega_a(\boldsymbol{\varphi}_1^a-\boldsymbol{\varphi}_2^a)\right|^2\right),
\end{aligned}
\tag{4.210}
$$

where the last line, obtained to leading order in d, makes explicit the coupling between the different auxiliary fields after integration of the positional degrees of freedom $\hat{\mathbf{r}}$. In the following, we neglect the scalar product between fields $\boldsymbol{\xi}_1$ and $\boldsymbol{\xi}_2$ as they are drawn independently from the same rationally invariant distribution and thus scale as $O(d^{-1/2})$ and perform the remaining Gaussian integrations. We thus obtain, following the notations introduced in the previous section,

$$
\begin{aligned}
I(\boldsymbol{\xi}_1,\boldsymbol{\xi}_2;h) =& \exp\left(\frac{\beta\hat{\tau}^2}{2\sigma^4}\widehat{U}'(h)^2\widehat{U}''(h)\left(Y_1^\alpha+Y_2^\alpha\right)\left(Y_1^\beta+Y_2^\beta\right)\left(iJ+\frac{\hat{\tau}\widehat{U}''(h)}{\sigma^2}(Q_1+Q_2)\right)^{-1}_{\alpha\beta}\right)\\
&\frac{\exp\left(-\frac{\beta\hat{\tau}\widehat{U}'(h)^2}{2\sigma^2}(\boldsymbol{\psi}_1^2+\boldsymbol{\psi}_2^2)\right)}{\sqrt{\det\left(iJ+\frac{\hat{\tau}\widehat{U}''(h)}{\sigma^2}(Q_1+Q_2)\right)}}.
\end{aligned}
\tag{4.211}
$$

with the matrix J being $2(n-1)\times 2(n-1)$ and given by block as

$$
J=\left[\begin{array}{c|c} \mathbb{1} & 0 \\ \hline 0 & -\mathbb{1}\end{array}\right]. \tag{4.212}
$$

Integrating over the fields $\boldsymbol{\xi}_1$, $\boldsymbol{\xi}_2$ thus yields the interacting part of the free energy

$$\begin{aligned}
\mathrm{g}_{int}[\rho,\Gamma(\boldsymbol{\xi})] =& -\frac{d\rho}{2}\widehat{\varphi}\int \mathrm{d}h\,\mathrm{e}^{h}\mathrm{d}\boldsymbol{\xi}_1\mathrm{d}\boldsymbol{\xi}_2\mathrm{e}^{d\Gamma(\boldsymbol{\xi}_1)}\mathrm{e}^{d\Gamma(\boldsymbol{\xi}_2)}\Bigg[-1+\exp\Big(-\beta\widehat{U}(h)\\
&+\frac{i\hat{\tau}}{2}\frac{\widehat{U}'(h)}{\sigma^2}\sum_a\left((\boldsymbol{\phi}_1^a)^2+(\boldsymbol{\phi}_2^a)^2-(\boldsymbol{\varphi}_1^a)^2-(\boldsymbol{\varphi}_2^a)^2\right)\Big)\,\mathrm{I}(\boldsymbol{\xi}_1,\boldsymbol{\xi}_2;h)\Bigg],\\
=& -\frac{d\rho}{2}\widehat{\varphi}\int \mathrm{d}h\,\mathrm{e}^{h}\Bigg\{-1+\frac{\exp\left(-\beta\widehat{U}(h)+i\hat{\tau}\frac{\widehat{U}'(h)}{\sigma^2}\sum_a(p_{aa}-q_{aa})-\frac{\beta\hat{\tau}\widehat{U}'(h)^2}{\sigma^2}m\right)}{\sqrt{\det\left(iJ+\frac{2\hat{\tau}\widehat{U}''(h)}{\sigma^2}Q_{sp}\right)}}\times\\
&\cdots\times\exp\left(2\frac{\beta\hat{\tau}^2}{\sigma^4}\widehat{U}'(h)^2\widehat{U}''(h)Z^\alpha Z^\beta\left(iJ+\frac{2\hat{\tau}\widehat{U}''(h)}{\sigma^2}Q_{sp}\right)^{-1}_{\alpha\beta}\right)\Bigg\}.
\end{aligned}\tag{4.213}$$

In the remainder of this work, we assume that the potential $\widehat{U}(h)$ is described by a single energy scale,

$$\widehat{U}(h)=u_0\mathrm{v}(h)\,,\tag{4.214}$$

with $\mathrm{v}(h)$ free of any parameter. As in Sec. 4.3.3 we introduce the two constants $c_1=2\tau u_0/\sigma^2$ and $c_2=\beta u_0$ on which depends the free energy. We remind that the later is the ratio between the pair potential energy scale and the effective temperature of the $\tau=0$ dynamics whereas $\sqrt{c_1/c_2}$ controls the ratio between the run length of the original non-interacting AOUPs dynamics to the size of a particle, often called the Péclet number in the literature. The free energy functional then writes

$$\mathrm{g}[\rho,\Gamma(\boldsymbol{\xi})]=[\rho(\ln\rho-1)-\mu\rho]-\frac{d\rho}{2}f(\widehat{\varphi},S_{sp})\tag{4.215}$$

with

$$\begin{aligned}
f(\widehat{\varphi},S_{sp}) =& \operatorname{Log}\det S_{sp}+(2n-1)-m-(\epsilon+i)\sum_a q_{aa}-(\epsilon-i)\sum_a p_{aa}\\
&+\widehat{\varphi}\int \mathrm{d}h\,\mathrm{e}^{h}\Bigg\{-1+\frac{\exp\left(-c_2\mathrm{v}(h)+\frac{ic_1}{2}\mathrm{v}'(h)\sum_a(p_{aa}-q_{aa})-\frac{c_1c_2}{2}\mathrm{v}'(h)^2m\right)}{\sqrt{\det\left(iJ+c_1\mathrm{v}''(h)Q_{sp}\right)}}\times\\
&\cdots\times\exp\left(\frac{c_2c_1^2}{2}\mathrm{v}'(h)^2\mathrm{v}''(h)Z^\alpha Z^\beta\left(iJ+c_1\mathrm{v}''(h)Q_{sp}\right)^{-1}_{\alpha\beta}\right)\Bigg\}.
\end{aligned}\tag{4.216}$$

We remark that, as claimed earlier, the free energy functional depends only on S_{sp}, the saddle-point matrix associated to the distribution $\mathrm{e}^{d\Gamma(S)}$. We are now in a position to obtain all the information we need about the one-body distribution $\mathrm{e}^{d\Gamma(S)}$ in order to predict the structure and the phase behavior of the UCNA model.

4.3.8 Saddle point equations

The physical one-body distribution is characterized by a saddle-point matrix S^* which is found through the stationarity equation

$$\partial_{S_{ij}} f(\widehat{\varphi}, S^*) = 0\,. \tag{4.217}$$

We denote the inverse matrix $(S^*)^{-1}$ as

$$(S^*)^{-1} = \left(\begin{array}{c|ccc} \tilde{m} & \tilde{Z}_1 & \cdots & \tilde{Z}_{2(n-1)} \\ \hline \tilde{Z}_1 & & & \\ \vdots & & \tilde{Q} & \\ \tilde{Z}_{2(n-1)} & & & \end{array}\right) \tag{4.218}$$

with

$$\tilde{Q} = \left[\begin{array}{c|c} \tilde{p}_{ab} & \tilde{r}_{ab} \\ \hline \tilde{r}_{ba} & \tilde{q}_{ab} \end{array}\right]\,, \tag{4.219}$$

$$\tag{4.220}$$

and furthermore introduce the reduced notation

$$\begin{aligned} \mathrm{A} = & -c_2 \mathrm{v}(h) + \frac{ic_1}{2}\mathrm{v}'(h)\sum_a (p_{aa} - q_{aa}) - \frac{c_1 c_2}{2}\mathrm{v}'(h)^2 m \\ & + \frac{c_2 c_1^2}{2}\mathrm{v}'(h)^2\mathrm{v}''(h) Z^\alpha Z^\beta \left(iJ + c_1\mathrm{v}''(h)Q\right)^{-1}_{\alpha\beta}\,, \end{aligned} \tag{4.221}$$

We use the convention that indices α, β run from 1 to $2(n-1)$ while indices a, b run from 1 to $n-1$. We thus obtain the stationarity equations as,

$$\tilde{m} - 1 - c_1 c_2 \frac{\widehat{\varphi}}{2}\int \mathrm{d}h\, \mathrm{e}^h \mathrm{v}'(h)^2 \frac{\exp(A)}{\sqrt{\det\left(iJ + c_1\mathrm{v}''(h)Q\right)}} = 0\,, \tag{4.222}$$

$$2\tilde{Z}^\alpha + \widehat{\varphi} c_2 c_1^2 Z^\beta \int \mathrm{d}h\, \mathrm{e}^h \mathrm{v}'(h)^2\mathrm{v}''(h)\left(iJ + c_1\mathrm{v}''(h)Q\right)^{-1}_{\alpha\beta} \frac{\exp(A)}{\sqrt{\det\left(iJ + c_1\mathrm{v}''(h)Q\right)}} = 0\,, \tag{4.223}$$

$$\begin{aligned} \tilde{p}_{ab} - (\epsilon - i)\,\delta_{ab} + \frac{\widehat{\varphi} c_1}{2}\int \mathrm{d}h\, \mathrm{e}^h \frac{\exp(A)}{\sqrt{\det\left(iJ + c_1\mathrm{v}''(h)Q\right)}} \Bigg[& i\delta_{ab}\mathrm{v}'(h) - \mathrm{v}''(h)\left(iJ + c_1\mathrm{v}''(h)Q\right)^{-1}_{ab} \\ & - c_2 c_1^2 \mathrm{v}'(h)^2\mathrm{v}''(h)^2 Z^\alpha Z^\beta \left(iJ + c_1\mathrm{v}''(h)Q\right)^{-1}_{a\alpha}\left(iJ + c_1\mathrm{v}''(h)Q\right)^{-1}_{b\beta} \Bigg] = 0\,, \end{aligned} \tag{4.224}$$

$$\begin{aligned} \tilde{q}_{ab} + \frac{\widehat{\varphi} c_1}{2}\int \mathrm{d}h\, \mathrm{e}^h \frac{\exp(A)}{\sqrt{\det\left(iJ + c_1\mathrm{v}''(h)Q\right)}} \Bigg[& i\delta_{ab}\mathrm{v}'(h) - \mathrm{v}''(h)\left(iJ + c_1\mathrm{v}''(h)Q\right)^{-1}_{n-1+a,n-1+b} \\ & - c_2 c_1^2 \mathrm{v}'(h)^2\mathrm{v}''(h)^2 Z^\alpha Z^\beta \left(iJ + c_1\mathrm{v}''(h)Q\right)^{-1}_{(n-1)+a\alpha}\left(iJ + c_1\mathrm{v}''(h)Q\right)^{-1}_{(n-1)+b\beta} \Bigg] - (\epsilon + i)\,\delta_{ab} = 0\,, \end{aligned} \tag{4.225}$$

$$\tilde{r}_{ab} - \frac{\widehat{\varphi} c_1}{2} \int \mathrm{d}h \, \mathrm{e}^h \frac{\exp(A)}{\sqrt{\det(iJ + c_1 \mathrm{v}''(h) Q)}} \Bigg[\mathrm{v}''(h) \left(iJ + c_1 \mathrm{v}''(h) Q\right)^{-1}_{a,n-1+b} + c_2 c_1^2 \mathrm{v}'(h)^2 \mathrm{v}''(h)^2 Z^\alpha Z^\beta \left(iJ + c_1 \mathrm{v}''(h) Q\right)^{-1}_{a\alpha} \left(iJ + c_1 \mathrm{v}''(h) Q\right)^{-1}_{n-1+b,\beta} \Bigg] = 0 \,, \tag{4.226}$$

4.3.9 Replica symmetric diagonal ansatz

In this work, we restrict ourselves to the study of the stationarity equations Eqs. (4.222)-(4.226) in the simplest possible ansatz, the replica symmetric diagonal one, *i.e*

$$\begin{aligned} Z^\alpha &= 0 \,, \\ r_{ab} &= 0 \,, \\ p_{ab} &= p \, \delta_{ab} \,, \\ q_{ab} &= q \, \delta_{ab} \,. \end{aligned} \tag{4.227}$$

Equations (4.223) and (4.226) are automatically solved within this ansatz. In the limit $\epsilon \to 0^+$, we look for $p = i\hat{p}$ and $q = -i\hat{q}$. As $n \to 0$, this yields

$$\frac{1}{m} = 1 + \frac{\widehat{\varphi} c_1 c_2}{2} \int \mathrm{d}h \, \mathrm{e}^h \mathrm{v}'(h)^2 \sqrt{(1 + c_1 \mathrm{v}''(h)\hat{p})(1 + c_1 \mathrm{v}''(h)\hat{q})} \exp\left(-c_2 \mathrm{v}(h) + \frac{c_1}{2} \mathrm{v}'(h)(\hat{p} + \hat{q}) - \frac{c_1 c_2}{2} \mathrm{v}'(h)^2 m \right) , \tag{4.228}$$

$$\frac{1}{\hat{p}} = 1 + \frac{\widehat{\varphi} c_1}{2} \int \mathrm{d}h \, \mathrm{e}^h \left[\mathrm{v}'(h) + \frac{\mathrm{v}''(h)}{1 + c_1 \mathrm{v}''(h)\hat{p}} \right] \sqrt{(1 + c_1 \mathrm{v}''(h)\hat{p})(1 + c_1 \mathrm{v}''(h)\hat{q})} \exp\left(-c_2 \mathrm{v}(h) + \frac{c_1}{2} \mathrm{v}'(h)(\hat{p} + \hat{q}) - \frac{c_1 c_2}{2} \mathrm{v}'(h)^2 m \right) , \tag{4.229}$$

$$\frac{1}{\hat{q}} = 1 + \frac{\widehat{\varphi} c_1}{2} \int \mathrm{d}h \, \mathrm{e}^h \left[\mathrm{v}'(h) + \frac{\mathrm{v}''(h)}{1 + c_1 \mathrm{v}''(h)\hat{q}} \right] \sqrt{(1 + c_1 \mathrm{v}''(h)\hat{p})(1 + c_1 \mathrm{v}''(h)\hat{q})} \exp\left(-c_2 \mathrm{v}(h) + \frac{c_1}{2} \mathrm{v}'(h)(\hat{p} + \hat{q}) - \frac{c_1 c_2}{2} \mathrm{v}'(h)^2 m \right) , \tag{4.230}$$

For the sake of simplicity, we assume that the interaction potential is that of harmonic spheres, *i.e.*

$$\mathrm{v}(h) = \frac{1}{2} h^2 \Theta(-h) \,. \tag{4.231}$$

We thus obtain the following equations for the order parameters $m, \hat{p}, \hat{q}$

$$\frac{1}{m} = 1 + \frac{\widehat{\varphi} c_1 c_2}{2} \sqrt{(1 + c_1\hat{p})(1 + c_1\hat{q})} \int_{-\infty}^0 \mathrm{d}h \, h^2 \exp\left(h \left(1 + \frac{c_1}{2}(\hat{p} + \hat{q}) \right) - \frac{h^2}{2} c_2 \left(1 + m c_1\right) \right) , \tag{4.232}$$

$$\frac{1}{\hat{p}} = 1 + \frac{\widehat{\varphi} c_1}{2} \sqrt{(1 + c_1\hat{p})(1 + c_1\hat{q})} \int_{-\infty}^0 \mathrm{d}h \, \left[h + \frac{1}{1 + c_1\hat{p}} \right] \exp\left(h \left(1 + \frac{c_1}{2}(\hat{p} + \hat{q}) \right) - \frac{h^2}{2} c_2 \left(1 + m c_1\right) \right) , \tag{4.233}$$

$$\frac{1}{\hat{q}} = 1 + \frac{\widehat{\varphi} c_1}{2}\sqrt{(1+c_1\hat{p})(1+c_1\hat{q})}\int_{-\infty}^{0} \mathrm{d}h \left[h + \frac{1}{1+c_1\hat{q}}\right] \exp\left(h\left(1+\frac{c_1}{2}(\hat{p}+\hat{q})\right) - \frac{h^2}{2}c_2\left(1+mc_1\right)\right), \tag{4.234}$$

We remark that we could have obtained the same equation upon assuming that the matrix H was positive-definite and representing its determinant with real-valued Gaussian integrals. This suggests, together with the computation of the effective pair-potential Eq. (4.157), that the matrix H is indeed positive definite in the large d limit, or at least that configurations leading to a non-positive definite one are statistically negligible.

4.3.10 The free energy again

Let m^*, p^* and q^* be the solutions of the stationarity equations (4.232)-(4.234). These are functions of the density $\widehat{\varphi}$, even though the argument has not been made explicit in order to lighten notations. The physical free energy per unit volume of a homogeneous phase can be obtained as a function of the density only by evaluating Eq. (4.215) at m^*, p^* and q^*, *i.e.*

$$\begin{aligned} \mathrm{g}(\widehat{\varphi}) &= \frac{d}{\mathcal{V}_d(\sigma)}\left[\widehat{\varphi}\ln\widehat{\varphi} + \widehat{\varphi}\ln\left(\frac{d\,\mathrm{e}^{\mu}}{\mathcal{V}_d(\sigma)}\right) - \frac{d\widehat{\varphi}}{2}f(\widehat{\varphi},m^*,p^*,q^*)\right], \\ &\simeq \frac{d}{\mathcal{V}_d(\sigma)}\left[\widehat{\varphi}\ln\left(\frac{d\,\mathrm{e}^{\mu}}{\mathcal{V}_d(\sigma)}\right) - \frac{d\widehat{\varphi}}{2}f(\widehat{\varphi},m^*,p^*,q^*)\right], \end{aligned} \tag{4.235}$$

where the last line is obtained to leading order in d and with, from Eq. (4.216),

$$\begin{aligned} f(\widehat{\varphi},m^*,p^*,q^*) &= \ln m^* - \ln p^* - \ln q^* - 1 - m^* + p^* + q^* \\ &+ \widehat{\varphi}\left[-1 + \sqrt{\frac{\pi}{2c_2(1+c_1m^*)}}\exp\left(\frac{(2+c_1(p^*+q^*))^2}{8c_2(1+c_1m^*)}\right)\mathrm{erfc}\left(\frac{2+c_1(p^*+q^*)}{\sqrt{8c_2(1+c_1m^*)}}\right)\right]. \end{aligned} \tag{4.236}$$

In some parameter range, Eqs. (4.232)-(4.234) have multiple solutions. By definition, these are all stationary points of the above expression seen as a function of m, p and q at fixed $\widehat{\varphi}$. We find numerically that these stationary points are all local minima of the free energy. In this case, we select the one with lowest free energy as we know is correct in the case where the grand-canonical partition functional involves only real parameters, see Sec. 3.2.2. The stability of these stationary points in the full replica space has however not been analyzed in this work.

Furthermore, as is standard in thermodynamics, the non-convexity of the free energy $g(\widehat{\varphi})$ seen as a function of the conserved field $\widehat{\varphi}$ indicates the occurrence of a phase separation in the system. From the second line of Eq. (4.235), we see that it is enough to study the convexity properties of $\hat{g} \equiv -\widehat{\varphi}f/2$ as the first term between the brackets is linear. When we claim to evaluate numerically the free energy in the following, note that it is actually $\hat{g}$ that we compute.

4.3.11 The two-point function again

Before solving numerically the stationarity equations (4.232)-(4.234), we compute here the position space two-point function. With an arbitrary pair potential v, it reads from Eq. (4.186),

$$g(h) = \sqrt{(1 + c_1 \mathrm{v}''(h)\hat{p})\,(1 + c_1 \mathrm{v}''(h)\hat{q})}\, \exp\left(-c_2 \mathrm{v}(h) - \frac{c_1 c_2}{2} \mathrm{v}'(h)^2 m + \frac{c_1}{2} \mathrm{v}'(h)\,(\hat{p} + \hat{q})\right). \tag{4.237}$$

The obtained result is similar to the zero density one in Eq. (4.157) with the different contributions but the equilibrium-like one renormalized in a density dependent way by the coefficients m, $\hat{p}$ and $\hat{q}$. Of course, one recovers Eq. (4.157) from Eq. (4.237) and Eqs. (4.232)-(4.234) as $\widehat{\varphi} \to 0$.

4.3.12 Phase diagram of the UCNA

Equations (4.232)-(4.234) are solved numerically. We restrict our subsequent study to $c_2 = 1$ and we vary c_1. This amounts to varying the persistence time of the original AOUPs dynamics while working at β constant. The impact of βu_0, *i.e.* the ratio between the energy scale of the potential over the temperature of the $\tau \to 0$ dynamics, on the phase diagram of the UCNA approximation is an interesting question left for future work.

For all c_1, and at small density $\widehat{\varphi}$, Eqs.(4.232)-(4.234) have a single solution characterized by a high degree of symmetry $m = \hat{p} = \hat{q}$. We remark that the $\hat{p} = \hat{q}$ symmetry is expected given Eq. (4.170). At zero density $\widehat{\varphi} = 0$, the solution is trivial and is given by $m = \hat{p} = \hat{q} = 1$. As the density increases, the three coefficients start to decrease. For $c_1 \lesssim 3.8$, two other branches of solution appear at high enough density. They are both characterized by a breaking of the $\hat{p} = \hat{q}$ symmetry (but are each twice degenerated because of the $\hat{p} \leftrightarrow \hat{q}$ correspondence). These two branches emerge from the same point but are not connected to the original one. The free energy Eq. (4.216) of these two new branches remains higher than that of the symmetric $m = \hat{p} = \hat{q}$ one. The system thus selects the latter even at these high densities. The situation is described in Fig. 4.13 for $c_1 = 3$. The original fully symmetric branch is depicted in blue. The two new branches appearing at $\widehat{\varphi} \gtrsim 8$ are drawn in orange and green. For these two degenerates branch, there is one solution with $\hat{p}$ selecting the high value and $\hat{q}$ the low as well as another solution where the situation is reversed.

The situation is different for $c_1 \gtrsim 3.8$ in which case the green branch of Fig. 4.13 merges onto the blue fully symmetric one thus leaving only two branches in the high density regime which are plotted in Fig. 4.14 for $c_1 = 4.86$. Their respective free energy is plotted in the left panel of Fig. 4.15. The orange branch in Fig. 4.14 emerges from the blue one and thus, at the point where the second one appears, the two branches have the same free energy. Upon increasing the density, the free energy of the orange branch becomes lower than that of the blue one. This corresponds to a continuous transition from the symmetric branch to the one with broken symmetry. Upon increasing the density again, the free energy of the orange branch crosses that of the blue one. This is the sign of a discontinuous transition from the branch with broken symmetry to the symmetric one. This is magnified in the inset of the

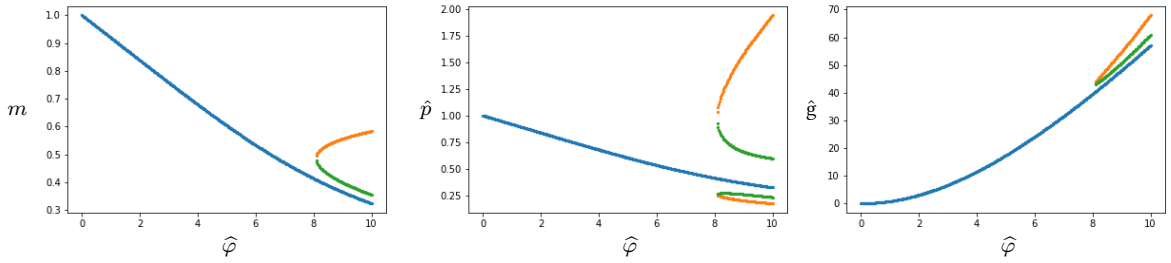

Figure 4.13: Solutions of the stationarity equations (4.232)-(4.234) at $c_2 = 1$ and $c_1 = 3$ as a function of the density $\widehat{\varphi}$. (**Left**) The solution m. (**Center**) The solution $\hat{p}$ (equivalently $\hat{q}$). For $\widehat{\varphi} \lesssim 8$, there exists a single solution with $m = \hat{p} = \hat{q}$ (blue). For $\widehat{\varphi} \gtrsim 8$, two new branches appear (orange and green). These break the $\hat{p} = \hat{q}$ symmetry. Along each one of them there is one solution with $\hat{p}$ selecting the high value of the branch and $\hat{q}$ selecting the low one and another solution where the reverse holds. (**Right**) The associated free energy of each branch is plotted. The symmetric one remains the lowest free energy one and is thus selected by the system.

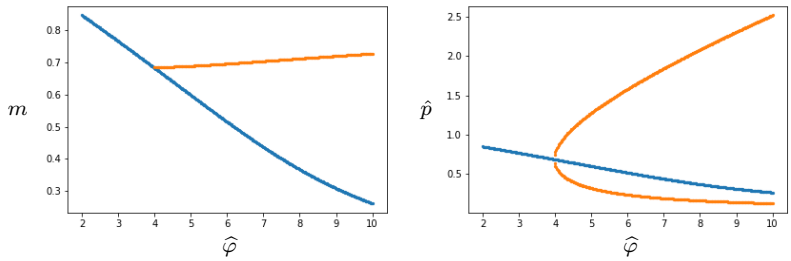

Figure 4.14: Solutions of the stationarity equations (4.232)-(4.234) at $c_2 = 1$ and $c_1 = 4.86$ as a function of the density $\widehat{\varphi}$. (**Left**) The solution m. (**Center**) The solution $\hat{p}$ (equivalently $\hat{q}$). For $\widehat{\varphi} \lesssim 8$, there exists a single solution with $m = \hat{p} = \hat{q}$ (blue). For $\widehat{\varphi} \gtrsim 8$, only one new branch appear (orange). It breaks the $\hat{p} = \hat{q}$ symmetry. Along it there is one solution with $\hat{p}$ selecting the high value of the branch and $\hat{q}$ selecting the low one and another solution where the reverse holds.

left panel of Fig.4.15 that shows the free energy of the blue branch minus that of the orange one. These two transitions are actually never observed except at the critical point where the low c_1 scenario of Fig. 4.13 merges into the high c_1 one of Fig. 4.14 and where the two above mentioned transitions merge in a single continuous one. Indeed, following the lowest free energy curve as a function of the density, we see that the latter becomes non convex around the two points at which the two branches cross each other. In the right panel of Fig. 4.15, we plot the convex hull of the lowest free energy curve. In the parts where the lowest free energy curve is convex we have indicated by the same color code as before the selected branch. Dashed red regions correspond to regions of non-convexity of the free energy. There, the system phase separates with coexisting densities given by the boundaries of these regions. We thus see emerging the phase diagram of the infinite dimensional UCNA within the replica symmetric diagonal ansatz as displayed in Fig. 4.16. At low $c_1 \lesssim 3.8$ activity, the

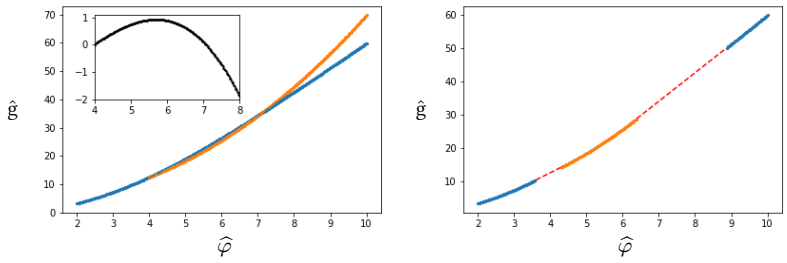

Figure 4.15: (**Left**) Free energy of the branches as a function of the density. The free energy difference of the blue branch minus that of the orange one is plotted in the inset. (**Right**) Convex hull of the curve of lowest free energy. The blue and orange parts correspond to convex regions and indicate which branch is selected by the system. In the two regions defined by the dashed red lines the free energy is non-convex and the system thus phase separates. The coexisting densities are given by the boundaries of the dashed regions. $c_2 = 1$ and $c_1 = 4.86$.

system is homogeneous and is described by a $(\hat{p}, \hat{q})$ symmetric phase. For $c_1 \gtrsim 3.8$ the latter still holds at low density. Above a certain density threshold, the system phase separates into a dense and a dilute phase. The latter is $(\hat{p}, \hat{q})$ symmetric while the symmetry is broken in the former. Upon increasing the density the system becomes homogeneous again but in a phase with broken $(\hat{p}, \hat{q})$ symmetry. Increasing the density again leads to a new phase separation: the low density phase is not symmetric while the high density one is. Finally, at high density, the system is in a symmetric homogeneous phase. As seen in Sec. 4.3.3, the whole phase behavior is completely missed if one restricts the stationary state to two-body interactions. We stress that it would be particularly interesting to have better insights into the physical real space implications of these auxiliary fields. Can we think of them as being related to the original speed degrees of freedom of the AOUPs dynamic ? Is it possible to distinguish with real-space observables only the symmetric phase from the one where the symmetry is broken ? In the end of App. E, in a completely different context, we demonstrate that a formally similar symmetry breaking accounts for the exponential growth of stationary points in a family of random dynamical systems.

4.4 Conclusion

Let us now add some concluding remarks to this work on active matter in infinite dimension. Some common features emerged from Sec. 4.2 and Sec. 4.3. First, in both case, the fluid structure, described by its n-point distribution functions, is equivalent to that of a standard equilibrium fluid with density dependent pair potential. This renormalization of the structure with the density is a signature of the steady state multibody interactions. Second, in the Kirkwood approximation of the RTP system, the self-propulsion velocity never vanishes and nor does the system undergo phase separation. Accordingly, in the UCNA approximation, keeping track only of two-body interactions prevents to account for the rich phase behavior of the system. This advocates for the generic importance of multi-

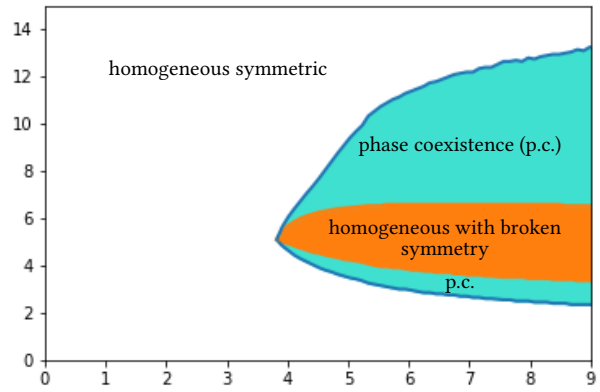

Figure 4.16: Phase diagram of the UCNA within the replica symmetric block diagonal ansatz. It displays two regions of homogeneous phases with different symmetries: one with the $\hat{p} = \hat{q}$ symmetry and one where this symmetry is broken (**Orange**). These are separated by two regions of phase coexistence (p.c.) with coexisting densities given by the boundaries of the turquoise domains (**Turquoise**). The critical point is located at $c_1 \simeq 3.8$ and $\widehat{\varphi} \simeq 4.8$.

body interactions at least at the mean-field level. Further insights could be gained in the future by applying the ideas of [142] to the UCNA and the RTP dynamics. In this work, inspired from an earlier proposal of [118], the authors study a slightly modified version of the standard equilibrium dynamics of pairwise interacting colloids with the pair interaction $\boldsymbol{\nabla}_{\mathbf{r}_i} U(\mathbf{r}_i - \mathbf{r}_j)$ replaced by $\boldsymbol{\nabla} U(\mathbf{r}_i - \mathbf{r}_j - \mathbf{A}_{ij})$ with $\mathbf{A}_{ij} = \mathbf{A}_{ji}$ a symmetric matrix of zero mean independent and identically distributed random vectors. When the variance of their norm becomes of the order of the system size, the system becomes mean-field like. As in the large d limit indeed, if particle i interacts with particle j and k then it is highly unlikely that particles j and k interact together. In fact, it can be proven that the system is then equivalent to its infinite dimensional counterpart, at least in equilibrium. These model have the great advantage to introduce a continuous parameter that allows to go from the standard regime to the mean-field one (the typical size of the vectors $\mathbf{A}_{ij}$) and are amenable to numerical simulations.

To conclude, we attempt to paint a broader picture. Sec. 4.3 suggests that if the many-body stationary distribution can be mapped, in an extended space, onto one with pairwise structure then the structure of the fluid will be (provided correct scalings can be taken) that of an equilibrium one with density dependent pair potential. Both Sec. 4.2 and Sec. 4.3 however show that there is no immediate recipe to predict the way interactions renormalize the two-point function. This scenario is actually a very generic one as such a mapping can indeed always be found in systems in which the dynamics is described in terms of pairwise forces. Consider the dynamical equations,

$$\dot{\mathbf{r}}_i = \boldsymbol{\eta}_i(t) - \sum_{j \neq i} \boldsymbol{\nabla}_{\mathbf{r}_i} U(\mathbf{r}_i - \mathbf{r}_j)\,, \tag{4.238}$$

where the $\boldsymbol{\eta}_i(t)$ are assumed to be independent and identically distributed noises. Then,

from any initial distribution P_0, the stationary distribution P_N can be obtained as

$$P_N(\{\mathbf{r}_i\}) = \lim_{T\to\infty} \int \prod_i \mathrm{d}\mathbf{r}_i^0 P\left[\{\mathbf{r}_i\} \,|\, \{\mathbf{r}_i^0\}\,; -T\right] P_0(\{\mathbf{r}_i^0\})\,, \tag{4.239}$$

with $P\left[\{\mathbf{r}_i\} \,|\, \{\mathbf{r}_i^0\}\,; -T\right]$ the transition probability to go from $\{\mathbf{r}_i^0\}$ at time $-T$ to $\{\mathbf{r}_i\}$ at time 0. Upon introducing the standard MSRJD response fields, the N-body stationary distribution reads

$$P_N(\{\mathbf{r}_i\}) = \lim_{T\to\infty} \int \prod_i \mathcal{D}\hat{\mathbf{r}}_i\, \mathcal{D}\mathbf{r}_i\, \mathrm{d}\mathbf{r}_i^0\, P_0(\{\mathbf{r}_i^0\}) \exp\left[-i \int_{-T}^0 \hat{\mathbf{r}}_i \cdot \left(\dot{\mathbf{r}}_i + \sum_{j\neq i} \boldsymbol{\nabla}_{\mathbf{r}_i} U(\mathbf{r}_i - \mathbf{r}_j)\right)\right] \times \cdots \times \left\langle \exp\left(i \int_{-T}^0 \hat{\mathbf{r}}_i \cdot \boldsymbol{\eta}_i\right)\right\rangle_{\boldsymbol{\eta}}\,. \tag{4.240}$$

Therefore, in this extended space comprising the trajectories of the original and of the response fields, the stationary distribution indeed has a pairwise structure (this becomes manifest upon choosing an initial distribution that has itself such a structure). This is at the basis of the derivation of the DMFT equations [2, 136]. However, in this framework, finding the two-point function amounts at solving the DMFT equations in the stationary state, a task which in general is out-of-reach. There also remain many open questions regarding to what extent does the two-point distribution function, if known, contain all the information needed to predict the behavior of the system. On the one hand, Sec. 4.2 suggests that the Franz-Parisi construction might actually be extended to some out-of-equilibrium dynamics with multibody interactions in steady for predicting their dynamical glass transition in infinite dimension. It would be nice to see if the DMFT framework can bring us insights into the validity of this statement. On the other hand, the actual free energy of the system is in general not given by that of its equilibrium pairwise interacting counterpart. As can be seen in Eq. (4.187), contributions coming from the entropy of the auxiliary degrees of freedom also have to be taken into account so that the position-space pair distribution alone does not control all the phase behavior of the system.

Chapter 5

Conclusion

We now conclude this part devoted to the study of the collective behavior of self-propelled particle systems. In Chap. 2, we have studied the case of one particle in an external potential. This case in which the complexity is reduced as much as possible is the first building block of our understanding of more complex macroscopic properties. We have first worked out the deviations from equilibrium in a model of AOUP at low persistence and in the presence of thermal noise. We have demonstrated a non-trivial interplay between the active and the thermal noises as it appears that increasing temperature does not generically push the system closer to equilibrium. We have then derived the properties of a single RTP first in a one-dimensional confining potential and second around a fixed spherical obstacle. These results illustrate the repulsion-induced attraction often referred to in active matter systems.

The remainder of our work was devoted to studying the collective properties of assemblies of self-propelled particles interacting via pairwise forces with a particular emphasis on the stationary state. These systems are known to combine the hurdles of nonequilibrium physics with those of strongly correlated liquids. The strategy we adopted in this manuscript was to use the limit of infinite dimension. The latter has indeed proven in the past to be a powerful tool to study the statics of equilibrium fluids [68] and the dynamics of generic dynamical systems interacting with pairwise forces [2]. We started by studying the Dynamical Mean Field Theory equations in the dilute limit for a generic class of sticky sphere potentials. In particular, we proved the proportionality, to first order in the density, between the long-time mean square displacement of a particle and the square of the effective velocity. We then studied these systems beyond the dilute limit which brought us to focus on the role of multibody interactions in the steady state. Their existence makes the stationary distribution of active matter systems genuinely different from that of standard equilibrium fluids. In an approximate resummation scheme of the BBGKY hierarchy presented in Sec. 4.2, we have computed the density dependence of the effective self-propulsion and of the radial pair distribution function of RTPs interacting via a sticky sphere potential. We have also introduced the notion of effective amplitude of potential interactions. In the purely hard sphere case, we have shown that, within this approximation, the pair correlation function is given by its dilute limit counterpart and that, in agreement with numerical simulations performed on finite dimensional systems [196], the effective self-

propulsion linearly decays with the density. This is however not a dilute limit result since the proposed resummation is non-perturbative in the density. For a generic sticky-sphere potential, we have shown that the spatial structure of the active fluid is the same as that of a passive one with a density dependent interaction potential. Remarkably, both the effective self-propulsion and the effective amplitude of potential interactions vanish at a crowding density $\widehat{\varphi}_{\rm cr}$ that equals the dynamical glass transition density $\widehat{\varphi}_d$ of the equilibrium colloidal system with an equivalent spatial structure. We pursued our investigation in Sec. 4.3 on the role of multibody interactions in the steady state by studying the phase behavior of the Unified Colored Noise Approximation of the AOUPs dynamics. Similarly to what we showed in Sec. 4.2, the spatial structure is similar to that of a passive fluid with a density dependent interaction potential. Furthermore, we obtained the rich phase diagram of the UCNA that displays two regions of phase separation and showed that an approximation keeping only track of two-body interactions could not account for it. We believe this advocates for the generic importance of multibody interactions in nonequilibrium systems as recently claimed in the case of three-dimensional ABPs [202].

This work leaves many open questions ahead of us. The relation between first the mean-square-displacement and second the effective self-propulsion remains to be properly understood. This would open the way towards a finer understanding of the links existing between the dynamical glass transition of equilibrium systems on the one side and the vanishing of the effective self-propulsion speed in active systems on the other. Our work suggests that some connection exists, at least at the mean-field level. Lastly, to what extent does the infinite dimensional phenomenology survives in two or three dimensional systems remains a debated issue [95] and deserves to be better understood in, and outside of, the context of active matter.

Part II

Stochastic calculus for path integration

Chapter 6

Introduction

Take a Langevin equation for a one-dimensional stochastic process $x(t)$ with multiplicative noise, whose generic form is

$$\frac{\mathrm{d}x}{\mathrm{d}t} = f(x(t)) + g(x(t))\eta(t)\,, \tag{6.1}$$

where η is a Gaussian white noise with correlations $\langle \eta(t)\eta(t')\rangle = \delta(t-t')$. It is a well-known feature of this equation that it must be considered with great care as the process $x(t)$ is not differentiable. One way to endow Eq. (6.1) with a well-defined mathematical meaning is to consider the infinitesimal increment of x between t and $t+\Delta t$, for $\Delta t \to 0$,

$$x(t+\Delta t) - x(t) = \Delta x = f\left(x(t)\right)\Delta t + g\left(x(t) + \alpha \Delta x\right)\Delta\eta\,, \tag{6.2}$$

with $0 \leq \alpha \leq 1$ and where $\Delta\eta$ is a zero mean Gaussian variable of variance Δt. This is known as the α-discretization scheme and each value of α generates a different process. The $\alpha = 0$ scheme is known as the Itō one, $\alpha = 1/2$ as the Stratonovich one, and $\alpha = 1$ as the Hänggi-Klimontovich one. Such an equation as Eq. (6.1) usually appears, in physics, after some coarse-graining procedure consisting in integrating out degrees of freedom of no direct interest. It also requires the existence of a separation of space and time scales between the degree of freedom of interest and the surrounding environment. It is the Markov approximation according to which the relaxation of the environment occurs over time scales much smaller than that of the degree of freedom of interest that is responsible for η to be δ correlated and therefore for the process x not to be differentiable. When the Markov limit is carefully taken in an equation of the form of Eq. (6.1) with a correlated noise, the increment of x between t and $t+\Delta t$ is shown to be given by the Stratonovich $\alpha = 1/2$ scheme. Of course, a process expressed in one of the α-discretized forms can always be expressed in terms of another α-discretized one,

$$\frac{\mathrm{d}x}{\mathrm{d}t} \overset{\alpha}{=} f(x) + g(x)\eta \iff \frac{\mathrm{d}x}{\mathrm{d}t} \overset{\alpha'}{=} f(x) + (\alpha - \alpha')g'g + g(x)\eta\,, \tag{6.3}$$

where the the $\overset{\alpha}{=}$ symbol means that the continuous-time equation must be understood according to the α-discretization of Eq. (6.2).

Given a smooth function $u(x)$, the process $U(t) = u(x(t))$ also evolves according to a Langevin equation. However, it is only when Eq. (6.1) is understood with the Stratonovich scheme that the usual chain rule of differential calculus holds and that

$$\frac{\mathrm{d}x}{\mathrm{d}t} \overset{1/2}{=} f(x) + g(x)\eta \implies \frac{\mathrm{d}U}{\mathrm{d}t} \overset{1/2}{=} F(U) + G(U)\eta\,, \tag{6.4}$$

where $F(U(t)) = u'f$ and $G(U) = u'g$. Instead, when Eq. (6.1) is understood in the Itō scheme, one has to use the celebrated Itō formula,

$$\frac{\mathrm{d}x}{\mathrm{d}t} \overset{0}{=} f(x) + g(x)\eta \implies \frac{\mathrm{d}U}{\mathrm{d}t} \overset{0}{=} u'\frac{\mathrm{d}x}{\mathrm{d}t} + \frac{1}{2}u''g^2\,, \tag{6.5}$$

While a discussion of the discretization scheme is irrelevant at the level of Eq. (6.1) whenever g is a constant (namely for a process with additive noise), it becomes a requirement when studying the evolution of a nonlinear function of x, as seen in Eqs. (6.4) and (6.5).

Physical approximations (coarse-graining and the Markov limit) need not be implemented at the level of the equations of motion. They can instead be applied to, say, a Liouville equation. In the Markov approximation, this results in a master equation, which, in the diffusive limit, is known as the Fokker-Planck (or as the Kolmogorov forward equation or the Smoluchowski equation). Instead of tracking individual fluctuating trajectories generated by Eq. (6.1) one focuses on the probability density $P(x,t)$ of the random process $x(t)$ and arrives at an equation of the form

$$\partial_t P = -\partial_x(fP) + \frac{1}{2}\partial_x^2(g^2P)\,, \tag{6.6}$$

which describes the same process as the one evolving according to Eq. (6.1) understood in the Itō sense with $\alpha = 0$. Within the framework of quantum mechanics in which randomness is intrinsic, *i.e.* not resulting from a loss of information, probability amplitudes are obtained from the Schrödinger equation. The latter, for a particle in a potential, also takes the form of a linear first-order in time, second-order in space, partial differential equation. This formal resemblance explains that tools developed in stochastic processes can be useful in quantum mechanics, and *vice versa*. Interestingly, there have even been attempts to cast quantum mechanics within the Langevin language [160].

This brings us to the topic of this work. There is a third description of random processes based on path integrals where the fundamental object is the probability distribution over random trajectories. Originally Wiener [208, 209] built them to analyze the properties of Brownian motion, but they became a central tool of theoretical physics after Feynman [52] reformulated quantum mechanics in terms of path integrals. After the work of Onsager and Machlup [165, 132], they became a cornerstone in the study of classical irreversible processes. In much the same way as in Langevin equations, in path integrals one manipulates non-differentiabile trajectories, and this comes with its share of mathematical difficulties first raised by Edwards and Gulyaev [45]. These are the ones we would like to discuss now. We begin by illustrating one of them by an example.

6.0.1 A Brownian particle

Consider a large particle of mass m in water, whose motion is modelled by the Langevin equation

$$m\frac{\mathrm{d}v}{\mathrm{d}t} = -\gamma v + \sqrt{2\gamma T}\eta,\ \langle \eta(t)\eta(t')\rangle = \delta(t-t')\,, \tag{6.7}$$

where γ is the friction coefficient and T is the temperature of the water bath. Starting from an initial condition where $v(0)=0$, the probability of observing a velocity v at time t can be obtained from a summation over all velocity trajectories going from $v(0)=0$ to $v(t)=v$:

$$P(v,t|0,0) = \int_{v(0)=0}^{v(t)=v} \mathcal{D}v \exp\left[-\frac{1}{4\gamma T}\int_0^t \mathrm{d}\tau \left(m\frac{\mathrm{d}v}{\mathrm{d}t}+\gamma v\right)^2\right]. \tag{6.8}$$

As for Langevin equations, expressions such as Eq. (6.8) acquire an unequivocal meaning when a discretization scheme is provided. Here we must understand Eq. (6.8) as the $\Delta t \to 0$ limit of

$$\prod_{i=1}^{t/\Delta t-1}\left(\frac{m}{\sqrt{4\pi\gamma T\Delta t}}\right)\mathrm{d}v_i \to \mathcal{D}v\,, \tag{6.9}$$

along with

$$\Delta t\sum_{i=0}^{t/\Delta t-1}\left(m\frac{v_{i+1}-v_i}{\Delta t}+\gamma v_i\right)^2 \to \int_0^t \mathrm{d}\tau\left(m\frac{\mathrm{d}v}{\mathrm{d}t}+\gamma v\right)^2, \tag{6.10}$$

with $v_0=0$ and $v_{t/\Delta t}=v$. These discretized expressions are the direct analogs of the Itō discretized form of the Langevin equation. Similarly, other schemes could be used, such as the Stratonovich one, leading to

$$P(v,t|0,0) = \int_{v(0)=0}^{v(t)=v} \mathcal{D}v \exp\left[-\frac{1}{4\gamma T}\int_0^t \mathrm{d}\tau \left(m\frac{\mathrm{d}v}{\mathrm{d}t}+\gamma v\right)^2 + \frac{\gamma}{2m}t\right], \tag{6.11}$$

with

$$\prod_{i=1}^{t/\Delta t-1}\left(\frac{m}{\sqrt{4\pi\gamma T\Delta t}}\right)\mathrm{d}v_i \to \mathcal{D}v\,, \tag{6.12}$$

and

$$\Delta t\sum_{i=0}^{t/\Delta t-1}\left(m\frac{v_{i+1}-v_i}{\Delta t}+\gamma\frac{v_i+v_{i+1}}{2}\right)^2 \to \int_0^t \mathrm{d}\tau\left(m\frac{\mathrm{d}v}{\mathrm{d}t}+\gamma v\right)^2. \tag{6.13}$$

While discretization issues are irrelevant for Langevin processes with additive noise, they play a manifest role for the corresponding path integral formulations, as can be seen from the difference between Eqs. (6.8) and (6.11).

We now ask about the statistics of the kinetic energy $K=\frac{m}{2}v^2$ of the particle and we denote by $Q(K,t|0,0)$ its probability density. At the level of Langevin equations the rules of stochastic calculus allow us to write that

$$\begin{aligned}\frac{\mathrm{d}K}{\mathrm{d}t} &\overset{1/2}{=} -\frac{2\gamma}{m}K + \sqrt{\frac{4\gamma TK}{m}}\eta\,,\\ &\overset{0}{=} -\frac{2\gamma}{m}K + \frac{\gamma T}{m} + \sqrt{\frac{4\gamma TK}{m}}\eta\,.\end{aligned} \tag{6.14}$$

Regarding the corresponding path-integral formulation, in the Itō scheme,

$$Q(K,t|0,0) = \int \mathcal{D}K \; \mathrm{e}^{-\frac{m}{8\gamma T}\int_0^t \mathrm{d}\tau \frac{1}{K}\left(\frac{\mathrm{d}K}{\mathrm{d}\tau}+\frac{2\gamma}{m}K-\frac{\gamma T}{m}\right)^2}, \tag{6.15}$$

where

$$\begin{aligned}
&\prod_{i=1}^{t/\Delta t-1}\left(\sqrt{\frac{m}{8\pi\gamma T\Delta t K_i}}\right)\mathrm{d}K_i \to \mathcal{D}K\,,\\
&\Delta t\sum_{i=0}^{t/\Delta t-1}\frac{1}{K_i}\left(\frac{K_{i+1}-K_i}{\Delta t}+\frac{2\gamma}{m}K_i-\frac{\gamma T}{m}\right)^2 \to \int_0^t \mathrm{d}\tau\frac{1}{K}\left(\frac{\mathrm{d}K}{\mathrm{d}\tau}+\frac{2\gamma}{m}K-\frac{\gamma T}{m}\right)^2,
\end{aligned} \tag{6.16}$$

while in the Stratonovich one,

$$Q(K,t|0,0) = \int \mathcal{D}K \mathrm{e}^{-\frac{m}{8\gamma T}\int_0^t \mathrm{d}\tau\left[\frac{1}{K}\left(\frac{\mathrm{d}K}{\mathrm{d}\tau}+\frac{2\gamma}{m}K\right)^2+\frac{2\gamma T}{mK}\frac{\mathrm{d}K}{\mathrm{d}\tau}-\frac{\gamma^2T^2}{m^2K}\right]+\frac{\gamma t}{2m}}, \tag{6.17}$$

where

$$\begin{aligned}
&\prod_{i=1}^{t/\Delta t-1}\left(\sqrt{\frac{m}{4\pi\gamma T\Delta t(K_i+K_{i+1})}}\right)\mathrm{d}K_i \to \mathcal{D}K\,,\\
&\Delta t\sum_{i=0}^{t/\Delta t-1}\left[\frac{2}{K_i+K_{i+1}}\left(\frac{K_{i+1}-K_i}{\Delta t}+\frac{\gamma}{m}(K_i+K_{i+1})\right)^2,\right.\\
&\qquad\left.+\frac{4\gamma T}{m(K_i+K_{i+1})}\frac{K_{i+1}-K_i}{\Delta t}-\frac{2\gamma^2T^2}{m^2(K_i+K_{i+1})}\right],\\
&\to\int_0^t\mathrm{d}\tau\left[\frac{1}{K}\left(\frac{\mathrm{d}K}{\mathrm{d}\tau}+\frac{2\gamma}{m}K\right)^2+\frac{2\gamma T}{mK}\frac{\mathrm{d}K}{\mathrm{d}\tau}-\frac{\gamma^2T^2}{m^2K}\right].
\end{aligned} \tag{6.18}$$

At the Langevin level, the Stratonovich discretization is consistent with differential calculus and switching from v to K can be done as if these functions were differentiable. However naively changing path from v to K starting from Eq. (6.11) would not lead to the correct expression Eq. (6.17) (the last two terms in the time integral would be absent). Similarly, using the Itō formula from Eq. (6.8) does not lead to the correct Itō discretized action for K shown in Eq. (6.15).

This simple example allows us to phrase the questions of interest throughout this work. Starting from an action in the Itō (or Stratonovich) form, can we extend the Itō lemma to path-integral calculus (without using Langevin equations as intermediate steps)? Is there a discretization scheme that allows to deal with functions in path integrals as if these were differentiable? These are really the two sides of the same coin: either one sticks to a given discretization and then the rules of differential calculus have to be adapted, or one imposes differential calculus to hold, but this requires finding the appropriate discretization schemes. Such questions have already been addressed and answered in the past. We review the existing literature, and further bring to the fore alternative answers to these old questions.

6.0.2 Motivations and outline

We have just illustrated the core of the mathematical problem we want to address. These technical aspects of path integrals are of interest in a wide array of sciences. Indeed, stochastic processes are ubiquitous in mathematical descriptions of the physical world. In situations where one focuses on a subset of degrees of freedom, information is lost, and this results in effective randomness. This applies to inflationary cosmology [146, 205], climate dynamics [85], colloidal particles in solvents [46], Bose-Einstein condensates [43], to name but a few. Phenomena outside the realm of physics, whether option pricing or myosin dynamics are also described by similar tools. Going down in scale one meets the quantum description of matter which is intrinsically random. A common mathematical tool that pervades these areas of science are stochastic differential equations and their path-integral representation. It is thus of paramount importance to understand the mathematical subtleties that pave their use.

The forthcoming results are the fruit of a collaboration with L. Cugliandolo and V. Lecomte. In Chap. 7, we review some useful results about first stochastic calculus in Sec. 7.1 and second path integral representation of stochastic differential equations in Sec. 7.2. In Chap. 8, this will allows us to clearly identify the origin of the problems encountered when changing variables at the level of continuous-time path integrals as already pointed out by many authors in the literature, *e.g.* in [28, 124]. We next present different strategies to circumvent the problem. In Sec. 8.1, we start by showing how to extend to usual rules of stochastic calculus of α-discretized stochastic differential equations in order to make them usable for performing changes of variables within α-discretized path integrals. Then, we present an alternative approach consisting in altering the discretization scheme of the path integral so as to make the continuous-time expression consistent with differential calculus. Historically, it is DeWitt [36] who first proposed a covariant extension of Feynman's path-integral formulation of quantum mechanics on curved space. A similar construction was then used by Graham [86, 87] for classical diffusive processes. In their formulation, the propagator of the process between two infinitesimally close times is expressed by means of the continuous-time action evaluated at the least-action trajectory. This requires solving the classical equation of motion over an infinistesimal time window with boundary conditions at x and $x + \Delta x$. We review these approaches in Sec. 8.2. The construction we propose in 8.3 is based on an extension of the Stratonovich discretization of Langevin equations. The continuous-time expressions we obtain are compatible with differential calculus, as already achieved by DeWitt and Graham, but this covariance property extends to the fully discretized level. Our scheme, that generalizes the work of [29], will probably appear more familiar in spirit to statistical physicists.

Chapter 7

Stochastic calculus and path integrals

Contents

This chapter is dedicated to reviewing some useful results about first stochastic calculus in Sec. 7.1 and second path integral representation of stochastic differential equations in Sec. 7.2. We will use them later in Chap. 8 to explain the difficulties linked to performing changes of variables in the path integral and to show how to circumvent them.

7.1 Stochastic calculus

This section reviews stochastic calculus at the level of the Langevin and Fokker-Planck equations without referring just yet to path integrals. The difficulties intrinsic to working in more than one space dimension are discussed.

7.1.1 Discretization of stochastic differential equations

As we shall review below, a stochastic differential equation involving a multiplicative noise (one in which the noise η appears to be multiplied by a state-dependent function g, as in Eq. (7.1) below), acquires a well-defined mathematical meaning once endowed with a corresponding discretization rule. Such equations with multiplicative noise are by no means a rarity. For instance, the mobility of a Brownian colloid diffusing in the vicinity of a wall depends on its distance to the wall [122, 5, 78, 174, 140]. The description of rotational Brownian motion [27] (with applications to dielectrics [129], magnetism [18], and active matter [24]) also involves, in order to enforce a spherical constraint, a multiplicative noise. Another celebrated example outside of the realm of physics is the Black and Scholes equation [98] proposed to model the evolution of some specific financial assets. Of course, any non-linear transformation of a stochastic variable evolving according to a Langevin equation with additive noise evolves according to a Langevin equation with multiplicative noise, as illustrated in our opening example, Eqs. (6.7) and (6.14). In the physical sciences, there are mostly two channels through which such Langevin equations arise [109]. In the first one, a large physical system is described by dynamical equations that couple the degrees of freedom of interest, hereafter denoted by $x(t)$, to some other external degrees of freedom referred to as a bath or an environment. Integrating out the latter generically yields a dynamical equation for $x(t)$ which features both colored noise and colored friction. It is then the Markov limit, in which the relaxation time of the external degrees of freedom is assumed to be much smaller than the typical timescale associated with the dynamics of $x(t)$, that defines the correct limiting stochastic differential equation and the associated discretization rule. In the second situation, physics is fundamentally described by master equations (derived *e.g.* from some Liouville equation). The correspondence between such a level of description with a stochastic differential equation also fixes the proper discretization scheme used to represent the stochastic process. Most of the discussion that follows can be found in classic textbooks such as Van Kampen's [108] or Gardiner's [75].

We now consider a dynamical variable $x(t)$ the evolution of which is assumed to be given by a stochastic differential equation with multiplicative noise

$$\frac{\mathrm{d}x}{\mathrm{d}t} \overset{\mathfrak{d}}{=} f(x(t)) + g(x(t))\eta(t)\,. \tag{7.1}$$

The noise $\eta(t)$ is Gaussian and white with zero mean,

$$\langle \eta(t) \rangle = 0\,, \qquad \langle \eta(t)\eta(t') \rangle = \delta(t'-t)\,. \tag{7.2}$$

The label $\mathfrak{d}$ above the equal sign stands for a reminder that Eq. (7.1) comes hand-in-hand with an accompanying discretization scheme (Van Kampen [109] refers to Eq. (7.1) as a pre-equation). Concretely, Eq. (7.1) should be understood as the continuous-time limit, *i.e.* the limit in which the time step Δt goes to zero, of the following discrete companion evolution rule

$$\Delta x(t) = x(t+\Delta t) - x(t) = f(\bar{x})\Delta t + g(\bar{x})\Delta\eta(t)\,, \tag{7.3}$$

where at each time step the $\Delta\eta(t)$ are independent and identically distributed Gaussian variables with zero mean and variance Δt. Notations-wise, we shall also use the discrete

sequence of steps $x_k = x(k\Delta t)$, $k = 0, \ldots, N$, $N = t_{\text{obs}}/\Delta t$ (here $[0, t_{\text{obs}}]$ refers to the time window over which we sample the random process) and of independent identically distributed Gaussian variables $\Delta\eta_k$ with unit variance and zero mean,

$$\Delta x_k = x_{k+1} - x_k = f(\bar{x}_k)\Delta t + g(\bar{x}_k)\Delta\eta_k \,, \tag{7.4}$$

In Eq. (7.3), f and g are evaluated at $\bar{x}$, a function of $x(t+\Delta t)$ and $x(t)$, the choice of which fully determines the discretization scheme (and $\bar{x}_k$ is $\bar{x}$ where $x(t)$ and $x(t+\Delta t)$ have been replaced with x_k and x_{k+1}). It is of paramount importance to notice that as a consequence of Eq. (7.3), as $\Delta t \to 0$, we have that

$$\Delta x(t) = O\left(\sqrt{\Delta t}\right) \,. \tag{7.5}$$

Therefore, the trajectories $x(t)$ obtained in the continuous-time limit $\Delta t \to 0$ are (almost surely) nowhere differentiable. This explains why, as we will see later, the discretization scheme of stochastic differential equations matters while it does not in the $\Delta t \to 0$ limit when discretizing ordinary differential equations. A common scheme [103] is the so-called α-discretization scheme in which

$$\bar{x} = x(t) + \alpha\Delta x(t) \,, \tag{7.6}$$

with $\alpha \in [0, 1]$. The Itō or pre-point convention corresponds to $\alpha = 0$ for which Eq. (7.3) provides an explicit expression for the increment $\Delta x(t)$. It moreover guarantees the statistical independence of $x(t)$ with respect to $\Delta\eta(t)$. The $\alpha = 1/2$ case corresponds to the Stratonovich or mid-point convention. The Stratonovich scheme is time-symmetric and, as we shall see further down, it allows the usual chain rule of differential calculus to hold. Finally, the $\alpha = 1$ discretization scheme is called the Hanggi-Klimontovich or the postpoint one and it has proved convenient in the study of relativistic Brownian motion [44]. In view of performing efficient numerical simulations, the question of finding the "best" discretization scheme is a very active one that goes well-beyond the present discussion. We refer the interested reader to recent reviews in that area [153, 154, 114, 139, 115]. We emphasize that, contrary to what holds for ordinary differential equations, different α-discretized companion processes sharing the same f and g functions lead to different stochastic processes in the $\Delta t \to 0$ limit, and are thus characterized by different distributions. This is best seen, using Eq. (7.5), by considering, for $\alpha \neq \alpha'$, the difference

$$\begin{aligned}\left[g(x(t) + \alpha\Delta x(t)) - g(x(t) + \alpha'\Delta x(t))\right]\Delta\eta(t) &= (\alpha - \alpha')g'(x(t))\Delta x(t)\Delta\eta(t) + O\left(\Delta t^{3/2}\right) \\ &= O(\Delta t) \,. \end{aligned} \tag{7.7}$$

Therefore, for two different α-discretization schemes, the difference in the increments $\Delta x(t)$ is of order $O(\Delta t)$, as is the contribution to the increments of the deterministic term, and thus cannot be neglected in the $\Delta t \to 0$ limit. Note that, by constrast,

$$\left[f(x(t) + \alpha\Delta x(t)) - f(x(t) + \alpha'\Delta x(t))\right]\Delta t = O\left(\Delta t^{3/2}\right) \,, \tag{7.8}$$

which expresses that the way the deterministic term is discretized does bear any influence on the $\Delta t \to 0$ limit. The sensitivity to the discretization scheme of course reflects on the

Fokker-Planck equation associated to Eq. (7.1) which in any α-discretization reads [74, 108, 125, 7]

$$\partial_t P(x,t) = -\partial_x[(f(x) + \alpha g(x)g'(x))P(x,t)] + \frac{1}{2}\,\partial_x^2[g^2(x)P(x,t)]\,. \tag{7.9}$$

It is a deterministic partial differential equation and it is thus immune to any discretization issues. Once supplemented with an initial condition $P(x,0)$, this equation describes the deterministic evolution of the probability density $P(x,t)$ of finding x at time t. Equation (7.9) can be written in the form of a continuity equation $\partial_t P + \partial_x J = 0$ and its stationary solution with vanishing current, $J = 0$, is

$$P_{\rm st}(x) = Z^{-1}\,[g(x)]^{2(\alpha-1)}\,\mathrm{e}^{2\int^x \mathrm{d}x'\,\frac{f(x')}{g^2(x')}}\,, \tag{7.10}$$

where $\int^x$ represents the indefinite integral over x' and Z is a normalization constant [74, 108]. The approach to this asymptotic form can be proven with the construction of an H-function or with the mapping of the Fokker-Planck operator onto a Schrödinger operator and the analysis of its eigenvalue problem [168]. That $P_{\rm st}$ depends on α and g explicitly shows that these ingredients affect the stationary properties of the system [97, 182, 197]. However, if we allow ourselves to consider the special 'drift force' [112]

$$f(x) = -g^2(x)V'(x) + (1-\alpha)g(x)g'(x)\,, \tag{7.11}$$

the dependence on α is eliminated from the FP equation

$$\partial_t P(x,t) = \partial_x\left(g^2(x)[V'(x)P(x,t) + \frac{1}{2}\,\partial_x P(x,t)]\right)\,, \tag{7.12}$$

and no observable depends on this parameter either. The asymptotic solution of the Fokker-Planck equation in Eq. (7.12) then reads

$$P_{\rm st}(x) = Z^{-1}\,\mathrm{e}^{-V(x)} = P_{\rm GB}(x)\,, \tag{7.13}$$

which is the standard Gibbs-Boltzmann distribution in the canonical ensemble, for a system with potential energy $V(x)$, independently of α and g.

Therefore, in order to describe the equilibrium Langevin dynamics of a multiplicative white noise system that samples the standard Gibbs-Boltzmann distribution, one needs to work with the following equation

$$\frac{\mathrm{d}x}{\mathrm{d}t} \overset{\alpha}{=} -g^2(x)V'(x) + (1-\alpha)g(x)g'(x) + g(x)\eta(t)\,, \tag{7.14}$$

using an α-prescription. Note the presence of a non-trivial additional 'drift force' even in the Stratonovich ($\alpha = 1/2$) prescription. It is only with a post-point prescription $\alpha = 1$ [89, 90, 91, 113] that this additional drift term vanishes.

While distinct discretizations of the same continuous-time expression lead to different processes, there are conversely distinct yet equivalent ways to describe the same physical process using a Langevin equation. To be more explicit, we consider an α-discretized stochastic differential equation of the form

$$\frac{\mathrm{d}x}{\mathrm{d}t} \overset{\alpha}{=} f(x) + g(x)\eta(t)\,, \tag{7.15}$$

which yields in discrete time

$$\Delta x = f(x)\Delta t + g(x + \alpha\Delta x)\Delta\eta(t)\,. \tag{7.16}$$

The latter evolution rule can be rewritten for any $\alpha' \in [0,1]$ as

$$\begin{aligned}\Delta x &= f(x)\Delta t + g(x + \alpha'\Delta x + (\alpha-\alpha')\Delta x)\Delta\eta(t)\,,\\ &= f(x)\Delta t + g(x+\alpha'\Delta x)\Delta\eta + (\alpha-\alpha')g'(x+\alpha'\Delta x)\Delta x\Delta\eta(t) + O(\Delta t^{3/2})\,,\\ &= f(x)\Delta t + g(x+\alpha'\Delta x)\Delta\eta + (\alpha-\alpha')g(x)g'(x)\Delta\eta(t)^2 + O(\Delta t^{3/2})\,.\end{aligned} \tag{7.17}$$

The evolution rule in Eq. (7.17) explicitely displays a $\Delta\eta(t)^2$ contribution, at odds with the original dynamics in Eq. (7.16). However, when computing the continuous-time Fokker-Planck equation associated with the $\Delta t \to 0$ limit of Eq. (7.17), one realizes that the $\Delta\eta(t)^2$ only contributes through it first moment $\langle\Delta\eta(t)^2\rangle = \Delta t$. One can thus rewrite

$$\Delta x := f(x)\Delta t + g(x+\alpha'\Delta x)\Delta\eta + (\alpha-\alpha')g(x)g'(x)\Delta t\,. \tag{7.18}$$

In Eq. (7.18), the $:=$ sign does not mean there is a point-wise equality between Eq. (7.17) and Eq. (7.18) but rather that these two discrete time evolution rules generate the same random process in the continuous-time limit. This is the first example of a substitution rule, a notion that we will shortly clarify. Therefore, in the continuous time limit, we can assert that

$$\begin{aligned}\frac{\mathrm{d}x}{\mathrm{d}t} &\overset{\alpha}{=} f(x) + g(x)\eta(t)\,,\\ &\overset{\alpha'}{=} f(x) + (\alpha-\alpha')g(x)g'(x) + g(x)\eta(t)\,.\end{aligned} \tag{7.19}$$

This concludes our review of the most common schemes used to discretize Langevin equations. We now wish to investigate how the rules of calculus—integration and differentiation—are affected by the singular nature of the paths generated by Langevin equations.

7.1.2 Integration

We now consider a random process $x(t)$ evolving according to the Langevin equation

$$\frac{\mathrm{d}x}{\mathrm{d}t} \overset{\alpha}{=} f(x) + g(x)\eta(t)\,, \tag{7.20}$$

understood as α-discretized. First, we wish to focus on observables of the form

$$\mathcal{O}_0 = \int_0^t \mathrm{d}s\, h(x(s))\,, \tag{7.21}$$

where h is a (smooth enough) arbitrary function, which, when expressed in terms of the discrete time companion process, writes

$$\mathcal{O}_0 = \lim_{\Delta t\to 0}\sum_{k=0}^{N}\Delta t\, h(x_k)\,, \tag{7.22}$$

where the notation x_k refers to the value of x at time step number k (at time $k\Delta t$). In the $\Delta t \to 0$ limit, one could also have written

$$\mathcal{O}_0 = \lim_{\Delta t \to 0} \sum_{k=0}^{N} \Delta t \, h(x_k + \alpha' \Delta x_k) \,, \tag{7.23}$$

for any $\alpha' \in [0, 1]$ with $\Delta x_k = x_{k+1} - x_k$. In other words, in the continuous time limit, the specific discretization scheme of the integral in Eq. (7.21) is irrelevant, as expected for such standard Riemann sums.

Other interesting observables that, for example, often arise in the field of stochastic thermodynamics [187, 188] are of the form

$$\mathcal{O}_1 \overset{\alpha'}{=} \int_0^t \dot{x} \, h(x(s)) \, \mathrm{d}s \,, \tag{7.24}$$

which in terms of the discrete time companion process reads

$$\mathcal{O}_1 = \lim_{\Delta t \to 0} \sum_{k=0}^{N-1} \Delta t \, \frac{\Delta x_k}{\Delta t} \, h\left(x_k + \alpha' \Delta x_k\right) \,. \tag{7.25}$$

This discretization has been made explicit above the equality sign by the α' label appearing in Eq (7.24). Due to the scaling $\Delta x_k = O(\sqrt{\Delta t})$, the discretization of the integral, namely the point at which the function h is evaluated, is relevant even in the $\Delta t \to 0$ limit. This statement is very similar to the fact that one needs to specify the discretization of g in the discrete time companion process of Eq. (7.20). Note that α and α' have nothing to do with each other: α determines the evolution of the companion process x while α' enters in the definition of the observable $\mathcal{O}_1$. Integrals of the form Eq. (7.24) with $\alpha' = 0$ (respectively $\alpha' = 1/2$) are referred to as Itō integrals (respectively as Stratonovich integrals).

To conclude this subsection devoted to integration, we wish to introduce a last class of observables. A quantity of the form $\int_0^t \mathrm{d}s \dot{x}^2 h(x(s))$, as can often been seen in the exponential weight entering a path integral, is strictly not defined. However, the attached observable $\mathcal{O}_2$, defined by its discrete expression as

$$\mathcal{O}_2 = \lim_{\Delta t \to 0} \sum_{k=0}^{N-1} \Delta t \, \frac{(\Delta x_k)^2}{\Delta t} \, h(x_k) \,, \tag{7.26}$$

is indeed finite in the $\Delta t \to 0$ limit. Furthermore, the discretization of h is irrelevant to define the continuous time limit. We recall that

$$\Delta x_k = f(x_k) \Delta t + g\left(x_k + \alpha \Delta x_k\right) \Delta \eta_k \,, \tag{7.27}$$

so that

$$\begin{aligned}\mathcal{O}_2 &= \lim_{\Delta t\to 0}\sum_{k=0}^{N-1}\Delta t\,\frac{\left(f(x_k)\Delta t + g\left(x_k+\alpha\Delta x_k\right)\Delta\eta_k\right)^2}{\Delta t}\,h(x_k)\,,\\ &= \lim_{\Delta t\to 0}\sum_{k=0}^{N-1}\Delta t\,\frac{\Delta\eta_k^2}{\Delta t}\,g^2\left(x_k+\alpha\Delta x_k\right)\,h(x_k)\,,\\ &= \lim_{\Delta t\to 0}\sum_{k=0}^{N-1}\Delta t\,\frac{\Delta\eta_k^2}{\Delta t}\,g^2\left(x_k\right)\,h(x_k)\,. \end{aligned} \tag{7.28}$$

Interestingly, in the L^2-norm sense, the statistical properties of $\mathcal{O}_2$ and $\mathcal{O}_2'$ defined by

$$\mathcal{O}_2' = \lim_{\Delta t\to 0}\sum_{k=0}^{N-1}\Delta t\,g^2\left(x_k\right)\,h(x_k)\,, \tag{7.29}$$

are the same, as can be checked by a direct computation

$$\begin{aligned}&\lim_{\Delta t\to 0}\left\langle\left(\sum_{k=0}^{N-1}\Delta t\,g^2\left(x_k\right)\,h(x_k)\left[1-\frac{\Delta\eta_k^2}{\Delta t}\right]\right)^2\right\rangle\,,\\ &= \lim_{\Delta t\to 0}\left\langle\sum_{k,k'=0}^{N-1}\Delta t^2\,g^2\left(x_k\right)g^2\left(x_k'\right)\,h(x_k)h(x_k')\left[1-\frac{\Delta\eta_k^2}{\Delta t}\right]\left[1-\frac{\Delta\eta_k'^2}{\Delta t}\right]\right\rangle\,,\\ &= \lim_{\Delta t\to 0}\left\langle\sum_{k=0}^{N-1}\Delta t^2\,g^4\left(x_k\right)\,h^2(x_k)\left[1-\frac{\Delta\eta_k^2}{\Delta t}\right]^2\right\rangle = 0\,. \end{aligned} \tag{7.30}$$

This justifies the substitution relation

$$\Delta x_k^2 := g^2(x_k)\Delta t\,, \tag{7.31}$$

or equivalently,

$$\Delta\eta_k^2 := \Delta t\,. \tag{7.32}$$

Accordingly, one can show following the same reasoning that

$$\Delta x_k^4 = 3g^4(x_k)\Delta t^2\,. \tag{7.33}$$

This substitution rules allows one for example to express $\mathcal{O}_1$ α'-discretized observables in terms of $\mathcal{O}_1$ α''-discretized ones as,

$$\begin{aligned}\mathcal{O}_1 &\overset{\alpha'}{=} \int_0^t \dot{x}\,h(x(s))\,\mathrm{d}s_,,\\ &= \lim_{\Delta t\to 0}\sum_{k=0}^{N-1}\Delta t\,\frac{\Delta x_k}{\Delta t}\,h\left(x_k+\alpha'\Delta x_k\right)\,,\\ &= \lim_{\Delta t\to 0}\sum_{k=0}^{N-1}\left[\Delta t\,\frac{\Delta x_k}{\Delta t}\,\left(h\left(x_k+\alpha''\Delta x_k\right)+\left(\alpha'-\alpha''\right)h'(x_k)\Delta x_k\right)+O(\Delta t^{3/2})\right]\,,\\ &\overset{\alpha''}{:=} \int_0^t \dot{x}\,h(x(s))\,\mathrm{d}s+\left(\alpha'-\alpha''\right)\int_0^t g^2(x(s))h(x(s))\,\mathrm{d}s\,. \end{aligned} \tag{7.34}$$

As a final comment, we stress that even though the point at which the function h is evaluated is irrelevant to determine the observable $\mathcal{O}_2$ in the $\Delta t \to 0$ limit, finite Δt corrections to $\mathcal{O}_2$, if needed (and they will be needed when we address path integration), depend on the value at which h is evaluated. Equivalently, this issue surfaces if we want to regularize integrals of the type $\int_0^t \mathrm{d}s \dot{x}^2 h(x(s))$. Indeed, as pointed out previously, it is clear that any observable of the form

$$\mathcal{O}_3 = \sum_k \Delta t \, h(x_k) \left(\frac{\Delta x_k^2}{\Delta t^2} \right) , \tag{7.35}$$

only has infinite moments when x_k is sampled from the companion process associated to Eq. (7.20) in the $\Delta t \to 0$ limit. Suppose, however, that our interest goes to the observable defined by

$$\mathcal{O}_3' = \sum_k \Delta t \, h(\bar{x}_k) \left(\frac{\Delta x_k^2}{\Delta t^2} \right) - \sum_k \Delta t \, h(x_k) \left(\frac{\Delta x_k^2}{\Delta t^2} \right) , \tag{7.36}$$

where $\bar{x}_k$ is again a function of x_k and x_{k+1} and where the diverging part in the continuous limit has been substracted. Owing to the scaling of Δx_k, namely,

$$\Delta x_k \sim \sqrt{\Delta t} \, , \tag{7.37}$$

one needs to know $h(\bar{x}_k)$ up to order $O(\Delta t)$ in order to collect all finite terms in the continuous time limit. This is in stark contrast with standard Itō or Stratonovich integrals (or any integral of the type $\mathcal{O}_1$) in which the function h needs to be known up to order $O(\sqrt{\Delta t})$ only. In particular, observables such as O_3 (that we will encounter when dealing with path integrals) are sensitive to higher-order terms in the discretization. To render this property more explicit, we introduce an α, β discretization scheme defined by

$$\bar{x}_k = x_k + \alpha \Delta x_k + \beta \Delta x_k^2 \, , \tag{7.38}$$

which gives

$$\begin{aligned}
\mathcal{O}_3' &= \sum_k \Delta t \, \left(h(x_k + \alpha \Delta x_k + \beta \Delta x_k^2) - h(x_k) \right) \left(\frac{\Delta x_k^2}{\Delta t^2} \right) , \\
&= \sum_k \Delta t \, \left(\alpha \, \Delta x_k \, h'(x_k) + \left(\beta h''(x_k) + \frac{\alpha^2}{2} h''(x_k) \right) \Delta x_k^2 \right) \left(\frac{\Delta x_k^2}{\Delta t^2} \right) , \\
&= \sum_k \alpha h'(x_k) \frac{\Delta x_k^3}{\Delta t} + \sum_k \left(\beta h'(x_k) + \frac{\alpha^2}{2} h''(x_k) \right) \frac{\Delta x_k^4}{\Delta t^2} \Delta t \, , \\
&:= \sum_k \alpha h'(x_k) \frac{\Delta x_k^3}{\Delta t} + 3 \sum_k g^4(x_k) \left(\beta h'(x_k) + \frac{\alpha^2}{2} h''(x_k) \right) \Delta t \, ,
\end{aligned} \tag{7.39}$$

where the last line is valid in the $\Delta t \to 0$ limit. A last comment is in order: stochastic calculus with white, yet non-Gaussian, noise η, is another instance in which higher order discretization schemes are required [167, 38, 37, 110, 61]. We shall say more on this in the sections to come.

The goal of this subsection was to provide the reader with a review of stochastic integration. We have discussed four types of integral observables, $\mathcal{O}_0$, $\mathcal{O}_1$, $\mathcal{O}_2$ and $\mathcal{O}_3$ that will each appear in the exponential weight of path integrals. We now turn to the differentiation of a stochastic path.

7.1.3 Differentiation

The other operation that we wish to extend to stochastic paths is differentiation. Going back to our intial equation

$$\frac{\mathrm{d}x}{\mathrm{d}t} \overset{\alpha}{=} f(x) + g(x)\eta(t)\,, \tag{7.40}$$

we now define the observable $u(t) = U(x(t))$ where U is some smooth invertible function. The discrete time companion x process evolves according to

$$\Delta x = f(x)\Delta t + g\left(x + \alpha\Delta x\right)\Delta\eta\,. \tag{7.41}$$

We therefore obtain, in discrete time, for the new variable u

$$\begin{aligned}
\Delta u &= u(t+\Delta t) - u(t) = U(x+\Delta x) - U(x)\,,\\
&= \Delta x U'(x) + \frac{1}{2}\alpha\Delta x^2 U''(x) + O\left(\Delta t^{3/2}\right)\,,\\
&= f(x)U'(x)\Delta t + \frac{1}{2}g^2(x)U''(x)\Delta\eta^2 + g(x+\alpha\Delta x)U'(x)\Delta\eta + O\left(\Delta t^{3/2}\right)\,,\\
&= f(x)U'(x)\Delta t + \left(\frac{1}{2}-\alpha\right)g^2(x)U''(x)\Delta\eta^2 + g(x+\alpha\Delta x)U'(x+\alpha\Delta x)\Delta\eta + O\left(\Delta t^{3/2}\right)\,.
\end{aligned} \tag{7.42}$$

We note that

$$x = U^{-1}(u)\,, \tag{7.43}$$

and that

$$x + \alpha\Delta x = U^{-1}(u + \alpha\Delta u) + O(\Delta t)\,. \tag{7.44}$$

Equation (7.42) thus becomes

$$\begin{aligned}
\Delta u &= F(u)\Delta t + \left(\frac{1}{2}-\alpha\right)g^2(U^{-1}(u))U''(U^{-1}(u))\Delta\eta^2 + G(u+\alpha\Delta u)\Delta\eta + O\left(\Delta t^{3/2}\right)\,,\\
&:= F(u)\Delta t + \left(\frac{1}{2}-\alpha\right)g^2(U^{-1}(u))U''(U^{-1}(u))\Delta t + G(u+\alpha\Delta u)\Delta\eta\,,
\end{aligned} \tag{7.45}$$

with

$$\begin{aligned}
F &= (fU')\circ U^{-1}\,,\\
G &= (gU')\circ U^{-1}\,,
\end{aligned} \tag{7.46}$$

and where the $:=$ notation expresses that the two discrete time processes generate the same process in the limit $\Delta t \to 0$ (this is not a pointwise equality). This can be established either by computing the Kramers-Moyal expansion of the u process and determining the Fokker-Planck equation associated with Eq. (7.45) in the continuous-time limit, or by resorting to the substitution rule Eq. (7.31). In the continuous time limit, we thus arrive at

$$\begin{aligned}\frac{\mathrm{d}u}{\mathrm{d}t} &\overset{\alpha}{=} U' \frac{\mathrm{d}x}{\mathrm{d}t} + \left(\frac{1}{2} - \alpha\right) g^2(U^{-1}(u))U''(U^{-1}(u))\,, \\ &\overset{\alpha}{=} F(u) + \left(\frac{1}{2} - \alpha\right) g^2(U^{-1}(u))U''(U^{-1}(u)) + G(u)\eta(t)\,. \end{aligned} \tag{7.47}$$

The above formula is at the core of stochastic calculus as it explicitely shows how working with paths generated by Eq. (7.20) modifies the chain rule of ordinary differential calculus. For $\alpha = 0$, Eq. (7.47) is the celebrated Itō's lemma. Note, however, that for $\alpha = 1/2$ the standard chain rule holds. This is one of the most important assets of Stratonovich discretized stochastic differential equations. An interesting consequence of formula Eq. (7.47) is that it is always possible (for a one-dimensional process) to perform a nonlinear change of variable so as to turn a process with multiplicative noise into a process with additive one. This is indeed easily seen if one starts from a Stratonovich discretized process (from Eq. (7.19) we know that any α-discretized stochastic differential equation can be turned into a Stratonovich discretized one) of the form

$$\frac{\mathrm{d}x}{\mathrm{d}t} \overset{1/2}{=} f(x) + g(x)\eta(t)\,. \tag{7.48}$$

Assuming g is a non vanishing function of x, we choose U to be such that

$$(gU') \circ U^{-1} = \mathrm{Id}\,, \tag{7.49}$$

namely we choose

$$U(x) = \exp\left(\int_{x_0}^{x} \frac{1}{g(x')}\mathrm{d}x'\right), \tag{7.50}$$

for some x_0. We therefore obtain for $u(t) = U(x(t))$,

$$\frac{\mathrm{d}u}{\mathrm{d}t} = F(u) + \eta(t)\,. \tag{7.51}$$

which has additive noise. The conversion of a multiplicative noise process into an additive noise process is a peculiarity of processes living on the real axis which does not in general extend to higher dimensions.

7.1.4 What changes in higher dimensions

We now introduce a d-dimensional stochastic process $\mathbf{x}(t)$ with components x^μ for $\mu \in [\![1, d]\!]$. Einstein summation convention is hereafter used throughout. The time evolution of $\mathbf{x}(t)$ is governed by

$$\frac{\mathrm{d}x^\mu}{\mathrm{d}t} \overset{\mathfrak{d}}{=} f^\mu(\mathbf{x}) + g^{\mu i}(\mathbf{x})\eta_i(t)\,, \tag{7.52}$$

where the $\mathfrak{d}$ accounts for the underlying discretization scheme and where the index i run from 1 to n with the n-dimensional Gaussian white noise $\boldsymbol{\eta}(t)$ having correlations

$$\langle \eta_i(t) \rangle = 0\,, \qquad\qquad \langle \eta_i(t)\eta_j(t') \rangle = \delta_{ij}\delta(t-t')\,. \tag{7.53}$$

In the α-discretization scheme, we have

$$\Delta x_k^\mu = x^\mu((k+1)\Delta t) - x^\mu(k\Delta t) = f^\mu(\mathbf{x}_k) + g^{\mu i}\left(\mathbf{x}_k + \alpha\Delta\mathbf{x}_k\right)\Delta\eta_{i,k}\,, \tag{7.54}$$

where the noise correlations are such that

$$\langle \Delta\eta_{i,k} \rangle = 0\,, \qquad\qquad \langle \Delta\eta_{i,k}\Delta\eta_{j,k'} \rangle = \Delta t\,\delta_{ij}\delta_{kk'}\,, \tag{7.55}$$

We furthermore introduce the $d \times d$ matrix $\omega^{\mu\nu}(x)$ defined by

$$\omega^{\mu\nu}(x) = \left(g(x)\,g(x)^T\right)^{\mu\nu}\,. \tag{7.56}$$

The substitution rules Eq. (7.31)- (7.33) are generalized as follows

$$\Delta x^\mu \Delta x^\nu := \omega^{\mu\nu}(x)\Delta t\,, \qquad\qquad \Delta\eta_i\Delta\eta_j := \Delta t\delta_{ij}\,, \tag{7.57}$$

and

$$\Delta x^\mu \Delta x^\nu \Delta x^\rho \Delta x^\sigma := \left(\omega^{\mu\nu}(x)\omega^{\rho\sigma}(x) + \omega^{\mu\rho}(x)\omega^{\nu\sigma}(x) + \omega^{\mu\sigma}(x)\omega^{\nu\rho}(x)\right)\Delta t^2\,. \tag{7.58}$$

From these rules, it is possible to derive the equivalence rules between α-discretized and α'-discretized stochastic differential equations, which reads

$$\begin{aligned}\frac{\mathrm{d}x^\mu}{\mathrm{d}t} &\overset{\alpha}{=} f^\mu + g^{\mu i}\eta_i(t)\,,\\ &\overset{\alpha'}{=} f^\mu + (\alpha-\alpha')\sum_i g^{\nu i}\,\partial_\nu g^{\mu i} + g^{\mu i}\eta_i(t)\,.\end{aligned} \tag{7.59}$$

Let us now investigate the issue of differentiation and changes of variables. Let $\mathbf{U} : \mathbb{R}^d \to \mathbb{R}^d$ be an invertible transformation ($\mathbf{U}$ is a diffeomorphism) and define the process $\mathbf{u}(t) = \mathbf{U}(\mathbf{x}(t))$. Assuming that $\mathbf{x}$ evolves according to Eq. (7.52) understood as α-discretized, we obtain

$$\frac{\mathrm{d}u^\mu}{\mathrm{d}t} \overset{\alpha}{=} \left[f^\rho\,\partial_\rho U^\mu\right]\circ\mathbf{U}^{-1}(u) + \left(\alpha - \frac{1}{2}\right)\left[\omega^{\rho\sigma}\,\partial_\rho\partial_\sigma U^\mu\right]\circ\mathbf{U}^{-1}(u) + \left[g^{\rho i}\,\partial_\rho U^\mu\right]\circ\mathbf{U}^{-1}(u)\,\eta_i(t)\,. \tag{7.60}$$

Therefore, as for one-dimensional systems, the rules of differential calculus hold in the Stratonovich discretization $\alpha = 1/2$. In such a discretization, Eq. (7.60) shows that under a change of coordinates (that is, a rerametrization of the variables describing the system), f^μ and $g^{\mu i}$ transform as contravariant vectors do in Riemann geometry regarding their μ index. Accordingly, $\omega^{\mu\nu}$ transforms as a rank-2 contravariant tensor. We will therefore borrow some of the language of Riemannian geometry to efficiently study transformations under a reparametrization of coordinates. Let us first write the Fokker-Planck equation associated to Eq. (7.52) in the Stratonovich discretization. It is given by

$$\partial_t P = -\partial_\mu\left(f^\mu + \frac{1}{2}\sum_i g^{\nu i}\,\partial_\nu g^{\mu i}\right)P + \frac{1}{2}\partial_\mu\partial_\nu\left(\omega^{\mu\nu}P\right)\,. \tag{7.61}$$

It is clear that $P(\mathbf{x},t)$ is not invariant under a change of coordinates. Indeed, the simplest scalar invariant object one can construct is the infinitesimal probability of finding the system in a box of size $\mathrm{d}^d x$ around $\mathbf{x}$ at time t that writes $\mathrm{d}^d x\, P(\mathbf{x},t)$. In what follows, we construct a scalar invariant probability density along the footsteps of [86]. This construction renders the connection to Riemannian geometry more explicit and it will serve as our starting point for constructing covariant path integral representations of stochastic differential equations. We first assume that $\omega^{\mu\nu}(\mathbf{x})$ is invertible. This requires, in particular, that $n \geq d$ (where n is the dimension of the noise space). Following standard conventions, we denote by $\omega_{\mu\nu}(\mathbf{x})$ the inverse of $\omega^{\mu\nu}(\mathbf{x})$ ($\omega^{\mu\rho}\omega_{\rho\nu} = \delta^\mu_\rho$). The matrix $\omega_{\mu\nu}(\mathbf{x})$ is symmetric, positive-definite and transforms as a rank-2 convariant tensor under a change of coordinates. It can thus be promoted as the metric tensor of a d-dimensional Riemann space. Denoting by $\omega(\mathbf{x})$ the determinant of $\omega_{\mu\nu}(\mathbf{x})$, we construct the invariant volume element

$$\mathrm{d}^d\mathbf{x}\sqrt{\omega(\mathbf{x})}\,, \tag{7.62}$$

and we introduce

$$K(\mathbf{x},t) = \frac{P(\mathbf{x},t)}{\sqrt{\omega(\mathbf{x})}}\,, \tag{7.63}$$

which is thus invariant under a change of coordinates. It can be shown [86] that $K(\mathbf{x},t)$ evolves according to the manifestly covariant equation

$$\partial_t K = -\nabla_\mu\left(h^\mu K\right) + \frac{1}{2}\nabla_\mu\nabla_\nu\left(\omega^{\mu\nu}K\right)\,, \tag{7.64}$$

where ∇_μ is the covariant derivative associated with the metric $\omega_{\mu\nu}$. While $\nabla_\mu = \partial_\mu$ when acting on a scalar, when applied to a contravariant vector A^ν, it acts as

$$\nabla_\mu A^\nu = \partial_\mu A^\nu + \Gamma^\rho_{\mu\nu}A_\rho\,, \tag{7.65}$$

and when applied to a contravariant rank-2 tensor $T^{\rho\sigma}$, it acts as

$$\nabla_\mu T^{\rho\sigma} = \partial_\mu T^{\rho\sigma} + \Gamma^\rho_{\mu\nu}T^{\nu\sigma} + \Gamma^\sigma_{\mu\nu}T^{\rho\nu}\,, \tag{7.66}$$

where $\Gamma^\mu_{\rho\sigma}$ is the corresponding Christoffel symbol,

$$\Gamma^\mu_{\rho\sigma} = \frac{1}{2}\omega^{\mu\nu}\left(\partial_\rho\omega_{\nu\sigma} + \partial_\sigma\omega_{\nu\rho} - \partial_\nu\omega_{\rho\sigma}\right)\,. \tag{7.67}$$

In addition, the vector h^μ appearing in Eq. (7.64) is defined by

$$h^\mu = f^\mu - \frac{1}{2}\,\Gamma^\rho_{\nu\rho}\omega^{\nu\mu} - \frac{1}{2}\partial_\nu g^{\nu i}g^{\mu j}\,\delta_{ij}\,, \tag{7.68}$$

which can be shown to transform as a vector under a change of coordinates. We also introduce, as it will prove useful in many parts of this work, the Ricci scalar curvature associated to the $\omega_{\mu\nu}$ metric

$$R = \omega^{\mu\nu}\left(\partial_\eta\Gamma^\eta_{\mu\nu} - \partial_\mu\Gamma^\eta_{\eta\nu} + \Gamma^\eta_{\mu\nu}\Gamma^\rho_{\eta\rho} - \Gamma^\eta_{\mu\rho}\Gamma^\rho_{\eta\nu}\right)\,. \tag{7.69}$$

Note that in this language, stochastic dynamics with additive noise is associated to a flat space and a null Ricci curvature. Therefore, quite unlike the one-dimensional case, a multi-dimensional stochastic process with a nonzero Ricci curvature cannot be mapped onto one with an additive form by a change of variables. However, similarly to the one-dimensional case, it is possible to generalize the α, β discretization scheme to higher space dimensions. This is done by introducing a three index quantity $M^{\mu}_{\rho\sigma}$,

$$\bar{x}^{\mu}_{k} = x^{\mu}_{k} + \alpha \Delta x^{\mu}_{k} + M^{\mu}_{\rho\sigma} \Delta x^{\rho} \Delta x^{\sigma} \, . \tag{7.70}$$

The stage is now set for investigating the additional subtleties that path integrals conceal.

7.2 Path integral representation of stochastic processes

This section reviews the standard construction of path integral representations for the transition probability of stochastic differential equations with Gaussian white noise. The simpler example of a one-dimensional process with additive noise is treated first. In line with the points raised in Sec. 7.1.2 for stochastic integrals, we show that one can resort to different discretizations to construct the path integral. We also recall the connection between the question of discretization of path integrals and the so-called operator ordering problem in quantum mechanics. We then turn to the more involved case of multi-dimensional processes with multiplicative noise for which we introduce the notion of covariant path integral representation and contruct explicitely the path integral in the α-discretization. At the end of this section, we show that the rules of differential calculus, while known to hold at the level of Stratonovich discretized stochastic differential equations, are not adequate for changing variables at the level of α-discretized continuous-time path integrals, including the Stratonovich case $\alpha = 1/2$.

7.2.1 The one-dimensional additive case

We start by implementing our program on the example of a one-dimensional stochastic process with additive noise

$$\frac{\mathrm{d}x}{\mathrm{d}t} = f + \eta(t) \, , \tag{7.71}$$

Let $\mathbb{P}\left[x, t_{obs}; x_0, t_0\right]$ be the propagator associated to Eq. (7.71), *i.e.* the probability to be at x at time t_{obs} given that the motion starts at x_0 at time t_0. We divide the interval $[t_0, t_{obs}]$ into N slices and we introduce the intermediate times $t_k = t_0 + k\Delta t$ with $\Delta t = (t_{obs} - t_0)/N$ and $t_N = t_{obs}$, $k = 0, \ldots, N$. We introduce the discrete-time companion process with time step Δt associated to Eq. (7.71),

$$\Delta x_k = f(x_k)\Delta t + \Delta \eta_k \, , \tag{7.72}$$

and define $\mathbb{P}_{\Delta t}\left[x, t_{obs}; x_0, t_0\right]$ the propagator associated to Eq. (7.72). We first use the equality of the two processes described above in the limit $\Delta t \to 0$ to state that:

$$\mathbb{P}\left[x, t_{obs}; x_0, t_0\right] = \lim_{N \to +\infty} \mathbb{P}_{\Delta t}\left[x, t_{obs}; x_0, t_0\right] \, . \tag{7.73}$$

Relying on the fact that the processes described here are Markovian, we use the Chapman-Kolmogorov equation over the intermediate time windows $[t_k, t_{k+1}]$ to obtain:

$$\mathbb{P}\left[x, t_{obs}; x_0, t_0\right] = \lim_{N\to+\infty} \int \prod_{k=1}^{N-1} \mathrm{d}x_k \prod_{k=0}^{N-1} \mathbb{P}_{\Delta t}\left[x_{k+1}, t_{k+1}; x_k, t_k\right] \ . \tag{7.74}$$

In Eq. (7.72), the $\Delta\eta_k$ are independent and identically distributed random variables with a normal probability density

$$P\left(\Delta\eta_k\right) = \frac{1}{\sqrt{2\pi\Delta t}} \mathrm{e}^{-\frac{\Delta\eta_k^2}{2\Delta t}} \ , \tag{7.75}$$

so that the one-step propagator is obtained as

$$\mathbb{P}_{\Delta t}\left[x_{k+1}, t_{k+1}; x_k, t_k\right] = \frac{1}{\sqrt{2\pi\Delta t}} \exp\left(-\frac{1}{2\Delta t}\left(\Delta x_k - f(x_k)\Delta t\right)^2\right) \ . \tag{7.76}$$

This result leads to writing the finite time propagator as:

$$\mathbb{P}\left[x, t; x_0, t_0\right] = \lim_{N\to+\infty} \frac{1}{\sqrt{2\pi\Delta t}} \int \prod_{k=1}^{N-1} \left(\frac{\mathrm{d}x_k}{\sqrt{2\pi\Delta t}}\right) \exp\left(-\frac{\Delta t}{2} \sum_{k=0}^{N-1} \left(\frac{\Delta x_k}{\Delta t} - f(x_k)\right)^2\right) \ , \tag{7.77}$$

$$= \int_{\mathcal{C}(x_0,t_0;x,t_{obs})} \mathcal{D}x \, \mathrm{e}^{-\mathcal{S}[x(t)]} \ , \tag{7.78}$$

In Eq. (7.78), the meaning of the formal continuous time writing is inferred from the limiting discrete-time expression where the path measure is expressed as:

$$\mathcal{D}x = \lim_{N\to+\infty} \frac{1}{\sqrt{2\pi\Delta t}} \prod_{k=1}^{N-1} \left(\frac{\mathrm{d}x_k}{\sqrt{2\pi\Delta t}}\right) \ , \tag{7.79}$$

and the action $\mathcal{S}[x(s)]$ as:

$$\mathcal{S}[x(s)] \overset{0}{=} \frac{1}{2} \int_{t_0}^{t_{obs}} \mathrm{d}t \, \left(\frac{\mathrm{d}x}{\mathrm{d}t} - f(x)\right)^2 \ , \tag{7.80}$$

where the superscript 0 above the equal sign is meant to specify the underlying time discretization. The notation $\mathcal{C}(x_0, t_0; x, t_{obs})$ appearing in the path integral sign in Eq. (7.78) refers to the set of continuous paths with appropriate boundary conditions.

Changing discretization

Exactly in the same way as the same integral observable can be expressed using different discretizations and can thus correspond to visually different continuous time expressions (see *e.g.* Eq. (7.34)), we wish to rewrite the path integral weight associated with the process in Eq. (7.71) not only as the limit of an Itō discretized sum but as the limit of an α-discretized one with $\alpha \in [0, 1]$. This will concretely illustrate that the underlying discretization scheme

must be prescribed in order to work with path integrals in an unambiguous way (see [94] for a review of the handling of path integrals in different discretizations). We start from the expression of the infinitesimal propagator Eq. (7.76) obtained in the previous section which we rewrite so as to evaluate f at $x + \alpha\Delta x$, rather than at x,

$$\begin{aligned}&\mathbb{P}_{\Delta t}\left[x+\Delta x, t+\Delta t; x, t\right]\\&= \frac{1}{\sqrt{2\pi\Delta t}} \exp\left(-\frac{\Delta t}{2}\left[\left(\frac{\Delta x}{\Delta t} - f(x+\alpha\Delta x)\right)^2 + 2\alpha\frac{\Delta x^2}{\Delta t} f'\left(x+\alpha\Delta x\right)\right]\right),\end{aligned} \tag{7.81}$$

up to negligible $O(\Delta t^{3/2})$ corrections in the exponential. Hence we obtain the following expression of the finite time propagator:

$$\begin{aligned}\mathbb{P}\left[x, t_{obs}; x_0, t_0\right] = \lim_{N\to+\infty} \frac{1}{\sqrt{2\pi\Delta t}} \int \prod_{k=1}^{N-1} \frac{\mathrm{d}x_k}{\sqrt{2\pi\Delta t}}\\ \exp\left(-\frac{\Delta t}{2}\left[\sum_{k=0}^{N-1}\left(\frac{x_{k+1}-x_k}{\Delta t} - f\left(x_k+\alpha\Delta x_k\right)\right)^2 + 2\alpha\frac{\Delta x_k^2}{\Delta t} f'\left(x_k+\alpha\Delta x_k\right)\right]\right),\end{aligned} \tag{7.82}$$

Isolating the kinetic term $\sum_{k=0}^{N-1}\left(\Delta x_k/\Delta t\right)^2$, we can rewrite the above equation as:

$$\mathbb{P}\left[x, t_{obs}; x_0, t_0\right] = \lim_{N\to+\infty} \left\langle \exp\left(-\frac{\Delta t}{2}\sum_{k=0}^{N-1} 2\alpha\frac{\Delta x_k^2}{\Delta t} f'\left(x_k+\alpha\Delta x_k\right) + \ldots\right)\right\rangle, \tag{7.83}$$

where the above average is taken with respect to free Brownian motion. We are now in position to use the substitution rule of Eq. (7.31) to write:

$$\begin{aligned}\mathbb{P}\left[x, t_{obs}; x_0, t_0\right] &= \lim_{N\to+\infty} \frac{1}{\sqrt{2\pi\Delta t}} \int \prod_{k=1}^{N-1}\left(\frac{\mathrm{d}x_k}{\sqrt{2\pi\Delta t}}\right)\\ &\qquad \exp\left(-\frac{\Delta t}{2}\left[\sum_{k=0}^{N-1}\left(\frac{\Delta x_k}{\Delta t} - f\left(x_k+\alpha\Delta x_k\right)\right)^2 + 2\alpha f'\left(x_k\right)\right]\right), \qquad (7.84)\\ &\overset{\alpha}{=} \int_{\mathcal{C}(x_0,t_0;x,t)} \mathcal{D}x\ \exp\left(-\frac{1}{2}\int_{t_0}^{t}\left(\dot{x} - f(x)\right)^2 + 2\alpha f'(x)\right),\end{aligned}$$

where the superscript α in the continuous writing stands for α-discretized integral.

Path integrals and operator ordering

For the sake of completeness, we present here another derivation of the path integral representation of the transition probability $\mathbb{P}\left[x, t_{obs}; x_0, t_0\right]$. This approach, which uses the Fokker-Planck equation as its starting point, instead of the Langevin equation, emphasizes the equivalence between the issue of the discretization of path integrals and the operator ordering problem in quantum mechanics. Using the standard momentum operator $\hat{p} = -i\frac{\mathrm{d}}{\mathrm{d}x}$ of quantum mechanics, we write the Fokker-Planck equation associated to Eq. (7.71) as

$$\partial_t P = -\hat{\mathrm{H}}_{FP} P\,, \tag{7.85}$$

with $\hat{\mathrm{H}}_{FP} = \frac{1}{2}\hat{p}^2 + i\hat{p}\hat{f}$. Introducing the usual position eigenvectors $|x\rangle$, the infinitesimal propagator then reads

$$\mathbb{P}\left[x+\Delta x, t+\Delta t; x, t\right] = \langle x+\Delta x| \, \mathrm{e}^{-\Delta t\left(\hat{p}^2/2 + i\hat{p}\hat{f}\right)} \, |x\rangle \ , \tag{7.86}$$

$$= \langle x+\Delta x| \, \mathrm{e}^{-\Delta t/2\hat{p}^2/2} \mathrm{e}^{-i\Delta t\hat{p}\hat{f}} \, |x\rangle \ , \tag{7.87}$$

where the last line is obtained using the first order of the Baker-Campbell-Hausdorff formula. In Sec. 8.3.1, we will prove that for any function G

$$\left(\exp\left(f(x)\Delta t\frac{\mathrm{d}}{\mathrm{d}x}\right)G\right)(x_0) = G\left(\exp\left(f(x)\Delta t\frac{\mathrm{d}}{\mathrm{d}x}\right)x_0\right) \ , \tag{7.88}$$

which in the present case translates into,

$$\exp\left(-i\hat{p}\hat{f}\Delta t\right)|x_0\rangle = \left|\exp\left(f(x)\Delta t\frac{\mathrm{d}}{\mathrm{d}x}\right)x_0\right\rangle = \left|x_0 + f(x_0)\Delta t + \mathcal{O}(\Delta t^2)\right\rangle \ . \tag{7.89}$$

We therefore obtain

$$\mathbb{P}\left[x+\Delta x, t+\Delta t; x, t\right] \simeq \langle x+\Delta x| \, \mathrm{e}^{-\Delta t/2\hat{p}^2} \, |x + f(x)\Delta t + ...\rangle \ , \tag{7.90}$$

$$\simeq \frac{1}{\sqrt{2\pi\Delta t}} \exp\left(-\frac{\Delta t}{2}\left(\frac{\Delta x}{\Delta t} - f(x)\right)^2\right) \ . \tag{7.91}$$

This expresses that a $\hat{p}\hat{x}$ or normal ordering of the Hamiltonian naturally leads to an Itō discretized path integral. We could nevertheless choose to order it differently, following for instance an α ordering, as in the following:

$$\begin{aligned}
&\mathbb{P}\left[x+\Delta x, t+\Delta t; x, t\right] = \langle x+\Delta x| \exp\left(-\frac{\hat{p}^2}{2}\Delta t - i\hat{p}\hat{f}\Delta t\right)|x\rangle \ , \\
&= \langle x+\Delta x| \exp\left(-\frac{\hat{p}^2}{2}\Delta t - i\left((1-\alpha)\hat{p}\hat{f} + \alpha\hat{f}\hat{p}\right)\Delta t - \alpha\hat{f}'\Delta t\right)|x\rangle \ , \\
&= \exp\left(-\alpha f'(x)\Delta t\right)\langle x+\Delta x| \exp\left(-i\alpha\Delta t\hat{f}\hat{p}\right)\exp\left(-\frac{\hat{p}^2}{2}\Delta t\right)\exp\left(-i(1-\alpha)\Delta t\hat{p}\hat{f}\right)|x\rangle \ , \\
&= \exp\left(-\alpha f'(x)\Delta t\right)\langle x+\Delta x - \alpha\Delta t f(x+\Delta x) + ...| \exp\left(-\frac{\hat{p}^2}{2}\Delta t\right)|x + (1-\alpha)\Delta t f(x) + ...\rangle \ , \\
&= \frac{1}{\sqrt{2\pi\Delta t}} \exp\left(-\alpha f'(x)\Delta t - \frac{\Delta t}{2}\left(\frac{\Delta x}{\Delta t} - f\left(x+\alpha\Delta x\right)\right)^2\right) \ .
\end{aligned} \tag{7.92}$$

Thus, the α ordering of the operator $\hat{p}\hat{f}$ naturally leads to an α-discretized path integral. In particular, the well known Weyl ordering corresponds to $\alpha = 1/2$ and leads to a Stratonovich-discretized path integral.

7.2.2 Multidimensional processes

We now turn to the more general case of multidimensional processes with multiplicative noise

$$\frac{\mathrm{d}x^\mu}{\mathrm{d}t} \overset{1/2}{=} f^\mu(\mathbf{x}) + g^{\mu i}(\mathbf{x})\eta_i(t) \, . \tag{7.93}$$

Without loss of generality, equation (7.93) is understood as Stratonovich-discretized. Furthermore, the matrix $g^{\mu i}(\mathbf{x})$ is hereafter assumed to be invertible of inverse $g_{i\mu}(\mathbf{x})$. This imposes the necessary condition $d = n$. In the same vein as the presentation above, we introduce the propagator $\mathbb{P}[\mathbf{x}, t_{obs}; \mathbf{x}_0, t_0]$ of Eq. (7.93) and its discrete-time companion process defined with a time step of duration $\Delta t = (t_{obs} - t_0)/N$, $N \in \mathbb{N}$. Accordingly we introduce the scalar invariant propagators of the original process

$$K[\mathbf{x}, t_{obs}; \mathbf{x}_0, t_0] = \frac{\mathbb{P}[\mathbf{x}, t_{obs}; \mathbf{x}_0, t_0]}{\sqrt{\omega(\mathbf{x})}}\,, \tag{7.94}$$

and of the companion process

$$K_{\Delta t}[\mathbf{x}, t_{obs}; \mathbf{x}_0, t_0] = \frac{\mathbb{P}_{\Delta t}[\mathbf{x}, t_{obs}; \mathbf{x}_0, t_0]\,.}{\sqrt{\omega(\mathbf{x})}} \tag{7.95}$$

We then write a time-sliced expression for the propagators:

$$\mathbb{P}[\mathbf{x}, t_{obs}; \mathbf{x}_0, t_0] = \lim_{N\to+\infty} \int \prod_{k=1}^{N-1} \mathrm{d}\mathbf{x}_k \prod_{k=0}^{N-1} \mathbb{P}_{\Delta t}[\mathbf{x}_{k+1}, t_{k+1}; \mathbf{x}_k, t_k]\,, \tag{7.96}$$

$$\Leftrightarrow K[\mathbf{x}, t_{obs}; \mathbf{x}_0, t_0] = \lim_{N\to+\infty} \int \prod_{k=1}^{N-1} \left\{ \mathrm{d}\mathbf{x}_k \sqrt{\omega(\mathbf{x}_k)} \right\} \prod_{k=0}^{N-1} \left\{ \frac{\mathbb{P}_{\Delta t}[\mathbf{x}_{k+1}, t_{k+1}; \mathbf{x}_k, t_k]}{\sqrt{\omega(\mathbf{x}_{k+1})}} \right\}\,, \tag{7.97}$$

$$= \lim_{N\to+\infty} \int \prod_{k=1}^{N-1} \left\{ \mathrm{d}\mathbf{x}_k \sqrt{\omega(\mathbf{x}_k)} \right\} \prod_{k=0}^{N-1} K_{\Delta t}[\mathbf{x}_{k+1}, t_{k+1}; \mathbf{x}_k, t_k]\,,$$

$$= \int_{\mathcal{C}(\mathbf{x}_0, t_0; \mathbf{x}, t_{obs})} \mathcal{D}\mathbf{x}\ \mathrm{e}^{-\mathcal{S}[\mathbf{x}(t)]}\,. \tag{7.98}$$

In the above expression, the meaning of the formal continuous-time writing is inferred from the limiting discrete time expression with the path measure

$$\mathcal{D}\mathbf{x} = \lim_{N\to+\infty} \left(\frac{1}{\sqrt{2\pi\Delta t}} \right)^d \int \prod_{k=1}^{N-1} \left\{ \frac{\mathrm{d}\mathbf{x}_k \sqrt{\omega(\mathbf{x}_k)}}{\sqrt{2\pi\Delta t}^{\,d}} \right\}\,, \tag{7.99}$$

and the action

$$\mathrm{e}^{-\mathcal{S}[\mathbf{x}(t)]} = \lim_{N\to+\infty} \prod_{k=0}^{N-1} (2\pi\Delta t)^{\frac{d}{2}}\ K_{\Delta t}[\mathbf{x}_{k+1}, t_{k+1}; \mathbf{x}_k, t_k]\,, \tag{7.100}$$

Note that different definitions of $\mathcal{D}x$ and $\mathcal{S}[x(s)]$ could give the same result in the $\Delta t \to 0$ limit, only the product of the two being prescribed. It is thus not uncommon in the literature to find different discretization of the path measure (see *e.g.* [126, 164]. This precise definition of $\mathcal{D}\mathbf{x}$ in Eq. (7.99), with the function ω being evaluated at $\mathbf{x}_k$, is however the only one providing a scalar invariant path measure $\mathcal{D}\mathbf{x}$. This is in contrast with the previous section where the noise was additive, and for which the discretization of the path measure $\mathcal{D}\mathbf{x}$ in Eq. (7.79) was not an issue. Different discretizations can be used to represent the same

action functional $\mathcal{S}[\mathbf{x}(t)]$, as was illustrated by our study of the one-dimensional additive case in Sec. 7.2.1. For a given discretization $\mathfrak{d}$, we write the action as the $\mathfrak{d}$-discretized integral of a Lagrangian

$$\mathcal{S}[\mathbf{x}(t)] \stackrel{\mathfrak{d}}{=} \int_{t_0}^{t_{obs}} \mathrm{d}t \; \mathcal{L}_{\mathfrak{d}}(\mathbf{x}(t), \dot{\mathbf{x}}(t)) \,, \tag{7.101}$$

where the $\mathfrak{d}$ subscript in $\mathcal{L}_{\mathfrak{d}}$ accounts for the fact that the functional form of the Lagrangian depends on the underlying discretization.

7.2.3 Covariant path integral representation of stochastic processes

In this section we define a central concept, that of a covariant path integral representation for multidimensional stochastic differential equations with multiplicative noise. Let $\mathcal{P}[\Omega]$ be the probability that the system is in some region Ω of the phase space at time t_{obs} while being at $\mathbf{x}_0$ at t_0. We have derived a path integral representation of this probability within a given discretization scheme $\mathfrak{d}$:

$$\mathcal{P}[\Omega] \stackrel{\mathfrak{d}}{=} \int_{\mathbf{x}(t_0)=\mathbf{x}_0}^{\mathbf{x}(t_f)\in\Omega} \mathcal{D}\mathbf{x} \; \exp\left(- \int_{t_0}^{t_{obs}} \mathrm{d}\tau \; \mathcal{L}^x_{\mathfrak{d}}[\mathbf{x}(\tau), \dot{\mathbf{x}}(\tau)] \right) \,. \tag{7.102}$$

where the superscript x stresses that this Lagrangian is associated with the variable $\mathbf{x}$. We are free to reparametrize the phase space and define new variables $\mathbf{u}$ through $\mathbf{u} = \mathbf{U}(\mathbf{x})$ where $\mathbf{U}$ is an invertible transformation from $\mathbb{R}^d$ to $\mathbb{R}^d$. Using this new parametrization, the probability $\mathcal{P}[\Omega]$ can be constructed accordingly:

$$\mathcal{P}[\Omega] \stackrel{\mathfrak{d}}{=} \int_{\mathbf{u}(t_0)=U(\mathbf{x}_0)}^{\mathbf{u}(t_f)\in U(\Omega)} \mathcal{D}\mathbf{u} \; \exp\left(- \int_{t_0}^{t_{obs}} \mathrm{d}\tau \; \mathcal{L}^u_{\mathfrak{d}}[\mathbf{u}(\tau), \dot{\mathbf{u}}(\tau)] \right) \,. \tag{7.103}$$

A path integral representation is said to be covariant if the following two conditions are fulfilled. First we must have

$$\mathcal{D}\mathbf{x} = \mathcal{D}\mathbf{u} \,, \tag{7.104}$$

which expresses that the measure is a scalar invariant under changes of coordinates, consistently with our construction. Second, we require that:

$$\mathcal{L}^x_{\mathfrak{d}}[\mathbf{x}, \dot{\mathbf{x}}] = \mathcal{L}^u_{\mathfrak{d}}[\mathbf{U}(\mathbf{x}), (\partial\mathbf{U}/\partial\mathbf{x}).\dot{\mathbf{x}}] \,. \tag{7.105}$$

which means that one is free to use the standard chain rule directly at the level of the continuous time Lagrangian. Stated otherwise, a discretization $\mathfrak{d}$ of the path integral is covariant if and only if the associated Lagrangian $\mathcal{L}^x_{\mathfrak{d}}[\mathbf{x}, \dot{\mathbf{x}}]$ is manifestly covariant. In the following section we will compute $\mathcal{L}^x_{\alpha}[\mathbf{x}, \dot{\mathbf{x}}]$, the continuous time α-discretized Lagrangian for all $\alpha \in [0, 1]$. A rapid visual inspection will then show us that none of these α-discretizations, not even the Stratonovich one which is nevertheless adapted to the use of the chain rule at the level of stochastic differential equations, are covariant: changing variables by applying blindly the chain rule at the level of the continuous time Lagrangian is not an option in these α-discretizations.

7.2.4 The α-discretized path integral

In this section, we construct the α-discretized path integral representation of the transition probability of Eq. (7.93). This amounts at computing, in the limit $\Delta t \to 0$, and up to $O(\Delta t)$ terms, the one step scalar propagator $K_{\Delta t}[\mathbf{x}_{k+1}, t_{k+1}; \mathbf{x}_k, t_k]$ associated to the Stratonovich-discretized equation:

$$\Delta x_k^\mu = f^\mu(\mathbf{x}_k)\Delta t + g^{\mu i}\left(\mathbf{x}_k + \frac{\Delta \mathbf{x}_k}{2}\right)\Delta \eta_{i,k}\,. \tag{7.106}$$

The later is straightforwardly given by:

$$(2\pi\Delta t)^{\frac{d}{2}}\, K_{\Delta t}[\mathbf{x}_{k+1}, t_{k+1}; \mathbf{x}_k, t_k] = (2\pi\Delta t)^{\frac{d}{2}} \left|\det\left(\frac{\partial \Delta\eta_{i,k}}{\partial \Delta x_k^\sigma}\right)\right| \frac{P[\Delta\eta_{i,k}]}{\sqrt{\omega(\mathbf{x}_{k+1})}}\,, \tag{7.107}$$

with $P[\Delta\eta_{i,k}]$ the probability distribution of the noise increments

$$P[\Delta\eta_{i,k}] = \left(\frac{1}{2\pi\Delta t}\right)^{\frac{d}{2}} \exp\left(-\frac{\Delta\eta_{i,k}\Delta\eta_{j,k}\delta^{ij}}{2\Delta t}\right)\,. \tag{7.108}$$

The point at which we choose to evaluate the functions appearing in $K_{\Delta t}[\mathbf{x}_{k+1}, t_{k+1}; \mathbf{x}_k, t_k]$ then sets the discretization scheme of the action $\mathcal{S}[x(s)]$. As we will show next, we can infer from Eq. (7.107) the expression of the α-discretized Lagrangian for any $\alpha \in [0,1]$. Following the notations introduced in Sec. 7.1.4, it reads:

$$\begin{aligned}\mathcal{L}_\alpha^x[\mathbf{x}, \dot{\mathbf{x}}] = \frac{1}{2}\Bigg[&\omega_{\mu\nu}\left(\frac{\mathrm{d}x^\mu}{\mathrm{d}t} - h^\mu\right)\left(\frac{\mathrm{d}x^\nu}{\mathrm{d}t} - h^\nu\right) + (1-2\alpha)\frac{\mathrm{d}x^\mu}{\mathrm{d}t}\left(\omega_{\mu\nu}\omega^{\rho\sigma}\Gamma^\nu_{\rho\sigma} + 2\Gamma^\alpha_{\mu\alpha}\right)\\ &+2\alpha\nabla_\mu h^\mu - (1-2\alpha)\omega_{\mu\nu}\omega^{\rho\sigma}\Gamma^\nu_{\rho\sigma}h^\mu + \left(\alpha - \frac{1}{2}\right)^2\omega_{\mu\nu}\omega^{\rho\sigma}\omega^{\alpha\beta}\Gamma^\mu_{\rho\sigma}\Gamma^\nu_{\alpha\beta} - \alpha\,(1-\alpha)\,R\\ &+\alpha\,(1-\alpha)\,\omega^{\mu\nu}\Gamma^\alpha_{\beta\mu}\Gamma^\beta_{\alpha\nu} + (1-3\alpha(1-\alpha))\,\omega^{\mu\nu}\partial_\nu\Gamma^\alpha_{\mu\alpha}\Bigg]\,.\end{aligned} \tag{7.109}$$

For the sake of completeness, we explicitely write here the expressions of the Itō-discretized Lagrangian,

$$\begin{aligned}\mathcal{L}_0^x[\mathbf{x}, \dot{\mathbf{x}}] = \frac{1}{2}\Bigg[&\omega_{\mu\nu}\left(\frac{\mathrm{d}x^\mu}{\mathrm{d}t} - h^\mu\right)\left(\frac{\mathrm{d}x^\nu}{\mathrm{d}t} - h^\nu\right) + \frac{\mathrm{d}x^\mu}{\mathrm{d}t}\left(\omega_{\mu\nu}\omega^{\rho\sigma}\Gamma^\nu_{\rho\sigma} + 2\Gamma^\alpha_{\mu\alpha}\right) - \omega_{\mu\nu}\omega^{\rho\sigma}\Gamma^\nu_{\rho\sigma}h^\mu\\ &+\frac{1}{4}\omega_{\mu\nu}\omega^{\rho\sigma}\omega^{\alpha\beta}\Gamma^\mu_{\rho\sigma}\Gamma^\nu_{\alpha\beta} + \omega^{\mu\nu}\partial_\nu\Gamma^\alpha_{\mu\alpha}\Bigg]\,,\end{aligned} \tag{7.110}$$

and of the Stratonovich-discretized one,

$$\mathcal{L}_{1/2}^x[\mathbf{x}, \dot{\mathbf{x}}] = \frac{1}{2}\left[\omega_{\mu\nu}\left(\frac{\mathrm{d}x^\mu}{\mathrm{d}t} - h^\mu\right)\left(\frac{\mathrm{d}x^\nu}{\mathrm{d}t} - h^\nu\right) + \nabla_\mu h^\mu - \frac{1}{4}R + \frac{1}{4}\omega^{\mu\nu}\Gamma^\alpha_{\beta\mu}\Gamma^\beta_{\alpha\nu} + \frac{1}{4}\omega^{\mu\nu}\partial_\nu\Gamma^\alpha_{\mu\alpha}\right]\,. \tag{7.111}$$

Before diving into the details of the computation of the Lagrangian in Eq. (7.109), note that there is no α such that its expression is manifestly covariant. This confirms our earlier claim that the chain rule can not correclty be blindly used in order to change variables at the level of an α-discretized continuous time action, even if it is Stratonovich discretized.

Derivation of the α-discretized Lagrangian

For a matter of convenience, in order to obtain a path integral representation of Eq. (7.93) where all functions in the infinitesimal propagator are evaluated at $\mathbf{x}_k + \alpha\Delta\mathbf{x}_k$, we start by expressing this process by the equivalent α-discretized stochastic differential equation:

$$\frac{\mathrm{d}x^\mu}{\mathrm{d}t} \overset{\alpha}{=} f^\mu_{(\alpha)} + g^{\mu i}\eta_i(t)\,, \tag{7.112}$$

with

$$f^\mu_{(\alpha)} = f^\mu + \left(\frac{1}{2} - \alpha\right) g^{\nu i}\partial_\nu g^{\mu j}\delta_{ij}\,. \tag{7.113}$$

In the discrete time companion process of Eq. (7.112), we express the noise increments in terms of the displacement $\Delta\mathbf{x}$ by

$$\Delta\eta_i = g_{i\nu}\left(x + \alpha\Delta x\right)\left(\Delta x^\nu - f^\nu_{(\alpha)}\left(x + \alpha\Delta x\right)\Delta t\right)\,, \tag{7.114}$$

from where we can deduce the expression of the Jacobian of the change of variables when going from the noise to the position

$$\left|\det\left(\frac{\partial\Delta\eta_i}{\partial\Delta x^\beta}\right)\right| = \sqrt{\omega(x+\alpha\Delta x)}\left|\det\left(\delta^\nu_\beta - \alpha\partial_\beta f^\nu_{(\alpha)}\Delta t + \alpha g^{\nu j}\partial_\beta g_{j\rho}\left(\Delta x^\rho - f^\rho\Delta t\right)\right)\right|\,. \tag{7.115}$$

Please note that in Eq. (7.115), and until the end of this section after Eq. (7.121), functions are assumed to be evaluated at $x + \alpha\Delta x$ unless explicitely stated otherwise. Following Eq. (7.107), we first express in Eq. (7.115) $\omega(x + \alpha\Delta x)$ in terms of $\omega(x + \Delta x)$ up to terms $O(\Delta t)$. We observe that

$$\begin{aligned}
\omega(x+\alpha\Delta x) &= \omega(x+\Delta x)\exp\left(\ln\omega(x+\alpha\Delta x) - \ln\omega(x+\Delta x)\right)\,,\\
&= \omega(x+\Delta x)\exp\left(-(1-\alpha)\Delta x^\mu\partial_\mu\ln\omega - \frac{(1-\alpha)^2}{2}\Delta x^\mu\Delta x^\nu\partial_\mu\partial_\nu\ln\omega\right)\,,\\
&:= \omega(x+\Delta x)\exp\left(-2(1-\alpha)\Delta x^\mu\Gamma^\alpha_{\mu\alpha} - (1-\alpha)^2\omega^{\mu\nu}\partial_\nu\Gamma^\alpha_{\mu\alpha}\Delta t\right)\,,
\end{aligned} \tag{7.116}$$

where the last line was obtained after using the substitution relation Eq. (7.57) and the formula for the derivative of the determinant of the metric

$$\partial_\mu\ln\omega = \omega^{\alpha\beta}\partial_\mu\omega_{\alpha\beta} = 2\Gamma^\alpha_{\mu\alpha}\,. \tag{7.117}$$

Using now the formula valid for any matrix H,

$$\det\left(1+\epsilon H\right) = \exp\left(\epsilon\, Tr(H) - \frac{\epsilon^2}{2}Tr\left(H^2\right)\right) + o\left(\epsilon^2\right)\,, \tag{7.118}$$

we can express the remaining determinant in Eq. (7.115) as

$$\begin{aligned}
&\left|\det\left(\delta^\nu_\beta - \alpha\partial_\beta f^\nu_{(\alpha)}\Delta t + \alpha g^{\nu j}\partial_\beta g_{j\rho}\left(\Delta x^\rho - f^\rho\Delta t\right)\right)\right|\\
&= \exp\left(-\alpha\partial_\nu f^\nu_{(\alpha)}\Delta t + \alpha g^{\nu j}\partial_\nu g_{j\rho}\left(\Delta x^\rho - f^\rho_{(\alpha)}\Delta t\right) - \frac{\alpha^2}{2}\partial_\beta g^{\nu j}\partial_\nu g^{\beta i}\delta_{ij}\Delta t\right)\,.
\end{aligned} \tag{7.119}$$

Grouping all terms and taking the continuum limit, this eventually allows us to express the α-discretized Lagrangian as

$$\begin{aligned}\mathcal{L}^x_\alpha[\mathbf{x},\dot{\mathbf{x}}] = \frac{\omega_{\mu\nu}}{2}\left(\frac{\mathrm{d}x^\mu}{\mathrm{d}t} - f^\mu_{(\alpha)}\right)\left(\frac{\mathrm{d}x^\nu}{\mathrm{d}t} - f^\nu_{(\alpha)}\right) + \frac{\mathrm{d}x^\mu}{\mathrm{d}t}\left(\alpha g^{\nu j}\partial_\nu g_{j\mu} - (1-\alpha)\Gamma^\alpha_{\mu\alpha}\right) \\ - \alpha\left(\partial_\nu f^\nu_{(\alpha)} + g^{\nu j}\partial_\nu g_{j\rho} f^\rho_{(\alpha)}\right) - \frac{(1-\alpha)^2}{2}\omega^{\mu\nu}\partial_\nu\Gamma^\alpha_{\mu\alpha} - \frac{\alpha^2}{2}\partial_\beta g^{\nu j}\partial_\nu g^{\beta i}\delta_{ij}\,.\end{aligned} \tag{7.120}$$

In order to from Eq. (7.120) to Eq. (7.109), we substitute for $f^\mu_{(\alpha)}$ in Eq. (7.120) its expression in function of h^μ as infered from Eq. (7.113) and Eq. (7.68),

$$\begin{aligned}f^\mu_{(\alpha)} &= h^\mu + \frac{1}{2}\Gamma^\rho_{\nu\rho}\omega^{\mu\nu} + \frac{1}{2}\partial_\nu g^{\nu i} g^{\mu j}\delta_{ij} + \left(\frac{1}{2} - \alpha\right) g^{\nu i}\partial_\nu g^{\mu j}\delta_{ij}\,, \\ &= h^\mu - \frac{1}{2}\Gamma^\mu_{\alpha\beta}\omega^{\alpha\beta} - \alpha g^{\nu i}\partial_\nu g^{\mu j}\delta_{ij}\,.\end{aligned} \tag{7.121}$$

The algebra is then tedious but straightforward to arrive at Eq. (7.109).

7.2.5 A free particle in the two-dimensional plane

Before delving in further mathematics, we illustrate the findings of this section on a simple example inspired from [45]. We take a close look at a two-dimensional Brownian motion, when changing from Cartesian to polar coordinates, and we shed light on where the difficulties lie in this specific example. We start by the equations of motion:

$$\frac{\mathrm{d}x}{\mathrm{d}t} = \eta_x,\ \frac{\mathrm{d}y}{\mathrm{d}t} = \eta_y\,, \tag{7.122}$$

where η_x and η_y are independent Gaussian white noises with correlations

$$\langle\eta_x(t)\eta_x(t')\rangle = \langle\eta_y(t)\eta_y(t')\rangle = \delta(t-t'). \tag{7.123}$$

In this case, the measure over trajectories simply reads

$$\int \mathcal{D}x\mathcal{D}y\,\mathrm{e}^{-\frac{1}{2}\int_0^t \mathrm{d}\tau\left[\dot{x}^2+\dot{y}^2\right]}\,. \tag{7.124}$$

Because the process in Eq. (7.122) has additive noise and vanishing drift, in writing Eq. (7.124) there is no discretization issues involved. Following the work of Edwards and Gulyaev [45] who first pinpointed these difficulties, we wish to rewrite the path probability in terms of the polar coordinates r and ϕ with $x = r\cos\phi$ and $y = r\sin\phi$. Assuming that we use a covariant discretization scheme, the chain rule applies by definition and the measure over the r,ϕ paths reads

$$\int \mathcal{D}r\,\mathcal{D}\phi\,\mathrm{e}^{-\frac{1}{2}\int_0^t \mathrm{d}\tau\left[\dot{r}^2+r^2\dot{\phi}^2\right]}\,, \tag{7.125}$$

with $\mathcal{D}r\,\mathcal{D}\phi$ the covariant volume element given from Eq. (7.99) as:

$$\mathcal{D}r\,\mathcal{D}\phi = \lim_{N\to+\infty}\frac{1}{2\pi\Delta t}\prod_{k=1}^{N-1}\left\{r_k\frac{\mathrm{d}r_k\mathrm{d}\phi_k}{2\pi\Delta t}\right\}\,. \tag{7.126}$$

This continuous-time expression of course differs from the ones that could be derived using an Itō discretization—which may not come as a surprise—but also with a Stratonovich discretization. The latter is perhaps more surprising given that, at the level of a Langevin equation, it is known to preserve differential calculus. In this particular problem, the vectorial drift h^μ vanishes and the flat Euclidean metric in polar coordinates is given by

$$\omega_{\mu\nu}(r,\phi) = \begin{pmatrix} 1 & 0 \\ 0 & r^2 \end{pmatrix} . \tag{7.127}$$

The corresponding Ricci scalar curvature vanishes and the only nonzero Christoffel symbols are given by:

$$\Gamma^r_{\phi\phi} = -r, \quad \Gamma^\phi_{r\phi} = \Gamma^\phi_{\phi r} = \frac{1}{r} . \tag{7.128}$$

Thus, from Eq. (7.109), the Itō Lagrangian writes

$$\mathcal{L}_0\left(r,\dot{r},\phi,\dot{\phi}\right) = \frac{1}{2}\left[\dot{r}^2 + r^2\dot{\phi}^2 + \frac{\dot{r}}{r} - \frac{3}{4r^2}\right] , \tag{7.129}$$

and the Stratonovich one writes

$$\mathcal{L}_{1/2}\left(r,\dot{r},\phi,\dot{\phi}\right) = \frac{1}{2}\left[\dot{r}^2 + r^2\dot{\phi}^2 - \frac{1}{2r^2}\right] . \tag{7.130}$$

None of the above actually matches the covariant expression obtained in Eq. (7.125). This concretely illustrates that neither the Itō scheme nor the Stratonovich one (nor any α scheme) are covariant discretization schemes of path integral weights. We defer to Secs. 8.2 and 8.3.1 the description of covariant discretization schemes.

Chapter 8

Stochastic calculus for path integrals

Contents

In this chapter, we study the crucial issue of changing variables within the Onsager-Machlup path integral. As we have seen in Sec. 7.1, the commonly used α-discretized path integrals are not compatible with the naive use of the chain rule in continuous time. In Sec. 8.1, we show that they are not compatible with the blind use of Itō's lemma neither. Working at the level of stochastic differential equations indeed involves dealing with the singular object $\dot{x}$ but working at the level of path integrals involves dealing with the even more singular object $\dot{x}^2$. This brings about higher order terms which need to be taken into account when performing changes of variables at the level of path integrals. For a generic α-discretized action and in any dimension d we explain in Sec. 8.1 how to extend Eq. (7.60) so as to make it compatible with path integration.

In Sec. 8.3 we change our point of view and discretize differently the path integral so as to make manifestly covariant and compatible with the use of the chain rule in continuous time. We first review the old proposal of DeWitt [36] in the field of quantum mechanics in curved space and its many extensions in the domain of classical stochastic processes [86, 35, 127]. We then introduce a discretization of the Langevin equation that is fully covariant in discrete time. The latter generalizes a proposal of [29] for one-dimensional processes. Building on it, we propose a higher-order discretization scheme of the path integral that makes it covariant.

Contributions

Section 8.1

- extension of Itō's lemma for the change of variables inside path integrals,
- proof of a third order substitution rule.

Section 8.3

- discretization of multidimensional Langevin equations that is fully covariant in discrete time
- higher-order discretization scheme that makes the path integral covariant.

8.1 Extensions of Itō's lemma for path integral calculus

As we have extensively discussed in the previous section Sec. 7.2, the chain rule does not operate at the level of a continuous-time α-discretized Lagrangian. For $\alpha \neq 1/2$, this is intuitively expected based on our knowledge of stochastic calculus performed at the level of Langevin equations for which the chain rule does not hold. In line with the findings of [28] where the authors focused on the one-dimensional case, we show in addition in this section that applying blindly Itō's lemma of α-discretized stochastic differential equations (7.47) to the continuous time α-discretized Lagrangians does not provide a correct result either. In explicit terms, this means that the differentiation rule

$$\frac{\mathrm{d}u^\mu}{\mathrm{d}t} = \partial_\rho U^\mu \frac{\mathrm{d}x^\rho}{\mathrm{d}t} + \left(\alpha - \frac{1}{2}\right) \omega^{\rho\sigma} \partial_\rho \partial_\sigma U^\mu \,, \tag{8.1}$$

for the evolution of the reparametrized process $\mathbf{u}(t) = \mathbf{U}(\mathbf{x}(t))$, cannot be use withing a Lagrangian. In the course of our derivation, we shall pinpoint the mathematical cause for these failures and we shall construct an extension of Itō's lemma for path integral calculus, which is the main result of this section. In the following, we consider the α-discretized infinitesimal propagator from which originates the Lagrangian in Eq. (7.109) and its transformation under the change of variable $\mathbf{x}(t) = \mathbf{X}(\mathbf{u}(t))$ where $\mathbf{X}$ denotes the functional inverse of $\mathbf{U}$.

8.1.1 Transformation of variables at the path integral level

The logarithm of the α-discretized scalar invariant infinitesimal propagator $K_{\Delta t}[\mathbf{x}+\Delta\mathbf{x}, t+\Delta t; \mathbf{x}, t]$, as can be read from the continuous-time α-Lagrangian in Eq. (7.109), contains, up to order $O(\Delta t)$, three types of terms. A first one is of the form

$$A_1 = T^{(0)}(\mathbf{x})\Delta t \,, \tag{8.2}$$

where the discretization point of $T^{(0)}$ is irrelevant to the order in Δt we consider. It transforms, under a change of variables, in a trivial fashion, namely

$$A_1 = T^{(0)}(\mathbf{X}(\mathbf{u}))\Delta t + O(\Delta t^{3/2}) \,. \tag{8.3}$$

Terms of the form

$$A_2 = T^{(1)}_\mu(\mathbf{x} + \alpha\Delta\mathbf{x})\Delta x^\mu \,. \tag{8.4}$$

which are $O(\Delta t^{1/2})$, are also encountered. In the continuous-time scalar propagator, these will give rise to a standard α-discretized integral of the type described in Eq. (7.24). As we hereafter argue, the expression inferred from the direct application of Itō's lemma Eq. (8.1) is actually correct. This means that A_2 transforms, under a change of variables, according to

$$\begin{aligned} A_2 = & \, T^{(1)}_\mu \left(\mathbf{X}(\mathbf{u} + \alpha\Delta\mathbf{u})\right) \partial_\nu X^\mu \left(\mathbf{u} + \alpha\Delta\mathbf{u}\right) \Delta u^\nu \\ & + \left(\alpha - \frac{1}{2}\right) T^{(1)}_\mu \left(\mathbf{X}(\mathbf{u})\right) \Omega^{\rho\sigma} \left(\mathbf{u}\right) \partial_\rho \partial_\sigma X^\mu \left(\mathbf{u}\right) \Delta t \,, \end{aligned} \tag{8.5}$$

with

$$\Omega^{\rho\sigma}\left(\mathbf{u}\right) = \omega^{\mu\nu}\left(\mathbf{X}(\mathbf{u})\right) \partial_\mu U^\rho \left(\mathbf{X}(\mathbf{u})\right) \partial_\nu U^\sigma \left(\mathbf{X}(\mathbf{u})\right) \,, \tag{8.6}$$

the inverse metric tensor associated to the $\mathbf{u}(t)$ process. The corresponding Christoffel symbols associated to this metric tensor will be denoted $\hat{\Gamma}$.

Finally, the last term inside the exponential of the α-discretized scalar invariant infinitesimal propagator is the kinetic one, of order $O(1)$ in terms of Δt,

$$A_3 = \omega_{\mu\nu}\left(\mathbf{x} + \alpha\Delta\mathbf{x}\right) \frac{\Delta x^\mu \Delta x^\nu}{\Delta t} \,, \tag{8.7}$$

where the $\frac{1}{2}$ prefactor was omitted for the sake of simplicity. Interestingly, and in the same vein as Eq. (7.39), in order to perform the change of variables in Eq. (8.7) and to collect all terms up to $O(\Delta t)$, we need to express Δx^α as a function of Δu^μ up to order $O\left(\Delta t^{3/2}\right)$. This is one order more in $\Delta t^{1/2}$ than what was needed earlier to establish Itō's lemma for stochastic differential equations. Furthermore, and this is a new feature to pay attention to, we also need to express $\omega_{\mu\nu}\left(\mathbf{x} + \alpha\Delta\mathbf{x}\right)$ in terms of $\Omega_{\rho\sigma}\left(\mathbf{u} + \alpha\Delta\mathbf{u}\right)$ up to order $O(\Delta t)$. The rest of this section will be devoted to establishing the transformation law of A_3 under a change of variable. We begin by plainly stating the result (where all functions are evaluated at $\mathbf{u} + \alpha\Delta\mathbf{u}$):

$$\begin{aligned} A_3 = & \, \Omega_{\mu\nu}\frac{\Delta u^\mu \Delta u^\nu}{\Delta t} + (1-2\alpha)\Big[3\Omega^{\eta\gamma}\partial_{(\eta}X^\mu\partial_\gamma\partial_{\delta)}X^\nu\omega_{\mu\nu}\Delta u^\delta \\ & -3\alpha\Omega^{\alpha\eta}\Omega^{\beta\delta}\hat{\Gamma}^\gamma_{\alpha\beta}\partial_{(\eta}X^\mu\partial_\gamma\partial_{\delta)}X^\nu\omega_{\mu\nu}\Delta t \\ & +3(1-2\alpha)\Omega^{\alpha\mu}\Omega^{\beta\nu}\Omega^{\gamma\rho}\left(\partial_{(\alpha}X^{\eta_1}\partial_\beta\partial_{\gamma)}X^{\eta_2}\omega_{\eta_1\eta_2}\right)\left(\partial_{(\rho}X^{\varphi_1}\partial_\mu\partial_{\nu)}X^{\varphi_2}\omega_{\varphi_1\varphi_2}\right)\Delta t \\ & +\frac{1-2\alpha}{4}\left(\Omega^{\eta_1\eta_2}\Omega^{\gamma_1\gamma_2}+2\Omega^{\eta_1\gamma_1}\Omega^{\eta_2\gamma_2}\right)\partial_{\eta_1}\partial_{\eta_2}X^\mu\partial_{\gamma_1}\partial_{\gamma_2}X^\nu\omega_{\mu\nu}\Delta t\Big] \\ & +\left(1-3\alpha(1-\alpha)\right)\Omega^{\eta\gamma_1}\Omega^{\gamma_2\gamma_3}\partial_\eta X^\mu\partial_{\gamma_1}\partial_{\gamma_2}\partial_{\gamma_3}X^\nu\omega_{\mu\nu}\Delta t \\ & +\frac{\alpha(1-\alpha)}{2}\left(\Omega^{\rho\sigma}\Omega^{\eta\gamma}+2\Omega^{\rho\gamma}\Omega^{\sigma\eta}\right)\partial_\rho\partial_\sigma X^\beta\partial_\eta X^\mu\partial_\gamma X^\nu\partial_\beta\omega_{\mu\nu}\Delta t + O(\Delta t^{3/2}) \,, \end{aligned} \tag{8.8}$$

where the notation $(\alpha\beta\gamma)$ means that the tensor is symmetrized with respect to these three indices. The above formula provides the correct transformation law under changes of variables of the kinetic term of the α-discretized Lagrangian. It thus extends, Itō's lemma for changing variables at the level of stochastic differential equations to path integral calculus. The issue of changing variables inside the continuous-time path integral has already been addressed in the past [150, 77, 124, 28]. Provided one uses the covariant discretization of the path measure shown in Eq. (7.99), formula (8.8) generalizes these contributions by making the transformation law of the kinetic term under a change of variable explicit in a generic α-discretization of the path integral weight and in any dimension d. Before proving this result, a few comments are in order. The first term of Eq. (8.8) arises from the standard chain rule. The terms in the bracket multiplied by $(1-2\alpha)$ emerge from the same terms in the expansion of Δx^μ as a function of Δu^ρ as the ones that lead to the standard Itō's lemma. Unsurprisingly, this contribution to the transformation law thus vanishes when $\alpha = 1/2$. Eventually, the last two terms arise from higher order terms in the expansions and are completely missed by a blind implementation of Itō's lemma at the level of the continuous time Lagrangian. Note that there exists no value of α such that these two contributions vanish. Hence, the formula inferred from Itō's lemma Eq. (8.1) never holds at the path integral level. Moreover, the discretization parameter α appears in the same combinations in the transformation law Eq. (8.8) and in the continuous time Lagrangian Eq. (7.109). This is to be expected since the non-manifestly covariant part of the transformation of $\mathcal{L}^x_\alpha[\mathbf{x}, \dot{\mathbf{x}}]$ should be compensated by all the terms coming in addition to those originating from the chain rule in Eq. (8.8) for the scalar invariant propagator to be, indeed, a proper scalar.

8.1.2 Elementary transformation rules

In order to establish formula (8.8), we need to express (i) Δx^α af a function of Δu^μ up to order $O\left(\Delta t^{3/2}\right)$ and (ii) $\omega_{\mu\nu}\left(\mathbf{x}+\alpha\Delta\mathbf{x}\right)$ in terms of $\Omega_{\rho\sigma}\left(\mathbf{u}+\alpha\Delta\mathbf{u}\right)$ up to order $O(\Delta t)$. We obtain first

$$\begin{aligned}\Delta x^\alpha &= X^\alpha(\mathbf{u}+\Delta\mathbf{u}) - X^\alpha(\mathbf{u}) \\ &= \partial_\mu X^\alpha\left(\mathbf{u}+\alpha\Delta\mathbf{u}\right)\Delta u^\mu + \left(\frac{1}{2}-\alpha\right)\partial_\mu\partial_\nu X^\alpha\left(\mathbf{u}+\alpha\Delta\mathbf{u}\right)\Delta u^\mu\Delta u^\nu \\ &\quad + \frac{1-3\alpha(1-\alpha)}{6}\partial_\mu\partial_\nu\partial_\rho X^\alpha\left(\mathbf{u}\right)\Delta u^\mu\Delta u^\nu\Delta u^\rho + O\left(\Delta u^4\right)\,.\end{aligned} \tag{8.9}$$

The first two terms in the right-hand side of the above Eq. (8.9), from which one can infer Itō's lemma, are sufficient to express Δx up to order $O(\Delta t)$, which is the desired precision when working at the level of stochastic differential equations. The higher order term is however necessary to study transformation laws at the path integral level. Next, for an arbitrary smooth function $\varphi(\mathbf{x})$ we have,

$$\begin{aligned}\varphi\left(\mathbf{x}+\alpha\Delta\mathbf{x}\right) &= \varphi\left(X(\mathbf{u}+\alpha\Delta\mathbf{u}-\alpha\Delta\mathbf{u})+\alpha\Delta x\right) \\ &= \varphi\left(X(\mathbf{u}+\alpha\Delta\mathbf{u})\right) + \frac{\alpha(1-\alpha)}{2}\partial_\rho\partial_\sigma X^\nu(\mathbf{u})\partial_\nu\varphi\left(X(\mathbf{u})\right)\,\Delta u^\rho\Delta u^\sigma + O(\Delta t^{3/2})\,.\end{aligned} \tag{8.10}$$

Note that the correcting term in Eq. (8.10) is of order $O(\Delta t)$ and was negligible when studying transformation properties of α-discretized stochastic differential equations. Note also

that we naturally find in Eq. (8.9) and Eq. (8.10) the same combinations of α as in Eq. (8.8) and Eq. (7.109). Using these last two equations, as well as the substitution rules for $\Delta u^\mu \Delta u^\nu$ and $\Delta u^\mu \Delta u^\nu \Delta u^\rho \Delta u^\sigma$, we obtain the following transformation rule for the kinetic term

$$\begin{aligned} A_3 =& \Omega_{\mu\nu} \frac{\Delta u^\mu \Delta u^\nu}{\Delta t} + (1-2\alpha) \partial_\eta X^\mu \partial_\gamma \partial_\delta X^\nu \omega_{\mu\nu} \frac{\Delta u^\eta \Delta u^\gamma \Delta u^\delta}{\Delta t} \\ &+ \left(\frac{1}{2} - \alpha\right)^2 \left[\Omega^{\eta_1}\Omega^{\eta_2}\Omega^{\gamma_1}\Omega^{\gamma_2} + 2\Omega^{\eta_1\gamma_1}\Omega^{\eta_2\gamma_2}\right] \partial_{\eta_1}\partial_{\eta_2} X^\mu \partial_{\gamma_1}\partial_{\gamma_2} X^\nu \omega_{\mu\nu} \Delta t \\ &+ (1 - 3\alpha(1-\alpha)) \, \Omega^{\eta\gamma_1}\Omega^{\gamma_2\gamma_3} \partial_\eta X^\mu \partial_{\gamma_1}\partial_{\gamma_2}\partial_{\gamma_3} X^\nu \omega_{\mu\nu} \Delta t \\ &+ \frac{\alpha(\alpha-1)}{2} \left(\Omega^{\rho\sigma}\Omega^{\eta\gamma} + 2\Omega^{\rho\gamma}\Omega^{\sigma\eta}\right) \partial_\rho \partial_\sigma X^\beta \partial_\eta X^\mu \partial_\gamma X^\nu \partial_\beta \omega_{\mu\nu} \Delta t + O(\Delta t^{3/2}) \, . \end{aligned} \tag{8.11}$$

As already noted by several authors [150, 77], the Stratonovich case $\alpha = 1/2$ is peculiar in that no third power of Δu appears in the transformation law of the kinetic term whereas they do for $\alpha \neq 1/2$. We show how to treat this terms in the following and derive a substitution rule paving the way to Eq. (8.8).

Third order substitution rule

In this section we derive a substitution rule for third order terms of the type

$$T_{\mu\nu\rho}\left(\mathbf{u} + \alpha \Delta \mathbf{u}\right) \frac{\Delta u^\mu \Delta u^\nu \Delta u^\rho}{\Delta t} \, , \tag{8.12}$$

i.e. a way to replace such terms in the path integral weight by contributions involving zeroth and first powers of $\Delta \mathbf{x}$ only. This substitution rule has a weaker meaning than the second and fourth order ones as it does not correspond to L^2 convergence but rather to a weaker convergence in distribution. In the same vein as Sec. 7.2.1, let us separate the kinetic term from the rest and write the infinitesimal propagator, up to order $O(\Delta t)$, as follows

$$\begin{aligned} &\mathcal{P}[\mathbf{x} + \Delta \mathbf{x}, t + \Delta t; \mathbf{x}, t] \\ &= \frac{\sqrt{\omega(\mathbf{x} + \Delta \mathbf{x})}}{(2\pi \Delta t)^{d/2}} \exp\left(-\frac{1}{2}\omega_{\mu\nu}\left(\mathbf{x} + \alpha \Delta \mathbf{x}\right) \frac{\Delta x^\mu \Delta x^\nu}{\Delta t}\right) \exp\left(T^{(0)}(\mathbf{x}) \Delta t + T^{(1)}_\mu(\mathbf{x} + \alpha \Delta \mathbf{x}) \Delta x^\mu \right. \\ &\left. + T^{(2)}_{\mu\nu}(\mathbf{x}) \Delta x^\mu \Delta x^\nu + T^{(3)}_{\mu\nu\rho}(\mathbf{x} + \alpha \Delta \mathbf{x}) \frac{\Delta x^\mu \Delta x^\nu \Delta x^\rho}{\Delta t} + T^{(4)}_{\mu\nu\rho\sigma}(\mathbf{x}) \frac{\Delta x^\mu \Delta x^\nu \Delta x^\rho \Delta x^\sigma}{\Delta t}\right) \, , \\ &= \frac{\sqrt{\omega(\mathbf{x} + \Delta \mathbf{x})}}{(2\pi \Delta t)^{d/2}} \exp\left(-\frac{1}{2}\omega_{\mu\nu}\left(\mathbf{x} + \alpha \Delta \mathbf{x}\right) \frac{\Delta x^\mu \Delta x^\nu}{2}\right) \left\{1 + T^{(0)}(\mathbf{x}) \Delta t + T^{(1)}_\mu(\mathbf{x} + \alpha \Delta \mathbf{x}) \Delta x^\mu \right. \\ &+ T^{(2)}_{\mu\nu}(\mathbf{x}) \Delta x^\mu \Delta x^\nu + T^{(3)}_{\mu\nu\rho}(\mathbf{x} + \alpha \Delta \mathbf{x}) \frac{\Delta x^\mu \Delta x^\nu \Delta x^\rho}{\Delta t} + T^{(4)}_{\mu\nu\rho\sigma}(\mathbf{x}) \frac{\Delta x^\mu \Delta x^\nu \Delta x^\rho \Delta x^\sigma}{\Delta t} \\ &+ \frac{1}{2} T^{(1)}_\mu(\mathbf{x}) T^{(1)}_\nu(\mathbf{x}) \Delta x^\mu \Delta x^\nu + \frac{1}{2} T^{(3)}_{\mu\nu\rho}(\mathbf{x}) T^{(3)}_{\alpha\beta\gamma}(\mathbf{x}) \frac{\Delta x^\mu \Delta x^\nu \Delta x^\rho}{\Delta t} \frac{\Delta x^\alpha \Delta x^\beta \Delta x^\gamma}{\Delta t} \\ &\left. + T^{(1)}_\mu(\mathbf{x}) T^{(3)}_{\alpha\beta\gamma}(\mathbf{x}) \frac{\Delta x^\mu \Delta x^\alpha \Delta x^\beta \Delta x^\gamma}{\Delta t} + O(\Delta t^{3/2})\right\} , \end{aligned} \tag{8.13}$$

where, for the sake of generality of the demonstration, we have kept all possible terms, including those for which we already know the subsitution relations. Without any loss of generality we furthermore assume that $T^{(3)}_{\mu\nu\rho}$ is fully symmetric and so as are $T^{(2)}$ and $T^{(4)}$. In the continuous time limit, the process is entirely described by the first two moments of the probability distribution Eq. (8.13) which read

$$\langle \Delta x^\mu \Delta x^\nu \rangle = \omega^{\mu\nu}(\mathbf{x})\Delta t + O(\Delta t^{3/2}) \,, \tag{8.14}$$

and

$$\langle \Delta x^\mu \rangle = \overline{\Delta x^\mu} + T^{(1)}_\nu(\mathbf{x})\omega^{\mu\nu}\Delta t + 3T^{(3)}_{\nu\sigma\rho}(\mathbf{x})\omega^{\mu\nu}\omega^{\sigma\rho}\Delta t + O(\Delta t^{3/2}) \,, \tag{8.15}$$

where $\overline{\Delta x^\mu}$, and accordingly for the bar notation in the following, stands for

$$\overline{\Delta x^\mu} = \int \mathrm{d}\Delta\mathbf{x} \frac{\sqrt{\omega(\mathbf{x}+\Delta\mathbf{x})}}{(2\pi\Delta t)^{d/2}} \exp\left(-\frac{1}{2}\omega_{\rho\sigma}\left(\mathbf{x}+\alpha\Delta\mathbf{x}\right)\frac{\Delta x^\rho \Delta x^\sigma}{2}\right)\Delta x^\mu \,. \tag{8.16}$$

Defining $\hat{T}^{(1)}_\nu(\mathbf{x}) = T^{(1)}_\nu(\mathbf{x}) + 3T^{(3)}_{\nu\sigma\rho}(\mathbf{x})\omega^{\sigma\rho}(\mathbf{x})$, one can thus rewrite the first moment equation as

$$\langle \Delta x^\mu \rangle = \overline{\Delta x^\mu} + \hat{T}^{(1)}_\nu(\mathbf{x})\omega^{\mu\nu}(\mathbf{x})\Delta t + O(\Delta t^{3/2}) \,. \tag{8.17}$$

From Eq. (8.17), however, one cannot naively deduce that the third order substitution relation reads at the level of the infinitesimal propagator

$$T^{(3)}_{\mu\nu\rho}(\mathbf{x}+\alpha\Delta\mathbf{x})\frac{\Delta x^\mu \Delta x^\nu \Delta x^\rho}{\Delta t} \to 3T^{(3)}_{\mu\nu\rho}(\mathbf{x}+\alpha\Delta\mathbf{x})\omega^{\mu\nu}(\mathbf{x}+\alpha\Delta\mathbf{x})\Delta x^\rho \,, \tag{8.18}$$

as that would not preserve the normalization of the infinitesimal propagator. Indeed, the latter is expressed as

$$\begin{aligned} 0 = \overline{1} - 1 + T^{(0)}\mathrm{d}t + \overline{T^{(1)}_\mu(\mathbf{x}+\alpha\Delta\mathbf{x})\Delta x^\mu} + T^{(2)}_{\mu\nu}\omega_{\mu\nu}\Delta t + \overline{T^{(3)}_{\mu\nu\rho}(\mathbf{x}+\alpha\Delta\mathbf{x})\frac{\Delta x^\mu \Delta x^\nu \Delta x^\rho}{\Delta t}} \\ + 3T^{(4)}_{\mu\nu\rho\sigma}\omega^{\mu\nu}\omega^{\rho\sigma}\Delta t + \frac{1}{2}T^{(1)}_\mu T^{(1)}_\nu \omega^{\mu\nu}\Delta t + \frac{1}{2}T^{(3)}_{\mu\nu\rho}T^{(3)}_{\alpha\beta\gamma}\left[6\omega^{\alpha\mu}\omega^{\beta\nu}\omega^{\gamma\rho} + 9\omega^{\alpha\beta}\omega^{\gamma\rho}\omega^{\mu\nu}\right]\Delta t \\ + 3T^{(1)}_\mu T^{(3)}_{\alpha\beta\gamma}\omega^{\alpha\beta}\omega^{\mu\gamma}\Delta t + O(\Delta t^{3/2}) \,, \end{aligned} \tag{8.19}$$

where the discretization points were omitted where irrelevant. First, we notice that the terms proportional to $T^{(2)}_{\mu\nu}$ and $T^{(4)}_{\mu\nu\rho\sigma}$ appear in the normalization equation only through their mean with respect to the process

$$\frac{\mathrm{d}\mathbf{x}^\mu}{\mathrm{d}t} \overset{0}{=} g^{\mu i}(\mathbf{x})\eta_i(t) \,, \tag{8.20}$$

which is yet another justification of the substitution relations we used so far. Hence, we group hereafter all the terms in Eq. (8.19) involving $T^{(0)}$, $T^{(2)}$ and $T^{(4)}$ under the label $\tilde{T}^{(0)}$. Upon replacing $T^{(1)}$ by its expression in terms of $\hat{T}^{(1)}$ given above Eq. (8.17), we obtain

$$0 = \overline{1} - 1 + \hat{T}^{(0)}\Delta t + \overline{\hat{T}^{(1)}_\mu(\mathbf{x}+\alpha\Delta\mathbf{x})\Delta x^\mu} + \frac{1}{2}\hat{T}^{(1)}_\mu \hat{T}^{(1)}_\nu \omega^{\mu\nu}\Delta t + O(\Delta t^{3/2}) \,, \tag{8.21}$$

with

$$\begin{aligned}\hat{T}^{(0)} =& \tilde{T}^{(0)} + 3T^{(3)}_{\alpha\beta\gamma}T^{(3)}_{\mu\nu\rho}\omega^{\alpha\mu}\omega^{\beta\nu}\omega^{\gamma\rho} + 6\alpha T^{(3)}_{\mu\nu\rho}\Gamma^{\mu}_{\gamma\sigma}\omega^{\rho\gamma}\omega\sigma\nu \\ & - 3T^{(3)}_{\mu\nu\rho}\omega^{\mu\nu}\frac{\overline{\Delta x^{\rho}}}{\Delta t} + T^{(3)}_{\mu\nu\rho}\frac{\overline{\Delta x^{\mu}\Delta x^{\nu}\Delta x^{\rho}}}{\Delta t^2}\,.\end{aligned} \tag{8.22}$$

The remaining two integrals can be evaluated and yield

$$\frac{\overline{\Delta x^{\rho}}}{\Delta t} = (1-2\alpha)\Gamma^{\nu}_{\mu\nu}\omega^{\mu\rho} - \alpha\Gamma_{\eta\gamma}\omega^{\eta\gamma}\,, \tag{8.23}$$

and

$$\frac{\overline{\Delta x^{\mu}\Delta x^{\nu}\Delta x^{\rho}}}{\Delta t^2} = 3(1-2\alpha)\Gamma^{\alpha}_{\sigma\alpha}\omega^{\mu\nu}\omega^{\sigma\rho} - 3\alpha\Gamma^{\rho}_{\alpha\beta}\omega^{\mu\nu}\omega^{\alpha\beta} - 9\alpha\Gamma^{\mu}_{\alpha\beta}\omega^{\rho\alpha}\omega^{\beta\nu}\,. \tag{8.24}$$

Inserting Eqs. (8.23)-(8.24) into Eq. (8.22), we obtain

$$\hat{T}^{(0)} = \tilde{T}^{(0)} + 3T^{(3)}_{\alpha\beta\gamma}T^{(3)}_{\mu\nu\rho}\omega^{\alpha\mu}\omega^{\beta\nu}\omega^{\gamma\rho} - 3\alpha T^{(3)}_{\mu\nu\rho}\omega^{\mu\eta}\omega^{\nu\delta}\Gamma^{\eta\delta}_{\rho}\,. \tag{8.25}$$

We are now in a position to infer the third order substitution rule. This amounts to replacing the cubic term in the infinitesimal propagator Eq. (8.13) by contributions involving zeroth and first powers of $\Delta\mathbf{x}$ only. Requiring that after substitution the first and second moments of the two distribution coincide, and that they remain correctly normalized, we obtain

$$\begin{aligned}T^{(3)}_{\mu\nu\rho}(\mathbf{x}+\alpha\Delta\mathbf{x})\frac{\Delta x^{\mu}\Delta x^{\nu}\Delta x^{\rho}}{\Delta t} :=& \, 3T^{(3)}_{\mu\nu\rho}(\mathbf{x}+\alpha\Delta\mathbf{x})\omega^{\mu\nu}(\mathbf{x}+\alpha\Delta\mathbf{x})\Delta x^{\rho} \\ & + \left[3T^{(3)}_{\alpha\beta\gamma}T^{(3)}_{\mu\nu\rho}\omega^{\alpha\mu}\omega^{\beta\nu}\omega^{\gamma\rho} - 3\alpha T^{(3)}_{\mu\nu\rho}\omega^{\mu\eta}\omega^{\nu\delta}\Gamma^{\rho}_{\eta\delta}\right]\Delta t\,.\end{aligned} \tag{8.26}$$

While this formula was proposed in dimension one [124, 28] by requiring the consistency of the two infinitesimal propagators obtained by (i) performing a change of variables inside the path integral weight as we did in Eq. (8.11) and (ii) performing the change of variables directly at the level of the Langevin equation, we do not know of any published direct proof such as that of the present section (at least in the physics literature). The use of the third order substitution rule then allows us to obtain from Eq. (8.11) the transformation law for the kinetic term of an α-discretized Lagrangian under a change of variable Eq. (8.8). We note that the authors of a very recent work [41] have shown that the the Itō rule for Itō-discretized stochastic differential equation given in Eq. (7.60) at $\alpha = 0$ could be used blindly within the Itō-discretized continuous-time path integral weight. This requires, at odds with the case studied here, the path measure not to be covariantly discretized as in Eq. (7.99) but rather to be defined as

$$\mathcal{D}\mathbf{x} = \lim_{N\to+\infty}\left(\frac{1}{\sqrt{2\pi\Delta t}}\right)^{d}\int\prod_{k=1}^{N-1}\left\{\frac{\mathrm{d}\mathbf{x}_k\sqrt{\omega(\mathbf{x}_{k-1})}}{\sqrt{2\pi\Delta t}^{\,d}}\right\}\,. \tag{8.27}$$

This way both the kinetic term of the path integral weight and the path measure transform non-trivially under a change of variable but the different contributions cancel out and only the ones induced by Itō's lemma survive.

8.2 Covariant path integral representation à la DeWitt

In the previous section, we have discussed the non covariance of the formal continuous-time Lagrangian associated to the α-discretized path integral representation of multidimensional stochastic equations. Designing constructions of path integrals that would naturally be manifestly covariant in continuous time thus became a challenge for the theoretical physics community, especially for those attempting to extend Feynman's path integral to quantum mechanics on curved spaces. In a seminal work [36], later complemented by the work of [150], DeWitt came up with a first answer to this question. In DeWitt's construction, which follows the very spirit of path integrals as introduced by Feynman in quantum mechanics [52], the infinitesimal propagator is given, up to a proportionality constant, as the exponential of the manifestly covariant action of a classical massive particle in curved space evaluated at the infinitesimal classical path with appropriate boundary conditions. In [36], it is then shown that such a path integral indeed propagates the solution of a Schrödinger equation with Hamiltonian given, up to an additional potential term proportional to the Ricci curvature of the embedding space, by that of a classical particle quantized in such a way that it remains covariant at the quantum level. This approach for defining the path integral was then later transposed to the context of diffusion processes as the ones we focus on in the present work by Graham [87] and later Graham and Deininghaus [35] who used a similar construction for the definition of path integrals for multidimensional diffusion processes. While in this section we mostly follow the lines of [127], we will comment on the difference with the approach of [86] in the end. We start by assuming that the process in Eq. (7.106) can be described by the following path integral propagator

$$K[\mathbf{x},t;\mathbf{x}_0,t_0] = \int_{\mathcal{C}(\mathbf{x}_0,t_0;\mathbf{x},t)} \mathcal{D}\mathbf{x}\ \exp\left(-\int_{t_0}^{t}\left(\frac{1}{2}\omega_{\mu\nu}\dot{x}^\mu\dot{x}^\nu + a_\mu\dot{x}^\mu + b\right)\mathrm{d}\tau\right), \tag{8.28}$$

where the path measure follows the definition in Eq. (7.99) and where the infinitesimal scalar invariant propagator reads

$$K[\mathbf{x}+\Delta\mathbf{x},t+\Delta t;\mathbf{x},t] = \exp -\frac{1}{2}\int_t^{t+\Delta t}(\omega_{\mu\nu}\dot{x}^\mu_{cl}\dot{x}^\nu_{cl} + a_\mu\dot{x}^\mu_{cl} + b)\,\mathrm{d}\tau\,. \tag{8.29}$$

In Eq. (8.29), $\mathbf{x}_{cl}(\tau)$ is the infinitesimal minimal action path such that $\mathbf{x}_{cl}(t) = \mathbf{x}$ and $\mathbf{x}_{cl}(t+\Delta t) = \mathbf{x}+\Delta\mathbf{x}$. The vector field $a_\mu(\mathbf{x})$ and the function $b(\mathbf{x})$ are then set by requiring agreement between the formula in Eq. (8.29) and the already known Stratonovich discretized infinitesimal propagator infered from Eq. (7.111). In the following, we evaluate the integral in the exponential of Eq. (7.111) and write the result in a Stratonovich discretized form amenable to immediate comparison. We write the classical trajectory as $x^\mu_{cl}(\tau) = x^\mu + \delta x^\mu(\tau)$ and due to boundary conditions we have $\delta x^\mu(\tau) \sim O(\sqrt{\Delta t})$ and $\dot{x}^\mu_{cl}(\tau) \sim O(\Delta t^{-1/2})$. The minimal action path satisfies the Euler-Lagrange equations:

$$\ddot{x}^\nu_{cl} + \Gamma^\nu_{\alpha\beta}\dot{x}^\alpha_{cl}\dot{x}^\beta_{cl} = \omega^{\nu\rho}\partial_\rho b + \omega^{\nu\rho}(\partial_\rho a_\mu - \partial_\mu a\rho)\dot{x}^\mu_{cl}\,. \tag{8.30}$$

Hence we have $\ddot{x}^\mu_{cl}(\tau) \sim O(\Delta t^{-1})$ and recursively the n^{th} time derivative scales as $x^{\mu,(n)}_{cl}(\tau) \sim O(\Delta t^{-n/2})$. Note that for $a_\mu = 0$ and $b = 0$, Eq. (8.30) is nothing more but a geodesic equation. First, from the above discussed scalings,

$$\int_t^{t+\Delta t} b(\mathbf{x}_{cl}(\tau))\mathrm{d}\tau = b(\mathbf{x})\Delta t + O(\Delta t^{3/2})\,. \tag{8.31}$$

Furthermore,

$$\begin{aligned}\int_t^{t+\Delta t} a_\mu\left(\mathbf{x}_{cl}(\tau)\right)\dot{x}^\mu(\tau)\mathrm{d}\tau &= \int_t^{t+\Delta t}\left(a_\mu(\mathbf{x})+\delta x^\nu\partial_\nu a_\mu(\mathbf{x})\right)\dot{x}^\mu(\tau)\mathrm{d}\tau+\mathcal{O}(\Delta t^{3/2})\,,\\ &= a_\mu(\mathbf{x})\Delta x^\mu+\partial_\nu a_\mu(\mathbf{x})\int_t^{k+1}\delta x^\nu(\tau)\dot{\delta x^\mu}(\tau)\mathrm{d}\tau+\mathcal{O}(\Delta t^{3/2})\,.\end{aligned} \tag{8.32}$$

We now use the expansions:

$$\begin{aligned}\delta x^\mu(\tau) &= (\tau-t)\dot{x}^\mu(t)+\mathcal{O}(\Delta t)\,,\\ \dot{x}^\mu_{cl}(\tau) &= \dot{x}^\mu_{cl}(t)+\mathcal{O}(1)\,,\end{aligned} \tag{8.33}$$

to conclude that to the desired order

$$\int_t^{t+\Delta t}\delta x^\nu(\tau)\dot{\delta x^\mu}(\tau)\mathrm{d}\tau=\frac{1}{2}\Delta x^\mu\Delta x^\nu+O(\Delta t^{3/2})\,, \tag{8.34}$$

and therefore we obtain the integral in Eq. (8.32) as

$$\int_t^{t+\Delta t} a_\mu\left(\mathbf{x}_{cl}(\tau)\right)\dot{x}^\mu(\tau)\mathrm{d}\tau=a_\mu(\mathbf{x}+\Delta\mathbf{x}/2)\Delta x^\mu+\mathcal{O}(\Delta t^{3/2})\,. \tag{8.35}$$

Finally, we want to integrate the kinetic term

$$\int_t^{t+\Delta t}\omega_{\mu\nu}(\mathbf{x}_{cl}(\tau))\dot{x}^\mu_{cl}(\tau)\dot{x}^\nu_{cl}(\tau)\mathrm{d}\tau\,. \tag{8.36}$$

First, note that the integrand, that would be strictly conserved over time along a geodesic, remains conserved in the presence of the fields a_μ and b to the desired order in Δt since

$$\frac{\mathrm{d}}{\mathrm{d}\tau}\left(\omega_{\mu\nu}\dot{x}^\mu_{cl}\dot{x}^\nu_{cl}\right)=2\dot{x}^\mu\partial_\mu b\,, \tag{8.37}$$

so that

$$\omega_{\mu\nu}(\mathbf{x}_{cl}(\tau))\dot{x}^\mu_{cl}(\tau)\dot{x}^\nu_{cl}(\tau)=\omega_{\mu\nu}(\mathbf{x})\dot{x}^\mu_{cl}(t)\dot{x}^\nu_{cl}(t)+O(\sqrt{\Delta t})\,. \tag{8.38}$$

Therefore,

$$\int_t^{t+\Delta t}\omega_{\mu\nu}(\mathbf{x}_{cl}(\tau))\dot{x}^\mu_{cl}(\tau)\dot{x}^\nu_{cl}(\tau)\mathrm{d}\tau=\omega_{\mu\nu}(\mathbf{x})\dot{x}^\mu(t)\dot{x}^\nu(t)\Delta t+O(\Delta t^{3/2})\,. \tag{8.39}$$

Next, we Taylor expand $\Delta x^\mu=\dot{x}^\mu(t)\Delta t+(1/2)\ddot{x}^\mu(t)\Delta t^2+(1/6)\dddot{x}^\mu(t)\Delta t^3+...$, and using Eqs. (8.30)-(8.33) we obtain

$$\begin{aligned}\frac{1}{2}\int_t^{t+\Delta t}\omega_{\mu\nu}(\mathbf{x}_{cl}(\tau))\dot{x}^\mu_{cl}(\tau)\dot{x}^\nu_{cl}(\tau)\mathrm{d}\tau &= \frac{1}{2}\omega_{\mu\nu}(\mathbf{x})\frac{\Delta x^\mu\Delta x^\nu}{\Delta t}+\frac{1}{4\Delta t}\partial_\alpha\omega_{\nu\beta}(\mathbf{x})\Delta x^\alpha\Delta x^\beta\Delta x^\nu\\ &+\frac{1}{\Delta t}\left\{\frac{1}{12}\partial_\mu\partial_\nu\omega_{\alpha\beta}(\mathbf{x})-\frac{1}{24}\Gamma^\rho_{\alpha\beta}(\mathbf{x})\Gamma^\sigma_{\mu\nu}(\mathbf{x})\omega_{\rho\sigma}(\mathbf{x})\right\}\Delta x^\alpha\Delta x^\beta\Delta x^\mu\Delta x^\nu+O(\Delta t^{3/2})\,,\end{aligned} \tag{8.40}$$

where all functions are evaluated at $\mathbf{x}$. The detail of the computation can be found in [26]. Note that to the desired order in Δt, the result is independent of a_μ and b. This means that evaluating the integral in Eq. (8.29) along the minimal action path or along the geodesic path with appropriate boundary conditions is completely equivalent. We can now expand all the functions around $\mathbf{x} + \Delta\mathbf{x}/2$ and use the substitution rules to compare the obtained result with the Stratonovich infinitesimal propagator obtained in the previous section. Agreement between the two requires:

$$a_\mu = -\omega_{\mu\nu} h^\nu \,, \tag{8.41}$$

$$b = \frac{1}{2}\omega_{\mu\nu} h^\mu h^\nu + \frac{1}{2}\nabla_\mu h^\mu + \frac{1}{6}R \,. \tag{8.42}$$

Thus the continuous time action that describes the stochastic process in Eq. (7.106) constructed using Eq. (8.29) takes, unsurprinsingly as it is build using covariant notions, a manifestly covariant form and reads:

$$\mathcal{S}[x(t)] = \int \mathrm{d}\tau \, \frac{1}{2}\omega_{\mu\nu}(\dot{x}^\mu - h^\mu)(\dot{x}^\nu - h^\nu) + \frac{1}{2}\nabla_\mu h^\mu + \frac{1}{6}R \,. \tag{8.43}$$

This way of constructing path integrals is therefore, in the continuous time limit, compatible with the naive use of the chain rule for performing changes of variables. In his 1977 paper [87], Graham derived the following manifestly continuous time action:

$$\mathcal{S}[x(t)] = \int \mathrm{d}\tau \, \frac{1}{2}\omega_{\mu\nu}(\dot{x}^\mu - h^\mu)(\dot{x}^\nu - h^\nu) + \frac{1}{2}\nabla_\mu h^\mu + \frac{1}{12}R \,, \tag{8.44}$$

where the curvature contribution has a coefficient $1/12$ instead of the $1/6$ of Eq. (8.43). The reason that this is so is that, in Graham's construction, and as was shown in [35], the infinitesimal propagator actually takes the WKB form

$$\begin{aligned} &K[\mathbf{x}_1 = \mathbf{x} + \Delta\mathbf{x}, t + \Delta t; \mathbf{x}, t] \\ &= (\Delta t)^{n/2} \left(\omega(\mathbf{x} + \Delta x)\omega(\mathbf{x})\right)^{-1/4} \sqrt{\det - \frac{\partial^2 \mathcal{S}[x_{cl}(t)]}{\partial x_0^\mu \partial x_1^\nu}} \exp -\mathcal{S}[x_{cl}(t)] \,, \end{aligned} \tag{8.45}$$

with the so called van Vleck-Pauli-Morette determinant [157] given by

$$(\Delta t)^{n/2} \left(\omega(\mathbf{x} + \Delta x)\omega(\mathbf{x})\right)^{-1/4} \sqrt{\det - \frac{\partial^2 \mathcal{S}[x_{cl}(t)]}{\partial x_0^\mu \partial x_1^\nu}} = \exp -\frac{1}{12} R\Delta t + O(\Delta t^{3/2}) \,. \tag{8.46}$$

The main difference between the two Lagrangian Eq. (8.43) and (8.44) thus lies in whether the WKB-type prefactor is incorporated or not within the action itself which results in the $R/6$ or $R/12$ contributions.

8.3 Higher-order discretization schemes for covariant path integrals

Our interest now goes into knowing if one can construct a discretized version of the path integral in the same way as in Sec. 7.2.4 that would be covariant in continuous time and therefore consistent with differential calculus. This requires using higher order discretization schemes for the so called kinetic term.

8.3.1 Covariant Langevin equation in discrete time

Consider a discrete time Stratonovich Langevin equation. As already discussed, this equation is covariant up to terms scaling as $O(\Delta t^{1/2})$. While this is enough to warrant the covariance of the Langevin equation obtained in the limit $\Delta t \to 0$, we have seen that midpoint discretized infinitesimal propagators have a non covariant formal continuous time limit due to these $O(\Delta t^{1/2})$ corrections. In this section, we introduce an alternative discretization of Langevin equations that describes the same process as the Stratonovich discretized one in the continuous time limit and that has the remarkable property of being covariant in discrete time to all orders in Δt in a way that will be made precise below. It extends the results previously obtained by L. Cugliandolo, V. Lecomte and F. van Wijland in [29] for one-dimensional systems to multidimensional ones. Lastly, we use this discretization as a guide to construct a new path integral representation of the continuous time process. We introduce the stochastic equation:

$$\Delta x^\alpha = \mathbb{T}_{\mathbf{f},\mathbf{g}} \cdot \left(f^\alpha \Delta t + g^{\alpha i} \Delta \eta_i \right) (\mathbf{x}) \tag{8.47}$$

with $\Delta \eta_i$ the same zero mean Gaussian noise as before and the operator $\mathbb{T}_{\mathbf{f},\mathbf{g}}$ defined by its action on function as

$$\mathbb{T}_{\mathbf{f},\mathbf{g}} \cdot h(\mathbf{x}) = \left(\frac{\exp\left(f^\mu \Delta t + g^{\mu i} \Delta \eta_i \right) \partial_{x^\mu} - 1}{\left(f^\mu \Delta t + g^{\mu i} \Delta \eta_i \right) \partial_{x^\mu}} \, h \right) (\mathbf{x}) \, . \tag{8.48}$$

Direct expansion of Eq. (8.47) shows that this process and the Stratonovich discretized one in Eq. (7.54) are equivalent in the limit $\Delta t \to 0$. This discretization scheme, inspired by the field of calculus with Poisson point processes [50], is transparent to the chain rule, to all orders in Δt in the sense that the process $\mathbf{u}(t) = \mathbf{U}(\mathbf{x}(t))$ evolves according to

$$\Delta u^\alpha = \mathbb{T}_{\mathbf{F},\mathbf{G}} \cdot \left(F^\alpha \Delta t + G^{\alpha i} \Delta \eta_i \right) (\mathbf{u}) \tag{8.49}$$

with

$$\begin{aligned} F^\alpha &= \partial_\beta U^\alpha f^\beta \, , \\ G^{\alpha i} &= \partial_\beta U^\alpha g^{\beta i} \, . \end{aligned} \tag{8.50}$$

This statement is proved in the next section.

Proving the covariance of the discretization scheme

Let $\mathbf{U}$, be an invertible transformation of the initial coordinates $\{x^\alpha\}$. We define the new process $\mathbf{u}(t) = \mathbf{U}(\mathbf{x}(t))$. Let's assume first that the chain rule holds with the discretization rule specified above. Then,

$$\begin{aligned} \Delta u^\sigma &= \left[\frac{\exp \frac{\partial U^\mu}{\partial x^\alpha} f^\alpha \Delta t + \frac{\partial U^\mu}{\partial x^\alpha} g^{\alpha i} \Delta \eta_i \partial_{u^\mu} - 1}{\left(\frac{\partial U^\mu}{\partial x^\alpha} f^\alpha \Delta t + \frac{\partial U^\mu}{\partial x^\alpha} g^{\alpha i} \Delta \eta_i \right) \partial_{u^\mu}} \right] \left(\frac{\partial U^\sigma}{\partial x^\beta} f^\beta \Delta t + \frac{\partial U^\sigma}{\partial x^\beta} g^{\beta i} \Delta \eta_i \right) \, , \\ &= \left[\frac{\exp f^\alpha \Delta t + g^{\alpha i} \Delta \eta_i \partial_{x^\alpha} - 1}{\left(f^\alpha \Delta t + g^{\alpha i} \Delta \eta_i \right) \partial_{x^\alpha}} \right] \left(\frac{\partial U^\sigma}{\partial x^\beta} f^\beta \Delta t + \frac{\partial U^\sigma}{\partial x^\beta} g^{\beta i} \Delta \eta_i \right) \, , \\ &= \left[\exp f^\alpha \Delta t + g^{\alpha i} \Delta \eta_i \partial_{x^\alpha} - 1 \right] U^\sigma \end{aligned} \tag{8.51}$$

On the other side, independently of the chain rule, we have

$$\Delta v^\sigma = V^\sigma\left(x^1+\Delta x^1,...\right) - V^\sigma\left(x^1,...\right)\,, \tag{8.52}$$

with moreover

$$\begin{aligned}\Delta x^\mu &= \left[\frac{\exp f^\alpha \Delta t + g^{\alpha i}\Delta\eta_i \partial_{x^\alpha} - 1}{\left(f^\alpha \Delta t + g^{\alpha i}\Delta\eta_i\right)\partial_{x^\alpha}}\right]\left(f^\mu \Delta t + g^{\mu i}\Delta\eta_i\right)\,,\\ &= \left[\frac{\exp f^\alpha \Delta t + g^{\alpha i}\Delta\eta_i \partial_{x^\alpha} - 1}{\left(f^\alpha \Delta t + g^{\alpha i}\Delta\eta_i\right)\partial_{x^\alpha}}\right]\left(\frac{\partial x^\mu}{\partial x^\nu} f^\nu \Delta t + \frac{\partial x^\mu}{\partial x^\nu} g^{\nu i}\Delta\eta_i\right)\,,\\ &= \left[\exp f^\alpha \Delta t + g^{\alpha i}\Delta\eta_i \partial_{x^\alpha} - 1\right] x^\mu\end{aligned} \tag{8.53}$$

Proving the validity of the chain rule in this discretization scheme amounts therefore to proving the following functional identity:

$$V^\sigma\left[\left(\exp f^\alpha \Delta t + g^{\alpha i}\Delta\eta_i\partial_{x^\alpha}\right)x^1,...\right] = \left[\exp f^\alpha \Delta t + g^{\alpha i}\Delta\eta_i\partial_{x^\alpha}\right] V^\sigma\left(x^1,...\right)\,, \tag{8.54}$$

which generalizes Eq. (7.88). In order to prove the previous equation, we follow the route taken in the 1-dimensional case [29] and we define :

$$\Psi(\alpha) = \exp\alpha\left(f^\mu\Delta t + g^{\mu i}\Delta\eta_i\right)\partial_{x^\mu}\left[V^\sigma(\chi_1(\alpha,\cdot),...)\right](x(t))\,, \tag{8.55}$$

with

$$\chi_\beta(\alpha,x) = \exp(1-\alpha)\left(f^\mu\Delta t + g^{\mu i}\Delta\eta_i\right)\partial_{x^\mu}x^\beta\,. \tag{8.56}$$

We can then prove that $\Psi'(\alpha)=0$, a property that then leads to

$$\Psi(0) = \Psi(1)\,, \tag{8.57}$$

so that the functional equation established earlier is verified. Indeed:

$$\begin{aligned}\Psi'(\alpha) =& \sum_{m\geq 1}\frac{\alpha^{m-1}}{(m-1)!}\left[\left(f^\mu\Delta t + g^{\mu j}\Delta\eta_j\right)\partial_{x^\mu}\right]^m\left[V^\sigma\left(\chi_1(\alpha,\cdot),...\right)\right](x)\\ &+\sum_{m\geq 0}\frac{\alpha^m}{m!}\left[\left(f^\mu\Delta t + g^{\mu j}\Delta\eta_j\right)\partial_{x^\mu}\right]^m\left[\frac{\partial V^\sigma}{\partial x^\beta}\left(\chi_1(\alpha,\cdot),...\right)\frac{\partial\chi^\beta}{\partial\alpha}\right](x)\,,\\ =&\sum_{m\geq 1}\frac{\alpha^{m-1}}{(m-1)!}\left[\left(f^\mu\Delta t + g^{\mu j}\Delta\eta_j\right)\partial_{x^\mu}\right]^m\left[V^\sigma\left(\chi_1(\alpha,\cdot),...\right)\right](x)\\ &-\sum_{m\geq 0}\frac{\alpha^m}{m!}\left[\left(f^\mu\Delta t + g^{\mu j}\Delta\eta_j\right)\partial_{x^\mu}\right]^m\left[\frac{\partial V^\sigma}{\partial x^\beta}\left(\chi_1(\alpha,\cdot),...\right)\left(f^\mu\Delta t + g^{\mu j}\Delta\eta_j\right)\frac{\partial\chi^\beta}{\partial x^\mu}\right](x)\,,\\ &=\sum_{m\geq 1}\frac{\alpha^{m-1}}{(m-1)!}\left[\left(f^\mu\Delta t + g^{\mu j}\Delta\eta_j\right)\partial_{x^\mu}\right]^m\left[V^\sigma\left(\chi_1(\alpha,\cdot),...\right)\right](x)\\ &-\sum_{m\geq 0}\frac{\alpha^m}{m!}\left[\left(f^\mu\Delta t + g^{\mu j}\Delta\eta_j\right)\partial_{x^\mu}\right]^m\left[\left(f^\mu\Delta t + g^{\mu j}\Delta\eta_j\right)\frac{\partial V^\sigma}{\partial x^\mu}\left(\chi_1(\alpha,\cdot),...\right)\right](x)\,,\\ &=0\,,\end{aligned} \tag{8.58}$$

which completes the proof.

Implicit discretization scheme of the Langevin equation

In order to use Eq. (8.47) as as a guide for building covariant path integral representations, we rewrite the latter in an implicit form more familiar to Eq. (7.54). We expand Eq. (8.47) neglecting terms of order $O(\Delta t^2)$ and obtain,

$$\Delta x^\mu = f^\mu\left(\mathbf{x}+\frac{\Delta\mathbf{x}}{2}\right)\Delta t + \left(g^{\mu i}\left(\mathbf{x}+\frac{\Delta\mathbf{x}}{2}\right) + M^{\mu i}_{\alpha\beta}\Delta x^\alpha\Delta x^\beta\right)\Delta\eta_i + O(\Delta t^2)\,, \quad (8.59)$$

with

$$M^{\mu i}_{\alpha\beta} = \frac{1}{24}\left(\partial_\alpha\partial_\beta g^{\mu i} - 2g_{\beta j}\partial_\alpha g^{\gamma j}\partial_\gamma g^{\mu i}\right)\,. \quad (8.60)$$

In the following, we introduce the notations

$$\bar{g}^{\mu i}\left(\mathbf{x},\Delta\mathbf{x}\right) = g^{\mu i}\left(\mathbf{x}+\frac{\Delta\mathbf{x}}{2}\right) + M^{\mu i}_{\alpha\beta}\Delta x^\alpha\Delta x^\beta\,, \quad (8.61)$$

and

$$\bar{g}_{i\mu}(\mathbf{x},\Delta\mathbf{x}) = \bar{g}_{i\mu}\left(\mathbf{x}+\frac{\Delta x}{2}\right) + T_{i\mu\alpha\beta}(\mathbf{x})\Delta x^\alpha\Delta x^\beta\,, \quad (8.62)$$

with

$$T_{i\mu\alpha\beta} = -g_{j\mu}g_{i\nu}M^{\nu j}_{\alpha\beta}\,, \quad (8.63)$$

so that

$$\bar{g}_{i\mu}(\mathbf{x},\Delta\mathbf{x})\bar{g}^{\mu j}(\mathbf{x},\Delta\mathbf{x}) = \delta^j_i + O(\Delta t^{3/2})\,. \quad (8.64)$$

Inverting Eq. (8.59) thus yields

$$\Delta\eta_i = \bar{g}_{i\mu}(\mathbf{x},\Delta\mathbf{x})\left(\Delta x^\mu - f^\mu\left(\mathbf{x}+\frac{\Delta\mathbf{x}}{2}\right)\Delta t\right) + O(\Delta t^2)\,. \quad (8.65)$$

Furthermore, for any invertible and smooth transformation $\mathbf{u}(t) = \mathbf{U}(\mathbf{x}(t))$ of the original variables, Eq. (8.49) tells us that similarly

$$\Delta\eta_i = \bar{G}_{i\mu}(\mathbf{u},\Delta\mathbf{u})\left(\Delta u^\mu - F^\mu\left(\mathbf{u}+\frac{\Delta\mathbf{u}}{2}\right)\Delta t\right) + O(\Delta t^2)\,, \quad (8.66)$$

where the notations follow Eq. (8.50). All in all, this warrants that the accordingly discretized kinetic term transform formally as a scalar under changes of variables up to corrections of order $O(\Delta t^{3/2})$. Indeed, we get from Eqs. (8.65)-(8.66)

$$\begin{aligned}
&\bar{G}_{i\mu}(\mathbf{u},\Delta\mathbf{u})\bar{G}_{j\nu}(\mathbf{u},\Delta\mathbf{u})\left(\frac{\Delta u^\mu}{\Delta t} - F^\mu\left(\mathbf{u}+\frac{\Delta\mathbf{u}}{2}\right)\right)\left(\frac{\Delta u^\nu}{\Delta t} - F^\nu\left(\mathbf{u}+\frac{\Delta\mathbf{u}}{2}\right)\right)\delta^{ij}\Delta t\\
&= \bar{g}_{i\mu}(\mathbf{x},\Delta\mathbf{x})\bar{g}_{j\nu}(\mathbf{x},\Delta\mathbf{x})\left(\frac{\Delta x^\mu}{\Delta t} - f^\mu\left(\mathbf{x}+\frac{\Delta\mathbf{x}}{2}\right)\right)\left(\frac{\Delta x^\nu}{\Delta t} - f^\nu\left(\mathbf{x}+\frac{\Delta\mathbf{x}}{2}\right)\right)\delta^{ij}\Delta t\\
&\quad + O(\Delta t^{3/2})\,.
\end{aligned} \quad (8.67)$$

The realization that in this implicit discretization scheme the infinitesimal propagator kinetic term transforms covariantly under the chain rule is a the basis of our subsequent construction of manifestly covariant path integrals.

8.3.2 A discretization scheme for covariant path integrals

In order to obtain a covariant discretization scheme in continuous time, Eq. (8.67) suggests to write the infinitesimal propagator under the following form

$$K[\mathbf{x}+\Delta\mathbf{x}, t+\Delta t; \mathbf{x}, t] = \exp\left(-\frac{1}{2}\left(\bar{g}_{i\mu}(\mathbf{x},\Delta\mathbf{x})\bar{g}_{j\nu}(\mathbf{x},\Delta\mathbf{x})\delta^{ij}\frac{\left(\Delta x^\mu - h^\mu\left(\mathbf{x}+\frac{\Delta\mathbf{x}}{2}\right)\Delta t\right)}{\Delta t}\times\right.\right.$$
$$\left.\left.\times\left(\Delta x^\nu - h^\nu\left(\mathbf{x}+\frac{\Delta\mathbf{x}}{2}\right)\Delta t\right) + b(\mathbf{x})\Delta t\right)\right), \tag{8.68}$$

where b is yet to be determined. In order to find b, the simplest way to proceed is to start from the already derived Stratonovich discretized infinitesimal propagator and put by hand the discretization suggested in Eq. (8.68). This yields,

$$\begin{aligned}
K[\mathbf{x}+\Delta\mathbf{x}, t+\Delta t; \mathbf{x}, t] =& \exp\left(-\frac{1}{2}\left(\bar{g}_{i\mu}(\mathbf{x},\Delta\mathbf{x}) - T_{i\mu\alpha\beta}\Delta x^\alpha\Delta x^\beta\right)\times\right.\\
&\times\left(\bar{g}_{j\nu}(\mathbf{x},\Delta\mathbf{x}) - T_{j\nu\rho\sigma}\Delta x^\alpha\Delta x^\beta\right)\delta^{ij}\frac{\left(\Delta x^\mu - h^\mu\left(\mathbf{x}+\frac{\Delta\mathbf{x}}{2}\right)\Delta t\right)\left(\Delta x^\nu - h^\nu\left(\mathbf{x}+\frac{\Delta\mathbf{x}}{2}\right)\Delta t\right)}{\Delta t}\\
&\left.-\frac{1}{2}\left(\nabla_\mu h^\mu - \frac{1}{4}R + \frac{1}{4}\left[\omega^{\mu\nu}\Gamma^\alpha_{\beta\mu}\Gamma^\beta_{\alpha\nu} + \omega^{\mu\nu}\partial_\nu\Gamma^\alpha_{\mu\alpha}\right]\right)\Delta t\right),\\
=& \exp\left(-\frac{1}{2}\bar{g}_{i\mu}(\mathbf{x},\Delta\mathbf{x})\bar{g}_{j\nu}(\mathbf{x},\Delta\mathbf{x})\delta^{ij}\frac{\left(\Delta x^\mu - h^\mu\left(\mathbf{x}+\frac{\Delta\mathbf{x}}{2}\right)\Delta t\right)\left(\Delta x^\nu - h^\nu\left(\mathbf{x}+\frac{\Delta\mathbf{x}}{2}\right)\Delta t\right)}{\Delta t}\right.\\
&\left.-\frac{1}{2}\left(\nabla_\mu h^\mu - \frac{1}{4}R + \frac{1}{4}\left[\omega^{\mu\nu}\Gamma^\alpha_{\beta\mu}\Gamma^\beta_{\alpha\nu} + \omega^{\mu\nu}\partial_\nu\Gamma^\alpha_{\mu\alpha}\right] + \Delta L\right)\Delta t\right),
\end{aligned} \tag{8.69}$$

with

$$\begin{aligned}
\Delta L &= -2T_{i\mu\alpha\beta}g_{j\nu}\delta^{ij}\frac{\Delta x^\mu\Delta x^\nu\Delta x^\alpha\Delta x^\beta}{\Delta t^2},\\
&= 2\omega_{\rho\mu}g_{k\nu}M^{\rho k}_{\alpha\beta}\frac{\Delta x^\mu\Delta x^\nu\Delta x^\alpha\Delta x^\beta}{\Delta t^2},\\
&:= 2\omega_{\rho\mu}g_{k\nu}M^{\rho k}_{\alpha\beta}\left(\omega^{\mu\nu}\omega^{\alpha\beta} + \omega^{\mu\alpha}\omega^{\nu\beta} + \omega^{\nu\alpha}\omega^{\mu\beta}\right).
\end{aligned} \tag{8.70}$$

The coefficient b can then be derived from the above equation and reads,

$$b = \nabla_\mu h^\mu - \frac{1}{4}R + \frac{1}{4}\left[\omega^{\mu\nu}\Gamma^\alpha_{\beta\mu}\Gamma^\beta_{\alpha\nu} + \omega^{\mu\nu}\partial_\nu\Gamma^\alpha_{\mu\alpha}\right] + 2\omega_{\rho\mu}g_{k\nu}M^{\rho k}_{\alpha\beta}\left(\omega^{\mu\nu}\omega^{\alpha\beta} + \omega^{\mu\alpha}\omega^{\nu\beta} + \omega^{\nu\alpha}\omega^{\mu\beta}\right). \tag{8.71}$$

Before using the particular form of M displayed in Eq. (8.60), let us pause for a second and remark that two discretizations of the form given in Eq. (8.68) together with Eq. (8.62) and characterized by two different $T'_{i\mu\alpha\beta}$ and $T''_{i\mu\alpha\beta}$ yield the same continuous time Lagrangian provided that

$$\omega_{\rho\mu}g_{k\nu}M'^{\rho k}_{\alpha\beta}\left(\omega^{\mu\nu}\omega^{\alpha\beta} + \omega^{\mu\alpha}\omega^{\nu\beta} + \omega^{\nu\alpha}\omega^{\mu\beta}\right) = \omega_{\rho\mu}g_{k\nu}M''^{\rho k}_{\alpha\beta}\left(\omega^{\mu\nu}\omega^{\alpha\beta} + \omega^{\mu\alpha}\omega^{\nu\beta} + \omega^{\nu\alpha}\omega^{\mu\beta}\right), \tag{8.72}$$

where the relation between M' and T' (respectively M'' and T'') can be read from Eq. (8.63). Remark that the relevant part of $M^{\rho k}_{\alpha\beta}$ (only the symmetric part in the down indices interests us) has $d^3(d+1)/2$ degrees of freedom while Eq. (8.72) imposes only one constraint. As soon as $d > 1$, there exists therefore a degeneracy in the higher order discretizations of the form Eq. (8.68) corresponding to a given continuous time Lagrangian. Let us now specify the result for M given in Eq. (8.60). Inserting the latter in Eq. (8.70) yields,

$$\Delta L = \frac{1}{12} g_{i\alpha}\omega^{\mu\nu}\partial_\mu\partial_\nu g^{\alpha i} + \frac{1}{6} g^{\mu i}\partial_\mu\partial_\nu g^{\nu j}\delta_{ij} + \frac{1}{6}\Gamma^\alpha_{\mu\alpha} g^{\nu i}\partial_\nu g^{\mu j}\delta_{ij} - \frac{1}{6} g_{\mu i}\partial_\nu g^{\alpha j}\partial_\alpha\omega^{\mu\nu} \,. \quad (8.73)$$

We therefore obtain

$$\begin{aligned} b =& \nabla_\mu h^\mu - \frac{1}{4}R + \frac{1}{4}\left[\omega^{\mu\nu}\Gamma^\alpha_{\beta\mu}\Gamma^\beta_{\alpha\nu} + \omega^{\mu\nu}\partial_\nu\Gamma^\alpha_{\mu\alpha}\right] + \frac{1}{12} g_{i\alpha}\omega^{\mu\nu}\partial_\mu\partial_\nu g^{\alpha i} + \frac{1}{6} g^{\mu i}\partial_\mu\partial_\nu g^{\nu j}\delta_{ij} \\ &+ \frac{1}{6}\Gamma^\alpha_{\mu\alpha} g^{\nu i}\partial_\nu g^{\mu j}\delta_{ij} - \frac{1}{6} g_{\mu i}\partial_\nu g^{\alpha j}\partial_\alpha\omega^{\mu\nu} \,. \end{aligned} \quad (8.74)$$

As expected, b can be put in a manifestly covariant form by noting that

$$\begin{aligned} \Delta L =& \frac{1}{12} g_{i\alpha}\omega^{\mu\nu}\nabla_\mu\nabla_\nu g^{\alpha i} + \frac{1}{6} g^{\mu i}\nabla_\mu\nabla_\nu g^{\nu j}\delta_{ij} - \left(\frac{1}{12}\omega^{\mu\nu}\partial_\mu\Gamma^\alpha_{\nu\alpha} + \frac{1}{6}\omega^{\mu\nu}\partial_\alpha\Gamma^\alpha_{\mu\nu} + \right. \\ & \left. \frac{1}{12}\omega^{\mu\nu}\Gamma^\alpha_{\mu\beta}\Gamma^\beta_{\nu\alpha} + \frac{1}{6}\omega^{\mu\nu}\Gamma^\alpha_{\alpha\beta}\Gamma^\beta_{\mu\nu}\right) \,, \end{aligned} \quad (8.75)$$

so that b writes

$$b = \nabla_\mu h^\mu - \frac{5}{12}R + \frac{1}{12} g_{i\alpha}\omega^{\mu\nu}\nabla_\mu\nabla_\nu g^{\alpha i} + \frac{1}{12} g_{i\alpha}\omega^{\mu\nu}\nabla_\mu\nabla_\nu g^{\alpha i} + \frac{1}{6} g^{\mu i}\nabla_\mu\nabla_\nu g^{\nu j}\delta_{ij} \,. \quad (8.76)$$

Note that while the expression of b is manifestly covariant, the rotational symmetry in the space of matrix $g^{\mu i}$ is not manifest in the obtained continuous time Lagrangian. This symmetry is indeed broken at the level of the discretization as can be seen by the expression of M in Eq. (8.60).

8.3.3 Higher order discretization point

The question we ask now is whether it is possible to cast the previous discretization into the form of an higher order one as described in Eq. (7.38), *i.e.* we look for $B^\mu_{\alpha\beta}$ such that discretizing the path integral at the point

$$\bar{x}^\mu = x^\mu + \frac{\Delta x^\mu}{2} + B^\mu_{\alpha\beta}\Delta x^\alpha \Delta x^\beta \,, \quad (8.77)$$

gives the same continuous time Lagrangian as the one infered from Eq. (8.68). In the notations of the previous section, this amounts at having

$$T_{i\mu\alpha\beta} = B^\nu_{\alpha\beta}\partial_\nu g_{i\mu} \,, \quad (8.78)$$

or equivalently

$$M^{\mu i}_{\alpha\beta} = B^\nu_{\alpha\beta}\partial_\nu g^{\mu i} \,. \quad (8.79)$$

From Eq. (8.72) we thus require that

$$\omega_{\rho\mu} g_{k\nu} \left(\omega^{\mu\nu} \omega^{\alpha\beta} + \omega^{\mu\alpha} \omega^{\nu\beta} + \omega^{\nu\alpha} \omega^{\mu\beta} \right) B^{\sigma}_{\alpha\beta} \partial_\sigma g^{\rho k} = \Delta L \,. \tag{8.80}$$

where ΔL was given in Eq. (8.70). This equation imposes only one constraints so that the solutions are in general degenerated. We look for a solution of the form

$$B^{\sigma}_{\alpha\beta} = \lambda \, \Gamma^{\sigma}_{\mu\nu} \omega^{\mu\nu} \omega_{\alpha\beta} \,. \tag{8.81}$$

Equation (8.80) thus becomes a scalar equation over the parameter λ,

$$\lambda = \frac{1}{\Gamma^{\rho}_{\sigma\rho} \Gamma^{\sigma}_{\mu\nu} \omega^{\mu\nu}} \left(\frac{\Delta L}{d+2} \right) \,. \tag{8.82}$$

Equation (8.82) together with Eq. (8.81) extend the results of [29] to multidimensional processes. Note that in the case where the Riemannian manifold defined from the metric $\omega_{\mu\nu}$ is locally flat around some point $\mathbf{x}_0$, *i.e.* with vanishing first derivatives of the metric but non-vanishing second ones, then we expect Eq. (8.80) to be singular and λ defined in Eq. (8.82) to diverge. The points in space at which this can occur are however expected to be isolated as if locally the metric has vanishing first and second derivatives then Eq. (8.80) is automatically satisfied for any B at that point. We have therefore constructed a higher-order discretization scheme generalizing that of [29] that allows to blindly use the chain rule at the level of continuous-time path integral weights. In this discretization, all function are evaluated at

$$\bar{x}^\mu = x^\mu + \frac{\Delta x^\mu}{2} + \frac{1}{\Gamma^{\rho}_{\sigma\rho} \Gamma^{\sigma}_{\omega\xi} \omega^{\omega\xi}} \left(\frac{\Delta L}{d+2} \right) \Gamma^{\mu}_{\eta\delta} \omega^{\eta\delta} \omega_{\alpha\beta} \Delta x^\alpha \Delta x^\beta \,, \tag{8.83}$$

and the associated continuous-time Lagrangian reads

$$\begin{aligned} \mathcal{L}^x[\mathbf{x}, \dot{\mathbf{x}}] = & \frac{1}{2} \omega_{\mu\nu} \left(\frac{\mathrm{d}x^\mu}{\mathrm{d}t} - h^\mu \right) \left(\frac{\mathrm{d}x^\nu}{\mathrm{d}t} - h^\nu \right) + \frac{1}{2} \nabla_\mu h^\mu - \frac{5}{24} R + \frac{1}{24} g_{i\alpha} \omega^{\mu\nu} \nabla_\mu \nabla_\nu g^{\alpha i} \\ & + \frac{1}{24} g_{i\alpha} \omega^{\mu\nu} \nabla_\mu \nabla_\nu g^{\alpha i} + \frac{1}{12} g^{\mu i} \nabla_\mu \nabla_\nu g^{\nu j} \delta_{ij} \,. \end{aligned} \tag{8.84}$$

These results bring new light on the mathematical subtleties associated to path integrals and the problems these can raise when manipulated improperly. The interest of formula (8.84) lies much more in its very existence, namely in the possibility of deriving such a covariant Lagrangian, than in its practical roll-out. While bringing answers to these questions for Onsager-Machlup path integrals in finite dimension, it certainly raises many questions for path integrals over fields where the internal dimension d is somehow sent to infinity. The fate of covariant derivatives and curvature contributions deserves to be explored.

Chapter 9

Conclusion

This part was devoted to the Onsager-Machlup path integral representation of the transition probability of diffusive systems and in particular to the issue of performing changes of variables directly at the level of the continuous time action. After reviewing the constructions of α-discretized path integrals in Sec. 7.1, we have explained that these were not compatible with the blind use of the chain rule, even in the Stratonovich discretization. Since the seminal work of Edwards and Gulyaev [45] this fact has raised the interest of communities working, given the ubiquity of path integrals, in a wide range of topics. In this work we hope to have answered some of these old and intriguing questions. In Sec. 8.1, we have shown that Itō's formula for changing variables at the level of stochastic differential equations could be extended to treat the very singular $\dot{x}^2$ term appearing in the path integral weight so as to become usable for changing variables inside an α-discretized continuous time action. We have then changed our point of view and, instead of changing the rules for changing variables while keeping the discretization scheme fixed, insisted on finding new discretization schemes of the path integral that would make it compatible with the use of the chain rule. We have reviewed DeWitt's and Graham's proposals in Sec. 8.2. There, the infinitesimal propagator is essentially expressed as the exponential of the classical action evaluated along the (infinitesimal) geodesic path with appropriate boundary conditions. In a way more similar in spirit to the usual α-discretization, we have then proposed in Sec. 8.3 a higher-order discretization scheme that extends the Stratonovich one and which has the property of being amenable to the use of the chain rule in continuous time.

These answers however come with their share of new questions which in the end all amount to wondering: "What can we actually do and what can we not do with path integrals?". For d-dimensional Gaussian processes, we have seen that performing a change of variable was already far from being trivial. Fortunately, in the small noise limit, everything becomes simple again. The blind use of the chain rule indeed then works in continuous time as all the higher-order terms of Eq. (8.8) yield negligible contributions. Apart from that limit, one however has to work more as we have shown in the present manuscript. Naturally, we can wonder about what happens to field theories regarding these issues and how does the geometrical picture we used throughout this work transform in the limit where d is sent to infinity. Another natural extension is the issue of non-Gaussian noises such

as Poisson processes where the Langevin equation is not available anymore as a guideline. The present work indeed suggests that in such cases an infinite number of terms should be kept in order to properly change variables inside the path integral. It also raises the related question of fields transforms of the Janssen-De Dominicis action that would mix both the original and the response fields as, for instance, the Cole-Hopf one. Finally, we stress that similar questions should arise in static field theories where, at least in $d = 1$, an action featuring a $\int \mathrm{d}x \left(\frac{\mathrm{d}\phi}{\mathrm{d}x}\right)^2$ contribution will be plagued by similar issues as the ones discussed in this part on stochastic calculus. All in all, there is much we still do not know and that remains to be discovered about path integrals.

Part III

Appendices

Appendix A

AOUP at small τ

We reproduce here the appendix of [143] that is associated to Sec.2.1 of the present manuscript.

A.1 Full steady-state distribution

In this appendix, we report the steady-state probability density $\mathcal{P}_s(x,v)$ up to order τ^2.

$$
\begin{aligned}
e^{\frac{\phi}{T+D}}\mathcal{P}_s(x,v) = c_0 + \sqrt{\tau}P_1(v)\frac{c_0\sqrt{D}\phi^{(1)}(x)}{T+D} + \tau P_0(v)\Bigg[-\frac{c_0 D\phi^{(1)2}}{2(T+D)^2} + c_2 + \frac{Dc_0\phi^{(2)}}{T+D} \\
-\frac{\sqrt{D}b_3}{T+D}\int_0^x e^{\frac{\phi(z)}{T+D}}dz\Bigg] + \tau^{\frac{3}{2}}\Bigg[\frac{P_3(v)c_0D^{\frac{3}{2}}}{\sqrt{6}}\left(\frac{\phi^{(1)3}}{(T+D)^3} - \frac{3\phi^{(1)}\phi^{(2)}}{(T+D)^2} + \frac{\phi^{(3)}}{T+D}\right) \\
+P_1(v)\left(\frac{b_3De^{\frac{\phi}{T+D}}}{T+D} - \frac{\phi^{(1)}b_3D}{(T+D)^2}\int_0^x e^{\frac{\phi(z)}{T+D}}dz + \frac{\sqrt{D}c_2\phi^{(1)}}{T+D} - \frac{c_0D^{\frac{3}{2}}\phi^{(1)3}}{2(T+D)^3}\right. \\
\left.+\frac{c_0\sqrt{D}(D^2-T^2)\phi^{(1)}\phi^{(2)}}{(T+D)^3} + \frac{c_0\sqrt{D}T\phi^{(3)}}{T+D}\right)\Bigg] + \tau^2P_0(v)\Bigg[\frac{c_2D\phi^{(2)}}{T+D} - \frac{c_2D\phi^{(1)2}}{2(T+D)^2} \\
-\frac{D^{\frac{3}{2}}b_3}{(T+D)^2}\int_0^x e^{\frac{\phi(z)}{T+D}}\phi^{(2)}(z)dz + \frac{c_0D^2}{8(T+D)^4}\phi^{(1)4} - \frac{c_0D(D-T)\phi^{(1)2}\phi^{(2)}}{2(T+D)^3} \\
+\frac{b_3D^{\frac{3}{2}}}{(T+D)^3}\int_0^x\left(\int_0^s e^{\frac{\phi(z)}{T+D}}dz\right)\left(\phi^{(1)}(s)\phi^{(2)}(s) - (T+D)\phi^{(3)}(s)\right)ds + c_4 \\
+\frac{Dc_0}{2(T+D)}\int_0^x \phi^{(1)2}(z)\phi^{(3)}(z)dz - \frac{Dc_0(D+2T)}{(T+D)^2}\phi^{(3)}\phi^{(1)} - \frac{\sqrt{D}b_5}{T+D}\int_0^x e^{\frac{\phi(z)}{T+D}}dz \\
+\frac{Dc_0(D-2T)\phi^{(2)2}}{4(T+D)^2} + \frac{Dc_0(D+2T)\phi^{(4)}}{2(T+D)}\Bigg].
\end{aligned}
\tag{A.1}
$$

In Eq. (A.1), c_0 is defined by Eq. (2.26) while c_2, c_4, b_3 and b_5 are integration constants whose expressions must be adapted to the boundary conditions. For a confining potential, $\mathcal{P}_s(x,v)$

must vanish for $x \to \pm\infty$, and thus $b_3 = b_5 = 0$ yielding the following spatial distribution:

$$e^{\frac{\phi}{T+D}}\mathcal{P}_s(x) = c_0 + \tau\left[-\frac{c_0 D\phi^{(1)2}}{2(T+D)^2} + c_2 + \frac{Dc_0\phi^{(2)}}{T+D}\right] + \tau^2\left[\frac{c_2 D\phi^{(2)}}{T+D} - \frac{c_2 D\phi^{(1)2}}{2(T+D)^2} + c_4 \right.$$
$$+\frac{c_0 D^2}{8(T+D)^4}\phi^{(1)4} - \frac{c_0 D(D-T)\phi^{(1)2}\phi^{(2)}}{2(T+D)^3} + \frac{Dc_0}{2(T+D)}\int_0^x \phi^{(1)2}(z)\phi^{(3)}(z)dz$$
$$\left. -\frac{Dc_0(D+2T)}{(T+D)^2}\phi^{(3)}\phi^{(1)} + \frac{Dc_0(D-2T)\phi^{(2)2}}{4(T+D)^2} + \frac{Dc_0(D+2T)\phi^{(4)}}{2(T+D)}\right]. \tag{A.2}$$

The integration constants c_2 and c_4 are finally found by normalization, requiring $\int_{-\infty}^{+\infty}\mathcal{P}_s(x)dx = 1$ at every order in τ. For a periodic potential of period L, the spatial distribution must respect $\mathcal{P}_s(x+L) = \mathcal{P}_s(x)$. This condition implies $b_3 = 0$, but $b_5 \neq 0$ and $\mathcal{P}_s$ reads:

$$e^{\frac{\phi}{T+D}}\mathcal{P}_s(x) = c_0 + \tau\left[-\frac{c_0 D\phi^{(1)2}}{2(T+D)^2} + c_2 + \frac{Dc_0\phi^{(2)}}{T+D}\right] + \tau^2\left[\frac{c_2 D\phi^{(2)}}{T+D} - \frac{c_2 D\phi^{(1)2}}{2(T+D)^2} + c_4 \right.$$
$$+\frac{c_0 D^2}{8(T+D)^4}\phi^{(1)4} - \frac{c_0 D(D-T)\phi^{(1)2}\phi^{(2)}}{2(T+D)^3} + \frac{Dc_0}{2(T+D)}\int_0^x \phi^{(1)2}(z)\phi^{(3)}(z)dz$$
$$-\frac{Dc_0(D+2T)}{(T+D)^2}\phi^{(3)}\phi^{(1)} + \frac{Dc_0(D-2T)\phi^{(2)2}}{4(T+D)^2} + \frac{Dc_0(D+2T)\phi^{(4)}}{2(T+D)}$$
$$\left. -\frac{\sqrt{D}b_5}{T+D}\int_0^x e^{\frac{\phi(z)}{T+D}}dz\right], \tag{A.3}$$

with b_5 given by

$$b_5 = \frac{D}{2(T+D)}\frac{\int_0^L \phi^{(1)2}\phi^{(3)}dx}{\int_0^L e^{\frac{\phi}{T+D}}dx\int_0^L e^{-\frac{\phi}{T+D}}dx}. \tag{A.4}$$

Once again, c_2 and c_4 are then found by normalization. Note that in expression Eq. (A.1), v corresponds to the rescaled variable $\tilde{v}$. To get the exact steady-state distribution associated to Eqs. (2.2)-(2.3), one thus has to make the change of variable $v \to \sqrt{\tau}v$.

A.2 Harmonic potential

We report hereafter the steady-state distribution for the special case of a harmonic potential $\phi(x) = \kappa x^2/2$

$$\mathcal{P}_s(x,v) = \frac{\sqrt{4ab-c^2}}{2\pi}e^{-ax^2-bv^2+cvx}, \tag{A.5}$$

with the constants a, b and c defined as:

$$a = \frac{\kappa(1+\kappa\tau)^2}{2(D+T(1+\kappa\tau)^2)} \quad b = \frac{D(1+\kappa\tau)+T(1+\kappa\tau)^2}{2D(D+T(1+\kappa\tau)^2)} \quad c = \frac{\kappa\sqrt{\tau}(1+\kappa\tau)}{D+T(1+\kappa\tau)^2}. \tag{A.6}$$

Note that in expression Eq. (A.5), v corresponds to the rescaled variable $\tilde{v}$. To get the exact steady-state distribution associated to Eqs. (2.2)-(2.3), one thus has to replace v with $\sqrt{\tau}v$ in Eq. (A.5) and to multiply Eq. (A.5) by $\sqrt{\tau}$. At $T = 0$, the distribution Eq. (A.5) corresponds to the result obtained in [198].

A.3 Computing the entropy production rate

As shown in Eq. (2.52), the entropy production rate can be expressed as

$$\sigma = \frac{2}{\tau}\left\langle \int_{-\infty}^{+\infty} dt\, G(t)\, \dot{x}(0)\, \phi'(x(t)) \right\rangle \ . \tag{A.7}$$

The small τ expansion of (A.7) is obtained by expanding it in powers of the particle displacement. In order to make this expansion in τ more explicit, we rescale time as $s = t/\tau$ and active force as $\hat{v} = v\sqrt{\tau}$. The entropy production rate then writes

$$\sigma = \frac{2}{\tau}\left\langle \int_{-\infty}^{+\infty} ds\, \hat{G}(s)\, \frac{dx}{ds}(0)\, \phi'(x(s)) \right\rangle \ , \tag{A.8}$$

with

$$\hat{G}(s) = \frac{D}{4T^2}\sqrt{\frac{T}{D+T}}\exp\left(-\sqrt{\frac{D+T}{T}}|s|\right) , \tag{A.9}$$

and the path measure $\langle \dots \rangle$ corresponding now to the process

$$\begin{aligned} \frac{dx}{ds} &= -\tau\phi'(x(s)) + \sqrt{\tau}\left(\hat{v}(s) + \sqrt{2T}\,\hat{\eta}_1(s)\right) \\ \frac{d\hat{v}}{ds} &= -\hat{v} + \sqrt{2D}\,\hat{\eta}_2(s) \ , \end{aligned} \tag{A.10}$$

where $\hat{\eta}_1(s)$ and $\hat{\eta}_1(s)$ are two independent Gaussian white noises. In order to keep notations simple we drop the hat in the following. We introduce the particle displacement during time s as

$$\Delta(s) = x(s) - x(0) \ . \tag{A.11}$$

Hence, we have

$$\sigma = \frac{2}{\tau}\int_{-\infty}^{\infty} ds\, G(s) \sum_{n=0}^{+\infty} \frac{1}{n!}\left\langle \dot{x}(0)\phi^{(n+1)}(x(0))\Delta(s)^n \right\rangle \ . \tag{A.12}$$

As usual in stochastic calculus, the underlying discretization of the various expressions at hand is crucial. Therefore, throughout this appendix, and for the sake of clarity of the presentation, we will sometimes go back to the discrete limiting expressions. For instance, Eq. (A.12) is understood in the Stratonovich sense, *i.e.* as the $\Delta t \to 0$ limit of the following discrete expression

$$\sigma = \frac{2}{\tau}\sum_{i=-\infty}^{+\infty} \Delta t\, G(i\Delta t) \sum_{n=0}^{+\infty} \frac{1}{n!}\left\langle \frac{\Delta x_0}{\Delta t}\, \phi^{(n+1)}\left(x_0 + \frac{\Delta x_0}{2}\right)\left(x_i - \left(x_0 + \frac{\Delta x_0}{2}\right)\right)^n \right\rangle , \tag{A.13}$$

with $\Delta x_i = x((i+1)\Delta t) - x(i\Delta t)$. The first term of the series involves the Stratonovich average $\langle \dot{x}(0)\phi'(x(0)) \rangle$ and thus vanishes. We now focus on the second one that we denote

by σ_1. We have

$$\begin{aligned}\sigma_1 &= \frac{2}{\tau}\int_{-\infty}^{+\infty} ds\, G(s)\left\langle \dot{x}(0)\phi^{(2)}(x(0))\Delta(s)\right\rangle \\ &= \frac{2}{\tau}\int_{0}^{+\infty} ds\, G(s)\left\langle \dot{x}(0)\phi^{(2)}(x(0))\left(\Delta(s)+\Delta(-s)\right)\right\rangle \\ &= \frac{2}{\tau}\int_{0}^{+\infty} ds\, G(s)\int_0^s ds'\,\left\langle \dot{x}(0)\phi^{(2)}(x(0))\left(\dot{x}(s')-\dot{x}(-s')\right)\right\rangle \\ &= \frac{2}{\tau}\int_{0}^{+\infty} ds\, G(s)\int_0^s ds'\,\left\langle \dot{x}(0)\dot{x}(s')\left(\phi^{(2)}(x(0))-\phi^{(2)}(x(s'))\right)\right\rangle\ ,\end{aligned}$$

where we have used time translation invariance in the steady state. The corresponding discretized expression writes

$$\sigma_1 = \frac{2}{\tau}\sum_{i=2}^{+\infty}\Delta t G(i\Delta t)\sum_{j=1}^{i-1}\left\langle \frac{\Delta x_0 \Delta x_j}{\Delta t}\left[\phi^{(2)}\left(x_0+\frac{\Delta x_0}{\Delta t}\right)-\phi^{(2)}\left(x_i+\frac{\Delta x_i}{\Delta t}\right)\right]\right\rangle \quad \text{(A.14)}$$

We now expand again Eq. (A.14) in powers of the displacement, which gives

$$\sigma_1 = -\frac{2}{\tau}\int_0^{+\infty} ds\, G(s)\int_0^s ds'\,\sum_{n=1}^{+\infty}\frac{1}{n!}\left\langle \dot{x}(0)\phi^{(n+2)}(x(0))\dot{x}(s')\Delta(s')^n\right\rangle\ . \quad \text{(A.15)}$$

In the Stratonovich discretization scheme we recognize a total derivative and we thus get

$$\sigma_1 = -\frac{2}{\tau}\int_0^{+\infty} ds G(s)\sum_{n=1}^{+\infty}\frac{1}{(n+1)!}\left\langle \dot{x}(0)\phi^{(n+2)}(x(0))\Delta(s)^{n+1}\right\rangle\ . \quad \text{(A.16)}$$

Eventually, when plugged back in Eq. (A.12), half of the terms cancel out and we obtain

$$\sigma = \frac{2}{\tau}\sum_{n=2}^{+\infty}\frac{1}{n!}\int_0^{+\infty} ds\, G(s)\left\langle \dot{x}(0)\phi^{(n+1)}(x(0))\Delta(-s)^n\right\rangle\ . \quad \text{(A.17)}$$

which is Eq. (2.53) of the main text. Once more, Eq. (A.17) should be understood in the Stratonovich sense, *i.e.* as the continuous time limit of

$$\sigma = \frac{2}{\tau}\sum_{i=1}^{+\infty}\Delta t\, G(i\Delta t)\sum_{n=2}^{+\infty}\frac{1}{n!}\left\langle \phi^{(n+1)}\left(x_0+\frac{\Delta x_0}{2}\right)\frac{\Delta x_0}{\Delta t}\left(x_{-i}-x_0-\frac{\Delta x_0}{2}\right)^n\right\rangle\ . \quad \text{(A.18)}$$

This first result justifies our claim that any additive Gaussian process in a harmonic potential has a vanishing entropy production rate. Since $\langle \eta(0)x(-s)\rangle = 0$ for any $s > 0$, we are now in position to integrate out the thermal noise appearing in $\dot{x}(0)$. This allows us to obtain an unambiguous continuous expression for the entropy production rate. Indeed, in (A.17),

$$\begin{aligned}&\left\langle \dot{x}(0)\phi^{(n+1)}(x(0))\Delta(-s)^n\right\rangle \\ &= \left\langle \left(-\tau\phi'(x(0))+\sqrt{\tau}v(0)+\sqrt{2T\tau}\,\eta(0)\right)\phi^{(n+1)}(x(0))\left(x(-s)-x(0)\right)^n\right\rangle \\ &= T\tau\left\langle \phi^{(n+2)}(x(0))\left(x(-s)-x(0)\right)^n - n\phi^{(n+1)}(x(0))\left(x(-s)-x(0)\right)^{n-1}\right\rangle \\ &+ \left\langle \left(-\tau\phi'(x(0))+\sqrt{\tau}v(0)\right)\phi^{(n+1)}(x(0))\left(x(-s)-x(0)\right)^n\right\rangle\ .\end{aligned}$$

Note that the first term yields a telescopic sum. Then, using time translation invariance, one obtains the entropy production rate as

$$\sigma = \frac{2}{\tau}\left\langle \int_0^{+\infty} ds\, G(s) \left[\sum_{n=2}^{+\infty} \frac{(-1)^n}{n!} \left(-\tau\phi'(x(s)) + \sqrt{\tau} v(s)\right) \phi^{(n+1)}(x(s))\Delta(s)^n \right] \right\rangle + \frac{2}{\tau}\left\langle \int_0^{+\infty} ds\, G(s) T\tau \phi^{(3)}(x(s))\Delta(s) \right\rangle .$$

So far this exact expression still involves two-time averages. In order to reduce the result to the evaluation of stationary state averages, we first expand again Eq. (A.19) in powers of $\Delta(s)$. The entropy production rate can thus be written as the sum of two contributions

$$\sigma = \sigma_a + \sigma_b \,, \tag{A.19}$$

with the first one given by

$$\begin{aligned} \sigma_a &= 2T \int_0^{+\infty} ds\, G(s) \left\langle \phi^{(3)}(x(s))\Delta(s) \right\rangle \\ &= 2T \sum_{n=0}^{+\infty} \int_0^{+\infty} ds\, G(s) \frac{\tau^{\frac{n+1}{2}}}{n!} \left\langle \phi^{(n+3)}(x(0)) \left(\frac{\Delta(s)}{\sqrt{\tau}}\right)^{n+1} \right\rangle , \end{aligned}$$

and the second one by

$$\sigma_b = \int_0^{+\infty} ds\, G(s) \sum_{n=2}^{+\infty} \frac{2(-1)^n}{\tau n!} \left\langle \left(-\tau\phi'(x(s)) + \sqrt{\tau} v(s)\right) \phi^{(n+1)}(x(s))\Delta(s)^n \right\rangle . \tag{A.20}$$

Taylor expanding Eq. (A.20) around $x(0)$, we further express σ_b as

$$\begin{aligned} \sigma_b = &\sum_{n=2}^{+\infty}\sum_{p=0}^{+\infty} \frac{2(-1)^n}{p!\, n!} \tau^{\frac{n+p}{2}} \int_0^{+\infty} ds G(s) \left\langle \partial_x^p \left[-\phi'(x)\phi^{(n+1)}(x)\right]\big|_{x(0)} \left(\frac{\Delta(s)}{\sqrt{\tau}}\right)^{n+p} \right\rangle \\ &+ \sum_{n=2}^{+\infty}\sum_{p=0}^{+\infty} \frac{2(-1)^n}{p!\, n!} \tau^{\frac{n+p-1}{2}} \int_0^{+\infty} ds G(s) \left\langle \left[v(s)\phi^{(n+1+p)}\right]\big|_{x(0)} \left(\frac{\Delta(s)}{\sqrt{\tau}}\right)^{n+p} \right\rangle . \end{aligned}$$

Note that in Eq. (A.21), the velocity is still evaluated at time s. This raises however no difficulty since the v equation of motion can be integrated exactly as

$$v(s) = v(0)e^{-s} + \sqrt{2D}e^{-s} \int_0^s ds'\, e^{s'} \eta_2(s') \,. \tag{A.21}$$

Finally, in order to be able to use only stationary state averages when computing the entropy production rate, one needs to express $\Delta(s)$ as a function of $x(0)$. This is done by integrating the equation of motion recursively in powers of τ,

$$\frac{\Delta(s)}{\sqrt{\tau}} = -\sqrt{\tau} \int_0^s ds'\, \phi'(x(s')) + \int_0^s ds' \left(v(s') + \sqrt{2T}\eta_1(s')\right) . \tag{A.22}$$

Applying Eq. (A.22) recursively in powers of τ allows us to compute $\Delta(s)$ up to order $\tau^{\frac{3}{2}}$

$$\begin{aligned}\frac{\Delta(s)}{\sqrt{\tau}} &= -\sqrt{\tau}s\phi'(x(0)) - \tau\int_0^s ds'\frac{\phi'(x(s'))-\phi'(x(0))}{\sqrt{\tau}} + \int_0^s ds'\left(v(s')+\sqrt{2T}\eta_1(s')\right)\\ &= \int_0^s ds'\left(v(s')+\sqrt{2T}\eta_1(s')\right) - \sqrt{\tau}s\phi'(x(0)) - \tau\phi^{(2)}(x(0))\int_0^s ds'\int_0^{s'} ds''v(s'')\\ &\quad - \tau\phi^{(2)}(x(0))\int_0^s ds'\int_0^{s'} ds''\sqrt{2T}\eta_1(s'') + O(\tau^{3/2})\end{aligned}$$

where the above order in the expansion is enough to collect all terms of order τ^2 in the entropy production rate. Equation Eq. (A.23) can then be plugged into Eq. (A.20) and Eq. (A.21). After averaging over the white noises $\eta_1(s)$ and $\eta_2(s)$, this allows us to obtain the entropy production rate, up to order τ^2, solely expressed in terms of stationary state averages over both x and v. Using Eq. (A.1), we directly obtain Eq. (2.54) of the main text.

A.4 Numerical methods

To simulate dynamics Eq. (2.2), we used a discretized Heun scheme while dynamics Eq. (2.3) was integrated exactly using Gillespie's method [79]. The obtained algorithm iterates as follows :

μ = $\exp(-\mathrm{dt}/\tau)$;
σ_x = $\sqrt{D(1-\mu^2)/\tau}$;
Y_1 = $\sqrt{2D\tau\,(\mathrm{dt}/\tau - 2(1-\mu) + 0.5(1-\mu^2)) - \tau D(1-\mu)^4/(1-\mu^2)}$;
Y_2 = $\sqrt{\tau D}(1-\mu)^2/\sqrt{1-\mu^2}$;
T_1 = $\sqrt{2T\mathrm{dt}}$;
Y = x = 0;
v = $\sqrt{D/\tau}$*normal_distribution(0,1);

```
while(t < totaltime){
  η1 = normal_distribution(0,1);
  η2 = normal_distribution(0,1);
  η3 = normal_distribution(0,1);
  Y = τ*v*(1-μ) + Y1*η2 + Y2*η1;
  v = v*μ + σx*η1;
  x1 = x - dt*∂xϕ(x) + Y + T1*η3;
  x += Y + T1*η3 -0.5*dt*( ∂xϕ(x) + ∂xϕ(x1) );
  t += dt;}
```

At step (17), x(t) is stored in the variable x. The steady-state marginal in space of the distribution $\mathcal{P}_s(x)$ was then obtained by recording the particle's position recurrently into an histogram. The current J was computed using the distance travelled by the particle divided by the duration of the simulation : the error bar on J thus corresponds to the standard deviation. Such a definition for the current was heuristically found to converge faster than computing $J = \langle -\partial_x\phi + v/\sqrt{\tau}\rangle$ with recurrent recordings.

Appendix B

Sticky hard spheres in the dilute and ballistic limit

We reproduce here the appendix of [176] that is associated to Sec.4.1 of the present manuscript.

B.1 Solving the two-body Fokker-Planck equation

In this Appendix, we solve Eq. (4.15) using the method of characteristics for the sticky-sphere potential. We start by establishing Eq. (4.19) and Eq. (4.20) of the main text which describe the $\lambda \to \infty$ limit of the stationary distribution. For $h > 1/\lambda$, we obtain first

$$w\,\partial_h P + \partial_w P = 0\,. \tag{B.1}$$

In the limit $\lambda \to \infty$, we thus recover Eq. (4.19) of the main text. Next, for $h < 1/\lambda$ and for any function $j(h)$ independent of λ we define

$$\Gamma_j^\lambda(w) = \int_{-\infty}^{1/\lambda} \mathrm{d}h\, e^h P(h,w) j(h)\,, \tag{B.2}$$

so that Eq. (4.15) yields

$$\begin{aligned} &-\widehat{v}_0 \partial_w \Gamma_j^\lambda(w) + \widehat{v}_0 w \Gamma_j^\lambda(w) - \widehat{v}_0 w \left(P\left(1/\lambda, w\right) j\left(1/\lambda\right) e^{1/\lambda}\right) + \widehat{v}_0 w \Gamma_{j'}^\lambda(w) \\ &- \int_{-\infty}^{1/\lambda} \mathrm{d}h\, e^h \frac{\widehat{U}'(h)}{\sigma} j'(h) P(h,w) = 0\,. \end{aligned} \tag{B.3}$$

In the limit $\lambda \to \infty$, the stationary distribution function decays to 0 as $h < 0$ over scales $O(1/\lambda)$ and we have

$$\Gamma_j^\lambda(w) \xrightarrow[\lambda\to\infty]{} j(0) \lim_{\lambda\to\infty} \int_{-\infty}^{1} \frac{\mathrm{d}h}{\lambda}\, e^{h/\lambda}\, P\left(\frac{h}{\lambda},\, w\right) = f(0)\,\Gamma(w)\,, \tag{B.4}$$

provided the previous limit exists. This justifies the functional form in Eq. (4.18) of the main text. Hence, on one hand, for a function j defined such that $j'(0) = 0$, Eq. (B.3) yields Eq. (4.20)

$$\Gamma'(w) - w\Gamma(w) = -w \lim_{\lambda\to\infty} P\left(1/\lambda, w\right) . \tag{B.5}$$

On the other hand, for a function j such that $j(0) = 0$, Eq. (B.3) yields the integrated version of Eq. (4.26)

$$\lim_{\lambda\to\infty} \int_{-\infty}^{1/\lambda} \mathrm{d}h\, e^h j'(h) \frac{\widehat{U}'(h)}{l} P(h, w) = \widehat{v}_0 w j'(0)\Gamma(w) , \tag{B.6}$$

which gives the limit of the product $\widehat{V}'(h)P(h, w)$ as $\lambda \to \infty$. Eventually, since $\widehat{V}'(h) < \widehat{v}_0 w_0$, we obtain from Eq. (B.6)

$$\Gamma(w)\,(w - w_0) \leq 0\,, \tag{B.7}$$

which, given the positivity of $\Gamma(w)$, yields

$$\Gamma(w > w_0) = 0\,. \tag{B.8}$$

We are now in position to solve Eq. (4.19) and Eq. (4.20). In Sec. 4.1.3, the same stationary distribution will be derived in an alternative way directly from the equations of motion. For $h > 0$, Eq. (4.19) tells us that $P^b(h, w)$ is constant along the characteristics $2h-w^2 = \text{cst}$ that correspond to deterministic trajectories. These characteristic lines are depicted in Fig. B.1. We solve the equations with the boundary condition

$$P^b(L, x < 0) = 1\,, \tag{B.9}$$

where L is some large length scale introduced to treat the boundary conditions that will eventually be sent to infinity. In the relative-particle-around-a-spherical-obstacle picture this corresponds to a homogeneous reservoir of incoming particles at $h = L$. As L is sent to infinity this expresses the isotropy of the stationary distribution at large distances. The

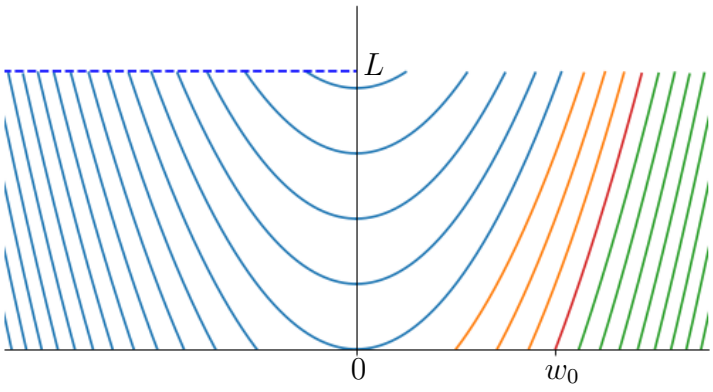

Figure B.1: Characteristics in the (w, h) plane.

blue domain in Fig. B.1, *i.e.* $\{w < 0, h\} \cup \{w > 0, 2h - w^2 > 0\}$, is made of characteristics that intersect the boundary half line $\{x < 0, h = L\}$. The quantity P^b is thus constant

and equal to one in this domain. On the contrary, P^b vanishes in the orange ($\{w > 0, 0 > 2h - w^2 > -w_0^2\}$) and green ($\{w > 0, 2h - w^2 < -w_0^2\}$) ones. Indeed, we have first $\Gamma(w > w_0) = 0$ so that Eq. (4.20) implies $P^b(0, w > w_0) = 0$ and the vanishing of P^b in the green domain. Then, we notice that the orange domain corresponds to trajectories in which the two particles escape from a collision event with $0 < w < w_0$. However, given the shape of the potential in Eq. (4.16), this never happens. Eventually, the red line $2h - w^2 = -w_0^2$ in Fig. B.1 plays a special role. Indeed, all trajectories leading to a collision event between the two particles collapse onto this line as they separate afterwards. We thus look for a solution of Eq. (4.19) of the form

$$P^b(h, w) = P_0(h, w) + f(h)\,\delta\left(h - \frac{w^2}{2} + \frac{w_0^2}{2}\right)\Theta(w)\,, \tag{B.10}$$

with $P_0(h, w)$ a piece-wise continuous function whose form was derived above. Equation (4.19) then yields

$$f'(h) = 0 \Rightarrow f(h) = f(0)\,. \tag{B.11}$$

The constant $f(0)$ is then found by integrating Eq. (4.20) between w_0^- and w_0^+. This yields

$$f(0) = \Gamma(w_0^-)\,. \tag{B.12}$$

We are now in position to solve Eq. (4.20). For $w < 0$, $P^b(0, w) = 1$ and we obtain

$$\Gamma'(w) - w\Gamma(w) = -w\,, \tag{B.13}$$

so that

$$\Gamma(w) = Ae^{w^2/2} + 1\,, \tag{B.14}$$

with A an integration constant that is set to 0 to ensure the integrability of $\Gamma(w)$ against $e^{-w^2/2}$. For $0 < w < w_0$, we have $P^b(0, w) = 0$ and thus

$$\Gamma(w) = e^{w^2/2}\,, \tag{B.15}$$

where the integration constant was chosen to ensure continuity at $w = 0$. We have therefore derived Eq.(4.21)

$$P_b(h, w) = \Theta(h)\left[1 - \Theta(w)\Theta\left(\frac{w^2}{2} - h\right) + \Theta(w)e^{\frac{w_0^2}{2}}\,\delta\left(h - \frac{w^2}{2} + \frac{w_0^2}{2}\right)\right] \tag{B.16}$$

and Eq. (4.22)

$$\Gamma(w) = \Theta(-w) + \Theta(w)\Theta(w_0 - w)e^{\frac{w^2}{2}} \tag{B.17}$$

of the main text.

B.2 Dynamical Mean-Field with a sticky potential

B.2.1 Trajectories

Here we solve the equation of motion of the rescaled gap $h(t)$ as defined in Eq. (4.41), for a sticky potential such as the one defined in Eq. (4.16). The trajectories start as

$$h_{01}(t) = h_0 + \xi_0 t + t^2/2 \,, \tag{B.18}$$

so, the attractive region is reached when $h(t) = 1/\lambda$ at time

$$t_1 = -\xi_0 - \sqrt{\xi_0^2 - 2(h_0 - 1/\lambda)} \,. \tag{B.19}$$

This happens for (ξ_0, h_0) such that

$$\xi_0 < 0 \quad \wedge \quad h_0 < \frac{1}{\lambda} + \frac{\xi_0^2}{2} \,. \tag{B.20}$$

For all other values of (ξ_0, h_0), the trajectory always stays in the noninteracting region. We therefore define the new variable $\alpha = \sqrt{\xi_0^2 - 2(h_0 - 1/\lambda)} > 0$, so that

$$t_1 = -\xi_0 - \alpha \,. \tag{B.21}$$

The condition $h_0 > 1/\lambda$ implies $\alpha < |\xi_0|$, and since $\xi_0 < 0$ for the trajectories of our interest we have

$$0 < \alpha < -\xi_0 \quad \wedge \quad \xi_0 < 0 \qquad \Leftrightarrow \qquad \alpha > 0 \quad \wedge \quad \xi_0 < -\alpha \,. \tag{B.22}$$

Finally, the weight in the integrals reduces to

$$\mathcal{D}\xi_0 \, \mathrm{d}h_0 \, e^{h_0} = \frac{1}{\sqrt{2\pi}} \mathrm{d}\xi_0 e^{-\xi_0^2/2} \, \alpha \, \mathrm{d}\alpha \, e^{1/\lambda + \xi_0^2/2 - \alpha^2/2} = \frac{e^{1/\lambda}}{\sqrt{2\pi}} \, \mathrm{d}\xi_0 \, \alpha \, \mathrm{d}\alpha \, e^{-\alpha^2/2} \,. \tag{B.23}$$

Tangential trajectories

Assuming we have entered the attractive region, we have the Cauchy problem

$$\begin{cases} \dot{h}(t) = \lambda w_0 h(t) - w_0 + \xi_0 + t \\ h(t_1) = \dfrac{1}{\lambda} \end{cases} , \tag{B.24}$$

which is valid for $0 < h(t) < 1/\lambda$. The analytical solution is

$$h_1(t) = \frac{1}{(\lambda w_0)^2} \left[-1 + \lambda w_0^2 + \lambda w_0 \alpha - \lambda w_0 (t - t_1) + e^{\lambda w_0 (t - t_1)} \left(1 - \lambda w_0 \alpha\right) \right] \,. \tag{B.25}$$

For later convenience, we define $z = \lambda w_0 \alpha - 1$ and $x = t - t_1$. Thus, we can rewrite

$$h_1(x = t - t_1) = \frac{1}{\lambda w_0} \left[w_0 - x - \frac{z}{\lambda w_0} \left(e^{\lambda w_0 x} - 1 \right) \right] . \tag{B.26}$$

There are now two possibilities:

1. the trajectory is tangential, $h_{\min}(t) > 0$ and therefore it crosses the attractive region and leaves it at a given time t_5;

2. the trajectory is colliding, therefore there is a positive $x = t - t_1$ at which $h(t) = 0$.

We need to solve the equation $h_1(t) = 0$. Its solution leads to

$$t - t_1 = \frac{1}{\lambda w_0}\left[\lambda w_0^2 + z - W\left(z e^{\lambda w_0^2 + z}\right)\right] , \tag{B.27}$$

where $W(x)$ is the Lambert function. The Lambert function has one branch for $x > 0$ and two branches for $-e^{-1} < x < 0$. Therefore, x exists if

$$\begin{aligned} & z e^{\lambda w_0^2 + z} > -e^{-1} \quad \Rightarrow \quad z e^z > -e^{-1-\lambda w_0^2} \\ & \Rightarrow \quad z < z_1 = W_{-1}\left(-e^{-1-\lambda w_0^2}\right) \vee z > z_2 = W_0\left(-e^{-1-\lambda w_0^2}\right) \end{aligned} \tag{B.28}$$

Given $z = \lambda w_0 \alpha - 1 > -1$ and $z_1 < -1$, the *colliding condition* reduces to $z > z_2$. We also note that $x = t - t_1 > 0$ for every z satisfying this condition. Indeed, if $z < 0$ there are two possible values of x, corresponding to the fact that the coefficient of the exponential in Eq. (B.26) is positive and therefore the *virtual* trajectory would cross the barrier twice and then diverge to $+\infty$; in this case, the primary branch of the Lambert function corresponds to the first intersection and the secondary branch to the second one.
On the other hand, if $z > 0$ there is only one intersection with the barrier because the virtual trajectory diverges to $-\infty$, corresponding to the unique branch of $W(x)$ for $x > 0$. This result further divides the (ξ_0, z) plane into the following cases

$$\begin{aligned} -1 < z < z_2 \quad & \Rightarrow \quad \text{tangential trajectory} \\ z > z_2 \quad & \Rightarrow \quad \text{colliding trajectory} \end{aligned} \tag{B.29}$$

Having found the values of z for which the trajectory is tangential, we can now compute the exit time t_5 (t_i with $i = 2, 3, 4$ will be reserved for colliding trajectories): we need indeed to solve the equation

$$h_1(t) = \frac{1}{\lambda} \quad \Rightarrow \quad \delta t_{15}(z) = t_5 - t_1 = \frac{1}{\lambda w_0}\left[z - W_{-1}\left(z e^z\right)\right] . \tag{B.30}$$

The two branches of $W(x)$ give two solutions: since $-1 < z < 0$, we have that $W_0(z e^z) = z$ and the solution above gives the trivial result $t_5 = t_1$; the second branch gives $W_{-1}(z e^z) < z$ and therefore a positive result for $\delta t_{15}(z)$.

So we have the trajectory from t_1 (entrance time) to t_5 (exit time), where the particle crosses the attractive region and contributes to the kernels.

Colliding trajectories

We now compute the colliding trajectories, which require $\xi_0 < -\alpha = -(1+z)/(\lambda w_0)$ and $z > z_2$.

Attractive region 1: zone 12 The motion in the attractive region towards the barrier has been already computed in Eq. (B.26). We recall the trajectory from Eq. (B.26) and the colliding time t_2 from Eq. (B.27), *i.e.*

$$h_1(x = t - t_1) = \frac{1}{\lambda w_0}\left[w_0 - x - \frac{z}{\lambda w_0}\left(e^{\lambda w_0 x} - 1\right)\right]. \tag{B.31}$$

$$\delta t_{12}(z) = t_2 - t_1 = \frac{1}{\lambda w_0}\left[\lambda w_0^2 + z - W_0\left(z e^{\lambda w_0^2 + z}\right)\right] . \tag{B.32}$$

Repulsive region: zone 23 The motion in the repulsive region needs the solution of the Cauchy problem

$$\begin{cases} \dot{h}(t) = -\lambda w_0 h(t) - w_0 + \xi_0 + t \\ h(t_2) = 0 \end{cases} \tag{B.33}$$

Its solution reads

$$h_2(x = t - t_2) = \frac{1}{\lambda w_0}\left[x - \frac{w(z)}{\lambda w_0}\left(1 - e^{-\lambda w_0 x}\right)\right] , \tag{B.34}$$

being $w(z) = 2 + W_0\left(z e^{\lambda f_0^2 + z}\right)$. Hence the exit time:

$$\delta t_{23}(z) = t_3 - t_2 = \frac{1}{\lambda w_0}\left[w(z) + W_0\left(-w(z)e^{-w(z)}\right)\right] . \tag{B.35}$$

Since $-w(z) < -1$, then $W_{-1}(-we^{-w}) = -w$ so the secondary branch gives the trivial solution $t_3 = t_2$; therefore we choose the primary branch W_0 into Eq. (B.35).

Attractive region 2: zone 34 For $t > t_3$, the particle enters back the attractive region, *i.e.*

$$\begin{cases} \dot{h}(t) = \lambda w_0 h(t) - w_0 + \xi_0 + t \\ h(t_3) = 0 \end{cases} , \tag{B.36}$$

yielding the solution

$$h_3(x = t - t_2) = \frac{1}{\lambda w_0}\left\{-x + \frac{1}{\lambda w_0}\left[2 + W_0\left(-w(z)e^{-w(z)}\right)\right]\left(e^{\lambda w_0 x} - 1\right)\right\} . \tag{B.37}$$

The exit time at which $h(t) = 1/\lambda$ is given by

$$\delta t_{34}(z) = t_4 - t_3 = -\frac{1}{\lambda w_0}\left\{w_{34}(z) + \lambda w_0^2 + W_{-1}\left[-w_{34}(z)e^{-\left(w_{34}(z) + \lambda w_0^2\right)}\right]\right\} , \tag{B.38}$$

having called $w_{34}(z) = 2 + W_0\left(-w(z)e^{-w(z)}\right)$. The secondary branch W_{-1} of the Lambert function has been chosen because of the condition $\delta t_{34} > 0$.

For $t > t_4$, the particle leaves the attractive region and diverges to $h \to \infty$ without giving any further contribution to the kernels.

B.2.2 Fluctuating response

Before proceeding with the computation of the kernels, we need to compute the fluctuating response $H(t,s)$ in any of the previously defined zones. In the dilute limit (first iteration), the dynamics of $H(t,s)$ in Eq. (4.33) reduces to (working in rescaled time)

$$\frac{\partial}{\partial t}H(t,s) = -\widehat{U}''(h(t))\left[H(t,s) - \delta(t-s)\right] \ . \tag{B.39}$$

We know that $H(t,s) = 0 \ \ \forall t < s$ because of causality. The delta term in the rhs is equivalent to an initial condition $H(t = s^+, s) = \widehat{U}''(h(s))$. Therefore, Eq. (B.39) has the general solution

$$H(t,s) = \begin{cases} 0 & t < s \\ \widehat{U}''(h(s)) \exp\left[-\int_s^t \mathrm{d}t' \widehat{U}''(h(t'))\right] & t > s \end{cases} . \tag{B.40}$$

The potential defined in Eq. (4.16) has a piece-wise constant second derivative; we can compute $H(t,s)$ as a piece-wise defined function depending only on the time zones. Since $H(t,s) > 0$ only if s is in a region where interaction is present, we can restrict the computation to these zones. Furthermore, the definition of $\mathcal{M}_R(t,s)$ in Eq. (4.32) shows that there is a contribution only at times t where the interaction is present, then we will consider only the cases $t_1 < s < t < t_5$ (tangential trajectories) and $t_1 < s < t < t_4$ (colliding trajectories).

Tangential trajectories

We have only one time zone, so $t_1 < s < t < t_5$. In this region the second derivative is constant and has $\widehat{U}''(h) = -\lambda w_0$, so

$$H_{15}(t,s) = -\lambda w_0 e^{\lambda w_0 (t-s)} \qquad t_1 < s < t < t_5 \ . \tag{B.41}$$

Colliding trajectories

Following the same reasoning as above and using Eq. (B.40), we can compute $H(t,s)$ for any possible combination of $t_1 < s < t < t_4$, which will include "self" terms (when s and t are in the same time zone) and "mixed" terms (when they belong to different zones). So, for the self terms we find

$$H_{12}(t,s) = -\lambda w_0 e^{\lambda w_0 (t-s)} \qquad t_1 < s < t < t_2 \ , \tag{B.42}$$

$$H_{23}(t,s) = \lambda w_0 e^{-\lambda w_0 (t-s)} \qquad t_2 < s < t < t_3 \ , \tag{B.43}$$

$$H_{34}(t,s) = -\lambda w_0 e^{\lambda w_0 (t-s)} \qquad t_3 < s < t < t_4 \ , \tag{B.44}$$

and for the mixed terms

$$H_{13}(t,s) = -\lambda w_0 e^{-\lambda w_0 (t-2t_2+s)} \qquad t_1 < s < t_2 < t < t_3 \ , \tag{B.45}$$

$$H_{14}(t,s) = -\lambda w_0 e^{\lambda w_0 (t-2t_3+2t_2-s)} \qquad t_1 < s < t_2 < t_3 < t < t_4 \ , \tag{B.46}$$

$$H_{24}(t,s) = \lambda w_0 e^{\lambda w_0 (t-2t_3+s)} \qquad t_2 < s < t_3 < t < t_4 \ . \tag{B.47}$$

B.2.3 Kernels

We now compute the dynamical kernels to the first order in the rescaled density $\widehat{\varphi}$, starting from the definitions given in Eq. (4.32).

First, we note that these can be computed as the sum of the kernels computed separately on the different time zones, namely

$$\kappa(t) = \kappa_{15}(t) + \kappa_{12}(t) + \kappa_{23}(t) + \kappa_{34}(t) \,, \tag{B.48}$$

and

$$\mathcal{M}_R(t,s) = \mathcal{M}_R^{15}(t,s)+\mathcal{M}_R^{12}(t,s)+\mathcal{M}_R^{23}(t,s)+\mathcal{M}_R^{34}(t,s)+\mathcal{M}_R^{13}(t,s)+\mathcal{M}_R^{14}(t,s)+\mathcal{M}_R^{24}(t,s)\,. \tag{B.49}$$

Second, as mentioned in Eq. (4.48) we assume that the retarded memory $\mathcal{M}_R(t,s)$ is short ranged because of the vanishing duration of a collision in the hard-core limit; we are therefore interested in computing the stiffness $\gamma(t)$ and the friction correction $\chi_1(t)$, defined as

$$\begin{aligned} \gamma(t) &= \kappa(t) - \int_0^t \mathrm{d}s\, \mathcal{M}_R(t,s) = \kappa(t) - \chi_0(t) \\ \chi_1(t) &= \int_0^t \mathrm{d}s\, \mathcal{M}_R(t,s)\,(t-s) \end{aligned} \tag{B.50}$$

We expect that $\gamma(t)$ vanishes in the steady state, so that $h(t)$ is not confined at long times (otherwise we would be in the glassy phase at any density) and that $\chi_1(t)$ goes to a constant depending on the density, giving us the first-order density correction to the activity and to the MSD.

We will show in Appendix B.2.4 that higher order terms do not contribute to the dynamics.

Change of variables

We perform the computation of the kernels in the (x,z) plane, being $x = t - t_i$ for every time zone starting in t_i and $z = \lambda w_0 \alpha - 1$, as defined in Sec. B.2.1. Since $t_1 = -\xi_0 - \alpha > 0$, then $\xi_0 = -\alpha - t_1 = -(1+z)/(\lambda w_0) - t_1$.
When performing the integrals over ξ_0 and z, we will choose the normal region $z > -1$ and $\xi_0 < -(1+z)/(\lambda w_0)$. The latter condition implies $t_1 > 0$.

This choice is particularly convenient to implement the time zone conditions *e.g.* $\Theta(t_i < t < t_j)$. The former actually translates to $0 < x < \delta t_{i,j}$ in every time region, where one typically has $j = i+1$. So we move from the integration over ξ_0 to the integration over $x = t - t_i = t - \delta t_{1i} - t_1 = t - \delta t_{1i} + \xi_0 + (1+z)/(\lambda w_0)$.
The condition $\xi_0 < -(1+z)/(\lambda w_0)$ then implies $x < t - \delta t_{1i}$. The typical times δt_{1i} are those computed in Appendix B.2.1; but since we are interested in the long-time limit, the assumption $t \to \infty$ automatically satisfies this condition; hence the integration region for

$\alpha > 0$, $\xi_0 < -\alpha$ and $t_i < t < t_j$ is equivalent in the long time limit to[1]

$$z > -1 \quad , \quad 0 < x < \delta t_{ij}(z) \, . \tag{B.51}$$

For tangential trajectories, we have $-1 < z < z_2$, while for colliding trajectories we have $z > z_2$.

The Gaussian weight in the integral then becomes

$$\frac{\widehat{\varphi}}{2} \frac{e^{1/\lambda}}{\sqrt{2\pi}} \alpha \, e^{-\alpha^2/2} \, \mathrm{d}\alpha \, \mathrm{d}\xi_0 = \frac{\widehat{\varphi}}{2} \frac{e^{1/\lambda}}{\sqrt{2\pi}} \frac{1+z}{(\lambda w_0)^2} \, e^{-(1+z)/(2(\lambda w_0)^2)} \, \mathrm{d}z \, \mathrm{d}x \equiv I_0(z) \, \mathrm{d}z \, \mathrm{d}x \, . \tag{B.52}$$

With all these precautions we can directly plug into the kernel integration the trajectories computed as functions of z, x in Sec. B.2.1. The computation is tedious but straightforward, and we will repeatedly apply the following formulas:

$$\begin{aligned} \kappa_{ij} &= \int \mathrm{d}z \, I_0(z) \int_0^{\delta t_{ij}(z)} \mathrm{d}x \, \left[\widehat{U}''(h(t)) + \widehat{U}'(h(t)) \right] \, , \\ \chi_n^{ij} &= \int \mathrm{d}z \, I_0(z) \int_0^{\delta t_{ij}(z)} \mathrm{d}x \, \widehat{U}''(h(t)) \int_0^t \mathrm{d}s \, H_{ij}(t,s)(t-s)^n \, \theta(t_i < s < t) \, , \end{aligned} \tag{B.53}$$

where ij are the time zone indices, integrating over the appropriate domain of z and recalling that $t = t_i + x$.

Tangential trajectories

For tangential trajectories we only have one time zone $t_1 < t < t_5$ and the tangential condition $-1 < z < z_2$: using Eqs. (B.26) and (B.41) we find

$$\gamma_{15} = \int_{-1}^{z_2} \mathrm{d}z \, I_0(z) \left[-\frac{z}{\lambda w_0} \delta t_{15}(z) + \frac{1}{2} \delta t_{15}^2(z) + \left(-1 + \frac{z}{(\lambda w_0)^2} \right) \left(e^{\lambda w_0 \delta t_{15}(z)} - 1 \right) \right] \, , \tag{B.54}$$

and

$$\chi_1^{15} = \int_{-1}^{z_2} \mathrm{d}z \, I_0(z) \left[\delta t_{15}(z) + \frac{2}{\lambda w_0} + \left(\delta t_{15}(z) - \frac{2}{\lambda w_0} \right) e^{\lambda w_0 \delta t_{15}(z)} \right] \, . \tag{B.55}$$

Colliding trajectories

We have now several time zones and the collisional condition $z > z_2$. We explicitly write the result for every time zone following Eq. (B.53).

[1] If one wants to recover the time dependence of the kernels, it is sufficient to substitute the upper bound of the integration over x with $\min(\delta t_{ij}(z), t - \delta t_{1i})(z)$.

Stiffness terms:

$$
\begin{aligned}
\gamma_{12} &= \int_{z_2}^{+\infty} \mathrm{d}z\, I_0(z) \left[-\frac{z}{\lambda w_0} \delta t_{12}(z) + \frac{1}{2} \delta t_{12}^2(z) + \left(-1 + \frac{z}{(\lambda w_0)^2} \right) \left(e^{\lambda w_0 \delta t_{12}(z)} - 1 \right) \right] , \\
\gamma_{23} &= \int_{z_2}^{+\infty} \mathrm{d}z\, I_0(z) \left[\left(w_0 - \frac{w(z)}{\lambda w_0} \right) \delta t_{23}(z) + \frac{1}{2} \delta t_{23}^2(z) + \left(1 + \frac{w(z)}{(\lambda w_0)^2} \right) \left(1 - e^{-\lambda w_0 \delta t_{23}(z)} \right) \right] , \\
\gamma_{34} &= \int_{z_2}^{+\infty} \mathrm{d}z\, I_0(z) \left[\left(w_0 + \frac{w_{34}(z)}{\lambda w_0} \right) \delta t_{34}(z) + \frac{1}{2} \delta t_{34}^2(z) + \left(-1 - \frac{w_{34}(z)}{(\lambda w_0)^2} \right) \left(e^{\lambda w_0 \delta t_{34}(z)} - 1 \right) \right] , \\
\gamma_{13} &= \int_{z_2}^{+\infty} \mathrm{d}z\, I_0(z) \left(e^{\lambda w_0 \delta t_{12}(z)} - 1 \right) \left(1 - e^{-\lambda w_0 \delta t_{23}(z)} \right) , \\
\gamma_{14} &= - \int_{z_2}^{+\infty} \mathrm{d}z\, I_0(z)\, e^{-\lambda w_0 \delta t_{23}(z)} \left(e^{\lambda w_0 \delta t_{34}(z)} - 1 \right) \left(e^{\lambda w_0 \delta t_{12}(z)} - 1 \right) , \\
\gamma_{24} &= \int_{z_2}^{+\infty} \mathrm{d}z\, I_0(z) \left(e^{\lambda w_0 \delta t_{34}(z)} - 1 \right) \left(1 - e^{-\lambda w_0 \delta t_{23}(z)} \right) .
\end{aligned}
\tag{B.56}
$$

Friction correction:

$$
\begin{aligned}
\chi_1^{12} &= \int_{z_2}^{+\infty} \mathrm{d}z\, I_0(z) \left[\delta t_{12}(z) + \frac{2}{\lambda w_0} + \left(\delta t_{12}(z) - \frac{2}{\lambda w_0} \right) e^{\lambda w_0 \delta t_{12}(z)} \right] , \\
\chi_1^{23} &= \int_{z_2}^{+\infty} \mathrm{d}z\, I_0(z) \left[\delta t_{23}(z) - \frac{2}{\lambda w_0} + \left(\delta t_{23}(z) + \frac{2}{\lambda w_0} \right) e^{-\lambda w_0 \delta t_{23}(z)} \right] , \\
\chi_1^{34} &= \int_{z_2}^{+\infty} \mathrm{d}z\, I_0(z) \left[\delta t_{34}(z) + \frac{2}{\lambda w_0} + \left(\delta t_{34}(z) - \frac{2}{\lambda w_0} \right) e^{\lambda w_0 \delta t_{34}(z)} \right] , \\
\chi_1^{13} &= \int_{z_2}^{+\infty} \mathrm{d}z\, I_0(z) \left[-\delta t_{12}(z) e^{\lambda w_0 \delta t_{12}(z)} - \delta t_{23}(z) e^{-\lambda w_0 \delta t_{23}(z)} + \delta t_{13}(z) e^{-\lambda w_0 [\delta t_{23}(z) - \delta t_{12}(z)]} \right] , \\
\chi_1^{14} &= \int_{z_2}^{+\infty} \mathrm{d}z\, I_0(z)\, e^{-\lambda w_0 \delta t_{23}(z)} \left[-\frac{2}{\lambda w_0} + \delta t_{23}(z) + \left(\frac{2}{\lambda w_0} - \delta t_{13}(z) \right) e^{\lambda w_0 \delta t_{12}(z)} \right. \\
&\qquad \left. + \left(\frac{2}{\lambda w_0} - \delta t_{24}(z) \right) e^{\lambda w_0 \delta t_{34}(z)} + \left(-\frac{2}{\lambda w_0} + \delta t_{14}(z) \right) e^{\lambda w_0 (\delta t_{12}(z) + \delta t_{34}(z))} \right] , \\
\chi_1^{24} &= \int_{z_2}^{+\infty} \mathrm{d}z\, I_0(z) \left[-\delta t_{23}(z) e^{-\lambda w_0 \delta t_{23}(z)} - \delta t_{34}(z) e^{\lambda w_0 \delta t_{34}(z)} + \delta t_{24}(z) e^{\lambda w_0 [\delta t_{34}(z) - \delta t_{23}(z)]} \right] .
\end{aligned}
\tag{B.57}
$$

B.2.4 Hard-sphere limit

The expressions written above are exact in the long-time limit. To obtain an analytical expression, we move to the hard-sphere limit $\lambda \to \infty$, which we use to approximate the behavior of the stiffness and of the friction correction.

The analytical computation requires the approximation of the Lambert function W in the different intervals of the integration over z. We computed the integrations in the previous equations both analytically and numerically; we omit the details of the computation

because they are tedious. Altogether, the only terms that survive when $\lambda \to \infty$ are

$$\gamma_{15} = -\gamma_{23} = -w_0^2/2 \,, \tag{B.58}$$

$$\chi_1^{15} = \frac{\widehat{\varphi}}{6\sqrt{2\pi}} w_0^3 \,, \quad \chi_1^{23} = \frac{\widehat{\varphi}}{4} \,. \tag{B.59}$$

This final result is crucial and tells us that (i) the elastic response $\gamma(t)$ vanishes in the long-time limit, and the particles can diffuse; (ii) the friction correction χ_1 leading to the effective self-propulsion has two contributions, one coming from the purely repulsive interaction $-\chi_1^{23}-$ and the other from the attractive region $-\chi_1^{15}-$, so that one finally finds

$$\chi_1 = \frac{\widehat{\varphi}}{4} \left(1 + \frac{\sqrt{2}}{3\sqrt{\pi}} w_0^3 \right) \,. \tag{B.60}$$

Vanishing terms

Here we sketch the reason why we stopped to the first-order in the expansion of the integrated response in Eq. (4.48): when we need to compute the integral $\int_{t_i}^{t} \mathrm{d}s \, H(t,s)(t-s)^n$, the fluctuating response has an exponential behavior and decays with a characteristic time $(\lambda w_0)^{-1}$. Therefore, when computing the instantaneous response κ and the zero-th order contribution χ_0, these both diverge separately as $\mathcal{O}(\lambda)$ in the hard-sphere limit but their difference has a finite limit. When computing χ_1, the first degree term $(t-s)$ in the integral lowers one degree in λ and its contribution is therefore finite.

This scheme repeats when computing χ_2, and lowering another degree in λ implies $\chi_2 = \mathcal{O}(\lambda^{-1})$, therefore all the χ_n vanish in the hard-sphere limit for $n \geq 2$.

Appendix C

Franz-Parisi approach to the glass transition with the potential inferred from active hard spheres

In this appendix, we show that equilibrium colloidal particles whose pair-potential is given in Eq. (4.140) of the main text experience a dynamical glass transition at the same density $\widehat{\varphi}_d$ as particles interacting through the standard Baxter potential

$$\mathrm{e}^{-\widehat{\beta}\widehat{U}_p(h)} = \theta(h) + \frac{1}{2}\delta(h)\,, \tag{C.1}$$

i.e. with a flat bulk distribution, for which $\widehat{\varphi}_d$ was computed in [190, 189] and reads $\widehat{\varphi}_d = 4$. In the Franz-Parisi approach [63], the ergodicity breaking is due to the appearance of long-lived metastable states. The latter is probed by studying the free energy of the system constrained to be at a distance a from a given liquid configuration which is then averaged out. At small densities, this average free energy, also called the Franz-Parisi potential, has a unique minimum at $a \to \infty$ suggesting that the system can diffuse away from any given liquid configuration. At higher densities, the existence of a local minimum at finite a is the sign of a caging effect: the system remains trapped in the vicinity of the reference liquid configuration. The smallest density at which this happens is the dynamical glass transition one $\widehat{\varphi}_d$. We stress that in the limit of infinite dimension, the predicted $\widehat{\varphi}_d$ in the Franz-Parisi approach equals the density at which the diffusion coefficient of the same equilibrium colloids vanishes [136].

Concretely, we want to find out $\widehat{\varphi}_d$ such that

$$\widehat{\varphi}_d^{-1} = \max_a \left[-a \int \mathrm{d}z \mathrm{e}^z \partial_a q(a,z) \ln q(a,z) \right] \tag{C.2}$$

and what the corresponding value of a is. In the above formula, we have introduced the function q defined by

$$q(a,z) = \int \mathrm{d}h g(h) \frac{\mathrm{e}^{-\frac{(h-z-a)^2}{4a}}}{\sqrt{4\pi a}} \tag{C.3}$$

The function $g(h)$ is the pair correlation function expressed in terms of the reduced space variable $h = d\frac{r-\sigma}{\sigma}$. In our case, we have $g(h) = \theta(h)f(h)+\frac{1}{2}\delta(h)$ with the bulk contribution

$$f(h) = \frac{\mathrm{e}^{-h}}{\sqrt{4\pi h}} + \frac{\mathrm{erf}(\sqrt{h})+1}{2}\,. \tag{C.4}$$

Numerical inspection of the expression in the right-hand side of Eq. (C.2) shows that the maximum is reached at $a = 0$ as in [190]. In the following, we therefore focus on the behavior of the above mentioned expression at leading order for $a \to 0$. Following [190], we find it convenient to rewrite q as

$$\begin{aligned} q(a,z) &= \int \mathrm{d}h' g(h'\sqrt{a}) \frac{\mathrm{e}^{-\frac{(h'-z'-\sqrt{a})^2}{4}}}{\sqrt{4\pi}} \\ &= \int \mathrm{d}h' f(h'\sqrt{a}) \frac{\mathrm{e}^{-\frac{(h'-z'-\sqrt{a})^2}{4}}}{\sqrt{4\pi}} + \frac{1}{2\sqrt{a}} \frac{\mathrm{e}^{-\frac{(z'+\sqrt{a})^2}{4}}}{\sqrt{4\pi}} \\ &= O(a^{-1/4}) + \frac{1}{2\sqrt{a}} \left[\frac{\mathrm{e}^{-\frac{z'^2}{4}}}{\sqrt{4\pi}} \right] \end{aligned} \tag{C.5}$$

with $z' = z/\sqrt{a}$ and $g(h'\sqrt{a}) = \theta(h')f(h')+\frac{1}{2\sqrt{a}}\delta(h')$ and $f(h') = \frac{1}{2}+\frac{\mathrm{erf}(a^{1/4}\sqrt{h'})}{2}+\frac{\mathrm{e}^{-\sqrt{a}h'}}{\sqrt{4\pi h' a^{1/4}}}$. As $a \to 0$ the leading contribution comes from the coefficient of the surface contribution $\delta(h')$. The condition for the structure captured by the function f to be negligible is that $x^2 f'(x) \to 0$ as $x \to 0$. Hence, to leading order as $a \to 0$, we have that

$$\ln q(a,z') = -\frac{1}{2}\ln a + \mathrm{cst} - \frac{z'^2}{4} + o(1) \tag{C.6}$$

and

$$\partial_a q(a,z') = -\frac{1}{4a^{3/2}} \frac{\mathrm{e}^{-\frac{z'^2}{4}}}{\sqrt{4\pi}} \left(1 - \frac{z'^2}{2}\right) + o(a^{-3/2}) \tag{C.7}$$

hence, to leading order as $a \to 0$,

$$\begin{aligned} -a \int \mathrm{d}z \mathrm{e}^z \partial_a q(a,z) \ln q(a,z) &= -\frac{1}{4} \int \mathrm{d}z' \frac{\mathrm{e}^{-\frac{z'^2}{4}}}{\sqrt{4\pi}} \left[\left(1 - \frac{z'^2}{2}\right) \frac{z'^2}{4} \right] \\ &= \frac{1}{4}\,, \end{aligned} \tag{C.8}$$

as the contribution given by the other terms of the log vanishes. Therefore, colloidal particles interacting through the dressed Baxter potential potential in Eq. (4.140) undergo a dynamical glass transition at $\widehat{\varphi}_d = 4$ with an associated cage size of 0 as do colloidal particles interacting via the standard Baxter one of Eq. (C.1). Remark that $\widehat{\varphi}_d$ is also the density at which the effective self-propulsion of the original RTP dynamics is predicted to vanish in our approximate resummation scheme.

Appendix D

Effective diffusion constant

In this appendix, we show the relation that exists between the long-time diffusion constant and the effective self-propulsion speed within our approximate resummation scheme of the hierarchy (see Sec. 4.2) in the ultraballistic limit. We consider an assembly of RTPs interacting via a hard sphere potential and initialized in the stationary state. We consider the infinite dimensional limit and the scalings are those of Sec. 4.2. For each particle we split its motion between a longitudinal contribution along $\mathbf{u}_i(t)$ and a transverse one,

$$\begin{aligned} \frac{\mathrm{d}\mathbf{r}_i}{\mathrm{d}t} &= v_0 \mathbf{u}_i(t) - \sum_{j\neq i} \boldsymbol{\nabla}_{\mathbf{r}_i} U(\mathbf{r}_i - \mathbf{r}_j)\,, \\ &= \dot{\mathbf{r}}_i^{\parallel}(t)\mathbf{u}_i(t) + \dot{\mathbf{r}}_i^{\perp}(t)\,, \end{aligned} \tag{D.1}$$

with

$$\dot{\mathbf{r}}_i^{\parallel} = \left[v_0 - \sum_{j\neq i} \boldsymbol{\nabla}_{\mathbf{r}_i} U(\mathbf{r}_i - \mathbf{r}_j) \cdot \mathbf{u}_i(t) \right]\,, \tag{D.2}$$

the longitudinal velocity, and

$$\dot{\mathbf{r}}_i^{\perp} = -\sum_{j\neq i} \boldsymbol{\nabla}_{\mathbf{r}_i} U(\mathbf{r}_i - \mathbf{r}_j) + \sum_{j\neq i} \left(\boldsymbol{\nabla}_{\mathbf{r}_i} U(\mathbf{r}_i - \mathbf{r}_j) \cdot \mathbf{u}_i(t)\right) \mathbf{u}_i(t)\,, \tag{D.3}$$

the transverse one. In the following, the notation $\langle \dots \rangle$ denotes an average over all the degrees of freedom of the system but the instantaneous self-propulsion vector $\mathbf{u}_i$ of particle i. At any time t, the probability distribution of the N-body system is the stationary one and hence the mean longitudinal velocity is given by,

$$\left\langle \dot{\mathbf{r}}_i^{\parallel}(t) \right\rangle = v(\widehat{\varphi})\,. \tag{D.4}$$

We now evaluate its one-time fluctuations. We have,

$$\begin{aligned}\left\langle \dot{\mathbf{r}}_i^{\parallel\,2}(t)\right\rangle - v(\widehat{\varphi})^2 &= v_0^2 + 2v_0(v(\widehat{\varphi})-v_0) - v(\widehat{\varphi})^2 \\ &\quad + \left\langle \sum_{j\neq i}\sum_{k\neq i} \left[\boldsymbol{\nabla}_{\mathbf{r}_i} U(\mathbf{r}_i-\mathbf{r}_j)\cdot\mathbf{u}_i(t)\right]\left[\boldsymbol{\nabla}_{\mathbf{r}_i} U(\mathbf{r}_i-\mathbf{r}_k)\cdot\mathbf{u}_i(t)\right]\right\rangle , \\ &= -(v_0 - v(\widehat{\varphi}))^2 + \sum_{j\neq i}\sum_{\substack{k\neq i\\ k\neq j}} \left\langle \left[\boldsymbol{\nabla}_{\mathbf{r}_i} U(\mathbf{r}_i-\mathbf{r}_j)\cdot\mathbf{u}_i(t)\right]\left[\boldsymbol{\nabla}_{\mathbf{r}_i} U(\mathbf{r}_i-\mathbf{r}_k)\cdot\mathbf{u}_i(t)\right]\right\rangle \\ &\quad + \sum_{j\neq i}\left\langle \left[\boldsymbol{\nabla}_{\mathbf{r}_i} U(\mathbf{r}_i-\mathbf{r}_j)\cdot\mathbf{u}_i(t)\right]^2\right\rangle .\end{aligned} \tag{D.5}$$

The last term yields contributions that are of order $O(d^2)$ and can therefore be dropped in the large d limit as all the other terms scale as $O(d^3)$. Evaluating the second one amounts at computing

$$\begin{aligned}&\rho^2 \int\int \mathrm{d}\mathbf{r}\mathrm{d}\mathbf{r}' \frac{\mathrm{d}\mathbf{u}}{\Omega_d}\frac{\mathrm{d}\mathbf{u}'}{\Omega_d} g^{(3)}(0,\mathbf{u}_1;\mathbf{r},\mathbf{u};\mathbf{r}',\mathbf{u}')\left[\boldsymbol{\nabla}_{\mathbf{r}} U(\mathbf{r})\cdot\mathbf{u}_1\right]\left[\boldsymbol{\nabla}_{\mathbf{r}'} U(\mathbf{r}')\cdot\mathbf{u}_1\right] , \\ &= \left(\rho\int \mathrm{d}\mathbf{r}\frac{\mathrm{d}\mathbf{u}}{\Omega_d} g^{(2)}(0,\mathbf{u}_1;\mathbf{r},\mathbf{u})\left[\boldsymbol{\nabla}_{\mathbf{r}} U(\mathbf{r})\cdot\mathbf{u}_1\right]\right)^2 , \\ &= \left(v_0 - v(\widehat{\varphi})\right)^2 .\end{aligned} \tag{D.6}$$

at leading order and where we have taken benefit from the weak correlations in the large d limit between different pairs of particles. Therefore at leading order,

$$\left\langle \dot{\mathbf{r}}_i^{\parallel\,2}(t)\right\rangle - v(\widehat{\varphi})^2 = 0 . \tag{D.7}$$

The fluctuations of the longitudinal velocity are hence negligible. Remark that this is a very general statement depending only on the scalings of the infinite dimensional limit and the weak correlations between the different pairs of particles, i.e. on the equality

$$g^{(3)}(0,\mathbf{u}_1;\mathbf{r},\mathbf{u};\mathbf{r}',\mathbf{u}') = g^{(2)}(0,\mathbf{u}_1;\mathbf{r},\mathbf{u})g^{(2)}(0,\mathbf{u}_1;\mathbf{r}',\mathbf{u}')g^{(2)}(\mathbf{r},\mathbf{u};\mathbf{r}',\mathbf{u}') + O\left(\frac{1}{\sqrt{d}}\right) . \tag{D.8}$$

We now turn to the study of the transverse velocity. We have the first moment

$$\left\langle \dot{\mathbf{r}}_i^{\perp}(t)\right\rangle = 0 . \tag{D.9}$$

At equal times, the second moment is given by

$$\begin{aligned}\left\langle \dot{\mathbf{r}}_i^{\perp}(t)\cdot\dot{\mathbf{r}}_i^{\perp}(t)\right\rangle &= \Bigg\langle -\sum_{j\neq i}\sum_{k\neq i}\left[\boldsymbol{\nabla}_{\mathbf{r}_i}U(\mathbf{r}_i-\mathbf{r}_j)\cdot\mathbf{u}_i\right]\left[\boldsymbol{\nabla}_{\mathbf{r}_i}V(\mathbf{r}_i-\mathbf{r}_k)\cdot\mathbf{u}_i\right] \\ &\qquad\qquad + \sum_{j\neq i}\sum_{k\neq i}\boldsymbol{\nabla}_{\mathbf{r}_i}U(\mathbf{r}_i-\mathbf{r}_j)\cdot\boldsymbol{\nabla}_{\mathbf{r}_i}U(\mathbf{r}_i-\mathbf{r}_k)\Bigg\rangle \\ &= -(v_0-v(\widehat{\varphi}))^2 + \Bigg\langle \sum_{j\neq i}\boldsymbol{\nabla}_{\mathbf{r}_i}U(\mathbf{r}_i-\mathbf{r}_j)^2 \\ &\qquad\qquad + \sum_{j\neq i}\sum_{\substack{k\neq i\\k\neq j}}\boldsymbol{\nabla}_{\mathbf{r}_i}U(\mathbf{r}_i-\mathbf{r}_j)\cdot\boldsymbol{\nabla}_{\mathbf{r}_i}U(\mathbf{r}_i-\mathbf{r}_k)\Bigg\rangle\end{aligned} \tag{D.10}$$

with

$$\begin{aligned}\left\langle \sum_{j\neq i}\boldsymbol{\nabla}_{\mathbf{r}_i}U(\mathbf{r}_i-\mathbf{r}_j)^2\right\rangle &= \rho\int \mathrm{d}\mathbf{r}'\frac{\mathrm{d}\mathbf{u}'}{\Omega_d}g(0,\mathbf{u};\mathbf{r}',\mathbf{u}')\partial_{r'}U(r')^2 \\ &= v_0^2\frac{\widehat{\varphi}}{4}\,.\end{aligned} \tag{D.11}$$

Eventually,

$$\begin{aligned}&\left\langle \sum_{j\neq i}\sum_{\substack{k\neq i\\k\neq j}}\boldsymbol{\nabla}_{\mathbf{r}_i}U(\mathbf{r}_i-\mathbf{r}_j)\cdot\boldsymbol{\nabla}_{\mathbf{r}_i}U(\mathbf{r}_i-\mathbf{r}_k)\right\rangle \\ &= \rho^2\int \mathrm{d}\mathbf{r}\,\mathrm{d}\mathbf{r}'\frac{\mathrm{d}\mathbf{u}\,\mathrm{d}\mathbf{u}'}{\Omega_d^2}g^{(3)}(0,\mathbf{u}_1;\mathbf{r},\mathbf{u};\mathbf{r}',\mathbf{u}')\boldsymbol{\nabla}_{\mathbf{r}'}U(\mathbf{r}')\cdot\boldsymbol{\nabla}_{\mathbf{r}}U(\mathbf{r}) \\ &= \rho\left(v(\widehat{\varphi})-v_0\right)\int \mathrm{d}\mathbf{r}\frac{\mathrm{d}\mathbf{u}}{\Omega_d}g^{(2)}(0,\mathbf{u}_1;\mathbf{r},\mathbf{u})\boldsymbol{\nabla}_{\mathbf{r}}U(\mathbf{r})\cdot\left[\mathbf{u}_1+\frac{\boldsymbol{\nabla}_{\mathbf{r}}U(\mathbf{r})}{v_0}\right] \\ &= 0\,.\end{aligned} \tag{D.12}$$

Hence the one-time fluctuations of the transverse velocity are given by

$$\left\langle \dot{\mathbf{r}}_i^{\perp}(t)\cdot\dot{\mathbf{r}}_i^{\perp}(t)\right\rangle = v(\widehat{\varphi})(v_0-v(\widehat{\varphi})) \tag{D.13}$$

They vanish at both $\widehat{\varphi}=0$ and $\widehat{\varphi}=\widehat{\varphi}_{cr}$, which is to be expected. Taking advantage of the absence of fluctuations in the longitudinal velocity, we can write in stationary state the effective dynamics of the one particle process as

$$\frac{\mathrm{d}\mathbf{r}_i}{\mathrm{d}t} = v(\widehat{\varphi})\mathbf{u}_i(t) + \dot{\mathbf{r}}_i^{\perp}(t) \tag{D.14}$$

with

$$\begin{cases}\left\langle \mathbf{u}_i(t)\cdot\mathbf{u}_i(t')\right\rangle = \mathrm{e}^{-\frac{|t-t'|}{\tau}} \\ \left\langle \dot{\mathbf{r}}_i^{\perp}(t)\cdot\dot{\mathbf{r}}_i^{\perp}(t')\right\rangle = v(\widehat{\varphi})(v_0-v(\widehat{\varphi}))f(t-t')\ \text{, with } f(0)=1\end{cases} \tag{D.15}$$

Following Sec. 4.1, let τ_0 be the typical time over which the transverse motion is correlated. In Sec. 4.1, we found at first order in $\widehat{\varphi}$ that τ_0 was given by the duration of a collision. In this scalings with $\zeta = 1$, this corresponds to a time scale of order $O(1/d^2)$. On the contrary, the longitudinal motion is correlated over the time scale τ. In the ultraballistic limit, $\tau = \widehat{\tau}/d \gg \tau_0$. In this limit, the long time diffusion constant is thus expected to be dominated by the contribution coming from the longitudinal motion *i.e.*

$$D = \frac{v(\widehat{\varphi})^2 \tau}{d}\,, \tag{D.16}$$

in line with our finding that $v(\widehat{\varphi})$ vanishes at a density $\widehat{\varphi}_{\rm cr}$ equal to the dynamical glass transition one obtained from the Franz-Parisi approach. Our computation suggests that the relation in Eq. (D.16) holds only in the limit where the persistence time is much larger than the interaction time between two particles. This would deserve further investigations.

Appendix E

Nonlinear analogue of the May-Wigner instability transition: a replica calculation

In this appendix, we show how a replica formulation of the absolute value of a determinant similar to that used in Sec. 4.3.4 allows to recover the findings of [70] about the number of stationary points in large random dynamical systems. Here we consider an N-dimensional dynamical system with degrees of freedom x_i for $i = 1, \dots, N$ evolving through

$$\frac{\mathrm{d}x_i}{\mathrm{d}t} = -\mu x_i + f_i(x_1, \dots, x_N)\,, \tag{E.1}$$

where the field $\mathbf{f}$ involves both gradients and solenoidal contributions,

$$f_i(\mathbf{x}) = \partial_{x_i} V(\mathbf{x}) + \frac{1}{\sqrt{N}} \sum_{j=1}^{N} \partial_{x_j} A_{ij}(\mathbf{x})\,, \tag{E.2}$$

with A_{ij} antisymmetric for the associated contribution in the equation of motion to be divergence free. Both $V(\mathbf{x})$ and $A_{ij}(\mathbf{x})$ are choosen to be independent Gaussian zero mean random fields with correlations

$$\begin{cases} \langle V(\mathbf{x})V(\mathbf{y})\rangle = v^2 \Gamma_V\left(|\mathbf{x}-\mathbf{y}|^2\right) \;,\; \Gamma_V''(0) = 1\,, \\ \langle A_{ij}(\mathbf{x})A_{mn}(\mathbf{y})\rangle = a^2 \Gamma_A\left(|\mathbf{x}-\mathbf{y}|^2\right)\left(\delta_{im}\delta_{jn} - \delta_{in}\delta_{jm}\right) \;,\; \Gamma_V''(0) = 1\,, \end{cases} \tag{E.3}$$

We eventually introduce the parameter $\tau = \frac{v^2}{v^2+a^2}$ that measures the relative strength of the gradient and solenoidal terms and $m = \frac{\mu}{2\sqrt{v^2+a^2}\sqrt{N}}$ comparing the amplitude of the linear contribution in Eq. (E.1) to the non-linear ones. The main result of [70] is that $\langle \mathcal{N} \rangle$, the mean number of stationary points of the dynamical system, undergoes at large N a phase transition from a regime where it is $O(1)$ at small m, *i.e.* in a regime where the harmonic potential dominates the dynamics, to a regime where it scales exponentially with the system size N. This is this result that we seek to recover using similar transformations to that of

Sec. 4.3.4. In a first part, we will actually use a slightly different representation than that of Sec. 4.3.4 as the matrix determinant we have to evaluate is that of a non-symmetric matrix. In the end, we study the $\tau = 1$ case corresponding to a purely gradient flow. This will allow us to use the same methods as in Sec. 4.3.4. In particular, we will show that the $(\hat{p}, \hat{q})$ symmetry breaking uncovered in the study of the UCNA phase diagram is associated in this context to the proliferation of an exponential number of stationary points.

Following [70], the mean number of stationary points of Eq. (E.1) can be obtained from the Kac-Rice formula and reads

$$\langle \mathcal{N} \rangle = \left\langle \left| \det \left(\delta_{ij} + \frac{J_{ij}}{\mu} \right) \right| \right\rangle , \tag{E.4}$$

The J_{ij}'s are the coefficients of an $N \times N$ zero mean Gaussian matrix with correlations

$$\langle J_{ij} J_{kl} \rangle = \alpha \left(\delta_{ik}\delta_{jl} + \tau \left(\delta_{ij}\delta_{kl} + \delta_{il}\delta_{jk} \right) \right) , \tag{E.5}$$

and with $\alpha = 2\sqrt{v^2 + a^2}$. We compute Eq. (E.4) through a replica calculation of the absolute value of a determinant. First, we use the identity valid for any real matrix

$$\left| \det \left(\mathbb{1} + J/\mu \right) \right| = \lim_{\epsilon \to 0^+} \lim_{n \to 0} I_\epsilon^{n-1} , \tag{E.6}$$

with

$$I_\epsilon = \int \prod_{i=1}^{N} \frac{\mathrm{d}\phi_i \mathrm{d}\varphi_i}{2\pi} \mathrm{e}^{-\frac{\epsilon}{2}\boldsymbol{\phi}^2 - \frac{\epsilon}{2}\boldsymbol{\varphi}^2 + i \sum_{i,j=1}^{N} \phi_i (\delta_{ij} + J_{ij}/\mu)\varphi_j} . \tag{E.7}$$

We therefore obtain,

$$\langle \mathcal{N} \rangle = \lim_{\epsilon \to 0^+} \lim_{n \to 0} \left\langle I_\epsilon^{n-1} \right\rangle . \tag{E.8}$$

$\langle I_\epsilon^{n-1} \rangle$ is then computed for $n \in \mathbb{N}$ with $n > 1$ and $\langle \mathcal{N} \rangle$ is obtained through analytical continuation to $n = 0$. The ability to perform this analytical continuation (*e.g.* à la Carlson) will not be checked here. Furthermore, as is usual in the use of the replica trick, we assume the limits $\lim_{N\to\infty}$ and $\lim_{\epsilon\to 0^+} \lim_{n\to 0}$ can be commuted. Hereafter, the different replicas are labeled by a, b. We obtain,

$$\begin{aligned}
\left\langle I_\epsilon^{n-1} \right\rangle &= \int \prod_{i=1}^{N} \prod_{a=1}^{n-1} \frac{\mathrm{d}\phi_i^a \mathrm{d}\varphi_i^a}{2\pi} \exp \left\{ N \left(-\frac{\epsilon}{2} \sum_a q_{aa} - \frac{\epsilon}{2} \sum_a p_{aa} + i \sum_a r_{aa} \right.\right. \\
&\qquad \left.\left. - \frac{1}{2m^2} \sum_{a,b} \left(q_{ab} p_{ab} + \tau \left(r_{aa} r_{bb} + r_{ab} r_{ba} \right) \right) \right) \right\} , \\
&= \int_{\{S>0\}} \prod_{a \le b} \mathrm{d}q_{ab} \mathrm{d}p_{ab} \prod_{a,b} \mathrm{d}r_{ab}\, \tilde{C}_{N,n}(S) \, \exp \left\{ N \left((n-1) + \frac{1}{2} \ln \det S \right.\right. \\
&\qquad \left.\left. - \frac{\epsilon}{2} \sum_a q_{aa} - \frac{\epsilon}{2} \sum_a p_{aa} + i \sum_a r_{aa} - \frac{1}{2m^2} \sum_{a,b} \left(q_{ab} p_{ab} + \tau \left(r_{aa} r_{bb} + r_{ab} r_{ba} \right) \right) \right) \right\} , \\
&= \int_{\{S>0\}} \prod_{a \le b} \mathrm{d}q_{ab} \mathrm{d}p_{ab} \prod_{a,b} \mathrm{d}r_{ab}\, \tilde{C}_{N,n}(S)\, \mathrm{e}^{N(n-1) f(S)} ,
\end{aligned} \tag{E.9}$$

which defines $f(S)$ and where

$$\begin{aligned} p_{ab} &= \frac{1}{N}\sum_i \varphi_i^a \varphi_i^b \,, \\ q_{ab} &= \frac{1}{N}\sum_i \phi_i^a \phi_i^b \,, \\ r_{ab} &= \frac{1}{N}\sum_i \varphi_i^a \phi_i^b \,. \end{aligned} \tag{E.10}$$

Eventually, S is the $2(n-1)\times 2(n-1)$ symmetric matrix defined by block as,

$$S = \left[\begin{array}{c|c} p_{ab} & r_{ab} \\ \hline r_{ba} & q_{ab} \end{array}\right] . \tag{E.11}$$

The integration domain is restricted to positive definite S matrices. Eventually, in the limit $N\to\infty$, the $\tilde{C}_{N,n}$ contribution coming from the Jacobian to go from the fields variables to the matrix of scalar products S reads [72]

$$\begin{aligned} \ln \tilde{C}_{N,n}(S) =& \frac{(n-1)(2n-1)}{2}\ln\frac{N}{2} - \frac{(n-1)(2n-3)}{2}\ln\pi - \frac{2n-1}{2}\ln\det S \\ & - (n-1)\ln(2\pi) + o(1)\,, \\ \underset{n\to 0}{=}& \frac{1}{2}\ln\frac{N}{2} - \frac{3}{2}\ln\pi + \frac{1}{2}\ln\det S + \ln 2\pi + o(1)\,. \end{aligned} \tag{E.12}$$

Going from the fields variables to the matrix S allows us in the end to evaluate the integral in Eq. (E.9) using the saddle-point approximation.

E.0.1 Saddle point equations

We denote S^{-1} the inverse of S by

$$S^{-1} = \left[\begin{array}{c|c} \tilde{p}_{ab} & \tilde{r}_{ab} \\ \hline \tilde{r}_{ba} & \tilde{q}_{ab} \end{array}\right] . \tag{E.13}$$

The saddle point equations associated to Eq. (E.9) then read

$$\begin{aligned} &\tilde{p}_{ab} - \frac{1}{m^2} q_{ab} - \epsilon\delta_{ab} = 0\,, \\ &\tilde{q}_{ab} - \frac{1}{m^2} p_{ab} - \epsilon\delta_{ab} = 0\,, \\ &\tilde{r}_{ab} + i\delta_{ab} - \frac{\tau}{m^2}\left(\delta_{ab}\sum_c r_{cc} + r_{ba}\right) = 0\,. \end{aligned} \tag{E.14}$$

E.0.2 Replica symmetric, block diagonal ansatz

We look for a solution of the saddle point equations Eq. (E.14) under the form of a replica symmetric block diagonal matrix

$$S = \left[\begin{array}{c|c} p\mathbb{1} & r\mathbb{1} \\ \hline r\mathbb{1} & q\mathbb{1} \end{array}\right] . \tag{E.15}$$

Eq. (E.14) then reduces to

$$\begin{aligned} &\frac{q}{pq-r^2} - \frac{q}{m^2} - \epsilon = 0 \,, \\ &\frac{p}{pq-r^2} - \frac{p}{m^2} - \epsilon = 0 \,, \\ &\frac{r}{pq-r^2} - i + \frac{n\tau}{m^2} r = 0 \,. \end{aligned} \tag{E.16}$$

Interestingly, in the limit $n \to 0$, the parameter τ disappears from the saddle point equations, thus suggesting the absence of τ dependence in the exponential weight of $\langle \mathcal{N} \rangle$. There exists three triplets of solutions, each of them with $p = q$. At exactly $\epsilon = 0$, there is a degeneracy along the hyperbola $pq = cst$ of the saddle point equations. Lifting the degeneracy is the purpose of the small ϵ parameter. As $\epsilon \to 0$, the solutions to the saddle point equations read

- $p = q = 0$ and $r = i$,
- $p = q = \pm\sqrt{m^2 - m^4}$ and $r = im^2$.

As $n \to 0$ and $\epsilon \to 0$ the saddle point value of the exponential weight respectively write

- $f(p = q = 0, r = i) = 0$,
- $f(p = q = \pm\sqrt{m^2 - m^4}, r = im^2) = \frac{1-m^2}{2} + \ln m$.

Note that $\forall m > 0$, $(1 - m^2)/2 + \ln m < 0$ and that the limit $n \to 0$ completely washes out the dependence on τ.

E.0.3 Saddle point selection

Here, we show that for $m > 1$ the first branch of the solution is selected while it is the second one that is selected for $m < 1$. Restricting the integral in Eq. (E.9) to the (p, r) plane, we obtain

$$\left\langle I_\epsilon^{n-1} \right\rangle \underset{N\to\infty}{\sim} \int_0^{+\infty} \mathrm{d}p \int_{-p}^{p} \mathrm{d}r \; \mathrm{e}^{N(n-1)g(p,r)} \tag{E.17}$$

with

$$\begin{aligned} g(p,r) &= 1 + \frac{1}{2}\ln(p^2 - r^2) - \epsilon p + ir - \frac{1}{2m^2}\left(p^2 + n\tau r^2\right) \\ &\underset{\substack{\epsilon\to 0\\ n\to 0}}{=} 1 + \frac{1}{2}\ln(p^2 - r^2) + ir - \frac{p^2}{2m^2} \end{aligned} \tag{E.18}$$

We change variables and introduce

$$\begin{aligned} p &= x\cosh\theta\,, \\ r &= x\sinh\theta\,, \end{aligned} \tag{E.19}$$

so that

$$\left\langle I_\epsilon^{n-1}\right\rangle \underset{N\to\infty}{\sim} \int_0^{+\infty} \mathrm{d}x \int_{-\infty}^{\infty} \mathrm{d}\theta \;\exp\left[N(n-1)\left(1 + \ln x + ix\sinh\theta - \frac{x^2}{2m^2}\cosh^2\theta\right)\right]. \tag{E.20}$$

Note that in Eq. (E.20), for the sake of simplicity of the expressions, we have already anticipated the $n \to 0$ limit in the function g but that, in order to get the proper analytical continuation to $n = 0$, we keep working with $N(n-1) > 0$. The saddle points of the θ integral are given by

$$\theta = i\left(\frac{\pi}{2} + s\pi\right),\ s \in \mathbb{N} \tag{E.21}$$

or

$$\begin{aligned} &\theta = i\arcsin\left(\frac{m^2}{x}\right) + 2is\pi,\ s\in\mathbb{N},\ \text{if}\ \frac{m^2}{x} < 1\,,\ \text{or} \\ &\theta = i\left(\pi - \arcsin\left(\frac{m^2}{x}\right)\right) + 2is\pi,\ s\in\mathbb{N},\ \text{if}\ \frac{m^2}{x} < 1\,,\ \text{or} \\ &\theta = \pm\text{arccosh}\left(\frac{m^2}{x}\right) + i\left(\frac{\pi}{2} + s\pi\right),\ s\in\mathbb{N},\ \text{if}\ \frac{m^2}{x} > 1\,. \end{aligned} \tag{E.22}$$

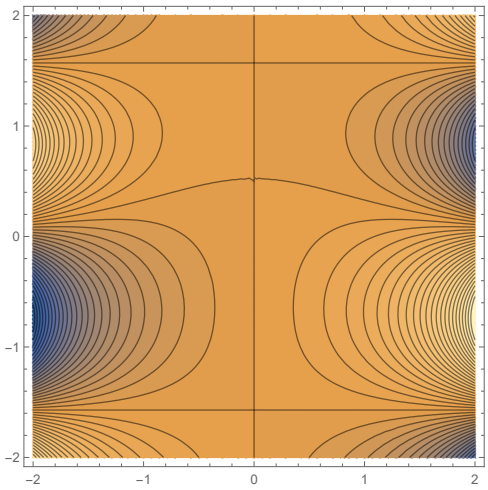

Fig.1. Lines of steepest descent/ascent of $\mathrm{Re}\,(g)$ for $m^2/x < 1$.

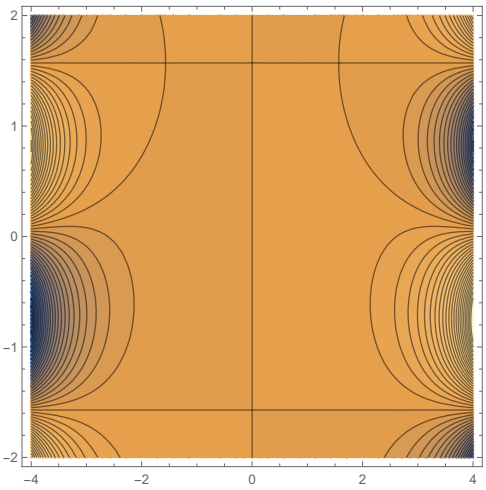

Fig.2. Lines of steepest descent/ascent of $\mathrm{Re}\,(g)$ for $m^2/x > 1$.

In both case, the θ integration path is deformed to the steepest descent path of 0 imaginary part passing through the saddles that can be seen respectively in Fig.1 and Fig.2. Notice that the saddle at $\theta = i\pi/2$ is only attained for $x < m^2$. We therefore obtain at the exponential level

$$\begin{aligned}\left\langle I_\epsilon^{n-1}\right\rangle \underset{N\to\infty}{\sim} &\int_{m^2}^{+\infty} \mathrm{d}x\, \exp\left[N(n-1)\left(1-\frac{m^2}{2}+\ln x-\frac{x^2}{2m^2}\right)\right] \\ &+\int_0^{m^2}\mathrm{d}x \exp\left[N(n-1)\left(1+\ln x-x\right)\right] \\ &+\int_0^{m^2}\mathrm{d}x\, \exp\left[N(n-1)\left(1-\frac{m^2}{2}+\ln x-\frac{x^2}{2m^2}\right)\right].\end{aligned} \tag{E.23}$$

Therefore, if $m > 1$, the result is dominated by the second integral and we have

$$\langle \mathcal{N}\rangle \sim 1\,, \tag{E.24}$$

and if $m < 1$, the result is dominated by the first one and we get after taking the $n \to 0$ limit

$$\langle \mathcal{N}\rangle \sim \exp\left(-N\left(\frac{1-m^2}{2}+\ln m\right)\right). \tag{E.25}$$

This is the main result of [70] showing a transition in the mean number of stationary points from a regime where it is $O(1)$ at $m < 1$ to a regime where it scales exponentially with the system size at $m > 1$. We stress here that at the exponential level $\mathcal{N}$ does not depend on τ, *i.e.* on the way the non-linearities are distributed between the solenoidal and potential contributions. We now attempt to recover the multiplicative constants appearing in front of these exponential contributions.

E.0.4 Multiplicative constants

In the limit $N \to \infty$, we assume the integral in Eq. (E.9) is dominated by a single saddle point S_0 which functional form was discussed earlier. We therefore obtain

$$\begin{aligned}\left\langle I_\epsilon^{n-1}\right\rangle &= \left(\frac{2\pi}{N}\right)^{\frac{(n-1)(2n-1)}{2}} \left(-\Delta_f(S_0)\right)^{-1/2}\tilde{C}_{N,n}(S_0)\mathrm{e}^{N(n-1)f(S_0)}\left[1+O(N^{-1})\right], \\ &\underset{n\to 0}{=} 2\sqrt{\det S_0}\left(-\Delta_f(S_0)\right)^{-1/2}\mathrm{e}^{-Nf(S_0)}\left[1+O(N^{-1})\right],\end{aligned} \tag{E.26}$$

with $\Delta_f(S_0)$ the value of the determinant of the Hessian of f at the saddle point. Note that the Hessian is here the Hessian in the full replica space. At the saddle point selected at $m > 1$, we have

$$\det S_0 = 1\,, \tag{E.27}$$

and we conjecture from a finite n inspection that the determinant of the Hessian writes

$$\begin{aligned}\Delta_f(S_0) &= (-1)^{n-1}\frac{(m^2-1)^{n(n-1)}\,(m^2-n\tau)(m^2-\tau)^{n(n-2)}}{4^{n-1}m^{2+n(2+4(n-2))}}\,,\\ &\underset{n\to 0}{=} -4\,.\end{aligned} \tag{E.28}$$

Therefore, we get for $m>1$

$$\langle \mathcal{N}\rangle = 1\,. \tag{E.29}$$

Furthermore, for $m<1$, we have

$$\det S_0 = m^{2(n-1)} \underset{n\to 0}{=} m^{-2}\,. \tag{E.30}$$

We now need to evaluate the determinant of the Hessian at the saddle point solution of Eq. (E.14) at finite ϵ. At $\epsilon=0$, it vanishes due to the aforementioned degeneracy of the saddle point equations. The ϵ dependence is as expected however washed out by the continuation to $n=0$. At the first, non vanishing order in ϵ, we conjecture from a finite n inspection that

$$\begin{aligned}\Delta_f(S_0) &= (-1)^{n-1}\epsilon^{\frac{n(n-1)}{2}}\frac{(1+n\tau)(1-\tau)^{\frac{(n-2)(n-1)}{2}}(1+\tau)^{\frac{(n-2)(n+1)}{2}}\,(1-m^2)^{\frac{n(n-1)}{4}}}{2^{\frac{(n-1)(4-n)}{2}}m^{\frac{3(n-1)+7(n-1)^2}{2}}}\,,\\ &\underset{n\to 0}{=} -\frac{4(1-\tau)}{m^2(1+\tau)}\,.\end{aligned} \tag{E.31}$$

Hence we obtain for $m<1$,

$$\langle \mathcal{N}\rangle = \sqrt{\frac{1+\tau}{1-\tau}}\mathrm{e}^{-N\left(\frac{1-m^2}{2}+\ln m\right)}\,. \tag{E.32}$$

Notice that there is a $\sqrt{2}$ discrepancy between our result and that of [70]. This might be due to the contributions of other saddle points. In a private communication, Prof. Fyodorov pointed out to me that it was not the first time troubles appeared at the level of the fluctuation determinant when trying to recover exact results from random matrix theory with the use of the replica trick [71].

E.0.5 The gradient-flow case $\tau = 0$

We now restrict our attention to the gradient flow case $\tau=0$ studied first in [69]. In this case, the mean number of stationary points can be expressed as

$$\langle \mathcal{N}\rangle = \left\langle \left|\det\left(\delta_{ij}+\frac{J_{ij}}{\mu}\right)\right|\right\rangle\,, \tag{E.33}$$

with J_{ij} a random Gaussian symmetric matrix with correlations

$$\langle J_{ij}J_{kl}\rangle = 2v^2\left(\delta_{ik}\delta_{jl}+\delta_{ij}\delta_{kl}+\delta_{il}\delta_{jk}\right)\,. \tag{E.34}$$

The same transformation as in Sec. 4.3.4 can then be applied in order to write $\langle \mathcal{N} \rangle$ as

$$\langle \mathcal{N} \rangle = \lim_{\epsilon \to 0^+} \lim_{n \to 0} \left\langle K_\epsilon^{n-1} \right\rangle , \tag{E.35}$$

with

$$\left\langle K_\epsilon^{n-1} \right\rangle = \int \prod_{i=1}^{N} \prod_{a=1}^{n-1} \frac{\mathrm{d}\phi_i^a \mathrm{d}\varphi_i^a}{2\pi} \exp \left\{ \frac{Ni}{2} \sum_a \left(p_{aa} - q_{aa} \right) - \frac{\epsilon N}{2} \sum_a \left(p_{aa} + q_{aa} \right) \right. \\ \left. - \frac{N}{8m^2} \sum_{a,b} \left(p_{aa} p_{bb} + q_{aa} q_{bb} - 2 p_{aa} q_{bb} + 2 p_{ab}^2 + 2 q_{ab}^2 - 4 r_{ab}^2 \right) \right\} . \tag{E.36}$$

where the notations p_{ab}, q_{ab} and r_{ab} were introduced in the above and with $m = \mu/(2v\sqrt{N})$. The above integral can then be computed through a saddle-point evaluation. Within the diagonal replica symmetric ansatz of Sec. 4.3.9,

$$\begin{cases} p_{ab} = i\hat{p}\delta_{ab} , \\ q_{ab} = -i\hat{q}\delta_{ab} , \\ r_{ab} = 0 , \end{cases} \tag{E.37}$$

the associated saddle point equations read

$$\begin{cases} \dfrac{1}{2} + \dfrac{\hat{q} - \hat{p}}{4m^2} - \dfrac{1}{2\hat{p}} = 0 , \\ \dfrac{1}{2} + \dfrac{\hat{p} - \hat{q}}{4m^2} - \dfrac{1}{2\hat{q}} = 0 , \end{cases} \tag{E.38}$$

The above system has three solutions. The first one is symmetric and reads

$$\hat{p} = \hat{q} = 1 . \tag{E.39}$$

If selected, it corresponds to

$$\mathcal{N} \sim 1 \tag{E.40}$$

The other two couple of solutions are real for $m > 1$. Each of these solution breaks the $\hat{p} \leftrightarrow \hat{q}$ symmetry. They read

$$\hat{p} = m \left(m - \sqrt{m^2 - 1} \right) , \hat{q} = m \left(m + \sqrt{m^2 - 1} \right) , \tag{E.41}$$

and

$$\hat{p} = m \left(m + \sqrt{m^2 - 1} \right) , \hat{q} = m \left(m - \sqrt{m^2 - 1} \right) , \tag{E.42}$$

If selected, they both correspond to

$$\langle \mathcal{N} \rangle \sim \exp \left(-N \left(\frac{1 - m^2}{2} + \ln m \right) \right) . \tag{E.43}$$

The issue of the saddle point selection can be tackled using arguments similar to those of the previous case. We have hence seen that the phase transition of [69] can be explained using the same replica representation of the absolute value of a determinant than the one used in Sec. 4.3.4. The diagonal replica symmetric ansatz perfectly accounts for this transition (at least at the exponential level and beside the fluctuating determinant problem raised in Sec. E.0.4). In the phase with exponentially many stationary points, the $\hat{p} \leftrightarrow \hat{q}$ symmetry is broken.

Bibliography

[1] Elisabeth Agoritsas. "Mean-field dynamics of infinite-dimensional particle systems: global shear versus random local forcing". In: *Journal of Statistical Mechanics: Theory and Experiment* 2021.3 (2021), p. 033501. DOI: 10.1088/1742-5468/abdd18. URL: https://doi.org/10.1088/1742-5468/abdd18.

[2] Elisabeth Agoritsas, Thibaud Maimbourg, and Francesco Zamponi. "Out-of-equilibrium dynamical equations of infinite-dimensional particle systems I. The isotropic case". In: *Journal of Physics A: Mathematical and Theoretical* 52.14 (2019), p. 144002. DOI: 10.1088/1751-8121/ab099d. URL: https://doi.org/10.1088%2F1751-8121%2Fab099d.

[3] Wylie W Ahmed et al. "Active mechanics reveal molecular-scale force kinetics in living oocytes". In: *Biophysical journal* 114.7 (2018), pp. 1667–1679.

[4] M Aldana, H Larralde, and B Vázquez. "On the emergence of collective order in swarming systems: a recent debate". In: *International Journal of Modern Physics B* 23.18 (2009), pp. 3661–3685.

[5] S. Andarwa, H. Basirat Tabrizi, and G. Ahmadi. "Effect of correcting near-wall forces on nanoparticle transport in a microchannel". In: *Particuology* 16 (2014), pp. 84–90. ISSN: 1674-2001. DOI: https://doi.org/10.1016/j.partic.2013.11.007. URL: https://www.sciencedirect.com/science/article/pii/S1674200114000170.

[6] Philip W Anderson. "More is different". In: *Science* 177.4047 (1972), pp. 393–396.

[7] Z. González Arenas and D. G. Barci. "Hidden symmetries and equilibrium properties of multiplicative white-noise stochastic processes". In: *J. Stat. Mech.* 2012 (2012), P12005.

[8] Vladimir I Arnol'd. "Proof of a theorem of AN Kolmogorov on the invariance of quasi-periodic motions under small perturbations of the Hamiltonian". In: *Russian Mathematical Surveys* 18.5 (1963), p. 9.

[9] Michele Ballerini et al. "Interaction ruling animal collective behavior depends on topological rather than metric distance: Evidence from a field study". In: *Proceedings of the national academy of sciences* 105.4 (2008), pp. 1232–1237.

[10] John Bardeen, Leon N Cooper, and John Robert Schrieffer. "Theory of superconductivity". In: *Physical review* 108.5 (1957), p. 1175.

[11] RJ Baxter. "Percus–Yevick equation for hard spheres with surface adhesion". In: *The Journal of chemical physics* 49.6 (1968), pp. 2770–2774.

[12] Eyal Ben-Isaac et al. "Effective temperature of red-blood-cell membrane fluctuations". In: *Physical review letters* 106.23 (2011), p. 238103.

[13] Howard C Berg and Douglas A Brown. “Chemotaxis in Escherichia coli analysed by three-dimensional tracking”. In: *Nature* 239.5374 (1972), pp. 500–504.

[14] John R Blake. “A spherical envelope approach to ciliary propulsion”. In: *Journal of Fluid Mechanics* 46.1 (1971), pp. 199–208.

[15] Luis L Bonilla. “Active ornstein-uhlenbeck particles”. In: *Physical Review E* 100.2 (2019), p. 022601.

[16] Christian Van den Broeck and Peter Hänggi. “Activation rates for nonlinear stochastic flows driven by non-Gaussian noise”. In: *Physical Review A* 30.5 (1984), p. 2730.

[17] Robert Brown. “XXVII. A brief account of microscopical observations made in the months of June, July and August 1827, on the particles contained in the pollen of plants; and on the general existence of active molecules in organic and inorganic bodies”. In: *The philosophical magazine* 4.21 (1828), pp. 161–173.

[18] William Fuller Brown Jr. “Thermal fluctuations of a single-domain particle”. In: *Physical review* 130.5 (1963), p. 1677.

[19] Ivo Buttinoni et al. “Dynamical Clustering and Phase Separation in Suspensions of Self-Propelled Colloidal Particles”. In: *Phys. Rev. Lett.* 110 (23 2013), p. 238301. DOI: 10.1103/PhysRevLett.110.238301. URL: https://link.aps.org/doi/10.1103/PhysRevLett.110.238301.

[20] Lorenzo Caprini, U Marini Bettolo Marconi, and Andrea Puglisi. “Spontaneous velocity alignment in motility-induced phase separation”. In: *Physical review letters* 124.7 (2020), p. 078001.

[21] Lorenzo Caprini et al. “Comment on “Entropy Production and Fluctuation Theorems for Active Matter””. In: *Physical review letters* 121.13 (2018), p. 139801.

[22] Lorenzo Caprini et al. “The entropy production of Ornstein–Uhlenbeck active particles: a path integral method for correlations”. In: *Journal of Statistical Mechanics: Theory and Experiment* 2019.5 (2019), p. 053203.

[23] John L Cardy and Peter Grassberger. “Epidemic models and percolation”. In: *Journal of Physics A: Mathematical and General* 18.6 (1985), p. L267.

[24] Michael E Cates and Julien Tailleur. “Motility-induced phase separation”. In: *Annu. Rev. Condens. Matter Phys.* 6.1 (2015), pp. 219–244.

[25] Andrea Cavagna. “Supercooled liquids for pedestrians”. In: *Physics Reports* 476.4-6 (2009), pp. 51–124.

[26] KS Cheng. “Quantization of a general dynamical system by Feynman’s path integration formulation”. In: *Journal of Mathematical Physics* 13.11 (1972), pp. 1723–1726.

[27] William Coffey and Yu P Kalmykov. *The Langevin equation: with applications to stochastic problems in physics, chemistry and electrical engineering*. Vol. 27. World Scientific, 2012.

[28] L. F. Cugliandolo and V. Lecomte. “Rules of calculus in the path integral representation of white noise Langevin equations: the Onsager–Machlup approach”. en. In: *J. Phys. A: Math. Theor.* 50.34 (2017), p. 345001. ISSN: 1751-8121. DOI: 10.1088/1751-8121/aa7dd6. (Visited on 05/04/2018).

[29] Leticia F Cugliandolo, Vivien Lecomte, and Frédéric Van Wijland. “Building a path-integral calculus: a covariant discretization approach”. In: *Journal of Physics A: Mathematical and Theoretical* 52.50 (2019), 50LT01.

[30] Lennart Dabelow, Stefano Bo, and Ralf Eichhorn. “How irreversible are steady-state trajectories of a trapped active particle?” In: *arXiv preprint arXiv:2012.05542* (2020).

[31] Lennart Dabelow, Stefano Bo, and Ralf Eichhorn. “Irreversibility in active matter systems: Fluctuation theorem and mutual information”. In: *Physical Review X* 9.2 (2019), p. 021009.

[32] Lokrshi Prawar Dadhichi, Ananyo Maitra, and Sriram Ramaswamy. “Origins and diagnostics of the nonequilibrium character of active systems”. In: *Journal of Statistical Mechanics: Theory and Experiment* 2018.12 (2018), p. 123201.

[33] Shibananda Das, Gerhard Gompper, and Roland G Winkler. “Confined active Brownian particles: theoretical description of propulsion-induced accumulation”. In: *New Journal of Physics* 20.1 (2018), p. 015001.

[34] M Deforet et al. “Emergence of collective modes and tri-dimensional structures from epithelial confinement”. In: *Nature communications* 5.1 (2014), pp. 1–9.

[35] U. Deininghaus and R. Graham. “Nonlinear point transformations and covariant interpretation of path integrals”. en. In: *Zeitschrift für Physik B Condensed Matter* 34.2 (June 1979), pp. 211–219. ISSN: 0722-3277, 1431-584X. DOI: 10.1007/BF01322143. URL: https://link.springer.com/article/10.1007/BF01322143 (visited on 05/11/2018).

[36] B. S. DeWitt. “Dynamical Theory in Curved Spaces. I. A Review of the Classical and Quantum Action Principles”. In: *Reviews of Modern Physics* 29.3 (July 1957), pp. 377–397. DOI: 10.1103/RevModPhys.29.377. URL: https://link.aps.org/doi/10.1103/RevModPhys.29.377 (visited on 04/26/2018).

[37] M. Di Paola and G. Falsone. “Ito and Stratonovich integrals for delta-correlated processes”. In: *Probabilistic Engineering Mechanics* 8.3 (Jan. 1993), pp. 197–208. ISSN: 0266-8920. DOI: 10.1016/0266-8920(93)90015-N. URL: http://www.sciencedirect.com/science/article/pii/026689209390015N (visited on 02/18/2018).

[38] M. Di Paola and G. Falsone. “Stochastic Dynamics of Nonlinear Systems Driven by Non-normal Delta-Correlated Processes”. In: *J. Appl. Mech* 60.1 (Mar. 1993), pp. 141–148. ISSN: 0021-8936. DOI: 10.1115/1.2900736. URL: http://dx.doi.org/10.1115/1.2900736 (visited on 02/18/2018).

[39] Pasquale Digregorio et al. "Full Phase Diagram of Active Brownian Disks: From Melting to Motility-Induced Phase Separation". In: *Phys. Rev. Lett.* 121 (9 2018), p. 098003. DOI: 10.1103/PhysRevLett.121.098003. URL: https://link.aps.org/doi/10.1103/PhysRevLett.121.098003.

[40] Pasquale Digregorio et al. "Full Phase Diagram of Active Brownian Disks: From Melting to Motility-Induced Phase Separation". In: *Phys. Rev. Lett.* 121 (9 2018), p. 098003. DOI: 10.1103/PhysRevLett.121.098003. URL: https://link.aps.org/doi/10.1103/PhysRevLett.121.098003.

[41] Mingnan Ding and Xiangjun Xing. *Time-Slicing Path-integral in Curved Space*. 2021. arXiv: 2107.14562 [cond-mat.stat-mech].

[42] Amin Doostmohammadi et al. "Active nematics". In: *Nature communications* 9.1 (2018), pp. 1–13.

[43] R. A. Duine and H. T. C. Stoof. "Stochastic dynamics of a trapped Bose-Einstein condensate". In: *Physical Review A* 65.1 (Dec. 2001), p. 013603. DOI: 10.1103/PhysRevA.65.013603. URL: https://link.aps.org/doi/10.1103/PhysRevA.65.013603 (visited on 05/02/2018).

[44] Jörn Dunkel and Peter Hänggi. "Theory of relativistic Brownian motion: the (1+ 1)-dimensional case". In: *Physical Review E* 71.1 (2005), p. 016124.

[45] S. F. Edwards and Y. V. Gulyaev. "Path integrals in polar co-ordinates". en. In: *Proc. R. Soc. Lond. A* 279.1377 (May 1964), pp. 229–235. ISSN: 0080-4630, 2053-9169. DOI: 10.1098/rspa.1964.0100. URL: http://rspa.royalsocietypublishing.org/content/279/1377/229 (visited on 05/11/2018).

[46] Albert Einstein. "Über die von der molekularkinetischen Theorie der Wärme geforderte Bewegung von in ruhenden Flüssigkeiten suspendierten Teilchen". In: *Annalen der physik* 4 (1905).

[47] Yves Elskens and Harry L. Frisch. "Kinetic theory of hard spheres in infinite dimensions". In: *Phys. Rev. A* 37 (11 1988), pp. 4351–4353. DOI: 10.1103/PhysRevA.37.4351. URL: https://link.aps.org/doi/10.1103/PhysRevA.37.4351.

[48] R. Evans. "The nature of the liquid-vapour interface and other topics in the statistical mechanics of non-uniform, classical fluids". In: *Advances in Physics* 28.2 (1979), pp. 143–200. DOI: 10.1080/00018737900101365. eprint: https://doi.org/10.1080/00018737900101365. URL: https://doi.org/10.1080/00018737900101365.

[49] Barath Ezhilan, Roberto Alonso-Matilla, and David Saintillan. "On the distribution and swim pressure of run-and-tumble particles in confinement". In: *Journal of Fluid Mechanics* 781 (2015).

[50] G Falsone. "Stochastic differential calculus for Gaussian and non-Gaussian noises: a critical review". In: *Communications in Nonlinear Science and Numerical Simulation* 56 (2018), pp. 198–216.

[51] Thomas FF Farage, Philip Krinninger, and Joseph M Brader. "Effective interactions in active Brownian suspensions". In: *Physical Review E* 91.4 (2015), p. 042310.

[52] R. P. Feynman. "Space-Time Approach to Non-Relativistic Quantum Mechanics". In: *Rev. Mod. Phys.* 20.2 (Apr. 1948), p. 367. DOI: 10.1103/RevModPhys.20.367. URL: http://link.aps.org/doi/10.1103/RevModPhys.20.367 (visited on 10/03/2011).

[53] Yaouen Fily. "Self-propelled particle in a nonconvex external potential: Persistent limit in one dimension". In: *The Journal of Chemical Physics* 150.17 (2019), p. 174906.

[54] Yaouen Fily and M. Cristina Marchetti. "Athermal Phase Separation of Self-Propelled Particles with No Alignment". In: *Phys. Rev. Lett.* 108 (23 2012), p. 235702. DOI: 10.1103/PhysRevLett.108.235702. URL: https://link.aps.org/doi/10.1103/PhysRevLett.108.235702.

[55] Yaouen Fily and M Cristina Marchetti. "Athermal phase separation of self-propelled particles with no alignment". In: *Physical review letters* 108.23 (2012), p. 235702.

[56] Elijah Flenner and Grzegorz Szamel. "Active matter: quantifying the departure from equilibrium". In: *arXiv preprint arXiv:2004.11925* (2020).

[57] Elijah Flenner and Grzegorz Szamel. "Active matter: Quantifying the departure from equilibrium". In: *Phys. Rev. E* 102 (2 2020), p. 022607. DOI: 10.1103/PhysRevE.102.022607. URL: https://link.aps.org/doi/10.1103/PhysRevE.102.022607.

[58] É Fodor et al. "Activity-driven fluctuations in living cells". In: *EPL (Europhysics Letters)* 110.4 (2015), p. 48005.

[59] Etienne Fodor et al. "How far from equilibrium active matter is ?" In: *Physical Review Letters* 117.3 (2016).

[60] Étienne Fodor et al. "How far from equilibrium is active matter?" In: *Physical review letters* 117.3 (2016), p. 038103.

[61] Étienne Fodor et al. "Non-Gaussian noise without memory in active matter". In: *Physical Review E* 98.6 (2018), p. 062610.

[62] Ronald F Fox. "Functional-calculus approach to stochastic differential equations". In: *Physical Review A* 33.1 (1986), p. 467.

[63] Silvio Franz and Giorgio Parisi. "Recipes for metastable states in spin glasses". In: *Journal de Physique I* 5.11 (1995), pp. 1401–1415.

[64] H. L. Frisch and J. K. Percus. "High dimensionality as an organizing device for classical fluids". In: *Phys. Rev. E* 60 (3 1999), pp. 2942–2948. DOI: 10.1103/PhysRevE.60.2942. URL: https://link.aps.org/doi/10.1103/PhysRevE.60.2942.

[65] H. L. Frisch and J. K. Percus. "Nonuniform classical fluid at high dimensionality". In: *Phys. Rev. A* 35 (11 1987), pp. 4696–4702. DOI: 10.1103/PhysRevA.35.4696. URL: https://link.aps.org/doi/10.1103/PhysRevA.35.4696.

[66] H. L. Frisch, N. Rivier, and D. Wyler. "Classical Hard-Sphere Fluid in Infinitely Many Dimensions". In: *Phys. Rev. Lett.* 54 (19 1985), pp. 2061–2063. DOI: 10.1103/PhysRevLett.54.2061. URL: https://link.aps.org/doi/10.1103/PhysRevLett.54.2061.

[67] HL Frisch and JK Percus. "High dimensionality as an organizing device for classical fluids". In: *Physical Review E* 60.3 (1999), p. 2942.

[68] HL Frisch, N Rivier, and D Wyler. "Classical hard-sphere fluid in infinitely many dimensions". In: *Physical review letters* 54.19 (1985), p. 2061.

[69] Yan V Fyodorov. "Complexity of random energy landscapes, glass transition, and absolute value of the spectral determinant of random matrices". In: *Physical review letters* 92.24 (2004), p. 240601.

[70] Yan V Fyodorov and Boris A Khoruzhenko. "Nonlinear analogue of the May- Wigner instability transition". In: *Proceedings of the National Academy of Sciences* 113.25 (2016), pp. 6827–6832.

[71] Yan V Fyodorov and Pierre Le Doussal. "Topology trivialization and large deviations for the minimum in the simplest random optimization". In: *Journal of Statistical Physics* 154.1 (2014), pp. 466–490.

[72] Yan V Fyodorov and H-J Sommers. "Classical particle in a box with random potential: exploiting rotational symmetry of replicated Hamiltonian". In: *Nuclear Physics B* 764.3 (2007), pp. 128–167.

[73] Peter Galajda et al. "A wall of funnels concentrates swimming bacteria". In: *Journal of bacteriology* 189.23 (2007), pp. 8704–8707.

[74] C. W. Gardiner. *Handbook of stochastic methods for physics, chemistry, and the natural sciences*. 2nd ed. Springer series in synergetics 13. Berlin ; New York: Springer-Verlag, 1994. ISBN: 978-3-540-15607-9 978-0-387-15607-1.

[75] Crispin W Gardiner et al. *Handbook of stochastic methods*. Vol. 3. springer Berlin, 1985.

[76] Elizabeth Gardner. "The space of interactions in neural network models". In: *Journal of physics A: Mathematical and general* 21.1 (1988), p. 257.

[77] J. L. Gervais and A. Jevicki. "Point canonical transformations in the path integral". In: *Nuclear Physics B* 110.1 (July 1976), pp. 93–112. ISSN: 0550-3213. DOI: 10.1016/0550-3213(76)90422-3. URL: http://www.sciencedirect.com/science/article/pii/0550321376904223 (visited on 11/22/2016).

[78] S. Ghosh, F. Mugele, and M. H. G. Duits. "Effects of shear and walls on the diffusion of colloids in microchannels". In: *Phys. Rev. E* 91 (5 2015), p. 052305. DOI: 10.1103/PhysRevE.91.052305. URL: https://link.aps.org/doi/10.1103/PhysRevE.91.052305.

[79] Daniel T Gillespie. "Exact numerical simulation of the Ornstein-Uhlenbeck process and its integral". In: *Physical review E* 54.2 (1996), p. 2084.

[80] Francesco Ginelli et al. "Intermittent collective dynamics emerge from conflicting imperatives in sheep herds". In: *Proceedings of the National Academy of Sciences* 112.41 (2015), pp. 12729–12734.

[81] Félix Ginot et al. "Nonequilibrium equation of state in suspensions of active colloids". In: *Physical Review X* 5.1 (2015), p. 011004.

[82] Luca Giomi et al. "Defect Annihilation and Proliferation in Active Nematics". In: *Phys. Rev. Lett.* 110 (22 2013), p. 228101. DOI: 10.1103/PhysRevLett.110.228101. URL: https://link.aps.org/doi/10.1103/PhysRevLett.110.228101.

[83] Nigel Goldenfeld. *Lectures on phase transitions and the renormalization group*. CRC Press, 2018.

[84] Koushik Goswami. "Work fluctuations in a generalized Gaussian active bath". In: *Physica A: Statistical Mechanics and its Applications* (2020), p. 125609.

[85] Georg A. Gottwald, Daan T. Crommelin, and Christian L. E. Franzke. "Stochastic Climate Theory". In: *Nonlinear and Stochastic Climate Dynamics*. Ed. by Christian L. E. Franzke and Terence J.Editors O'Kane. Cambridge University Press, 2017, 209–240. DOI: 10.1017/9781316339251.009.

[86] R. Graham. "Covariant formulation of non-equilibrium statistical thermodynamics". en. In: *Zeitschrift für Physik B Condensed Matter* 26.4 (Dec. 1977), pp. 397–405. ISSN: 0722-3277, 1431-584X. DOI: 10.1007/BF01570750. URL: https://link.springer.com/article/10.1007/BF01570750 (visited on 06/18/2018).

[87] R. Graham. "Path integral formulation of general diffusion processes". en. In: *Zeitschrift für Physik B Condensed Matter* 26.3 (Sept. 1977), pp. 281–290. ISSN: 0722-3277, 1431-584X. DOI: 10.1007/BF01312935. URL: https://link.springer.com/article/10.1007/BF01312935 (visited on 05/11/2018).

[88] Vincent Hakim and Pascal Silberzan. "Collective cell migration: a physics perspective". In: *Reports on Progress in Physics* 80.7 (2017), p. 076601.

[89] P. Hänggi. "Connection between Deterministic and Stochastic Descriptions of Nonlinear Systems". In: *Helv. Phys. Acta* 53 (1980), p. 491.

[90] P. Hänggi. "Stochastic Processes I: Asymptotic Behaviour and Symmetries". In: *Helv. Phys. Acta* 51 (1978), p. 183.

[91] P. Hänggi and H. Thomas. "Stochastic Processes: Time-Evolution, Symmetries and Linear Response". In: *Phys. Rep.* 88 (1982), p. 207.

[92] Jean-Pierre Hansen and Ian R McDonald. *Theory of simple liquids*. Elsevier, 1990.

[93] Andreas Härtel, David Richard, and Thomas Speck. "Three-body correlations and conditional forces in suspensions of active hard disks". In: *Physical Review E* 97.1 (2018), p. 012606.

[94] John A Hertz, Yasser Roudi, and Peter Sollich. "Path integral methods for the dynamics of stochastic and disordered systems". In: *Journal of Physics A: Mathematical and Theoretical* 50.3 (2016), p. 033001.

[95] C. L. Hicks et al. "Gardner Transition in Physical Dimensions". In: *Phys. Rev. Lett.* 120 (22 2018), p. 225501. DOI: 10.1103/PhysRevLett.120.225501. URL: https://link.aps.org/doi/10.1103/PhysRevLett.120.225501.

[96] P. C. Hohenberg. "Existence of Long-Range Order in One and Two Dimensions". In: *Phys. Rev.* 158 (2 1967), pp. 383–386. DOI: 10.1103/PhysRev.158.383. URL: https://link.aps.org/doi/10.1103/PhysRev.158.383.

[97] W. Horsthemke and R. Lefever. *Noise induced phase transitions*. Springer, Berlin, 1984.

[98] John Hull et al. *Options, futures and other derivatives/John C. Hull*. Upper Saddle River, NJ: Prentice Hall, 2009.

[99] Atsushi Ikeda and Kunimasa Miyazaki. "Mode-Coupling Theory as a Mean-Field Description of the Glass Transition". In: *Phys. Rev. Lett.* 104 (25 2010), p. 255704. DOI: 10.1103/PhysRevLett.104.255704. URL: https://link.aps.org/doi/10.1103/PhysRevLett.104.255704.

[100] Wolfram Research, Inc. *Mathematica, Version 12.1*. Champaign, IL, 2020. URL: https://www.wolfram.com/mathematica.

[101] Ernst Ising. "Contribution to the Theory of Ferromagnetism". In: *Z. Phys.* 31 (1925), pp. 253–258. DOI: 10.1007/BF02980577.

[102] Hugo Jacquin. "Glass and jamming transition of simple liquids: static and dynamic theory". In: *arXiv preprint arXiv:1307.3997* (2013).

[103] H. K. Janssen. "On the renormalized field theory of nonlinear critical relaxation". In: *From Phase Transitions to Chaos*. World Scientific, Apr. 1992, pp. 68–91. ISBN: 978-981-02-0938-4.

[104] Hans-Karl Janssen. "On the nonequilibrium phase transition in reaction-diffusion systems with an absorbing stationary state". In: *Zeitschrift für Physik B Condensed Matter* 42.2 (1981), pp. 151–154.

[105] Peter Jung and Peter Hänggi. "Dynamical systems: a unified colored-noise approximation". In: *Physical review A* 35.10 (1987), p. 4464.

[106] Peter Jung and Peter Hänggi. "Dynamical systems: A unified colored-noise approximation". In: *Phys. Rev. A* 35 (10 1987), pp. 4464–4466. DOI: 10.1103/PhysRevA.35.4464. URL: https://link.aps.org/doi/10.1103/PhysRevA.35.4464.

[107] Mark Kac. "A stochastic model related to the telegrapher's equation". In: *The Rocky Mountain Journal of Mathematics* 4.3 (1974), pp. 497–509.

[108] N. G. van Kampen. *Stochastic processes in physics and chemistry*. 3rd ed. North-Holland personal library. Amsterdam ; Boston: Elsevier, 2007. ISBN: 978-0-444-52965-7.

[109] N. G. van Kampen. "Itô versus Stratonovich". en. In: *J Stat Phys* 24.1 (Jan. 1981), pp. 175–187. ISSN: 0022-4715, 1572-9613. DOI: 10.1007/BF01007642. URL: https://link.springer.com/article/10.1007/BF01007642 (visited on 03/06/2017).

[110] K. Kanazawa, T. Sagawa, and H. Hayakawa. "Stochastic Energetics for Non-Gaussian Processes". In: *Phys. Rev. Lett.* 108.21 (May 2012), p. 210601. DOI: 10.1103/PhysRevLett.108.210601. URL: https://link.aps.org/doi/10.1103/PhysRevLett.108.210601 (visited on 02/18/2018).

[111] Yael Katz et al. "Inferring the structure and dynamics of interactions in schooling fish". In: *Proceedings of the National Academy of Sciences* 108.46 (2011), pp. 18720–18725.

[112] Y. Klimontovich. "Ito, stratonovich and kinetic forms of stochastic equations". In: *Phys. A* 163 (1990), p. 515.

[113] Y. L. Klimontovich. "Nonlinear Brownian motion". In: *Physics-Uspekhi* 37 (1994), p. 737.

[114] P. E. Kloeden and E. Platen. *Numerical solution of stochastic differential equations*. 2nd corr. print. Applications of mathematics 23. Berlin ; New York: Springer, 1995. ISBN: 978-3-540-54062-5 978-0-387-54062-7.

[115] P. E. Kloeden, E. Platen, and H. Schurz. *Numerical solution of SDE through computer experiments*. Springer Science & Business Media, 2012.

[116] AN Kolmogorov. "On the conservation of conditionally periodic motions under small perturbation of the Hamiltonian". In: *Dokl. Akad. Nauk. SSR*. Vol. 98. 527. 1954, pp. 2–3.

[117] N Koumakis, C Maggi, and R Di Leonardo. "Directed transport of active particles over asymmetric energy barriers". In: *Soft matter* 10.31 (2014), pp. 5695–5701.

[118] Robert H Kraichnan. "Stochastic Models for Many-Body Systems. I. Infinite Systems in Thermal Equilibrium". In: *Journal of Mathematical Physics* 3.3 (1962), pp. 475–495.

[119] Jorge Kurchan, Thibaud Maimbourg, and Francesco Zamponi. "Statics and dynamics of infinite-dimensional liquids and glasses: a parallel and compact derivation". In: *Journal of Statistical Mechanics: Theory and Experiment* 2016.3 (2016), p. 033210.

[120] Jorge Kurchan, Giorgio Parisi, and Francesco Zamponi. "Exact theory of dense amorphous hard spheres in high dimension I. The free energy". In: *Journal of Statistical Mechanics: Theory and Experiment* 2012.10 (2012), P10012. DOI: 10.1088/1742-5468/2012/10/p10012. URL: https://doi.org/10.1088%2F1742-5468%2F2012%2F10%2Fp10012.

[121] Christina Kurzthaler et al. "Probing the spatiotemporal dynamics of catalytic Janus particles with single-particle tracking and differential dynamic microscopy". In: *Physical review letters* 121.7 (2018), p. 078001.

[122] K. H. Lan, N. Ostrowsky, and D. Sornette. "Brownian dynamics close to a wall studied by photon correlation spectroscopy from an evanescent wave". In: *Phys. Rev. Lett.* 57 (1 1986), pp. 17–20. DOI: 10.1103/PhysRevLett.57.17. URL: https://link.aps.org/doi/10.1103/PhysRevLett.57.17.

[123] Paul Langevin. "Sur la théorie du mouvement brownien". In: *Compt. Rendus* 146 (1908), pp. 530–533.

[124] F Langouche, D Roekaerts, and E Tirapegui. "Functional integral methods for random fields". In: *Stochastic Processes in Nonequilibrium Systems*. Springer, 1978, pp. 316–329.

[125] F. Langouche, D. Roekaerts, and E. Tirapegui. "Functional integrals and the Fokker-Planck equation". en. In: *Nuovo Cim. B* 53.1 (Sept. 1979), pp. 135–159. ISSN: 1826-9877. DOI: 10.1007/BF02739307. (Visited on 04/04/2017).

[126] F. Langouche, D. Roekaerts, and E. Tirapegui. "General Langevin equations and functional integration". In: *Field Theory, Quantization and Statistical Physics: in Memory of Bernard Jouvet*. Dordrecht: Springer, 1981.

[127] F Langouche, D Roekaerts, and E Tirapegui. "Short derivation of Feynman Lagrangian for general diffusion processes". In: *Journal of Physics A: Mathematical and General* 13.2 (1980), p. 449.

[128] François A Lavergne et al. "Group formation and cohesion of active particles with visual perception–dependent motility". In: *Science* 364.6435 (2019), pp. 70–74.

[129] J. T. Lewis, James McConnell, and B. K. P. Scaife. "Relaxation Effects in Rotational Brownian Motion". In: *Proceedings of the Royal Irish Academy. Section A: Mathematical and Physical Sciences* 76 (1976), pp. 43–69. ISSN: 00358975. URL: http://www.jstor.org/stable/20489032.

[130] Chen Liu et al. *On the Dynamics of Liquids in the Large-Dimensional Limit*. 2021. arXiv: 2108.02378 [cond-mat.stat-mech].

[131] Hartmut Löwen. "Fun with Hard Spheres". In: *Statistical Physics and Spatial Statistics*. Ed. by Klaus R. Mecke and Dietrich Stoyan. Berlin, Heidelberg: Springer Berlin Heidelberg, 2000, pp. 295–331. ISBN: 978-3-540-45043-6.

[132] S. Machlup and L. Onsager. "Fluctuations and Irreversible Process. II. Systems with Kinetic Energy". In: *Phys. Rev.* 91.6 (Sept. 1953), pp. 1512–1515. DOI: 10.1103/PhysRev.91.1512. URL: http://link.aps.org/doi/10.1103/PhysRev.91.1512 (visited on 03/07/2017).

[133] Claudio Maggi et al. "Generalized energy equipartition in harmonic oscillators driven by active baths". In: *Physical review letters* 113.23 (2014), p. 238303.

[134] Claudio Maggi et al. "Multidimensional stationary probability distribution for interacting active particles". In: *Scientific reports* 5.1 (2015), pp. 1–7.

[135] Thibaud Maimbourg. "Théorie des liquides et verres en dimension infinie". PhD thesis. Université Paris sciences et lettres, 2016.

[136] Thibaud Maimbourg, Jorge Kurchan, and Francesco Zamponi. "Solution of the Dynamics of Liquids in the Large-Dimensional Limit". In: *Phys. Rev. Lett.* 116 (1 2016), p. 015902. DOI: 10.1103/PhysRevLett.116.015902. URL: https://link.aps.org/doi/10.1103/PhysRevLett.116.015902.

[137] Kanaya Malakar et al. "Steady state, relaxation and first-passage properties of a run-and-tumble particle in one-dimension". In: *Journal of Statistical Mechanics: Theory and Experiment* 2018.4 (2018), p. 043215.

[138] Alessandro Manacorda, Grégory Schehr, and Francesco Zamponi. "Numerical solution of the dynamical mean field theory of infinite-dimensional equilibrium liquids". In: *The Journal of Chemical Physics* 152.16 (2020), p. 164506. DOI: 10.1063/5.0007036. eprint: https://doi.org/10.1063/5.0007036. URL: https://doi.org/10.1063/5.0007036.

[139] R. Mannella. "Integration of stochastic differential equations on a computer". In: *International Journal of Modern Physics C* 13.09 (Nov. 2002), pp. 1177–1194. ISSN: 0129-1831. DOI: 10.1142/S0129183102004042. URL: https://www.worldscientific.com/doi/abs/10.1142/S0129183102004042 (visited on 11/09/2018).

[140] Sophie Marbach, David S Dean, and Lydéric Bocquet. "Transport and dispersion across wiggling nanopores". In: *Nature Physics* 14.11 (2018), pp. 1108–1113.

[141] Umberto Marini Bettolo Marconi, Matteo Paoluzzi, and Claudio Maggi. "Effective potential method for active particles". In: *Molecular Physics* 114.16-17 (2016), pp. 2400–2410.

[142] Romain Mari and Jorge Kurchan. "Dynamical transition of glasses: From exact to approximate". In: *The Journal of Chemical Physics* 135.12 (2011), p. 124504. DOI: 10.1063/1.3626802. eprint: https://doi.org/10.1063/1.3626802. URL: https://doi.org/10.1063/1.3626802.

[143] David Martin and Thibaut Arnoulx de Pirey. "AOUP in the presence of Brownian noise: a perturbative approach". In: *Journal of Statistical Mechanics: Theory and Experiment* 2021.4 (2021), p. 043205.

[144] David Martin et al. “Statistical Mechanics of Active Ornstein Uhlenbeck Particles”. In: *arXiv preprint arXiv:2008.12972v1* (2020).

[145] David Martin et al. “Statistical mechanics of active Ornstein-Uhlenbeck particles”. In: *Physical Review E* 103.3 (2021), p. 032607.

[146] A. Matacz. “A new theory of stochastic inflation”. In: *Physical Review D* 55.4 (Feb. 1997), pp. 1860–1874. DOI: 10.1103/PhysRevD.55.1860. URL: https://link.aps.org/doi/10.1103/PhysRevD.55.1860 (visited on 05/02/2018).

[147] Robert M May. “Will a large complex system be stable?” In: *Nature* 238.5364 (1972), pp. 413–414.

[148] JE Mayer and MG Mayer. “Statistical Mechanics QViley”. In: *New York* (1940).

[149] Joseph Edward Mayer and Maria Goeppert Mayer. *Statistical mechanics*. 2d ed. Wiley New York, 1977. ISBN: 0471579858.

[150] D. W. McLaughlin and L. S. Schulman. “Path Integrals in Curved Spaces”. en. In: *Journal of Mathematical Physics* 12.12 (Dec. 1971), pp. 2520–2524. ISSN: 0022-2488, 1089-7658. DOI: 10.1063/1.1665567. URL: http://aip.scitation.org/doi/10.1063/1.1665567 (visited on 04/26/2018).

[151] N David Mermin and Herbert Wagner. “Absence of ferromagnetism or antiferromagnetism in one-or two-dimensional isotropic Heisenberg models”. In: *Physical Review Letters* 17.22 (1966), p. 1133.

[152] Marc Mézard, Giorgio Parisi, and Miguel Angel Virasoro. *Spin glass theory and beyond: An Introduction to the Replica Method and Its Applications*. Vol. 9. World Scientific Publishing Company, 1987.

[153] G. Mil’shtejn. “Approximate Integration of Stochastic Differential Equations”. In: *Teor. Veroyatnost. i Primenen.* 19.3 (June 1974), pp. 583–588. ISSN: 0040-585X. URL: http://www.mathnet.ru/php/archive.phtml?wshow=paper&jrnid=tvp&paperid=2929&option_lang=eng (visited on 06/21/2019).

[154] G. Mil’shtejn. “Approximate Integration of Stochastic Differential Equations”. In: *Theory Probab. Appl.* 19.3 (June 1975), pp. 557–562. ISSN: 0040-585X. DOI: 10.1137/1119062. URL: https://epubs.siam.org/doi/10.1137/1119062 (visited on 06/21/2019).

[155] Ruoyang Mo, Qinyi Liao, and Ning Xu. “Rheological similarities between dense self-propelled and sheared particulate systems”. In: *Soft Matter* 16 (15 2020), pp. 3642–3648. DOI: 10.1039/D0SM00101E. URL: http://dx.doi.org/10.1039/D0SM00101E.

[156] José Moran and Jean-Philippe Bouchaud. “May’s instability in large economies”. In: *Phys. Rev. E* 100 (3 2019), p. 032307. DOI: 10.1103/PhysRevE.100.032307. URL: https://link.aps.org/doi/10.1103/PhysRevE.100.032307.

[157] Cécile Morette. "On the definition and approximation of Feynman's path integrals". In: *Physical Review* 81.5 (1951), p. 848.

[158] Tohru Morita and Kazuo Hiroike. "A new approach to the theory of classical fluids. III: general treatment of classical systems". In: *Progress of Theoretical Physics* 25.4 (1961), pp. 537–578.

[159] Jürgen K Moser. "On invariant curves of area-preserving mapping of an annulus". In: *Matematika* 6.5 (1962), pp. 51–68.

[160] E. Nelson. *Quantum fluctuations*. Princeton series in physics. Princeton, N.J: Princeton University Press, 1985. ISBN: 978-0-691-08378-0 978-0-691-08379-7.

[161] Jérémy O'Byrne et al. *Time-(ir)reversibility in active matter: from micro to macro*. 2021. arXiv: 2104.03030 [cond-mat.stat-mech].

[162] Ahmad K Omar et al. "Phase Diagram of Active Brownian Spheres: Crystallization and the Metastability of Motility-Induced Phase Separation". In: *Physical Review Letters* 126.18 (2021), p. 188002.

[163] Ahmad K. Omar et al. *Tuning Nonequilibrium Phase Transitions with Inertia*. 2021. arXiv: 2108.10278 [cond-mat.soft].

[164] Minoru Omote. "Point canonical transformations and the path integral". In: *Nuclear Physics B* 120.2 (1977), pp. 325–332.

[165] L. Onsager and S. Machlup. "Fluctuations and Irreversible Processes". In: *Phys. Rev.* 91.6 (Sept. 1953), pp. 1505–1512. DOI: 10.1103/PhysRev.91.1505. URL: http://link.aps.org/doi/10.1103/PhysRev.91.1505 (visited on 03/07/2017).

[166] Leonard S Ornstein. "Accidental deviations of density and opalescence at the critical point of a single substance". In: *Proc. Akad. Sci.* 17 (1914), p. 793.

[167] M. Di Paola and G. Falsone. "Stochastic Response on Non-Linear Systems under Parametric Non-Gaussian Agencies". en. In: *Nonlinear Stochastic Mechanics*. IUTAM Symposia. Springer, Berlin, Heidelberg, 1992, pp. 155–166. ISBN: 978-3-642-84791-2 978-3-642-84789-9. URL: https://link.springer.com/chapter/10.1007/978-3-642-84789-9_13 (visited on 02/18/2018).

[168] G. Parisi. *Statistical Field Theory*. New York: Addison-Wesley, 1988.

[169] Giorgio Parisi, Pierfrancesco Urbani, and Francesco Zamponi. *Theory of simple glasses: exact solutions in infinite dimensions*. Cambridge University Press, 2020.

[170] Giorgio Parisi and Francesco Zamponi. "Amorphous packings of hard spheres for large space dimension". In: *Journal of Statistical Mechanics: Theory and Experiment* 2006.03 (2006), P03017–P03017. DOI: 10.1088/1742-5468/2006/03/p03017. URL: https://doi.org/10.1088%2F1742-5468%2F2006%2F03%2Fp03017.

[171] Giorgio Parisi and Francesco Zamponi. "Mean-field theory of hard sphere glasses and jamming". In: *Reviews of Modern Physics* 82.1 (2010), p. 789.

[172] Giorgio Parisi and Francesco Zamponi. "Mean-field theory of hard sphere glasses and jamming". In: *Rev. Mod. Phys.* 82 (1 2010), pp. 789–845. DOI: 10.1103/RevModPhys.82.789. URL: https://link.aps.org/doi/10.1103/RevModPhys.82.789.

[173] Fernando Peruani et al. "Collective Motion and Nonequilibrium Cluster Formation in Colonies of Gliding Bacteria". In: *Phys. Rev. Lett.* 108 (9 2012), p. 098102. DOI: 10.1103/PhysRevLett.108.098102. URL: https://link.aps.org/doi/10.1103/PhysRevLett.108.098102.

[174] S. Pieprzyk, D. M. Heyes, and A. C. Brańka. "Spatially dependent diffusion coefficient as a model for pH sensitive microgel particles in microchannels". In: *Biomicrofluidics* 10.5 (2016), p. 054118. DOI: 10.1063/1.4964935. eprint: https://doi.org/10.1063/1.4964935. URL: https://doi.org/10.1063/1.4964935.

[175] Thibaut Arnoulx de Pirey, Gustavo Lozano, and Frédéric van Wijland. "Active hard spheres in infinitely many dimensions". In: *Physical review letters* 123.26 (2019), p. 260602.

[176] Thibaut Arnoulx de Pirey et al. *Active matter in infinite dimensions: Fokker-Planck equation and dynamical mean-field theory at low density*. 2021. arXiv: 2108.02407 [cond-mat.stat-mech].

[177] *Private communications with Yongjoo Baek.*

[178] Sriram Ramaswamy. "The mechanics and statistics of active matter". In: *Annu. Rev. Condens. Matter Phys.* 1.1 (2010), pp. 323–345.

[179] Markus Rein and Thomas Speck. "Applicability of effective pair potentials for active Brownian particles". In: *The European Physical Journal E* 39.9 (2016), pp. 1–9.

[180] John Shipley Rowlinson. *Cohesion: a scientific history of intermolecular forces*. Cambridge University Press, 2005.

[181] F Roy et al. "Numerical implementation of dynamical mean field theory for disordered systems: application to the Lotka–Volterra model of ecosystems". In: *Journal of Physics A: Mathematical and Theoretical* 52.48 (2019), p. 484001.

[182] F. Sagués, J. M. Sancho, and J. García-Ojalvo. "Spatiotemporal order out of noise". In: *Rev. Mod. Phys.* 79 (2007), p. 829.

[183] David Saintillan and Michael J. Shelley. "Instabilities and Pattern Formation in Active Particle Suspensions: Kinetic Theory and Continuum Simulations". In: *Phys. Rev. Lett.* 100 (17 2008), p. 178103. DOI: 10.1103/PhysRevLett.100.178103. URL: https://link.aps.org/doi/10.1103/PhysRevLett.100.178103.

[184] Paolo Sartori et al. “Wall accumulation of bacteria with different motility patterns”. In: *Physical Review E* 97.2 (2018), p. 022610.

[185] Bernhard Schmid and Rolf Schilling. “Glass transition of hard spheres in high dimensions”. In: *Phys. Rev. E* 81 (4 2010), p. 041502. DOI: 10.1103/PhysRevE.81.041502. URL: https://link.aps.org/doi/10.1103/PhysRevE.81.041502.

[186] Mark J. Schnitzer. “Theory of continuum random walks and application to chemotaxis”. In: *Phys. Rev. E* 48 (4 1993), pp. 2553–2568. DOI: 10.1103/PhysRevE.48.2553. URL: https://link.aps.org/doi/10.1103/PhysRevE.48.2553.

[187] Udo Seifert. “Stochastic thermodynamics, fluctuation theorems and molecular machines”. In: *Reports on progress in physics* 75.12 (2012), p. 126001.

[188] Ken Sekimoto. *Stochastic energetics*. Vol. 799. Springer, 2010.

[189] Mauro Sellitto and Francesco Zamponi. “A thermodynamic description of colloidal glasses”. In: *EPL (Europhysics Letters)* 103.4 (2013), p. 46005.

[190] Mauro Sellitto and Francesco Zamponi. “Packing hard spheres with short-range attraction in infinite dimension: phase structure and algorithmic implications”. In: *Journal of Physics: Conference Series*. Vol. 473. 1. IOP Publishing. 2013, p. 012020.

[191] Yakov G Sinai. “Dynamical systems with elastic reflections”. In: *Russian Mathematical Surveys* 25.2 (1970), p. 137.

[192] Alexandre P Solon et al. “Generalized thermodynamics of motility-induced phase separation: phase equilibria, Laplace pressure, and change of ensembles”. In: *New Journal of Physics* 20.7 (2018), p. 075001.

[193] Alexandre P Solon et al. “Pressure and phase equilibria in interacting active Brownian spheres”. In: *Physical review letters* 114.19 (2015), p. 198301.

[194] Alexandre P Solon et al. “Pressure is not a state function for generic active fluids”. In: *Nature Physics* 11.8 (2015), pp. 673–678.

[195] Vanessa Sperandio, Alfredo G Torres, and James B Kaper. “Quorum sensing Escherichia coli regulators B and C (QseBC): a novel two-component regulatory system involved in the regulation of flagella and motility by quorum sensing in E. coli”. In: *Molecular microbiology* 43.3 (2002), pp. 809–821.

[196] Joakim Stenhammar et al. “Phase behaviour of active Brownian particles: the role of dimensionality”. In: *Soft matter* 10.10 (2014), pp. 1489–1499.

[197] R. L. Stratonovich. *Nonlinear Nonequilibrium Thermodynamics I*. Berlin: Springer, 1992.

[198] Grzegorz Szamel. “Self-propelled particle in an external potential: Existence of an effective temperature”. In: *Physical Review E* 90.1 (2014), p. 012111.

[199] J. Tailleur and M. E. Cates. "Sedimentation, trapping, and rectification of dilute bacteria". In: *EPL (Europhysics Letters)* 86.6 (2009), p. 60002. ISSN: 1286-4854. DOI: 10.1209/0295-5075/86/60002. URL: http://dx.doi.org/10.1209/0295-5075/86/60002.

[200] J. Tailleur and M. E. Cates. "Statistical Mechanics of Interacting Run-and-Tumble Bacteria". In: *Phys. Rev. Lett.* 100 (21 2008), p. 218103. DOI: 10.1103/PhysRevLett.100.218103. URL: https://link.aps.org/doi/10.1103/PhysRevLett.100.218103.

[201] John Toner and Yuhai Tu. "Flocks, herds, and schools: A quantitative theory of flocking". In: *Phys. Rev. E* 58 (4 1998), pp. 4828–4858. DOI: 10.1103/PhysRevE.58.4828. URL: https://link.aps.org/doi/10.1103/PhysRevE.58.4828.

[202] Francesco Turci and Nigel B Wilding. "Phase separation and multibody effects in three-dimensional active brownian particles". In: *Physical Review Letters* 126.3 (2021), p. 038002.

[203] Hervé Turlier et al. "Equilibrium physics breakdown reveals the active nature of red blood cell flickering". In: *Nature physics* 12.5 (2016), pp. 513–519.

[204] Robin Van Damme et al. "Interparticle torques suppress motility-induced phase separation for rodlike particles". In: *The Journal of chemical physics* 150.16 (2019), p. 164501.

[205] V. Vennin and A. A. Starobinsky. "Correlation functions in stochastic inflation". en. In: *The European Physical Journal C* 75.9 (Sept. 2015), p. 413. ISSN: 1434-6044, 1434-6052. DOI: 10.1140/epjc/s10052-015-3643-y. URL: https://link.springer.com/article/10.1140/epjc/s10052-015-3643-y (visited on 04/26/2018).

[206] Tamás Vicsek et al. "Novel Type of Phase Transition in a System of Self-Driven Particles". In: *Phys. Rev. Lett.* 75 (6 1995), pp. 1226–1229. DOI: 10.1103/PhysRevLett.75.1226. URL: https://link.aps.org/doi/10.1103/PhysRevLett.75.1226.

[207] Andreas Walther and Axel HE Müller. "Janus particles". In: *Soft Matter* 4.4 (2008), pp. 663–668.

[208] N. Wiener. "Differential-Space". en. In: *Journal of Mathematics and Physics* 2.1-4 (1923), pp. 131–174. ISSN: 00971421. DOI: 10.1002/sapm192321131. URL: http://doi.wiley.com/10.1002/sapm192321131 (visited on 04/25/2018).

[209] N. Wiener. "The Average value of a Functional". en. In: *Proceedings of the London Mathematical Society* s2-22.1 (1924), pp. 454–467. ISSN: 00246115. DOI: 10.1112/plms/s2-22.1.454. URL: http://doi.wiley.com/10.1112/plms/s2-22.1.454 (visited on 04/25/2018).

[210] Claire Wilhelm. "Out-of-equilibrium microrheology inside living cells". In: *Physical review letters* 101.2 (2008), p. 028101.

[211] René Wittmann et al. "Effective equilibrium states in the colored-noise model for active matter I. Pairwise forces in the Fox and unified colored noise approximations". In: *Journal of Statistical Mechanics: Theory and Experiment* 2017.11 (2017), p. 113207.

[212] Eric Woillez, Yariv Kafri, and Vivien Lecomte. "Nonlocal stationary probability distributions and escape rates for an active Ornstein–Uhlenbeck particle". In: *Journal of Statistical Mechanics: Theory and Experiment* 2020.6 (2020), p. 063204.

[213] D. Wyler, N. Rivier, and H. L. Frisch. "Hard-sphere fluid in infinite dimensions". In: *Phys. Rev. A* 36 (5 1987), pp. 2422–2431. DOI: 10.1103/PhysRevA.36.2422. URL: https://link.aps.org/doi/10.1103/PhysRevA.36.2422.

[214] Natsuhiko Yoshinaga and Tanniemola B Liverpool. "Hydrodynamic interactions in dense active suspensions: From polar order to dynamical clusters". In: *Physical Review E* 96.2 (2017), p. 020603.

[215] Jean Zinn-Justin. *Quantum field theory and critical phenomena*. Vol. 171. Oxford university press, 2021.

[216] Andreas Zöttl and Holger Stark. "Hydrodynamics Determines Collective Motion and Phase Behavior of Active Colloids in Quasi-Two-Dimensional Confinement". In: *Phys. Rev. Lett.* 112 (11 2014), p. 118101. DOI: 10.1103/PhysRevLett.112.118101. URL: https://link.aps.org/doi/10.1103/PhysRevLett.112.118101.

[217] Robert Zwanzig. *Nonequilibrium statistical mechanics*. Oxford university press, 2001.